PERSPECTIVES OF CHEMICALS SYNTHESIS AS A GREEN ALTERNATIVE TO FOSSIL FUELS

EDITED BY: Luis Puigjaner, Antonio Espuña, Mar Pérez-Fortes and
Ana Somoza-Tornos

PUBLISHED IN: Frontiers in Energy Research

frontiers Research Topics

Frontiers eBook Copyright Statement

ISSN 1664-8714
ISBN 978-2-88971-945-7
DOI 10.3389/978-2-88971-945-7

About Frontiers

Frontiers is more than just an open-access publisher of scholarly articles: it is a pioneering approach to the world of academia, radically improving the way scholarly research is managed. The grand vision of Frontiers is a world where all people have an equal opportunity to seek, share and generate knowledge. Frontiers provides immediate and permanent online open access to all its publications, but this alone is not enough to realize our grand goals.

Frontiers Journal Series

The Frontiers Journal Series is a multi-tier and interdisciplinary set of open-access, online journals, promising a paradigm shift from the current review, selection and dissemination processes in academic publishing. All Frontiers journals are driven by researchers for researchers; therefore, they constitute a service to the scholarly community. At the same time, the Frontiers Journal Series operates on a revolutionary invention, the tiered publishing system, initially addressing specific communities of scholars, and gradually climbing up to broader public understanding, thus serving the interests of the lay society, too.

Dedication to Quality

Each Frontiers article is a landmark of the highest quality, thanks to genuinely collaborative interactions between authors and review editors, who include some of the world's best academicians. Research must be certified by peers before entering a stream of knowledge that may eventually reach the public - and shape society; therefore, Frontiers only applies the most rigorous and unbiased reviews.
Frontiers revolutionizes research publishing by freely delivering the most outstanding research, evaluated with no bias from both the academic and social point of view. By applying the most advanced information technologies, Frontiers is catapulting scholarly publishing into a new generation.

What are Frontiers Research Topics?

Frontiers Research Topics are very popular trademarks of the Frontiers Journals Series: they are collections of at least ten articles, all centered on a particular subject. With their unique mix of varied contributions from Original Research to Review Articles, Frontiers Research Topics unify the most influential researchers, the latest key findings and historical advances in a hot research area! Find out more on how to host your own Frontiers Research Topic or contribute to one as an author by contacting the Frontiers Editorial Office: frontiersin.org/about/contact

PERSPECTIVES OF CHEMICALS SYNTHESIS AS A GREEN ALTERNATIVE TO FOSSIL FUELS

Topic Editors:
Luis Puigjaner, Universitat Politecnica de Catalunya, Spain
Antonio Espuña, Universitat Politecnica de Catalunya, Spain
Mar Pérez-Fortes, Delft University of Technology, Netherlands
Ana Somoza-Tornos, University of Colorado Boulder, United States

Citation: Puigjaner, L., Espuña, A., Pérez-Fortes, M., Somoza-Tornos, A., eds. (2021). Perspectives of Chemicals Synthesis as a Green Alternative to Fossil Fuels. Lausanne: Frontiers Media SA. doi: 10.3389/978-2-88971-945-7

Table of Contents

frontiers
in Energy Research

EDITORIAL
published: 05 November 2021
doi: 10.3389/fenrg.2021.780533

Editorial: Perspectives of Chemicals Synthesis as a Green Alternative to Fossil Fuels

Luis Puigjaner[1]*, Mar Pérez-Fortes[2], Ana Somoza-Tornos[1,3] and Antonio Espuña[1]

[1]Department of Chemical Engineering, Universitat Politècnica de Catalunya, Campus Diagonal-Besòs, Barcelona, Spain, [2]Department of Engineering Systems and Services, Faculty of Technology, Policy and Management, Delft University of Technology, Delft, Netherlands, [3]Renewable and Sustainable Energy Institute (RASEI), University of Colorado Boulder, Boulder, CO, United States

Keywords: green fuels, circular economy, low carbon processes, sustainable development, process systems engineering, LCA, economic competitiveness

OPEN ACCESS

Edited and reviewed by:
Francois M. A. Marechal,
École Polytechnique Fédérale de Lausanne, Switzerland

****Correspondence:***
Luis Puigjaner
luis.puigjaner@upc.edu

Specialty section:
This article was submitted to Process and Energy Systems Engineering, a section of the Frontiers in Energy Research.

Received: *21 September 2021*
Accepted: *19 October 2021*
Published: *05 November 2021*

Citation:
Puigjaner L, Pérez-Fortes M, Somoza-Tornos A and Espuña A (2021) Editorial: Perspectives of Chemicals Synthesis as a Green Alternative to Fossil Fuels. Front. Energy Res. 9:780533. doi: 10.3389/fenrg.2021.780533

Editorial on the Research Topic

Perspectives of Chemicals Synthesis as a Green Alternative to Fossil Fuels

Renewable energy sources and more efficient and integrated processes are needed to avoid resource depletion and climate change. The production of chemicals, fuels, and materials has to change from a primarily linear synthesis pathway to closed-loop alternatives based on circular economy approaches and rely on green and low carbon synthesis processes while supporting their economic competitiveness in the upcoming years. Green and low-carbon chemicals, fuels, and materials constitute the base for the transition towards a sustainable financial system. Important sectors that need to decrease their dependence on fossil fuels in terms of raw materials and energy consumption are, for instance, plastics, construction, packaging, textile, electronics, batteries, or transport.

Advance towards implementing novel circular approaches and green and low carbon processes urges to move towards techniques that eliminate waste, use renewable sources, or generate fewer emissions (are more efficient) than the overall benchmark processes. Process modeling and assessment stand as powerful tools to evaluate the economic characteristics (business cases) and the environmental benefit of the proposed options. Given the impressive advances in mathematical programming techniques during the last decades, a process systems engineering (PSE) approach is suitable for dealing with synthesis problems, systems analysis, and life cycle analysis (LCA). Besides, the significant advances achieved in solving enormous challenges, particularly for linear and mixed-integer linear programming techniques, offer unique possibilities to deal with this Research Topic.

The focus of this Research Topic is on chemicals, fuels, and materials synthesis processes; circular approaches, green, low carbon, and transitional solutions towards more environmentally friendly options. We look for Original Research, Review, or Mini-Review papers that discuss these issues. Themes of interest include, but are not limited to:

- Techno-economic and life cycle analyses of synthesis of green/low carbon chemicals, fuels, and materials;
- Evaluation, process design, and optimization of new synthesis pathways of chemicals, fuels, and materials;
- Analysis of the implementation of green/low carbon chemicals, fuels, and materials;
- Circular economy, carbon dioxide utilization, and electrochemistry for chemicals synthesis.

In the following, you will find selected contributions (Original research. Perspectives, and Review) to this research topic. They bring novel solution approaches accompanied by rich case studies and examples of practical interest.

ORIGINAL RESEARCH

The articles in this Special Issue examine different facets of alternative fuels' synthesis from the point of view of fuels as an end product. Contribution by Antonio Argüelles et al. should be of interest to the petroleum industry, companies and researchers. It reports a lack of information about the environmental impacts of renewable diesel production. The authors conduct attributional life cycle assessment (LCA) of green diesel obtained by hydrodeoxygenation (HEFA). Results demonstrate that biofuel significantly reduces GHG emissions than its fossil counterpart by about 110%. Renewable diesel (RD) production by HEFA has lower emissions than conventional diesel in the following categories: acidification, ozone layer depletion, and photochemical smog, while in the human toxicity and eutrophication categories, it has a significant environmental impact. Whenever RD has poor cold flow properties, it becomes necessary to mix it with ULSD.

Pacheco-López et al. also analyze the implications of the different end products. They present a techno-economic and environmental comparison of existing liquid fuels and their emerging renewable substitutes from biomass or the chemical recycling of plastic waste. They find that plastic waste pyrolysis oil performs better than diesel in cost (25% reduction) and environmental impacts. Their study also includes assessing bioethanol and ethanol from plastic waste pyrolysis as an alternative to gasoline additives, showing higher costs and variable results regarding the life cycle impacts. Thus, they analyze the effect of these results on gasoline blends and conclude that blends with ethanol from plastic pyrolysis can reduce the impact on human health and ecosystems. In contrast, blends with bioethanol have a lower impact on resource scarcity and better economic profitability.

Conversely, some of the works focus on the processes. Biomass waste used as fuel essentially provides a circular approach, and the following four papers consider organic waste as raw material.

The contribution by Castro-Amoedo et al. analyzes different biomass transformation technologies. The authors present a systematic approach for designing, evaluating, and ranking biomass-to-X production strategies under uncertain market conditions. Their framework includes a bi-level mixed-integer linear programming formulation to identify and assess current and promising robustness and resilient designs strategies. After studying the integration of anaerobic digestion of food and green waste biomass in the current Swiss market, they stress energy integration and poly-generation as critical factors for the energy transition.

In a similar light, Mahmud and Rosentrater examine the particulars of biomass pretreatment methods. They test low moisture anhydrous ammonia pretreatment to overcome the drawbacks of standard pretreatment methods. Once subjecting Distillers Dried Grains with Solubles, corn gluten feed, corn fiber, and oil palm frond (OPF) with different moisture contents to this pretreatment process, they find out a decreased lignin content of the materials, increased their percentage of α-cellulose, and improved enzymatic digestibility.

Shafinas and Rosentrater's article reveals the concern of food waste (FW) impacting the environment, societies, and economies, triggering research to find alternative ways to utilize such materials. FW may contain sugars (e.g., glucose) susceptible for conversion into value-added products such as highly demanded ethanol by industries like fuel, beverages, pharmaceuticals, and other industrial applications. To challenge the lower price of ethanol produced from corn, the authors propose an integrated system: a conventional fermentation plant integrated with a novel combined heat and power (CHP) system that reduces utility costs thanks to the recovery of energy from waste (FW). Using techno-economic analysis (TEA), the authors find it more economical and attractive at the commercial scale.

The energy transition needs alternative fuels, more efficient and integrated power plants. The following two papers use solid oxide cells as a technology that can use and provide renewable electricity in a highly efficient manner. From a plant system perspective, in the contribution by Pérez-Fortes et al., the authors apply scenario analysis, and multi-objective optimization to the design of a pilot integrated biomass waste gasifier—solid oxide fuel cell (SOFC) plant. The results in the paper summarize the most optimal operating conditions and provide an optimal plant layout (with anode off-gas recirculation and hot gas cleaning units) and a heat exchanger network. Combined heat and power efficiency can go up to 82%.

From a broader system perspective, the article by Carbone et al. evaluates the use of organic waste to power a reversible solid oxide cell (rSOC) via gasification to support the electricity grid. The rSOC system operated in electrolysis mode uses excess renewable electricity to synthesize methane. On the other side, the rSOC system operated in fuel cell mode supplies power when needed by the grid by oxidizing syngas. The paper uses hourly real large-scale energy storage needs and biomass waste generation for the southern Italian peninsula in 2030. The methodology can be of use in other case studies (locations and technologies). For the current situation, the authors calculated the yearly used biomass waste and the yearly electricity storage and generation needs provided by the gasification-rSOC system.

The chemical industry and particularly energy-intensive industries like steel production have inherent CO_2 emissions. Industrial symbiosis, Circular, in essence, industrial symbiosis aims at using waste from an industrial process as feedstock for another one, thus reducing raw materials and resources needs. The article by Collis et al. evaluates the potential of using the three flue gases from conventional steel production (blast furnace gas, essential oxygen furnace gas, and coke oven gas, with different ranges of CO, $CO_{2,}$ and H_2), currently used to produced internal heat and power, as raw material or fuel for other companies. One can extrapolate the applied methodology to other industrial plants and flue gases, and the results compare economic and environmental indicators of the proposed alternatives versus the benchmark situation.

Carbon dioxide may be a potential raw material whose use is, in essence, circular. Existing literature focuses on the potential environmental benefits while pointing out the technological and economic challenges. CO_2-based products need to be not only competitive with current fossil fuel options, but public acceptance and social willingness to change current behavior are crucial. The social perspective has had less attention, and the work by Simons et al. studies the acceptance of CO_2-based fuels for aviation synthesized *via* Carbon Capture and Utilization (CCU). Here, professionally treated social factors, affective evaluation, and benefit perception of CCU to ultimate consequences: public information and information strategies. A case study of innovative technologies corroborates the interest of this contribution. Here, materials and products manufactured through the reuse of CO2-based jet fuels in the context of CCU represent an ultimate technological approach receiving increasing attention on the path to meeting climate targets.

PERSPECTIVE

Styring et al.'s considers a systemic approach to using synthetic fuels in a transport energy transition. Using a Theory of Change, the authors show synthetic CO2-derived fuels to fill the gaps in the shift towards a fully electric vehicle fleet for ground transit. Then, it includes a deep reflection of the pros/cons of the various alternatives considered in the use of Synthetic Fuels in a Transport Transition. Comments on the effects of fossil fuel replacement on air quality showing the importance of atmospheric chemistry consideration as the transition to electric vehicles progresses, concluding on the impact of conventional fuels prohibition on social justice.

REVIEW

Karka et al.'s format also takes rich Encyclopedic background. The authors present relatively mature technological options' current and future potential (e.g., TRL > 6). It looks for greening existing industrial infrastructures in liquid biofuels, which have not yet found actual application at a commercial scale. This context systematically analyses these integration options concerning the present and future opportunities, barriers to overcome, real-world industrial examples, and feasibility to scale up. The material can be used as a reference point for the 2020 status in this research and contribute to coordination and support actions/projects." Otherwise, it can be of substantial interest to decision-makers in industrial practice, as shown through real-world industrial examples.

The Review by Styring et al. analyses the use of dimethyl ether (DME) from sustainable feedstock as a future non-fossil fuel alternative for road transportation, compared to oxymethylene ether and synthetic diesel through Fischer-Tropsch reactions. DME can replace diesel in a compression ignition engine (engines requiring well-known modifications), and it can be produced from CO_2 and carbon-containing waste materials. In its comparison, DME can be produced needing less hydrogen than the other routes. Towards diesel produces lower NOx, soot, and particulate matter. The authors conclude that DME can be then one of the fuels used in the future mobility sector.

CONCLUSION

The articles in this Research Topic represent a selected sample of precious contributions to various Perspectives of Chemicals Synthesis as a Green Alternative to Fossil Fuels. The necessary presence of Renewable Diesel in the Petroleum Industry and the need for emerging renewable substitutes of liquid fuels, thus yielding to different biomass transformation technologies. Carbon Capture and Utilization is under examination in the light of novel factors. Food waste novel reevaluation permits the production of competitive ethanol. The techno-economic analysis uncovers more efficient novel combined alternatives recovering energy from waste. A novel Perspective on Fuels in a Transport Transition under examining Theory of Change reveals the impact of conventional fuels prohibition on social justice. A wealthy Review looks for greening existing industrial infrastructures in liquid biofuels, which have not yet found actual application at a commercial scale. Carbon-containing waste as raw material and fuel and more efficient energy conversion and chemical processes are needed towards a net-zero emissions society. And, as a sample of the future community, the current special issue compiles many different greener alternatives; society will require technological options adapted to each specific context.

The authors of this Editorial want it to be of use to its readers and inspiration to many.

AUTHOR CONTRIBUTIONS

All authors listed have made a substantial, direct, and intellectual contribution to the work and approved it for publication.

ACKNOWLEDGMENTS

Authors would like to acknowledge the support of CEPIMA (UPC) Barcelona, Spain.

Conflict of Interest: The authors declare that the research was conducted in the absence of any commercial or financial relationships that could be construed as a potential conflict of interest.

frontiers in Energy Research

ORIGINAL RESEARCH
published: 17 February 2021
doi: 10.3389/fenrg.2021.618229

Potential Deployment of Reversible Solid-Oxide Cell Systems to Valorise Organic Waste, Balance the Power Grid and Produce Renewable Methane: A Case Study in the Southern Italian Peninsula

Claudio Carbone[1]*, Francesco Gracceva[1], Nicola Pierro[1], Vincenzo Motola[1], Yi Zong[2], Shi You[2], Mar Pérez-Fortes[3], Ligang Wang[3,4] and Alessandro Agostini[1]

[1]Italian National Agency for New Technologies, Energy and Sustainable Economic Development (ENEA), Rome, Italy, [2]Centre for Electric Power and Energy, Technical University of Denmark (DTU), Copenhagen, Denmark, [3]Group of Energy Materials, Swiss Federal Institute of Technology in Lausanne (EPFL), Lausanne, Switzerland, [4]Innovation Research Institute of Energy and Power, North China Electric Power University, Beijing, China

Edited by:
Valerie Eveloy,
Khalifa University, United Arab Emirates

Reviewed by:
Yusuf Bicer,
Hamad Bin Khalifa University, Qatar
Aniruddha Pramod Kulkarni,
Commonwealth Scientific and Industrial Research Organisation (CSIRO), Australia

***Correspondence:**
Claudio Carbone
claudio.carbone@enea.it

Specialty section:
This article was submitted to Process and Energy Systems Engineering, a section of the journal Frontiers in Energy Research

Received: 16 October 2020
Accepted: 12 January 2021
Published: 17 February 2021

Citation:
Carbone C, Gracceva F, Pierro N, Motola V, Zong Y, You S, Pérez-Fortes M, Wang L and Agostini A (2021) Potential Deployment of Reversible Solid-Oxide Cell Systems to Valorise Organic Waste, Balance the Power Grid and Produce Renewable Methane: A Case Study in the Southern Italian Peninsula. Front. Energy Res. 9:618229. doi: 10.3389/fenrg.2021.618229

The large market penetration of non-dispatchable renewable power sources (vRES), i.e., wind and photovoltaic, may be hampered by an increasing need for large scale energy storage capacity and the challenges of balancing the power grid. Novel technologies integrating waste gasification with reversible Solid-Oxide Cell systems have been proposed to provide flexible grid balancing services. The rSOC system operated in electrolysis mode uses excess power from vRES to generate hydrogen (H_2), which is combined with syngas derived from waste gasification to produce methane (CH_4). The rSOC system can also be operated in fuel cell mode by oxidising syngas to produce electricity. This paper presents a well-defined case study which aimed to estimate the potential deployment of a novel rSOC technology in a future power system dominated by intermittent renewables. The hourly power grid residual loads (i.e., the difference between load and vRES power generation) and the availability of low-grade organic waste and residues are quantified and matched for the southern Italian peninsula in 2030. The results show that the theoretical grid flexibility needs approximately 10 TW h of overproduction and 5 TW h of underproduction in 2030 to ensure the complete disposal of the municipal organic waste generated in 2030 (6.7 Mt) and that production of renewable CH_4 will need to be 1.4–2.4 Mt, pointing to an intriguing perspective for the deployment of rSOC systems at a large scale. The multifunctionality of the system proposed is an added value that can make it a convenient and efficient piece of the puzzle of technologies

---

Abbreviations: LHV, Low Heating Value; PowGen mode, Power Generation mode of the rSOC; PowNeu mode, Power Neutral mode of the rSOC; PowSto mode, Power Storage mode of the rSOC; PV, photovoltaic; RED, Renewable Energy Directive of the European Parliament; RES, renewable energy resources; RES-dominated zone, areas characterized by high penetration of renewable energy resources; rSOC, reversible Solid-Oxide Cell; SOEC, Solid-Oxide Electrolysis Cell; SOFC, Solid-Oxide Fuel Cell; t.d.m., tons of dry matter; TSO, Transmission System Operator; vRES, non-dispatchable/variable renewable energy power resources; SUD, The identified RES-dominated zone for Italy, including four political regions in the South of Italy (Basilicata, Calabria, Molise, Puglia); W2G, Waste2GridS Project/Technology.

required in a climate-neutral and circular economy. The results and methods here presented are intended to form the basis for estimations of future potential deployment and economic and environmental assessments of competing technologies.

Keywords: solid oxide fuel cell, solid oxide electrolysis cell, biomethane production, waste valorization, grid adequacy, hydrogen, renewable energy recources

1 INTRODUCTION

The member states of the European Union (EU) have signed and ratified the Paris agreement to keep global warming "well below 2°C above preindustrial levels, and to pursue efforts to limit the temperature increase even further to 1.5°C". To meet this challenging target, the EU has put forward the ambitious Green Deal, a growth strategy that transforms the Union into a modern, resource-efficient, and competitive economy. Specific goals are (1) no net emissions of greenhouse gases by 2050, (2) decoupling economic growth from resource use, and (3) leaving no person and no place behind. The European Green Deal is the roadmap for making the EU's economy sustainable (European Commission, 2019).

The greenhouse gas (GHG) emissions resulting from the provision of energy services have contributed significantly to historic anthropogenic climate change, impacting the energy budget of the atmosphere. Since approximately 1850, the global use of fossil fuels (coal, oil, and gas) has increased. These resources now dominate energy supply, which has resulted in the rapid growth in emissions of climate forcers, e.g., GHGs (Edenhofer et al., 2011). Demand for energy and associated services to meet social and economic development and improve human welfare and health is increasing. All societies require energy services to meet basic human needs and to serve productive processes. Historically, economic development has been strongly correlated with increasing energy use and growth of GHG emissions, and renewable energy can help decouple that correlation (Edenhofer et al., 2011).

In its EU2020 climate and energy package of 2009, the EU passed The Renewable Energy Directive (RED) (European Parliament, 2009). The RED set targets for renewable energy at 20% by 2020. In November 2016, the European Commission published the so-called winter package, a set of measures that is part of the 'Clean Energy for all Europeans' initiative. A recast of the RED was included in the package. In 2018, the EU agreed on a set of ambitious targets in its 2030 energy union strategy, with renewables expected to cover 32% of total energy consumption (European Commission, 2018b). To reach such an overall renewable energy target, by 2030, the EU needs to meet more than 50% of its gross electricity generation needs through renewable energy sources (RES) because it is easier (and cheaper) to decouple the power sector from fossil fuels than other systems (e.g., transport) (Banja et al., 2017).

Variable/non-dispatchable renewable energy resources (vRES), namely wind and solar photovoltaic (PV) sources, grew over four-fold in capacity in Europe between 2007 and 2016, from 62 to 260 GW (IRENA, 2020), and are still increasing. The costs associated with RES technologies have been decreasing abruptly, especially for solar PV and wind, which have resulted in high levels of competitiveness for RES on a more levelized general power market (IRENA, 2019). However, the large penetration of intermittent, weather-dependent vRES poses serious threats to system operation, such as increased interconnector flows, greater need for balancing and storage, as well as curtailment of vRES (Collins et al., 2018).

The large penetration of vRES on some electric grids has resulted in curtailment in recent years. Studies of renewable energy grid integration have found that curtailment levels may grow as wind and solar energy generation penetration increases (Bird et al., 2016). Collins et al., (2018) found that variable renewable curtailment increased linearly beyond 20% penetration of vRES and that it is an inherent part of highly variable renewable power systems. This is due to operational inefficiency and the costs associated with additional transmission infrastructure and the storage systems needed to avoid curtailment. This challenge could be addressed by trading with neighboring countries/regions or adding more flexible options, depending, case by case, on what is more secure and economically viable.

A broad spectrum of energy storage technologies are currently being evaluated as candidates for transferring surpluses from the electricity grid to the gas grid or a gas-consuming process. The importance of gas technologies for handling high shares of vRES and complying with future curtailment of generation is being discussed at length. Simonis and Newborough (2017) modeled excess wind power in the Emden region of Germany between 2015 and 2020. The study is based on time series data for wind generation and electricity demand, exhibiting that excess renewable electricity levels will reach about 40 MW and 45 GW h per annum by 2020. They concluded that achieving a progression in power-to-gas capacity in the preceding period is necessary.

In this context, rSOC technologies may play a pivotal role in the transition toward the decarbonization of the power grid. The rSOC system can be operated in electrolysis mode using excess power from vRES to generate H_2 or in fuel cell mode by oxidising an H_2 rich energy carrier to produce electricity. As energy convertors, rSOC systems may enable the penetration of large amounts of vRES in the power grid by offering balancing services and producing renewable fuels for the industry, transport, and heating and cooling sectors, which are the hardest sectors to decouple from fossil fuels. Hutty et al., (2020) presented a successful proof-of-concept application of rSOC systems to real microgrid cases. They found that rSOC systems may reduce the import of grid power and reach up to 50% of grid independence while attaining cost-effectiveness.

Although various technologies exist to provide additional energy storage to the grid, each technology works with a distinct and strict time and energy capacity range (Olsen et al., 2020). Indeed, energy storage systems based on rSOC technology present some key advantages in flexibility, adaptability, capability, and efficiency, where more pronounced balancing needs are observed. The rSOC systems boast easy scalability (e.g., kW to MW) and can be used hourly up to monthly timescales. They can therefore be deployed at different locations, where they can either store energy as fuels or chemicals or be connected to the natural gas grid. The round trip efficiency for these systems is close to 70%, and it is anticipated that this could rise to 80% (Peters et al., 2015). Furthermore, because of the solid feature of solid-oxide stacks, there is limited risk of electrolyte leakage. On the other hand, there are safety issues in terms of fuel utilization, such as: risk of corrosion of materials, carbon deposition and nickel oxidation; the presence of impurities and gas cleaning; balance-of-plant (BoP) modifications and/or new burner and heat exchanger installation. These issues are expected to be resolved and/or fine-tuned to achieve full integration of rSOC systems with gasifiers for large scale deployment (Liu et al., 2013).

A case study for applying a multifunctional system, named Waste2Grids (W2G) hereafter, is proposed. A W2G plant is a combination of an rSOC system with a waste biomass gasifier connected to natural gas and power grids (W2G Project). In a W2G system, the H_2 is produced with an rSOC operated as an electrolyser, using excess power from vRES. The H_2 is then combined with syngas from biowaste and residue gasification to produce synthetic CH_4. The rSOC system can also be operated in fuel cell mode by oxidising syngas to produce electricity.

CH_4 is considered an optimal final chemical product due to its large-scale distribution, storage infrastructures and applications. The amount of H_2 that could be directly injected into the gas grid is limited by country specific standards and regulations to a maximum of 0–12 vol% (Götz et al., 2016). In contrast, synthetic CH_4 may exploit existing natural gas infrastructures for storage in large quantities over long periods of time (in Europe alone, storage capacity is about 1 PW h, i.e., ca. 20% of the total annual consumption) (GIE, 2018). The direct methanation of biogas using hydrogen from electrolysis is another promising pathway for the seasonal storage of renewables in the natural gas network in terms of cost savings (Calbry-muzyka and Schildhauer, 2020). Because it has a large storage and distribution infrastructure already available, CH_4 is an optimal energy and carbon carrier that could make vRES available to a large portfolio of final uses due to its intensive integration with other well-established natural gas sectors and facilities, i.e., mobility, as compressed natural gas (CNG) motor fuel, industry or space heating and cooling. An efficient combustion natural gas has low tailpipe or stack emissions. If used in fuel cells, there is virtually no emission of harmful pollutants in the operation phase (Schreiber et al., 2020). This combination of biowaste and residue gasification with the rSOC provides the added value of efficiently disposing and valorizing organic waste, thus limiting environmental impact.

Wang et al. (Wang et al., 2020) originally presented the concept and developed the thermodynamic performance of the novel W2G technology. Building upon these findings, the present study develops and presents an overall methodology for the identification and potential deployment of this technology in specific areas by applying it to an Italian case study. The present study investigates Italian power market zones to identify the areas with the highest penetration of vRES (i.e., vRES-dominated zone) and need storage capacity and flexibility/adequacy in the power system. Based on the historical data of vRES generation and load in the Italian power market and the planned penetration of intermittent renewables, we developed residual load scenario simulations for 2030. These were calculated and matched with biowaste availability, considering the efficiencies of a representative set of novel W2G systems and the maximum technical W2G deployment potential. This study also estimates the hourly power grid balancing needs in 2030 based on NECP projections, along with the spatial distribution and availability of biowaste.

2 MATERIALS AND METHODS

The overall goal of the W2G technology is to facilitate the penetration of vRES power in RES-dominated areas and efficiently dispose of organic waste by balancing the grid and, at the same time, synthesising a renewable chemical. The first step involves converting various types of carbon-containing waste (e.g., industrial and municipal organic waste, secondary and tertiary biomass) into syngas, a mixture of H_2/carbon monoxide (CO)/carbon dioxide (CO_2), via gasification. The syngas is then cleaned and further conditioned (if necessary) to meet the requirements of the rSOC unit. It works in Solid-Oxide Fuel Cell (SOFC) mode for power generation (PowGen) and Solid-Oxide Electrolysis Cell (SOEC) mode for power storage (PowSto). This two-mode operation, as defined in W2G, requires interaction with an electrical grid to capture electricity storage and generation needs. However, there might be times when the amount of generated and demanded power are close to each other, i.e., when the corresponding residual loads are limited. To keep the system in continuous operation and avoid the costly and inefficient shutdown and start-up phases, a third operation mode, the power neutral mode, has been introduced (PowNeu). In PowNeu mode, the power produced internally in SOFC mode is also used internally to produce CH_4 in SOEC mode. Thus, the plant can be considered as isolated from the electrical grid but remains under operation and can quickly be back-in-service for the electrical grid by switching from the PowNeu mode to PowGen or PowSto modes.

The schematics of the energy flows of the three modes are shown in **Figure 1**. The gasification process operates all the time, while the solid-oxide cell switches among the three operating modes, depending on the balancing scenarios. In order to allow the operation of the three modes in a single plant, the solid-oxide cell stacks are split into two blocks, Block A and B. Both blocks can switch between SOFC (PowGen) and SOEC (PowSto) modes. The PowGen mode converts the cleaned syngas from the gasification process into power with the fuel cell operation of the solid-oxide cell stack (both Block A and B) and delivers the

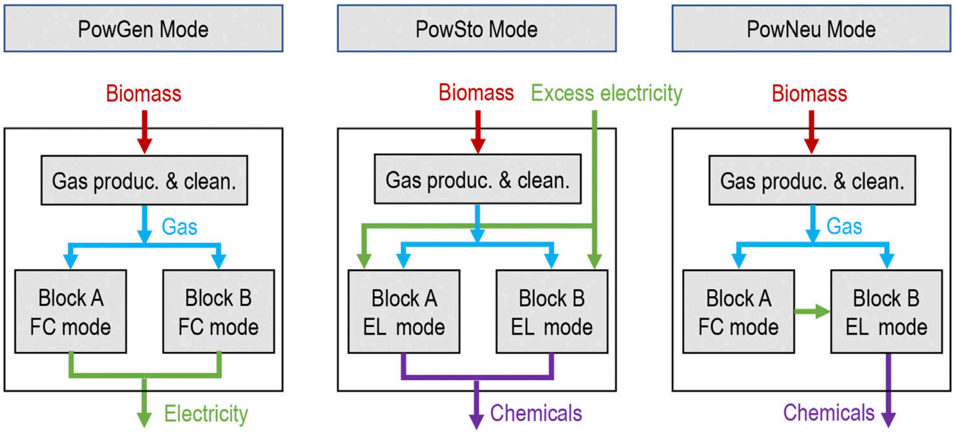

FIGURE 1 | Schematic illustration of the energy flows of the three modes for W2G plants. The red arrows stand for energy flows related to biomass fed into the plant and the syngas generated from the gasification processes; the green arrows represent power/electricity flows; the blue arrows indicate energy flows related to water and steam; the purple arrows are the energy flows related to the CH_4 produced. The rSOC stacks are split into two blocks—Block A and Block B, to allow for the operation of the three modes in one single plant; Gas production and clean.: gasification and cleaning; FC: fuel cell operation; EC: electrolyzer operation. The Figure is only a simple illustration and does not represent a detailed flowchart.

electricity produced to the grid. The PowSto mode imports electricity from the grid and converts the syngas from the gasification process into CH_4 with the electrolyser operation of the solid-oxide cell stack (both Block A and B), and sends the CH_4 produced to the natural gas grid. In the PowNeu mode, a part of the syngas is converted in Block A (SOFC operation) into power to drive the Block B (SOEC operation) so that the remaining syngas can be converted into CH_4. The overall process is exothermic with a considerable amount of excess heat at the intermediate temperature levels, which can be used by an additional steam cycle to enhance the efficiency of each mode. The concept and thermodynamic performances of W2G technology are described in full detail by Wang et al., (2020).

2.1 General Methodology to Assess the Potential Deployment of Waste2GridS Systems

The methodology for estimating the potential technical deployment of W2G systems in 2030 involves three main tasks (**Figure 2**). In the first task, an analysis of historical disaggregated data is carried out to quantify the current dispatchable and flexible generation needs (residual loads) in the different market zones with high vRES penetration and the expected development of residual loads in 2030 according to the expected penetration of wind and PV. The second parallel task involves a geographically explicit assessment of the available biomass in the selected areas and feedstock to support the deployment of the W2G technology. The last task involves the identification of the maximum potential deployment of the W2G technology, based on the future availability of waste and residues and the expected theoretical balancing needs of the power system, due to the higher penetration of vRES in 2030.

2.1.1 Analysis of Current and Future Power Balancing Needs

The current and 2030 balancing scenarios were developed for different electrical zones in Italy to identify the optimal case study (see **Section 3.1**), based on a statistical analysis of historical/forecasted data provided by the Italian Transmission System Operator (TSO) (Terna, 2019a). The data for the 2030 scenario estimate were obtained by scaling the current power profiles in Italy to the planned expectations for 2030, based on growth targets and trajectories for the renewable share of the electricity sector according to the Italian National Energy and Climate Plan -NECP (Ministero dello Sviluppo Economico et al., 2019). The different zones are assumed to increase proportionally to Italy as a whole. **Table 1** reports the expected increase of RES penetration in the time horizon 2016–2030 in Italy, provided by NECP.

The electricity grid balancing power profiles were estimated based on dispatchable and flexible generation needs. These were defined in terms of residual loads, namely, the imbalance between gross consumption and vRES generation (the sum of wind and solar power generation). The energy balance of the electrical system was calculated on an hourly basis. The residual load was defined hour by hour as the difference between the foreseen load (total electricity demand) and the production from vRES. A positive residual load implies the need for energy sources other than PV and wind to fulfill the grid requirements. A negative residual load occurs when the grid cannot fully absorb the available vRES. The resultant overproduction would be curtailed or fed to a power storage system. The PowGen and PowSto modes of the W2G rSOC system would then be used to balance the positive and negative residual loads, respectively.

To allow for year-to-year fluctuations in the climatological drivers affecting wind and solar PV capacity factors and generation trends, the current power generation profile.

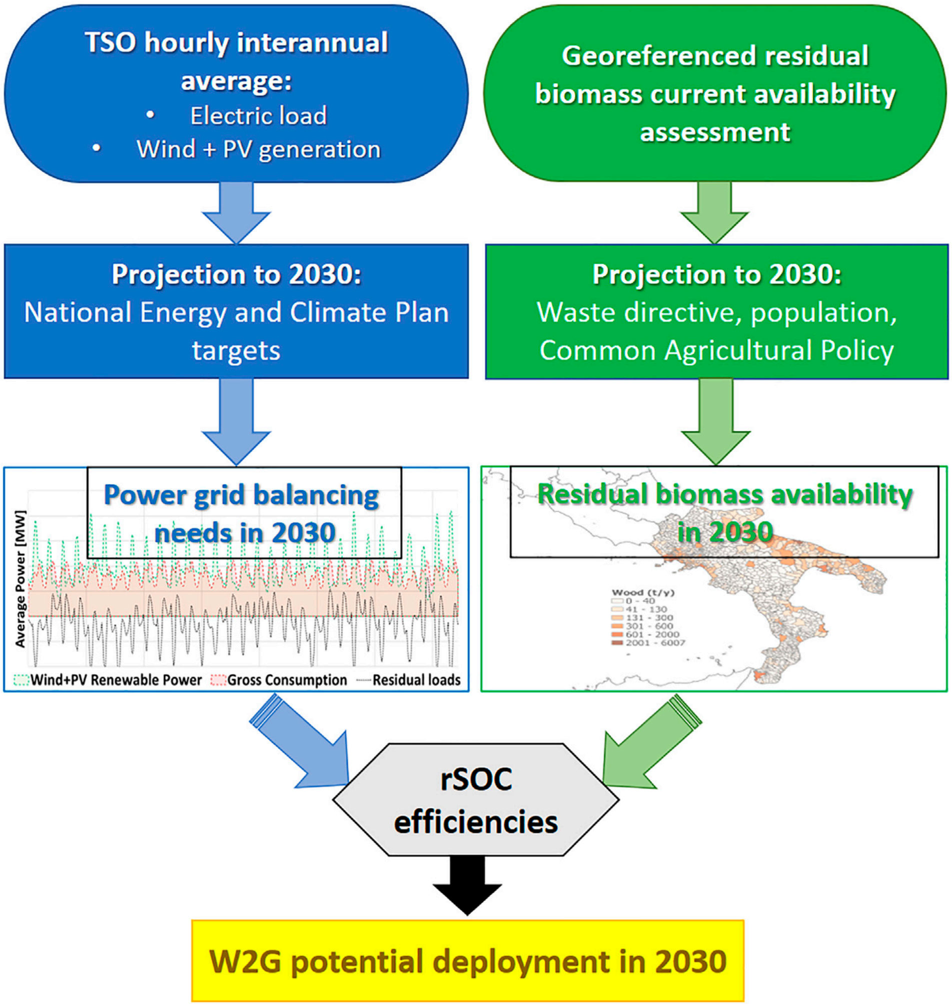

FIGURE 2 | Exemplification of the methodology adopted in this work to determine the potential deployment of the W2G systems in specific RES-dominated areas.

TABLE 1 | Italian electric energy mix for RES, in terms of installed capacity (MW) and electricity production (TW h), normalized according to the Directive 2009/28/CE, source: NECP (Ministero dello Sviluppo Economico et al., 2019).

	2016		2017		2025		2030	
	Installed capacity (MW)	**Electricity production (TW h)**	**Installed capacity (MW)**	**Electricity production (TW h)**	**Installed capacity (MW)**	**Electricity production (TW h)**	**Installed capacity (MW)**	**Electricity production (TW h)**
Hydro	18,641	46.2	18,863	46.0	19,140	49.0	19,200	49.3
Geothermal	815	6.3	813	6.2	920	6.9	950	7.1
Wind	9,410	16.5	9,766	17.2	15,950 (300 off-shore)	31	19,300 (900 off-shore)	41.5
Bioenergy	4,124	19.4	4,135	19.3	3,570	16	3,760	15.7
Solar-PV	19,269	22.1	19,682	24.4	28,550 (250 CSP)	40.1	52,000 (800 CSP)	73.1
RES share (%)		34.0%		34.1%		42.6%		55.0%

Resultant capacity factor average values were applied to up-to-date installed capacity rates for 2018, to determine current vRES energy production. Even though the use of the average capacity factor values may lead to peak shaving and, consequently, underestimate the maximum capacity of the vRES system, this approach was the best compromise, to overcome the inadequacy

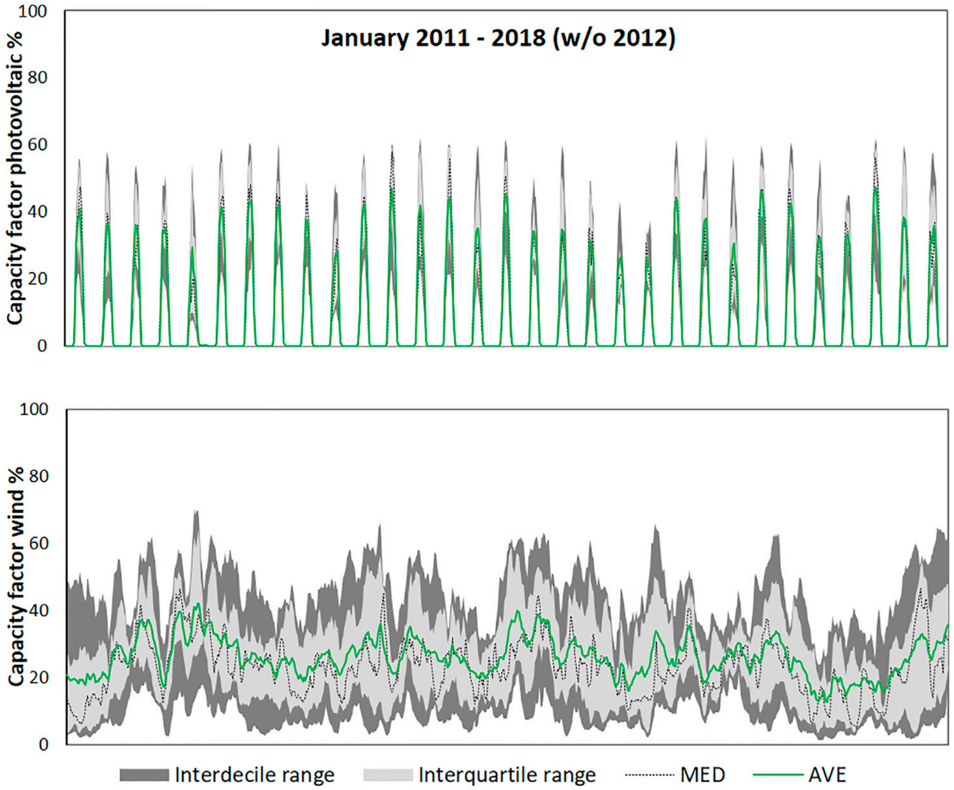

FIGURE 3 | Statistics of 2011–2018 (w/o 2012) historical hourly based data of capacity factors for PV **(A)** and wind **(B)** corresponding to January (cold season). Interdecile range, interquartile range, median (MED), and average (AVE) values are plotted.

of one single year representativeness in depicting the inter-annual variability. Load profiles are elaborated accordingly. The inter-annual time-series are compared as a function of working and non-working days to consider the bias caused by the load reduction occurring systematically during weekends.

Figures 3, **4** show the inter-annual variation of historical data relating to capacity factors for wind and solar PV 2011–2018 (w/o 2012) for two months from each year, referring to the selected electrical Italian zone (see **Section 3.1**) in Southern Italy. The two months reported are January and July, as they were considered representative of the cold and warm seasons. The green line indicates the averaged values taken as current status to calculate power generation according to the installed capacity reported for 2018.

Wind power production exhibits no clear diurnal pattern but a favorable seasonal profile with much more intensity and variation and a consequent higher production during the cold season. Solar PV is characterized by its typical daily pattern, with multi-peak daily trends with higher intensity in the middle of the day and steep changes in concomitance with sunrise and sunset, as well as a higher contribution in the warm season.

To estimate the expected residual loads in 2030, the current hourly-based generation profiles and the electrical load patterns were generated for the entire annual timescale. The dataset was then scaled to 2030 based on the targets provided by NECP (Ministero dello Sviluppo Economico et al., 2019). The applied increase coefficients are assumed, in comparison to 2018 installed capacity, as 222.7, 276.5, and 102.1%, for wind, PV generation, and load, respectively.

2.1.2 Biomass Assessment

In combination with evaluating the grid balancing needs in 2030, we also characterized the biomass availability to fuel the W2G technology. There are many biomass classification schemes available worldwide.

The scheme adopted in this work was developed by the EU BEE Project (Biomass Energy Europe Project, 2020), which aimed to harmonize methodologies for biomass resource assessments for energy purposes in Europe and its neighboring countries. This approach to biomass assessment is in compliance with the EU S2Biom Project (S2Biom Project, 2020). Accordingly, biomass resources were evaluated as follows:

Energy crops: wood energy crops (short rotation forestry, i.e., willow, eucalyptus, poplar), grass energy crops (miscanthus, hemp), oilseed crops (rape, linseed, sunflower), hydroponics (lake weed, kelp algae).

Wood, wood residues and by-products: wood and wood branches from forest, wood residues from the industrial sector (sawmills, construction, furniture).

Agricultural residues: wheat or barley straw, corn stover, pruning (fruit, vineyard).

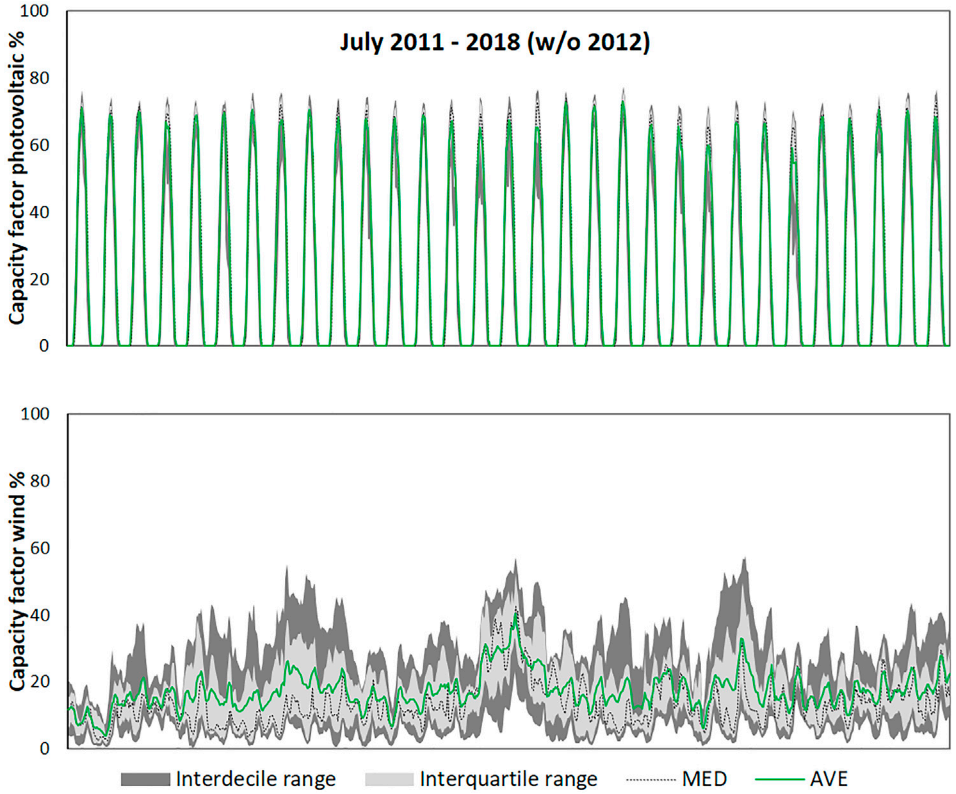

FIGURE 4 | Statistics of 2011–2018 (w/o 2012) historical hourly based data of capacity factors for PV **(A)** and wind **(B)** corresponding to July (warm season). Interdecile range, interquartile range, median (MED), and average (AVE) values are plotted.

Livestock: pig and cattle slurry, sheep manure, grass silage, poultry litter.
Agro-industrial residues: residues and waste from various processes in the distillery, dairy, meat, fish, oils, fruit and vegetable sectors.
Waste: sewage sludge, organic fraction of MSW.

Taking into account the technology investigated and the characteristics of the examined areas, the following biowaste categories are considered:

Agricultural residues: cereal straw, fruits tree pruning.
Waste: MSW organic fractions, waste wood, and waste paper.

The Italian National Institute of Statistics (ISTAT a, 2020) reports annual grain and fruit production and their cultivated areas at the EU NUTS 2 level (European Commission, 2018c). The annual straw and pruning are computed at the NUTS 2 level and then allocated on the NUTS 3 level using information from the Italian Agriculture Census (ISTAT b, 2020) as a proxy, enabling a higher spatial resolution at the scale of Italian municipalities. Straw and pruning residues are then quantified by applying specific empirical conversion factors, taken from (ENAMA, 2011), to the annual production of grain and fruits.

MSW data are provided by the Italian Institute for Environmental Protection and Research (ISPRA) (ISPRA Waste database, 2020), the public Italian authority in charge of monitoring waste management, which elaborates on the annual MSW report, a database containing quantitative data on all the fractions of the MSW at NUTS3 level. The 2018 report was considered (reference year 2017), and three different MSW fractions—i.e., organic, paper, and wood–are quantified for the municipalities of interest. MSW quantification for the year 2030 was performed according to the mandatory goals set by the Waste Directive (EU) 2018/851 (European Commission, 2018). The MSW was therefore considered as separated at origin in its organic fraction.

Annual straw, pruning, waste paper, waste wood, and MSW data are elaborated and then computed by employing the Q-GIS (Quantum Geographical Information System) software and raster algorithms (QGIS, 2020) to produce a georeferenced dataset on the spatial distribution and availability of organic waste. The georeferenced datasets ensure data interoperability, Standard Query Language (SQL) query capabilities, and dynamic visualization.

The ratio underpinning this shortlist is that the gasification technology, though it may work with many more feedstock types, is more reliable and efficient with low moisture feedstock (Sikarwar et al., 2016). In addition, dry feedstocks are more easily transported and stored. Low grade waste streams were also considered, as hypothetically, these will suffer from less competition from other uses in a future bio-based economy and have a lower, and in some cases, negative cost.

Environmental aspects also contributed to the identification of the feedstocks considered. Fruit tree pruning often involves field burning, causing the emission of air pollutants. Though it may be considered a residue, cereal straw provides benefits to soil health, ecosystem services, and removes carbon from the atmosphere (Giuntoli et al., 2016). Energy crops were excluded for their competition for agricultural land (European Commission, 2015) and their environmental impact, which involves using machinery, fertilizers, and pesticides on a large-scale (Agostini et al., 2015).

Several other sources consider the net annual increment (NAI) of the forest biomass to be available for bioenergy production, at least partially (e.g., both Biomass Energy Europe Project; S2Biom Project). However, forest biomass was also excluded from the present study as we focus on low grade residual biomass, and because the appropriation of the forest NAI for bioenergy production would instantaneously release this carbon into the atmosphere, thus cannot be considered carbon neutral, but rather as a foregone sequestration (Pan et al., 2011; Maxwell et al., 2019).

Manures were excluded from the present study due to their moisture content and the difficult and costly processes involved with handling, transporting, and storing it.

2.1.3 Potential Deployment

We also considered the efficiency of the W2G system to assess whether the amount of residual biomass and waste estimated for the 2030 scenario would be sufficient to cover the full grid balancing needs of the examined area.

There are degrees of freedom in the design of W2G plants. Each plant itself comprises the processes of onsite biomass pre-treatment, gasification, syngas cleaning, rSOC stacks, methanator, heat exchanger network, and steam turbine network (for heat recovery). The sections of biomass pre-treatment, gasification and syngas cleaning were considered to operate at full load all the time without load shifting in order to continuously provide the same amount of clean syngas for the rSOC stack and methanation subsystems. The coordination of the two rSOC blocks (**Figure 1**) and the methanator enables the plant to switch between the PowGen/PowSto/PowNeu modes. Therefore, the operating strategy of each subsystem mentioned above is as follows:

PowGen: biomass pre-treatment, gasification, syngas cleaning, rSOC block A (SOFC mode), rSOC block B (SOFC mode), methanator (hot standby), heat exchanger network, and steam turbine network.

PowSto: biomass pre-treatment, gasification, syngas cleaning, rSOC block A (SOFC mode), rSOC block B (SOEC mode), methanator (partial-load operation), heat exchanger network, and steam turbine network.

PowNeu: biomass pre-treatment, gasification, syngas cleaning, rSOC block A (SOEC mode), rSOC block B (SOEC mode), methanator (full-load operation), heat exchanger network, and steam turbine network.

The plant design can be varied by changing (1) the combination of gasification technology (entrained flow gasifier or circulating fluidized bed gasifier), syngas cleaning technology (hot/cold), electrolysis mode (steam electrolysis or co-electrolysis), and (2) the design operating points of the key components, particularly the stacks (under both SOFC and SOEC modes). For this paper, the technology combination was selected as it is a fast-internally circulating fluidized bed gasifier, hot syngas cleaning, and fuel-electrode supported cell stack. All the aspects mentioned above were implemented into an optimization platform to derive a set of optimal plant designs (design pool). They show the trade-off between mode-efficiency (i.e., PowGen, PowSto) and capital expenditure (CAPEX), or specific cell area per kW-LHV of the processed biomass. For the purpose of this work, five options are shortlisted from the pool of the optimal designs, which we considered sufficient to enable a good coverage of the overall characteristics of the W2G technology. Other design freedoms can be automatically optimized by considering different process configurations, as detailed in Wang et al., (2020).

The key stack design points for the five designs selected are listed in **Table 2**. The energy content of the biomass needed as input to produce the specified amounts of electricity or CH4, and the corresponding efficiency values in PowSto and PowGen modes are also reported.

The energy content of the available feedstocks was quantified by applying the same lower heating values (LHV) used by the European Commission for the calculation of the default values of the RED (Giuntoli et al., 2017).

By combining the waste availability and process design efficiencies, the constraints to the deployment of the W2G technology were identified in terms of maximum power utilization in the PowSto mode and the PowGen mode.

3 RESULTS

In this section, the results of the biowaste availability, power grid balancing needs, and potential deployment of the W2G technology are reported. All these estimates represent the technical sustainable potential, they do not account for competition with other uses of the biomass and waste, as these depend on the economic performance of the technology and markets and policies that are not accounted for in this work. Furthermore, they do not account for the potential use of other technologies for the stabilization of the power grid or connectivity with other power markets to dispose of the excess power from vRES.

3.1 Identification of vRES-Dominated Areas and Future Dispatchable and Flexible Power Generation Needs

The Italian power market uses zonal management systems, which reflect grid limitations in transmission capacity. The stretched shape of the Italian Peninsula, dominated by the Apennines, a mountain chain extending from the North-West to South-East,

TABLE 2 | Key stack design points, energy flows needed as input to produce the specified amounts of electricity or CH_4, and the corresponding efficiency values in PowSto and PowGen modes, for the five optimal designs selected.

	SOFC mode					SOEC mode						
Design options	**Utilisation factor**	**Current density** ($A\ cm^{-2}$)	**Oxygen side flow rate** ($sccm\ cm^{-2}$)	**Electricity produced** (kW h)	**PowGen efficiency*** (%)	**Utilisation factor** ($A\ cm^{-2}$)	**Current density** ($A\ cm^{-2}$)	**Oxygen side flow rate** ($sccm\ cm^{-2}$)	**Methanation pressure** (bar)	**Electricity consumed** (kW h)	**Power stored in methane** (kW h)	**PowSto efficiency**** (%)
1	0.58	0.38	68.1	21,862	43.6	0.55	0.61	5.63	24	24,287	41,959	56.4
2	0.75	0.3	53.1	23,756	47.4	0.57	0.61	8.24	19	48,533	67,836	68.8
3	0.88	0.27	51.3	25,149	50.2	0.72	0.56	1.08	27	47,692	67,836	69.4
4	0.78	0.33	61.4	25,564	51	0.78	0.35	0.47	19	19,044	38,588	55.8
5	0.9	0.23	41.7	26,986	53.9	0.64	0.37	1.27	23	49,638	67,879	68.1

*According to the energy flows of the plant shown in **Figure 1**, the PowGen efficiency is defined as $\eta_{PowGen} = \frac{\dot{E}_{ele,out}}{\dot{E}^{lhv}_{bio,in}}$, where $\dot{E}_{ele,out}$ is the net electricity exported to the electrical grid and $\dot{E}^{lhv}_{bio,in}$ is the biomass energy input based on lower heating value (LHV).

According to the energy flows of the plant shown in **Figure 1, the PowSto efficiency is defined as $\eta_{PowSto} = \frac{\dot{E}^{lhv}_{sng,out}}{\dot{E}^{lhv}_{bio,in}+\dot{E}_{ele,in}}$, where $\dot{E}^{lhv}_{sng,out}$ is the SNG exported to the gas grid based on lower heating value, $\dot{E}^{lhv}_{bio,in}$ is the biomass energy input based on lower heating value (LHV), and $\dot{E}_{ele,in}$ is the electricity imported from the electrical grid.

FIGURE 5 | Zones in the Italian electricity system (adapted from Terna, 2019b).

bordered by narrow coastlands across the middle of the country, limits the possibility of achieving a full meshed grid integration, especially between North and South of Italy. The Italian electricity market implemented a zonal structure in which the zones are defined as parts of the National power grid, where physical limits exist for electricity transfers to/from other geographical areas. The six geographical zones of the national network are shown in **Figure 5**: Northern Italy (NORD), Central-Northern Italy (CNOR), Central-Southern Italy (CSUD), Southern Italy (SUD), Sicily (SICI), and Sardinia (SARD). It is likely that in the future, there will be more investment in the grid to help increase the flexibility of the overall system, reduce curtailments and local congestion. However, the short- to mid- term deployment of local storage systems could play an important role in a transition to high-vRES scenarios.

In Italy, at the end of 2017, the installed capacity of wind and solar PV was approximately 9.8 and 19.7 GW, corresponding to 17.2 and 24.4 TW h of electricity generation, respectively. This represents a total renewable energy penetration of 12.5%, which is expected to increase over the next few years. The NECP envisages a central role for vRES in the future Italian power energy mix, with PV expected to account for more than a half of the power capacity by the end of the decade, (i.e., 50 GW installed capacity by 2030). In NECP projections, RES estimate an electricity generation of 186.8 TW h, including 74.5 and 40.1 TW h of PV and wind power, respectively. In this study the 2018 data provided by TERNA, the Italian TSO in charge of high voltage electricity transmission networks and the auxiliary services market throughout the country, were explored and disaggregated into the six market zones. The 2018 renewable penetration rates for wind and PV power are 5, 10, 16, 27, 28, and 54%, in NORD, CNOR, CSUD. SARD, SICI, and SUD, respectively (Ministero dello Sviluppo Economico et al., 2019).

Figure 6 shows the distribution of the PV and wind power installed capacity in Italy in provinces and regions, respectively. Most wind power plants (more than 95%) are located in the south of Italy, while solar PV plants are distributed more uniformly throughout the country, with a slightly higher contribution in northern regions. In terms of power generation, the higher productivity of the PV plants in the South is due to more than 2000 h of sunshine per year, counterbalanced by a higher number of proper sites for distributed generation in the North (e.g., civil and industrial building roofs). However, Northern regions, being more densely populated and industrialized, exhibit a less pronounced overproduction from vRES (Guandalini et al., 2017), indicating that Southern areas will be

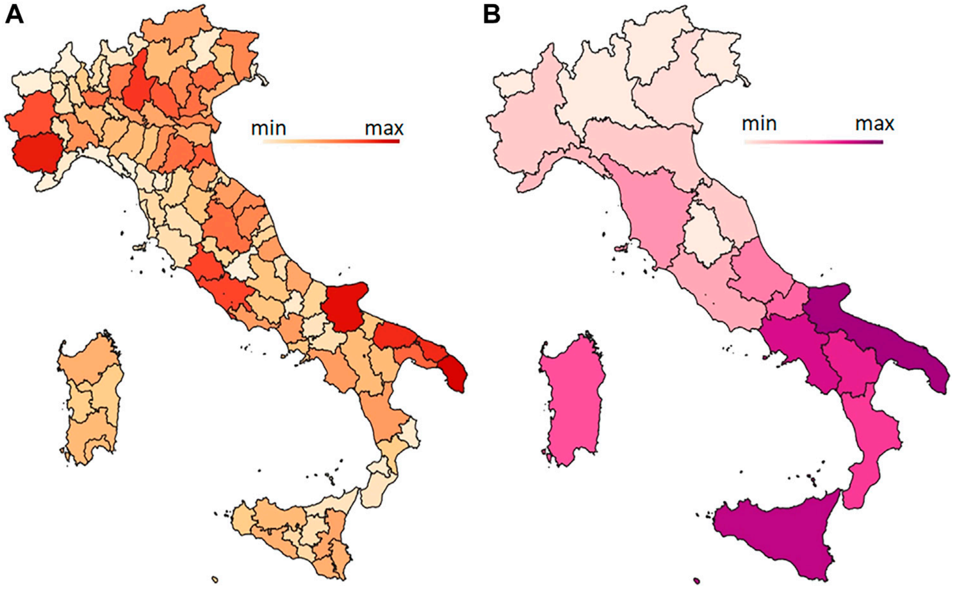

FIGURE 6 | Distribution of the installed capacity for wind **(A)** 2018 and PV **(B)** 2019 power.

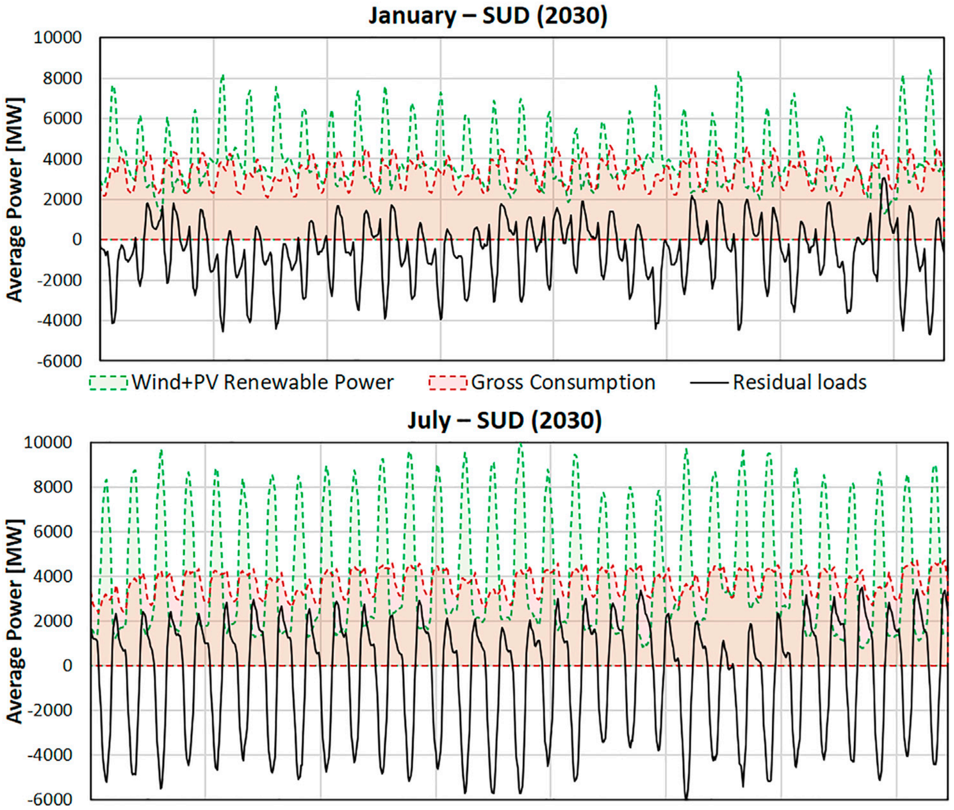

FIGURE 7 | The total variable renewable generation (PV and wind) and residual load (hourly-based) in January **(A)** and July **(B)** for the RES-dominated regions in Italy, namely the SUD zone as here defined. Expected scenarios in 2030.

TABLE 3 | Summary of overproduction in different zones of the Italian electrical power system, according to TSO data and our projections.

	Hours in overproduction		
Zones	**2018**	**Multiannual hourly average**	**2030**
SUD	1,240	350	4,715
SICI	1	0	1,498
SARD	200	0	1,659
NORD	0	0	4
CNORD	0	0	102
CSUD	0	0	119

*The multiannual scenario refers to the current scenario, i.e., the hourly inter-annual mean from 2011 to 2018 (2012 was not available). The electrical zones are geographically visualized on the map in **Figure 5**.*

more impacted by transmission congestion and energy curtailments in the future.

A recent analysis of the Italian authority for power system management shows that vRES penetration has already determined an increasing wind curtailment in Italy. In 2019, the wind power energy curtailment was estimated at 6,067 GW h (3% of the total wind production), 62% of which is concentrated in the South of Italy (ARERA, 2020).

The Italian lockdown in spring 2020 due to the Covid-19 pandemic can be considered a sort of real-scale laboratory experiment of the expected conditions of the electricity system in 2030. According to preliminary estimations (ENEA, 2020), wind curtailment could have reached ca. 60 GW h in a single week (April 27–May 3, 2020), corresponding to 10% of the total wind curtailment in 2019, and providing important warning signals about the adequacy of the future power system.

This is reflected by our 2030 power grid balancing scenarios. **Figure 7** shows hourly-based residual loads patterns for SUD; the zone exhibiting the highest negative residual loads. The plots refer only to two months, i.e., January and July, reported as representative of the cold and warm seasons. They show that a low frequency of positive residual loads and a large overproduction of vRES power are expected (i.e., flexibility needs dominated by PowSto), without significant seasonal fluctuations. In SUD. The influence of heating and lightning requirements during winter is counterbalanced by cooling system consumption during summer, resulting in a limited annual variation in electricity demand.

Table 3 reports our estimations, calculated from the same dataset, of hours in overproduction for 2030 in Italy. They evidence a much more pronounced overproduction for SUD with respect to the other zones, corresponding to a large increase in installed vRES capacity, which drives a strong mismatch between production and load. This points to significant storage requirements in the time horizon 2020–2030, with large capacity combined with rapid charge/discharge periods, which could potentially be matched by the W2G technology.

Molise, Puglia, Basilicata, and Calabria, the four regions in the SUD zone, were therefore identified as the main RES-dominated Italian areas, and SUD was selected as the case study in the present work.

3.2 Residual Biomass Availability in 2030

The amount of biomass available that could be converted to syngas and enable the operation of W2G technology in the RES-dominated zone SUD was quantified by building a Geographical Information System (GIS) geodatabase that spatially covers the areas identified as the power market zone SUD (i.e., the regions Molise, Puglia, Basilicata, and Calabria) and the region Campania. The neighboring region of Campania was added for the biomass availability quantification because of the high potential of municipal solid waste (MSW) production from the city of Naples and its surrounding area and their lack of disposal capacity (i.e., issues experienced with illegal waste disposal and export to other regions) (Ripa et al., 2017). The georeferenced database was used as input to evaluate the feasibility of the proposed technology and to estimate the size of future plants with the scope of balancing the 2030 electricity grid by recycling waste, taking into account its 2030 targets in compliance with the RED recast (European Comission, 2018) directive and the EU Circular Economy package (European Comission, 2018).

The agricultural residues considered include cereals, straw, and fruit trees pruning, as these were identified as the most relevant agricultural residues in the selected southern regions. SUD presents a total area of 62,531 km^2, of which 17,550 and 9,962 km^2 are covered by cereal crop cultivation and fruit tree plantations, respectively.

For the regions under evaluation, the crops chosen for the straw biomass availability assessment were Wheat, Barley, Oat, Rice, Corn, and horticulture. These cultivation areas for these crops amount to 1,755,020 ha. The fruit trees with more relevant production in the selected regions were olives, vineyards, peaches, apricots, cherries, and oranges, for the reference year 2018, totaling an area equal to 996,234 ha.

The sustainability standards for agricultural forestry and land management deriving from the Common Agricultural Policy (CAP) (European Commission, 2018a) were taken into account to elaborate the 2030 projections for agricultural farming practices, land management, and agreed (national and regional) forestry management plans.

The CAP sustainable agricultural farming practices include applying conservation of Soil Organic Carbon (SOC) practices (e.g., Cross Compliance issues of ‘maintaining agricultural land in good farming and management condition’ and avoiding soil erosion). Moreover, there may be market constraints, as straw is already used for livestock bedding, animal feed, and in the future could be used in biorefineries, building biomaterials, and second-generation biofuel (ENAMA Biomass Project, 2020). Therefore, to account for the impact on soil health, ecosystem services, storage of carbon in the soil, and competition with other markets, only a conservative 30% of total straw production was estimated to be available in 2030.

Fruit tree pruning currently has limited uses. They can be used for conventional combustion. However, given the very high moisture content (about 60%), high bark and ashe content, low spatial density (2–4 t d.m./ha), and the high collection bailing and transport costs, they are not competitive on the market. Currently, pruning offcuts are left in the fields or burned to preserve fruit trees from infection (ENAMA

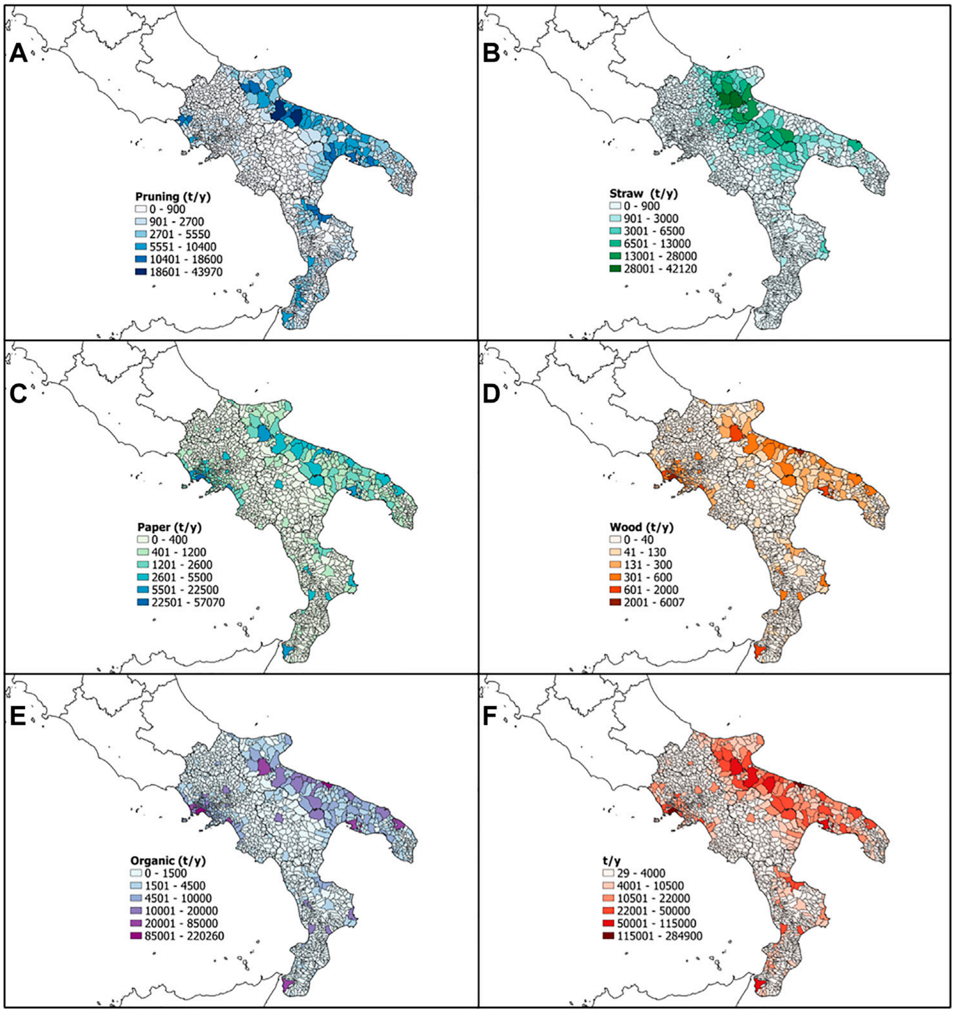

FIGURE 8 | Georeferenced maps of 2030 projections, technical potential for **(A)** pruning, **(B)** straw **(C)** wood, **(D)** paper **(E)** municipal organic waste, and **(F)** total feedstocks availability.

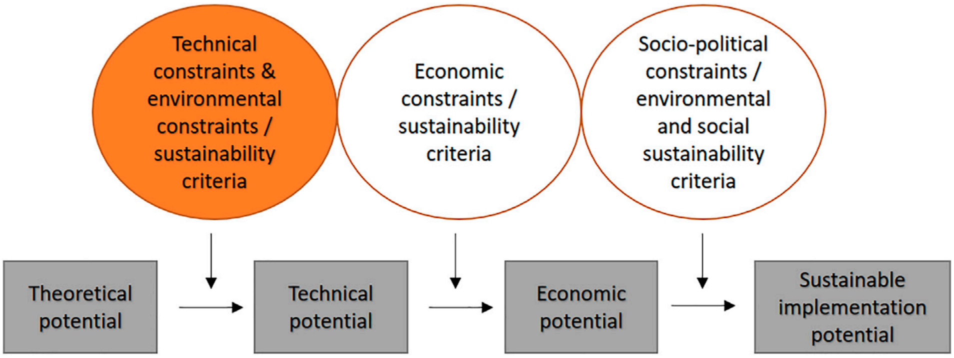

FIGURE 9 | Biomass potential classification, adapted from (S2Biom Project).

TABLE 4 | Technical potential of the feedstock in 2030.

Feedstock		Availability in 2030 (t)	Moisture %*	Energy content LHV (MJ/kg dry)**	Energy content (kWh of the dry part)
Agricultural residues	Pruning	1,221,102		18.0	6,105,510
	Straw	826,384		17.2	3,948,279
Municipal Solid Waste—MSW, separated at origin	Organic	3,721,023	50	20.7	10,697,941
	Paper	796,697	10	18.0	3,585,137
	Wood	86,110	10	18.0	387,495
	Total				24,724,362

*Average, from (TNO, 2020).

**(Giuntoli et al., 2017).

Biomass Project, 2020). The real limitation for the use of this resource in the year 2030 is likely to be feedstock market prices, in case of pruning for syngas conversion, as no significant environmental constraints were present. For the year 2030, the base potential is considered 90% of the potential calculated for 2018.

The 2030 waste stream availability was estimated based on demographic projection and the goals outlined in the Circular Economy Package Directive (European Commission, 2018).

Figures 8A–E show georeferenced maps of expected waste and residue availability in 2030, indicating pruning, straw, waste paper, waste wood, and MSW, respectively. **Figure 8F** shows the total waste and residue availability for gasification in a W2G plant in 2030.

The potential obtained was thus considered as sustainable technical potential (**Figure 9**). It does not include any economic aspects, in particular, regarding alternative uses of the same feedstocks in a future European bioeconomy. While this methodological approach tends to overestimate the availability of waste and residue, limiting the waste and supply area to the region under analysis has an opposite impact on estimates, as it excludes potential imports. Residue (and waste in particular) are often transported for long distances, e.g., a large percentage of the waste produced in the Central and Southern regions of Italy are treated in plants located in the Northern regions, indicating a national movement of waste from South to North (Malinauskaite et al., 2017). Transboundary transport is common as well. In extraordinary cases, large amounts are transported between countries (The New York Times, 2020. A Whiff of Naples Arrives in Hamburg, 2008). Thus, in the framework of this study, we referred to the technical potential to account for at least current sustainability constraints, refraining from any economic analysis and market and policy issues, such as future competing uses. The georeferenced organic waste stream database and the power grid data have been made available online (W2G Project).

Table 4 provides the total technical potential of residues and waste available for SUD in 2030 and the corresponding energy content. The energy content refers to the dry part of the biomass. This approach reflects the limited impact of water content on gasification processes, which contrasts with combustion, where the moisture content of the fuel was determined. For the year 2018, the maximum technical potential of straw was estimated at 2,754,612 t d.m./year, while the maximum technical potential of pruning was 1,356,780 t d.m./year.

TABLE 5 | Comparison between the residual loads and the local (in-around SUD) biomass waste and residue availability, in terms of energy content, by adopting W2G technology in the five proposed designs.

	Design 1	Design 2	Design 3	Design 4	Design 5
Biomass need PowSto (GWh)	19,485	9,750	9,922	24,849	9,534
Biomass need PowGen (GWh)	12,697	11,684	11,037	10,858	10,286
Total biomass need (GWh)	32,182	21,435	20,960	35,707	19,819
Total biomass available (GWh)	24,724	24,724	24,724	24,724	24,724
Total need/total available (%)	130%	87%	85%	144%	80%
PowSto need/total available (%)	79%	39%	40%	101%	39%
PowGen need/total available (%)	51%	47%	45%	44%	42%

The cases in which the biomass is not sufficient to fully balance the residual loads are highlighted in red.

3.3 Potential Deployment of Waste2GridS Technology in the Italian Case Study

The maximum potential installed capacity is identified for the RES-dominated zone SUD, both in PowGen and PowSto modes.

Table 5 presents the results, comparing the residual loads expected in 2030 with the maximum power capacity of the W2G technology, which can be matched by the biomass waste and residues available (**Table 4**) in those regions. The five best performing designs—D1, D2, D3, D4, and D5—and the corresponding efficiencies were taken into account (**Table 2**). Data are reported in terms of availability of biomass with respect to the energy needs for the two examined modes of operation, i.e., PowGen mode and PowSto mode, for SUD. The total waste availability is the total energy content of waste and residues, expressed in MW h.

Biomass needs PowGen is the amount of biomass required as gasification feedstock to fuel the PowGen operation required to balance the power grid. Biomass need PowSto, shows the total amount of biomass needed to produce the amount of syngas required to match the amount of excess electricity in the power grid, and stoichiometrically produce enough CH_4 to be injected into the gas grid. The total biomass need corresponds to the sum of Biomass need PowSto, and Biomass need PowGen.

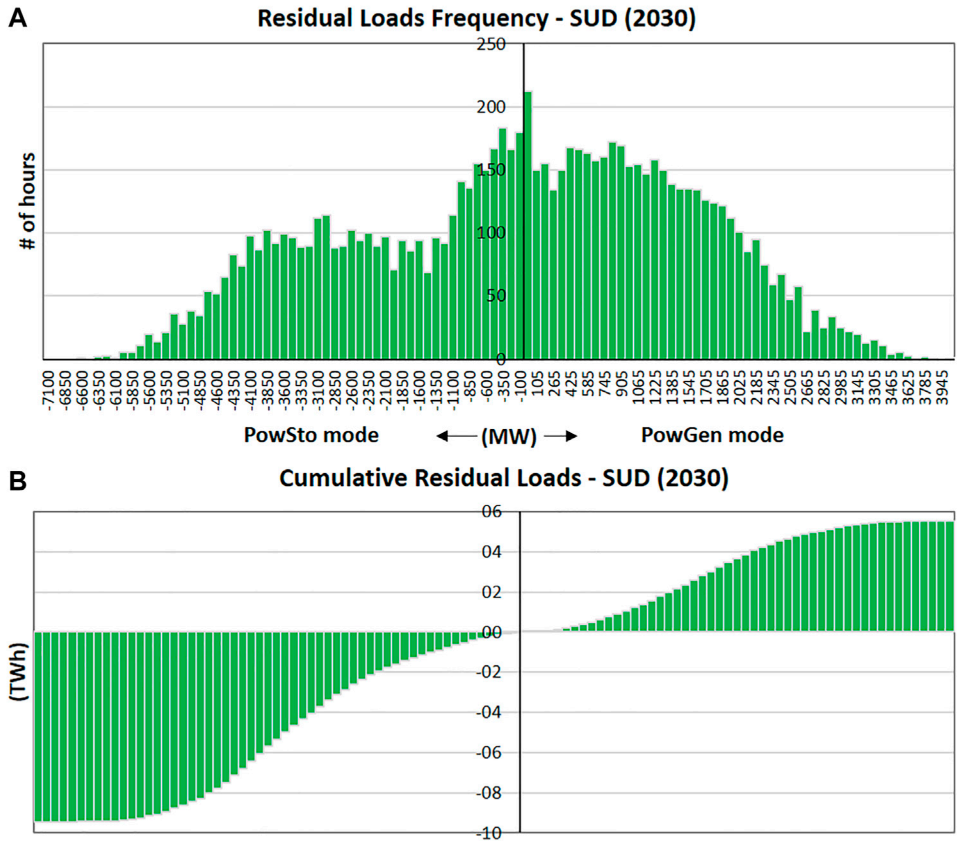

FIGURE 10 | Frequency histogram of the hourly PowGen/PowSto power capacity **(A)**. Energy content of waste and residues needed to support W2G technology deployed in the vRES-dominated zone **(B)**. 2030 scenario in Southern Italy (SUD zone).

If the total biomass need is larger than the total biomass availability, this implies a surplus of biomass. The only constraint to W2G technology deployment is the flexibility needs of the power grid. The cells in red highlight the cases in which the residue and waste are not sufficient to cover the balancing and flexibility demands of the power grid.

Histograms in **Figure 10** show the frequency and capacity of hourly balancing needs for the power grid system analysis in 2030 (A) and the cumulative residual load in terms of power consumption or production (B). The cumulative residual load represents the potential operation of W2G systems in PowGen and PowSto modes, to fully satisfy the dispatchable and flexible generation needs of the power grid.

In PowGen mode, the amount of available biomass satisfies the energy demand for all the configurations. The biomass availability is not a constraint to the operation of the PowGen mode. The local biomass would be able to balance the excess electricity in the power grid in SUD. The same is true in PowSto mode for D1, D2, D3, and D5, whereas the amount of biomass is sufficient to run a maximum capacity of 4225 MW in PowSto mode, D4. These results correspond to the production of renewable CH_4 in the range 1.4–2.4 Mt. The total biomass required to balance the power grid in both modes of operation is considerably higher than the amount of biomass potentially available in 2030, resulting in not enough in D1 and D4 designs.

The methodology applied in this work show that incorporating the 2030 expectations of wind and solar power penetration into the existing electricity system in SUD, would result in large and frequent surpluses and deficits that are attributable to the patterns of vRES variability. In order to satisfy the magnitude of the surplus and deficits, corresponding in total to ca. 5.5 and 9.4 TW h, respectively, a 4,025 and 6,600 MW of maximum potential installed capacity are identified when the system is operated as PowGen and PowSto, respectively.

4 DISCUSSION

W2G systems are rSOC combined with the gasification of waste and residues. The overall approach of the system was conceived in this perspective to provide grid-balancing flexible services with the ability to fulfill upward and downward power adjustments that are able to operate both as SOFC and SOEC. The scope of this work aimed to estimate the potential role of the W2G system in fulfilling the reasonably predicted 2030 power grid balancing needs for a well-defined case study of a specific geographical zone in terms of biomass availability and vRES penetration.

In the first step of the analysis, the 2030 dispatchable and flexible power generation needs were estimated by the high penetration of intermittent, weather dependent vRES in Italy. Based on these results, the power market zone SUD (**Figure 5**) was identified as the RES-dominated zone for Italy. In the second step, the low-grade residual biomass availability in the same area was quantified. In the third and last step, the power grid balancing needs were matched with biowaste availability by considering the efficiency of optimized W2G systems.

Based on statistically high resolution historical data and a plausible estimation of power generation and load in 2030, this work provides the characterization of specific power grid balancing needs and a detailed georeferenced biowaste availability assessment, to explore the maximum potential capacities of W2G technology both in power storage mode and power generation mode.

In the power storage mode, the W2G system uses excess power from vRES combined with syngas from waste gasification to produce CH_4, which is then injected into the natural gas grid for transport and storage. This operational mode is a key asset of the technology as it offers a multiplicity of added values:

it allows a higher penetration of renewables by absorbing the excess power, which can cause grid unbalances or renewables power generation curtailment;
it produces an energy and carbon carrier which has already a large distribution network and storage capacity;
it can provide long term seasonal storage of the excess renewables power;
it produces an energy carrier which may be used to decouple fossil fuels fromall sectors of the economy (transport, space heating, industry and others);
it contributes to solving the issue of organic waste disposal.

In power generation mode, the syngas produced from waste is used as SOFC to produce renewable power and dispose of organic wastes and residues.

On top of that, the plant's reversibility enables continuous operation, improving efficiency and economic costs by avoiding both unproductive phases and the ramp-up and down (or warming and cooling) time of single mode power generation or storage technologies.

The results indicated that the amount of waste and residue in the examined Italian region was enough to match the power storage balancing needs of the power grid. In the power generation mode, the residue and waste were sufficient to generate all the electricity need by the power grid in most design configurations. The potential for the deployment of W2G technology is impressive, with an order of magnitude of the rSOC capacity of approximately 4 and 7 GW when the rSOC operates in power generation and power storage modes, respectively. The operation of the W2G systems would correspond to about 5.5 TW h of power generated and 9.6 TW h of energy absorbed from the grid, and approximately 1.4–2.4 Mt of methane produced; while, at the same time, disposing of 6.7 Mt of biowaste. In agreement with our estimate, at least as an order of magnitude, the Italian TSO, in its adequacy analysis of the NECP scenario, reports projections of a need of approximately 6 GW additional to centralized storage capacity, mainly in the South, for 2030 (Terna, 2019c). These potentials are theoretical upper limits to the deployment of the W2G systems, as merely the sustainable technical potential of biowaste and power grid estimated balancing needs are considered.

5 CONCLUSION

The power sector is one of the main contributors to global warming, and RES may play a key role in its decarbonization. The transition toward a climate-neutral energy system requires higher penetration of vRES, namely wind, and PV. The EU aims at achieving a 96–99% renewable energy share in the power sector by 2050 (EU energy roadmap 2050). This paper proposes a case study for the potential deployment of the novel W2G rSOC system in the so-called RES-dominated area in Italy, to enable such a renewable penetration in the power sector.

The results showed that the power overproduction from intermittent renewables might be an opportunity instead of an issue. The W2G technology could dispose of all the organic waste of a RES-dominated zone and fully balancing the power grid. In the long term (summer-winter), it could produce valuable renewable fuels (i.e., syngas, $H_{2,}$ and CH_4) and a chemical building block for the other sectors of the economy (transport, space heating, industry).

The research question underpinning the methodology proposed in this work is 'what is the potential deployment of the W2G technology'. To answer that question, the two other questions to answer are 'what is the balancing need of the power grid in 2030?' and 'what is the availability of biowaste in 2030?'. This study has presented a methodological approach that answers these questions. The same approach could also be applied to other areas characterized by overproduction of vRES and potentially interested in applying similar technologies to dispose of the organic waste and balance the power grid.

The results of the present study show sustainable technical potentials. They are not meant to represent an optimal solution but rather indicate the maximum potential deployment of the technology and support the identification of an optimal design and scale for future studies. This paper provides insights into potential operating parameters and locations where W2G-like technologies could be used to treat biowaste and/or balance the power grid. This prospective case study does not provide a final resolution for the application of rSOC technology in the transition toward a 100% renewable energy power sector in Italy as it did not account for the economic and political factors that drive wholesale prices and the total system costs of the power grid.

This work contributes to understanding of biowaste availability and which power sector features are needed to implement overall EU energy targets. Further to the methodological approach outlined, our datasets on waste flow availability and power grid balancing needs provide the basis for similar studies and/or market/techno-economic optimization modeling in the future.

DATA AVAILABILITY STATEMENT

The raw data supporting the conclusions of this article were made available by the authors, without undue reservation, and can be found in the ZENODO repository at: 1) waste stream dataset: https://zenodo.org/record/3629527#.X-x-v9hKiUk; 2) power grid (renewables and consumption) dataset: https://zenodo.org/record/3625882#.X-x-1dhKiUk.

AUTHOR CONTRIBUTIONS

AA, LW, MP-F, YZ, and SY undertook funding acquisition, designed the research project and the overall methodology. CC, AA, and FG analyzed power generation and load data. NP and VM performed the biomass assessment in Italy. CC and AA wrote the paper. All authors contributed to review and editing of the manuscript.

FUNDING

This work was supported by the European Union Horizon 2020 Grant Agreement No. 826161 Waste2GridS Project, and by the Fuel Cells and Hydrogen Joint Undertaking Program.

REFERENCES

Agostini, A., Battini, F., Giuntoli, J., Tabaglio, V., Padella, M., Baxter, D., et al. (2015). Environmentally sustainable biogas? The key role of manure co-digestion with energy crops. *Energies.* 14, 33–39. doi:10.3390/en8065234

ARERA. (2020). Report. Available at https://www.arera.it/it/docs/20/321-20.htm.

Banja, M., and Jégard, M. (2017). Renewable technologies in the EU electricity sector trends and projections: analysis in the framework of the EU 2030 climate and energy strategy. doi:10.2760/733769(online)

Biomass Energy Europe Project. (2020). Biomass Energy Europe Project. Available at http://www.eu-bee.eu/. (Accessed).

Bird, L., Lew, D., Milligan, M., Carlini, E. M., Estanqueiro, A., Flynn, D., et al. (2016). Wind and solar energy curtailment: a review of international experience. *Renew. Sustain. Energy Rev.* 65, 577–586. doi:10.1016/j.rser.2016.06.082

Biswas, S., Kulkarni, A. P., Giddey, S., and Bhattacharya, S. (2020). A review on synthesis of methane as a pathway for renewable energy storage with a focus on solid oxide electrolytic cell-based processes. *Front. Energy Res.* 8, 64. doi:10.3389/fenrg.2020.570112

Calbry-muzyka, A. S., and Schildhauer, T. J. (2020). Direct methanation of biogas—technical challenges and recent progress. doi:10.3389/fenrg.2020.570887

Collins, S., Deane, P., Ó Gallachóir, B., Pfenninger, S., and Staffell, I. (2018). Impacts of inter-annual wind and solar variations on the European power system. *Joule* 2, 2076–2090. doi:10.1016/j.joule.2018.06.020

Davies, J., Dolci, F., Klassek-Bajorek, D., Ortiz Cebolla, R., and Weidner, E. (2020). Current status of chemical energy storage technologies. doi:10.2760/280873

Edenhofer, O., Pichs-Madruga, R., Sokona, Y., Seyboth, K., Eickemeier, P., Matschoss, P., et al. (2011). IPCC special report on renewable energy sources and climate change mitigation summary for policymakers and technical summary. doi:10.5860/CHOICE.49-6309

ENAMA Biomass Project. (2020). Biomass project. Available at https://www.enama.it/progetto-biomasse/sccc7227d. (Accessed).

ENAMA. (2011). Report. Available at https://www.progettobiomasse.it/it/pdf/studio/p1c2.pdf.

ENEA. (2020). Report 02/2020. Available at https://www.enea.it/it/seguici/pubblicazioni/analisi-trimestrale-del-sistema-energetico-italiano.

European Comission. (2018). Directive (EU) 2018/851. doi:10.1023/A:1009932427938

European Commission. (2018a). COM(2018) 392. Available at https://eur-lex.europa.eu/resource.html?uri=cellar:aa85fa9a-65a0-11e8-ab9c-01aa75ed71a1.0003.02/DOC_1&format=PDF.

European Commission. (2015). Directive (EU) 2015/1513. *Off. J. Eur. Union* 2014, 20–30.

European Commission. (2018b). Directive (EU) 2018/2001.

European Commission. (2018c). Regulation 1059/2003. Available at https://eur-lex.europa.eu/legal-content/EN/TXT/PDF/?uri=CELEX:02003R1059-20180118&from=EN.

European Commission. (2019). The European green deal. doi:10.1017/CBO9781107415324.004

European Parliament. (2009). Directive 2009/28/EC of the European parliament and of the council of april 23 2009. doi:10.3000/17252555.L_2009.140.eng

GIE. (2018). GIE Existing gas storage capacity in Europe exceeded one petawatthour in 2018, shrinked against 2016-GIE. Available at https://www.gie.eu/index.php/gie-media/press-releases/ (Accessed).

Giuntoli, J., Agostini, A., Caserini, S., Lugato, E., Baxter, D., and Marelli, L. (2016). Climate change impacts of power generation from residual biomass. *Biomass Bioenergy* 89, 146–158. doi:10.1016/j.biombioe.2016.02.024

Giuntoli, J., Agostini, A., Edwards, R., and Marelli, L. (2017). Solid and gaseous bioenergy pathways : input values and GHG emissions. Calculated according to the methodology set in COM(2016) 767 (EUR 27215). doi:10.2790/27486

Götz, M., Lefebvre, J., Mörs, F., McDaniel Koch, A., Graf, F., Bajohr, S., et al. (2016). Renewable Power-to-Gas: a technological and economic review. *Renew. Energy* 85, 1371–1390. doi:10.1016/j.renene.2015.07.066

Guandalini, G., Robinius, M., Grube, T., Campanari, S., and Stolten, D. (2017). Long-term power-to-gas potential from wind and solar power: a country analysis for Italy. *Int. J. Hydrogen Energy* 42, 13389–13406. doi:10.1016/j.ijhydene.2017.03.081

Hutty, T., Dong, S., and Brown, S. (2020). Suitability of energy storage with reversible solid oxide cells for microgrid applications. *Energy Convers. Manag.* 226, 113499. doi:10.1016/j.enconman.2020.113499

IRENA. (2019). Report. Available at https://www.irena.org/publications/2019/Mar/Renewable-Capacity-Statistics-2019.

IRENA. (2020). Report. Available at https://www.irena.org/publications/2020/Jun/Renewable-Power-Costs-in-2019.

ISTAT a. (2020). Download data. Available at http://dati.istat.it/ (Accessed).

ISTAT b. (2020). Download data. Available at http://dati-censimentoagricoltura.istat.it/Index.aspx (Accessed).

Liu, M., Lanzini, A., Halliop, W., Cobas, V. R. M., Verkooijen, A. H. M., and Aravind, P. V. (2013). Anode recirculation behavior of a solid oxide fuel cell system: a safety analysis and a performance optimization. *Int. J. Hydrogen Energy* 38, 2868–2883. doi:10.1016/j.ijhydene.2012.12.070

Malinauskaite, J., Jouhara, H., Czajczyńska, D., Stanchev, P., Katsou, E., Rostkowski, P., et al. (2017). Municipal solid waste management and waste-to-energy in the context of a circular economy and energy recycling in Europe. *Energy* 141, 2013–2044. doi:10.1016/j.energy.2017.11.128

Maxwell, S. L., Evans, T., Watson, J. E. M., Morel, A., Grantham, H., Duncan, A., et al. (2019). Degradation and forgone removals increase the carbon impact of intact forest loss by 626%. *Sci. Adv.* 5, 2546. doi:10.1126/sciadv.aax2546

Ministero dello Sviluppo Economico. (2019). Ministero dell'Ambiente e della Tutela del Territorio e del Mare, and Ministero delle Infrastrutture e dei Trasporti. Piano Nazionale Integrato per l'Energia e il Clima.

Olsen, K. P., Zong, Y., You, S., Bindner, H., Koivisto, M., and Gea-Bermúdez, J. (2020). Multi-timescale data-driven method identifying flexibility requirements for scenarios with high penetration of renewables. *Appl. Energy* 264, 33. doi:10.1016/j.apenergy.2020.114702

Pan, Y., Birdsey, R. A., Fang, J., Houghton, R., Kauppi, P. E., Kurz, W. A., et al. (2011). A large and persistent carbon sink in the world's forests. *Science* 333, 988–993. doi:10.1126/science.1201609

Peters, R., Deja, R., Blum, L., Nguyen, V. N., Fang, Q., and Stolten, D. (2015). Influence of operating parameters on overall system efficiencies using solid oxide electrolysis technology. *Int. J. Hydrogen Energy* 40, 7103–7113. doi:10.1016/j.ijhydene.2015.04.011

QGIS. (2020). QGIS project. Available at https://www.qgis.org/en/site/. (Accessed).

Ripa, M., Fiorentino, G., Vacca, V., and Ulgiati, S. (2017). The relevance of site-specific data in Life Cycle Assessment (LCA). The case of the municipal solid waste management in the metropolitan city of Naples (Italy). *J. Clean. Prod.* 142, 445–460. doi:10.1016/j.jclepro.2016.09.149

S2Biom Project. (2020). S2Biom Project. Available at https://www.s2biom.eu/en/. (Accessed).

Schreiber, A., Peschel, A., Hentschel, B., and Zapp, P. (2020). Life cycle assessment of power-to-syngas: comparing high temperature Co-electrolysis and steam methane reforming. *Front. Energy Res.* 8, 1–17. doi:10.3389/fenrg.2020.533850

Sikarwar, V. S., Zhao, M., Clough, P., Yao, J., Zhong, X., Memon, M. Z., et al. (2016). An overview of advances in biomass gasification. *Energy Environ. Sci.* 9, 2939–2977. doi:10.1039/c6ee00935b

Simonis, B., and Newborough, M. (2017). Sizing and operating power-to-gas systems to absorb excess renewable electricity.. *Int. J. Hydrogen Energy* 42, 21635–21647. doi:10.1016/j.ijhydene.2017.07.121

Terna. (2019a). Download data. Available at https://www.terna.it/it/sistema-elettrico/transparency-report/download-center. (Accessed).

Terna. (2019b). Download data. ed evoluzione del Sistema Elettrico_8d75639fa148d01.pdf. Available at: https://download.terna.it/terna/Contesto. (Accessed).

Terna. (2019c). Rapporto adeguatezza italia Adeguatezza Italia 2019_8d71cb7ff32ad37.pdf. Available at: https://download.terna.it/terna/Rapporto.

The New York Times. (2020). A Whiff of Naples Arrives in Hamburg (2008). Available at https://www.nytimes.com/2008/06/09/world/europe/09trash.html.

TNO. (2020). Phyllis2 Download data. Available at https://phyllis.nl/.

W2G Project (2020). W2G Projectat. Available at https://www.waste2gridsproject.net/publications/.

Wang, L., Zhang, Y., Li, C., Pérez-Fortes, M., Lin, T. E., Maréchal, F., et al. (2020). Triple-mode grid-balancing plants via biomass gasification and reversible solid-oxide cell stack: concept and thermodynamic performance. *Appl. Energy* 280, 115987. doi:10.1016/j.apenergy.2020.115987

ISPRA Waste database. (2020). Available at https://www.isprambiente.gov.it/en/databases/data-base-collection/waste.

Wulf, C., Zapp, P., and Schreiber, A. (2020). Review of power-to-X demonstration projects in Europe. *Front. Energy Res.* 8, 1–12. doi:10.3389/fenrg.2020.00191

Conflict of Interest: The authors declare that the research was conducted in the absence of any commercial or financial relationships that could be construed as a potential conflict of interest.

frontiers
in Energy Research

REVIEW
published: 06 April 2021
doi: 10.3389/fenrg.2021.636782

Perspectives for Greening European Fossil-Fuel Infrastructures Through Use of Biomass: The Case of Liquid Biofuels Based on Lignocellulosic Resources

*Paraskevi Karka, Filip Johnsson and Stavros Papadokonstantakis**

Department of Space, Earth and Environment, Division of Energy Technology, Chalmers University of Technology, Gothenburg, Sweden

OPEN ACCESS

Edited by:
Luis Puigjaner,
Universitat Politecnica de Catalunya, Spain

Reviewed by:
Elisabeth Wetterlund,
Luleå University of Technology, Sweden
Pinaki Dey,
Karunya Institute of Technology and Sciences, India
Jay Prakash Verma,
Banaras Hindu University, India

****Correspondence:***
Stavros Papadokonstantakis
stavros.papadokonstantakis@chamers.se

Specialty section:
This article was submitted to Process and Energy Systems Engineering, a section of the journal Frontiers in Energy Research

Received: *02 December 2020*
Accepted: *08 March 2021*
Published: *06 April 2021*

Citation:
Karka P, Johnsson F and Papadokonstantakis S (2021) Perspectives for Greening European Fossil-Fuel Infrastructures Through Use of Biomass: The Case of Liquid Biofuels Based on Lignocellulosic Resources. Front. Energy Res. 9:636782. doi: 10.3389/fenrg.2021.636782

Given the importance of climate change it is vital to find a transition away from fossil fuels. The transition will include electrification of several sectors, for example road transport, but considering the strong dependency on carbon-based fuels and associated infrastructures, it is reasonable to assume that biomass-based hydrocarbon will play a key role to smoothen the transition away from fossil fuels. This study provides an analysis of direct and indirect technological options for liquid biofuels based on lignocellulosic resources in the context of greening European fossil-fuel infrastructures. Direct options are those which result in integration of biogenic feedstock in a fossil-based process and then co-processing in a downstream conventional unit or substituting a conventional part of the production chain of a liquid fuel by a bio-based one. Indirect options are those which pave the way for ramping-up biomass supply chain in the form of infrastructure and market. Examples of direct options in the focus of this study are biomass gasification for production of intermediates and biomass pyrolysis substituting fossil feedstock. Examples of indirect options are co-firing biomass in coal-fired power plants and integrating biomass gasification plants with district heating (DH) networks. Such options are important for establishing biomass supply chains and markets. This study also assesses the potential of biomass use in other industrial sectors not directly related with fossil-based fuel or energy production, such as the pulp and paper industry and the iron and steel industry. In this context, opportunities and barriers for both direct and indirect greening options are discussed, focusing mainly on technological and logistic aspects. It is highlighted that fossil-fuel infrastructures can act as drivers for the development of advanced biofuels production as they can reduce the initial risks, in terms of cost and technological maturity, offering the opportunity to increase gradually the demand for biomass, and develop the logistic infrastructure. It is, however, important to make sure that such biofuel production processes are part of a long-term strategy, which needs incentives to overcome current barriers and eventually phase out fossil infrastructures.

Keywords: integration, bioeconomy, gasification, pyrolysis, district heating, lignocellulosic biomass, advanced fuels, co-firing

INTRODUCTION

The European Union (EU) aims at the transition toward a climate neutral economy in order to reach the goals of the Paris Agreement (United Nations Climate Change, 2016) adopting various action plans and strategies. In short term the "2030 climate and energy framework" (European Commission, 2030 climate & energy framework, Climate Action[1]) includes EU-wide targets and policy objectives targeting at the reduction of greenhouse gas (GHG) emissions, increased share of renewable energy and improvement in energy efficiency. In long term, EU targets at climate neutrality by 2050 (European Commission, 2050 long-term strategy, Climate Action[2]) in the framework of the European Green Deal (European Commission, A European Green Deal[3]), which includes action plans toward a resource efficient, circular economy, restoration of biodiversity, and pollution reduction. In this context, it is likely that in the foreseeable future the fossil-fuel infrastructure will involve significant downsizing. A combination of measures will be most likely needed to compensate this reduced dependency on fossil fuels, such as change of end-user consumption patterns, evolution of engines, more efficient logistics, promotion of direct and indirect electrification, and use of liquid biofuels, either as drop-in or in blending. Whereas, passenger and light duty road transportation could be benefitted from electrification aviation, shipping, and long-haul road transportation are expected to—at least to a large share—rely on over the next decades (Gudde et al., 2019).

With respect to increasing the share of liquid (advanced) biofuels, a major challenge is their production cost in relation to the fossil fuel alternatives. This is of fundamental importance, since drastic reductions in production costs of biofuels cannot be expected, while the cost of the biomass feedstock remains a substantial part of the fuel price (Thunman et al., 2018; IEA Bioenergy Report, 2020). Both governmental support for supporting investments to scale-up the production of biofuels and long-term market conditions in favor of biofuels are required. The current regulations in energy use and climate change have not so far created an environment of long-term stability to reduce capital risk and unlock massive large-scale investments on renewable sources (Fuels Europe, 2018). Two representative policies have a significant impact on the future of transportation fuels: Fuel Quality Directive (European Commission, Fuel Quality[4]) with 6% emissions reductions target by 2020 using biofuels, electricity, e-fuels, and upstream emissions reduction and the Renewable Energy Directive—Recast to 2030 (European Commission, Renewable Energy—Recast to 2030 (RED II), EU Science Hub[5]) including targets for road and rail transport sub-sectors by 2030 and requiring a minimum of 14% of the energy consumed as renewable energy. The Emissions Trading System [European Commission, EU Emissions Trading System (EU ETS), Climate Action[6]] is also expanded for the aviation sector (Fuels Europe, 2018).

Eventually, such policies should be effective at the development of efficient biomass supply logistics, which is a vital factor for the success of liquid biofuels. There is significant potential for establishing biomass supply systems for different types of lignocellulosic feedstock such as from forests and short rotation crops. For instance, EU countries like Sweden and Finland have well-developed forest industry including production of some liquid biofuels (e.g., bio-ethanol) and development of biorefineries (Scarlat et al., 2011; Kumar et al., 2021). Since biomass transportation costs influence the total biomass fuel costs, production site selection for new biomass facilities is an important factor when designing biomass supply networks (Awudu and Zhang, 2012; Yue et al., 2014; Atashbar et al., 2016). Numerous studies have focused on mathematical programming and simulation approaches to optimize bio-based supply chains and support decision making of biofuels or bioenergy production (Elia et al., 2011; Pérez-Fortes et al., 2012; You et al., 2012; Yilmaz Balaman and Selim, 2014; O'Neill and Maravelias, 2021). In such studies, besides the proximity factor between biomass resources and biofuel production plants, another factor that should be considered is the potential of using existing infrastructures for fossil-based fuel production. Potential benefits may arise from reductions in capital costs, shared utility infrastructures, and use of existing logistics networks. Moreover, a description of the employment effects, also for personnel in existing fossil infrastructures, from the construction and operation of biofuel supply chains can be found in the study of Yue et al. (2014).

Thus, the identification of synergies between the existing fossil infrastructure and liquid biofuel production can play a significant role toward a realistic gradual phase-out of fossil fuel production. However, on the technology level, most publications about liquid fuels production have focused either on facilities that can operate in isolation (Phillips et al., 2007; Hu and Lu, 2012; Dimitriou et al., 2018) or as parts of value chains for diverse biorefinery configurations (Parker et al., 2010; Sadhukhan et al., 2014; Karka et al., 2017; Doliente and Samsatli, 2020). This study, instead, focuses specifically on technological opportunities for "greening" conventional infrastructures with advanced biofuels processes based on lignocellulosic feedstock which are at a relatively high technology readiness level (TRL>6). This can be a win-win situation, contributing to both a realistic, gradual phase-out of fossil infrastructures, and to increasing the TRL of biomass conversion technologies from demonstration to commercial scale facilities. This perspective also includes more generic options

---

Abbreviations: bio-SNG, bio-synthetic natural gas; BFB, bubbling fluidized bed; BTL, biomass-to-liquids; CCS, carbon capture and storage; CFB, circulating fluidized bed; CTL, coal-to-liquids; DFB, dual fluidized bed; DME, dimethyl ether; DH, district heating; EU, European Union; FCC, fluid catalytic cracking; FT, Fischer-Tropsch; GHG, greenhouse gas; HDO, hydrodeoxygenation; HEFA, hydrotreated ester and fatty acids; LBG, liquified biogas; LPG, liquefied petroleum gas; TMP, thermo-mechanical pulp; TRL, technology readiness level; VGO, vacuum gas oil.

[1] https://ec.europa.eu/clima/policies/strategies/2030_en

[2] https://ec.europa.eu/clima/policies/strategies/2050_en

[3] https://ec.europa.eu/info/strategy/priorities-2019-2024/european-green-deal_en

[4] European Commission, Fuel Quality. https://ec.europa.eu/clima/policies/transport/fuel_en

[5] https://ec.europa.eu/jrc/en/jec/renewable-energy-recast-2030-red-ii

[6] https://ec.europa.eu/clima/policies/ets_en

for integrating biomass toward a carbon-neutral energy sector, such as co-combustion and co-gasification of biomass and coal (Lainez-Aguirre et al., 2015; Puigjaner et al., 2015; Cintas et al., 2018). Thus, this study also includes steppingstone options, which may be especially relevant for regions with limited or no experience in biomass logistics. In this regard, a mapping of relevant European fossil-based and conventional facilities is also considered. This includes data for capacities of oil refineries, fossil-based power plants in Europe and potential of technologies that can be converted to produce liquid biofuels due to technical feasibility (e.g., biomass boilers converted to gasifiers). Each greening option is followed by a summary of the corresponding opportunities and barriers. This refers to economic, technological, and generic supply chain related factors which promote or impede the incorporation of these bio-based technologies in conventional infrastructures. Notwithstanding the importance of other factors, such as rigorous optimization of industrial site selection and supply chains as well as influence of national and international policies, such studies require detailed case-specific data, which lies outside the scope of the study. Instead, this study aims at providing the short- to mid-term perspectives for greening fossil infrastructures in the context of the most advanced biomass conversion technologies for liquid biofuels from lignocellulosic feedstock, based on an overview of the generic technology status, available capacities, and important techno-economic aspects.

FRAMEWORK OF ANALYSIS

In the framework of the current study, the possibilities for integrating biofuel production are divided in two categories, direct and indirect options, as shown in **Figure 1**.

1. "Direct" are characterized those technological options which lead to the incorporation of renewable carbon in the final molecule of the fuels. In practice, the substitution is achieved by:
   - drop-in (blending) of a biogenic feedstock in a fossil-based process stream and then co-processing in a downstream conventional unit
   - substituting a conventional part of the production chain of a liquid fuel by a bio-based one.

In both cases, the biogenic feedstock (or intermediate stream) can be produced, either within the system boundaries of the fossil-fuel infrastructure or in a decentralized way and then transported to the fossil-fuel infrastructure for processing. According to Bunting et al. (2010) and DOE/EERE (2013) three possible insertion ways for biofuel to entry the petroleum infrastructure are identified: a bio-crude that can be co-processed with conventional crude oil, refinery-ready intermediates that are compatible with specific refinery streams for further processing at the refinery, and a near-finished fuel or blend stock that will be minimally processed at the refinery. The latter direct option is rather trivial from technology integration perspective, especially if it refers to pure mixing of the fuel product of a stand-alone biorefinery with the corresponding fuel of an oil refinery (e.g., mixing of bio-gasoline from the bio-methanol to gasoline process with oil refinery gasoline). As this case of greening refers to utilizing an existing fuel distribution-to-end-user infrastructure rather than the fossil fuel production infrastructure, it lies outside the focus of the present study.

2. "Indirect" are characterized those technological options which fall into one of the following two categories: steppingstone options which do not focus on the development of liquid biofuels infrastructures but on other energy related systems for short-term development of biomass supply infrastructures and mid-term potential of conversion to biofuel production, and other integration options which refer to the development of biomass supply infrastructures or liquid biofuels production through various non-fossil carbon-based industrial sectors such as 1st generation bio-ethanol plants, saw-mills and pulp and paper industry, and steel industry.

Figure 2 gives an overview of different routes from lignocellulosic biomass to fuel through various conversion technologies which refer to direct options and indirect options as described in **Figure 1**. Lignocellulosic biomass is one of the most abundant forms of biomass, including wood and residues from forestry, waste-wood from industry, agricultural residues such as straw and stover, and energy-crops such as willow or miscanthus. The various conversion technologies of biomass (Sims et al., 2010; Nanda et al., 2014; Sikarwar et al., 2017) can be roughly categorized in:

- Biochemical pathways, which include processes such as fermentation in which enzymes and other micro-organisms are used to convert cellulose and hemicellulose to sugars and alcohols.
- Thermochemical pathways including combustion, gasification, liquefaction, hydrogenation, and pyrolysis.

In the first category of biochemical pathways, the lignocellulosic ethanol pathway (also known as 2nd generation ethanol) is the advanced biofuel technology with the higher TRL (IEA Bioenergy Report, 2020). However, it has only limited applications for integration with refinery infrastructures, mainly via utilities and logistics. Thus, despite the potential penetration of higher ethanol blending rates in the future (e.g., gasoline blending), heat integration with 1st generation ethanol plants is the main other integration options (i.e., categorized as indirect option in this study). Other options of lower TRL than those studied herein include the fermentation toward higher alcohols, the acetone-butanol-ethanol fermentation process being under ongoing research. The main target is to optimize the fermentation process and identify bacteria that maximize the butanol yields, which at the moment hinder the scale-up toward commercial scale for fuel relevant quantities. In general, fewer industrial actors are optimizing lignocellulosic production processes for butanol than for ethanol (IRENA, 2016).

In the second category of thermochemical pathways, bio-oil and syngas, as presented in **Figure 2**, are intermediate products for producing a wide range of fuels and chemicals through various processing paths (Canabarro et al., 2013). These two products provide opportunities for utilizing existing facilities,

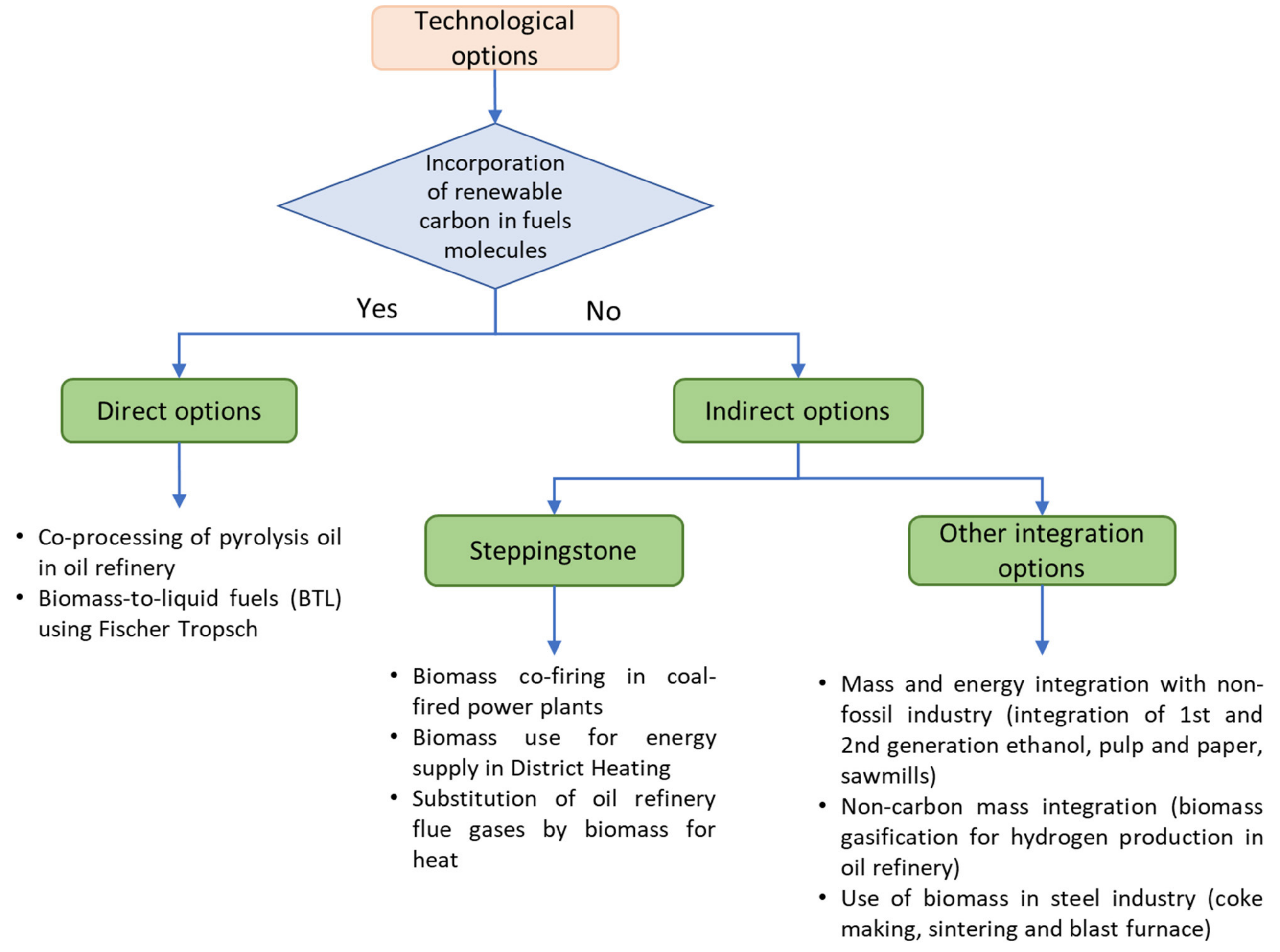

FIGURE 1 | Technological options which can facilitate biomass use toward greener fossil fuel infrastructures.

such as bio-oil hydrocracking, hydrotreating, gasification, and chemical synthesis. These intermediates can be produced within refinery sites or at other locations, for example in connection to existing power or combined heat and power plants (Cintas et al., 2018), which are considered points with potential to introduce biomass use.

The gasification-based pathways comprise synthesis reactions toward methanol, DME (Hannula and Kurkela, 2013), ethanol and higher alcohols (Villanueva Perales et al., 2011), liquefied methane (Thunman et al., 2018), and gasoline, diesel, and kerosene through FT synthesis (Swanson et al., 2010). Biomass gasification with FT synthesis [i.e., Biomass-To-Liquids (BTL) technology] can have a greening effect in oil refineries through FT syncrude co-processing and heat integration. The case of the substitution/conversion of Coal-To-Liquids (CTL) and Gas-To-Liquids (GTL) to BTL and combined feedstock options is also considered in this study.

In **Figure 2**, two conversion technologies are highlighted as direct options. The first is the case of biomass pyrolysis for co-processing bio-oil in Fluid Catalytic Cracking (FCC) units. The pyrolysis-based pathways focus on the upgrading of pyrolysis oil via hydrotreatment and cracking toward gasoline, diesel, and kerosene, and liquefied methane. Thus, greening fossil infrastructures may refer to the partial substitution and blending of pyrolysis oil into existing oil refineries. The second is the case of syngas via gasification which can replace syngas from coal or natural gas for downstream FT synthesis. In addition, this path can provide waste heat in existing district heating (DH) networks.

Hydrothermal liquefaction (HTL) is another thermochemical liquefaction process, alternative to pyrolysis, that produces bio-oil. Xing et al. (2019) and Sharma et al. (2020) studied the co-processing of HTL bio-oil with fossil fuels (e.g., VGO and straight-run gas oil, respectively). The study of Xing et al. (2019) showed that HTL bio-oils from woody biomass have significantly less oxygen (typically <15 wt %) than pyrolysis bio-oils and are more thermally stable, making them more amenable for co-processing in refining. Nevertheless, there is limited experience with processing HTL biocrudes, mostly because HTL technologies are in the transient state from lab-pilot scale to pilot-industrial scale (Gollakota et al., 2016). For this reason the HTL

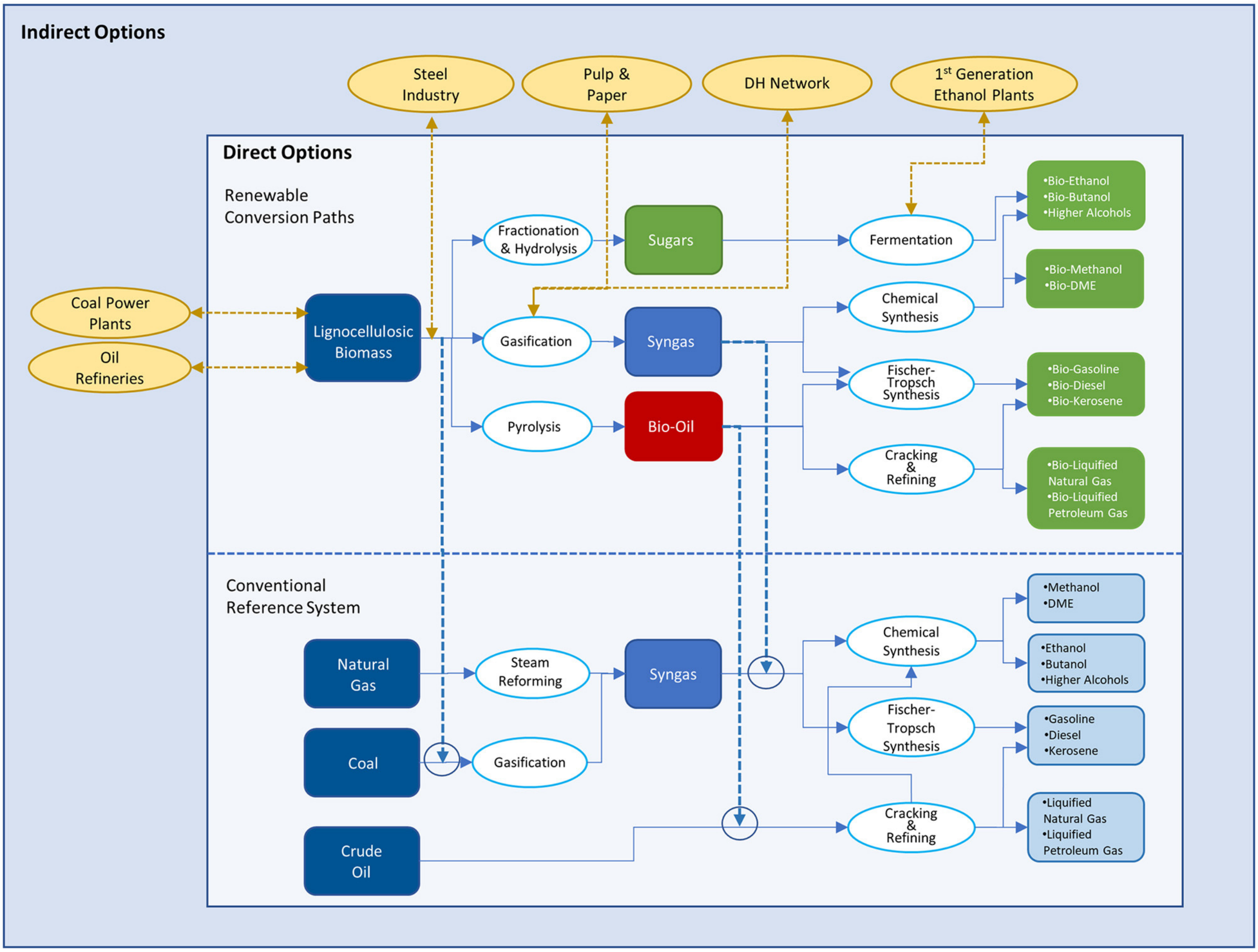

FIGURE 2 | Overview of different routes from biomass to fuel through various conversion technologies which refer to direct and indirect options.

pathway is not considered to satisfy the constraint of TRL>6 and it is not further studied herein.

Indirect steppingstone ways to implement greening of fossil infrastructures and enhance biomass use mainly refer to taking advantage of existing energy infrastructure of industrial facilities, onsite and offsite of power plants and combined heat and power plants, by starting with co-firing of biomass or by exploiting excess heat from biomass gasification plants in DH networks. The concept is that when the existing power plants using fossil feedstock are phased out (i.e., by other renewable energy sources), the sites can be partially or fully replaced by biomass pyrolysis, gasification, or other emerging biomass conversion technologies (e.g., HTL) for the production of intermediates which can be transported to refineries as analyzed by Cintas et al. (2018). To use existing infrastructure also includes taking advantage of existing knowledge and know-how on thermal processes as well as utilizing existing sites which keeps transportation costs low. Wherever it is difficult to build greenfield plants due to various constraints (e.g., financial, legal, technical, etc.), new biomass-conversion plants could be built in already existing industrialized areas to benefit from existing process know how in energy plants and refineries.

DIRECT OPTIONS FOR GREENING FOSSIL-FUEL INFRASTRUCTURES

Incorporation of Bio-Oil Feedstock Into Existing Oil Refineries

Given that it is rather difficult to establish a specific way to provide a stable biomass feedstock (i.e., in terms of composition, properties, etc.), it is quite effective to transform it into bio-oil. However, bio-oil is reported to have high oxygen content ranging from 8 to 63 % (dry basis) depending on feedstocks and pyrolysis conditions (Gollakota et al., 2016), with typical values ranging from 35 to 40% (dry basis) (Lehto et al., 2013), reducing the energy content of the fuel. Regarding further limitations of bio-oil use, it is rather immiscible with hydrocarbon fuels because of the high polarity of oxygenated compounds impeding it from direct use in the FCC process. Other relevant bio-oil properties are its chemical instability, low volatility, high viscosity, and corrosiveness. Nevertheless, the liquid nature of bio-oil is quite advantageous compared to handling solid biomass (Melero et al., 2012).

In terms of utilizing existing infrastructures, oil refineries can be suitable infrastructures for processing of bio-intermediate streams depending on the composition of the intermediate product. Many of the biocrudes may contain larger molecules of phenols, catechols, etc., which motivates co-processing in oil refinery units such as FCC, hydrocracker, or thermal cracking. However, the direct use of bio-oils in refineries by direct mixing with petroleum liquids is not technologically favorable and a way to tackle the insertion of bio-oils in a conventional refinery is by hydrotreating it. The hydrotreatment conditioning step results in partial hydrodeoxygenation (HDO) where the acidity and the oxygen content of the stream are reduced. Deoxygenation is applied up to a point which meets the minimum requirements of the refinery since approaching oxygen-free bio-oil can be expensive (van Dyk et al., 2019). Thus, the degree of HDO varies depending on the co-processing insertion point at the refinery (Karatzos et al., 2014). In this context, the PNNL study (Freeman et al., 2013) categorized US oil refineries in response to their conversion capability (i.e., ability to process biomass intermediates and convert higher boiling range into lower boiling range materials) which can be achieved through FCC or hydrocracking.

Co-processing of bio-oil in FCC together with vacuum gas oil (VGO) removes oxygen present in feedstocks in the form of water, CO, and CO_2 via simultaneous dehydration, decarboxylation, and decarbonylation. Co-processing in an FCC unit has an advantage compared to other processing units in a refinery as additional hydrogen or energy inputs are typically not required, saving both costs and additional GHG emissions. FCC is more profitable than thermal cracking and also minimizes the yield toward by-products such as gases, coke, and heavy fractions while maximizing the production of the liquid fraction suitable for use as transport fuel (Melero et al., 2012). Moreover, catalysts are more tolerant than hydrocracking catalysts in higher oxygen levels (Agblevor et al., 2012). The study of van Dyk et al. (2019) refers that hydrotreatment units are sensitive to oxygen and unlikely to be used to process bio-oils with an oxygen content that exceeds 5% at blending ratios of more than 10%. It should be noted that there is limited experimental data on co-feeding of real bio-oils with petroleum feeds in hydrotreating units.

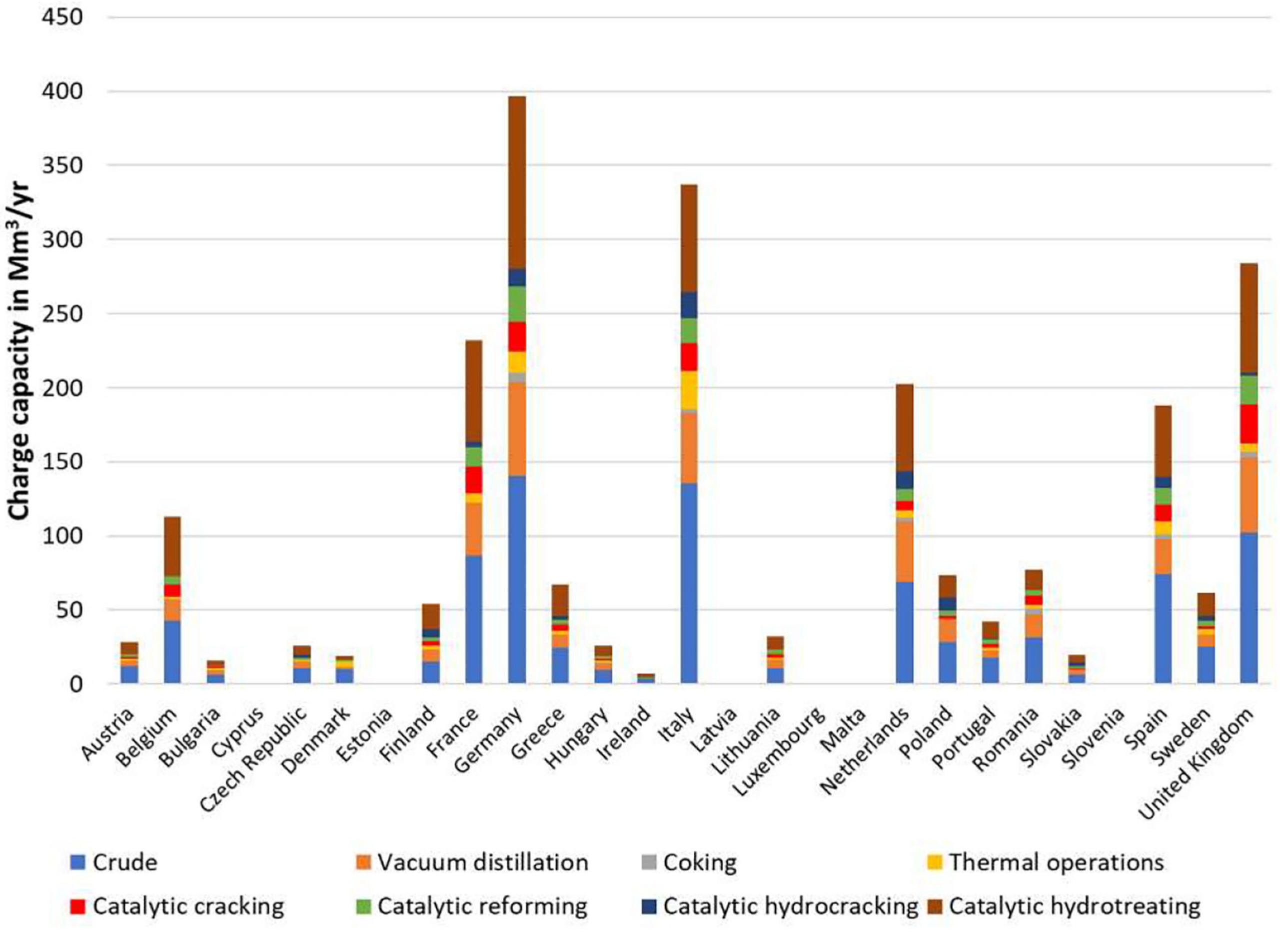

FIGURE 3 | EU 27 capacity for mineral oil refining (source: Barthe et al., 2015).

Current Technology Status

In contrast with the lack of commercial, lignocellulosic based fuels, which are basically at demonstration scale, the oleochemical route (e.g., feedstocks of vegetable oils and animal fats) to produce drop-in biofuels, is the most commercialized process. Oleochemical feedstocks due to their low oxygen content are easily converted to fuels (Melero et al., 2012), whereas lipid hydrotreatment has recently become a well-established technology with a few stand-alone operations (Neste, 2020). Even though this type of feedstock is out of scope for the particular study, some case studies are referred to herein as they can be considered as a good knowledge source about technological opportunities and constrains of co-processing renewable feedstocks in oil-refineries. Some examples of hydroprocessing oleochemicals feedstocks in EU are presented in literature (de Jong and Jungmeier, 2015): Neste Oil operated since 2013 three Hydrotreated Ester and Fatty Acids (HEFA) facilities in Finland, Rotterdam, and Singapore with an annual total capacity of 2.4 billion liters of palm oil-derived diesel marketed as "NexBTL" (Neste, 2020). Preem (Sweden) has started to produce diesel (330,000 m^3 diesel per year) with 30% renewable content (i.e., the renewable feedstock is raw tall oil, a byproduct from kraft pulp mills) in a modified mild hydrocracker unit (Sandén and Pettersson, 2013; Karatzos et al., 2014).

There are no cases of co-processing bio-oil in oil refineries at commercial scale. Stefanidis et al. (2018) discussed the possible insertion of bio-oil and biocrudes in the fluid catalytic cracker, whereas the increased coking and reactor plugging due to char and coke formation make upgrading of raw bio-oil through hydrotreatment necessary to remove oxygen. The results of this experimental set-up, of which the conditions did not resemble a real FCC, led to different conclusions when using a pilot-scale FCC under more realistic conditions. The same aspect of scaling up is discussed as a challenge in accurately predicting product distribution by Pinho et al. (2017), who presented an application of the use of lignocellulosic raw materials in a conventional refining scheme by the co-processing of raw bio-oils from pine woodchips with standard Brazilian VGO commercially processed in Petrobras FCC unit. In their study, two different bio-oil/VGO weight ratios were tested, 5/95 and 10/90. This pilot scale study was tested in a 200 kg/h FCC demonstration-scale unit using a commercial FCC equilibrium catalyst and bio-oil was fed directly without any other pre-processing in order to test the sensitivity of production yields in diesel, gasoline, coke, CO, and CO_2. In all cases, about 30% of renewable carbon in pyrolysis oil ends up in total liquid products and bottoms.

Potential for Integration Options of Oil Refineries With Biomass Use

The refining sector in the EU comprises 85 refineries (according to data from years 2015–2016), spread across 22 Member States, Norway, and Switzerland. In total, EU has a combined throughput capacity of over 14.5 Mb/d, accounting for roughly 14.5% of global refining capacity in 2015. Overall, the sector exhibits a wide variety in levels of configuration, integration, and production with capacity ranges between 40 and 425 Kb/d. Europe's largest refineries (>250 Kb/d) are located in the Netherlands, Poland, Germany, Belgium, Italy, UK, and Spain (Nivard and Kreijkes, 2017).

According to the data provided by Nivard and Kreijkes (2017), the oil refineries, spread across 22 of the EU Member States, Switzerland, and Norway are mainly developed near major seaports, large rivers or pipelines. The distribution in terms of number of refineries is more even across EU compared to refining capacity which is more concentrated in the North-Western part of the EU close to the North Sea crude oil sources (European Commission, 2016a,b,c).

Since most refineries in the EU are equipped with FCC units according to the values for oil refinery installations for 2013, these units can be considered as a potential infrastructure for co-processing pyrolysis oil (Barthe et al., 2015). **Figure 3** presents various processing techniques of the European oil refineries (EU 27) and the existence of FCC per country indicates a potential of co-processing bio-oil. Of course, many other factors may play significant role in the application of this "greening" possibility such as supply chain infrastructures, policies which enhance the development of renewable infrastructures, technological constraints, and the existence of financial support instruments.

According to the reported ranges of 2–10% of blending bio-oil in FCC units (where the 10% would refer to the case of HDO bio-oil) an estimation of the potential HDO bio-oil is possible. The potentially used HDO bio-oil would be approximately 10 Mm^3/year HDO to be blended in the FCC units for the whole FCC capacity in Europe. This corresponds to approximately 6,400 MW bio-oil production (e.g., 64 plants in Europe of 100 MW each). This would require 10,000–11,000 MW of lignocellulosic biomass (e.g., woody residues) in total in Europe to be converted in this bio-oil. These estimations are based on LHV of approximately 20 MJ/l for bio oil and a blend ratio of 10%.

Bio-based Syngas for Liquid Fuels (BTL) Including Fischer-Tropsch Synthesis

The gasification pathway via the intermediate synthesis gas utilizes technologies already commercialized for production of methanol, diesel, and jet from natural gas and coal. Synthesis gas conversion to methanol is very well-established in the chemical industry, methanol being mainly reported as a fuel in marine applications in the form of blends (10% in methanol) (Paulauskiene et al., 2019) or in light and heavy duty vehicles (e.g., in China) (Schröder et al., 2020). Using synthesis gas with FT synthesis to produce liquid hydrocarbons, where crude oil is not readily available, is also well known for exploiting coal or natural gas resources (Gudde et al., 2019). Thus, it is the synthesis gas production and cleaning via biomass gasification technology that determines the performance of the BTL pathways compared to gasification of other resources or natural gas steam reforming (Dimitriou et al., 2018).

Current Technology Status

Several CTL and GTL FT plants are running or planned, while biomass-based conversion for production of FT fuels is only at pilot or demonstration scale (Luque et al., 2012). The FT process is currently being operated at an industrial scale by two main fossil fuel companies: Sasol in South Africa (producing 160,000 bpd of FT-diesel from coal derived syngas and converting of one of its CTL facilities to accept natural gas) and Qatar (34,000 bpd Oryx GTL facility) and Shell[7] in Malaysia [world's first commercial-scale Gas-To-Liquid (GTL) plant based on FT synthesis producing 15,000 bpd of middle distillates and specialty products] and Qatar (in collaboration with Qatar Petroleum producing 260,000 barrels of GTL products).

Over the last several decades, a continuous effort to improve catalyst activity, selectivity, and stability has been carried out in these fossil-based GTL and CTL technologies. Thus, similar challenges should be expected for BTL technologies utilizing FT synthesis with respect to the suitability of biomass syngas using the existing catalysts (Luque et al., 2012). It should be noted that data from FT plants mostly come from engineering studies or cost estimates for plants currently under construction or commissioning according to IEA Bioenergy Report (2020). It has been suggested that when a BTL process is compared to a GTL one, the main challenges are related to processing a more heterogeneous biomass feedstock, production of a lower quality syngas, and the feedstock availability risks (Hileman et al., 2009).

Potential Integrations With Fossil Infrastructures

While the FT process does not depend on how the syngas is produced, as long as its composition depending on the feedstock fulfills the downstream specifications, the gasification technology is the key technological step to the integration of CTL and BTL processes. In order to take advantage of the economy of scale when using biomass, significant efforts are being made to test CBTL processes, namely co-gasification of coal and biomass (Shah, 2013).

Even though GTL and CTL have reached commercial scale, the BTL process has not been completely commercially established. There are various examples of pilot and demonstration plants or discontinued BTL projects in Europe, such as the Choren Carbo-V!Process producing light FT products (now out of operation) in Frieberg Saxony in Germany and the BioTfuel pilot project in France which produces biodiesel and biokerosene based on biomass gasification (ETIP bioenergy[8], Biofuels Barometer, 2017).

NSE Biofuels Oy operated a 12 MW_{th} (656 tons/year of fuels) BTL demonstration plant in Finland from 2009 to 2011, which employed a circulating fluidized bed (CFB) gasifier developed by Foster Wheeler (Dimitriou et al., 2018). The GoBiGas plant in Sweden, which is a first-of-its-kind industrial installation for advanced biofuel production via gasification, converted woody biomass to biomethane (Thunman et al., 2018, 2019). These plants can be considered as a proof-of-concept for the production of liquid biofuels via gasification.

Biomass gasification process is usually limited to small scale due to biomass availability and logistics constraints, negatively influenced by seasonality, moisture, and low density, unlike coal and natural gas. Thus, biomass gasification processes tend to have high capital (fixed) cost, present lower thermal efficiency than coal-fired plants, and are subject to long term supporting policies. Their theoretical optimum capacity is frequently limited by biomass logistics issues.

The mixture of coal and biomass in co-gasification could be a steppingstone measure to develop biomass facilities in case of CTL existing infrastructures; however, the CTL technology is generally lacking in EU countries. Success stories of co-gasification is the NUON power plant at Buggenum (Netherlands) and Schwarze Pumpe (Germany), in which large proportions of biomass and coal have been co-gasified for liquid fuel and syngas (Kamble et al., 2019; IEA Bioenergy Agreement, Task 33[9]). This integration option provides a stable and reliable feed supply and potential feedstock disturbances of biomass supply cause less consequences in the production (Shah, 2013). NERL (National Energy Technology Laboratory) reported that the use of 30% switchgrass with coal for producing diesel (CBTL) with carbon capture and storage technology (CCS) produced 63% less GHG emissions compared to a fossil-derived diesel. Greenhouse gas emissions can further be decreased up to 75% by using more aggressive capturing technique of auto-thermal reformer in CCS (Brar et al., 2012).

Representative disadvantages of co-gasification are feed preparation and complex feed systems which can be expensive. The choice of gasifier operation parameters (temperature, gasifying agent, and catalysts) determine product gas composition and quality. Biomass decomposition occurs at a lower temperature than coal and, therefore, different reactors (fluidized bed or downdraft gasifier) compatible to the feedstock mixture are required. Also, at high temperature, alkali present in biomass can cause corrosion problems in downstream pipes. Biomass containing alkali oxides and salts with ash content above 5% causes clinkering/slagging problems (Brar et al., 2012).

The Concawe Report (2020) gives some numerical estimations and order of magnitude analysis regarding the potential quantities of biomass requirements and liquid products in the case of co-feeding a conventional gasifier of an oil refinery with a renewable feedstock. In EU only 6 refineries have been reported with gasifiers which convert residual oil to syngas for further production of methanol, hydrogen, and power and can be considered as potential points for biomass co-feeding. The estimations of Concawe report consider the case of a large-scale refinery-based gasifier which consumes ∼1 Mt/a of residue and point out that such a modification to receive biomass or bio-intermediate streams for units of this scale is a challenging matter. If a gasifier of that scale (i.e., ∼1 Mt/a) is co-fed with 5% biomass, thus requiring ∼50 kt/a of biomass, this can result in a rather small quantity of 25 kt/a of liquid product, whereas higher co-feeding ratios up to 50% would be a matter of significant technological and economic challenges (Gudde et al., 2019).

Table 1 summarizes the aforementioned direct options of biomass to liquid fuels in existing fossil infrastructures. The options are characterized with respect to opportunities and

---

[7] *Shell*. https://www.shell.com/about-us/major-projects/pearl-gtl/the-world-s-largest-gas-to-liquids-plant.html

[8] https://www.etipbioenergy.eu/value-chains/conversion-technologies/advanced-technologies/biomass-to-liquids

[9] IEA Bioenergy Agreement: Task 33, Thermal gasification of biomass. task33.ieabioenergy.com

TABLE 1 | Direct integration options of biomass to liquid fuels in fossil infrastructures.

Integration option	Opportunities	Barriers	Real world examples	References/Supplementary data	Feasibility to scale up (low, medium, high)
Bio-oil co-processing within an oil refinery	**Technological** • TRL of biomass pyrolysis: 6 or higher ETIP Bioenergy, 2020 **Economic** • Co-processing bio renewable feeds and fuels in existing refinery units is more profitable than the stand-alone case Jones et al., 2009; Beims et al., 2017; Bhatt et al., 2020 **Supply chain** • Established infrastructure of refineries for long-distance sea transport • Bio-oil imports can be facilitated together with oil imports Doug, 2006; Cintas et al., 2018	**Technological** • Current blending ratios of 2–10% lead to rather low scaleup feasibility Directorate-General for Mobility Transport, 2018 • Presence of water and oxygenated organic compounds affects yields and conversion rates Air Resources Board, 2017 • Alkali metals deactivate FCC catalysts Air Resources Board, 2017; Pinho et al., 2017 • Differences in yields when scaling-up from pilot to commercial scale projects Pinho et al., 2017; Stefanidis et al., 2018 **Economic** • Co-processing is highly sensitive to the crude prices and refinery feed rates **Supply chain** • Discontinuous production, variety and storage of biomass feedstock transportation chains, required pretreatments to accomplish energy densification • Challenge of the decentralized production of pyrolysis oil and its transfer to the oil refineries as the physical properties change during storage and transportation Yang et al., 2015	• IEA Bioenergy Agreement, Task 39[a] • Petrobras/NREL CRADA international partnership • Co-processing of pine-based bio-oil with petroleum-based fuel intermediate oil in the fluidized catalytic cracking process (FCC) • No other commercial case studies exist, just demonstration cases • **Other cases but not from pyrolysis of lignocellulosic feedstock** Biodiesel production from tall oil (a byproduct of the kraft processing of pinewood for pulp and paper), as a result of co-processing in oil refinery (https://www.etipbioenergy.eu/value-chains/feedstocks/waste/tall-oil)	• **Capacities of all European refineries:** (Nivard and Kreijkes, The European Refining Sector: A Diversity of Markets?, 2017) • Data for FCC units Barthe et al., 2015 • Other research studies suggesting co-processing of up to 20% wt bio-oil with VGO in FCC units Fogassy et al., 2010 • Example of estimation of co-processing and production of bio-renewable fuel potential in California Air Resources Board, 2017 • Study of co-locating a plant of hybrid poplar for gasoline and diesel production from fast pyrolysis with an existing refinery in the USA including capital investment data Jones et al., 2009 • Co-location of fast pyrolysis with an oil refinery to eliminate the need for pressure swing adsorption unit in the hydrotreating unit, with off-gas from hydrotreater being sent to refinery hydrogen generation • Economic analysis of co-processing bio-oil in an FCC unit in petroleum refinery Ali et al., 2018	• Low[b] (with respect to the technologies of upgrading bio-oil to advanced liquid fuels, both in a fully integrated plant or by co-processing with fossil fuels, typically validated at lab scale, reaching TRL 4–6)

(Continued)

TABLE 1 | Continued

Integration option	Opportunities	Barriers	Real world examples	References/Supplementary data	Feasibility to scale up (low, medium, high)
Biomass-to-liquid fuels (BTL) via Fischer-Tropsch	**Technological** • Co-gasification of biomass and coal can build upon experience for biofuels production • Fischer-Tropsch (FT) synthesis is an established technology, and many components are mature in CTL and GTL plants • Gasification plants can reach, after modifications, theoretical efficiency yields in commercial scale and have achieved continuous operation **Economic** • Technical advances in the FT process regarding yield and conditions can make biofuels competitive depending on crude oil prices Luque et al., 2012	**Technological** • A fully scaled-up commercial BTL process is not completely established until today. Luque et al., 2012 • Application of the corresponding process using biomass has yet to be fully optimized • Gasification technologies require development, especially regarding feedstock pretreatment and logistics **Economic** • Cost of feed preparation and logistics of biomass for an optimum size of a BTL plant can become an important factor in the scale of BTL process • No tax for fossil fuels and high production costs impede biofuel to be competitive • Fixed cost for BTL plant is generally 60% higher than the one required for GTL plant of the same size Lee, 2013 **Supply chain** • Biomass is difficult to transport and store • No consistent supply	• The case of Sweden's GoBiGas plant which is a 32MW$_{th}$ gasifier and produces SNG. Potential scaling up in 200MW could produce liquid fuels Thunman et al., 2018	• **Database of facilities for the production of advanced liquid and gaseous biofuels** for transport per country and TRL (https://demoplants.bioenergy2020.eu) • The capital cost estimates for a first-of-its-kind commercial gasification-based facility (2000 tons of biomass (dry basis) per day) are in the region of USD $600-900 million which is favored from economies of scale Karatzos et al. (2014) • **Overview of FT units in EU countries** (Luque et al; 2012) • The size of FT process depends on the size of the gasifier for an integrated process. For example, a BTL plant producing 2,100 bbld will require a gasifier producing 250 MW$_{th}$ Lee, 2013	Low[c] (with respect to scaling up gasification)

---

[a] *IEA Bioenergy Agreement, Task 39. https://demoplants.bioenergy2020.eu/.*

[b] *Based on the argument that significant challenges need to be resolved such as matching the scale, sizing and catalyst design for two distinctly different feedstocks [bulky and reactive solid biomass versus relatively inert petroleum liquids (crude oil)].*

[c] *Due to biomass related infrastructures for processing and logistic issues.*

barriers for integration together with real world examples with some references. For the bio-oil processing, the most important constraints are the upgrading steps of bio-oil (catalyst deactivation and high oxygen content) even though pyrolysis is a well-established technology. Economic parameters are also important in implementing this upgrading and require minimum capital costs to retrofit petroleum refinery units in order to be compatible with the insertion points (Tong et al., 2013a,b). Regarding the BTL processes, FT is an established technology, and many components of the system are already technologically mature in CTL or GTL plants. What remains unproven is the BTL processes at a commercial scale due to technical barriers of gasification and scale up constraints. The overall greening impact is further restricted by the significantly smaller capacities of FT plants compared to oil refineries.

With respect to the supply chain barriers of these solutions, which are mainly related to the potential variability of the biomass feedstock in quantity and quality, it should be noted that these greening opportunities of the existing infrastructure are advantageous compared to newly built stand-alone biofuel plants. The reason is that such stand-alone plants would have to be considerably oversized, at least in the first phase of their operation, to reduce the risk of interruption in sellable products. Obviously, this risk is inherently reduced when the biofuel plants are integrated into existing operating facilities. In general, an important factor related with using the opportunities and overcoming barriers in **Table 1** is related with regional and international policy support, including financial instruments.

A successful deployment of liquid biofuels plants can be achieved on the basis of a holistic approach able to identify technical, economic, and supply chain related challenges and the policy gaps to overcome these challenges. Thus, a set of policy interventions including regulations, financing, and information provision mechanisms can better capture the different challenges along the biomass value chains and allow optimizing performance for all stages. This policy dimension lies outside of the scope of the current analysis, as more detailed information can be found elsewhere (ADVANCEFUEL, 2020a,b; Panoutsou et al., 2021; Singh et al., 2021).

Another barrier, outside of the scope of the current analysis, is the challenges related to the plant-to-end user distribution network of liquid biofuels and the availability of the adequate infrastructure. Fuels such as 1st generation ethanol present incompatibility with fossil fuels in common supply systems such as pipelines and require dedicated fuel distribution systems. On the other hand, drop in fuels would gain easier market acceptance whereas a challenging point is their integration with petroleum refineries in terms of capacity expansion and efforts to coordinate with fossil production (Yue et al., 2014).

INDIRECT OPTIONS FOR GREENING FOSSIL-FUEL INFRASTRUCTURES—STEPPINGSTONE OPTIONS

The following paragraphs describe two indirect steppingstone options: integration of biofuels production in DH networks and co-firing of biomass and coal for power production. These two options enhance the biomass supply conditions for the development of logistics for liquid biofuels or they can lead to higher system efficiency from biofuels plants in the case of potential integration schemes (e.g., retrofitting of existing DH boilers in gasifiers).

Integration of Biofuel Production Into Existing District Heating Infrastructure

This option refers to the case of biomass gasification with subsequent synthesis to biofuels such as FT diesel, DME, methanol, and methane. This option prerequisites the existence of a DH network. In this case, these biofuel plants generate excess heat and energy efficiency can be succeeded if using the excess heat in DH systems. Therefore, heat integration of biofuel plants with DH networks can improve the economic and environmental performance of the integrated system, especially when replacing decommissioned heat generation capacity for existing DH systems or when investments are made to extend the DH systems. Broad implementation of gasification-based biofuel production in European DH systems is discussed by Berndes et al. (2010), who concluded that a heat source-sink matching between the excess heat from biomass gasification plants for the production of transport biofuels according to the EU 2020 target and the DH systems in EU is not subject to any sink constraints (i.e., the heat sink of the DH systems would be in this case more than sufficient).

Current Technology Status

As fossil fuels dominate the energy supply for DH, there is a strong potential for the transition in other renewable sources such as biomass. The Swedish example represents the gradual incorporation of biomass in existing infrastructures and highlights the possibility for the development of infrastructures for the production of liquid biofuels (e.g., the case of GoBiGas plant as reported by Thunman et al., 2018) which can be favored from the existence of a DH network.

District heating supplies 12% of space heating and domestic hot water demand for buildings in EU. From 1990 until 2015, the use of gas was expanded contributing to around 1/3 of the total DH supply whereas, during the same period, biofuels use expanded its share to 20% and renewables account for 6% of the DH production (Mathiesen et al., 2019). In 2015, the total heat supplied to EU DH was 2.3 EJ, of which around 30% of the DH supply came from coal and coal products, 4.5% from oil, 35% from natural gas, 26% from biomass and waste, and 4.5% from other sources (Werner, 2017). Regarding the technology providing this amount of heat to the DH system, this is mainly produced (54%) from recycled heat, fossil CHP, and industries, 19.5% from recycled heat and renewable CHP, 9% from renewables (geothermal and waste), and 17.5% from fossil direct use (fossil boilers). The value of heat supply from fossil boilers corresponds to 0.4 EJ/year (or equivalently to 111 TWh/year) and the scenario of replacing them by heat from biomass gasifiers is analyzed in the section Potential Future Applications of DH Based on Biofuel Plants.

To this end, one should also consider the competition from excess heat from other major industrial sectors. Heat Roadmap

Europe 2050[10] provides information per country for major industrial plants regarding five typical energy intensive industrial sub-sectors having excess heat, namely chemical/petrochemical, iron and steel, non-ferrous metals, non-metallic minerals, pulp, and paper production and oil refineries. An overview of these heat streams for 2008 indicates 0.3 TWh in France, 4.9 TWh in Sweden, 0.8 TWh in Denmark, 0.9 TWh in Germany, and 0.03 TWh in Italy. These volumes add up to approximately 6.9 TWh for EU27. Moreover, the Stratego project (http://stratego-project.eu) provides a sectoral analysis within which fuel supply and refineries represent highest annual excess heat availabilities (9% of the total excess heat volume and 36% of total industrial sectors volumes), while non-metallic minerals facilities account for 5% of the total excess heat volume and 20% of total industrial sectors volumes.

Potential Future Applications of DH Based on Biofuel Plants

Introducing biomass in DH will create a supply system which later may be used for biofuels plants for transportation. The aforementioned study of Berndes et al. (2010) illustrated the size of the current DH systems in EU25 in relation to the EU biofuels for transportation targets for 2020. It was calculated that if 10% of the projected transport energy demand in EU by 2020 was to be met with biofuels from biofuel production units integrated in the DH system, and that these would deliver 0.2 energy units of DH heat per energy unit of biofuel produced, these biofuel plants would cover roughly 15% of the total heat demand in the current DH systems in EU25.

This statement could be applied in the case of biofuels contribution to the transport energy mix for 2030 and 2050 according to the scenarios developed in the framework of the ADVANCEFUEL project (ADVANCEFUEL, 2020a,b, http://www.advancefuel.eu/) and the European Commission (2018). According to the previous profile of technologies supplying heat to DH, it is assumed that fossil boilers, accounting for approximately 111 TWh/year in European DH systems, are decommissioned and they are replaced by biomass gasifiers. In the framework of ADVANCEFUEL, a scenario is formulated assuming a strong growth of biofuels and a breakthrough of advanced biofuels in the transport sector and a low diffusion of electric vehicles. This scenario corresponds to maximum penetration of liquid biofuels in the transportations sector, and thus it is useful to analyze potential excess heat to heat sink constraints, with respect to the DH capacity. In this scenario, the installed capacity of biofuels production is assumed to be around 44 GW in 2030 and up to almost 191 GW in 2050, with large roles for bioethanol and alcohol-to-jet fuel (19% of installed capacity in 2030 and 33% in 2050) and thermochemical production routes (40% of installed capacity in 2030 and 58% in 2050). If, the thermochemical production is considered as a source of liquid biofuels, then 17.6 GW (154 TWh/year) of fuels from thermochemical route are produced. If 20% of this energy can be delivered to DH network (Berndes et al., 2010), 30.8 TWh/year would be provided as excess heat. Accordingly, for 2050, 110 GW (964 TWh/year) would be produced and assuming that 20% of this energy can be delivered to DH network, 192.8 TWh/year can be delivered to the DH network.

According to another baseline scenario reported for the EU transportation mix in 2050 (European Commission, 2018), liquid biofuels consumption is projected to be 6% of the total fuels consumed. This results in 188 TWh/year of liquid biofuels consumption with a potential of providing at maximum 37.6 TWh/year excess heat to DH network, if all the liquid biofuels come from thermochemical biomass conversion technologies. Other scenarios of this report for more extended penetration of liquid biofuels in the transportation mix, result in heat delivered ranging between 58.2 and 110 TWh/year. All these values for heat delivered to the DH network are directly comparable to the value of 111 TWh/year which is the current heat supplied by fossil boilers, as well as to the 6.9 TWh/year which is the currently available excess heat from the main industrial sectors in EU. The comparison clearly shows that for most of these scenarios the DH system has presently more than the required capacity to be efficiently used as heat sink for the excess heat from future biofuel production. This is also not constrained by the competition with industrial excess heat. These conclusions are also in agreement with the argument of Berndes et al. (2010). Only the scenario of the ADVANCEFUEL project for maximum penetration of liquid biofuels in 2050 with limited use of electricity in the transportation mix results in an excess of this DH system capacity (i.e., 192.8 TWh/year compared to 111 TWh/year, respectively). However, the corresponding liquid biofuel production of this scenario should be considered as a theoretical maximum since limited use of electricity in the transportation is not currently considered as a very likely scenario.

Thus, replacing part of the fossil boilers for DH systems by biomass boilers, with the intention of converting these biomass boilers later into gasification systems for biofuel production with simultaneous use of the excess heat for DH systems to increase the overall system efficiency, is a promising steppingstone option. Of course, the potential of this integration option may be reduced if the competitiveness against other heat supply technologies is considered (e.g., CHP systems which currently dominate the DH heat supply in most Member States). Another aspect that can affect the economic feasibility is the extent to which the DH integrated biofuel plant becomes a base load heat provider for the DH system (Berndes et al., 2010).

The study of Thunman et al. (2018) presents a potential strategy of how fluidized bed boilers can be retrofitted to biomass gasifiers which can then be operated for integrated production of fuels with DH systems heat delivery. As an example, the fluidized boilers [CFB and bubbling fluidized bed (BFB)] currently installed in the Swedish energy system can be operated as Dual Fluidized Bed (DFB) gasifiers. This scenario represents a low-cost, low risk option for large penetration of biofuel production. Retrofit of biomass boiler for combined production of electricity and DH to a gasifier with upgrading synthesis steps would reduce investment cost by 10–20% compared to a new stand-alone plant. But equally important, this is an example of how the existing energy infrastructure, including knowledge and competence, could be utilized for fast introduction of biofuel production.

---

[10] Heat Roadmap Europe 2050. https://heatroadmap.eu

Thunman et al. (2018) presented the potential in a numerical estimation: to the 6,400-MW_{th} installed boilers, the required boiler capacity that needs to be added is 6,800 MW_{th} to create a gasification potential of 35,000 MW. This correspond to a fuel demand of 280 TWh of biomass or equivalently 59 million dry tons of biomass per year (8,000 h annual operation), which can produce between 170 and 200 TWh (14.6–17.2 MTOE) of advanced biofuels. This is significantly greater (i.e., about 5 times) than the Swedish target for biofuel production required to reach the Swedish goal of fossil free nation in Year 2045. Considering logistic constraints lowers this potential. Thus, for most locations it is not feasible to have units with fuel inputs $>$500 MW (2,500 dry tons of biomass/day) which lowers the annual potential fuel demand by around 30% (i.e., to 200 TWh or equivalently 42 million dry tons of biomass). This is, nevertheless, a substantial demand for fuel (i.e., approximately equal to the total forest growth in Sweden), implying that biomass must be imported if this scenario is to be realized. In other words, there is a low risk option for introduction of biofuel production to an extent that is in fact the national biomass supply, which limits the amount of fuel production even if Sweden has large amounts of forestry derived biomass.

The Refuel project (Berndes et al., 2008) suggested criteria for a country to be candidate for introducing cogeneration of BTL fuels and heat for DH such as the existence of a large and possibly expanding DH system and a presently small share of heat from renewable and recyclable heat. Indicatively, Poland and Slovenia were proposed as the most interesting for introducing co-generation of BTL fuels and heat due to their high use of coal and oil, whereas Italy, France, UK, and Belgium were considered as countries that is easier to introduce the BTL fuels integrated with the DH option in a system that is expanding.

It should also be noted that establishing a biomass supply chain for providing heat as steppingstone is not restricted to DH systems. Another strategy is to incorporate biomass use in the form of biomass boiler infrastructure in oil refineries, where there is a large steam demand that is currently covered by combusting the gases produced from the internal distillation or conversion processes. The composition of these gases is similar to the one of gases produced in a biomass gasifier and can be mixed for fuels production. Thus, a low cost and low risk option is to install a biomass boiler for part of steam production. This first step of greening the fossil-based refinery infrastructure aims to increase gradually the demand for biomass and to build up the logistic infrastructure needed to receive biomass at the plant by starting with the installation of a CFB boiler. After the development of an established biomass infrastructure is accomplished, the CFB boiler can be later upgraded in a biomass gasification system through its connection to a BFB boiler in the form of an indirect dual-bed gasifier.

Biomass Co-firing With Coal

This is included as an indirect option since biomass co-firing is a low risk option to produce renewable electricity (and heat) for regions without any developed biomass supply infrastructure but with coal-fired power plants. Thus, this option takes advantage of existing energy infrastructures in the form of power plants and combined heat and power plants. Once the biomass supply infrastructure has been established, the fossil fuel plant with associated fossil-fuel infrastructure can be replaced with a biomass-only process such as a biofuel production unit in the form of a gasification or pyrolysis unit. It should be stressed that the biomass co-firing option should not be used as an excuse of maintaining the fossil fuel units (lock-in effect); instead, the option should go hand in hand with a clear plan on how to phase out the fossil fuel use in the longer run.

Co-firing biomass in existing coal-fired power plants offers the possibility of significantly increasing the share of biomass through a relatively small boiler-upgrade investment and impact on the overall efficiency compared to biomass-only plants, where alkali-related high-temperature corrosion can limit steam properties. Typically, 10% co-firing shares reduce the risk of alkali-related high-temperature corrosion (Al-Mansour and Zuwala, 2010; Cintas et al., 2018), while uncertain biomass supply can be handled by varying the share of co-feeding ratios (Berndes et al., 2010; IEA-ETSAP and IRENA Technology Brief E21, 2013). Thus, co-firing biomass in coal plants can provide a near-term biomass market (Cintas et al., 2018) that effectively reduces GHG emissions from coal-fired plants in short-term and motivates the development of biomass supply infrastructure that can later facilitate further development of advanced biofuel production technologies toward sufficiently high TRL.

Current Technology Status

In 2016, European Union had an installed coal power capacity of 164 GW, which generates 24.5% of the total electricity mix (Cintas et al., 2018). Worldwide, approximately 230 power and combined heat and power plants are in operation which apply co-firing with a significant proportion in Europe. In particular, the study of Roni et al. (2017) reports many EU countries that use biomass co-firing technologies in their power plants. For instance, Denmark has five co-combustion plants in which straw, wood chips, and wood pellets are the predominant co-firing fuels and relies heavily on importing wood pellets from external markets (Canada and Eastern Europe). Fourteen biomass co-firing plants are in Finland, whereas in Belgium there are seven co-firing plants, the initiation of which for electricity production started after the "green certificate" implementation in 2001. Thirty co-firing plants are reported in Germany, sewage sludge being used in approximately 50% of all plants. There are five co-firing power plants in Austria which in their majority use pulverized coal as primary fuel, whereas wood chips, mostly bark, are used as biomass. On the other hand, in Sweden, the biomass infrastructure is already well-developed and there is also not significant use of coal for electricity and heat production, making this steppingstone option not particularly interesting there.

The Potential of Greening Coal-Fired Plants in EU

Figure 4 shows that countries most reliant on coal are Germany, Poland, and the United Kingdom, the latter having a significant part of capacity retired or switching fuel during the last years (Europe Beyond Coal[11]). Germany and Poland alone are jointly

---

[11] https://beyond-coal.eu/database

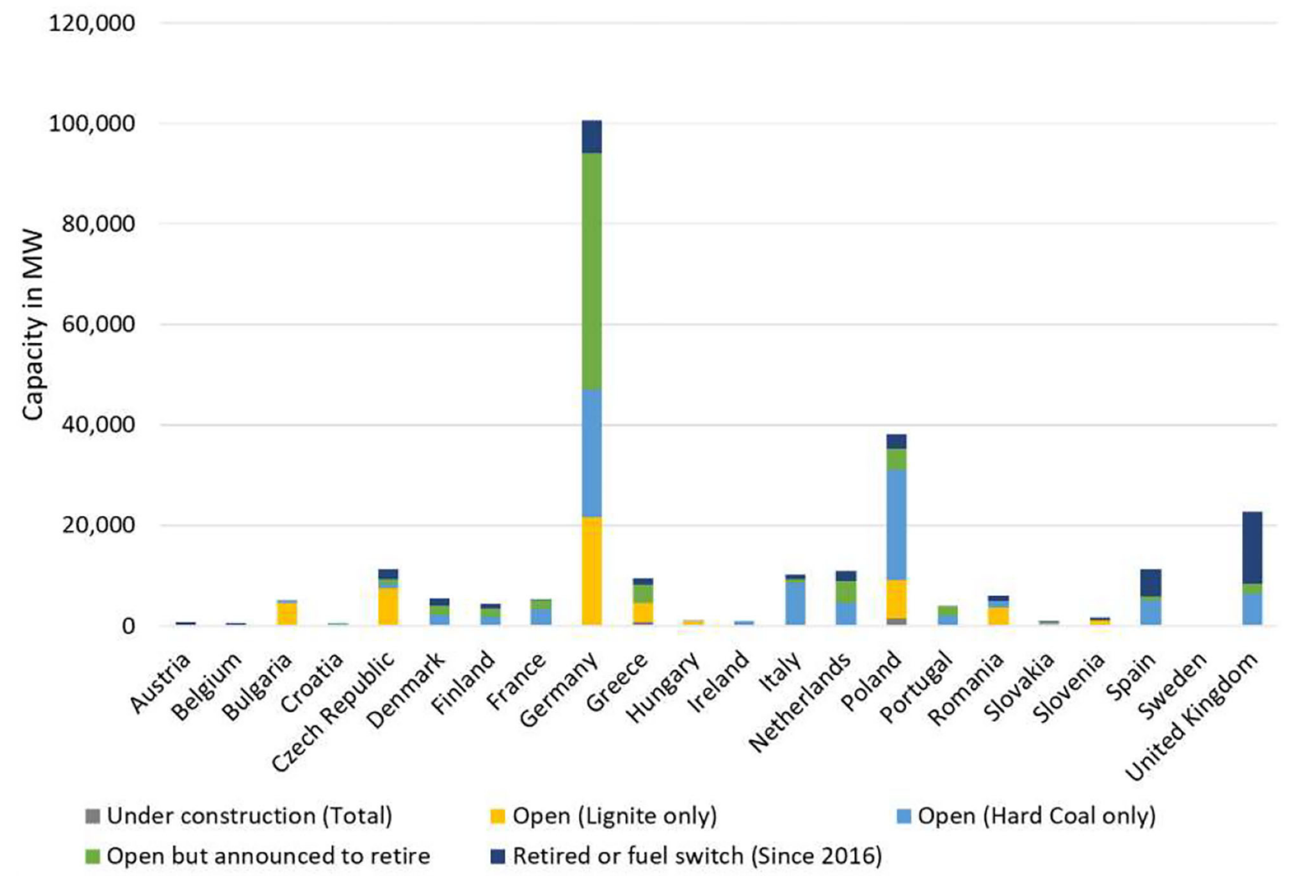

FIGURE 4 | Coal Fired plants in EU for 2019 (source: Europe Beyond Coal, https://beyond-coal.eu/database).

responsible for 51% of the EU's installed coal capacity and 54% of emissions from coal (https://climateanalytics.org/briefings/eu-coal-phase-out/); clearly, the long history in coal mining and extensive use of coal as fuel in power generation make some countries more than others prone to "carbon lock-in" and impedes carbon phase out (Rentier et al., 2019). Countries with power plants which announced to retire or already retired most or a significant part of the coal based power generation can be considered as candidate points of developing biofuels processes making use of the phased-out infrastructures to meet the EU climate and energy targets (EU Emissions Trading System—EU ETS).

Hansson et al. (2009) assessed biomass co-firing with coal in existing coal-fired power plants in EU-27, and Bertrand et al. (2014) matched the demand for biomass-based electricity with the potential biomass supply in Europe considering scenarios for both biomass co-firing in coal plants and dedicated biomass power plants. The study of Cintas et al. (2018) provides two scenarios for potential greening of existing coal-fired plants in EU countries, either converting the power plants to 100% biomass-firing plants (Scenario 1) or using the sites of the power plants to establish pyrolysis units for producing a raw bio-oil to be transported to petroleum refineries (Scenario 2), which was discussed as a direct option for the production of biofuels. Scenario 1 assumes that all existing co-firing plants and the coal-fired power plants identified as suitable for co-firing will be retrofitted to allow coal to be completely substituted by biomass; the plants will only use biomass, provided it is available. This kind of transition has been seen in the United Kingdom (UK), for instance, where three coal plants were converted to biomass fired plants (Roni et al., 2017). Suitable plants in the same study are economically feasible if the plant was constructed after 1990. In Scenario 2, it is assumed that pyrolysis units are built on current coal power plant sites. All coal power plants available were assumed to represent suitable sites for bio-oil production. Then, existing refineries with hydrocrackers are assumed to shift from petroleum to bio-based oil. The capacity of each pyrolysis unit is set to 100 MW bio-oil, corresponding to the planned size of the GoBiGas phase two project (100 MW bio-methane) (Alamia et al., 2017). In the same study, it was shown in GIS maps where residues can be collected to meet the biomass demand in each country.

The results of this analysis showed that bio-oil plants (each 100 MW) are built on all the existing coal power plant sites, producing 970 PJ of bio-oil and using about 1,493 PJ biomass. Results also showed that the largest bio-oil producers are naturally the countries with most coal power plants, namely Poland (97 units), Germany (93), the Czech Republic (43), Spain (20), Romania (17), Italy (15), and the UK.

Table 2 summarizes the options for indirect integration of biomass to liquid fuels technologies into existing fossil infrastructures, mainly contributing to the development of the logistics systems. The information is arranged in order to be clear what the current status, opportunities, and barriers for the integration of these technologies into existing fossil infrastructures are. For co-firing of coal-fired plants with biomass the basic opportunity of greening refers to the near term adaptation of specific areas in biomass supply and logistics infrastructures. Thus, this strategy prepares the ground for biofuel plants after the phasing out of fossil-fuel infrastructures. Even though this is a low-risk transition toward biomass use, a series of technical and economic factors may act as barriers in the long-term strategies for biofuel plants implementation, mainly due to lock-in effects and the lack of incentives of the energy markets toward radical changes for other renewable technologies.

Regarding the effect of DH networks, one can differentiate between regions with existing DH infrastructure and potential expansion plans and those with plans for new DH infrastructure. Those regions with existing DH networks and biomass fluidized bed boilers, thus having already biomass supply chains and consequently already having realized this steppingstone option, can be considered as drivers for other regions with only fossil-based DH networks or only DH network construction plans. This steppingstone serves the technological opportunity to convert the biomass boilers to dual fluidized gasifiers as excess heat sources, restricted of course from the uncertainty of the future evolution of the heat supply technologies and the expansion potential of the DH network in each EU country.

INDIRECT OPTIONS FOR GREENING FOSSIL-FUEL INFRASTRUCTURES—OTHER INTEGRATION OPTIONS

Co-location of biomass processing plants at existing industrial process sites offers interesting integration opportunities for heat and material flows, as well as the possibility to make use of the existing infrastructure. Some opportunities of this kind are presented here for four industrial sectors: oil, steel, pulp and paper, and 1st generation ethanol plants.

Oil Refineries and Petrochemical Industry

Based on the increasing demand of hydrogen in the oil refinery several studies refer to the production of hydrogen by biomass gasification in on-site installations of gasification units. Integrated configurations with gasification plants is investigated, for example, by Arellano Garcia et al. (2017), who analyzed the integration of biorefineries and oil refineries for the reduction of CO_2 emissions. The study investigates the case of a gasification unit that is fed with pyrolysis oil, biodiesel, and refinery residue, upgrading the syngas composition with water-gas shift reaction, before proceeding to production of clean hydrogen or liquid hydrocarbon fuels via FT synthesis.

In the study of Johansson et al. (2012) the integration of different biomass gasification technologies with an oil refinery for production of hydrogen is investigated through scenarios which assess the CO_2 emissions balance of the system. In the same context, Brau et al. (2013) studied the substitution of existing fossil fuel-based hydrogen production units in a refinery with a process based on indirect steam gasification of woody biomass. Furthermore, Johansson et al. (2014) investigated the integration of bio-FT fuels into a complex oil refinery, either by co-feeding the FT syncrude with crude oil in existing oil refinery facilities or by investing in new units for the FT syncrude processing and achieving heat and mass flow integration (e.g., off gases exploitation for energy sufficiency instead of natural gas).

Steel Industry

The opportunities to use biomass in iron and steel industry is to replace fossil carbon with carbon from biomass in coke making (in blends of 2–10%), sintering (for production of bio-sinter enabling replacement ratio of coal up to 60%), in blast furnace (partially replacement of coke from biomass as a reducing agent) or as a fuel in heating furnaces (Mousa et al., 2016). For instance, Mandova et al. (2018) developed the Global Suitability Index as an assessment methodology to identify countries which are potentially suitable for integrating biomass into their iron and steel making processes via the integrated blast furnace-basic oxygen furnace route, which provides 73% of the world's steel.

Industrial symbiosis opportunities may occur between a stand-alone biorefinery and a steel industry where excess heat from the iron and steel industry can be used in processes at the biorefinery (Sandén and Pettersson, 2013). An example can be found in the study of Ljungstedt et al. (2011), where heat and mass integration opportunities are investigated; excess heat from the steel plant can be used by an ethanol plant and the ethanol can be used as reducing agent in the blast furnace or as transportation fuel in the steel plant's vehicles. Ahlström et al. (2020) investigated the possibility to replace fossil fuels used for heating in the case of the Swedish iron and steel industry with liquefied biomethane (LBG) produced through gasification of forest residues. In this study, competition issues of LBG use were considered, such as using LBG for transportation, that influence the economic potential of LBG production.

Johansson (2013) investigated the profitability for a steel plant to produce bio-synthetic natural gas (bio-SNG) in a biomass gasifier and to substitute liquefied petroleum gas (LPG) with bio-SNG as fuel in reheating furnaces, for various energy price and carbon balance scenarios, not always ending up to profitable solutions. Lundgren et al. (2013) investigated the opportunities for methanol production from steelwork off-gases and biomass gasification in a steel plant, considering the SSAB steel plant in the town of Luleå, Sweden as a basis for the study. The results of this option, which could also be characterized as direct greening, showed that integration of methanol production in steel plants could be economically favorable and result in

TABLE 2 | Indirect integrated options of biomass use in fossil infrastructures.

Integration option	Opportunities	Barriers	Real world examples	References/Supplementary data	Feasibility to scale up (Low, Medium, High)
Biomass co-firing with coal	**Technological** • Exploiting existing infrastructures as a steppingstone for establishing biomass-supply infrastructure where it is lacking • Large number of coal-fired power plants makes biomass co-firing an option in many EU countries Roni et al., 2017 • 20% co-firing (as energy content) is currently applicable and more than 50% is technically feasible, whereas a usual biomass share today is below 5% IEA-ETSAP and IRENA Technology Brief E21, 2013 **Economic** • Main factors affecting the co-firing potential are the biomass price, carbon price and alkali index Cutz et al., 2019 • Cost of retrofitting a coal-based plant is lower than a dedicated 100% biomass plant IEA-ETSAP and IRENA Technology Brief E21, 2013 **Supply chain** • Starts up biomass supply chains, potentially suitable as feedstock for 2nd generation biofuels • Uncertain biomass supplies do not jeopardize the fuel supply for power plant	**Technological** • Risk of delaying the phase-out of fossil-fuel power plants • A steady growing biomass demand for co-firing may be considered a lock-in risk Berndes et al., 2010 **Economic** • Cost of collection, handling, preparation and transportation of biomass, in comparison with the relatively low cost of coal **Supply chain** • Cost of co-firing is affected by the plant location and the key cost element is the biomass feedstock IEA-ETSAP and IRENA Technology Brief E21, 2013 • A substantial increase in biomass co-firing could increase competition with other biomass uses	• Data for **location and capacity of coal co-fired power plants** in the EU member states Berndes et al., 2010 • **Biomass co-firing projects and costs in China and the US** Xu et al., 2020 • **Reporting of the existing co-firing plants** with technologies and availability of biomass resources in different countries of the world Roni et al., 2017	• **Database with information on coal power plants in EU** (Europe Beyond Coal, https://beyond-coal.eu/database/) • The costs of retrofitting an existing coal-fired power plant for co-firing range between USD300-700/kW with European estimates around €220/kW IEA-ETSAP and IRENA Technology Brief E21, 2013	High[a] (with respect to the preparation of the biomass market and infrastructure)
Integration of DH with biofuel production processes based on biomass gasification with subsequent synthesis to biofuels	**Technological** • Integration of biofuel plants with DH systems would improve the cost-competitiveness of these biofuels • Potential to convert fluidized bed boilers to dual fluidized gasifiers (e.g., in Sweden) **Economic** • By retrofitting an existing boiler from district heating to a gasifier producing advanced biofuels the cost of the investment would be reduced by 10–20% compared to a new stand-alone plant Thunman et al., 2018 **Supply chain** • Starts up biomass supply chains, potentially suitable as feedstock for 2nd generation biofuels	**Technological** • Highly dependent on the competitiveness against other heat supply options and in particularly CHP, which is dominating the DH heat supply in most EU member states **Economic** • Dependence on existence of financial incentives to retrofit boilers into gasifiers **Supply chain** • The development of biomass logistics is based on the other existing competitive technologies for energy supply in DH systems	• The case of Sweden's GoBiGas plant in a region with an established DH network Thunman et al., 2018	• Data for DH supply technologies and respective fuels used, for selected EU countries for 2012 (EC, 2016) • DH share in final heating demand for space heating and data on DH profiles in EU countries Mathiesen et al., 2019	High[a] (with respect to the preparation of the biomass market and infrastructure)

[a] *A near-term option to displace fossil fuels and pave the way for 2^{nd} generation biofuels.*

CO_2 emissions reductions and improvement of the overall plant energy efficiency.

Pulp and Paper and Saw-Mills

Synergies among pulp and paper industry and biorefineries mainly take advantage of the fact that both type of facilities use biomass resources and, thus, can exploit an existing mature infrastructure and know-how for handling large volumes of biomass. Other opportunities refer to access of heat integration practices. Sandén and Pettersson (2013) provided an overview of opportunities for developing biofuels production in the pulp and paper industry, including the extraction of hemicelluloses prior to pulping for upgrading toward fuels and chemicals, lignin extraction from black liquor for heating purposes replacing fossil fuels or upgrading, black liquor gasification for production of biofuels or electricity generation, and conversion of an existing pulp mill or one of the fiber lines to an ethanol production plant through cellulose extraction before pulping. Mongkhonsiri et al. (2018) also investigated possible pathways for a biorefinery integration with an existing pulp mill toward production of biofuels and value-added chemicals.

Saw-mills can be integrated with bio-SNG production according to the studies of Ahlström et al. (2017) and Zetterholm et al. (2020). Liquified Biogas (LBG) production is an effective way for a saw-mill to utilize its by-products and the policy and financial support were assessed in order to facilitate large-scale investments and maintain high production levels in saw-mill integrated production of LBG. Isaksson et al. (2012) and Tunå et al. (2012) investigated energy integration schemes among gasification plants and pulp and paper plants and assessed CO_2 emissions. The former study was based on the integration among three possible biomass gasification-based energy mills with an existing thermo-mechanical pulp (TMP) mill, co-located with a saw-mill producing electricity, methanol or FT liquids. The latter study assessed various gasification technologies with a possible portfolio of products (e.g., methanol, DME, FT fuels). The study of Jafri et al. (2020) presents a techno-economic and GHG emissions performance of five drop-in biofuel pathways based on black liquor lignin separation with hydrotreatment (i.e., where lignin and VGO mixture can be conveyed to the refinery and co-processed with crude oil derivatives) or black liquor gasification with catalytic synthesis (i.e., via syngas upgrading to "stabilized" methanol and then methanol to gasoline synthesis at a petroleum refinery). However, lignin separation pathways lower the entire TRL ranging between 4 and 6, making these configurations out of scope for the current study. Moreover, technologies facilitating the mixing of the final product fuel with the corresponding oil refinery fuel (e.g., methanol to gasoline such as in the case of black liquor gasification-catalytic synthesis route and mixing the gasoline with the oil refinery one) are also outside the scope of this study, as mentioned in the boundaries of the framework for this analysis.

Integration of 1st and 2nd Generation Bioethanol Plants

Several 2nd generation biofuel facilities (e.g., in Brazil, Finland, US) are already co-located with 1st generation biofuel production facilities. Moreover, an increasing number of US 1st generation biofuel companies are exploring how to retrofit their processes to incorporate cellulosic feedstocks into their production lines (IEA-RETD, 2016). Various studies have focused on the integration of 1st and 2nd generation of biofuels, either based on material and equipment integration or heat integration. For instance, the study of Lennartsson et al. (2014) investigated the integration of a 2nd generation ethanol (lignocellulosic) into 1st generation ethanol at the fermentation stage and the fungal cultivation stage. Other studies focused on the development of alternative configurations schemes in the form of process flowsheets (Dias et al., 2012) or heat integration showing that the heating and cooling energy demands could be reduced to a great extent (Joelsson et al., 2014). These studies demonstrate the benefits of sharing the existing infrastructures, logistics, and utilities.

Table 3 summarizes the indirect options for BTL fuels technologies into various existing process industries. The options are characterized with respect to opportunities and barriers for integration together with real world examples with some references. The opportunities refer to the development of biofuels plants close to industrial facilities, including non-fossil industry. The benefit arises from mass and energy integration between the advanced biofuel plant and the corresponding industrial infrastructure, including non-carbon mass integration through hydrogen production from biomass or heat integration with biomass being used for heating needs. Additionally, this co-location of advanced biofuel plants with potential retrofitting of existing facilities is benefited from utilities infrastructures in a total site analysis perspective, sharing of experienced personnel, and market penetration in already known market conditions (e.g., for 1st and 2nd generation ethanol plants). Challenges may be connected to the technical barriers of using biomass but also to bringing a totally new material (i.e., biomass) to industrial sites, such as the case of biomass and coal coke mixing in steel industry. Other techno-economical barriers refer to the low efficiency of 2nd generation ethanol plants and the lower TRL of lignin utilization toward a wider product portfolio.

CONCLUSIONS

To ramp up biofuels production processes and be part of a long-term climate strategy requires incentives and the overcoming of technological barriers. Although strongly decreasing the dependence on fossil-based resources is an indispensable part of climate strategies, in short- to mid-term using existing fossil-fuel infrastructures to incorporate the use of biomass is a low-risk option. Greening of fossil fuels infrastructures to enhance the deployment of liquid biofuels production is in line with the action plans of European Green Deal and the Sustainable Development Goals (e.g., SDG7—Affordable & Clean Energy, SDG 8—Decent work and economic growth, and SDG9—Industry, Innovation, and Infrastructure). However, avoiding lock-in effects should also be part of any proposed solution for greening fossil-based infrastructures.

The development of the thermochemical biomass conversion technologies to produce liquid fuels is currently lacking

TABLE 3 | Indirect integrated options of biomass use in processing industries.

Integration option	Opportunities	Barriers	Real world examples	References/Supplementary Data	Feasibility to scale up (Low, Medium, High)
Biomass use in industrial plants	**Technological** • Exploiting existing infrastructures as a steppingstone for establishing biomass-supply infrastructure where such is lacking • Lignocellulosic ethanol is on the verge of being commercial exploiting integration in early operations with 1st generation plants • Black liquor production is part of a pulp and paper industry facilitating exploitation routes close to commercialization such as gasification **Economic** • Potential heating and cooling demand reduction through heat integration • Share of existing infrastructures and no-need of investments anew **Supply chain** • Starts up biomass supply chains, potentially suitable as feedstock for advanced biofuels	**Technological** • The production of bio-coke (coal and biomass blend) with desired physical and chemical properties is still challenging Mousa et al., 2016 • Constraints of the development of 2nd generation ethanol Lennartsson et al., 2014: • Need for relatively severe pretreatments of the feedstock due to recalcitrance of biomass inhibiting fermentation • Production of cost competitive enzymes to hydrolyze the cellulose • Relatively low concentrations which increase the cost of distillation and wastewater treatment • Some exploitation steps in pulp and paper are of low TRL e.g., lignin separation and hydrotreatment restricting the options of integration with other industries e.g., oil refineries **Economic** • Economic assessment of integrations does not give always profitable results, e.g., the case of bio-synthetic gas in a biomass gasifier to substitute LPG for a steel plant (Johansson, 2013) and scenarios of various biorefinery concepts for an existing pulp and paper process Mongkhonsiri et al., 2018 • Scales of liquid biofuel plants are constrained and highly dependent on the capacity of the main industrial facility. This affects also the economic profitability of the new investment **Supply chain** • Competition with other uses of biomass and development of alternative fuels for the transportation and power sector will play an important role • Possible disadvantages of co-location of bio-processes with the pulping industry could be long distances among plants, lack of knowledge about the products and markets, and limited possibilities to deliver low-temperature excess heat to DH networks Sandén and Pettersson, 2013	• The status of lignocellulosic ethanol plants in EU can be found in the report of IEA Bioenergy Report (2020) • Two reported facilities producing bioethanol from cellulose via the biochemical route are the plant in Crescentino, Italy, constructed by Beta Renewables, and the plant Kajaani/St1 in Finland, by Cellunolix technology	• Data for pilot, demonstration and commercial plants with references on synergies with industrial sectors can be found in Landälv et al. (2017a,b) and IEA Bioenergy Report (2020) • Overview of the European steel industry, including crude steel production capacity per EU country for 2019 EUROFER, 2020 • Data for total pulp production, and paper and board production per EU country for 2019 CEPI, 2020	Medium to High[a] (with respect to the preparation of the biomass market and infrastructure)

[a] *A near-term option to displace fossil fuels and pave the way for 2nd generation biofuels.*

the experience of operating at large scale, namely at commercially relevant capacities for liquid biofuels. For instance, BTL production is mainly constrained by the biomass gasification technology and the catalytic upgrading technologies of the biomass pyrolysis oil, respectively. Integrating these technologies within oil-refineries provides mixing opportunities of intermediates, exploiting at the same time logistics infrastructure and engineering know-how and may significantly reduce the capital investment risk compared to stand alone biofuel plants. However, technological barriers still exist, mainly with respect to bio-oil quality for co-processing with refinery gas-oils and large-scale operation and syngas cleaning for the biomass gasification option. The biomass feedstock variability can be more easily handled when biomass conversion technologies are integrated into fossil infrastructures, however the cost of the biomass feedstock will still require dedicated support policies to reduce production costs.

Geographical aspects are also of importance with respect to available capacities, feedstock availability and supply chain constraints. Clearly, not all greening solutions are relevant or efficient for different regions. EU has significant FCC capacities in oil refineries for co-processing bio-oil but not so many FT synthesis plants which could provide additional options for integrating BTL processes. On the other hand, the overall system efficiency can be increased by exploiting excess heat from gasification plants to DH systems in EU, which represent a large heat sink. Thus, extending the use of biomass boilers in existing, under construction or planned DH systems can together with co-firing of biomass in coal-fired power plants prepare the conditions for regions where biomass infrastructure is missing.

It is important to note that greening fossil infrastructures should still be viewed as part of a more long-term strategy targeting at phasing out the fossil-fuel infrastructure and needs financial and legislative incentives to facilitate further technological improvement. Thus, the policy dimension, regional or international, should be incorporated for further analysis of the greening options. This includes identification of policy mechanisms and proper funding for innovation across the advanced biofuels value chain, including the potential of using fossil infrastructures. Such an analysis could identify current shortcomings in existing policies toward a more stable and efficient policy framework for the transportation sector and provide a clear direction for increasing investor confidence and successful market uptake.

AUTHOR CONTRIBUTIONS

PK performed the literature search, contributed to the organization of the material, contributed to the critical discussion of the findings, and to the final edition of the manuscript. FJ contributed to the critical discussion of the findings. SP contributed to the organization of the material, and to the critical discussion of the findings and the final edition of the findings. All authors contributed to the article and approved the submitted version.

ACKNOWLEDGMENTS

The authors would like to acknowledge financial support from the European Union's Horizon 2020 research and innovation programme under grant agreement N° 764799.

REFERENCES

ADVANCEFUEL (2020a). *Key Needs for Development and Potential for Innovations for Highly Efficient and Low Risk Biomass Conversion Technologies, Including Required Financial Instruments*. Available online at: http://www.advancefuel.eu/contents/reports/d33-potential-for-innovations-for-biomass-conversion-technologies.pdf

ADVANCEFUEL (2020b). *Socio-Economic Assessment Total System Costs of RESfuel Scenarios and the Employment Impacts of Biofuel Production*. Available online at: http://www.advancefuel.eu/contents/reports/d63-socioeconomic-analysis-final.pdf (accessed February 27, 2021)

Agblevor, F. A., Mante, O., McClung, R., and Oyama, S. T. (2012). Co-processing of standard gas oil and biocrude oil to hydrocarbon fuels. *Biomass Bioenergy* 45, 130–137. doi: 10.1016/j.biombioe.2012.05.024

Ahlström, J., Zetterholm, J., Pettersson, K., Harvey, S., and Wetterlund, E. (2020). Economic potential for substitution of fossil fuels with liquefied biomethane in Swedish iron and steel industry – synergy and competition with other sectors. *Energy Conver. Manage.* 209:112641. doi: 10.1016/j.enconman.2020.112641

Ahlström, J. M., Pettersson, K., Wetterlund, E., and Harvey, S. (2017). Value chains for integrated production of liquefied bio-SNG at sawmill sites – techno-economic and carbon footprint evaluation. *Appl. Energy* 206, 1590–1608. doi: 10.1016/j.apenergy.2017.09.104

Air Resources Board (2017). *Co-processing of Biogenic Feedstocks in Petroleum Refineries*. Available online at: https://ww2.arb.ca.gov/sites/default/files/classic//fuels/lcfs/lcfs_meetings/020717_staffdiscussionpaper.pdf

Alamia, A., Larsson, A., Breitholtz, C., and Thunman, H. (2017). Performance of large-scale biomass gasifiers in a biorefinery, a state-of-the-art reference. *Int. J. Energy Res.* 41, 2001–2019. doi: 10.1002/er.3758

Ali, A. M. A., Mustafa, A., and Yassin, K. E. (2018). A techno-economic evaluation of bio-oil co- processing within a petroleum refinery. *Biofuels*. doi: 10.1080/17597269.2018.1519758

Al-Mansour, F., and Zuwala, J. (2010). An evaluation of biomass co-firing in Europe. *Biomass Bioenergy* 34, 620–629. doi: 10.1016/j.biombioe.2010.01.004

Arellano Garcia, H., Ketabchi, E., and Reina, T. (2017). "Integration of biorefinery concepts in oil refineries," in *Proceedings of the 27th European Symposium on Computer Aided Process Engineering – ESCAPE 27* (Barcelona).

Atashbar, N. Z., Labadie, N., and Prins, C. (2016). Modeling and optimization of biomass supply chains: a review and a critical look. *IFAC PapersOnLine* 49, 604–615. doi: 10.1016/j.ifacol.2016.07.742

Awudu, A., and Zhang, J. (2012). Uncertainties and sustainability concepts in biofuel supply chain management: a review. *Renew. Sustain. Energy Rev.* 16, 1359–1368. doi: 10.1016/j.rser.2011.10.016

Barthe, P., Chaugny, M., Roudier, S., and Sancho, L. D. (2015). *Best Available Techniques (BAT) Reference Document for the Refining of Mineral Oil and Gas.* Seville: European Commission.

Beims, R., Bertoli, S., Botton, V., Ender, L., Simionatto, E., Meier, et al. (2017). Co-processing of thermal cracking bio-oil at petroleum refineries. *Brazilian J. Petrol. Gas* 11, 99–113. doi: 10.5419/bjpg2017-0009

Berndes, G., Hansson, J., Egeskog, A., and Johnsson, F. (2010). Strategies for 2nd generation biofuels in EU – co-firing to stimulate feedstock supply development and process integration to improve energy efficiency and economic competitiveness. *Biomass Bioenergy* 34, 227–236. doi: 10.1016/j.biombioe.2009.07.007

Berndes, G., Hansson, J., Egeskog, A., and Werner, S. (2008). *Bioenergy Expansion Strategies for Europe. Cost Effective Biomass Allocation and Biofuel Steppingstones. REFUEL WP5 Final Report*. Available online at: https://ec.europa.eu/energy/intelligent/projects/sites/iee-projects/files/projects/documents/refuel_bieoenergy_expansion_strategy_for_europe.pdf

Bertrand, V., Dequiedt, B., and Le Cadre, E. (2014). Biomass for electricity in the EU-27: potential demand, CO_2 abatements and break even prices for co-firing. *Energy Policy* 73, 631–644. doi: 10.1016/j.enpol.2014.06.007

Bhatt, A. H., Zhang, Y., and Heath, G. (2020). Bio-oil co-processing can substantially contribute to renewable fuel production potential and meet air quality standards. *Appl. Energy* 268:114937. doi: 10.1016/j.apenergy.2020.114937

Biofuels Barometer (2017). Available online at: https://www.eurobserv-er.org/biofuels-barometer-2017

Brar, J. S., Singh, K., Wang, J., and Kumar, S. (2012). Cogasification of coal and biomass: a review. *Int. J. Forest. Res.* 2012:363058. doi: 10.1155/2012/363058

Brau, J. F., Morandin, M., and Berntsson, T. (2013). Hydrogen for oil refining via biomass indirect steam gasification: energy and environmental targets. *Clean Technol. Environ. Policy* 15, 501–512. doi: 10.1007/s10098-013-0591-9

Bunting, B., Bunce, M., Barone, T., and Storey, J. (2010). *Fungible and Compatible Biofuels: Literature Search, Summary, and Recommendations.* Oak Ridge, TN: Oak Ridge National Laboratory, Fuels, Engines, and Emissions Research Center. Available online at: https://www.energy.gov/sites/prod/files/2014/03/f14/20110512135206-0.pdf

Canabarro, N., Soares, J. F., Anchieta, C. G., Kelling, C. S., and Mazutti, M. A. (2013). Thermochemical processes for biofuels production from biomass. *Sustain. Chem. Proc*. 1:22. doi: 10.1186/2043-7129-1-22

CEPI (2020). *Key Statistics 2019 European Pulp and Paper Industry*. Available online at: https://www.cepi.org/wp-content/uploads/2020/07/Final-Key-Statistics-2019.pdf

Cintas, O., Berndes, G., Englund, O., Cutz, L., and Johnsson, F. (2018). Geospatial supply–demand modeling of biomass residues for co- firing in European coal power plants. *Bioenergy* 10, 786–803. doi: 10.1111/gcbb.12532

Concawe Report (2020). *Concawe Review 29.* Available online at: https://www.concawe.eu/wp-content/uploads/Concawe-Review-29-1-web-resolution-PDF.pdf

Cutz, L., Berndes, G., and Johnsson, F. (2019). A techno-economic assessment of biomass co-firing in Czech Republic, France, Germany and Poland. *Biofuels Bioprod. Biorefin.* 13, 1289–1305. doi: 10.1002/bbb.2034

de Jong, E., and Jungmeier, G. (2015). "Chapter 1: Biorefinery concepts in comparison to petrochemical refineries in industrial biorefineries and white biotechnology," in *Industrial Biorefineries and White Biotechnology*, eds A. Pandey, R. Höfer, C. Larroche, M. Taherzadeh, and M. Nampoothiri (Amsterdam; Oxford: Elsevier), 3–33. doi: 10.1016/B978-0-444-63453-5.00001-X

Dias, M. O. S., Junqueira, T. L., Jesus, C. D. F., Rossell, C. E. V., Maciel Filho, R., and Bonomi, A. (2012). Improving second generation ethanol production through optimization of first generation production process from sugarcane. *Energy* 43, 246–252. doi: 10.1016/j.energy.2012.04.034

Dimitriou, I., Goldingay, H., and Bridgwater, A. (2018). Techno-economic and uncertainty analysis of biomass to liquid (BTL) systems for transport fuel production. *Renew. Sustain. Energy Rev.* 88, 160–175. doi: 10.1016/j.rser.2018.02.023

Directorate-General for Mobility and Transport (2018). *Building Up the Future, Cost of Biofuel*. Luxembourg: EU Publications.

DOE/EERE (2013). *Replacing the Whole Barrel: To Reduce U.S. Dependence on Oil*. U.S. Department of Energy, Office of Energy Efficiency & Renewable Energy. Available online at: https://www1.eere.energy.gov/bioenergy/pdfs/replacing_barrel_overview.pdf

Doliente, S., and Samsatli, S. (2020). Integrated production of fuels, energy and chemicals from *Jatropha Curcas*: multiobjective optimisation of sustainable value chains. *Chem. Eng. Trans.* 80, 343–348. doi: 10.3303/CET2080058

Doug, B. (2006). *European Market Study for Bio Oil (Pyrolysis Oil).* Ottawa, ON: Climate Change Solutions National Team Leader- IEA Bioenergy Task 40- Bio-trade. Available online at: http://www.unecefaoiufro.lsu.edu/biofuels/documents/2007July/SRN_009.pdf

Elia, J. A., Baliban, R. C., Xiao, X., and Floudas, C. A. (2011). Optimal energy supply network determination and life cycle analysis for hybrid coal, biomass, and natural gas to liquid (CBGTL) plants using carbon-based hydrogen production. *Comput. Chem. Eng.* 35, 1399–1430. doi: 10.1016/j.compchemeng.2011.01.019

ETIP Bioenergy (2020). ETIP Bioenergy Working Group 2 – Conversion Processes and ETIP-B-SABS2 Project Team (2020) *Current Status of Advanced Biofuels Demonstrations in Europe*. Available online at: https://www.etipbioenergy.eu/images/ETIP-B-SABS2_WG2_Current_Status_of_Adv_Biofuels_Demonstrations_in_Europe_Mar2020_final.pdf

EUROFER (2020). *European Steel in Figures 2020*. Available online at: https://www.eurofer.eu/publications/brochures-booklets-and-factsheets/european-steel-in-figures-2020/

European Commission (2016a). *COM, An EU Strategy on Heating and Cooling*. https://ec.europa.eu/energy/sites/ener/files/documents/1_EN_ACT_part1_v14.pdf

European Commission (2016b). *Mapping and Analyses of the Current and Future (2020–2030) heat-ing/cooling fuel deployment (fossil/renewables),* Final Report. Available online at: https://ec.europa.eu/energy/studies/mapping-and-analyses-current-and-future-2020-2030-heatingcooling-fuel-deployment_en

European Commission (2016c). *Sectoral Fitness Check for the Petroleum Refining Sector.* Commission Staff Working Document, Brussels. Available online at: https://ec.europa.eu/energy/sites/ener/files/documents/SWD_2015_284_F2_STAFF_WORKING_PAPER_EN_V4_P1_835479.pdf

European Commission (2018). *In-Depth Analysis in Support of the COM(2018): A Clean Planet for all - A European Strategic Long-Term Vision for a Prosperous, Modern, Competitive and Climate Neutral Economy*. Available online at: https://knowledge4policy.ec.europa.eu/publication/depth-analysis-support-com2018-773-clean-planet-all-european-strategic-long-term-vision_en

Fogassy, G., Thegarid, N., Toussaint, G., van Veen, A. C., Schuurman, Y., and Mirodatos, C. (2010). Biomass derived feedstock co-processing with vacuum gas oil for second-generation fuel production in FCC units. *Appl. Catal. B Environ.* 96, 476–485. doi: 10.1016/j.apcatb.2010.03.008

Freeman, C. J., Jones, S. B., Padmaperuma, A. B., Santosa, M., Valkenburg, C., and Shinn, J. (2013). *Initial Assessment of US Refineries for Purposes of Potential Bio-Based Oil Insertions*. U.S. Department of Energy. Available online at: https://www.pnnl.gov/main/publications/external/technical_reports/PNNL-22432.pdf

Fuels Europe (2018). *Vision 2050: A Pathway for the Evolution of the Refining Industry and Liquid Fuels*. Available online at: https://www.fuelseurope.eu/wp-content/uploads/DEF_2018_V2050_Narratives_EN_digital.pdf

Gollakota, A. R., Reddy, M., Subramanyam, M. D., and Kishore, N. (2016). A review on the upgradation techniques of pyrolysis oil. *Renew. Sustain. Energy Rev.* 58, 1543–1568. doi: 10.1016/j.rser.2015.12.180

Gudde, N., Larivé, J., and Yugo, M. (2019). *Refinery 2050: Conceptual Assessment*. Brussels, Concawe: Concawe Special Task Force Refinery 2050.

Hannula, I., and Kurkela, E. (2013). *Liquid Transportation Fuels via Large-Scale Fluidised-Bed Gasification of Lignocellulosic Biomass*. VTT Technical Research Center of Finland. Available online at: https://www.vtt.fi/inf/pdf/technology/2013/T91.pdf

Hansson, J., Berndes, G., Johnsson, F., and KJärsrtad, J. (2009). Co-firing biomass with coal for electricity generation – an assessment of the potential in EU27. *Energy Policy* 37, 1444–1455. doi: 10.1016/j.enpol.2008.12.007

Hileman, J. I., Ortiz, D. S., Bartis, J. T., Wong, H. M., Donohoo, P. E., Weiss, M. A., et al. (2009). *Near-Term Feasibility of Alternative Jet fuels*. Technical report, RAND Infrastructure, Safety and Environment. Available online at: https://www.rand.org/pubs/technical_reports/TR554.html

Hu, J., and Lu, Y. (2012). Application of Fischer–Tropsch synthesis in biomass to liquid conversion. *Catalysts* 2, 303–326. doi: 10.3390/catal2020303

IEA Bioenergy Report (2020). *Advanced Biofuels – Potential for Cost Reduction.* Available online at: https://www.ieabioenergy.com/blog/publications/new-publication-advanced-biofuels-potential-for-cost-reduction/

IEA-ETSAP and IRENA Technology Brief E21 (2013). *Biomass Co-firing Technology Brief*. Available online at: https://irena.org/-/media/Files/IRENA/Agency/Publication/2013/IRENA-ETSAP-Tech-Brief-E21-Biomass-Co-firing.pdf

IEA-RETD (2016). *Towards Advanced Biofuels – Options for Integrating Conventional and Advanced Biofuel Production Sites (RES-T-BIOPLANT).*

Available online at: http://iea-retd.org/wp-content/uploads/2016/08/20160202-IEA-RETD-RES-T-BIOPLANT-1.pdf

IRENA (2016). *Innovation Outlook – Advanced Liquid Bioguels*. Available online at: https://www.irena.org/-/media/Files/IRENA/Agency/Publication/2016/IRENA_Innovation_Outlook_Advanced_Liquid_Biofuels_2016.pdf

Isaksson, J., Pettersson, K., Mahmoudkhani, M., Asblad, A., and Berntsson, T. (2012). Integration of biomass gasification with a Scandinavian mechanical pulp and paper mill – consequences for mass and energy balances and global CO_2 emissions. *Energy* 44, 420–428. doi: 10.1016/j.energy.2012.06.013

Jafri, Y., Wetterlund, E., Mesfun, S., Rådberg, H., Mossberg, J., Hulteberg, C., et al. (2020). Combining expansion in pulp capacity with production of sustainable biofuels – techno-economic and greenhouse gas emissions assessment of drop-in fuels from black liquor part-streams. *Appl. Energy* 279:115879. doi: 10.1016/j.apenergy.2020.115879

Joelsson, E., Galbe, M., and Wallberg, O. (2014). Heat integration pf combined 1st and 2nd generation ethanol production from wheat kernels and wheat straw. *Sustain. Chem. Process.* 2:20. doi: 10.1186/s40508-014-0020-3

Johansson, D., Berntsson, T., and Franck, P.-Å. (2014). Integration of Fischer-Tropsch fuel production with a complex oil refinery. *Int. J. Environ. Sustain. Dev.* 13, 50–73. doi: 10.1504/IJESD.2014.056413

Johansson, D., Franck, P.-Å., and Berntsson, T. (2012). Hydrogen production from biomass gasification in the oil refining industry – a system analysis. *Energy* 38, 212–227. doi: 10.1016/j.energy.2011.12.011

Johansson, M. T. (2013). Bio-synthetic natural gas as fuel in steel industry reheating furnaces – a case study of economic performance and effects on global CO_2 emissions. *Energy* 57, 699–708. doi: 10.1016/j.energy.2013.06.010

Jones, S., Valkenburg, C., Walton, C., Elliott, D., Holladay, J., Stevens, D., et al. (2009). *Production of Gasoline and Diesel from Biomass via Fast Pyrolysis, Hydrotreating and Hydrocracking: A Design Case.* Washington, DC: Pacific Northwest National Laboratory. doi: 10.2172/950728

Kamble, A. D., Saxena, V. K., Chavan, P. K., and Mendhe, V. A. (2019). Co-gasification of coal and biomass an emerging clean technology: status and prospects of development in Indian context. *In. J. Min. Sci. Technol.* 2, 171–186. doi: 10.1016/j.ijmst.2018.03.011

Karatzos, S., McMillan, J. D., and Saddler, J. N. (2014). *The Potential and Challenges of Drop-in Biofuels.* A Report by IEA Bioenergy Task 39. Available online at: http://task39.sites.olt.ubc.ca/files/2014/01/Task-39-Drop-in-Biofuels-Report-FINAL-2-Oct-2014-ecopy.pdf

Karka, P., Papadokonstantakis, S., and Kokossis, A. (2017). Cradle-to-gate assessment of environmental impacts for a broad set of biomass-to-product process chains. *Int. J. Life Cycle Assess.* 22, 1418–1440. doi: 10.1007/s11367-017-1262-6

Kumar, A., Adamopoulos, S., Jones, D., and Amiandamhen, S. O. (2021). Forest biomass availability and utilization potential in Sweden: a review. *Waste Biomass Valor.* 12, 65–80. doi: 10.1007/s12649-020-00947-0

Lainez-Aguirre, J. M., Pérez-Fortes, M., and Puigjaner, L. (2015). Strategic planning of biomass supply chain networks for co-combustion plants. *Comput. Aid. Chem. Eng.* 36, 453–474 doi: 10.1016/B978-0-444-63472-6.00018-5

Landälv, I., Maniatis, K., Waldheim, L., van den Heuvel, E., and Kalligeros, S. (2017a). *Building up the Future – Cost of Biofuel*. European Commission. Sub-Group on Advanced Biofuels. Sustainable Transport Forum.

Landälv, I., Maniatis, K., Waldheim, L., van den Heuvel, E., and Kalligeros, S. (2017b). *Building up the Future – Technology Status and Reliability of the Value Chain*. European Commission. Sub-Group on Advanced Biofuels. Sustainable Transport Forum.

Lee, J. W. (2013). *Advanced Biofuels and Bioproducts*. New York, NY: Springer. doi: 10.1007/978-1-4614-3348-4

Lehto, J., Oasmaa, A., Solantausta, Y., Kytö, M., and Chiaramonti, C. (2013). *Fuel Oil Quality and Combustion of Fast Pyrolysis Bio-Oils.* VTT Technical Research Centre of Finland. Available online at: https://www.vttresearch.com/sites/default/files/pdf/technology/2013/T87.pdf

Lennartsson, P. R., Erlandsson, P., and Taherzadeh, M. J. (2014). Integration of the first and second generation bioethanol processes and the importance of by-products. *Bioresour. Technol.* 165, 3–8. doi: 10.1016/j.biortech.2014.01.127

Ljungstedt, H., Johansson, D., Johansson, M. T., and Karltorp, K. (2011). "Options for increased use and refining of biomass – the case of energy-intensive industry in Sweden," in *Proceedings of World Renewable Energy Congress* (Linköping). doi: 10.3384/ecp1105717

Lundgren, J., Ekbom, T., Hulteberg, C., Larsson, M., Grip, C. E., Nilsson, L., et al. (2013). Methanol production from steel-work off-gases and biomass based synthesis gas. *Appl. Energy* 112, 431–439. doi: 10.1016/j.apenergy.2013.03.010

Luque, R., de la Osa, A., Campelo, J., Romero, A., Valverde, J., and Sanchez, P. (2012). Design and development of catalysts for biomass-to-liquid Fischer–Tropsch (BTL-FT) processes for biofuels production. *Energy Environ. Sci.* 5, 5186–5202. doi: 10.1039/C1EE02238E

Mandova, H., Gale, W. F., Williams, A., Heyes, A. L., Hodgson, P., and Miah, K. H. (2018). Global assessment of biomass suitability for ironmaking – opportunities for co-location of sustainable biomass, iron and steel production and supportive policies. *Sustain. Energy Technol. Assess.* 27, 23–39. doi: 10.1016/j.seta.2018.03.001

Mathiesen, B. V., Bertelsen, N., Schneider, N. C. A., García, L. S., Paardekooper, S., Thellufsen, J. Z., et al. (2019). *Towards a Decarbonised Heating and Cooling Sector in Europe: Unlocking the Potential of Energy Efficiency and District Energy*. Aalborg Universitet. Available online at: https://vbn.aau.dk/ws/portalfiles/portal/316535596/Towards_a_decarbonised_H_C_sector_in_EU_Final_Report.pdf

Melero, J., Iglesias, J., and Garcia, A. (2012). Biomass as renewable feedstock in standard refinery units. Feasibility, opportunities and challenges. *Energy Environ. Sci.* 5, 7393–7420. doi: 10.1039/c2ee21231e

Mongkhonsiri, G., Gani, R., Malakul, P., and Assabumrungrata, S. (2018). Integration of the biorefinery concept for the development of sustainable processes for pulp and paper industry. *Comput. Chem. Eng.* 119, 70–84. doi: 10.1016/j.compchemeng.2018.07.019

Mousa, E., Wang, C., Riesbeck, J., and Mikael Larsson, M. (2016). Biomass applications in iron and steel industry: an overview of challenges and opportunities. *Renew. Sustain. Energy Rev.* 65, 1247–1266. doi: 10.1016/j.rser.2016.07.061

Nanda, S., Mohammad, J., Reddy, S. N., Kozinski, J. A., and Dalai, A. K. (2014). Pathways of lignocellulosic biomass conversion to renewable fuels. *Biomass Convers. Biorefin.* 4, 157–191. doi: 10.1007/s13399-013-0097-z

Neste (2020). *Neste Renewable Diesel Handbook*. Espoo: Neste. Available online at: https://www.neste.com/sites/default/files/attachments/neste_renewable_diesel_handbook.pdf

Nivard, M., and Kreijkes, M. (2017). *The European Refining Sector: A Diversity of Markets?* Clingendael International Energy Programme (CIEP). Available online at: https://www.clingendaelenergy.com/inc/upload/files/CIEP_paper_2017-02_web.pdf

O'Neill, E. G., and Maravelias, C. T. (2021). Towards integrated landscape design and biofuel supply chain optimization. *Curr. Opin. Chem. Eng.* 31:1006. doi: 10.1016/j.coche.2020.100666

Panoutsou, C., Germer, S., Karka, P., Papadokonstantakis, S., Kroyan, Y., Wojcieszyk, M., et al. (2021). Advanced biofuels to decarbonise european transport by 2030: markets, challenges, and policies that impact their successful market uptake. *Energy Strategy Reviews*. 34:100633.

Parker, N., Tittmann, P., Hart, Q., Nelson, R., Skog, K., Schmidt, A., et al. (2010). Development of a biorefinery optimized biofuel supply curve for the Western United States. *Biomass Bioenergy* 11, 1597–1607. doi: 10.1016/j.biombioe.2010.06.007

Paulauskiene, T., Bucas, M., and Laukinaite, A. (2019). Alternative fuels for marine applications: biomethanol-biodiesel-diesel blends. *Fuel*, 248, 161–167. doi: 10.1016/j.fuel.2019.03.082

Pérez-Fortes, M., Laínez-Aguirre, J. M., Arranz-Piera, P., Velo, E., and Puigjaner, L. (2012). Design of regional and sustainable bio-based networks for electricity generation using a multi-objective MILP approach. *Energy* 44, 79–95. doi: 10.1016/j.energy.2012.01.033

Phillips, S., Aden, A., Jechura, J., and Dayton, D. (2007). *Thermochemical Ethanol via Indirect Gasification and Mixed Alcohol Synthesis of Lignocellulosic Biomass*. Technical Report NREL/TP-510-41168. Available online at: https://www.nrel.gov/docs/fy07osti/41168.pdf

Pinho, A. D., de Almeida, M. B., Mendes, F. L., Casavechia, L. C., Talmadge, M. S., Kinchin, C. M., et al. (2017). Fast pyrolysis oil from pinewood chips co-processing with vacuum gas oil in an FCC unit for second generation fuel production. *Fuel* 188, 462–473. doi: 10.1016/j.fuel.2016.10.032

Puigjaner, L., Pérez-Fortes, M., and Laínez-Aguirre, J. M. (2015). Towards a carbon-neutral energy sector: opportunities and challenges of coordinated bioenergy supply chains - A PSE approach. *Energies* 8, 5613–5660. doi: 10.3390/en8065613

Rentier, G., Lelieveldt, H., and Kramer, G. (2019). Varieties of coal-fired power phase-out across Europe. *Energy Policy* 132, 620–632. doi: 10.1016/j.enpol.2019.05.042

Roni, M., Chowdhury, S., Mamun, S., Marufuzzaman, M., Lein, W., and Johnson, S. (2017). Biomass co-firing technology with policies, challenges, and opportunities: a global review. *Renew. Sustain. Energy Rev.* 78, 1089–1101. doi: 10.1016/j.rser.2017.05.023

Sadhukhan, J., Ng, K., and Martinez-Hernandez, E. (2014). *Biorefineries and Chemical Processes: Design, Integration and Sustainability Analysis.* Chichester: Wiley. doi: 10.1002/9781118698129

Sandén, B., and Pettersson, K. (2013). *Systems Perspectives on Biorefineries.* Chalmers University of Technology. Available online at: http://www.chalmers.se/en/areas-of-advance/energy/Documents/Systems%20Perspectives%20on/Systems_Perspectives_on_Biorefineries_2014_v3.1b.pdf

Scarlat, N., Dallemand, J.-F., Skjelhaugen, O., Asplund, D., and Nesheim, L. (2011). An overview of the biomass resource potential of Norway for bioenergy use. *Renew. Sustain. Energy Rev.* 15, 3388–3398. doi: 10.1016/j.rser.2011.04.028

Schröder, J., Müller-Langer, F., Aakko-Saksa, P., Winther, K., Baumgarten, W., and Lindgren, M. (2020). "Methanol as motor fuel - summary report," in *Annex 56, A Report from the Advanced Motor Fuels Technology Collaboration Programme by IEA*. Available online at: https://www.iea-amf.org/app/webroot/files/file/Annex%20Reports/AMF_Annex_56.pdf

Shah, Y. T. (2013). "Chapter 12: Biomass to liquid fuel via Fischer–Tropsch and related syntheses," in *Advanced Biofuels and Bioproducts* (Norfolk, VA: Springer New York Heidelberg Dordrecht London), 185–208. doi: 10.1007/978-1-4614-3348-4_12

Sharma, K., Pedersen, T. H., Toor, S. S., Schuurman, Y., and Rosendahl, L. A. (2020). Detailed investigation of compatibility of hydrothermal liquefaction derived biocrude oil with fossil fuel for corefining to drop-in biofuels through structural and compositional analysis. *ACS Sustain. Chem. Eng.* 8, 8111–8123. doi: 10.1021/acssuschemeng.9b06253

Sikarwar, V. S., Zhao, M., Fennell, P. S., Shah, N., and Anthony, E. J. (2017). Progress in biofuel production from gasification. *Prog. Energy Combust. Sci.* 61, 189–248. doi: 10.1016/j.pecs.2017.04.001

Sims, R. E. H., Mabee, W., Saddler, J. N., and Taylor, M. (2010). An overview of second generation biofuel technologies. *Bioresour. Technol.* 101, 1570–1580. doi: 10.1016/j.biortech.2009.11.046

Singh, A., Christensen, T., and Panoutsou, C. (2021). Policy review for biomass value chains in the European bioeconomy. *Global Trans.* 3, 13–42. doi: 10.1016/j.glt.2020.11.003

Stefanidis, S. D., Kalogiannis, K. G., and Lappas, A. A. (2018). Co-processing bio-oil in the refinery for drop-in biofuels via fluid catalytic cracking. *WIREs Energy Environ.* 7:e281. doi: 10.1002/wene.281

Swanson, R. M., Satrio, J. A., Brown, R. C., Platon, A., and Hsu, D. D. (2010). *Techno-Economic Analysis of Biofuels Production Based on Gasification*. Technical report, NREL/TP-6A20-46587. Available online at: https://www.nrel.gov/docs/fy11osti/46587.pdf

Thunman, H., Gustavsson, C., Larsson, A., Gunnarsson, I., and Tengberg, F. (2019). Economic assessment of advanced biofuel production via gasification using cost data from the GoBiGas plant. *Energy Sci. Eng.* 7, 217–229. doi: 10.1002/ese3.271

Thunman, H., Seemann, M., Berdugo Vilches, T., Maric, J., Pallares, D., Str?m, H., et al. (2018). Advanced biofuel production via gasification – lessons learned from 200 man-years of research activity with Chalmers' research gasifier and the GoBiGas demonstration plant. *Energy Sci. Eng.* 6, 6–34. doi: 10.1002/ese3.188

Tong, K., Gleeson, M. J., Rong, G., and You, F. (2013a). Optimal design ofadvanced 'drop-in' hydrocarbon biofuel supply chain integrating with existing petroleum refineries under uncertainty. *Biomass Bioenergy* 60, 108–120. doi: 10.1016/j.biombioe.2013.10.023

Tong, K., Gong, J., Yue, D., and You, F. (2013b). Stochastic programming approach to optimal design and operations of integrated hydrocarbon biofuel and petroleum supply chains. *ACS Sustain. Chem. Eng.* 2, 49–61. doi: 10.1021/sc400267t

Tunå, P., Hulteberg, C., Hansson, J., Åsblad, A., and Andersson, E. (2012). Synergies from combined pulp and paper and fuel production. *Biomass Bioenergy* 40, 174–180. doi: 10.1016/j.biombioe.2012.02.020

United Nations Climate Change (2016). *The Paris Agreement*. Available online at: https://unfccc.int/process-and-meetings/the-paris-agreement/the-paris-agreement

van Dyk, S., Su, J., McMillan, J., and Saddler, J. (2019). Potential synergies of drop-in biofuel production with further co-processing at oil refineries. *Biofuels Bioprod. Biorefin.* 13, 760–775. doi: 10.1002/bbb.1974

Villanueva Perales, A. L., Reyes Valle, C., and Gomez-Barea, A. (2011). Technoeconomic assessment of ethanol production via thermochemical conversion of biomass by entrained flow gasification. *Energy* 36, 4097–4108. doi: 10.1016/j.energy.2011.04.037

Werner, S. (2017). International review of district heating and cooling. *Energy* 137, 617–631. doi: 10.1016/j.energy.2017.04.045

Xing, T., Alvarez-Majmutov, A., Gieleciak, R., and Chen J. (2019). Co-hydroprocessing HTL biocrude from waste biomass with bitumen-derived vacuum gas oil. *Energy Fuels* 33, 11135–11144. doi: 10.1021/acs.energyfuels.9b02711

Xu, Y., Yang, K., Zhou, J., and Zhao, G. (2020). Coal-biomass co-firing power generation technology: current status, challenges, and policy implications. *Sustainability* 12:3692. doi: 10.3390/su12093692

Yang, Z., Kumar, A., and Huhnke, R. L. (2015). Review of recent developments to improve storage and transportation stability of bio-oil. *Renew. Sustain. Energy Rev.* 50, 859–870. doi: 10.1016/j.rser.2015.05.025

Yilmaz Balaman, S., and Selim, H. (2014). A fuzzy multiobjective linear programming model for design and management of anaerobic digestion based bioenergy supply chains. *Energy* 74, 928–940. doi: 10.1016/j.energy.2014.07.073

You, F., Tao, L., Graziano, D. J., and Snyder, S. W. (2012). Optimal design of sustainable cellulosic biofuel supply chains: multiobjective optimization coupled with life cycle assessment and input-output analysis. *AIChE J.* 58, 1157–1179. doi: 10.1002/aic.12637

Yue, D., You, F., and Snyder, S. W. (2014). Biomass-to-bioenergy and biofuel supply chain optimization: overview, key issues and challenges. *Comput. Chem. Eng.* 66, 36–56. doi: 10.1016/j.compchemeng.2013.11.016

Zetterholm, J., Ahlstrom, J., and Bryngemark, E. (2020). Large-scale introduction of forest-based biorefineries: Actor perspectives and the impacts of a dynamic biomass market. *Biomass Bioenergy*. 142:105782. doi: 10.1016/j.biombioe.2020.105782

Conflict of Interest: The authors declare that the research was conducted in the absence of any commercial or financial relationships that could be construed as a potential conflict of interest.

frontiers
in Energy Research

ORIGINAL RESEARCH
published: 19 May 2021
doi: 10.3389/fenrg.2021.642162

Deriving Economic Potential and GHG Emissions of Steel Mill Gas for Chemical Industry

Jason Collis[1], Till Strunge[2,3], Bernhard Steubing[4], Arno Zimmermann[1] and Reinhard Schomäcker[1]*

[1] Technische Chemie, Institute of Chemistry, Technische Universität Berlin, Berlin, Germany, [2] Research Centre for Carbon Solutions, School of Engineering and Physical Sciences, Heriot-Watt University, Edinburgh, United Kingdom, [3] Institute for Advanced Sustainability Studies e.V., Potsdam, Germany, [4] Institute of Environmental Sciences (CML), Leiden University, Leiden, Netherlands

OPEN ACCESS

Edited by:
Mar Pérez-Fortes,
Delft University of Technology,
Netherlands

Reviewed by:
Michael Martin,
IVL – Swedish Environmental
Research Institute, Sweden
Bin Xu,
Clemson University, United States
Gengyuan Liu,
Beijing Normal University, China

***Correspondence:**
Reinhard Schomäcker
schomaecker@tu-berlin.de

Specialty section:
This article was submitted to
Process and Energy Systems
Engineering,
a section of the journal
Frontiers in Energy Research

Received: *15 December 2020*
Accepted: *13 April 2021*
Published: *19 May 2021*

Citation:
Collis J, Strunge T, Steubing B, Zimmermann A and Schomäcker R (2021) Deriving Economic Potential and GHG Emissions of Steel Mill Gas for Chemical Industry. Front. Energy Res. 9:642162. doi: 10.3389/fenrg.2021.642162

To combat global warming, industry needs to find ways to reduce its carbon footprint. One way this can be done is by re-use of industrial flue gases to produce value-added chemicals. Prime example feedstocks for the chemical industry are the three flue gases produced during conventional steel production: blast furnace gas (BFG), basic oxygen furnace gas (BOFG), and coke oven gas (COG), due to their relatively high CO, CO_2, or H_2 content, allowing the production of carbon-based chemicals such as methanol or polymers. It is essential to know for decision-makers if using steel mill gas as a feedstock is more economically favorable and offers a lower global warming impact than benchmark CO and H_2. Also, crucial information is which of the three steel mill gases is the most favorable and under what conditions. This study presents a method for the estimation of the economic value and global warming impact of steel mill gases, depending on the amount of steel mill gas being utilized by the steel production plant for different purposes at a given time and the economic cost and greenhouse gas (GHG) emissions required to replace these usages. Furthermore, this paper investigates storage solutions for steel mill gas. Replacement cost per ton of CO is found to be less than the benchmark for both BFG (50–70 €/ton) and BOFG (100–130 €/ton), and replacement cost per ton of H_2 (1800–2100 €/ton) is slightly less than the benchmark for COG. Of the three kinds of steel mill gas, blast furnace gas is found to be the most economically favorable while also requiring the least emissions to replace per ton of CO and CO_2. The GHG emissions replacement required to use BFG (0.43–0.55 tons-CO_2-eq./ton CO) is less than for conventional processes to produce CO and CO_2, and therefore BFG, in particular, is a potentially desirable chemical feedstock. The method used by this model could also easily be used to determine the value of flue gases from other industrial plants.

Keywords: steel, flue gas, life cycle assesment, techno-economic assessment, CCU, CO_2 utilization

---

Abbreviations: BFG, blast furnace gas; BOFG, basic oxygen furnace gas; COG, coke oven gas; CHP, combined heat and power plant; GHG, greenhouse gas; LCA, life cycle assessment; TEA, techno-economic assessment.

INTRODUCTION

Greenhouse gas (GHG) emissions such as CO_2 from industry continue to rise worldwide despite efforts to decrease emissions, such as stated in the 2015 Paris agreement, which aims to limit global warming to 2°C and make efforts to limit it to 1.5°C (Jarraud and Steiner, 2014; IEA, 2017; Rogelj et al., 2018). The steel industry is one of the major emitters of CO_2, with the sector being responsible for around 6% of total CO_2 emissions globally, making it also the largest industrial emitter. Additionally, the industry grew by 6.9% annually between 2000 and 2014 (He and Wang, 2017; World Steel Association, 2020) and is expected to reach 2200 Mt of crude steel production in 2050 (Bellevrat and Menanteau, 2009), primarily due to demand in developing countries for infrastructure. Therefore, the industry's emissions are predicted to increase naturally in the mid-term future. Consequently, to meet the Paris agreement's emissions requirements, the emissions of steel production must be significantly lowered or completely stopped.

There are many possible process routes for decarbonizing the steel industry (He and Wang, 2017), [(Hasanbeigi et al., 2014), both in the iron-making and steelmaking parts of the process. However, these are yet to see actual implementation and often end up stuck in the development stage. Most of these pathways are not economically feasible without implementing a carbon tax or other subsidy (Fischedick et al., 2014). Investment cycles in the industry are comparably long due to a combination of factors such as the age and conservative nature of the industry, the fact that the steelmaking process has not changed significantly in a long time, and the vast investment costs required to build a steel plant, as well as the lifetime of the plant (Arens et al., 2017). Unfortunately, this makes it challenging to implement process changes that reduce emissions within the Paris agreement's time scales. Therefore, to meet the goal of sufficient GHG reductions in the steel industry in the short to mid-term future, the CO_2 emissions from steel mills must be captured and either sequestrated or utilized (Gabrielli et al., 2020).

One method of reducing emissions is utilizing emitted steel mill gas for chemical products, requiring industrial symbiosis between the steel and chemical industry (Zimmermann and Kant, 2017). While the chemical industry's emissions are smaller than those of the steel industry, it is regardless a large emitter being directly responsible for around 2% of global GHG emissions (Leimkühler, 2010). Similar to the steel industry, the chemical industry is thus under political pressure to cut emissions. As most chemical feedstocks consume hydrocarbons, producing chemicals from industrial waste gases instead of fossil fuels could be a viable way to decrease total CO_2 emissions; this is because CO_2 from flue gas, which otherwise would have been emitted, ends up in a chemical product instead (Abanades et al., 2017; Rogelj et al., 2018; Gabrielli et al., 2020). Although this CO_2 will be released into the atmosphere at the end of life of the chemical, flue gas utilization can reduce the chemical's overall emissions as it reuses carbon and thereby reduces the consumption of additional fossil carbon (Artz et al., 2018). Flue gas utilization (in particular CO_2) is a growing field, and many chemical producers have been investigating industrial waste gases as an alternative feedstock (Bruhn et al., 2016; SAPEA, 2018). In steel mill gas, CO or H_2 are more likely to be the most desirable components for most chemical producers than CO_2. However, the utilization of these also saves CO_2 emissions, as the CO would be combusted to CO_2 and released into the atmosphere if unused, and conventional methods of H_2 production produce relatively high CO_2 emissions (Dufour et al., 2011).

One instance is the Carbon4PUR project, which aims to use the CO and CO_2 in steel mill gas as a feedstock to produce polyurethanes (Carbon4PUR, 2020a). In this process, steel mill gases are used without separation or purification of the desirable components. Although the feedstock is less pure, expensive separation is avoided. An important question for both the chemical and steel producers in Carbon4PUR and similar projects is how much these steel mill gases are worth. Chemical producers must know how much their potential feedstock costs for economic planning purposes; likewise, steel producers need to ensure they receive adequate compensation for the waste gas in order to avoid a loss. Although some papers have assessed the usage of steel mill gas for chemical processes and its calorific value (Joseck et al., 2008; Chen et al., 2011; Lundgren et al., 2013; Uribe-Soto et al., 2017; Frey et al., 2018), literature has not yet evaluated in detail the economic and environmental impact, and most research on processes using steel mill gases as a feedstock either do not account for any direct purchase cost (Ou et al., 2013) or just assume a static standard cost that may not accurately represent the value that steel mill gas provides to the steel mill (Lundgren et al., 2013; Yildirim et al., 2018).

Therefore, developing a framework or model to estimate the value of the waste gas is crucial information for both industries. Ideally, the framework should be replicable and easily alterable for all steel plants and chemical producers, and potentially other sectors both producing and looking to utilize waste gases as well. It should thus be based on parameters that are as generic as possible, for example usage of the waste gases in the steel mill, production capacity of the chemical company, and composition of the waste gas, all of which affect the value of the gas. Essentially, the economic value of the waste gas depends upon what the steel mill uses it for and the financial benefit the plant gains from this usage. Determination of this benefit is key to estimating the cost of the waste gas for other parties and therefore also its synergetic potential. As well as the economic benefit, environmental benefit in terms of greenhouse gas (GHG) emissions avoided is also essential information, as the usual motivation behind flue gas utilization processes is a reduction of emissions. Decision-makers could also base decisions on how much GHG emissions they want to avoid or a combined economic and environmental indicator such as the "cost of CO_2 avoided" (Zimmermann et al., 2020a). For such processes, integrated economic and environmental reporting is necessary for decision-makers to make a fully informed judgment (Zimmermann and Schomäcker, 2017; Wunderlich et al., 2020). In addition to simply knowing the cost of the steel mill gases, in order for it to be properly competitive, it must be economically and/or environmentally favorable when compared to conventional feedstocks.

BACKGROUND

Steelmaking Process

Steel is predominantly produced using an integrated steel mill, which combines iron production in a blast furnace (BF) and steel production in a basic oxygen furnace (BOF), and is responsible for 74.3% of worldwide steel production (Uribe-Soto et al., 2017). The second most commonly used process route is the electric arc furnace, and in the future other steel-making routes such as direct reduction based on H_2 are expected to be extensively adopted (Mazumdar and Evans, 2009; PwC, 2016; Arens et al., 2017). The European Steel Association classifies technological pathways for CO_2 emissions reduction into two main groups: Smart Carbon Usage, which includes CO_2 and CO utilization and storage with little change to the actual steel-making process, and Carbon Direct Avoidance, which are major changes to the process route, such as the use of H_2, biomass, or electricity as the reduction agent for iron ore, instead of CO from coal as is used presently in the integrated steel mill (Wei et al., 2013; EUROFER, 2019). Forecasts suggest that while new carbon-avoiding process routes will eventually make up a significant fraction of European steel production, it is likely that more than 50% of steel being produced in 2050 will still be produced by the integrated BF-BOF route, largely due to the long investment cycles and lifetime of steel mills, and that flue gas utilization and storage will be required in 2050 (Arens et al., 2017; EUROFER, 2019). Therefore, this work focuses primarily on the integrated steel mill route.

Firstly, coke is produced from heating coal in an oxygen-deprived coke oven. Iron ores, which are iron oxides, are fed into the BF as pellets, lump ores, or sinter. There they are reduced to pig iron with a carbon content of about 4.5% using reducing agents such as CO from the oxidization of coke in hot air. Limestone is also introduced to the BF to reduce impurities like silicon or phosphorus. The pig iron is then turned to steel in the BOF. Oxygen is used to lower the carbon content in the steel to around 0.1%, as well as to remove further impurities such as nickel and chromium (Ho et al., 2013). The integrated steel mill process is shown in **Figure 1**, along with the three different steel mill gases produced – coke oven gas (COG), blast furnace gas (BFG), and basic oxygen furnace gas (BOFG); the compositions and relative amounts of these gases are shown in **Table 1**. BFG is by far the largest stream, with a share of around 85 vol% of the produced gas. However, COG and BOFG are also potentially useful gases as a chemical feedstock due to the comparably high H_2 and carbon content, respectively (Joseck et al., 2008).

Current Usages for Steel Mill Gases

As steel mill gases are only partially combusted, they provide energy for different usages in the plant. These can be clustered as follows, two of which provide useful energy and one for emergencies:

Electricity Generation

The steel mill gases are used to generate electricity or steam while being co-fired with natural gas or coal in a power plant. The electricity can be used on-site or sold to the electricity grid.

Heat Generation

The steel mill gases are burned in burners on-site for heat generation within the plant.

Flaring

In some emergency situations, such as a build-up in gas pressure or failure of equipment, the gas must be flared (Damodara, 2018). The flared gas is not useful in any way to the steel producer.

Most steel mill gases (73.3% when averaged across all three gases) are used for the generation of electricity, with the bulk of the rest being used for heating, although this differs from plant to plant. Often, the usage of the gases can be switched on short notice, particularly if they are being combusted in a combined heat and power plant (CHP). The amount of gas flared varies

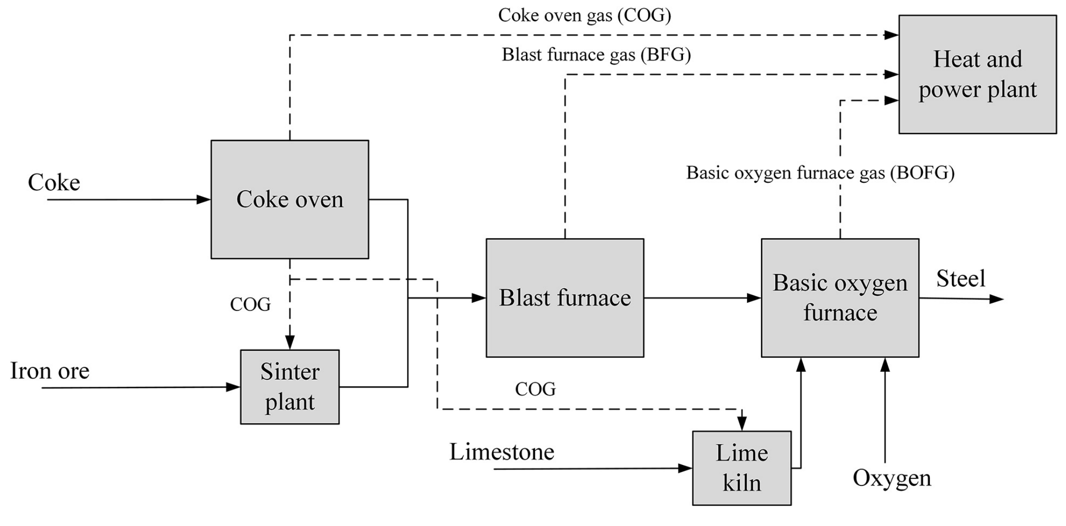

FIGURE 1 | Diagram of an integrated steel mill, showing the main unit operations and where the three steel mill gases are produced. Adapted from Wiley et al. (2011).

TABLE 1 | Compositions and other key values for each steel mill gas for a modern steel mill producing 6 Mt of steel per year (**Uribe-Soto et al., 2017**).

Mole composition	BFG	BOFG	COG	Mix of all 3
CO	23.5	54	4.1	23.9
CO_2	21.6	20	1.2	20.5
H_2	3.7	3.2	60.7	6.5
CH_4	0	0	22.0	1.1
C_xH_y	0	0	2	0.1
N_2	46.6	18.1	5.9	43.3
H_2O	4.0	4	4	4
Ar + O_2	0.6	0.7	0.2	0.6
Flow rate (Nm^3/h)	730,000	35,000	40,000	805,000
LHV (kJ/Nm^3)	3,365	7,163	15,660	4,141
Thermal power (MW)	682	70	174	926

from around 0.1 vol% to 22 vol% (U.S. Department of Energy [DOE], 2010; Lundgren et al., 2013), with the average European steel plant flaring 2 vol% of their gas. Flare rates above 5 vol% typically only occur in modern plants where there is a failure or maintenance on one of the pipelines or power plant components. All three types of steel mill gas can be used for any of these purposes using a gas management system (U.S. Department of Energy [DOE], 2010; Lundgren et al., 2013; Sadlowski and Van Beek, 2020), although BFG is usually only used for heating in particular uses such as the coke plant or in combination with another fuel due to its lower flame temperature (Hou et al., 2011). The usage of the gas for either heating or electricity generation by the steel mill depends on factors unique to each steel mill, such as the presence of cold rolling or coating lines or the location of the coke oven within the plant (Carbon4PUR, 2020b).

Chemical Uses for Steel Mill Gases

The chemical industry currently depends significantly on fossil fuels for chemical production, leading to high carbon footprints (and fossil depletion) of chemical products. Due to the relatively high CO, CO_2, and H_2 content in steel mill gases, they are a potentially attractive alternative as a feedstock for the chemical industry. Desired molecules could be captured, or products could be produced directly from the gas, leading to an extensive range of possible chemical products (Stießel et al., 2018). Although there have been many studies on producing basic chemicals from pure CO_2 (Aresta, 2010; Quadrelli et al., 2011; Artz et al., 2018; Chauvy et al., 2019), there has been hardly any work focusing on using combinations of CO and CO_2 (as is present in BFG). If steel mill gases could be directly used, it could be economically beneficial as it would avoid expensive separation and purification of the gas. Both the CO and CO_2 present can be reacted with H_2 to produce valuable hydrocarbons. Economic assessments could then be performed to determine if the benefit from a purer feed stream outweighs the cost of separation for a particular process, as is the case in Carbon4PUR.

Many chemical syntheses from pure CO_2 are limited environmentally and economically due to the amount of H_2 required to produce products. For CO_2 utilization to be environmentally advantageous, this H_2 has to be provided by a low-emissions source (such as electrolysis based on renewable electricity), which is still comparatively expensive (6700 €/ton), despite efforts to reduce cost (Saur and Ramsden, 2011; Gielen et al., 2019; IEA, 2019). H_2 from COG could be captured using pressure swing adsorption and used for this purpose (Flores-Granobles and Saeys, 2020). A summary of some possible utilization options from steel mill gases is shown in **Figure 2**. It is estimated that the entire demand for methanol and ethanol in Europe could be met if 77% of the steel mill gases produced in Europe were used for chemical production (CORESYM, 2017).

The largest barrier facing the utilization of steel mill gases for chemical production at the present is mostly the technological development of processes that are both economically and environmentally competitive with conventional processes. Other problems are logistical in nature, such as finding locations where chemical plants are in close proximity to steel mills, or who would take ownership of the chemical plant if a new one was to be constructed on the site of the steel mill. The Carbon4PUR consortium addresses these problems with specialized work packages (Carbon4PUR, 2020a).

Current Literature on Steel Mill Gas Valuation

Although there have been many techno-economic and life cycle assessments on the use of steel mill gases as a feedstock for chemical processes, most do not take into account any cost or GHG emissions for using steel mill gas as a feedstock, despite the gas providing energetic value to the steel mill. Ou et al. (2013) justify this by assuming that the steel mill gas used for their chemical process is gas that would otherwise have been flared; while this may be a valid assumption in China, where flaring rates are very high, this is not a valid assumption for a continuous process in Western Europe as the amount of flared gas ranges from 0.1 to 22 vol%, averaging around 2 vol% (Lundgren et al., 2013; Carbon4PUR, 2020b). Other studies do not provide any justification for their assumption of zero replacement cost or emissions (CORESYM, 2017; Deng and Adams, 2020). Those studies that do assume a purchase cost for steel mill gases usually assume a constant cost that may not accurately compensate the steel mill for the real value that steel mill gases provide for a given plant. Lundgren et al. (2013) assume a constant cost of 22.4 €/MWh for COG, while BFG and BOFG are assumed to be free. Yildirim et al. (2018) assume that COG will be replaced by natural gas within the plant, and the purchase cost of COG is effectively the cost of natural gas required to replace it. While this is an informed assumption, it neglects the other usages of steel mill gases (electricity generation and flaring) and how that varies dynamically, and again no purchase cost for BFG or BOFG is assumed. Lee et al. (2020) is the only study found to assume a purchase cost for BOFG as well as COG, using a static value for the cost of natural gas required to replace their energetic value. Likewise, the life cycle assessment conducted by Thonemann et al. (2018) assume natural gas replaces all steel mill gases consumed. No studies found have thus far considered replacing the electricity generated at the power plant, nor considered a dynamic model where the cost is based on the real-time steel

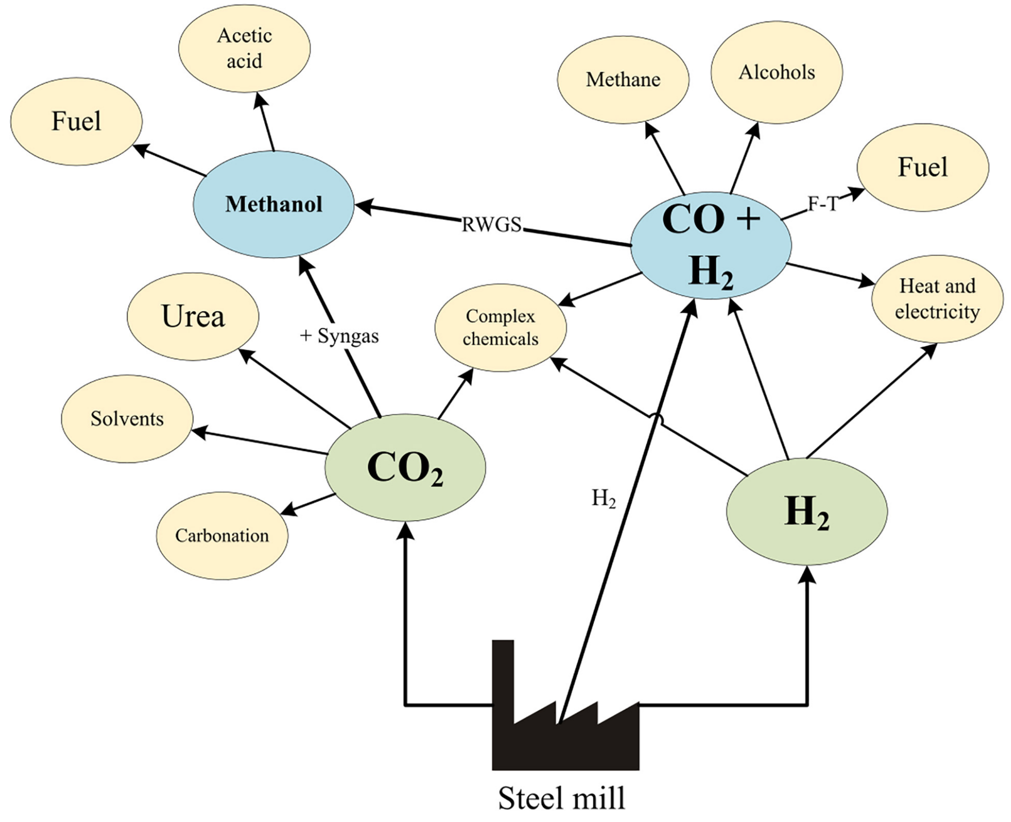

FIGURE 2 | Summary of possible utilization options from steel mill gas adapted from Milani et al. (2015) and Hernández et al. (2017).

mill gas usages and the prices of the utilities required to replace them. More accurate estimates for the cost of steel mill gas that fairly reflect the value it provides to the steel mill are beneficial to both the chemical and steel producer to ensure adequate compensation for the steel mill gas and to allow for more precise techno-economic and life cycle assessments on future technologies.

GOAL AND SCOPE

The main goal of the study is to investigate the economic cost and environmental implication of using steel mill gases as a chemical feedstock in order to assess its synergetic potential. As a first step, the value of the gases to the steel mill must be derived. The steel producer gains energy in the form of heat and electricity from burning the steel mill gases, which can be used on-site or sold to the grid. Knowing the value this gas generates is crucial in order to derive the cost the chemical producer must pay for the steel mill gases, which they aim to use as a substitute for other feedstocks to produce and sell chemicals. Secondly, to be considered as a potential feedstock by a chemical company, utilization of the steel mill gases has to be more economically and/or environmentally attractive than conventional feedstocks. The benchmarks for the study are discussed in detail in **Benchmark Definition**. The findings of this study could then be used as an input to further, more specific techno-economic and life-cycle assessments on a particular chemical process. Intermediate gas storage will also be considered and assessed for potential economic and environmental benefits. A storage tank could be implemented to increase the amounts of flare gas used, which would decrease the replacement cost and global warming impact. The scope of the study includes the steel mill gas usages, from the moment the gases are produced to their consumption for heat or power generation, as shown in **Figure 3**. Any chemical processes or gas processing, transport of the gases, separation, or treatment needed for such processes is not included in the scope of this study. The goal is to determine the value of the "feedstock stream" as shown in **Figure 3** which also provides an indication of the purchase cost for the chemical producer, by using an estimate for the cost of replacing the energetic value the steel mill gas provides to the steel mill. The environmental analysis aims to then study the associated GHG emissions of the replacement.

Benchmark Definition

For the utilization of steel mill gases as a feedstock to become adopted, it must perform better than conventional feedstocks at whichever economic or environmental metrics are considered important by individual decision-makers. Benchmark feedstocks

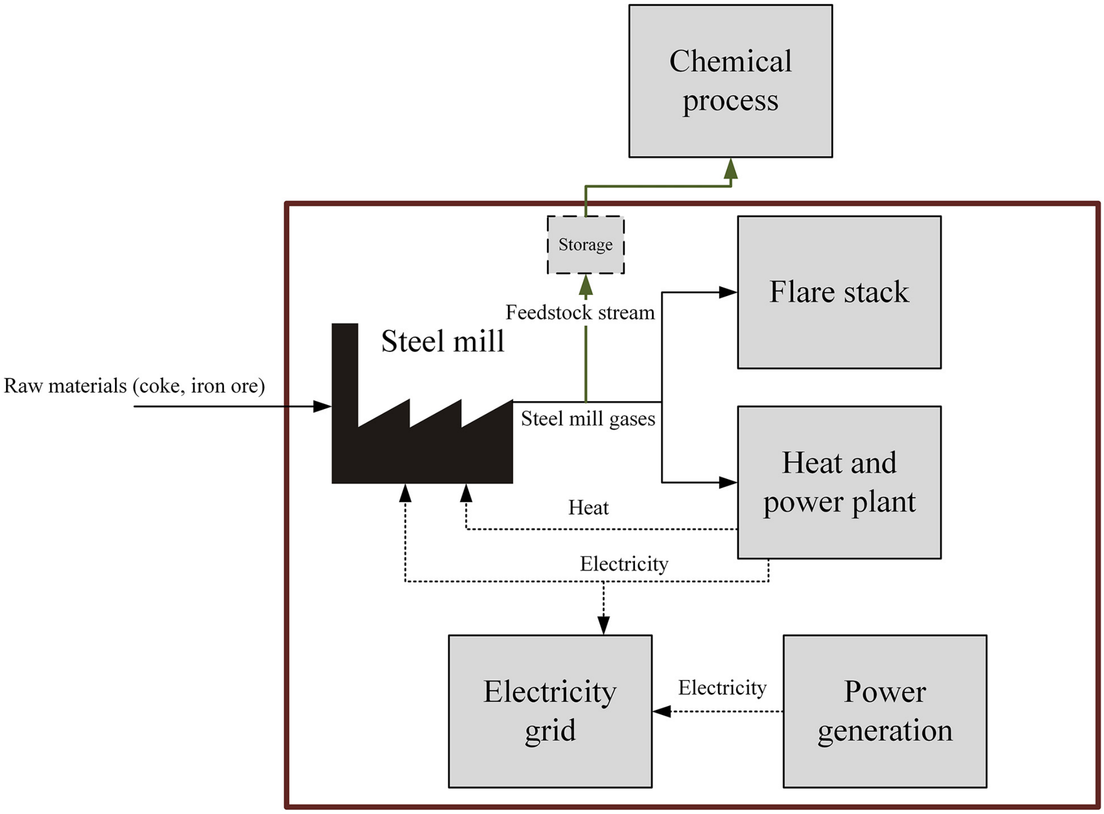

FIGURE 3 | The scope of the study, including the usages of the steel mill gases and their replacements. Optional storage is shown in dashed lines.

for steel mill gases are the base chemicals that are the most valuable components in each steel mill gas – CO for BFG and BOFG, and H_2 for COG. Although CO_2 is also a potentially valuable component of BFG and BOFG for CO_2 utilization processes, if it was desired as the only product, it could simply be taken from the waste steel mill gases after combustion in the CHP at a higher concentration. Therefore, it will only be considered as a "secondary" feedstock or benchmark, useful in such processes that are designed to use both CO and CO_2. However, although CO_2 is more likely to be used as an additional feedstock than the main one, if it is used in a process alongside CO, such as the Carbon4PUR process, knowing the replacement cost is valuable information.

The benchmark for CO is defined to be CO produced from fossil fuels through coal gasification, which has production costs of around 440 €/ton (Pei et al., 2016) and a GHG emissions impact of approximately 1.25 kg-CO_2-eq./kg CO (Wernet et al., 2016) for a cradle-to-gate system boundary.

For H_2, two benchmarks are defined: firstly, a steam reforming process, representing conventional, fossil-based H_2 production, and a solar-powered electrolyzer process, representing an alternative non-fossil-based production method. The steam reforming process has production costs of around 2200 €/ton, and the electrolysis method currently around 6700 €/ton (Gielen et al., 2019). Steam reforming has a GHG emissions impact of 4.8 kg-CO_2-eq./kg H_2 (Dufour et al., 2011) and solar-powered electrolysis of around 2.0 kg-CO_2-eq./kg H_2 (Bhandari et al., 2014) when taking into account cradle-to-gate emissions.

As well as a comparison to conventional benchmark feedstocks, from an environmental perspective, usage of steel mill gases should reduce overall emissions from the system, i.e., replacing the heat and electricity to the steel mill should not generate more emissions than the steel mill gases otherwise would have. Therefore, the emissions results from this study are also compared to a "viability point," above which emissions are no longer saved when steel mill gases are used.

Scenario Definition

The base scenario is defined as a mid-flaring, mid-capacity steel mill in the year 2017 in France using BFG. Variables that are altered and compared are done so from this base scenario. For example, if differing capacities are being compared, they are done so at a mid-flaring level in 2017. In most cases, both countries studied are also compared directly.

Germany and France are selected as the studied countries because they are both large economies with substantial chemical and steel industry (Statista, 2020), as well as containing particular locations where such a symbiosis could take place (*Fos sur Mer* in France, *Ruhrgebiet* in Germany). There is a large difference in how electricity is produced for the grid in each country, making both economic and environmental comparisons interesting. France's electricity grid has one of the lowest GHG emissions intensities in Western Europe, while Germany has one of the highest, making it possible to see results for both "best" and "worst" case scenarios.

The gas feedstock capacities are selected based on appropriate amounts required for example processes, as mentioned in the list below. The maximum capacity for BOFG and COG is around 400 and 250 kt/a, respectively, and therefore that was the upper limit that was simulated for them. The average flare rate in European steel mills is around 2 vol%, and this was consequently chosen as the value for the base scenario. Boundaries as low as 0.5 vol% and as high as 5 vol% were also simulated to ensure the limits of most modern steel mills are covered.

All three types of steel mill gas are considered in this study. For smaller chemical syntheses, solely BOFG or COG could be used for the feedstock, but using BFG is required for larger plant capacities. It is believed that most steel mill flue gas utilization processes will focus on solely using BFG, as it accounts for roughly 85% of the emitted steel mill gases. However, some processes utilizing multiple gas streams are under research, such as the production of syngas by mixing BFG and COG (Lundgren et al., 2013).

The year 2017 is chosen as the base year of the study as initial research was started this year; neither grid prices nor emissions factors have significantly altered since then. As a future scenario, the year 2050 is selected due to the relative abundance of data available for grid emissions predictions for this time; as well as this, many countries and industries have set specific emissions-related goals for 2050. Forecasts predict that the majority of steel produced in 2050 will still be by the integrated steel mill route and that steel mill gas utilization will be required to meet 2050 emissions targets (EUROFER, 2019). This scenario only analyses GHG emissions; utility price predictions 30 years in the future are too uncertain to be used.

In summary, the following possibilities for each variable were thereby derived:

Location:

- *France.*
- *Germany.*

Gas capacity:

- *Low capacity – 25 kt/a* – Very small industrial plant (e.g., specialty chemicals such as rubbers).
- *Mid capacity – 100 kt/a* – Medium-sized industrial plant (e.g., common polymers, intermediate chemicals such as polyethylene).
- *High capacity* – the highest feasible scale of gas usage *(BFG: 1000 kt/a* **or** *BOFG: 400 kt/a* **or** *COG: 250 kt/a)* – very large industrial plant (e.g., large scale base chemicals such as methanol) (different plant sizes here are due to the three gases having different quantities).

Type of steel mill gas used as feedstock:

- *BFG* – Used for most flue gas utilization processes studied thus far due to very large capacity.
- *BOFG* – Useful if gas is desired with slightly higher carbon content than BFG.
- *COG* – Useful if H_2 or CH_4 is desired.

Mill flaring rates:

- *Low flaring – 0.5 vol%* – more likely in modern plants.
- *Mid flaring – 2 vol%* – average flaring rate for European steel mills.
- *High flaring – 5 vol%* – could happen in circumstances with ongoing maintenance or broken parts in the power plant or heat generation systems.

Year:

- *2017* – Reflecting present time grid emissions intensity.
- *2050* – Reflecting future grid emissions intensity (from ecoinvent 3.6, 450 2050 scenario).

Any of these variables can be changed to create a multitude of possible unique scenarios, one "branch" of which is demonstrated in **Figure 4**.

DATA COLLECTION AND MANIPULATION

Data Collection and Assumptions

Data were obtained from a major steel producer from two of their steel mills detailing how much gas is used for electricity generation, heating, or is flared. One of the datasets covers a representative 2-month period on a 10 min basis, while the other has measurements on an hourly basis over a complete year. One of these mills (hereafter referred to as the "non-efficient case") had a particularly high flaring rate due to technical issues (one of the highest flaring rates in Western Europe), and the other ("efficient case") had one of the lowest flaring rates in Western Europe.

The spot market prices for both electricity and natural gas in both Germany and France were obtained for the year 2017. It is assumed that these prices have not greatly varied since 2017 and that the random fluctuations present in the price are of the order of magnitude that can also be found in previous or later years.

The greenhouse gas emissions are calculated using LCA data on global warming impact from ecoinvent 3.6 (cut-off system model) *[tons-CO_2-eq,/kWh]* (Wernet et al., 2016). The share of electricity generated in Germany and France from each source type (coal, wind, etc.) was found for every hour over the year 2017 (Bundesministerium für Umwelt, 2020; ENTSOE, 2020; Fraunhofer, 2020; RTE, 2020; Umweltbundesamt, 2020). For the scenarios set in 2050, data for the predicted carbon intensity of the grid, again in *[tons-CO_2-eq,/kWh]*, was also obtained from ecoinvent 3.6 (Stehfest et al., 2014; Mendoza Beltran et al., 2020).

It is important to note that the power plant and burner efficiency has an impact on the value the gas provides for electricity generation or heating purposes (Worrell et al., 2010). The power plants in steel mills have efficiencies that vary from 0.3 to 0.5 (Kim and Lee, 2018). An efficiency of 0.36 is commonly used in literature (Harvey et al., 1995; Kim and Lee, 2018), and the same value was chosen for this study after discussion with a

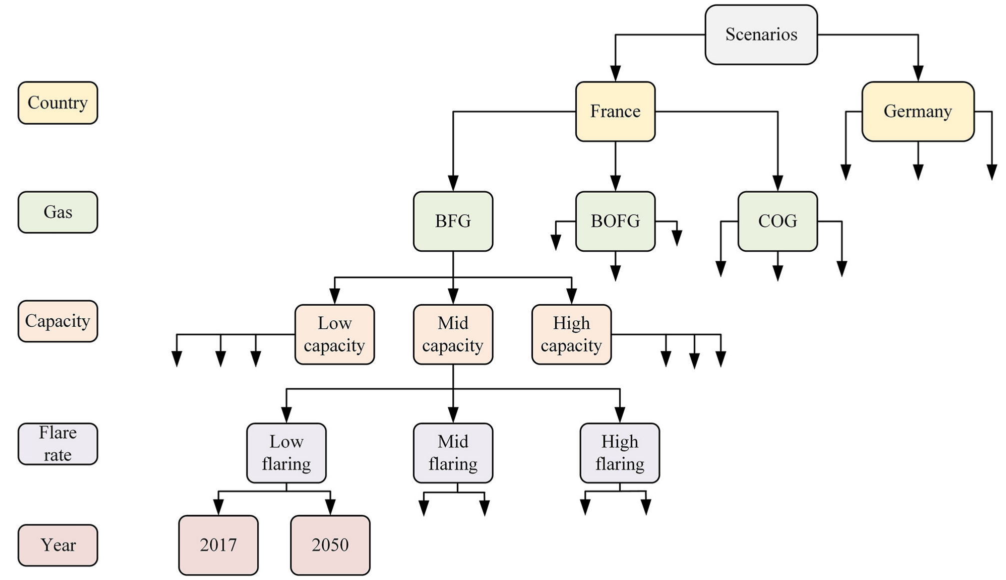

FIGURE 4 | Tree diagram of the different scenarios possible by changing model parameters. Only one "branch" is shown for diagram simplicity.

steel manufacturer. Higher efficiencies mean that more electricity or heat can be generated for a certain amount of steel mill gases in the power plants, resulting in the steel mill gases being more valuable.

Simulation of Steel Mill Flaring Data

From the flaring patterns in the data obtained from the steel mill, a flaring pattern for an average Western European steel mill is simulated. As the "non-efficient case" has a very atypical flaring pattern due to technical issues, the simulation for the study was based on the patterns in the data set from the "efficient case." It is assumed that the flaring pattern for the average case would look similar to the efficient case but simply scaled up.

A discrete-time Markov chain is implemented to simulate flaring patterns across a range of potential steel plants (Mcbratney and Everitt, 2002; Towers, 2016; Gagniuc, 2017). Three Markov transition matrices are created from the amount of gas being flared every hour, wherein the first bin of the first matrix contains the second Markov transition matrix, and likewise with the second to the third, as illustrated in **Figure 5**. With this method, both appropriate resolution and probability of flaring events are retained from the original data. Two variables are considered to be critical to the replication of realistic flaring data: the frequency of times when flaring is zero and the overall average volume of gases flared (essentially equal to flaring rate). Realistic ranges for these variables were created using linear regression from the data provided by the steel manufacturer for multiple steel mills. The heat maps of the Markov transition matrices highlight the moderate probability of a given flaring amount maintaining a similar amount into the next hour, as well as the high likelihood of a flaring event going to zero. Flaring events usually last a few hours or days and do not change between non-zero values too erratically.

MODEL DESCRIPTION

Modeling the Replacement Cost of Steel Mill Gases

The economic value of the steel mill gases depends directly on the economic value that it supplies to the steel producer. This economic value is entirely based on the energy gained from the combustion of the gas. As mentioned in **Current Usages of Steel Mill Gas**, the steel mill gases are either combusted for electricity generation, heat, or are flared. Each of these options provides a different economic value. Essentially, the steel mill gases' economic value can be viewed as the cost to replace these usages by another source. For example, if steel mill gases that would otherwise have been used to generate electricity were instead used as a chemical feedstock, the electricity that would have been generated needs to be replaced by another source. This electricity could either be purchased from the local grid or generated on-site by other means. Likewise, for heating, the heat that would have been generated by steel mill gas that is now used instead as a chemical feedstock could be generated instead by natural gas or other means.

A single-objective cost-minimization model was created in the programming platform MATLAB that follows the following logic tree shown in **Figure 6**. The model is run according to a logical hierarchy: first, if there is enough gas being flared at a particular moment to supply the feedstock demands for a specific chemical plant, then the gas could be obtained effectively at zero cost by the chemical producer. Second, when there is not enough flare gas to meet demand, the electricity gas is taken next, which is replaced by either buying electricity from the grid or generating that electricity with natural gas directly. Third, when there is not enough electricity gas or flaring gas to meet the demand, heating gas is chosen, and natural gas is burned to replace heat that would

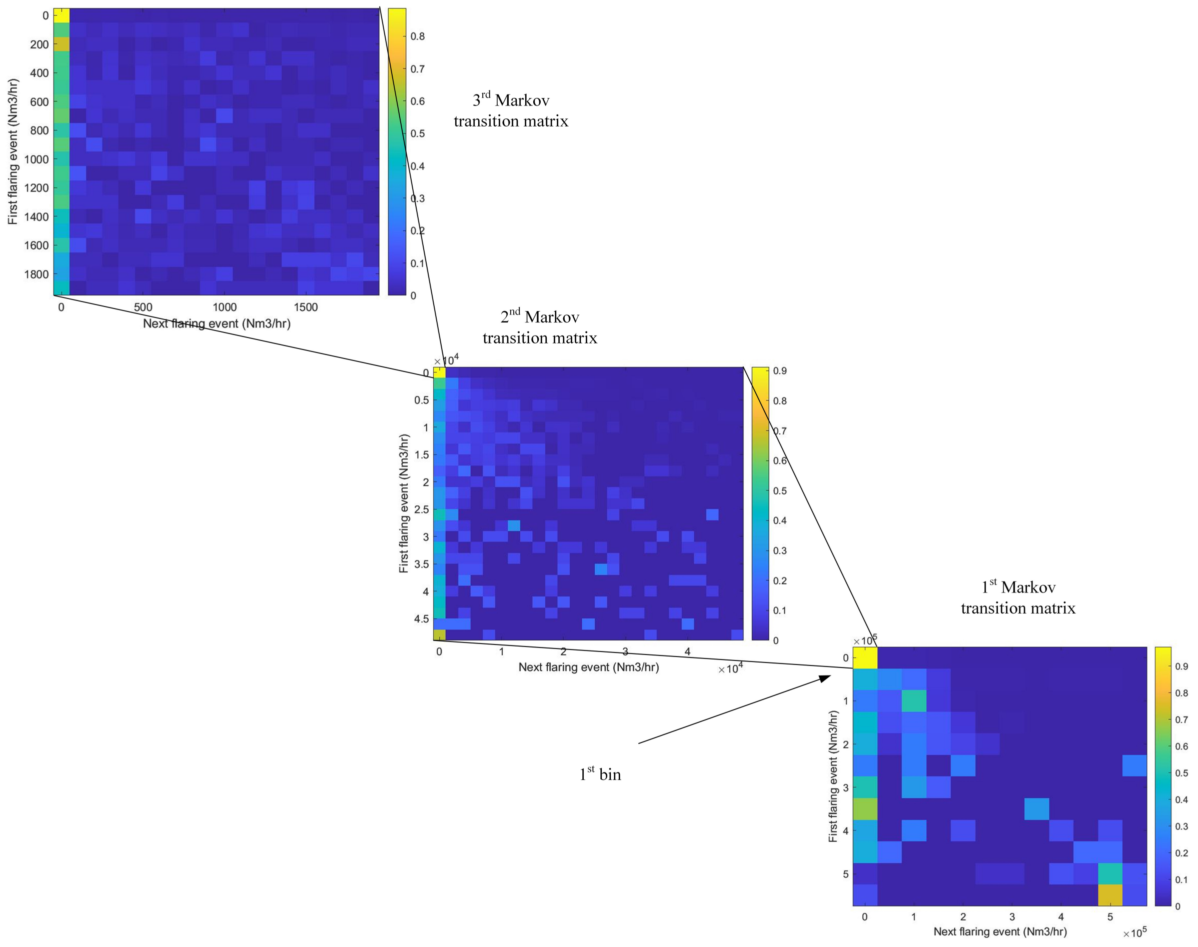

FIGURE 5 | Heat map of the Markov transition matrices, indicating probability of the flaring amount (Nm^3) at the next hour given the amount at the current hour. The first bin of the first Markov transition matrix leads to the second transition matrix, and vice versa for the second to third. Data is shown here for a 2% average flare rate steel mill.

otherwise have been generated by the steel mill gases. The model allows for varying the plant capacity (and therefore the amount of steel mill gases used), the input dataset from the steel mill (or another industrial plant), the electricity and natural gas prices, the efficiency of the steel mill, the flaring rate in volume and the frequency of flaring of the steel mill.

The most desirable steel mill gases to take for chemical feedstocks are gases that would have otherwise been flared (hereafter referred to as "flare gas"). In flaring, no energy is recovered, so no value can be gained. Regarding costs, most flare stacks are usually required to constantly burn a natural gas ignition flame, meaning that operating costs are not expected to differ noticeably during periods where gas is flared or not (Damodara, 2018). As flaring provides no economic benefit or value to the steel producer, the replacement cost of flaring gas (RC_{flare}) is zero, independent of time:

$$RC_{flare} = 0$$

Consequently, for the chemical producer, the gas is essentially free from a material cost basis (capital infrastructure and transport costs are discussed in section "Estimation of Storage Potential") and is the top priority for feedstock gas.

Feedstock gas that would otherwise be used for electricity generation (hereafter referred to as "electricity gas") does provide economic value to the steel producer. Another source must replace this electricity (or at least the economic value it provides). In this study, two sources are considered: purchasing electricity from the grid, and producing electricity directly from natural gas. Natural gas is already co-fired with BFG in many power plants due to the comparatively low energetic value of BFG. Therefore, this process does not require any extra process units nor incur higher operating costs outside of the cost of natural gas. Steel mills have a gas management system that allows for the usage of the gas to be altered on short notice. The replacement cost of electricity gas ($RC_{\mathrm{electricity}}$ at a particular time (t) is the cheaper of the two alternatives at that time:

$$RC_{electricity}\ (t) = \min[RC_E(t),\ RC_{NG}(t)]$$

It might also be the case that the steel mill would not buy energy directly from the grid if that is the cheapest option, as electricity

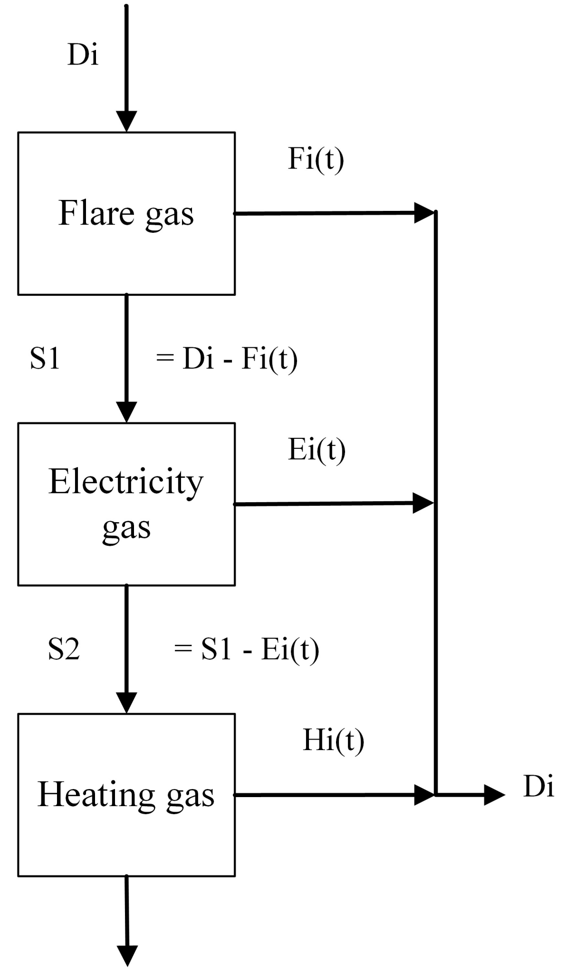

FIGURE 6 | The three different potential usages of steel mill gases and how the amount of each one is decided. $F_i(t)$, $E_i(t)$, and $H_i(t)$ are the amounts of steel mill gas that are taken from flaring, electricity production and heating, respectively. D_i is the total gas demand. S_1 is the amount of gas that cannot be met by flared gas, and S_2 is the amount that cannot be met by flaring or electricity gas.

is usually produced in excess by the steel mill and sold to the grid. The chemical company would simply then reimburse the lost revenue of the steel company, which is essentially the price of that amount of electricity from the grid at that time.

Feedstock gas that would be otherwise used for heating (hereafter referred to as heating gas) can only be easily replaced by natural gas. Burners in a steel mill already have natural gas present to co-fire with steel mill gases when required, so that the mill can maintain production in the case of a lack of steel mill gases due to maintenance or failure in the gas distribution system. Therefore, the replacement cost of heating gas ($RC_{heating}$) at a particular time (t) is equal to the natural gas price at that time:

$$RC_{heating}(t) = RC_{NG}(t)$$

Note that this does not mean that the same volume of natural gas has to be purchased as that of the steel mill gases that were taken for feedstock; only the amount of natural gas that replaces the energetic value that the steel mill gases would have provided.

To calculate the overall replacement cost (RC_T), the amount of steel mill gas taken from each source is multiplied by the cost to replace it for each source. For detailed calculations on how the replacement costs are calculated, refer to the **Supplementary Material section** "Calculations for the Choice of Steel Mill Gas Source." It is assumed that the steel mill can change between these options on an hourly basis, based on the fact that they can burn natural gas in the burners currently with little planning (Sadlowski and Van Beek, 2020).

Estimation of the GHG Emissions of Steel Mill Gases Usage

To assess the global warming impact of steel mill gas utilization, the GHG emissions of the dynamic stream determined by the cost-minimization model in **Modeling the Replacement Cost of Steel Mill Gases** must be calculated. For the year 2017, if electricity from the grid is used to replace the electricity generation of the steel mill gases, the amount of grid electricity that is required at a given hour [$E_R(t)$] is multiplied by the share of each gas (x_i) and the emissions intensity data for the respective source (EI_i) from ecoinvent, giving a total amount of GHG emissions for that hour from electricity [$GHG_{E,17}(t)$] in the unit of *[tons-CO$_2$-eq.]*:

$$GHG_{ET,17}\,(t) = E_R(t)\sum_i x_i(t)\,EI_i$$

If natural gas is used, either to replace electricity or for heating, the GHG emissions for that hour from natural gas [$GHG_{NG,17}(t)$] are determined by multiplying the amount of natural gas required [$NG_R(t)$] by the emissions factor for natural gas (EI_{NG}).

$$GHG_{NG,17}(t) = NG_R(t)\,EI_{NG}$$

The total GHG emissions for a given hour [$GHG_{T,17}(t)$] is then the sum of both the GHG emissions from electricity and those from natural gas:

$$GHG_{T,17}(t) = GHG_{NG,17}(t) + GHG_{E,17}(t)$$

For the year 2050, it is assumed that grid electricity would be cheaper to use than natural gas to replace electricity generated by steel mill gases due to carbon taxes and renewable energy development. Therefore, only grid electricity is used to replace electricity generated by the steel mill gases. This amount of electricity required to replace the electricity generation of the used steel mill gases [$E_R(t)$] is multiplied by the carbon intensity of the grid (EI_G) to give the total GHG emissions for that hour [$GHG_{T,50}(t)$] in *[tons-CO$_2$-eq.]*.

$$GHG_{T,50}(t) = E_R(t)\,EI_G$$

It should be noted that in the year 2050 it is unclear if heating in the steel mill will still be conducted by natural gas or if it will be replaced by lower-emission forms of heating.

Some of the solutions currently being investigated include using bio-methane or biomass, H_2 that is produced from BFG for specially developed burners, inductive heating from steel strips for coating, or simply capturing and storing the emitted CO_2 from heating with natural gas (Carbon4PUR, 2020b). However, these technologies are at a low technology readiness level and require further development. Due to the very different and unknown costs and emissions associated with each of these, as well as the uncertainty of which technology is the most likely to become widely adopted, these possibilities are not considered in this analysis. Therefore, GHG emissions for the 2050 scenario could be considered as a conservative estimate; emissions from steel mill heating will likely be reduced in some capacity by the year 2050.

It is assumed that the emissions from the rest of the value chain outside of the scope of the study remain constant and do not change between a scenario where steel mill gases are used for chemical production and one where no steel mill gases are used (for example, that the same amount of steel is produced, and the same amount of coal is required). In this case, the emissions determined in this study can be directly compared to the cradle-to-gate emissions of the benchmarks. As the emissions required to produce the steel do not change, the only emissions that can be allocated to steel mill gases as a feedstock are those emissions required to replace the usage of the steel mill gases. The end "gate" of the study is the same point as the benchmarks, which is when a ready feedstock is produced. The steel will be produced with or without steel mill gas utilization, and therefore all other and previous emissions are allocated to the steel production itself, which is the main product of a steel mill.

Estimation of Storage Potential

If gas storage is to be used, it should be optimally sized for the given gas capacity. If the storage is too large or small, the capital investment required might outweigh the savings gained by reducing steel mill gas replacement costs. The storage size was an alterable variable in the model, and if gas was flared, it was taken into the storage until the storage was either full or there was no more flare gas to be used. At this point, electricity gas was taken into storage, and finally heating gas if no more electricity gas was available. This ensures a much higher ratio of flare gas is used and therefore lowers both cost and emissions required to replace the steel mill gases. The cost of the storage tank was determined as follows (Sinnott and Towler, 2009), with a general empirical formula for equipment cost of unit operations.

$$C_e = a + bS^n \ in \ [\frac{€}{a}]$$

Where a = 97,000, b = 2,800, n = 0.65, and S = size in m^3 between 100 and 10,000 m^3.

The size was then varied to find the optimum storage size for a particular steel mill. This optimum was found at the lowest total cost when the annualized equipment cost for the storage was added to the cost per year of steel mill gas. The investment cost was then annualized (Chiuta et al., 2016):

$$annualized \ CapEx = CapEx \ \frac{i}{1-(1+i)^{-L}} \quad in \ [\frac{€}{a}]$$

RESULTS

Replacement Costs From an Energy Perspective

This section discusses the average replacement costs in 2017 Euros from an energy perspective by former usage options across the year 2017; results are shown in **Table 2**. Both the type of gas chosen and its usage have drastic impacts on the economic value it provides to the steel mill, and therefore also on its replacement cost. BFG has a relatively low replacement cost for both power generation (15 €/ton in France) and heating (21 €/ton in France). BOFG has a higher calorific value due to its higher CO content, resulting in a replacement cost of 52 €/ton for electricity generation. COG has the highest calorific value as a result of the large H_2 and CH_4 content and therefore has also the highest replacement cost (205 €/ton for electricity generation in France).

Gases used for heating also have about 40% higher replacement costs than gases used for electricity generation on average, due to the higher costs of natural gas. Therefore, it will usually be more beneficial to take feedstock gas from the stream to the power plant than the stream used for heating. Germany has a higher replacement cost for electricity generation (about 5%) in all three gases, and likewise lower for heating (14%), which directly results from the difference in prices for electricity and natural gas between the two countries.

Figure 7 details which gases are most frequently used for which purpose in vol%. BFG is flared the most at 20%, while COG and BOFG are flared at around 5%. Non-flared BFG is almost exclusively used in the power plant, while COG is used only for heating. BOFG is spread more evenly, with a 68% share used in the power plant and 25% used for heating. The higher flared volume in BFG is a positive indication that BFG is likely to perform better economically and have a lower global warming impact than the other gases.

Replacement Costs From a Chemical Feedstock Perspective

This section discusses the costs from a feedstock perspective; the analysis assumes that the respective steel mill gases are used as

TABLE 2 | Average replacement costs over the year 2017 for the different steel mill gases and respective usages.

Steel mill gas/former usage	BFG *(€/ton)*		BOFG *(€/ton)*		COG *(€/ton)*	
	France	Germany	France	Germany	France	Germany
RC_{flare}	0	0	0	0	0	0
$RC_{electricity}$	15.2	16.6	53.2	58.1	205.4	224.2
$RC_{heating}$	21.3	18.7	74.2	65.4	286.6	252.7

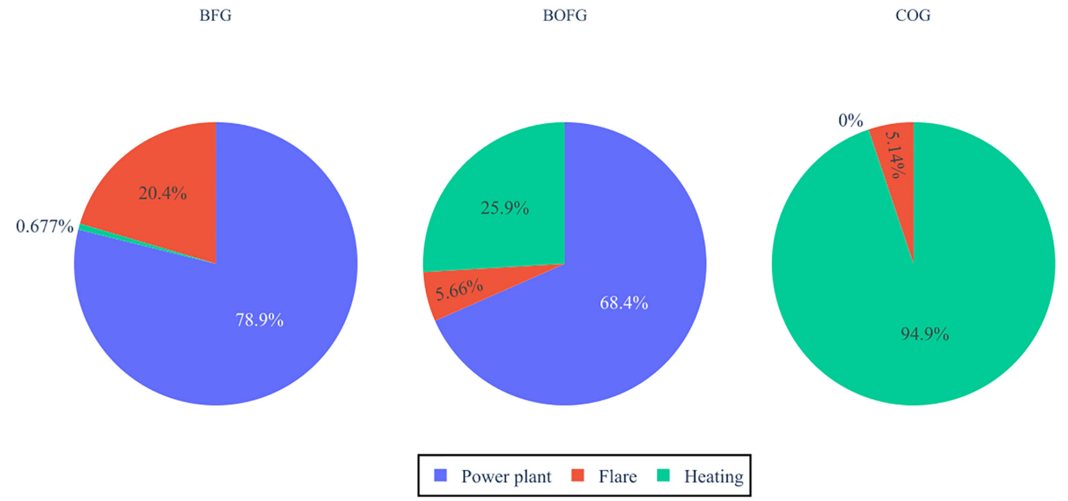

FIGURE 7 | Usages of each steel mill gas for the baseline system if they would have been used in the steel mill conventionally.

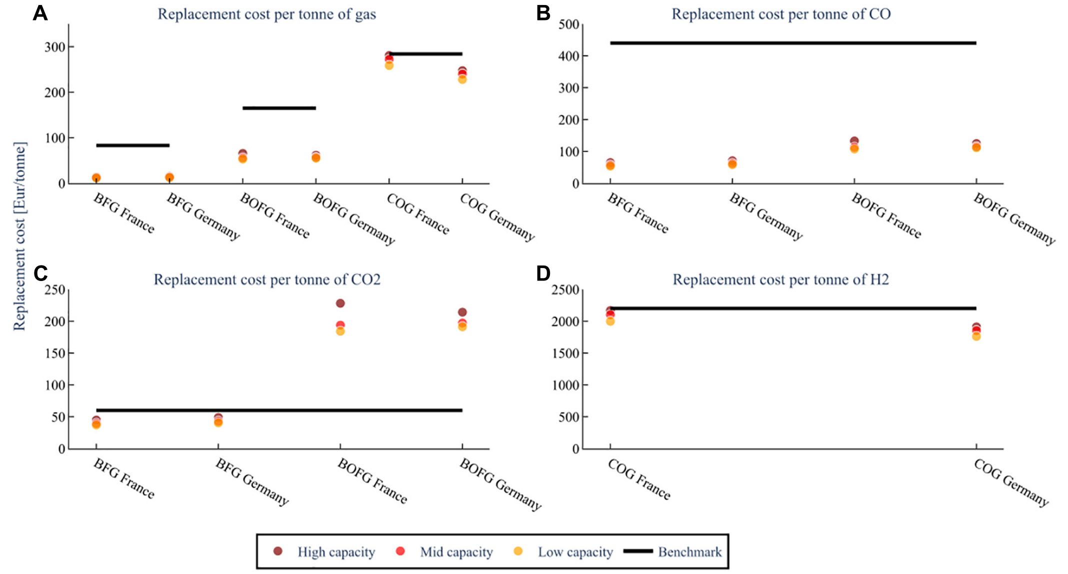

FIGURE 8 | The replacement cost of the steel mill gases when using them as chemical feedstocks for different capacity scenarios; low capacity (25 kt), mid capacity (100 kt), high capacity (1000 kt/a BFG or 400 kt BOFG or 250 kt COG, at a flare rate of 2%. The costs for **(A)** assume both CO and CO_2 are used. The costs for **(B–D)** are assuming that feedstock is the only one used. The benchmark is the cost of the feedstock when produced from conventional sources.

feedstocks in the chemical industry for a CO and CO_2 mix (A), and CO (B), CO_2 (C), and H_2 (D). Results are shown for each capacity scenario in **Figure 8**. For example, when BOFG serves as a feedstock for CO and CO_2 in France at high capacity, the steel mill has to cover replacement costs of 70 €/ton. COG is not shown in subplots B and C because it contains very minor amounts of CO and CO_2; likewise, BFG and BOFG only contain small amounts of H_2 and are therefore omitted from subplot D.

Subfigure A assumes that the steel mill gases are used as feedstocks for both CO and CO_2. In this case, both replacement costs for BFG (11–15 €/ton) and BOFG (52–65 €/ton) are considerably lower than their benchmarks (83 and 165 €/ton, respectively). Although BOFG has only a slightly higher CO content than BFG, the fact that it is flared much less (5% compared to 20% by volume) results in a significantly higher gas price. The replacement costs for COG are just slightly lower than the benchmark (284 €/ton) for France (258–280 €/ton) and about 15–20% lower for Germany (227–247 €/ton). These results are a positive indication that BFG and BOFG are economically viable when both CO and CO_2 are utilized.

In subfigure B, it is assumed that the steel mill gases are used as feedstocks for CO only. Compared to the benchmark

(440 €/ton), the replacement costs of both BFG (50–70 €/ton) and BOFG (100–130 €/ton) are significantly lower, which is a positive indication that usage of CO from steel mill gases is more economically favorable than conventional CO for all scenarios. Usage of BFG and BOFG for CO is especially interesting for chemical processes that do not require a pure CO stream.

In subfigure C, it is assumed that the steel mill gases are used as feedstocks for CO_2 only. The costs for CO_2 from BFG are 37–48 €/ton, which is lower than the benchmark (60 €/ton). For BOFG, however, the costs are significantly higher (184–228 €/ton). Using CO_2 from BFG is therefore economically viable, even if CO were also not used. It is not recommended to use BOFG to obtain CO_2 as a feedstock.

In subfigure D, it is assumed that COG is used as feedstocks for H_2 only. The replacement costs for H_2 for the base scenario are about 2100 €/ton, varying from 2168 €/ton for 250 kt/a COG to 1877 €/ton for 25 kt/a COG. This is also on par or slightly less than the benchmark's price, conventionally produced H_2 from steam reforming (2200 €/ton) (Gielen et al., 2019). Therefore, usage of H_2 from COG could be economically feasible for a small or medium-sized chemical process plant. It is important to note that H_2 separation costs should be added if the H_2 is desired pure.

The replacement costs were also calculated with the different flaring scenarios; however, different flare rates have a smaller impact on the replacement cost of the steel mill gases than different capacities [see the **Supplementary Material Section** "Results for Differing Flare Rate Scenarios"]. The viability compared to benchmarks for the flaring scenarios are similar to that described above for the capacity scenarios. It should be noted that all replacement costs mentioned here do not include separation or purification of the feedstock, transport, or additional costs imposed by the steel producer.

Replacement Greenhouse Gas Emissions From a Chemical Feedstock Perspective in 2017

The amount of GHG emissions (tons-CO_2-eq.) required to replace the steel mill gases used is shown in **Figure 9** for the three capacity scenarios for a CO and CO_2 mix (A), and CO (B), CO_2 (C), and H_2 (D). For example, the number of emissions required to replace the electricity and heat that a high capacity BOFG scenario in France is about 0.75 tons-CO_2-eq/ton of BOFG.

If both CO_2 and CO are used, as is effectively shown in subfigure A, then the viability point for BFG (0.64 tons-CO_2-eq/ton BFG) and BOFG (1.06 tons-CO_2-eq/ton BOFG) are both well above the replacement emissions (0.02–0.11 tons-CO_2-eq/ton BFG and 0.26–0.84 tons-CO_2-eq/ton BOFG) required. Their use is therefore viable from an emissions standpoint. However, in all scenarios, BFG requires fewer emissions than BOFG and France less than Germany. BFG also clearly has much fewer emissions than the benchmark (0.64 tons-CO_2-eq/ton BFG and 0.82 tons-CO_2-eq/ton BOFG). In comparison, BOFG has fewer emissions for all scenarios in France and the lower and mid-capacity scenarios in Germany. COG has much higher emissions (3.9–4.2 tons-CO_2-eq/ton COG) than both the viability point and the benchmark for all capacity scenarios and countries.

For both countries, when using BFG (about 0.1 tons-CO_2-eq./ton CO for France and 0.43–0.55 tons-CO_2-eq./ton CO for Germany), the replacement emissions required per ton of CO (shown for BFG and BOFG in subfigure B) are lower than for the benchmark method of obtaining CO [1.25 tons-CO_2-eq./ton CO (Wernet et al., 2016)]. Also, for the low and mid-capacity scenarios for BOFG when located in France (0.53–0.71 tons-CO_2-eq./ton CO) and Germany (1.07–1.20 tons-CO_2-eq./ton CO),

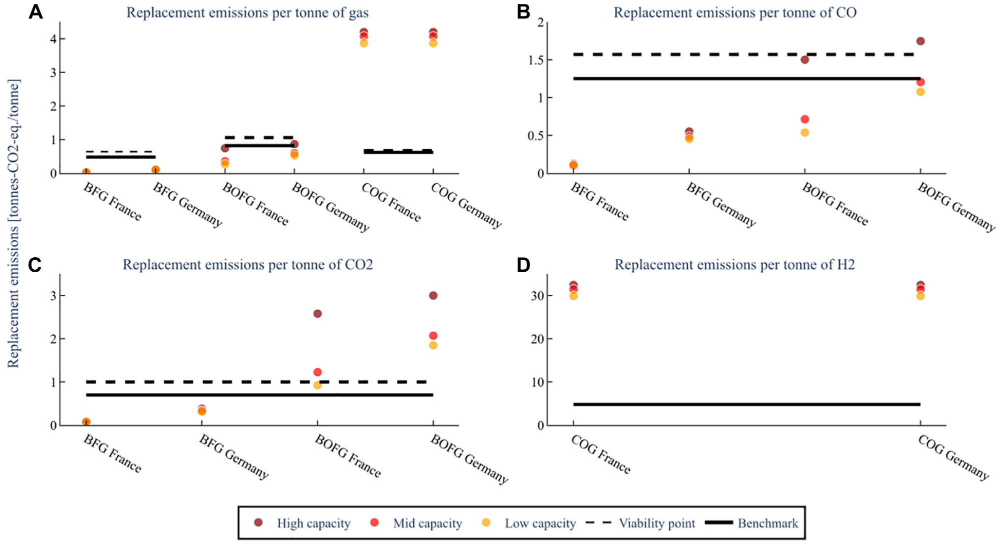

FIGURE 9 | The GHG emissions required to replace the energy provided to the steel mill by the steel mill gases for the three capacity scenarios; low capacity (25 kt), mid capacity (100 kt), high capacity (1000 kt/a BFG or 400 kt BOFG or 250 kt COG), at a flare rate of 2%. The replacement emissions for **(A)** assume both CO and CO_2 are used. The replacement emissions for **(B–D)** are assuming that feedstock is the only one used. The benchmark is the global warming impact of the feedstock when produced from conventional sources.

the emissions required to replace the steel mill gases are lower than the benchmark. However, for the high capacity scenario located in France (1.5 tons-CO_2-eq./ton CO) or Germany (1.75 tons-CO_2-eq./ton CO), the emissions required are higher than the benchmark.

For CO_2 (shown for BFG and BOFG in subfigure C), only the usage of BFG is lower than conventional methods [0.75 tons-CO_2-eq./ton CO_2 (Wernet et al., 2016)]. It should be noted that in the event of CO_2-only usage, replacement emissions of more than one ton-CO_2-eq./ton CO_2 means that the use of this CO_2 is not viable from the standpoint of reducing GHG emissions. This shows that while BFG is viable in both Germany and France, BOFG is only viable in France and then only at smaller to medium-sized plants.

The replacement emissions required per ton of H_2 (subfigure D) are extraordinarily high, around 31 tons-CO_2-eq. per ton of H_2 obtained, and the overall usage of H_2 results in emissions of around 27 tons-CO_2-eq. per ton of H_2 even when the emissions saved from avoiding combustion are taken into account. As even H_2 produced from conventional methods has a much lower emissions intensity ranging from 1.6 tons-CO_2-eq. per ton of H_2 for coal gasification (Wernet et al., 2016) to 4.8 tons-CO_2-eq. per ton of H_2 for steam reforming (Dufour et al., 2011), it is not recommended to use COG to obtain H_2 from a GHG emissions perspective.

The simulation for the different flaring scenarios (0.5–5% for BFG and BOFG, and 0.5–2% for COG) instead of capacities is shown in the **Supplementary Material section** "Results for Differing Flare Rate Scenarios," **Figure 4**). As with the replacement cost, changes in the flare rate do not have as large an impact as changes to the plant's capacity.

Replacement Greenhouse Gas Emissions From a Chemical Feedstock Perspective in 2050

It is important to consider that electricity grid mixes in the future could be vastly different from current grid mixes. Therefore, the same simulations for GHG emissions were completed with the predicted grid emissions intensity for the year 2050 in order to estimate the replacement emissions. The results are shown in **Figure 10**.

In the 2050 scenario, a large decrease in the replacement emissions is seen for Germany for all scenarios, but for France, only a very slight decrease is observed due to the already low emissions intensity of the electricity grid in France. Both Germany and France are predicted to have similarly low grid emissions intensities by 2050 (<0.1 tons-CO_2-eq./MWh) (Wernet et al., 2016). The plot for the various flaring scenarios is shown in the **Supplementary Material section** "Results for Differing Flare Rate Scenarios," **Figure 5**).

Replacement Costs and Greenhouse Gas Emissions When Gas Storage Is Used

A time-series plot of the replacement cost over the year 2017 for both Germany and France is shown in **Figure 11**. The replacement cost fluctuates quite significantly both on longer timescales throughout the year as a result of the electricity and natural gas prices, but also on much shorter timescales (days or hours) due to the steel mill gas usages (particularly the flaring volume, which often drives the replacement cost to zero). It could thus be beneficial to build gas storage, which could be filled when lower-valued flare gas is being drawn from the steel

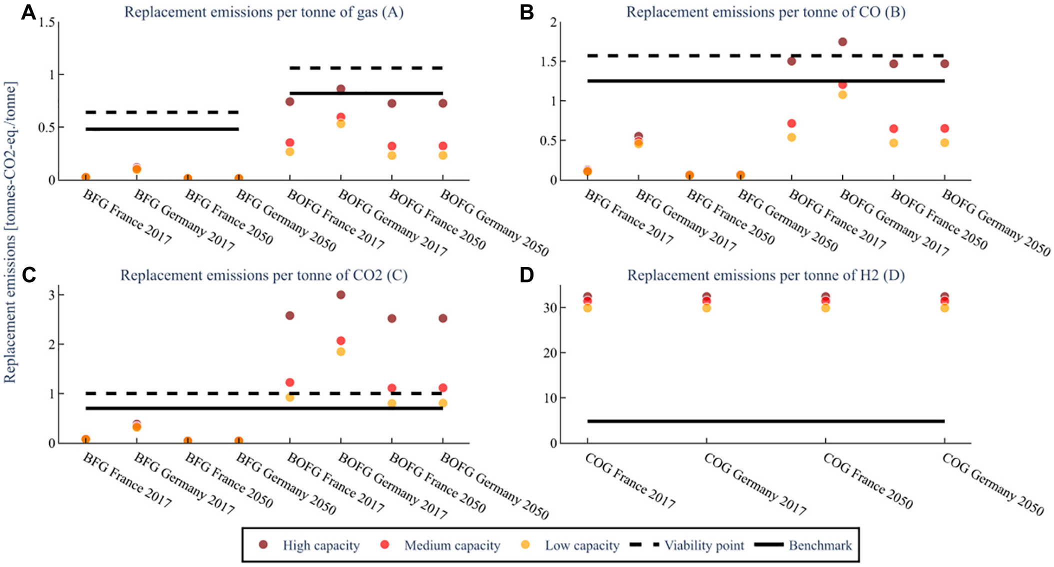

FIGURE 10 | The GHG emissions required to replace the energy provided to the steel mill by the steel mill gases for the three capacity scenarios in 2050; low capacity (25 kt), mid capacity (100 kt), high capacity (1000 kt/a BFG or 400 kt BOFG or 250 kt COG), at a flare rate of 2%. The replacement emissions for **(A)** assume both CO and CO_2 are used. The replacement emissions for **(B–D)** are assuming that feedstock is the only one used. The benchmark is the global warming impact of the feedstock when produced from conventional sources.

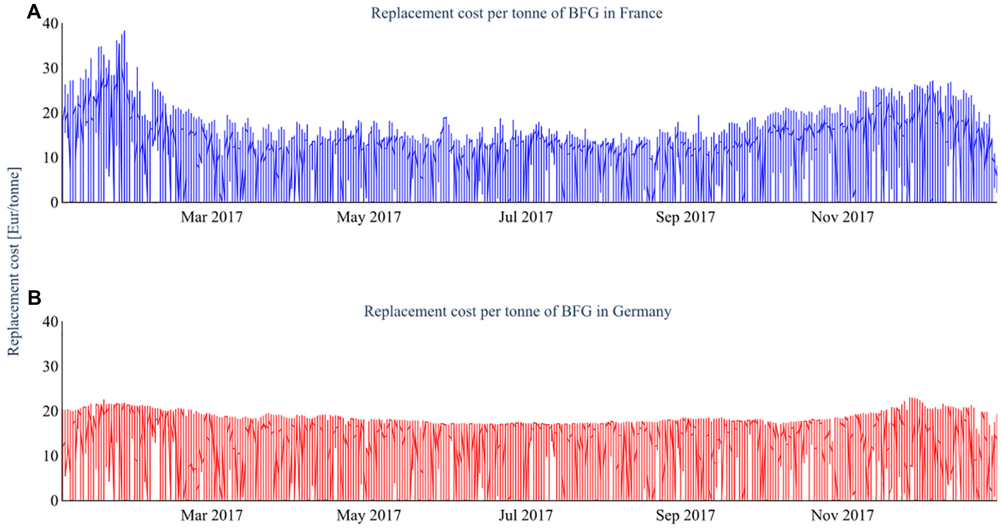

FIGURE 11 | Time-series plot of replacement cost over the year 2017 for the base scenario (flare rate 2%, capacity 100 kt BFG) for both France **(A)** and Germany **(B)**.

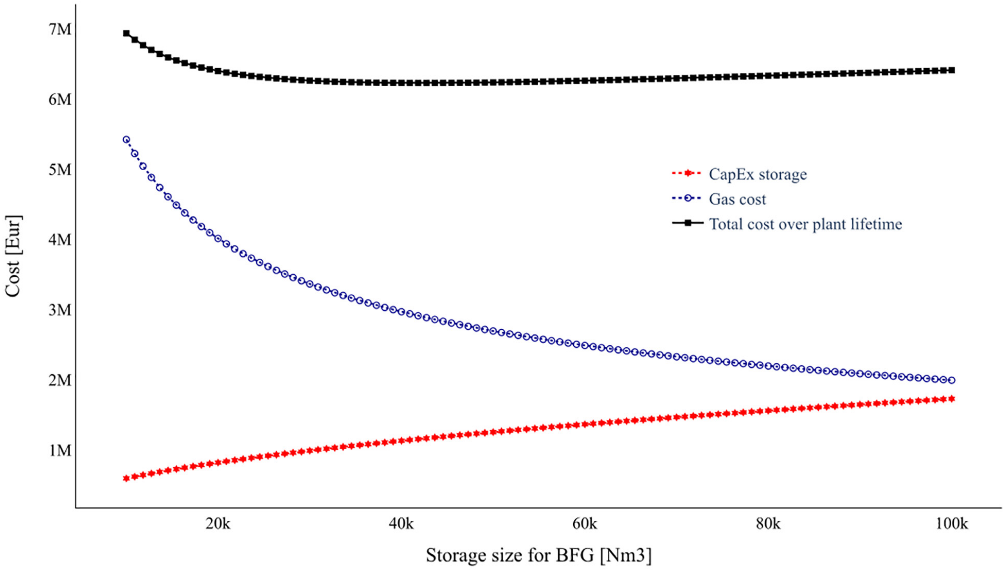

FIGURE 12 | Optimization of storage size for the base scenario (flare rate 2%, capacity 100 kt BFG).

mill, and used up when there is no flaring and higher value electricity or heating gas is being drawn, taking advantage of these short-term fluctuations.

The capital cost of the storage was taken into account using commonly used capital cost estimation equations for a storage tank, based on the capacity of the storage (Sinnott and Towler, 2009). Storage size was plotted against annualized capital cost, yearly feedstock cost of the steel mill gas, and the sum of the two to find the minimum of this sum, which is the optimal storage size from an economic perspective and is shown in **Figure 12**.

The optimum storage size for the base scenario was compared to the base scenario in Germany without storage. A comparison of the replacement cost is shown in **Figure 13**. For example, without storage, BFG has a replacement cost of about 13 €/ton. When the optimally sized storage is used, it drops to about 6 €/ton. A similar result can be seen when looking at the GHG emissions for the same scenarios in **Figure 14**, with even more significantly reduced GHG emissions for BFG and only a slight reduction for BOFG. The results show that optimally sized storage is advantageous for reducing both the replacement cost and GHG emissions impact of BFG by around 50% and is therefore recommended for BFG. On the other hand, negligible cost differences are seen for BOFG and COG, and therefore storage is not recommended for BOFG or COG.

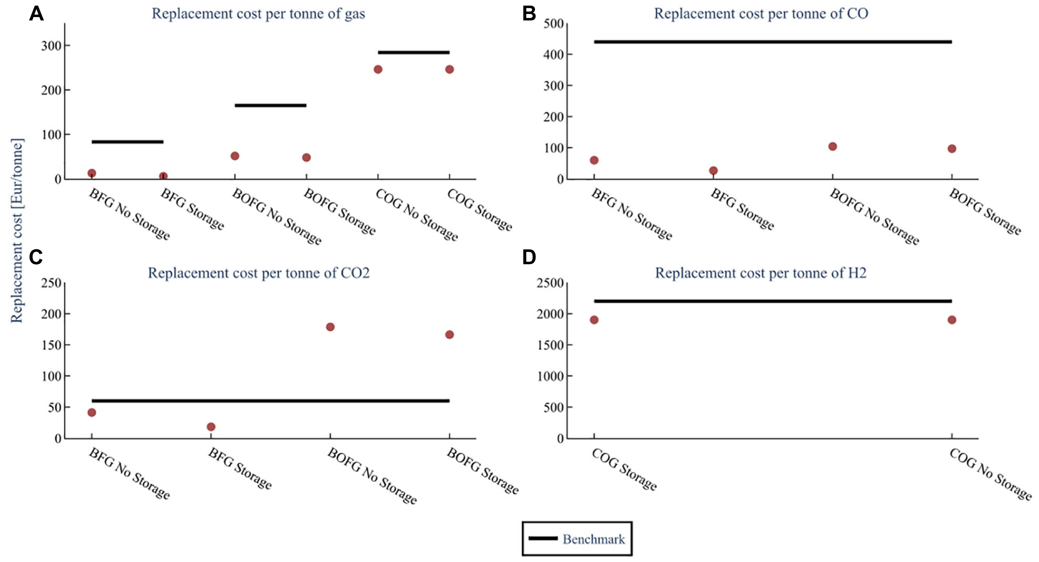

FIGURE 13 | Replacement cost comparison of the three steel mill gases with no storage vs 90 kt storage (optimal) for the base scenario (flare rate 2%, capacity 100 kt BFG). The costs for **(A)** assume both CO and CO_2 are used. The costs for **(B–D)** are assuming that feedstock is the only one used. The benchmark is the cost of the feedstock when produced from conventional sources.

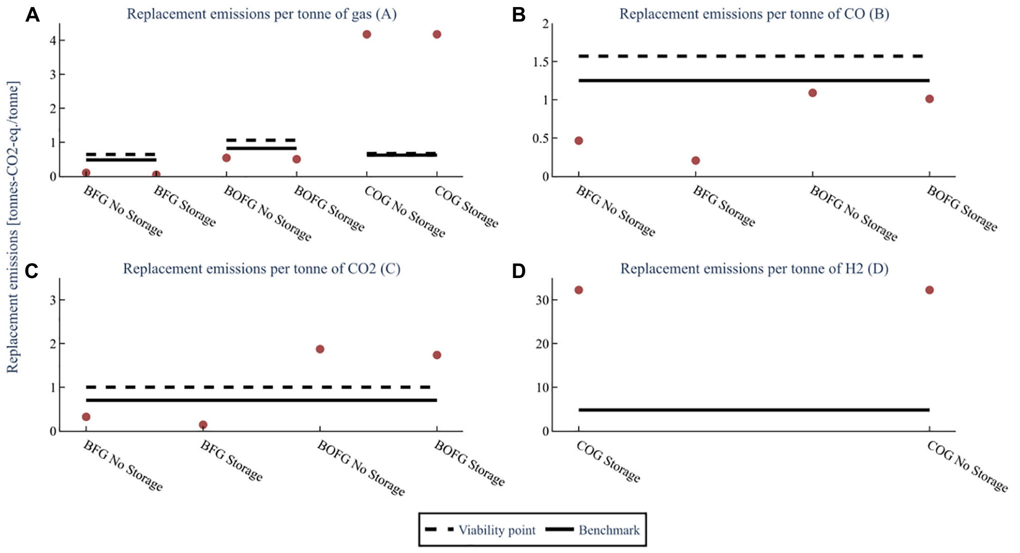

FIGURE 14 | GHG emissions comparison of the three steel mill gases with no storage vs. 90kt storage (optimal) for the base scenario (flare rate 2%, capacity 100 kt BFG). The replacement emissions for **(A)** assume both CO and CO_2 are used. The replacement emissions for **(B–D)** are assuming that feedstock is the only one used. The benchmark is the global warming impact of the feedstock when produced from conventional sources.

DISCUSSION

Energy Results

The replacement costs for BFG for both heating and electricity generation are the lowest, followed by BOFG and finally COG, directly correlated to the gases' calorific value. Heating has a lower replacement cost in Germany than in France, and vice versa for electricity. Electricity taxes and tariffs are significantly higher in Germany than in France, resulting in a more expensive electricity price. However, the price for natural gas in Germany is on average lower than for France. Subsequently, in Germany, only 53.4% of the time grid electricity is used to replace steel mill gases that would otherwise be used in the power plant, compared to 95.4% of the time for France. These values are not expected to vary significantly year on year due to limited changes in the electricity and natural gas price and no significant changes in the average European steel mill. Therefore, the assumption that 2017 data could be used as an effective proxy for steel mill gas replacement costs for other years is reasonable. Naturally, when looking more than 5–10 years into the future, updated electricity and natural gas price data should be used if available.

The different usages of each gas, shown in **Figure 7**, are less certain to change in other circumstances. The major potential source of uncertainty is the data obtained from the steel producer; although flaring data was obtained from multiple plants and manipulated to try and obtain European average flaring data, it is still inherently based on steel mills from one company, and therefore it is hard to say how accurately they portray flaring patterns for steel mills from other companies. While all steel mills using the conventional route of steel production should be similar, there could be deviations in locations of parts of the plant, making usage of one of the steel mill gases more favorable for heating, for instance. The model used in this study was designed in such a way that enables it to be used for any industrial flue gas stream for which end usage data is available. Therefore, it is recommended to use this model or perform a similar calculation for each steel mill and flue gas utilization scenario desired due to these individual mill differences.

Economic Results

The replacement costs of CO are significantly lower than the benchmark for all scenarios of BFG and BOFG, and the replacement costs for H_2 from COG are slightly lower than the benchmark. Both BFG and BOFG show good economic potential for use as feedstocks for the chemical industry. COG shows good promise as an economically viable H_2 source if it is not required pure; if it is, then the costs of separation would likely put the total cost of H_2 from COG above the benchmark cost. This section discusses and analyses the results based on gas composition, capacity, flare rate, and country.

When used as feedstock for CO, the replacement costs for BFG are about half when compared to the replacement costs for BOFG. When used as feedstock for CO_2, this difference becomes even more pronounced, with BFG's replacement costs being about four times cheaper per ton of CO_2 obtained. This variance results from the compositional differences of the gases; BOFG has a higher CO composition than BFG and a larger ratio of CO to CO_2 than BFG. BFG has a similar replacement cost per ton of CO or CO_2, whereas obtaining CO from BOFG is about 75% cheaper than obtaining CO_2.

This study finds that larger steel mill gas usage results in a slight increase in replacement cost per unit of feedstock, as shown in **Figure 8**. As the feedstock requirement increases, there will be fewer times when the flared gas is enough to meet the complete feedstock demand, thus requiring more electricity or heating gas and therefore increasing the value of the gas. For BFG and BOFG, the cost is relatively low and does not vary markedly with respect to capacity. However, this increase in the replacement costs of steel mill gases at increased capacities is low. It should not affect the economic viability of a subsequent chemical production process, especially when taking into account expected decreases in capital costs when building larger plants. COG is comparatively expensive, although it also does not fluctuate too much as capacity changes.

Changes in the flare rate do not have as large an impact on replacement cost as changes in the plant's capacity (**Supplementary Material** "Results for Differing Flare Rate Scenarios," **Figure 3**). The lack of variation is mainly because steel mill gases are not flared very often, but when they is flared, it is in large amounts, which are more than the required feedstock amount. Although the frequency of flaring increases slightly when the volumetric flare rate increases, this increase is not substantial enough to notice a considerable reduction in gas replacement cost when the flare rate is increased. In general, for both changing flare rates and capacities, the change in the replacement cost of the gas is usually around 10–20% and is not expected to significantly affect a flue gas utilization process's economic viability. The lack of variation is similar when looking at replacement cost per ton of CO, CO_2, or H_2, where smaller variations are seen with changing flare rate than with changing capacity.

France has lower costs for BFG than Germany and has a broader variation with a similar average cost for BOFG. This wider variation is because BOFG, unlike BFG or COG, is used for electricity generation and heating. Therefore, at lower capacities, BOFG will use mostly electricity gas, which is cheaper in France than in Germany. However, at higher capacities, heating gas must be taken and then natural gas used as a replacement, which is less expensive in Germany. Germany has a lower cost difference between natural gas and electricity, meaning that the cost variation with respect to capacity is smaller.

Costs for the two fossil-fuel-based feedstocks, CO and H_2 from steam reforming, are expected to stay relatively stable as they are established processes. However, with decreasing solar power costs, the production cost of H_2 from electrolysis is expected to drop sharply in the coming decade.

Transportation costs and other capital infrastructure required, such as holding tanks, are not considered in this model. Such costs depend heavily on the distance between the steel mill and the chemical plant, as well as other location-specific logistical factors. Ideally, the chemical plant would be located on or next to the steel mill's premises, heavily reducing transport costs to almost nothing. In most scenarios, a pipeline would be used to transport the goods. Another source of uncertainty is the profit margin applied by the steel producer, which must be small enough that the cost for the chemical producer is not greater than other feedstocks.

Many previous studies on other chemical processes from steel mill gases do not assume any purchase cost for the gases. This may have a large impact on process economics, particularly for the more valuable COG and BOFG. Even studies that assume zero cost for BFG neglect a cost of multiple million euros per year for mid to large capacity plants. Studies such as Yildirim et al. (2018) that assume COG is to be replaced by natural gas is a more accurate assumption. Taking an average price across 2017 for natural gas in France (31.4 €/MWh) would then result in a replacement cost for COG of 324 €/ton, which is similar to the replacement cost calculated in this study (258 – 280 €/ton), as most COG is used for heating and it has a relatively low flaring rate. It is a slight overestimate due to the share of flare gas that can be used, which does not require a replacement and is not taken into consideration with a static replacement cost assumption. However, if steel mill gas usage data is unavailable, it is a reasonable assumption to make for the replacement cost of COG. Lee et al. (2020) assume that BOFG, as well as COG, will be replaced by natural gas, resulting in a cost for BOFG of 145 €/ton if the study was conducted in France in 2017. This assumption results in a much higher replacement cost than the results presented in this study of 52 – 65 €/ton. This is because only 25% of BOFG is used for heating, while 68% is used for electricity generation; therefore, it would have been more accurate to assume a replacement by grid electricity if a static assumption was desired. As for COG, flaring gas is again neglected, overestimating the replacement cost. The more accurate replacement costs that dynamic cost-minimization models provide could help refine future studies investigating the usage of steel mill gases.

Greenhouse Gas Emissions Results

The GHG emissions required to replace CO from BFG are less than the benchmark and viability point for all three capacity and flaring scenarios, while for BOFG they were only less for the low and mid-capacity scenarios. Therefore, usage of BFG as a feedstock for CO, in particular, is highly recommended from an environmental perspective, reducing the global warming impact of chemical processes. The emissions required to replace H_2 are exceptionally high, about 6 times more than the fossil-fuel-based benchmark. It is not recommended to use COG to obtain H_2 as a feedstock from a global warming impact perspective. In this section, the GHG emissions results will be discussed and analyzed from the standpoint of gas capacity, feedstock, flare rate, and country.

In all scenarios, BFG has low replacement GHG emissions due to its low calorific value; this means less grid electricity or natural gas is required to replace BFG than BOFG or COG. Furthermore, BFG has low replacement GHG emissions due to its comparatively higher share of flare gas, which does not require a replacement. Meanwhile, the replacement emissions when using BOFG as feedstock for CO are about 3–5 times as high as BFG; when using BOFG as a feedstock for CO_2, replacement emissions are 6–10 times as high as BFG. When both are used, the replacement emissions are between 10 and 30 times as high.

As well as for the cost, higher capacities require larger GHG emissions per ton to replace. At low capacities, usage of BOFG for CO can result in a reasonably large emissions savings per ton of CO. Still, the overall capacity is often so low that the total GHG emissions saved are relatively insignificant. As BOFG is the most evenly split between flare gas, electricity gas, and heating gas (see **Figure 7**), it has the largest range in all scenarios. Smaller capacities use mostly flare gas (which does not require any replacement emissions) and electricity gas, which requires relatively little emissions to replace. Larger capacities use mostly electricity gas and heating gas, which requires moderately high GHG emissions to replace. This is in contrast with BFG, where most of the feedstock comes from either flare gas or electricity gas, resulting in much smaller variations as capacity changes.

As heating gas can only be replaced by natural gas, France has a more extensive range than Germany, due to the considerable average difference in GHG emissions between the electricity grid and natural gas. COG usage results in the same GHG emissions for both Germany and France because no COG is used for electricity generation. Therefore, it is always replaced by natural gas, and the range is due to changes in the amount of flare gas used for different capacities. In the case that COG would also be used for electricity production, perhaps its usage as a feedstock could have a lower global warming potential.

Changes in the flare rate [shown in the **Supplementary Material section** "Results for Differing Flare Rate Scenarios," **Figure 3**)] do not have as large an impact as changes in the plant's capacity. Again, this is because the frequency of zero flaring does not change drastically, even as the total volumetric flare rate over the year changes significantly.

A source of uncertainty common to industrial symbiosis is which of the two partners should get any credits or certificates for reducing emissions. It may be that due to European regulations, one partner is unable to claim credit for reducing emissions. In all likelihood, any subsidies or avoidance of taxes will likely be passed from one consumer to the other; for instance, the steel mill could claim an emissions reduction and use the money saved to reduce the feedstock costs for the chemical producer.

Previous LCA studies such as Ou et al. (2013) that assume all steel mill gas taken would have otherwise been flared (or give no justification for their assumption of zero replacement emissions) neglect a significant emissions source of 0.26–0.84 tons-CO_2-eq/ton BOFG. COG in particular requires a lot of replacement emissions and would be a large oversight if completely neglected. On the other hand, studies such as Thonemann et al. (2018) that assume natural gas as a replacement for all steel mill gas emissions overestimate the replacement emissions required, particularly for BFG (0.94 tons-CO_2-eq/ton BFG if natural gas was to replace all BFG in France in 2017 compared to 0.02-0.11 tons-CO_2-eq/ton BFG) and BOFG (2.26 tons-CO_2-eq/ton BOFG compared to 0.26–0.84 tons-CO_2-eq/ton BOFG), because most BFG and BOFG are used to generate electricity, and are therefore instead replaced by the electricity grid, which has a lower emissions intensity (particularly in France). As well, the static assumption of natural gas as a replacement does not consider flared gas, which does not need any replacement and therefore lowers the overall replacement emissions. This assumption, however, does not severely overestimate the replacement emissions for COG (5.05 tons-CO_2-eq/ton COG compared to 3.9–4.2 tons-CO_2-eq/ton COG), because COG is mostly used for heating, which is in turn replaced by natural gas. The smaller deviation is due to the amount of flaring gas that can be used, which a dynamic model takes into account. These discrepancies in turn could result in an overestimate for the total emissions estimation for the chemical processes investigated.

It is also important to point out that simply because the replacement emissions required are lower than the emissions that gas would have produced, that does not indicate that every process using this gas as a feedstock will be environmentally favorable. Further processing steps and chemicals needed for a flue gas utilization process will also contain their own emissions footprint, which could make them unviable. The values presented in these plots can simply be used for the replacement emissions required when using steel mill gases as a feedstock in a flue gas utilization process.

2050 Greenhouse Gas Emissions Results

Unlike the economic utility price data, it is expected that the emissions intensity of the electricity grid will change significantly in the future for most countries, particularly for Germany. Although France already has a low emissions-intensity grid, which is not predicted to change greatly until 2050, Germany's grid has a relatively high emissions intensity, which is expected to decrease drastically by 2050 to levels similar to France. To account for this, the study also analyzed usages for steel mill gases in the 2050 scenarios. If studies into the shorter-term future are desired (such as 2030), the model should be re-run at the expected grid emissions intensities for that year and country. In **Figure 10**, a strong decrease in the GHG replacement emissions are seen for BFG in Germany between the 2017 (0.43–0.55 tons-CO_2-eq./ton CO) and 2050 (∼0.05–0.06) tons-CO_2-eq./ton CO) scenarios; as most of the BFG is used for electricity generation, changes to the emissions intensity of the grid have a large impact on the replacement emissions required to substitute BFG. The replacement emissions for BOFG in Germany also decrease from 2017 (1.07 – 1.75 tons-CO_2-eq./ton CO) to 2050 (0.47 – 1.47), although not as substantially as for BFG. This is because a smaller fraction of BOFG is used for electricity generation than BFG, so changes to the grid emissions intensity have a smaller effect. Changes in France are not very pronounced for any scenario, due to the small change expected in grid emissions intensity between 2017 and 2050.

Although natural gas was still used in the model for the 2050 scenarios, in reality, it is unlikely to be the most common heating method in 2050. As mentioned in **Modeling the Replacement Cost of Steel Mill Gases**, a variety of other methods are being investigated that aim to reduce emissions from heating in steel mills. For this reason, the results for the 2050 scenarios are relatively uncertain, with large differences in uncertainty between the three kinds of steel mill gas. The 2050 values for BFG have a higher certainty because very little BFG is used for heating. For BOFG, of which up to 25% used for heating, the uncertainty regarding future heating emissions has a greater effect. COG is even more uncertain, as it is effectively only used for heating. Therefore, the replacement emissions required for BOFG and COG in 2050 could decrease drastically if low-emissions heating technologies are widespread. Likewise, for higher capacity or higher flaring scenarios where more flaring gas is used, the uncertainty decreases, as the fraction of heating gas is lower.

Storage Potential

Use of storage shows substantial reductions in both the replacement costs and emissions for BFG while having a negligible effect for COG and BOFG, because of the larger frequency of flaring for BFG compared to COG and BOFG. As BFG is flared about four times more frequently, the storage tank can be more often replenished with flare gas for BFG than for BOFG and COG. As BFG is not flared in very high frequencies, but large amounts on the occasions when it is flared, utilization of a storage tank allows the possibility to use more flare gas than a scenario without storage.

This result positively highlights the economic and environmental benefits of storage when BFG is used. Although BOFG and COG do not show a substantial decrease in cost or emissions, this could also be different on steel mills that flare these gases more regularly. It is recommended that the idea of storage for BOFG and COG not be discarded, but the model should be run on the data from the particular steel mill that is being considered for a flue gas utilization process.

Data, Scenario, and Model Analysis

As the model directly uses the replacement costs of the steel mill gases to determine the economic value and as an estimate for the cost the chemical producer would pay for the gas, it is robust and versatile and can be used for a range of industrial plants and scenarios beyond what has been investigated in this study. It can be directly used to estimate the economic and environmental feasibility of novel flue gas utilization processes from steel mills, which thus far have not taken into account the economic and environmental cost of utilizing steel mill gases. These processes can be analyzed by using data from published techno-economic or life cycle assessments. Often, this data has to be adapted to fit the novel process. Several parameters are important to note, such as plant capacity, plant location, and the year the study was conducted. As long as the plant's capacity in the published TEA is also of industrial scale, it is usually possible to directly up-scale the costs according to commonly used factorial methods (Sinnott and Towler, 2009). If much of the process is novel, as is often the case for flue gas utilization processes, it will usually not be possible to conduct a cost estimation based on published literature. In this case, a complete TEA will have to be performed. This TEA can be performed according to standardized guidelines and methods found in literature (Peters et al., 2003; Sinnott and Towler, 2009; Buchner et al., 2018; Zimmermann et al., 2020a,b).

The scenarios chosen for the study were selected to best represent the realistic range of European steel mills, with high, low, and mid flaring rates and gas capacities. Germany and France were selected as they have a large chemical and steel industry, while also having a considerable difference in the electricity grid emissions intensity. Performing the study in different countries could also have a great impact on results, due to the changing grid emissions and utility prices; however, it is likely that Germany and France continue to have substantial chemical and steel industries in the future. The greatest source of uncertainty in the key parameters chosen for the model is the predicted grid emissions intensity for the 2050 scenario; many developments or changes in policy and technology are possible until 2050 that could greatly affect the future grid emission intensity. Therefore, the future grid emissions intensity is quite uncertain. Another potential source of uncertainty is the flaring rate. It is possible that with technological improvements to the integrated steel mill route that flare rates decrease in the future. Decreases in the flare rate would increase the cost of steel mill gases, as less flare gas could be used as feedstock. As well, differences between the flaring rates of individual steel mills could significantly affect the cost of steel mill gases. While the current certainty of flare rates is relatively high, future values are very uncertain. More certain are the gas capacities selected for the study; while process improvements could slightly reduce the amount of steel mill gas required as feedstock for a chemical plant, or slightly larger plants could be built in the future with, respectively, larger feedstocks required, many of these processes are limited stoichiometrically and therefore require at minimum a set amount of a particular component. Therefore, it is expected that the capacities chosen remain relevant for future studies.

A limitation is that the model's scope does not include any gas separation or purification that may be required for a particular process to use the gas. Many chemical processes may require purer CO or CO_2 or need one or more components removed to avoid interference with desired reactions. However, many chemical processes do not require pure components, such as the Carbon4PUR process, which uses BFG directly (Carbon4PUR, 2020a). An interesting future study would be investigating the costs and emissions involved in the separation and purification of the essential components, such as CO or H_2, as perhaps a more accurate comparison to the benchmarks for processes that require pure component feedstocks.

CONCLUSION

A promising solution to reduce GHG emissions in the steel industry is industrial symbiosis, using steel mill gases as a feedstock for chemical processes. To correctly estimate such processes' economic and environmental impact, a model was created to evaluate both the costs and global warming impact of replacing the **Current Usages of Steel Mill Gases**. The valuable feedstocks from steel mill gases such as CO and H_2 are compared to conventionally produced benchmarks to assess their economic and environmental viability.

The results from this model show that the usage of steel mill gases requires a replacement cost for their current usages in addition to a potential need for separation and purification steps, which lie beyond the scope of this paper. Overall, however, they are a viable source for certain desired feedstocks. BFG in particular is viable as a source of CO and CO_2 from both an economic and environmental perspective with replacement costs between 50 and 70 €/ton CO and GHG emissions between 0.43 and 0.55 tons-CO_2-eq./ton CO, which is both cheaper and less impactful than benchmark feedstocks. BOFG is also recommended as a feedstock in most scenarios, but especially in cases where all the BFG is already being consumed. While it generally performs better than benchmark feedstocks, it performs worse than BFG in most metrics and has a much lower total gas flow than BFG. COG offers the potential for a slight reduction in H_2 cost (1800–2100 €/ton) when compared to conventional production but at the expense of much greater emissions (31 tons-CO_2-eq./ton H_2). BFG can be optimally used in most scenarios with the addition of intermittent storage, allowing for a higher ratio of desirable flare gas to be used.

Potentially interesting future studies could include investigating the economic and GHG emissions cost of gas separation and purification of the feedstocks in order to best compare the results to those of conventional benchmarks. As well, exploring a range of further scenarios such as different future grid emissions intensities, other countries, or additional sources of industrial flue gases.

DATA AVAILABILITY STATEMENT

The raw data supporting the conclusions of this article will be made available by the authors, without undue reservation.

AUTHOR CONTRIBUTIONS

TS envisaged and developed the methodology and initial model used for economic analysis. BS developed the idea and provided data and guidance for the environmental model. JC performed literature research, data preparation, further advanced the economic model and created the environmental model, and was the main author of all text. AZ and RS provided guidance and structure to the manuscript. All authors read, commented, developed structure, and approved the final manuscript.

FUNDING

This research was carried out within the project Carbon4PUR, which received funding from the European Union's Horizon 2020 research and innovation program under grant agreement no. 768919. Furthermore, the research was funded by EIT Climate-KIC, a body of the European Union, project number 180409. The European Commission is neither responsible nor liable for the content of this document.

ACKNOWLEDGMENTS

The authors would like to thank Natalya Tsoy (Universiteit Leiden) for her help in initializing ideas for the greenhouse gas emissions calculations and finding publicly available data sources for the electricity grid production sources of France. The authors would also like to thank Prof. Sherry Towers for her kind advice.

SUPPLEMENTARY MATERIAL

The Supplementary Material for this article can be found online at: https://www.frontiersin.org/articles/10.3389/fenrg.2021.642162/full#supplementary-material

REFERENCES

Abanades, J. C., Rubin, E. S., Mazzotti, M., and Herzog, H. J. (2017). On the climate change mitigation potential of CO2 conversion to fuels. *Energy Environ. Sci.* 10, 2491–2499. doi: 10.1039/c7ee02819a

Arens, M., Worrell, E., Eichhammer, W., Hasanbeigi, A., and Zhang, Q. (2017). Pathways to a low-carbon iron and steel industry in the medium-term – the case of Germany. *J. Clean. Prod.* 163, 84–98. doi: 10.1016/j.jclepro.2015.12.097

Aresta, M. (2010). *Carbon Dioxide as Chemical Feedstock*. Weinheim: WILEY-VCH.

Artz, J., Müller, T. E., Thenert, K., Kleinekorte, J., Meys, R., Sternberg, A., et al. (2018). Sustainable conversion of carbon dioxide: an integrated review of catalysis and life cycle assessment. *Chem. Rev.* 118, 434–504. doi: 10.1021/acs.chemrev.7b00435

Bellevrat, E., and Menanteau, P. (2009). Introducing carbon constraint in the steel sector: ULCOS scenarios and economic modeling. *Rev. Met. Paris* 106, 318–324. doi: 10.1051/metal/2009059

Bhandari, R., Trudewind, C. A., and Zapp, P. (2014). Life cycle assessment of hydrogen production via electrolysis - a review. *J. Clean. Prod.* 85, 151–163. doi: 10.1016/j.jclepro.2013.07.048

Bruhn, T., Naims, H., and Olfe-Kräutlein, B. (2016). Separating the debate on CO2 utilisation from carbon capture and storage. *Environ. Sci. Policy* 60, 38–43. doi: 10.1016/j.envsci.2016.03.001

Buchner, G. A., Zimmermann, A. W., Hohgr, A. E., äve, and Schomäcker, R. (2018). Techno-economic assessment framework for the chemical industry—based on technology readiness levels. *Ind. Eng. Chem. Res.* 57, 8502–8517. doi: 10.1021/acs.iecr.8b01248

Bundesministerium für Umwelt (2020). *Schadstoffregister*. Available online at: https://www.bmu.de/themen/bildung-beteiligung/umweltinformation/schadstoffregister/ (accessed on 4 Nov 2020)

Carbon4PUR (2020a). *Carbon4PUR*. Available online at: https://www.carbon4pur.eu/ (accessed on: 03 December 2020)

Carbon4PUR (2020b). *Expert communication was conducted in 2020*.

Chauvy, R., Meunier, N., Thomas, D., and De Weireld, G. (2019). Selecting emerging CO2 utilization products for short- to mid-term deployment. *Appl. Energy* 236, 662–680. doi: 10.1016/j.apenergy.2018.11.096

Chen, W. H., Lin, M. R., Leu, T. S., and Du, S. W. (2011). An evaluation of hydrogen production from the perspective of using blast furnace gas and coke oven gas as feedstocks. *Int. J. Hydrogen Energy* 36, 11727–11737. doi: 10.1016/j.ijhydene.2011.06.049

Chiuta, S., Engelbrecht, N., Human, G., and Bessarabov, D. G. (2016). Techno-economic assessment of power-to-methane and power-to-syngas business models for sustainable carbon dioxide utilization in coal-to-liquid facilities. *J. CO2 Util.* 16, 399–411. doi: 10.1016/j.jcou.2016.10.001

CORESYM (2017). *CarbOn-Monoxide RE-Use Through Industrial Symbiosis Between Steel and Chemical Industries*. Available online at: https://www.metabolic.nl/projects/coresym-industrial-symbiosis/ (accessed November 20, 2021).

Damodara, V. D. (2018). Numerical modelling of soot emission and flare efficiencies. *Int. J. Spray Combust. Dyn.* 8, 1–3.

Deng, L., and Adams, T. A. (2020). Comparison of steel manufacturing off-gas utilization methods via life cycle analysis. *J. Clean. Prod.* 277:123568. doi: 10.1016/j.jclepro.2020.123568

Dufour, J., Serrano, D. P., Gálvez, J. L., Moreno, J., and González, A. (2011). Hydrogen production from fossil fuels: life cycle assessment of technologies with low greenhouse gas emissions. *Energy Fuels* 25, 2194–2202. doi: 10.1021/ef200124d

ENTSOE (2020). *Actual Generation Per Production Type*. Available online at: https://transparency.entsoe.eu/ (Accessed on 04 Nov 2020).

EUROFER (2019). *Pathways to a CO2-Neutral European Steel Industry*. Brussels: EUROFER.

Fischedick, M., Marzinkowski, J., Winzer, P., and Weigel, M. (2014). Techno-economic evaluation of innovative steel production technologies. *J. Clean. Prod.* 84, 563–580. doi: 10.1016/j.jclepro.2014.05.063

Flores-Granobles, M., and Saeys, M. (2020). Minimizing CO 2 emissions with renewable energy: a comparative study of emerging technologies in the steel industry †. *Energy Environ. Sci.* 13, 1923–1932. doi: 10.1039/d0ee00787k

Fraunhofer (2020). *Energy Charts*. Munich: Fraunhofer.

Frey, A., Goeke, V., and Voss, C. (2018). Steel gases as ancient and modern challenging resource; historical review, description of the present, and a daring vision. *Chem. Ingen. Tech.* 90, 1384–1391. doi: 10.1002/cite.201800046

Gabrielli, P., Gazzani, M., and Mazzotti, M. (2020). The role of carbon capture and utilization, carbon capture and storage, and biomass to enable a Net-Zero-CO2 emissions chemical industry. *Ind. Eng. Chem. Res.* 59, 7033–7045. doi: 10.1021/acs.iecr.9b06579

Gagniuc, P. A. (2017). *Markov Chains: From Theory to Implementation and Experimentation*. Hoboken, NJ: John Wiley & Sons, Inc.

Gielen, D., Taibi, E., and Miranda, R. (2019). *Hydrogen: A Renewable Energy Perspective*. Abu Dhabi: International Renewable Energy Agency.

Harvey, S. P., Knoche, K. F., and Richter, H. J. (1995). Reduction of combustion irreversibility in a gas turbine power plant through off-gas recycling. *J. Eng. Gas Turb. Power* 117, 24–30. doi: 10.1115/1.2812776

Hasanbeigi, A., Arens, M., and Price, L. (2014). Alternative emerging ironmaking technologies for energy-efficiency and carbon dioxide emissions reduction: a technical review. *Renew. Sustain. Energy Rev.* 33, 645–658. doi: 10.1016/j.rser.2014.02.031

He, K., and Wang, L. (2017). A review of energy use and energy-efficient technologies for the iron and steel industry. *Renew. Sustain. Energy Rev.* 70, 1022–1039. doi: 10.1016/j.rser.2016.12.007

Hernández, S., Farkhondehfal, M. A., Sastre, F., Makkee, M., Saracco, G., and Russo, N. (2017). Syngas production from electrochemical reduction of CO2: current status and prospective implementation. *Green Chem.* 19, 2326–2346. doi: 10.1039/c7gc00398f

Ho, M. T., Bustamante, A., and Wiley, D. E. (2013). Comparison of CO2 capture economics for iron and steel mills. *Int. J. Greenh. Gas Control* 19, 145–159. doi: 10.1016/j.ijggc.2013.08.003

Hou, S. S., Chen, C. H., Chang, C. Y., Wu, C. W., Ou, J. J., and Lin, T. H. (2011). Firing blast furnace gas without support fuel in steel mill boilers. *Energy Convers. Manag.* 52, 2758–2767. doi: 10.1016/j.enconman.2011.02.009

IEA (2017). *Global Energy and CO2 Status Report*. Paris: IEA.

IEA (2019). *The Future of Hydrogen*. Paris: IEA.

Jarraud, M., and Steiner, A. (2014). *Climate Change 2014: Synthesis Report*. Geneva: IPCC.

Joseck, F., Wang, M., and Wu, Y. (2008). Potential energy and greenhouse gas emission effects of hydrogen production from coke oven gas in U.S. steel mills. *Int. J. Hydrogen Energy* 33, 1445–1454. doi: 10.1016/j.ijhydene.2007.10.022

Kim, Y. K., and Lee, E. B. (2018). Optimization simulation, using steel plant off-gas for power generation: a life-cycle cost analysis approach. *Energies* 11, 2884. doi: 10.3390/en11112884

Lee, J. K., Shin, S., Kwak, G. J., Lee, M. K., Lee, I. B., and Yoon, Y. S. (2020). Techno-economic evaluation of polygeneration system for olefins and power by using steel-mill off-gases. *Energy Convers. Manag.* 224:113316. doi: 10.1016/j.enconman.2020.113316

Leimkühler, H.-J. (2010). *Trends in Energy and CO2 Reduction in the Chemical Process Industry*. Weinheim: Wiley-VCH Verlag GmbH & Co.

Lundgren, J., Ekbom, T., Hulteberg, C., Larsson, M., Grip, C.-E., Nilsson, L., et al. (2013). Methanol production from steel-work off-gases and biomass based synthesis gas. *Appl. Energy* 112, 431–439. doi: 10.1016/j.apenergy.2013.03.010

Mazumdar, D., and Evans, J. W. (2009). *Modeling of Steelmaking Processes*. Boca Raton, FL: CRC Press.

Mcbratney, A., and Everitt, B. S. (2002). *Geoderma* 121, 155–156.

Mendoza Beltran, A., Cox, B., Chris, M., van Vuuren, D. P., Font Vivanco, D., Deetman, S., et al. (2020). When the background matters: using scenarios from integrated assessment models in prospective life cycle assessment. *J. Ind. Ecol.* 24, 64–79. doi: 10.1111/jiec.12825

Milani, D., Khalilpour, R., Zahedi, G., and Abbas, A. (2015). A model-based analysis of CO2 utilization in methanol synthesis plant. *J. CO2 Util.* 10, 12–22. doi: 10.1016/j.jcou.2015.02.003

Ou, X., Zhang, X., Zhang, Q., and Zhang, X. (2013). Life-cycle analysis of energy use and greenhouse gas emissions of gas-to-liquid fuel pathway from steel mill off-gas in China by the LanzaTech process. *Front. Energy* 7:263–270. doi: 10.1007/s11708-013-0263-9

Pei, P., Korom, S. F., Ling, K., and Nasah, J. (2016). Cost comparison of syngas production from natural gas conversion and underground coal gasification. *Mitig. Adapt. Strateg. Glob. Change* 21, 629–643. doi: 10.1007/s11027-014-9588-x

Peters, M. S., Timmerhaus, K. D., and West, R. E. (2003). *Plant Design and Economics for Chemical Engineers*, 5th Edn. New York, NY: McGraw-Hill Education.

PwC (2016). *Comparison of Electricity and Gas Prices for Large Industrial Consumers*. London: PwC.

Quadrelli, E. A., Centi, G., Duplan, J.-L. L., and Perathoner, S. (2011). Carbon dioxide recycling: emerging large-scale technologies with industrial potential. *ChemSusChem* 4, 1194–1215. doi: 10.1002/cssc.201100473

Rogelj, J., Shindell, D., Jiang, K., Fifita, S., Forster, P., Ginzburg, V., et al. (2018). "Mitigation pathways compatible with 1.5°C in the context of sustainable development," in *Global Warming of 1.5°C. An IPCC Special Report on the Impacts of Global Warming of 1.5°C Above Pre-Industrial Levels and Related Global Greenhouse Gas Emission Pathways, in the Context of Strengthening the Global Response to the Threat of Climate Change, Sustainable Development, and Efforts to Eradicate Poverty*, eds V. Masson-Delmotte, P. Zhai, H. O. Pörtner, D. Roberts, J. Skea, and P. R. Shukla (Geneva: IPCC).

RTE (2020). *Le réseau de Transport de l'électricité*. Paris: RTE.

Sadlowski, M., and Van Beek, M. (2020). Ecologic potential for flexible methanol production from steel mill off-gases. *Chem. Ingen. Tech.* 92, 1416–1424. doi: 10.1002/cite.202000085

SAPEA (2018). *Novel Carbon Capture and Utilisation Technologies, no. 2*. Berlin: SAPEA.

Saur, G., and Ramsden, T. (2011). *Wind Electrolysis: Hydrogen Cost Optimisation*. Washington, DC: Genevieve Saur.

Sinnott, R., and Towler, G. (2009). *Chemical Engineering Design*. Amsterdam: Elsevier Ltd.

Statista. (2020). *Steel Industry in Europe - Statistics & Facts 2020*. Available online at: https://www.statista.com/topics/6045/steel-industry-in-europe/ (accessed on 18 Nov 2020)

Stehfest, E., Van Vuuren, D., Kram, T., Bouwman, L., Alkemade, R., Bakkenes, M., et al. (2014). *Integrated Assessment of Global Environmental Change with IMAGE 3.0. Model Description and Policy Applications*. Nairobi: BESnet.

Stießel, S., Berger, A., Fernández Sanchis, E. M., and Ziegmann, M. (2018). Methodology for the evaluation of CO2-based syntheses by coupling steel industry with chemical industry. *Chem. Ingen. Tech.* 90, 1392–1408. doi: 10.1002/cite.201800030

Thonemann, N., Maga, D., and Petermann, C. (2018). Handling of multi-functionality in life cycle assessments for steel mill gas based chemical production. *Chem. Ingen. Tech.* 90, 1576–1586. doi: 10.1002/cite.201800025

Towers, S. (2016). *Stochastic Compartmental Modelling With Markov Chain Monte Carlo: Part I*. Available online at: http://sherrytowers.com/2016/01/02/stochastic-compartmental-modelling-with-markov-chain-monte-carlo/ (accessed July 17, 2020).

U.S. Department of Energy [DOE] (2010). *Final Environmental Assessment for the Blast Furnace Gas Flare Capture Project at the ArcelorMittal USA, Inc*. East Chicago: Indiana Harbor Steel Mill.

Umweltbundesamt (2020). *Für Mensch und Umwelt*. Available online at: https://www.umweltbundesamt.de/en (Accessed on 04 Nov 2020)

Uribe-Soto, W., Portha, J. F., Commenge, J. M., and Falk, L. (2017). A review of thermochemical processes and technologies to use steelworks off-gases. *Renew. Sustain. Energy Rev.* 74, 809–823. doi: 10.1016/j.rser.2017.03.008

Wei, W., Mellin, P., Yang, W., Wang, C., Hultgren, A., and Salman, H. (2013). *Utilization of Biomass for Blast Furnace in Sweden*. Stockholm: KTH Royal Institute of Technology.

Wernet, G., Bauer, C., Steubing, B., Reinhard, J., Moreno-Ruiz, E., et al. (2016). The ecoinvent database version 3 (part I): overview and methodology. *Int. J. Life Cycle Assess.* 21, 1218–1230. doi: 10.1007/s11367-016-1087-8

Wiley, D. E., Ho, M. T., and Bustamante, A. (2011). Assessment of opportunities for CO2 capture at iron and steel mills: an Australian perspective. *Energy Proc.* 4, 2654–2661. doi: 10.1016/j.egypro.2011.02.165

World Steel Association (2020). *World Steel in Figures*. Brussels: World Steel Association.

Worrell, E., Blinde, P., Neelis, M., Blomen, E., and Masanet, E. (2010). *Energy Efficiency Improvement and Cost Saving Opportunities in the Fruit and Vegetable Processing Industry - An ENERGY STAR Guide for Energy and Plant Managers*. Berkeley, CA: Lawrence Berkeley National Laboratory.

Wunderlich, J., Armstrong, K., Buchner, G. A., Styring, P., and Schomäcker, R. (2020). Integration of techno-economic and life cycle assessment: defining and applying integration types for chemical technology development. *J. Clean. Prod.* 287:125021. doi: 10.1016/j.jclepro.2020.125021

Yildirim, Ö, Nölker, K., Büker, K., and Kleinschmidt, R. (2018). Chemical conversion of steel mill gases to urea: an analysis of plant capacity. *Chem. Ingen. Tech.* 90, 1529–1535. doi: 10.1002/cite.201800019

Zimmermann, A., and Kant, M. (2017). *CO2 Utilisation Today*. Available online at: https://www.depositonce.tu-berlin.de/handle/11303/6247 (accessed October 10, 2020).

Zimmermann, A. W., Jan Müller, L., Marxen, A., Armstrong, K., Buchner, G. A., Wunderlich, J., et al. (2020a). *Techno-Economic Assessment & Life Cycle Assessment Guidelines for CO2 Utilization (Version 1.1)*, 2nd Edn. Ann Arbor, MI: University of Michigan Library.

Zimmermann, A. W., and Schomäcker, R. (2017). Assessing early-stage CO2 utilization technologies—comparing apples and oranges? *Energy Technol.* 5, 850–860. doi: 10.1002/ente.201600805

Zimmermann, A. W., Wunderlich, J., Müller, L., Buchner, G. A., Marxen, A., Michailos, S., et al. (2020b). Techno-economic assessment guidelines for CO2 utilization. *Front. Energy Res*. 8:5. doi: 10.3389/fenrg.2020.00005

Conflict of Interest: The authors declare that the research was conducted in the absence of any commercial or financial relationships that could be construed as a potential conflict of interest.

frontiers in Energy Research

REVIEW
published: 28 May 2021
doi: 10.3389/fenrg.2021.663331

Synthetic Fuels Based on Dimethyl Ether as a Future Non-Fossil Fuel for Road Transport From Sustainable Feedstocks

Peter Styring, George R. M. Dowson and Isabel O. Tozer*

UK Centre for Carbon Dioxide Utilisation, Chemical & Biological Engineering, Sir Robert Hadfield Building, The University of Sheffield, Sheffield, United Kingdom

In this review we consider the important future of the synthetic fuel, dimethyl ether (DME). We compare DME to two alternatives [oxymethylene ether (OME_x) and synthetic diesel through Fischer-Tropsch (FT) reactions]. Finally, we explore a range of methodologies and processes for the synthesis of DME.

DME is an alternative diesel fuel for use in compression ignition (CI) engines and may be produced from a range of waste feedstocks, thereby avoiding new fossil carbon from entering the supply chain. DME is characterised by low CO_2, low NOx and low particulate matter (PM) emissions. Its high cetane number means it can be used in CI engines with minimal modifications. The key to creating a circular fuels economy is integrating multiple waste streams into an economically and environmentally sustainable supply chain. Therefore, we also consider the availability and nature of low-carbon fuels and hydrogen production. Reliable carbon dioxide sources are also essential if CO_2 utilisation processes are to become commercially viable. The location of DME plants will depend on the local ecosystems and ideally should be co-located on or near waste emitters and low-carbon energy sources. Alternative liquid fuels are considered interesting in the medium term, while renewable electricity and hydrogen are considered as reliable long-term solutions for the future transport sector. DME may be considered as a circular hydrogen carrier which will also be able to store energy for use at times of low renewable power generation.

The chemistry of the individual steps within the supply chain is generally well known and usually relies on the use of cheap and Earth-abundant metal catalysts. The thermodynamics of these processes are also well-characterised. So overcoming the challenge now relies on the expertise of chemical engineers to put the fundamentals into commercial practice. It is important that a whole systems approach is adopted as interventions can have detrimental unintended consequences unless close monitoring is applied. This review shows that while DME production has been achieved and shows great promise, there is considerable effort needed if we are to reach true net zero emissions in the transport sector, particularly long-haul road use, in the require timescales.

Keywords: dimethyl ether, diesel, net zero carbon, de-fossilise, synthetic fuel, e-fuels

Edited by:
Mar Pérez-Fortes,
Delft University of Technology,
Netherlands

Reviewed by:
Enrico Catizzone,
ENEA—Centro Ricerche Trisaia, Italy
Yusuf Bicer,
Hamad bin Khalifa University, Qatar

****Correspondence:***
Peter Styring
p.styring@sheffield.ac.uk

Specialty section:
This article was submitted to
Process and Energy Systems
Engineering,
a section of the journal
Frontiers in Energy Research

Received: *02 February 2021*
Accepted: *06 May 2021*
Published: *28 May 2021*

Citation:
Styring P, Dowson GRM and Tozer IO (2021) Synthetic Fuels Based on Dimethyl Ether as a Future Non-Fossil Fuel for Road Transport From Sustainable Feedstocks. Front. Energy Res. 9:663331. doi: 10.3389/fenrg.2021.663331

INTRODUCTION

The drive towards 'net zero' policies in the United Kingdom, and indeed globally, has led to a re-evaluation of energy policies. While the obvious sectors needed to maximise emissions reductions are electricity and heating, a considerable quantity of energy is consumed by the transportation sector, including road, rail, aviation and maritime. The urgent need to de-carbonise, or more correctly, de-fossilise, the transport sector is a huge challenge. Internal combustion engines (ICEs) have been developed and optimised over many decades and represent the most abundant form of mobility powertrains. While there has been a governmental drive in the United Kingdom to replace ICEs with electric vehicles (EVs), a recent report by the Royal Society (Royal Society, 2019) has also considered policies surrounding a migration to synthetic transport fuels. The reason is partly because a transition to an EV infrastructure would require a complete overhaul of the electricity supply chain and economics. While plug-in battery electric vehicles (BEVs) provide zero tailpipe emissions, the energy required to power them needs to be generated elsewhere.

In the current electrical energy grid mix the amount of renewable power available is dependent on many factors including weather and demand. In the United Kingdom, low carbon energy (including nuclear) accounts for 55% of the electricity generated on average across a year (2019 figures, UK Department for Business, Energy and Industrial Strategy, 2020). This means that nearly half of the electricity remains fossil-derived and so the emissions for BEVs are deferred to the power generator. Therefore, BEVs cannot truly be considered as zero-emissions vehicles if a complete life cycle is carried out to include deferred electricity generation within the system boundaries. Furthermore, it is also necessary to include the battery manufacture and disposal of end-of-life units in the environmental analyses (Wang and Yu, 2021).

In a transition to net zero emissions, due to the economic inertia of the existing supply infrastructure and logistics, it is well-worth considering a graduated transition rather than attempting a step change. For example, in compression ignition vehicles (CIVs) such as diesel, it is not the engine that is the problem but the fuels. Rather than significantly redesigning the engine, can we instead redesign the fuels? In the case of diesel replacement, one fuel that is attracting considerable attention is dimethyl ether (DME) and the family of oxymethylene ethers (OME_x) where DME is equivalent to OME_0 and x is the number of additional oxymethylene units (-CH_2-O-) within the molecule. Alternative liquid fuels are interesting in the medium term, while renewable electricity and hydrogen are considered as reliable long-term solutions for the future transport sector. DME may be considered as a circular hydrogen carrier which will also be able to store energy for use at times of low renewable power generation.

Work by Willems at Ford has shown that in engine tests, not only is there zero SOx emissions associated with DME fuels (because the fuel is not fossil-derived) but due to the reduced carbon content in the molecules compared to diesel, CO_2 emissions can be as low as 3 g/km, compared to EU 2020 standard diesel car emissions of 95 g/km (European Council directive, 443/2009; European Council directive, 443/2009). Furthermore, as less air is needed and the flame temperature is lower there are practically zero NOx emissions, and because there are no C-C bonds in the ether molecules particulate matter (PM or soot) is also practically zero (Lee et al., 2016). Therefore, compared to current electricity grid mixes and emissions in power generation for EVs, the full scope life cycle emissions for DME-CIVs could be considerably lower.

We recently published a review on the synthesis of oxygenated transport fuels from carbon dioxide (Styring and Dowson, 2021), including DME which prompted us to consider expanding the range of feedstocks to include other materials considered to be waste. Unilever have recently announced their ambitions to remove fossil-based carbon materials from their supply chain by using waste materials described by Unilever as a 'Carbon Rainbow' (Unilever, 2020). This includes 'Purple' carbon (CO_2), 'Green' carbons (bio-based), 'Blue' carbons (marine based) and 'Grey' carbons (general waste including plastics). Using these principles, we present an up-to-date analysis of routes to DME/OME_x using waste feedstocks to eliminate fossil-carbon from the fuels supply chain.

This paper aims to show that DME is a useful mobility fuel that can be used as a diesel drop-in fuel that requires only slight modifications to existing combustion engines. This will allow low-emissions fuels to be used in legacy combustion engines while the industry and society transitions to electric vehicles in the mid- to long-term. Comparisons are made to FT and OME ethers which may also be used as drop-in fuels. We consider the technology available, and the feedstocks needed to assure a just and economically viable move to synthetic fuels.

CARBON NEUTRAL FUELLING OPTIONS

Carbon neutrality, or the aim to reach a net zero state, refers to the balance between reducing carbon dioxide emissions as far as possible and removing the remaining of carbon dioxide from the atmosphere. The European Union has committed to climate neutrality by 2050 which includes the goal of being a society with net-zero greenhouse gases. This commitment is also in line with the legally binding Paris agreement as signed by 190 parties (United Nations, 2015).

Transport is fundamental to modern living and is a key stimulator for societal improvement and economic growth. However, the negative externalities surrounding the emissions caused by transport indicate that it is a key sector for improvement to reach a net zero state.

In order to create carbon neutral transport, a multitude of options need to be considered for the many different forms of transport. The breakdown of global CO_2 emissions per transport division can be seen in **Figure 1** (Our World in Data, 2020).

Some transport sectors have already been optimised to reduce CO_2 emissions. For example, the majority of passenger rail links across the globe have been, or are in the process of being, electrified (IEA, 2019). Thus, rail emissions only contribute to 1% of the global CO_2 emissions from transport (Our World in Data, 2020).

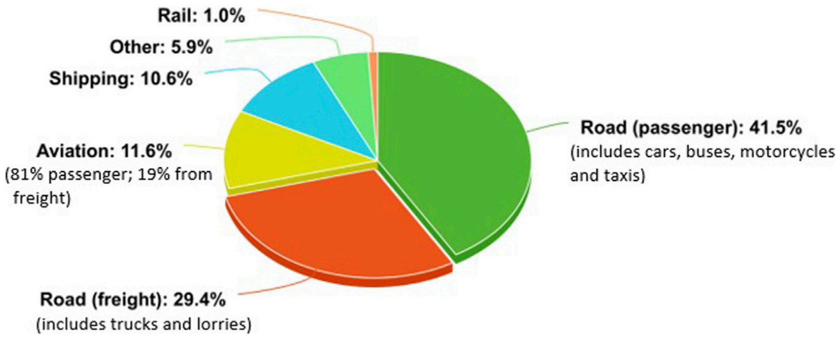

FIGURE 1 | Breakdown of global CO_2 emissions per transport division.

When looking at electrification and carbon neutrality, again it is important to recognise that in order to be truly carbon neutral the electricity source must also be made in a carbon sustainable manner. Carbon sustainable electricity sources include renewables such as energy retrieved from solar and wind farms, or energy options form sources such as nuclear which has a negligible direct production of CO_2 (IEA, 2020a). Concentrating on road transport which dominates an estimated 71% of the transport CO_2 emissions, there are two key sectors, passenger and freight. In order to reach net zero, carbon neutral fuel options need to be considered and implemented in both these sectors. However, the same methods can not necessarily be used for each sector, due to their different working requirements.

The main driving force in United Kingdom passenger transport is the electrification of the vehicle fleet, with the United Kingdom government promising to ban the sale of new combustion-engine vehicles by 2030 (Johnson, 2020). This United Kingdom policy however does not cover freight and heavy goods vehicles (HGVs) as there are many issues surrounding their electrification. The barriers that would need to be overcome by an advance in battery technology in order to electrify the HGV fleet include the long charging time and limited driving range of existing batteries. An increase in the size of the battery to solve these problems, rather than an increase in efficiency, would lead to the weight and size of the battery being too much to make it a viable and cost-effective option (Sia Partners, 2016). Current research on using BEVs to support large heavy goods vehicles over 15 tonnes, shows low feasibility for a conventional vehicle configuration due to their increased loads and the longer trip distances required. The possibility of BEVs supporting lighter medium goods vehicles (3.5–7.5 tonnes) and smaller heavy goods vehicles (7.5–15 tonnes) would require multiple charging events a day which would decrease sector efficiency and require a massive infrastructure change (Forrest et al., 2020). While fast charging of large battery-powered goods vehicles may be possible in principle, this will require enormous electrical power availability at major recharging stations (such as motorway services), especially when multiple heavy goods vehicles will need to be charged simultaneously. We have calculated that to allow fast charging (1 h charge) of upcoming battery goods vehicles such as the Freightliner eCascadia or the Tesla Semi (long range), power supplies between 0.56–0.68 and 1.12–1.36 megawatts per vehicle respectively would need to be made available at recharging stations. This is based on battery sizes of 500 and 1,000 kWh in these vehicles and a 64–88% charging efficiency (Apostolaki-Isofidou et al., 2017), which may be lower when fast charging such large batteries (Michaelides, 2020). Note that a single full charge of the larger battery, enough for a truck to drive for a full 9-hour day (approximately 500 miles), requires around a third of the electricity the average United Kingdom household will use in a year (O'Mahoney, 2020). Indeed, the scale of challenges facing electrification of larger heavy goods vehicles by using batteries has promoted the alternative concept of electrification by use of overhead cables and cabin-mounted pantographs in the United Kingdom and abroad (Ainalis et al., 2020), eliminating much of the battery weight.

Other on-board storage strategies include hydrogen fuel cell technology. However, there is still a lack of the technology and supply infrastructure that would be required to allow for widespread adoption of this technology. Depending on the production method used, the cost of producing hydrogen is up to seven times more than that of petrol and diesel (Abbasi and Abbasi, 2011). Furthermore, introducing hydrogen fuel cell technology would also require a mass investment in and restructure of fuelling infrastructure due to the necessity for new fuelling stations and pipelines (Popov et al., 2018).

As alternative on-board power sources (such as hydrogen fuel cell technology) require entirely new fleets of vehicles together with significant and very costly infrastructure changes, there is a gap in the market for synthetic fuels or biofuels, particularly those which can be fed into the existing supply infrastructure. Furthermore, synthetic fuels such as DME are circular hydrogen carriers and utilise hydrogen as a method of storing energy in a vector form that can be transported and stored with more ease and safety than using hydrogen as the singular fuel source (Catizzone et al., 2021).

Biofuels are fossil replacement transport fuels made directly from biomass, instead of from fossil-based carbon sources. The most widely used biofuels for transport are bioethanol and biodiesel. Bioethanol can be produced from first generation feedstock e.g. sugarcane as well as second generation feedstock such as lignocellulose. The complexity of the process increases

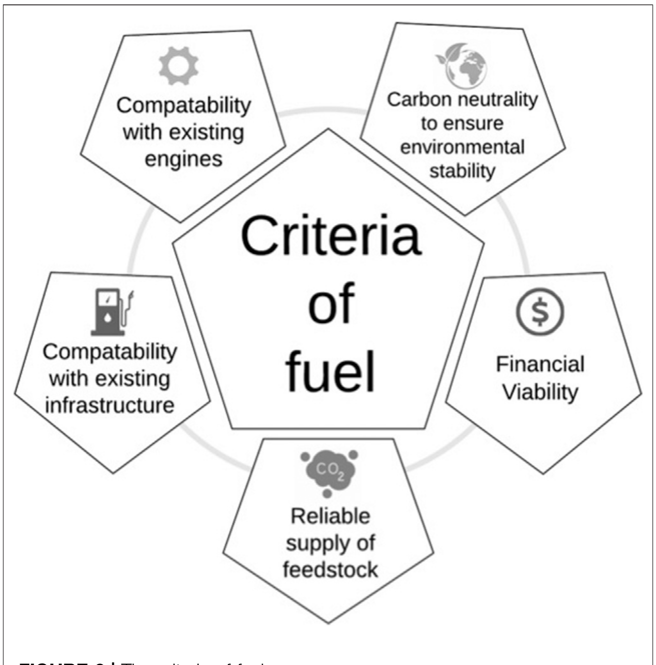

FIGURE 2 | The criteria of fuel.

as you go from 1st → 2nd → 3rd generation, however the movement away from 1st generation feedstock avoids a key barrier for the production of biofuels, namely the food vs fuel argument (Prasad and Ingle, 2019). Biodiesel manufactured mainly in the EU is produced by the transesterification and esterification of vegetable oils or animal fats with alcohols such as methanol (Brito Cruz et al., 2014). Although regarded as one of the most viable options for the reduction of CO_2 in transport, biofuels only acquired around a 3% share of total global transport fuel demand in 2018 (IEA, 2020b) due to limitations such as raw material supply insufficiency, the low mitigation of CO_2 and low-cost competitiveness (Oh et al., 2018). In order for biofuels to cope with the increasing demand for carbon neutral fuelling options, development in advanced biofuels using inedible biomass looks to be a promising solution.

It is clear that there is no single "silver bullet" solution to decarbonisation of existing transport modes, including long haul transport, aviation and maritime transport, that does not, in turn, have further issues in terms of either public or private financing, raw material availability or technology readiness. While conventional fossil diesel fuel may be eventually banned, starting with the elimination of new diesel passenger vehicles in the United Kingdom in 2030 (Johnson, 2020), engines that currently burn diesel and kerosene are still very likely to be used and needed much further into the future. Indeed, the legacy vehicles purchased before 2030 will still require fuels until they reach their end of life. While this could be fossil-based petrol and diesel, there is an opportunity to introduce alternative fossil-free fuels such as DME to accelerate the de-fossilisation of the passenger transport fleet while EVs become more established.

CRITERIA OF THE FUEL

For a synthetic liquid fuel to be the best option to move freight vehicles to a carbon neutral transport source, it needs to fulfil the 'fuel criteria'. This includes the environmental cost, referring primarily to whether it can be made sustainably in order to make it carbon neutral, but also other environmental factors (such as resource depletion, water use and generation of other pollutants) which must be considered in detailed life cycle assessment. It also refers to whether the fuel itself can be made in a financially viable manner so that the industry can continue to work profitably without continued reliance on substantial government subsidies. Additional criteria include the supply and scope of the new fuel and the reliability of supply. Compatibility with the existing global infrastructure and combustion engines is also essential. Finally, it would be advantageous if it were possible to mix the new fuel with existing fuels. This would allow immediate introduction of the new fuel and therefore an immediate transition towards carbon neutrality. This has the added advantage that it would either comply with existing legislation or fall within the scope of realistically foreseeable future legislation. These criteria are illustrated in **Figure 2**.

Synthetic liquid fuels in this setting work from the principle of defossilisation rather than decarbonisation. This is due to the fuel still being a carbon combustion source. The feedstock material being captured carbon dioxide which is utilised (CCU) or other sustainable carbon resource to synthesise the fuels (Global Alliance Powerfuels, 2020). Defossilisation acknowledges that it is not just carbon atoms being present in the atmosphere which cause dangerous climate change but rather the increase in the overall concentration of the carbon atoms. Thus, it is the carbon atoms derived from fossil sources that need to be prevented from reaching the atmosphere (ETIP PV, 2020). Although during the use phase of using synthetic liquid fuels carbon will be a factored emission in such forms as CO_2 and lesser so carbon particulates within the life cycle of the fuel, the circular nature of CO_2 being both the initial feedstock and final product in the forms of emissions, leads the fuel to have similar inclusive carbon emissions as carbon free fuels such as hydrogen and ammonia. This minimises the environmental concerns. Further environmental concerns coming from conventional fuels can also be diminished. This is because certain liquid synthetic fuels can reduce other emissions such as NOx, whereas carbon-free fuels currently being researched in a dual-fuel capacity show high NOx emissions and unburnt ammonia due to the fuel-bound nitrogen (Dimitriou and Javaid, 2020).

In order to maintain a carbon neutral fuel source, the carbon atoms that are taken away from the atmosphere in the form of the material feedstock need to be equal in number to the carbon atoms released when the fuel is burnt, with no additional fossil carbon used. Subsequently, the energy-intensive processes of synthesising the fuels need to be powered by renewable energy sources, such as wind, solar and hydro. Nuclear fuel, although not considered renewable, is a low-carbon source of energy suitable for clean electricity provision for the production of synthetic fuels. It should also be noted that recent research considered extracting uranium from seawater, making nuclear power a significantly more sustainable and egalitarian energy source (Parker et al., 2018). It has also been suggested that as there is growing demand for renewable energy sources and as the sources are not always constant, the use of excess-energy during low periods of demand can be used to produce synthetic fuels (Luo et al., 2015) rather than being "wasted" by curtailment. In this way the liquid fuels acts as an energy vector that can be stored using existing facilities and infrastructure. This could boost the financial value of the renewable energy source. To determine and demonstrate the true carbon neutrality of a fuel an environmental lifecycle assessment can be used (Zimmermann et al., 2020).

A viable synthetic fuel also needs to a financially sound investment. Here, the variables that contribute into the cost of the fuel are the feedstock materials, production costs and the fuel-to-vehicle transport, otherwise known as the fuelling infrastructure. As previously mentioned, for a synthetic liquid fuel to be financially viable in comparison to other fuelling methods, one main component is that the fuel would be compatible with current pipelines, infrastructure and combustion engines (Willems, 2018).

To be financially viable, the synthesis route also needs to be cost-effective. This may differ depending on the country in which country the fuel is produced. For example, the cost of producing electricity in France is low due to the high use of low-cost nuclear energy sources (Nuclear Power in France | French Nuclear Energy - World-nuclear.org, 2020). If the low cost of nuclear electricity production could be exploited, it could be more realistic for France to use the energy intensive hydrolysis method of hydrogen production. The specific route for the generation of the fuel from sustainable carbon and how that carbon is acquired or captured will be compared in a later section.

Finally, to be the answer to the carbon neutral fuelling crisis, ideally the synthetic fuel would be compatible with current combustion engines as this would mean that current trucks and HGVs could be made carbon neutral by just changing the fuelling source instead of changing the engine or having to build a new fleet of HGVs entirely. This would give an enormous advantage because of the existing fuelling infrastructure. If this is the case, and the new fuel can be mixed with conventional fuels, this allows a gradual transition towards higher concentrations of the low carbon fuel whist the supply line is developed and ramped in scale sufficiently to replace the current supply demands. However, mixing of fuels and using different fuels in existing engines and within existing infrastructure may encounter legislation restrictions which may need to be changed in order to make a smooth and complete legal shift (European Council directive 2018/2001). this will depend on a variety of factors from the degree of blending and the nature of the new fuel to the intended use of the fuel.

TYPE OF SYNTHETIC FUEL CONSIDERED

For the reasons explained above we are interested in fuels that have a possibility of being "drop-in" compatible with diesel combustion engines (the most common in goods vehicles) and which would only require limited retrofitting of existing engines (such as replacing the fuel tank) rather than the development of a completely new engine. Accordingly, we have not focussed on hydrogen directly as a synthetic fuel, because an additional fuel cell or significant change to HGVs' internal combustion engines would be required.

The fuels that best meet most or all of these criteria are dimethyl ether (DME), oxymethylene ether (OME_x) and potentially synthetic diesel through Fischer-Tropsch (FT) reactions. These are considered individually below.

Dimethyl Ether

DME is a liquefied gas that has been identified as a potential diesel fuel replacement. It has a chemical formula of CH_3OCH_3. Its structure is illustrated in **Figure 3**.

Using DME as a fuel significantly reduces NOx output in comparison to conventional diesel engines due to lower flame temperatures and more efficient combustion. Additionally, DME combustion produces far less particulate matter (Pélerin et al., 2020), which is a significant concern in major cities around the world. The lack of particulate matter is due to the absence of C-C bonds in DME, this results in the clean burning and the shorter ignition delay compared to diesel (Kajitani et al., 1997). Rather than C-C bonds, the abundance of C-O bonds leads to a vast reduction in unburnt hydrocarbon fuel exhaust. This is because the extra presence of oxygen in the combustion leads to complete combustion and results in less carbon monoxide and unburnt carbon (soot) being produced. The additional oxygen in the molecular structure also reduces the amount of air required for the same energy output in the engine, which further reduces NOx generation. The particulate yields for DME are 0.013% compared to that of regular diesel (0.026%) or biodiesel engines (0.51%) (Sidhu et al., 2001).

The liquefied gas has a boiling point of −25.05°C. This, in combination with the differences in other physical properties, such as the viscosity and calorific value, means that some changes to a vehicle would be required to make DME a suitable replacement for diesel (Willems et al., 2020). In order to retrofit existing diesel HGVs either low level retrofitting (replacing the tank for on-board blending) or high-level retrofitting (low level plus the additional replacement of the injection system and air path modification) is required; these come at an estimated additional cost to consumers of ≈4 k€/truck or ≈7 k€/truck respectively (INERIS, 2020).

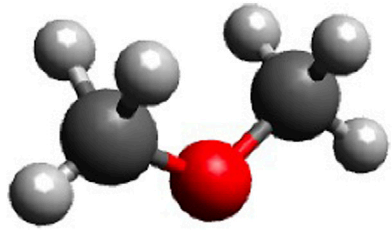

FIGURE 3 | The structure of DME (built in Avogadro, 2021).

TABLE 1 | The comparison between the properties of DME, diesel and methanol can be seen in (Arcoumanis et al., 2008), (Worldwide Fuel Charter Committee, 2019), (Wang et al., 2020), (US deperatment of energy, 2021):

Property (unit/condition)	Unit	Diesel	DME	Methanol
Chemical structure		Av. $C_{15}H_{28}$ Range $C_{12}-C_{20}$	CH_3-O-CH_3	CH_3OH
Oxygen content	Mass%	0	34.8	50
Final boiling point	°C	365	−25.05	64.7
Density at 15°C	kg/m^3	815–850	667	797
Cetane number		>51	>55	5.0
Lower heating value	MJ/kg	43.8	27.6	22.7
Volume required for diesel equivalence	m^3/m^3	1	1.8	2.2

As shown in **Table 1**, DME has a higher cetane number than diesel. This allows it to perform well as a fuel alternative since the low auto-ignition temperature in combination with the low boiling point means that the fuel, once injected into the system, vaporises almost instantly leading to reduced ignition delay and good cold-starting properties (Teng et al., 2001).

However, a consideration for fuel substitution is that due to the lower heating value (LHV) of DME in comparison with diesel, the equivalent fuel volume of DME to diesel is 1:1.8 L proficiently (McKone et al., 2015). Thus, larger fuel tanks are needed to fulfil the same distance requirements, and these fuel tanks must be designed to handle the gaseous fuel. This, along with other vehicle changes such as timing, air fuel mixture ratios and alternative lubrication methods encompass most of the modest modifications required to allow conventional diesel engines to run using DME.

However, while pure DME is not compatible with gasoline or petrol engines that use spark ignition, it can be used in a 30% DME/70% liquified petroleum gas (LPG) ratio, potentially also allowing some non-diesel vehicles to run up to 30% cleaner in terms of CO_2 emissions (IDA Fact Sheet No. 2, 2010).

Although a gas at room temperature, DME has a comparable vapour-pressure interaction to LPG which forms a liquid phase above 0.5 MPa (5 bar). Therefore, DME has similar characteristics to LPG, which is widely transported (Verbeek and Van der Weide, 1997) and so would be compatible with existing transport infrastructure. Additionally, DME can be used as a carbon neutral feedstock for production of olefins using a zeolite catalyst. This provides an innovative mechanism for making carbon neutral polymers and other products that are usually derived from petrochemicals (Galanova et al., 2021).

The colourless DME gas has no negative health effects. Even at high vapour concentrations the human reaction is only that of a small narcotic response (Arcoumanis et al., 2008). Due to historical usage of DME as an aerosol propellent, the safety aspects of DME exposure have been evaluated extensively (McKone et al., 2015).

Dimethyl Ether Efficiency

The basic cycle of carbon-based greenhouses gases and other sustainable carbon sources to produce DME fuels follows CO_2/CH_4 capture and storage from a variety of sources including, but not limited to, power, steel, cement and other industrial plants, landfill sites, waste to gas by anaerobic digestion and potentially air-captured CO_2. The well-to-miles or well-to-wheel cost compares different fuelling solutions and their impact on climate change through greenhouse gas emissions (Semelsberger et al., 2006). DME has shown high well-to-wheel efficiency, demonstrated using a fleet of DME-fuelled Volvo vehicles operating on sustainable feedstocks (IDA Fact Sheet No. 2, 2010). Well-to-tank efficiencies have varying values from various sources as this is dependent on the designation of affecting variables. The higher values of well-to-tank efficiencies come with the assumption of total vehicle efficiency of 40%, with the well-to-tank portion calculated at 27%, whereas a well-to-wheel efficiency of 18% was calculated using conventional technology (Semelsberger et al., 2006). The efficiencies will also change depending on the source of the carbon dioxide.

'Well-to-miles' calculations show a 2% overall change when comparing air as a carbon dioxide source in comparison to biogas in passenger vehicles (Hänggi et al., 2019). Although the well-to-miles efficiency is lower than that in conventional diesel and petrol engines due to the high well-to-tank efficiency of these established processes, DME fuel has an equivalent or higher efficiency than all other alternative transport fuels in the study (Semelsberger et al., 2006). If DME becomes a conventional feedstock, the well-to-tank efficiency would increase as technology is developed and perfected.

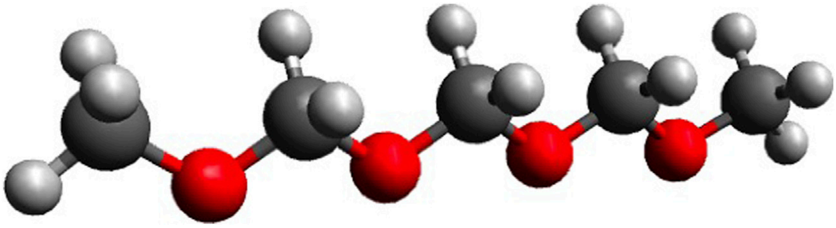

FIGURE 4 | The structure of OME_3 (built in Avogadro, 2021).

TABLE 2 | Comparison of OME_x and diesel properties.

Property (unit/condition)	Unit	Diesel	OME_1	OME_2	OME_3	OME_4	OME_5
Chemical structure		Av. $C_{15}H_{28}$ Range C_{12}—C_{20}	$C_3H_6O_2$	$C_4H_{10}O_3$	$C_5H_{12}O_4$	$C_6H_{14}O_4$	$C_7H_{16}O_6$
Oxygen content	Mass%	0	42.1	45.2	47	48.1	48.9
Final boiling point	°C	365	42	105	156	202	242
Density at 15°C	kg/m^3	815–850	860	980	1,030	1,070	1,110
Cetane number		>51	29	63	67	76	90
Lower heating value	MJ/kg	43.8	22.4	20.6	19.4	18.7	18.1
Volume required for diesel equivalence	m^3/m^3	1	1.77	1.75	1.7	1.7	1.7

Oxymethylene Ethers (OME_x/OME_n)

OME_x are related to DME with the chemical formula of CH_3O-$(CH_2O)_x$-CH_3, x = 1–8 (Ouda et al., 2018). OME_x as DME derivatives have similar properties but a higher molecular mass and boiling points. An example of the chemical structure of an OME_3 molecule is illustrated in (**Figure 4**).

The oligomer length of the OME has a significant effect on the physical properties of the fuel. However, due to the increased length and higher boiling point in comparison to DME, the fuel acts similarly to LPG but has physical, chemical and fuel-properties similar to conventional diesel (Deutsch et al., 2017). The similarities allow conventional diesel supply structures to be used without significant alterations (Oestreich et al., 2018). This allows OME to be a direct replacement for fossil fuels as an immediate "drop in" replacement (Deutz et al., 2018).

OME_x also have no C-C bonds so are clean burning as discussed above in relation to DME. Similarly, precursors for soot such as C_2H_2 are inhibited in the combustion cycles (Sun et al., 2017). Another advantage of minimal particulate matter production is that there is a reduction in fouling in engine parts such as in the exhaust gas recirculation system (Härtl et al., 2017).

As the oligomer lengths affect the fuel properties, the compatibility and suitability of OMEx as a diesel replacement is dependent on oligomer length. Properties of different oligomer length OMEs and a comparison to diesel properties are shown in **Table 2** (Worldwide Fuel Charter Committee, 2019), (Härtl, et al., 2017).

The operating efficiency of a modern diesel engine will decrease if the cetane number is not higher than 51. Therefore, OME_1 is not a viable candidate as a replacement for diesel fuels.

An increase in the length of the oligomer sees a decrease in the lower heating value. The lower heating value determines the rate of flow of fuel required into the engine needed for the defined output energy from the engine. If a fuel has a lower heating value a high volume of fuel is required to meet the same energy output. The increase in density with oligomer length does help combat this issue. The volume of fuel needed for fuel equivalence is 1.7x that of diesel m^3/m^3.

Fischer-Trospch Diesel

Fischer-Trospch (FT) diesel is produced from syngas condensation (CO/H_2) and post-processing to create a synthetic fuel that has a similar long chain hydrocarbon structure to conventional diesel. However, the fuel properties can vary from batch to batch due to the changing of process temperatures, catalysts and feedstock quality (Alleman and McCormick, 2003) with variations that can be used to tailor the fuels to the end-users needs (Gill et al., 2011).

Although very similar to conventional diesel, FT diesel has virtually no sulfur or aromatic hydrocarbons (Abu-Jrai et al., 2006). Although this decreases emissions such as SOx, the sulphur and aromatic contents of conventional diesel provide it with natural lubricity, which is absent in FT diesel. However, this can be rectified by commercial additives (Rodríguez-Fernández et al., 2019). The high cetane number of fuels that can be derived from the F-T process also show a high potential for reducing the NOx/PM trade-off seen in conventional diesel engines (Rounce et al., 2009).

SYNTHESIS ROUTES

Fischer-Tropsch Diesel

FT synthesis is classified into high temperature (310–340°C) and low temperature (210–260°C) reactions (Leckel, 2009). The low temperature and high temperature methods give different compositional outcomes. Low temperature provides a higher cetane number and paraffinic compounds more suitable as diesel fuels. High temperature FT is more suitable as a gasoline substitute. One draw-back to the low temperature product is the lower density than conventional diesel which may lead to a need to reconfigure the fuel injection strategy and hardware (Larsson and Denbratt, 2007). The catalytic FT process to produce diesel fuels is shown in the following reactions:

Syngas production

$$H_2O + CO \rightarrow H_2 + CO_2 \quad (water\ gas\ shift) \tag{1}$$

$$H_2O + CH_4 \rightarrow CO + 3H_2 \quad (steam\ reforming\ methane) \tag{2}$$

FT Process

$$nCO + (2n+1)H_2 \rightarrow C_nH_{(2n+2)} + nH_2O \quad (paraffins) \tag{3}$$

$$nCO + 2nH_2 \rightarrow C_nH_{2n} + nH_2O \quad (olefins) \tag{4}$$

The complete diesel production process, including post-production, is complex with numerous reactors and processes required. This is because direct FT products are a range of carbon numbers requiring upgrading to reach the desired carbon number for a homogenous fuel. This is less of an issue for OME_x fuels due to their limited range of products and even less of an issue for DME production as a single component fuel, which requires a simple distillation.

According to (Becker et al., 2012) and (Hänggi et al., 2019) it takes 80 kJ/mol of electrical energy to transform 1 mol of CO into the desired diesel product. Although only 85% of the initial FT products can be formulated into the desired diesel product (Oscar et al., 2009), the other 15% can be burnt as a heat source for processes such as distillation or the water gas shift reaction. The excess heat provided also provides the thermal requirements for the diesel production process (Hänggi et al., 2019). Due to the additional refining processes in FT synthesis, the well-to-miles efficiency is lower than for DME production. The energy consumed in the production is approximately 25% more (Hänggi et al., 2019) than that of DME (Oscar et al., 2009). On the other hand, FT fuels benefit from the lack of changes to the IC engine and the diesel supply infrastructure. However, these may not be significant enough to establish FT diesel as a more promising fuel for the decarbonisation of HGVs than DME.

Oxymethylene Ether Synthesis

From DME or methanol there are a variety of different synthesis pathways to OME as shown in **Figure 5** (inspired by Baranowski, et al., 2017).

The most common synthesis pathway uses formaldehyde, as shown. However, the additional step required to synthesise formaldehyde, while it can be produced sustainably through partial oxidation of the MeOH (Ouda et al., 2017), decreases the well-to-wheel efficiency. The efficiency and economic viability of the process, no matter what route is taken, is also significantly reduced due to the many energy intensive fractional distillation processes required to separate the OMEs in order to make a fuel of equivalent compositions (Lautenschütz et al., 2016).

$$2MeOH + FA \overset{H^+}{\rightleftharpoons} OME_1 + H_2O \tag{5}$$

$$OME_{n-1} + FA \overset{H^+}{\rightleftharpoons} OME_n \tag{6}$$

$$HF_n + MeOH \overset{H^+}{\rightleftharpoons} OME_n + H_2O \tag{7}$$

Due to the increased complexity of the process and due to the required separation processes, OME synthesis has a lower exergy efficiency and a lower total fuel energy obtained from the same amount of CO_2 and H_2 in comparison to other synthetic fuels such as DME. However, it is comparable on this basis to that of FT diesel (Burre et al., 2019). Thus, unless and until further research and development leads to increased efficiency of the precursor of OME, DME appears to be a more efficient energy source.

Dimethyl Ether Synthesis

Dimethyl Ether From CO_2

DME can be synthesised from CO_2 via two main routes. By Route 1 it can be synthesised through the formation of syngas in the reverse water gas shift reaction (RWGSR) where it is then converted to DME through direct or indirect synthesis. Route 2 involves the synthesis of DME directly from CO_2. **Figure 6** shows a selection of potential routes to produce sustainable DME from a variety of sustainable carbon sources, with the key ‘steppingstones’ of most pathways, namely syngas and methanol, highlighted in green. This gives considerable scope for process development and new chemistries.

The Korean institute of Science and Technology developed a reactor sequence using the formation of syngas. It claimed that the reduction in the size of the methanol synthesis reactor

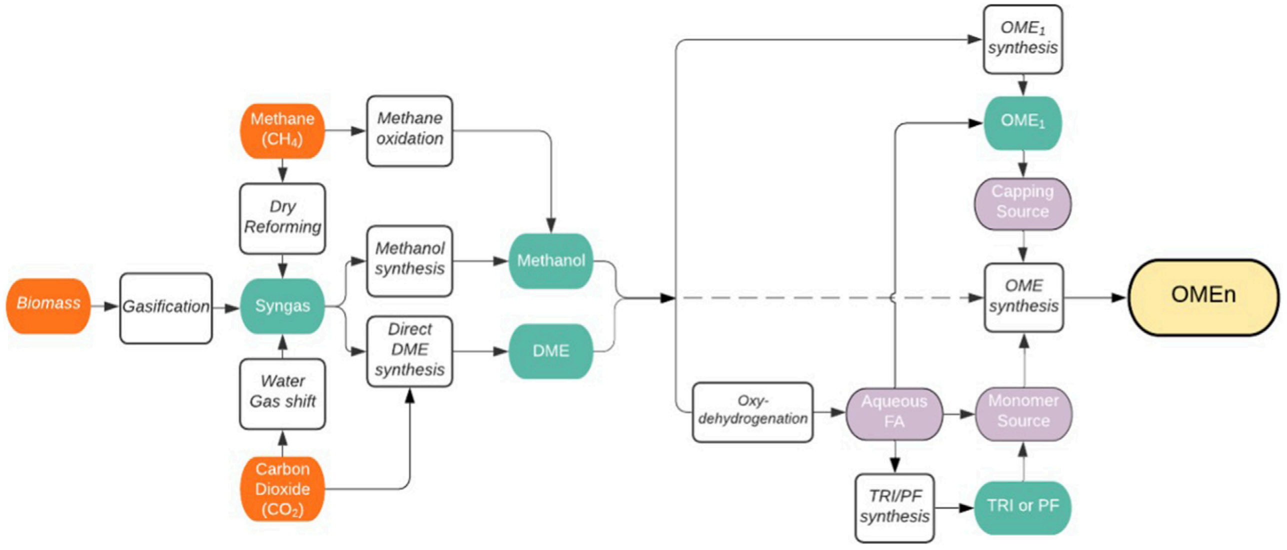

FIGURE 5 | Liquid phase synthesis of polyoxymethylene dimethyl ethers (OME) via methanol (derived from various sources) and DME. The depicted routes and reactants have been reported to be used for the production of OME_n with n > 1: OME_1 = dimethoxymethane, TRI = trioxane, PF = paraformaldehyde, FA = formaldehyde, DME = dimethyl ether.

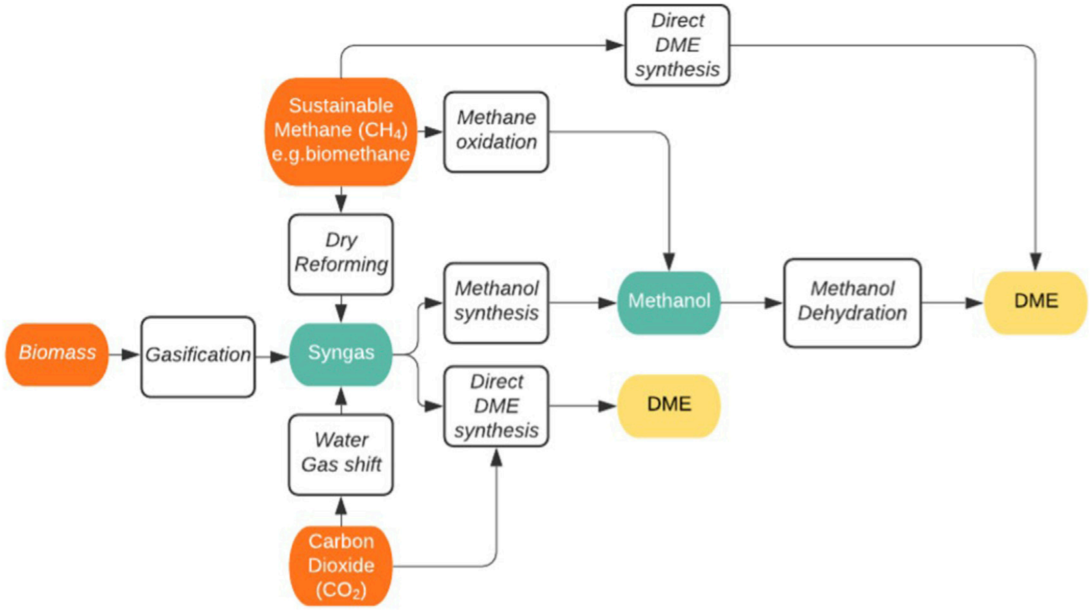

FIGURE 6 | Synthesis of DME using different carbon feedstocks.

and the increased efficiency in the production of methanol in this reactor led to the two-step procedure being the optimal method (Joo et al., 1999; Goeppert et al., 2014). Although the water produced during CO_2 hydrogenation limited the formation and dehydration of methanol, thus resulting in a lower DME yield in comparison to CO (Azizi et al., 2014), more recent studies show that the higher oxidation power of CO_2 in comparison to CO positively affects the active state of the catalyst for methanol formation, thus increasing the methanol yield, making it an equally viable pathway (Centi and Perathoner, 2013).

Evaluation of intermediate syngas production is not within the scope of this review. However, DME synthesis from CO_2 without syngas can also be categorised into a single-step process (direct synthesis) or a two-step process (indirect synthesis) (Asthana et al., 2016). The basic principle of DME formation from CO_2 is hydrogenation of CO_2 to form methanol then the dehydration of methanol to form DME. In the indirect process two reactors and two catalysts are used, whereas in the direct process a single reactor and a bifunctional catalyst is used; the bi-functional catalyst carries two active sites, one for methanol formation and one for dehydration (Álvarez et al., 2017). The reactions for the formation of DME from CO_2 are the hydrogenation of CO_2, the reverse water gas shift reaction and the dehydration of methanol:

$$CO_2 + 3H_2 \rightleftarrows CH_3OH + H_2O \quad -49.5\text{kJ}/\text{mol}_{CO_2} \tag{8}$$
$$CO_2 + H_2 \rightleftarrows CO + H_2 \quad +41.2\text{kJ}/\text{mol}_{CO_2} \tag{9}$$
$$CO + 2H_2 \rightleftarrows CH_3OH \quad -90.6\text{kJ}/\text{mol}_{CO} \tag{10}$$
$$2CH_3OH \rightleftarrows CH_3OCH_3 + H_2O \quad -23.4\text{kJ}/\text{mol}_{DME} \tag{11}$$

The combination gives the overall rection:

$$2CO_2 + 6H_2 \rightleftarrows CH_3OCH_3 + 3H_2O \tag{12}$$

In indirect synthesis, as methanol is synthesised separately and requires purification before the DME synthesis in a separate reactor, the economic viability of methanol production compared to DME is the main issue (Takeishi and Akaike, 2016). The dehydration/condensation of methanol to produce DME as a distinct step is discussed later. For the direct synthesis of DME using a ‘one-pot’ method, referring to simultaneous CO_2 hydrogenation and methanol dehydration, the bifunctional catalyst requires a redox function to catalyse the CO_2 and an acidic function to convert methanol to DME (Álvarez et al., 2017). The direct synthesis is theoretically more efficient and economical than the indirect method due to the reduction in process complexity and the thermodynamic equilibrium limitation of methanol synthesis decreasing by the consumption of methanol in the dehydration reaction. This moves the equilibrium in the forward direction (Vakili et al., 2011; Catizzone et al., 2017). As a result, the methanol purification unit required by indirect synthesis can be discarded as only one reactor is required in direct synthesis (Mollavali et al., 2008) and higher DME selectivity can be achieved (Aguayo et al., 2007).

The bifunctional catalyst historically used for DME synthesis is made up of $CuO/ZnO/Al_2O_3$ (CZA) for the CO_2 hydrogenation and has been proven to be highly active (Ali et al., 2015) working alongside a solid acid catalyst HZSM-5 or γ-Al_2O_3 for the methanol dehydration to DME (Ren et al., 2019). As one of the key features that limits the effectiveness of bifunctional catalysts is the water production from the use of CO_2 instead of CO, recent research has been conducted to improve the stability of the hydrogenation catalyst. Zirconium modified

CZA catalysts (Ren et al., 2020) and zeolite surface interaction with CuO-ZnO-ZrO_2 (Bonura et al., 2020) have both been shown to increase the stability of the catalysts with significant improvements on catalytic stabilities being recorded.

Thermodynamic Considerations

According to Le Chatelier's principle and equations, using a lower temperature and higher pressure should promote the formation of the desired products as the exothermic nature of both methanol and DME production favour lower temperatures, whilst the endothermic nature of the reverse water gas shift reaction favours higher temperatures and is independent of pressure. As DME is synthesised with methanol as an intermediary product, the thermodynamic profiles are closely related with, as previously mentioned, the limitation of the CO_2 conversion being removed by carrying out the methanol dehydration within the same catalytic system. Although the formation of olefins is possible in the production of DME from CO_2, these can be minimised by optimising the catalysts (Catizzone et al., 2017) and shortening the residence time in the reactor (Moulijn et al., 2013) and therefore are not taken into thermodynamic consideration.

Thermodynamic profiling by (Shen et al., 2000) show that the combination of methanol synthesis and dehydration to DME indeed gave a consistently higher CO_2 equilibrium conversion than the singular CO_2 hydrogenation to methanol process. Kinetic modelling of this process (Aguayo et al., 2007; Qin et al., 2015) concluded, that the rate-determining step in DME synthesis was the methanol synthesis. Use of a Gibbs free energy minimisation approach verified this and supported Le Chatelier's principle, concluding that CO_2 conversion and DME selectivity also increases with increasing total pressure (Ahmad and Upadhyayula, 2018). Although CO_2 conversion increases with temperature above 350°C, this signifies the move from equilibrium to kinetics controlling state of reaction completion. As a result of these competing influences, complete conversion to DME is close to impossible and there will always be a mixture of methanol and DME at equilibrium, meaning a separation process will always be required (Stangeland et al., 2018).

Dimethyl Ether From Methane

Rather than using CO_2 as the direct source of the carbon for the DME, sustainably derived methane can alternatively be reformed or oxidized to form syngas or methanol respectively as shown previously in **Figure 6**. Either product can then be used to derive the DME fuel. The sustainably derived methane is generated by two main routes, anaerobic digestion or the Sabatier reaction of waste organic material, which will naturally in turn have been generated from photosynthetic air-captured CO_2 at some point in the past. The Sabatier route involves the gasification of carbon-rich resources to generate pyrolysis gases; CO_2, CO, H_2, CH_4 and hydrocarbons, that can be further converted to commercially useful grades of methane using hydrogen and nickel-based catalysts (Sabatier and Senderens, 1902). The reactions are typically carried out at elevated temperatures and pressures (400°C and 30 bar) and proceed *via* complete hydrogenation of the carbon-species present:

$$CO_2 + 4H_2 \rightleftarrows CH_4 + 2H_2O \quad + 165\text{kJ/mol} \tag{13}$$

$$CO + 3H_2 \rightleftarrows CH_4 + H_2O \quad + 206\text{kJ/mol} \tag{14}$$

Side reactions typically include the generation of short hydrocarbon chains and elemental carbon.

A small number of plants using this principle have been operating for decades, converting coal into synthetic natural gas. Nevertheless, only one remains (in Beulah North Dakota) as low-cost shale gas has grown to dominate the non-sustainable fossil fuel market for natural gas (Kopyscinski et al., 2010; De Simio et al., 2013). New opportunities in this area remain, such as the possibility of using sustainable waste carbon resources like woodchip and other biomass which allow for the generation of renewable natural gas as a distinct product that can be immediately injected into the local national grid (Uchida and Harada, 2019; Vogt et al., 2019). By contrast, methane production from anaerobic digestion is widespread and typically carried out in individual small-scale digesters and on-site generation in suitable locations, particularly landfill sites. In the US in 2020, the total production of renewable natural gas via anaerobic digestion reached approximately 1.2 Mt (Mintz and Voss, 2020). The methane produced through anaerobic digestion, by contrast to that produced in the Sabatier reaction, is typically mixed with significant quantities of CO_2 and has a high water content. However, biogas drying and sweetening either by removal of this (originally biogenic) CO_2 (Aepli et al., 2020) or by further conversion of that CO_2 to more methane using renewable energy sources (Cave, 2020) is a developing industry.

While it may initially seem to be a circuitous route to generate DME from CO_2-derived methane, given that methane is in a lower oxidation state than the DME, the potential benefit of using methane as an intermediate may be practical. For example, methane is readily transported by the existing natural gas pipeline networks in most developed economies. Furthermore, existing, highly developed and commercialised processes such as those used for drying natural gas, can be used directly. The initial cost-savings of being able to use this existing infrastructure have been discussed previously and it holds significant benefit, avoiding the necessity of the generation of a new fuel transport infrastructure. The sustainable methane, delivered *via* pipeline, could then be converted into DME at the desired site, allowing flexible development of the technology by separation of the direct or indirect CO_2 utilisation from the fuel production. Once there is a supply of sustainable methane, it may be partially oxidized to methanol or syngas and then converted into DME as detailed previously, or even directly converted into DME by other means. For either partial oxidation route, selectivity to the desired product can be controlled by the reaction temperature. High reaction temperatures favour the production of syngas, whereas lower reaction temperatures promote the formation of methanol (Khirsariya and Mewada, 2013). However, the low reactivity of methane also makes the activation of the selective oxidation route challenging at low temperatures, resulting in a trade-off between reaction rate and selectivity to methanol. Supported copper-based catalysts have however shown promise, especially with water included or even used as the oxidant (Shi et al., 2018; Koishybay and Shantz, 2020).

Once the methanol is obtained, the formation of DME is carried out over a variety of acidic solid catalysts at 200–300°C and typically gives DME in high yield and selectivity through methanol dehydration. Example catalysts include supported iron and copper oxides and copper/zinc/zirconica catalysts, typically used in CO_2 hydrogenation to methanol (Armenta et al., 2020). These catalysts can approach the maximum theoretical yields and selectivities for the reaction, which are limited by the presence of water (Migliori et al., 2020). Methane partial oxidation or reforming into syngas is a highly active area of research, both for hydrogen production and for further chemical synthesis, *via* syngas, from methane sources. The former is usually carried out by steam reforming, generating three molar equivalents of hydrogen per molecule of methane, with an additional molecule of hydrogen available from RWGS in tri-reforming. The latter route, where syngas with a lower hydrogen concentration is desired, can be achieved through dry autothermal reforming, which uses further carbon dioxide with the methane at high temperatures to generate 1:1 syngas.

$$CH_4 + H_2O \rightleftarrows 3H_2 + CO \quad \text{Steam Reforming} \tag{15}$$

$$CH_4 + 2H_2O \rightleftarrows 4H_2 + CO_2 \quad \text{Tri Reforming} \tag{16}$$

$$2CH_4 + O_2 + CO_2 \rightleftarrows 3H_2 + 3CO + H_2O \quad \text{Autothermal Reforming} \tag{17}$$

This is carried out using a wide variety of catalysts, typically including supported nickel but also iron, calcium, zinc and cerium-based catalysts (Gao et al., 2020a; Ugwu et al., 2020; Dang et al., 2021; Shah et al., 2021) among others. Along with this variety of catalysts, a wide variety of conditions are also used with temperatures ranging from 550°C to 2,000°C, however very high yields (>95%) and selectivities (>95%) are typically achieved. The subsequent conversion of syngas to DME proceeds as detailed in the previous section on the direct route for DME from CO_2.

Finally, it is also possible to use methane as a direct precursor, rather than as a syngas or methanol source. This involves the activation of methane using a halogen radical to generate the methyl halide, followed by a precious-metal catalysed hydration-dimerisation process. Of note here is the potential for a low-temperature route to DME, with the hydration-dimerisation of methyl bromide to DME shown to occur with good yield and selectivity at just 150–180°C using a simple ruthenium catalyst (Xu et al., 2005). While the initial bromination step in that research required temperatures of 530–560°C, which were achieved through self-heating by partial methane combustion, the dimerization process could also be fuelled by low temperature methane halogenation through photochemical, electrochemical or even mechanochemical means, where a chlorine-rich substrate is milled in the presence of methane to selectively generate methyl chloride at temperatures below 150°C (Bilke, et al., 2019). Indeed, this route has been recently demonstrated for an electrochemical methane-to-methanol conversion at 130°C and 46.5 bar CH_4 over platinum which proceeds *via* a methyl chloride intermediate in a similar fashion (Kim and Surendranath, 2019).

HYDROGEN SOURCES

In order for these synthetic routes to be truly carbon neutral, the hydrogen sources also need to be derived from non-fossil sources. These sources include thermochemical water decomposition (Mehrpooya and Habibi, 2020), water electrolysis and biomass gasification (Badwal et al., 2014) as shown in **Figure 7**. As mentioned earlier, any energy required in the production of hydrogen and the synthesis of the DME must also be derived from non-fossil, renewable energy sources. The synthesis of DME from CO_2 requires the addition of hydrogen, as six hydrogen molecules are required for every two molecules of CO_2 to produce one molecule of DME. The highest heating value for H_2 is 142 MJ/kg (Chen et al., 2011), which compares well with other known fuels and is why it is seen as not only a feedstock for making other synthetic fuels but as a potential fuel itself.

As mentioned previously, in order to ensure that the DME produced is carbon neutral the source of the hydrogen and any electricity/heat energy used in the production must come from renewable sources (Kothari et al., 2008). This means that conventional hydrogen production from heavy hydrocarbons, coal gasification and fossil natural gas steam reforming cannot be considered, as CO_2 is the largest emission from the process (Kothari et al., 2004). With only 5% of hydrogen currently being produced by sources other than natural gas and coal (IRENA, 2019) and the leading practice being electrolysis of water, which is also the most energy consuming route (Holladay et al., 2009), it is necessary to look at other methods such as producing hydrogen from biomass and to compare their efficiencies.

It can be seen that water is always crucial for hydrogen generation, however, in many of these cases a very high purity of water is required for good conversion yields (Gandia, et al., 2013). Since globally clean water is an 'under-pressure resource', especially in arid areas which also contain solar primary energy resources (Saleth and Dinar, 2004), the location and distribution of any putative large scale sustainable hydrogen production requires serious consideration.

Hydrogen From Water

Water splitting or cracking to produce hydrogen is completed through three predominant methods; electrolysis, thermolysis and photo-electrolysis. The simple base principle is water is divided into its individual components; oxygen and hydrogen—requiring either free energy or high temperatures (Kothari et al., 2004). The basis of water electrolysis is the movement of ions promoted by an external circuit through an electrolyte to promote the splitting of water in an electrolysis cell (electrolyser) (**Eq. 20**) (Bhandari et al., 2014). In the electrolyser,

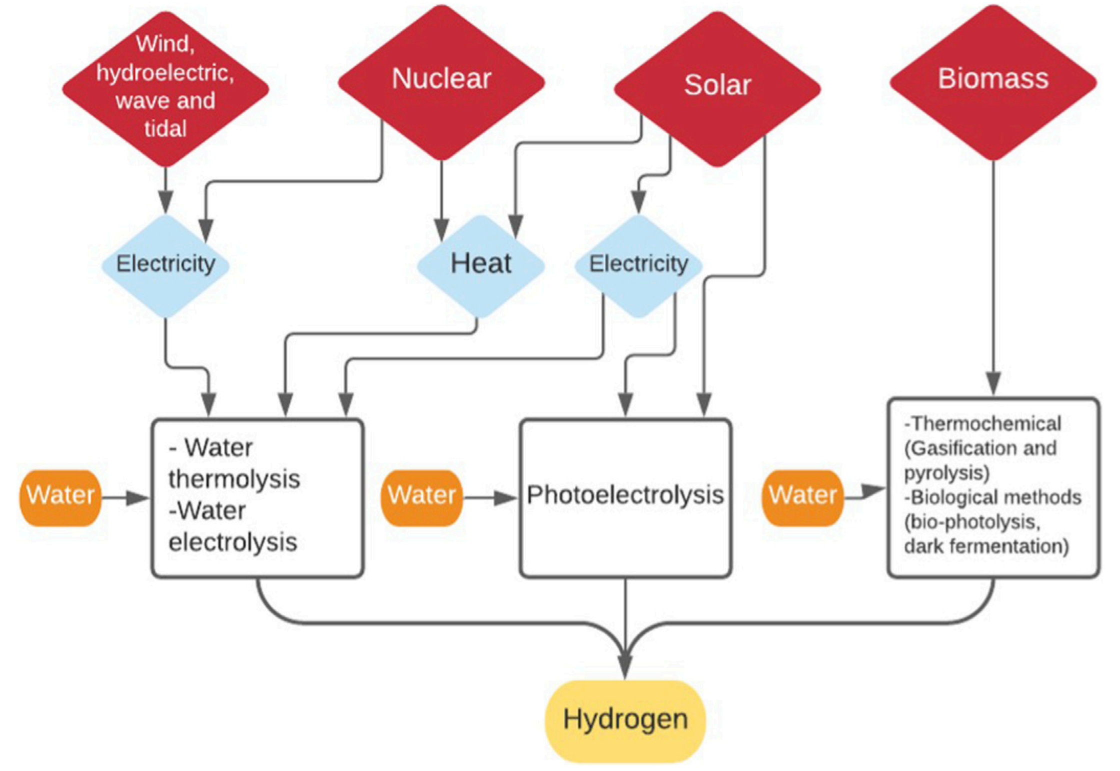

FIGURE 7 | Various routes for the sustainable (or low-carbon) production of hydrogen

two electrodes are placed in the water thus facilitating the external circuit and the formation of ions/electrons on either electrode:

$$Cathode: 2H_2O + 2e^- \rightarrow H_2 + 2OH^- \quad (18)$$

$$Anode: 4OH^- \rightarrow O_2 + 2H_2O + 4e^- \quad (19)$$

$$Overall: H_2O + direct\ current\ electricity \rightarrow H_2 + \frac{1}{2}O_2 \quad (20)$$

There are different types of electrolysis cells, such as polymeric electrolyte membrane electrolysers, alkaline electrolysers and solid oxide electrolysers among those in production and development. Although similar in their goal they use slightly different methods, catalysts and materials to try to formulate the most efficient and cheapest process, whilst also achieving the purity of hydrogen required. As low-temperature water electrolysis can take advantage of relatively low space requirements and exploiting the existing infrastructure for the electricity and water use, it can rapidly be added to an existing plant (FreedomCAR and Fuel Partnership, 2009). The downside of water electrolysis is its efficiency of 60–80% (Shiva Kumar and Himabindu, 2019) and the high capital cost due to catalyst/membrane poisoning depending on the water source and the low hydrogen evolution rate compared to the high energy consumption, especially prevalent if sea water is used (Shi et al., 2020). This means its economic compatibility is low. The energetic efficiency (energy obtained from the hydrogen fuel per unit of electrical energy required) is around 56–73% (Turner et al., 2008). In 2008, the cost of producing sustainable hydrogen to reach an equivalent fuel price to that of fossil-derived hydrogen required access to electricity prices as low as \$0.045-\$0.055 kWh^{-1} (Turner et al., 2008), no transportation of energy costs to be included, and the hydrogen being produced at a local wind power site as the primary energy source.

Water electrolysis requires 47.99 kWh per kg H_2 (Martínez-Rodríguez and Abánades, 2020). This is around four times higher than the energy required to produce hydrogen through steam reforming. Although research and development are leading to more energy efficient electrolysers, this still proves a barrier to an economically viable production method.

Thermolysis is the direct one-step method of decomposing water into its constituent molecules governed by homogenous kinetic mechanisms (da Silva Veras et al., 2017).

$$H_2O + heat \rightarrow H_2 + \frac{1}{2}O_2 \quad (21)$$

In order to achieve the thermal decomposition, the temperature needs to reach over 2,500 K (Dincer and Acar, 2015), which theoretically allows a >4% dissociation level at atmospheric pressure (Baykara, 2004). This increases at even higher temperatures, with 64% dissociation achieved at 3,000 K and 1 bar, (Dincer and Acar, 2015). As this is a reversible reaction, the recombination of the end products needs to be avoided. Common methods include rapid cooling of the gaseous mixture through direct contact with cold fluid (Lede et al., 1982). Having temperatures in both extremes increases the running cost of the facility thus increasing the cost of the hydrogen produced. In order not to require extreme cooling, the use of palladium membranes can be used to avoid the recombination of H_2 and O_2 (Dincer and Acar, 2015).

In order to obtain the high temperature required for this process, the renewable energy sources need to be evaluated. However, the scaling up of the process is believed to increase thermal efficiency (Holladay et al., 2009). The only renewable energy or low carbon sources currently generally capable of producing the heat required for this process are nuclear energy and concentrated solar power providing high temperature steam (Dincer and Acar, 2015; Dincer and Safari, 2020). The overall efficiency of the process is dependent on the renewable energy source and can vary between 17–45%, with a nuclear heat source providing a higher overall efficiency than a solar heat source (Nikolaidis and Poullikkas, 2017). As heat energy and electrical energy are not equivalent, with 1 J of electrical energy being equal to around 4 J of heat energy a kWh per kg H_2, comparison is not effective. However, comparisons based on cost of the hydrogen produced can be made at 2.17–2.63 United States $ per kg H_2. If it were decided to incorporate a hydrogen production plant into the DME production plant instead of outsourcing the hydrogen production, the excess heat released from the exothermic DME synthesis reactions could, in principle, contribute towards the heat require for thermolysis.

Photo-electrolysis or the photoelectrochemical (PEC) splitting of water, uses the absorption of photons from sunlight to directly decompose water on irradiation, using semiconductors. An advantage of the PEC cell is that it combines the water electrolysis and solar energy absorption into a single monolithic device (Chaubey et al., 2013; Dincer and Safari 2020).

$$H_2O + photons + electricity \rightarrow H_2 + \frac{1}{2}O_2 \tag{22}$$

The basis of PEC is that a photoelectrode absorbs photons from solar irradiation with enough energy to excite the electrons from the valence shell to the conduction band (Yang et al., 2017). The semiconductor is immersed in a water-based electrolyte where the energy released when the electrons return to the valence band is used to energise the water and facilitate the hydrogen production as water is split on the semiconductor surface (Turner et al., 2008). Depending on the conductor material, the density of the electric current produced varies between 10 and 30 mA cm^2 of the semiconductor. This facilitates a lower voltage requirement that leads to higher efficiencies (Christopher and Dimitrios, 2012). A minimum energy of 1.36 eV is required to split a water molecule and, including the electron transfer induced losses, a photon of 1.6–2.4 eV is required to be absorbed for effective photo-electrolysis (Roger, Shipman and Symes, 2017). This corresponds to wavelengths within the visible light spectrum, thus providing a potentially reliable energy feedstock and electrolysis efficiency levels reaching 91% (Christopher and Dimitrios, 2012). The overall hydrogen production efficiency of 10–12.4% (Turner et al., 2008; Christopher and Dimitrios, 2012) is promising for future production possibilities, with this efficiency level in 2007 corresponding to only requiring 4,000 square miles of photoreceptors for the entire United States vehicle fleet.

Hydrogen From Biomass

The two major categories of hydrogen production from biomass are thermochemical technology routes [which include gasification and pyrolysis (Zhang, 2010; Sanna, 2013)] and biological treatments [which includes bio-photolysis and fermentation (non-exclusively) (Levin, 2004)]. The thermochemical conversion of biomass to hydrogen is the most advanced and established technological production method (Lepage et al., 2021). Lignocellulosic biomass is the main feedstock for these processes, although it is currently expensive to produce, thus contributing to the higher production cost of hydrogen from thermochemical biomass. There is an indication that these prices will reduce in the future as a result of the environmental policy price impact on fossil resources (Fiorese et al., 2014). As the hydrogen content of biomass is only 6–6.5% depending on the feedstock, in comparison to 25% in natural gas (Kothari, et al., 2004), previously there has not been economic reason to make the swap to biomass. However, reduction in net CO_2 makes this a feasible production option.

Biomass gasification is a mature technology which adopts the same principles as coal gasification. Gasification and pyrolysis are related processes where the thermochemical conversion of solid biomass fuel into syngas uses steam, oxygen or air as a medium for gas generation at a level lower than that required for full stoichiometric combustion (Holladay et al., 2009; Sansaniwal et al., 2017). Gasification is a highly endothermic process, operating at temperatures between 500–1,400°C and from atmospheric pressure up to 33 bar depending on plant scale, type of reactor, initial feedstock material and the function of the syngas produced (Iribarren et al., 2014). Within biomass gasification, the biomass mass goes through three phases: drying, pyrolysis and reduction (Lepage et al., 2021). The gasification reaction can be achieved using air, oxygen and oxygen enriched air.

It is possible for a biorefinery to stop processing the biomass after pyrolysis producing three products; syngas, bio-oils and char. This allows the products to be separated and used for multiple end products such as such as the products of light olefins from the catalytic cracking of bio-oil (Arregi et al., 2018). However, as the required output is the hydrogen, for maximum biomass to hydrogen efficiency, full gasification must take place. Although hydrogen is a direct product of gasification, in order for the maximum hydrogen content to be extracted from this process, thus making it more efficient, the syngas received from gasification then goes through a water gas shift reactor to obtain the maximum hydrogen possible (Holladay et al., 2009).

Any excess products can be burnt as a cheap source of electricity or heat. This contributes to the lower cost of hydrogen production of 1.21–3.5 United States $/kg H_2 (Lepage et al., 2021), depending on the feedstock, scale of production, catalyst and methods used. Efficiencies can vary from 30–70% based on the LHV (Binder et al., 2018).

Biological treatments or processes are methods to produce hydrogen which depends on the use of enzymes to catalyse hydrogen formation (Levin, 2004). The biological treatments can be spilt into the biological splitting of water (direct and indirect bio-photolysis) and the fermentation of biomass to produce hydrogen. In comparison to the thermochemical biological methods to produce hydrogen, biological treatments tend to operate at atmospheric pressure and temperatures between 30–60°C (Lepage et al., 2021). Taking account of the ability of the microorganism to be regenerated by replication (Henstra et al., 2007) reduces the catalyst turnover resulting from degradation in high temperatures through thermochemical processes.

Bio-photolysis

Bio-photolysis utilises the photosynthetic abilities in green algae or cyanobacteria in a method adapted for the generation of hydrogen gas instead of carbon containing biomass (Kothari et al., 2004). The process is split into two methods direct and indirect photolysis. Direct bio-photolysis is the process of green algae splitting water via photosynthesis into a hydrogen ion and oxygen, using the ability of the algae to transform solar energy into chemical energy (Melis et al., 2000). The reaction is governed by two photosynthetic systems PS I and PS II (**Figure 8**). These systems harvest light energy under anaerobic conditions, transferring H_2O electrons to ferredoxin (Kim and Kim, 2011). The hydrogenase enzyme then catalyses the reaction of the reduced ferredoxin acting as an electron donor providing an electron to the hydrogen ion, forming hydrogen gas (Eroglu and Melis, 2011). This can be categorised in the following reaction scheme (Bičáková and Straka, 2012):

The major disadvantage of this system for producing hydrogen is that in order for the hydrogenase to function efficiently, anaerobic conditions are required as it is very sensitive to oxygen (Prince and Kheshgi, 2005). However, the reaction also produces oxygen as a product so maintaining complete anaerobic conditions is a priority for researchers. Research is on-going to increase the yield of hydrogen by depleting the production of oxygen, however current methods such as the addition of a sulphate solution also supresses hydrogen production (Williams and Bees, 2013). Progress has been made with recent research leading to an increase in light utilisation energy from 5 to 15%, with further room for improvement possible by increasing the scale of the algal bioreactors (Show et al., 2011). As the process does not require vast amounts of electricity, the price of the hydrogen produced is around 2.13 \$/kg H_2 (Hallenbeck and Benemann, 2002; Kayfeci et al., 2019) this is comparable to some fossil-based methods, however production on a large scale remains a barrier to mass rollout.

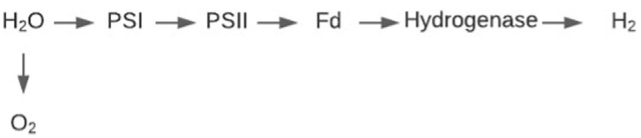

FIGURE 8 | Photosynthetic reaction scheme for bio-photolysis hydrogen production.

Indirect bio-photolysis is sometimes also referred to as aerobic dark fermentation as it consists of two major steps. The first comprises of the photosynthesis of cyanobacteria to produce glucose in a conventional manor. The second, involves the aerobic dark fermentation of the glucose to produce hydrogen as seen in **Eqs 23**, **24** (Chaubey et al., 2013):

$$6H_2O + 6CO_2 + photons \rightarrow (C_6H_{12}O_6)_n + 6O_2 \tag{23}$$

$$(C_6H_{12}O_6)_n + 12H_2O + photons \rightarrow H_2 + 6CO_2 \tag{24}$$

The reactions are catalysed by both hydrogenase and nitrogenase, as cyanobacteria are capable of fixing atmospheric nitrogen (Benemann, 2000). Cyanobacteria are the ideal candidates for this process with a maximum of 16.35% light efficiency (Prince and Kheshgi, 2005), however in practice efficiency is only 1–2%, so further development is required before this process can become commercially viable (Chaubey et al., 2013). Although the low efficiency leaves this method in its conceptual phase, calculations have been carried out which place the price of hydrogen needed to make the processes economically viable at 1.42 \$/kg of H_2 (Hallenbeck and Benemann, 2002; Kayfeci et al., 2019).

Dark Fermentation

Dark fermentation is the process of producing hydrogen through anaerobic bacteria being grown on carbohydrate rich substrates without accesses to light (Levin, 2004; Ghavam et al., 2021). It requires temperatures between 25°C and 80°C (Lepage et al., 2021) depending on the strains. The products of this process are mostly CO_2 and H_2 with other gas products being released such as CH_4 and H_2S. The combination of products and their ratios depends on the quality of the substrate used. Due to the production of other products, the H_2 yield is lower than that of bio-photolysis, thus contributing to the lower efficiency of the process (Soares et al., 2020). Glucose could be an ideal feedstock, however due to its high price it makes the process uneconomical. Lignocellulosic biomass has been identified as a promising feedstock although the requirement of pre-treatment increases the price of the hydrogen required to make the process economically viable (Soares et al., 2020). The amount of hydrogen produced also depends on the pH of the fermentation atmosphere with the maximum hydrogen yields occurring at a pH of 5–6 (Fang and Liu, 2002).

Dark fermentation has significant advantages such as being a light independent. It does not require large land use (such as those depending on solar energy), it can capitalise on being able to use a multitude of different feedstocks and it has high rates of hydrogen production unsurpassed by other biological processes (Chaubey et al., 2013; Soares et al., 2020) with values ranging from 184 to 2,710 ml hydrogen $L^{-1}h^{-1}$ reported (Turner et al., 2008). Dark fermentation has a biomass conversion efficiency of 60–80% assuming that the maximum yield of glucose as a feedstock is catabolised (Kovacs et al., 2006), which contributes to a hydrogen cost of 2.57 \$/kg Nikolaidis and Poullikkas, 2017).

The optimal hydrogen source for DME production will vary depending on the location of the plant, the availability of the feedstock and the price and availability of the primary energy source. This can change depending on location, for example (as

TABLE 3 | Hydrogen cost as a function of different processes (Kayfeci et al., 2019; Nikolaidis and Poullikkas, 2017; Kayfeci et al., 2019 and Lepage et al., 2021).

Process	Energy source	Feedstock	Hydrogen cost $/hg
Water electrolysis	Wind	Water	5.89–6.03
	Nuclear	Water	2.35–7.0
Thermolysis	Solar	Water	2.17–2.63
	Nuclear	Water	7.98–8.40
Photo electrolysis	Solar	Water	10.36
Biomass gasification	Internally generated steam	Biomass	1.21–3.5
Direct bio-photolysis	Solar	Algal biomass + water	2.13
Indirect bio-photolysis	Solar	Algal biomass + water	1.42
Dark fermentation		Organic biomass	2.37–2.80

explained above) France produces a lot of low-carbon electricity due to their vast nuclear programme. Producing hydrogen through water electrolysis from a nuclear source will be cheaper as the sustainable electricity is cheaper. The hydrogen sources discussed in this review are non-exhaustive and are meant to provide a brief overview. Comparisons can be seen in **Table 3**.

CARBON CAPTURE AND UTILISATION TECHNOLOGIES

In order to access CO_2, vital as the required feedstock for DME synthesis, it initially needs to be captured, compressed and transported from CO_2 point sources. As global political pressure regarding CO_2 output has increased on energy and industrial processes, there has been increased research and implementation of carbon capture and storage (CCS) technologies. This involves the selective removal of CO_2 from gas streams, after which it is then compressed and transported to geological storage solutions such as exhausted natural gas reservoirs and saline aquifers, where in principle the CO_2 can be stored for geological periods, instead of adding to the growing atmospheric concentration (Al-Mamoori et al., 2017). However, in spite of government subsidies, the high costs of CCS (with 75% of the total cost coming from the primary capture and compression of the CO_2) have inhibited large scale industrial roll-out. Therefore, Carbon Capture and Utilisation (CCU), where the CO_2 is used as a feedstock after capture and possibly compression and can be used by the industrial and energy sector as a valuable product instead of an expensive waste; a concept that makse it a much more attractive alternative (Styring et al., 2011; Styring et al., 2014; North and Styring, 2019a; North and Styring, 2019b).

The industrial sector accounted for almost 40% of global CO_2 emissions in 2018 (after allocating electricity and heat emissions across final sectors) (IEA, 2020a). This makes the industrial sector the prime location to install CCU technologies for the production of CO_2 as a valuable feedstock, along with fossil-fuel power plants (Markewitz et al., 2012). As well as offsetting CO_2 emissions by utilising the CO_2 for chemical synthesis of other products, in this case DME, it has been suggested that CCU can further reduce the emissions by forgoing conventional production strategies. For example, the use of 1 kg CO_2 for the production of CO_2-based polymers can overall reduce emissions totalling 3 kg CO_2 when compared to the non-CCU route (von der Assen and Bardow, 2014; Kätelhön et al., 2019). Michailos et al. (2019) have also considered the techno-economics of integrated carbon capture and DME production in the context of a positive life cycle impact.

Generally, there are three main methods for CO_2 capture from industry; pre-conversion/combustion, post-conversion/combustion and oxy-fuel combustion (Kanniche et al., 2010). These can be seen in **Figure 9**, adapted from Cuéllar-Franca and Azapagic, (2015):

Post-combustion carbon capture involves the separation of CO_2 from the waste gas stream after the combustion of the carbon source, or conversion of the carbon source in the formation of the target product, e.g. energy or steel. When used in power plants, the process is known as post-combustion capture, however when used in industrial plants it can be referred to as post-conversion capture. Post-conversion CCU requires the least amount of retrofitting to the existing facilities and is typically regarded as the most efficient strategy (Gao et al., 2020b). Using aqueous amine solution to capture CO_2 through absorption is the current industrial standard for post-combustion carbon capture (Nwaoha et al., 2017). However, as the solution has a high heat capacity and results in significant material losses, it causes elevated costs leading to a need for a more economical system (Patel, Byun and Yavuz, 2017). Many other post combustion methods have been developed as alternatives to amine solution separation such as absorption in other solvents, adsorption by solid sorbents (Patel, Byun and Yavuz, 2017), separation via membranes and cryogenic separations. The optimum overall strategy will depend on available energy at the CO_2 source. For example, the energy requirement needed for monoethanolamine (MEA) absorption can be met to facilitate lower energy costs if the plant has a combined heat and production feature. However, this is not the case in some industrial processes such as cement plants, as insufficient heat is produced (Kuramochi et al., 2012). An issue that needs to be addressed is that the separation processes can be challenging due to the low partial pressure of CO_2 in flue gas resulting in a low CO_2 driving force and a large volume of gas to be treated (Zhang et al., 2019). For the process to be truly carbon neutral, the energy required for CCU either needs to come from the process itself in the form of waste heat or from a renewable energy source.

Pre-combustion/conversion carbon capture purifies CO_2 generated during an intermediate process, resulting in the production of less end-CO_2. Examples include the gasification

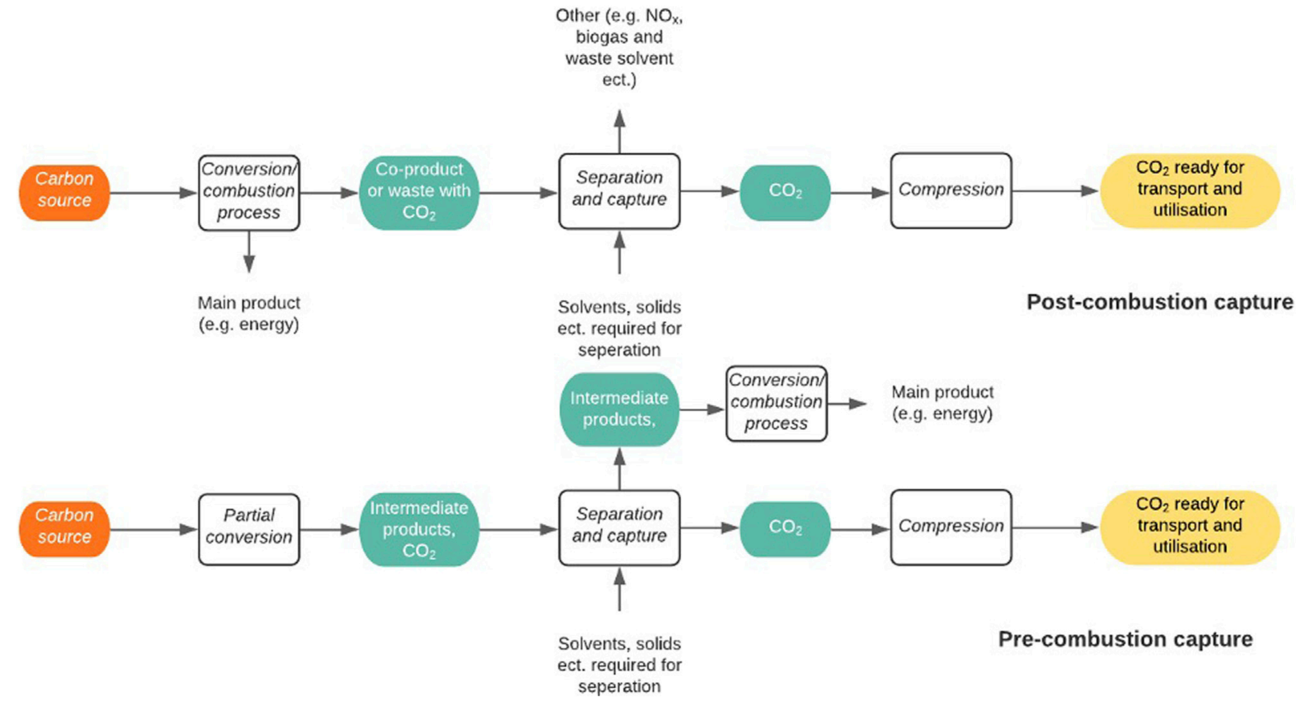

FIGURE 9 | CO_2 capture pathways for CCS and CCU.

of coal, reforming of natural gas and the production of ammonia (Jansen et al., 2015). As the majority of pre-combustion carbon capture involves the removal of CO_2 from syngas, the prime separation method will be dependent on the partial pressure of CO_2 in the treated gas. An example of industrial utilisation is the separation of CO_2 from H_2 before it can be used in ammonia synthesis. This usually occurs with the use of MEA as the absorption mechanism (Global Carbon Capture and Storage Institute, 2012). However, these methods are similarly disadvantaged to post-conversion/combustion technologies in that the regeneration of chemical solvents such as MEA cause an incurred energy penalty to the system, thus decreasing the overall efficiency (Cuéllar-Franca and Azapagic, 2015). The use of physical solvents decreases the energy required for the CO_2 capture. It is therefore the primary method for integrated gasification in combined cycle plants, which are being used to produce 'clean coal', where the physical solvents such as Selexol and Rectisol are used (Porter et al., 2017). For all CCU methods, it needs to be noted that any energy being supplied to the system to aid in the carbon capture needs to be renewable and therefore not be a process that itself produces CO_2.

Oxy-fuel combustion does not have a conversion alternative as it can only be applied to processes involving combustion. The principle uses pure oxygen for the combustion instead of air. This avoids the dilution of the flue gas with other gasses such as nitrogen, resulting in an exhaust gas with a significantly increased partial pressure of CO_2 (Borgert and Rubin, 2017). Partial recycling of the flue gas into the boiler is required to moderate the flame temperature which would otherwise burn excessively high as a result of burning in pure oxygen (Porter et al., 2017). Although the CO_2 does have a much higher partial pressure in the exhaust gas, there are still traces of water vapour, particulate matter and other pollution gases, which require a separation process before the CO_2 can be dried and compressed for transport (Najera et al., 2011). In order to retrofit a plant for oxy-fuel combustion carbon capture, it requires an air separation unit (which is often cryogenic) to provide pure oxygen from air and a CO_2 compression and separation unit and an exhaust gas recycle (Porter et al., 2017).

Although these three methods are not the only methods to capture CO_2 for utilisation, they are the main methods used from industrial and energy producing sources. Other sources include the CO_2 produced from biological processes and brewing sources, however these come with their barriers for the making of synthetic fuels. Biological sources of CO_2 come with more sulfur and a higher moisture content than energy and industrial sources (Thema et al., 2019). There is competition for the high purity of CO_2 produced from brewing for use in the fizzy drink industry, driving up the price of the CO_2, making this CO_2 not economically viable for synthetic fuel production. Porter et al. (2017) produced a comparative report of the cost and performance of carbon capture methods based on the three methods discussed in this review.

Once the CO_2 has been compressed and purified to the specification required by the consumer, in this case to produce DME, the CO_2 must be transported to the synthetic fuel plant. As any transportation of CO_2 will incur costs, the most economical option would be to synthesise the DME on the same site as the CO_2 is captured. This approach can also take advantage of the economies of scale of the existing plant where the CO_2 is being captured, as well as any excess heat from the plant, recycled where necessary in the DME synthesis process. If the CO_2 does need to be transported, a pipeline infrastructure is required, and currently there is no CO_2 infrastructure in the United Kingdom for CO_2 from industrial flue gases (Ecofys, 2017). However, CO_2 transportation plans exist in Europe and retrofitting of existing infrastructure by repurposing oil and gas pipelines is being considered. This approach represents a cost of around 1–10% of the cost of building an entirely new CO_2 pipeline (IOGP, 2019). While implanting CCU decreases the overall plant efficiency for the initial product, the addition of CCU creates another valued product whilst complying with strict government regulation imposed to reduce the level of CO_2 emissions to the atmosphere.

CONCLUSION

Dimethyl ether (DME) is discussed in this review as a future fuel that can help facilitate the transition from a fossil-fuel based economy to a net zero economy. DME is a single molecule fuel (unlike fossil fuels which are complex mixtures) and while having half the energy density of diesel it has several benefits.

- It contains only two carbon atoms and so burns almost completely, so NOx emissions are low.
- As the fuel is non-fossil-based there are also no SOx emissions.
- Because there are no carbon-carbon (C-C) bonds, only carbon-oxygen (C-O) bonds, there is no soot formation and so low PM emissions.
- Furthermore, due to its favourable cetane number it can be used directly in CI engines.
- Some fuel delivery modifications are needed as DME is a gas, but the interventions are similar to those already available for LPG fuels.
- Oxymethylene ethers (OMEx) are higher homologues where x represents additional oxymenthylene ($-CH_2O-$) groups, and where x = 3-5 possess liquid properties similar to diesel.

DME can be produced from carbon dioxide and other carbon-containing waste materials. However, it also needs additional resources such as electricity, water and ultimately hydrogen, which must be sustainably obtained. Strategies to produce hydrogen from low-carbon energy sources were therefore reviewed. The processes that facilitate DME from waste feedstocks have been presented and the routes considered over the complete system. DME and OMEx production and properties have been put into a synthetic fuel context through comparison to the production of Fisher-Tropsch synthetic diesel. The ether route represents a low hydrogen and so lower overall energy route to a useful synthetic fuel. While we do not consider the use of DME as a silver bullet in a transport energy transition, we do not consider that any single solution technology will provide the answer. The clue lies in the word transition. We need to move away from fossil fuels in a way that is sustainable environmentally, financially, and socially. Whatever technology or suite of technologies are used, this needs to be introduced sensitively and must avoid creating transport fuel poverty where members of society are denied mobility as a consequence of a fuel ideology. This review demonstrates that in spite of the need for further innovation and development, DME has an important role to play in this transition as an energy vector, with the availability to store surplus or curtailed renewable energy over seasons.

AUTHOR CONTRIBUTIONS

Each author contributed to the literature review and analysis and to the writing of the paper. IOT was a Master's student who led the data acquisition and analysis and produced the first draft of the manuscript. PS was the research supervisor and GRMD Postdoctoral Research Associate and project co-supervisor.

FUNDING

The work was funded as part of the UKRI-Engineering and Physical Sciences (EPSRC) SUSTAIN Manufacturing Hub (EP/S018107/1) and CO2Chem Network (EP/P026435/1) projects.

REFERENCES

Abbasi, T., and Abbasi, S. A. (2011). 'Renewable' Hydrogen: Prospects and Challenges. *Renew. Sustain. Energ. Rev.* 15, 3034–3040. doi:10.1016/j.rser.2011.02.026

Abu-Jrai, A., Tsolakis, A., Theinnoi, K., Cracknell, R., Megaritis, A., Wyszynski, M. L., et al. (2006). Effect of Gas-To-Liquid Diesel Fuels on Combustion Characteristics, Engine Emissions, and Exhaust Gas Fuel Reforming. Comparative Study. *Energy Fuels* 20, 2377–2384. doi:10.1021/ef060332a

Aepli, L., Frankiewics, T., and Meyer, E. (2020). *An Overview of Renewable Natural Gas from Biogas*. Washington DC, USA: US Environmental Protection Agency, Landfill Methane Outreach Program.

Aguayo, A. T., Ereña, J., Mier, D., Arandes, J. M., Olazar, M., and Bilbao, J. (2007). Kinetic Modeling of Dimethyl Ether Synthesis in a Single Step on a CuO–ZnO–Al2O3/γ-Al2O3 Catalyst. *Ind. Eng. Chem. Res.* 46, 5522–5530. doi:10.1021/ie070269s

Ahmad, K., and Upadhyayula, S. (2018). Greenhouse Gas CO2 Hydrogenation to Fuels: A Thermodynamic Analysis. *Environ. Prog. Sustain. Energ.* 38, 98–111. doi:10.1002/ep.13028

Ainalis, D. T., Thorne, C., and Cebon, D. (2020). Technical Report White Paper: Decarbonising the UK's Long-Haul Rod Freight at Minimum Economic Cost, Centre for Sustainable Road Freight. Available at: http://www.csrf.ac.uk/wp-content/uploads/2020/07./SRF-WP-UKEMS-v2.pdf.

Al-Mamoori, A., Krishnamurthy, A., Rownaghi, A. A., and Rezaei, F. (2017). Carbon Capture and Utilization Update. *Energy Technol.* 5, 834–849. doi:10.1002/ente.201600747

Ali, K. A., Abdullah, A. Z., and Mohamed, A. R. (2015). Recent Development in Catalytic Technologies for Methanol Synthesis from Renewable Sources: A Critical Review. *Renew. Sustain. Energ. Rev.* 44, 508–518. doi:10.1016/j.rser.2015.01.010

Alleman, T., and McCormick, R. (2003). "Fischer-Tropsch Diesel Fuels - Properties and Exhaust Emissions: A Literature Review,". Technical Paper 2003-01-0763 (SAE International).

Álvarez, A., Bansode, A., Urakawa, A., Bavykina, A. V., Wezendonk, T. A., Makkee, M., et al. (2017). Challenges in the Greener Production of Formates/Formic Acid, Methanol, and DME by Heterogeneously Catalyzed CO2 Hydrogenation Processes. *Chem. Rev.* 117, 9804–9838. doi:10.1021/acs.chemrev.6b00816

Apostolaki-Isofidou, E., Codani, P., and Kempton, W. (2017). Measurement of Power Loss during Electric Vehicle Charging and Discharging. *Energy* 127, 730–742. doi:10.1016/j.energy.2017.03.015

Arcoumanis, C., Bae, C., Crookes, R., and Kinoshita, E. (2008). The Potential of Dimethyl Ether (DME) as an Alternative Fuel for Compression-Ignition Engines: A Review. *Fuel* 87, 1014–1030. doi:10.1016/j.fuel.2007.06.007

Armenta, M. A., Maytorena, V. M., Flores–Sánchez, L. A., Quintana, J. M., Valdez, R., and Olivas, A. (2020). Dimethyl Ether Production via Methanol Dehydration Using Fe3O4 and CuO over γ-χ-Al2O3 Nanocatalysts. *Fuel* 280, 118545. doi:10.1016/j.fuel.2020.118545

Arregi, A., Amutio, M., Lopez, G., Bilbao, J., and Olazar, M. (2018). Evaluation of Thermochemical Routes for Hydrogen Production from Biomass: A Review. *Energ. Convers. Manage.* 165, 696–719. doi:10.1016/j.enconman.2018.03.089

Asthana, S., Samanta, C., Bhaumik, A., Banerjee, B., Voolapalli, R. K., and Saha, B. (2016). Direct Synthesis of Dimethyl Ether from Syngas over Cu-Based Catalysts: Enhanced Selectivity in the Presence of MgO. *J. Catal.* 334, 89–101. doi:10.1016/j.jcat.2015.10.020

Avogadro (2021). Avogadro: an Open-Source Molecular Builder and Visualization Tool. Version 1.2.0. http://avogadro.openmolecules.net/ (Accessed May 12, 2021).

Azizi, Z., Rezaeimanesh, M., Tohidian, T., and Rahimpour, M. R. (2014). Dimethyl Ether: A Review of Technologies and Production Challenges. *Chem. Eng. Process. Process Intensification* 82, 150–172. doi:10.1016/j.cep.2014.06.007

Badwal, S., Giddey, S., Munnings, C., Bhatt, A., and Hollenkamp, A. (2014). Emerging Electrochemical Energy Conversion and Storage Technologies. *Front. Chem.* 2 (79), 1–28. doi:10.3389/fchem.2014.00079

Baranowski, C. J., Bahmanpour, A. M., and Kröcher, O. (2017). Catalytic Synthesis of Polyoxymethylene Dimethyl Ethers (OME): A Review. *Appl. Catal. B: Environ.* 217, 407–420. doi:10.1016/j.apcatb.2017.06.007

Baykara, S. (2004). Experimental Solar Water Thermolysis. *Int. J. Hydrogen Energ.* 29, 1459–1469. doi:10.1016/j.ijhydene.2004.02.011

Becker, W. L., Braun, R. J., Penev, M., and Melaina, M. (2012). Production of Fischer-Tropsch Liquid Fuels from High Temperature Solid Oxide Co-electrolysis Units. *Energy* 47 (1), 99–115. doi:10.1016/j.energy.2012.08.047

Benemann, J. R. (2000). Hydrogen Production by Microalgae. *J. Appl. Phycol.* 12, 291–300. doi:10.1023/a:1008175112704

Bhandari, R., Trudewind, C. A., and Zapp, P. (2014). Life Cycle Assessment of Hydrogen Production via Electrolysis - a Review. *J. Clean. Prod.* 85, 151–163. doi:10.1016/j.jclepro.2013.07.048

Bičáková, O., and Straka, P. (2012). Production of Hydrogen from Renewable Resources and its Effectiveness. *Int. J. Hydrogen Energ.* 37, 11563–11578. doi:10.1016/j.ijhydene.2012.05.047

Bilke, M., Losch, P., Vozniuk, O., Bodach, A., and Schüth, F. (2019). Methane to Chloromethane by Mechanochemical Activation: A Selective Radical Pathway. *J. Am. Chem. Soc.* 141, 11212–11218. doi:10.1021/jacs.9b04413

Binder, M., Kraussler, M., Kuba, M., and Luisser, M. (2018). Hydrogen from Biomass Gasification. [online] IEA Bioenergy. Available at: https://www.ieabioenergy.com/wp-content/uploads/2019/01/Wasserstoffstudie_IEA-final.pdf (Accessed May 12, 2021).

Bonura, G., Cannilla, C., Frusteri, L., Catizzone, E., Todaro, S., Migliori, M., et al. (2020). Interaction Effects between CuO-ZnO-ZrO2 Methanol Phase and Zeolite Surface Affecting Stability of Hybrid Systems during One-step CO2 Hydrogenation to DME. *Catal. Today* 345, 175–182. doi:10.1016/j.cattod.2019.08.014

Borgert, K. J., and Rubin, E. S. (2017). Oxy-combustion Carbon Capture for Pulverized Coal in the Integrated Environmental Control Model. *Energ. Proced.* 114, 522–529. doi:10.1016/j.egypro.2017.03.1194

Brito Cruz, C. H., Souza, G. M., and Barbosa Cortez, L. A. (2014). "Biofuels for Transport," in *Future Energy*. Editor T. Letcher (Durban, South Africa: Elsevier), 215–244.

Burre, J., Bongartz, D., and Mitsos, A. (2019). Production of oxymethylene dimethyl ethers from hydrogen and carbon dioxide –part II: modeling and analysis for OME3 -5. *Ind. Eng. Chem. Res.* 58 (14), 5567–5578. doi:10.1021/acs.iecr.8b05577

Catizzone, E., Bonura, G., Migliori, M., Frusteri, F., and Giordano, G. (2017). CO2 Recycling to Dimethyl Ether: State-Of-The-Art and Perspectives. Molecules, [online] 23(1), p.31. Available at: https://www.mdpi.com/1420-3049/23/1/31/pdf-vor (Accessed May 12, 2021).

Catizzone, E., Freda, C., Braccio, G., Frusteri, F., and Bonura, G. (2021). Dimethyl Ether as Circular Hydrogen Carrier: Catalytic Aspects of Hydrogenation/dehydrogenation Steps. *J. Energ. Chem.* 58, 55–77. doi:10.1016/j.jechem.2020.09.040

Cave, E. (2020). Utilization of CO_2 Emissions to Make Renewable Fuels and Chemicals SoCalGas Research Webinar. *SoCalGas and Opus 12.* Available at: www.gasworld.com/consortium-to-convert-co2-into-renewable-fuel/2019355.article (Accessed May 12, 2021).

Centi, G., and Perathoner, S. (2013). "Advances in Catalysts and Processes for Methanol Synthesis from CO_2," in *CO_2: A Valuable Source of Carbon. Green Energy and Technology*. Editors M. Falco, G. Iaquaniello, and G. Centi (London: Springer), 147–169. doi:10.1007/978-1-4471-5119-7_9

Chaubey, R., Sahu, S., James, O. O., and Maity, S. (2013). A Review on Development of Industrial Processes and Emerging Techniques for Production of Hydrogen from Renewable and Sustainable Sources. *Renew. Sustain. Energ. Rev.* 23, 443–462. doi:10.1016/j.rser.2013.02.019

Chen, C.-Y., Liu, C.-H., Lo, Y.-C., and Chang, J.-S. (2011). Perspectives on Cultivation Strategies and Photobioreactor Designs for Photo-Fermentative Hydrogen Production. *Bioresour. Technol.* 102, 8484–8492. doi:10.1016/j.biortech.2011.05.082

Christopher, K., and Dimitrios, R. (2012). A Review on Exergy Comparison of Hydrogen Production Methods from Renewable Energy Sources. *Energy Environ. Sci.* 5, 6640–6651. doi:10.1039/C2EE01098D

Cuéllar-Franca, R. M., and Azapagic, A. (2015). Carbon Capture, Storage and Utilisation Technologies: A Critical Analysis and Comparison of Their Life Cycle Environmental Impacts. *J. CO2 Utilization* 9, 82–102. doi:10.1016/j.jcou.2014.12.001

da Silva Veras, T., Mozer, T. S., da Costa Rubim Messeder dos Santos, D., and da Silva César, A. (2017). Hydrogen: Trends, Production and Characterization of the Main Process Worldwide. *Int. J. Hydrogen Energ.* 42, 2018–2033. doi:10.1016/j.ijhydene.2016.08.219

Dang, C., Long, J., Li, H., Cai, W., and Yu, H. (2021). Pd-promoted Ni-Ca-Al Bi-functional Catalyst for Integrated Sorption-Enhanced Steam Reforming of Glycerol and Methane Reforming of Carbonate. *Chem. Eng. Sci.* 230, 116226. doi:10.1016/j.ces.2020.116226

De Simio, L., Gambino, M., and Iannaccone, S. (2013). Possible Transport Energy Sources for the Future. *Transport Policy* 27, 1–10. doi:10.1016/j.tranpol.2013.01.006

Deutsch, D., Oestreich, D., Lautenschütz, L., Haltenort, P., Arnold, U., and Sauer, J. (2017). High Purity Oligomeric Oxymethylene Ethers as Diesel Fuels. *Chem. Ingenieur Technik* 89 (4), 486–489. doi:10.1002/cite.201600158

Deutz, S., Bongartz, D., Heuser, B., Kätelhön, A., Schulze Langenhorst, L., Omari, A., et al. (2018). Cleaner Production of Cleaner Fuels: Wind-To-Wheel - Environmental Assessment of CO2-based Oxymethylene Ether as a Drop-In Fuel. *Energ. Environ. Sci.* 11, 331–343. doi:10.1039/C7EE01657C

Dimitriou, P., and Javaid, R. (2020). A Review of Ammonia as a Compression Ignition Engine Fuel. *Int. J. Hydrogen Energ.* 45 (11), 7098–7118. doi:10.1016/j.ijhydene.2019.12.209

Dincer, I., and Acar, C. (2015). Review and Evaluation of Hydrogen Production Methods for Better Sustainability. *Int. J. Hydrogen Energ.* 40, 11094–11111. doi:10.1016/j.ijhydene.2014.12.035

Dincer, I., and Safari, F. (2020). A Review and Comparative Evaluation of Thermochemical Water Splitting Cycles for Hydrogen Production,. *Energ. Convers. Manage.* 205, 112182. doi:10.1016/j.enconman.2019.112182

Ecofys (2017). Assessing the Potential of CO_2 Utilisation in the UK. [online] Ecofys 2017 by order of: UK Department for Business, Energy & Industrial Strategy (BEIS). Available at: https://assets.publishing.service.gov.uk/government/uploads/system/uploads/attachment_data/file/799293/SISUK17099AssessingCO2_utilisationUK_ReportFinal_260517v2__1_.pdf (Accessed January 31, 2021).

Eroglu, E., and Melis, A. (2011). Photobiological Hydrogen Production: Recent Advances and State of the Art. *Bioresour. Technol.* 102, 8403–8413. doi:10.1016/j.biortech.2011.03.026

ETIP PVEuropean Photovoltaic Technology and Innovation Platform (2020). PHOTOVOLTAIC SOLAR ENERGY: BIG and beyond, Sustainable Energy to Limit Global Warming to 1.5 Degrees. [online] Available at: https://www.buildup.eu/sites/default/files/content/photovoltaic-solar-energy-big-and-beyond.pdf (Accessed January 5, 2021).

European Council directive 443/2009. Regulation (EC) No 443/2009 of 23 April 2009, Setting Emissions Performance Standards for New Passenger Cars, L 140/1–15

Fang, H. H. P., and Liu, H. (2002). Effect of pH on Hydrogen Production from Glucose by a Mixed Culture. *Bioresour. Technol.* 82 (1), 87–93. doi:10.1016/s0960-8524(01)00110-9

Fiorese, G., Catenacci, M., Bosetti, V., and Verdolini, E. (2014). The Power of Biomass: Experts Disclose the Potential for success of Bioenergy Technologies. *Energy Policy* 65, 94–114. doi:10.1016/j.enpol.2013.10.015

Forrest, K., Mac Kinnon, M., Tarroja, B., and Samuelsen, S. (2020). Estimating the Technical Feasibility of Fuel Cell and Battery Electric Vehicles for the Medium and Heavy Duty Sectors in California. *Appl. Energ.* 276, 115439. doi:10.1016/j.apenergy.2020.115439

FreedomCAR and Fuel Partnership (2009). Hydrogen Production - Overview of Technology Options. [online] Available at: https://www1.eere.energy.gov/hydrogenandfuelcells/pdfs/h2_tech_roadmap.pdf (Accessed January 18, 2021).

Galanova, E. G., Magomedova, M. V., Afokin, M. I., Starozhitskaya, A. V., and Maximov, A. L. (2021). Synthesis of Olefins from Dimethyl Ether in a Synthesis Gas Atmosphere. *Catal. Commun.* 153, 106297. doi:10.1016/j.catcom.2021.106297

Gandia, L., Arzamedi, G., Dieguez, P., and Luis, M. G. (2013). *Renewable Hydrogen Technologies*. Pamplona, Spain: Elsevier Science & Technology.

Gao, N., Cheng, M., Quan, C., and Zheng, Y. (2020a). Syngas Production via Combined Dry and Steam Reforming of Methane over Ni-Ce/ZSM-5 Catalyst. *Fuel* 273, 11770. doi:10.1016/j.fuel.2020.117702

Gao, W., Liang, S., Wang, R., Jiang, Q., Zhang, Y., Zheng, Q., et al. (2020b). Industrial Carbon Dioxide Capture and Utilization: State of the Art and Future Challenges. *Chem. Soc. Rev.* 49, 8584–8686. doi:10.1039/D0CS00025F

Ghavam, S., Taylor, C. M., and Styring, P. (2021). Modeling and Simulation of a Novel Sustainable Ammonia Production Process from Food Waste and Brown Water. *Front. Energy Res.* 9, 600071. doi:10.3389/fenrg.2021.600071

Gill, S. S., Tsolakis, A., Dearn, K. D., and Rodríguez-Fernández, J. (2011). Combustion Characteristics and Emissions of Fischer-Tropsch Diesel Fuels in IC Engines. *Prog. Energ. Combustion Sci.* 37, 503–523. doi:10.1016/j.pecs.2010.09.001

Global Alliance Powerfuels (2020). *Carbon Sources for Powerfuels Production*. Berlin, Germany.

Global Carbon Capture and Storage Institute (2012). Pre Combustion Capture. CO_2 Capture Technologies. [online] Palo Alto. Available at: https://www.globalccsinstitute.com/archive/hub/publications/29756/co2-capture-technologies-pre-combustion-capture.pdf.

Goeppert, A., Czaun, M., Jones, J.-P., Surya Prakash, G. K., and Olah, G. A. (2014). Recycling of Carbon Dioxide to Methanol and Derived Products - Closing the Loop. *Chem. Soc. Rev.* 43 (23), 7995–8048. doi:10.1039/c4cs00122b10.1039/c4cs00122b

Hallenbeck, P., and Benemann, J. R. (2002). Biological Hydrogen Production; Fundamentals and Limiting Processes. *Int. J. Hydrogen Energ.* 27, 1185–1193. doi:10.1016/S0360-3199(02)00131-3

Hänggi, S., Elbert, P., Bütler, T., Cabalzar, U., Teske, S., Bach, C., et al. (2019). A Review of Synthetic Fuels for Passenger Vehicles. *Energ. Rep.* 5, 555–569. doi:10.1016/j.egyr.2019.04.007

Härtl, M., Gaukel, K., Pélerin, D., and Wachtmeister, G. (2017). Oxymethylene Ether as Potentially CO2-neutral Fuel for Clean Diesel Engines Part 1: Engine Testing. *MTZ Worldw* 78 (2), 52–59. doi:10.1007/s38313-016-0163-6

Henstra, A. M., Sipma, J., Rinzema, A., and Stams, A. J. (2007). Microbiology of Synthesis Gas Fermentation for Biofuel Production. *Curr. Opin. Biotechnol.* 18, 200–206. doi:10.1016/j.copbio.2007.03.008

Holladay, J. D., Hu, J., King, D. L., and Wang, Y. (2009). An Overview of Hydrogen Production Technologies. *Catal. Today* 139, 244–260. doi:10.1016/j.cattod.2008.08.039

IDA Fact Sheet No. 2 (2010). *International DME Association*. Available at: www.aboutdme.org/aboutdme/files/ccLibraryFiles/Filename/000000001520/IDA_Fact_Sheet_2_Transportation_Fuel.pdf (Accessed May 12, 2021).

IEA (2020a). CO2 Emissions from Fuel Combustion: Overview, IEA, Paris. Available at: https://www.iea.org/reports/co2-emissions-from-fuel-combustion-overview (Accessed April 11, 2021).

IEA (2019). The Future of Rail, IEA, Paris. Available at: https://www.iea.org/reports/the-future-of-rail (Accessed April 11, 2021).

IEA (2020b). Transport Biofuels. [online] Paris: IEA. Available at: https://www.iea.org/reports/transport-biofuels (Accessed March 24, 2021).

INERIS (2020). Socio-economic Analysis of Biomass Based DME Production and Use. [online] Verneuil-en-Halatte: L'Institut National de l'Environnement Industriel et des Risques. Available at: http://www.fledged.eu/wp-content/uploads/Downloads/Presentations/FinalWebinar/A6_FLEDGED%20webinar%20-%20Shucht%20-%20Socio%20economic%20assessment.pdf (Accessed March 25, 2021).

IOGP (2019). The Potential for CCS and CCU in Europe. REPORT to the THIRTY SECOND MEETING of the EUROPEAN GAS REGULATORY FORUM 5–6 JUNE 2019. [online] Available at: https://ec.europa.eu/info/sites/info/files/iogp_-_report_-_ccs_ccu.pdf (Accessed January 31, 2021).

IRENA (2019). HYDROGEN: A RENEWABLE ENERGY PERSPECTIVE. Report Prepared for the 2nd Hydrogen Energy Ministerial Meeting. [online] Tokyo: The International Renewable Energy Agency (IRENA). Available at: https://www.irena.org/-/media/Files/IRENA/Agency/Publication/2019/Sep/IRENA_Hydrogen_2019.pdf (Accessed March 24, 2021).

Iribarren, D., Susmozas, A., Petrakopoulou, F., and Dufour, J. (2014). Environmental and Exergetic Evaluation of Hydrogen Production via Lignocellulosic Biomass Gasification. *J. Clean. Prod.* 69, 165–175. doi:10.1016/j.jclepro.2014.01.068

Jansen, D., Gazzani, M., Manzolini, G., Dijk, E. v., and Carbo, M. (2015). Pre-combustion CO2 Capture. *Int. J. Greenhouse Gas Control.* 40, 167–187. doi:10.1016/j.ijggc.2015.05.028

Johnson, B. (2020). Boris Johnson: Now Is the Time to Plan Our green Recovery. Financial Times. [online], 17 November, Available at: https://www.ft.com/content/6c112691-fa2f-491a-85b2-b03fc2e38a30 (Accessed January 4, 2021).

Joo, O.-S., Jung, K.-D., Moon, I., Rozovskii, A. Y., Lin, G. I., Han, S.-H., et al. (1999). Carbon Dioxide Hydrogenation to Form Methanol via a Reverse-Water-Gas-Shift Reaction (The CAMERE Process). *Ind. Eng. Chem. Res.* 38, 1808–1812. doi:10.1021/ie9806848

Kajitani, S., Chen, Z., Konno, M., and Rhee, K. (1997). "Engine Performance and Exhaust Characteristics of Direct-Injection Diesel Engine Operated with DME,". Technical Paper 972973 (SAE International).

Kanniche, M., Gros-Bonnivard, R., Jaud, P., Valle-Marcos, J., Amann, J.-M., and Bouallou, C. (2010). Pre-combustion, post-combustion and Oxy-Combustion in thermal Power Plant for CO2 Capture. *Appl. Therm. Eng.* 30, 53–62. doi:10.1016/j.applthermaleng.2009.05.005

Kätelhön, A., Meys, R., Deutz, S., Suh, S., and Bardow, A. (2019). Climate Change Mitigation Potential of Carbon Capture and Utilization in the Chemical Industry. *Proc. Natl. Acad. Sci. USA* 116, 11187–11194. doi:10.1073/pnas.1821029116

Kayfeci, M., Keçebaş, A., and Bayat, M. (2019). "Hydrogen Production," in *Solar Hydrogen Production* (Naples, Italy: Academic Press), 45–83. doi:10.1016/B978-0-12-814853-2.00003-5

Khirsariya, P., and Mewada, R. K. (2013). Single Step Oxidation of Methane to Methanol-Towards Better Understanding. *Proced. Eng.* 51, 409–415. doi:10.1016/j.proeng.2013.01.057

Kim, D.-H., and Kim, M.-S. (2011). Hydrogenases for Biological Hydrogen Production. *Bioresour. Technol.* 102 (18), 8423–8431. doi:10.1016/j.biortech.2011.02.113

Kim, R. S., and Surendranath, Y. (2019). Electrochemical Reoxidation Enables Continuous Methane-To-Methanol Catalysis with Aqueous Pt Salts. *ACS Cent. Sci.* 5, 1179–1186. doi:10.1021/acscentsci.9b00273

Koishybay, A., and Shantz, D. F. (2020). Water Is the Oxygen Source for Methanol Produced in Partial Oxidation of Methane in a Flow Reactor over Cu-SSZ-13. *J. Am. Chem. Soc.* 142 (28), 11962–11966. doi:10.1021/jacs.0c03283

Kopyscinski, J., Schildhauer, T. J., and Biollaz, S. M. A. (2010). Production of Synthetic Natural Gas (SNG) from Coal and Dry Biomass - A Technology Review from 1950 to 2009. *Fuel* 89, 1763–1783. doi:10.1016/j.fuel.2010.01.027

Kothari, R., Buddhi, D., and Sawhney, R. L. (2008). Comparison of Environmental and Economic Aspects of Various Hydrogen Production Methods. *Renew. Sustain. Energ. Rev.* 12, 553–563. doi:10.1016/j.rser.2006.07.012

Kothari, R., Buddhi, D., and Sawhney, R. L. (2004). Sources and Technology for Hydrogen Production: a Review. *Int. J. Glob. Energ. Issues* 21, 154. doi:10.1504/ijgei.2004.004707

Kovacs, K., Maroti, G., and Rakhely, G. (2006). A Novel Approach for Biohydrogen Production. *Int. J. Hydrogen Energ.* 31, 1460–1468. doi:10.1016/j.ijhydene.2006.06.011

Kuramochi, T., Ramírez, A., Turkenburg, W., and Faaij, A. (2012). Comparative Assessment of CO2 Capture Technologies for Carbon-Intensive Industrial Processes. *Prog. Energ. Combustion Sci.* 38, 87–112. doi:10.1016/j.pecs.2011.05.001

Larsson, M., and Denbratt, I. (2007). "An Experimental Investigation of Fischer-Tropsch Fuels in a Light-Duty Diesel Engine,". Technical Paper Series, 2007-01-0030 (SAE International).

Lautenschütz, L., Oestreich, D., Seidenspinner, P., Arnold, U., Dinjus, E., and Sauer, J. (2016). Physico-chemical Properties and Fuel Characteristics of Oxymethylene Dialkyl Ethers. *Fuel* 173, 129–137. doi:10.1016/j.fuel.2016.01.060

Leckel, D. (2009). Diesel Production from Fischer–Tropsch: The Past, the Present, and New Concepts. *Energy Fuels* 23, 2342–2358. doi:10.1021/ef900064c

Lede, J., Lapicque, F., Villermaux, J., Cales, B., Ounalli, A., Baumard, J., et al. (1982). Production of Hydrogen by Direct thermal Decomposition of Water: Preliminary Investigations. *Int. J. Hydrogen Energ.* 7, 939–950. doi:10.1016/0360-3199(82)90162-8

Lee, U., Han, J., Wang, M., Ward, J., Hicks, E., Goodwin, D., et al. (2016). Well-to-Wheels Emissions of Greenhouse Gases and Air Pollutants of Dimethyl Ether from Natural Gas and Renewable Feedstocks in Comparison with Petroleum Gasoline and Diesel in the United States and Europe. *SAE Int. J. Fuels Lubr.* 9, 546–557. doi:10.4271/2016-01-2209

Lepage, T., Kammoun, M., Schmetz, Q., and Richel, A. (2021). Biomass-to-hydrogen: A Review of Main Routes Production, Processes Evaluation and Techno-Economical Assessment. *Biomass and Bioenergy* 144, 105920. doi:10.1016/j.biombioe.2020.105920

Levin, D. (2004). Biohydrogen Production: Prospects and Limitations to Practical Application. *Int. J. Hydrogen Energ.* 29, 173–185. doi:10.1016/s0360-3199(03)00094-6

Luo, X., Wang, J., Dooner, M., and Clarke, J. (2015). Overview of Current Development in Electrical Energy Storage Technologies and the Application Potential in Power System Operation. *Appl. Energ.* 137, 511–536. doi:10.1016/j.apenergy.2014.09.081

Markewitz, P., Kuckshinrichs, W., Leitner, W., Linssen, J., Zapp, P., Bongartz, R., et al. (2012). Worldwide Innovations in the Development of Carbon Capture Technologies and the Utilization of CO2. *Energ. Environ. Sci.* 5, 7281–7305. doi:10.1039/C2EE03403D

Martínez-Rodríguez, A., and Abánades, A. (2020). Comparative Analysis of Energy and Exergy Performance of Hydrogen Production Methods. *Entropy* 22, 1286. doi:10.3390/e22111286

McKone, T., Rice, D., Ginn, T., Levy, D. A., Syz, B. A., and Boudreaux, R. (2015). Dimethyl Ether Multimedia Evaluation Tier I, Report for the California Environmental Protection Agency Multimedia Working Group. Available at: https://www.arb.ca.gov/fuels/multimedia/meetings/DMETierIReport_Feb2015.pdf (Accessed May 12, 2021).

Mehrpooya, M., and Habibi, R. (2020). A Review on Hydrogen Production Thermochemical Water-Splitting Cycles. *J. Clean. Prod.* 275, 123836. doi:10.1016/j.jclepro.2020.123836

Melis, A., Zhang, L., Forestier, M., Ghirardi, M. L., and Seibert, M. (2000). Sustained Photobiological Hydrogen Gas Production upon Reversible Inactivation of Oxygen Evolution in the Green AlgaChlamydomonas Reinhardtii. *Plant Physiol.* 122, 127–136. doi:10.1104/pp.122.1.127

Michaelides, E. E. (2020). Thermodynamics and Energy Usage of Electric Vehicles. *Energ. Convers. Manage.* 203, 112246. doi:10.1016/j.enconman.2019.112246

Michailos, S., McCord, S., Sick, V., Stokes, G., and Styring, P. (2019). Dimethyl Ether Synthesis via Captured CO2 Hydrogenation within the Power to Liquids Concept: A Techno-Economic Assessment. *Energ. Convers. Manage.* 184, 262–276. doi:10.1016/j.enconman.2019.01.046

Migliori, M., Condello, A., Dalena, F., Catizzone, E., and Giordano, G. (2020). CuZnZr-Zeolite Hybrid Grains for DME Synthesis: New Evidence on the Role of Metal-Acidic Features on the Methanol Conversion Step. *Catalysts* 10, 671. doi:10.3390/catal10060671

Mintz, M., and Voss, P. (2020). Database of Renewable Natural Gas (RNG) Projects: 2020 Update, Argonne National Laboratory, October 2020. Figure Calculated from MMBtu Figure Using the Ratio 1 MMBtu : 21.10 Kg Natural Gas. Available at: www.anl.gov/es/reference/renewable-natural-gas-database (Accessed April 11, 2020).

Mollavali, M., Yaripour, F., Atashi, H., and Sahebdelfar, S. (2008). Intrinsic Kinetics Study of Dimethyl Ether Synthesis from Methanol on γ-Al2O3Catalysts. *Ind. Eng. Chem. Res.* 47, 3265–3273. doi:10.1021/ie800051h

Moulijn, J., Makkee, M., and Diepen, A. (2013). *Chemical Process Technology*. 2nd ed. Chichester: John Wiley & Sons Ltd. Hoboken, NJ, USA.

Najera, M., Solunke, R., Gardner, T., and Veser, G. (2011). Carbon Capture and Utilization via Chemical Looping Dry Reforming. *Chem. Eng. Res. Des.* 89, 1533–1543. doi:10.1016/j.cherd.2010.12.017

Nikolaidis, P., and Poullikkas, A. (2017). A Comparative Overview of Hydrogen Production Processes. *Renew. Sustain. Energ. Rev.* 67, 597–611. doi:10.1016/j.rser.2016.09.044

North, M., and Styring, P. (2019b). *Carbon Dioxide Utilisation Volume 2: Transformations*. Berlin; Boston: De Gruyter.

North, M., and Styring, P. (2019a). *Carbon Dioxide Utilisation: Fundamentals*. Berlin: Berlin/Boston De Gruyter.

Nwaoha, C., Supap, T., Idem, R., Saiwan, C., Tontiwachwuthikul, P., AL-Marri, M. J., et al. (2017). Advancement and New Perspectives of Using Formulated Reactive Amine Blends for post-combustion Carbon Dioxide (CO2) Capture Technologies. *Petroleum* 3, 10–36. doi:10.1016/j.petlm.2016.11.002

Oestreich, D., Lautenschütz, L., Arnold, U., and Sauer, J. (2018). Production of Oxymethylene Dimethyl Ether (OME)-hydrocarbon Fuel Blends in a One-step Synthesis/extraction Procedure. *Fuel* 214, 39–44. doi:10.1016/j.fuel.2017.10.116

Oh, Y.-K., Hwang, K.-R., Kim, C., Kim, J. R., and Lee, J.-S. (2018). Recent Developments and Key Barriers to Advanced Biofuels: A Short Review. *Bioresour. Technol.* 257, 320–333. doi:10.1016/j.biortech.2018.02.089

O'Mahoney, A. (2020). Ofgem Letter to Stakeholders on Revised Typical Domestic Consumption Values for Gas and Electricity and Economy 7 Consumption Split, UK Government. Available at: https://www.ofgem.gov.uk/system/files/docs/2020/01/tdcvs_2020_decision_letter_0.pdf (Accessed April 11, 2021).

Oscar, P. R. van. Vliet., André, P. C. F., and Wim, C. T. (2009). Fischer-Tropsch Diesel Production in a Well-To-Wheel Perspective: A Carbon, Energy Flow and Cost Analysis. *Energ. Convers. Manage.* 50, 855–876. doi:10.1016/j.enconman.2009.01.008

Ouda, M., Mantei, F. K., Elmehlawy, M., White, R. J., Klein, H., and Fateen, S.-E. K. (2018). Describing Oxymethylene Ether Synthesis Based on the Application of Non-stoichiomsetric Gibbs Minimisation. *React. Chem. Eng.* 3, 277–292. doi:10.1039/C8RE00006A

Ouda, M., Yarce, G., White, R. J., Hadrich, M., Himmel, D., Schaadt, A., et al. (2017). Poly(oxymethylene) Dimethyl Ether Synthesis - a Combined Chemical Equilibrium Investigation towards an Increasingly Efficient and Potentially Sustainable Synthetic Route. *React. Chem. Eng.* 2, 50–59. doi:10.1039/C6RE00145A

Our World in Data (2020). Cars, Planes, Trains: Where Do CO2 Emissions from Transport Come from?. [online] Available at: https://ourworldindata.org/co2-emissions-from-transport (Accessed January 2, 2021).

Parker, B. F., Zhang, Z., Rao, L., and Arnold, J. (2018). An Overview and Recent Progress in the Chemistry of Uranium Extraction from Seawater. *Dalton Trans.* 47, 639–644. doi:10.1039/C7DT04058J

Patel, H. A., Byun, J., and Yavuz, C. T. (2017). Carbon Dioxide Capture Adsorbents: Chemistry and Methods. *ChemSusChem* 10 (7), 1303–1317. doi:10.1002/cssc.201601545

Pélerin, D., Gaukel, K., Härtl, M., and Wachtmeister, G. (2020). "Nitrogen Oxide Reduction Potentials Using Dimethyl Ether and Oxymethylene Ether in a Heavy-Duty Diesel Engine,". Technical Paper 2020-01-5084 (SAE).

Popov, B. N., Lee, J.-W., and Djukic, M. B. (2018). "Hydrogen Permeation and Hydrogen-Induced Cracking," in *Handbook of Environmental Degradation of Materials*. Editor M. Kutz. Third Edition (William Andrew Publishing), 133–162.

Porter, R. T. J., Fairweather, M., Kolster, C., Mac Dowell, N., Shah, N., and Woolley, R. M. (2017). Cost and Performance of Some Carbon Capture Technology Options for Producing Different Quality CO 2 Product Streams. *Int. J. Greenhouse Gas Control.* 57, 185–195. doi:10.1016/j.ijggc.2016.11.020

Prasad, S., and Ingle, A. P. (2019). *Sustainable Bioenergy*. London, UK: Elsevier, 327–346.Impacts of Sustainable Biofuels Production from Biomass

Prince, R. C., and Kheshgi, H. S. (2005). The Photobiological Production of Hydrogen: Potential Efficiency and Effectiveness as a Renewable Fuel. *Crit. Rev. Microbiol.* 31, 19–31. doi:10.1080/10408410590912961

Qin, Z.-z., Su, T.-m., Ji, H.-b., Jiang, Y.-x., Liu, R.-w., and Chen, J.-h. (2015). Experimental and Theoretical Study of the Intrinsic Kinetics for Dimethyl Ether Synthesis from CO2over Cu-Fe-Zr/HZSM-5. *Aiche J.* 61, 1613–1627. doi:10.1002/aic.14743

Ren, S., Fan, X., Shang, Z., Shoemaker, W. R., Ma, L., Wu, T., et al. (2020). Enhanced Catalytic Performance of Zr Modified CuO/ZnO/Al2O3 Catalyst for Methanol and DME Synthesis via CO2 Hydrogenation. *J. CO2 Utilization* 36, 82–95. doi:10.1016/j.jcou.2019.11.013

Ren, S., Li, S., Klinghoffer, N., Yu, M., and Liang, X. (2019). Effects of Mixing Methods of Bifunctional Catalysts on Catalyst Stability of DME Synthesis via CO2 Hydrogenation. *Carbon Resour. Convers.* 2, 85–94. doi:10.1016/j.crcon.2019.03.002

Rodríguez-Fernández, J., Ramos, A., Sánchez-Valdepeñas, J., and Serrano, J. (2019). Lubricity of Paraffinic Fuels Additivated with Conventional and Non-conventional Methyl Esters. *Adv. Mech. Eng.* 11, 1–8. doi:10.1177/1687814019877077

Roger, I., Shipman, M., and Symes, M. (2017). Earth-abundant Catalysts for Electrochemical and Photoelectrochemical Water Splitting. *Nat. Rev. Chem.* 1, 1–13. doi:10.1038/s41570-016-000310.1038/s41570-016-0003

Rounce, P., Tsolakis, A., Rodríguez-Fernández, J., York, A., Cracknell, R., and Clark, R. (2009). Diesel Engine Performance and Emissions when First Generation Meets Next Generation Biodiesel. *SAE Tech. Paper Ser.* doi:10.4271/2009-01-1935

Royal Society (2019). Sustainable Synthetic Carbon Based Fuels for Transport, Policy Briefing Document. Available at: https://royalsociety.org/topics-policy/projects/low-carbon-energy-programme/sustainable-synthetic-carbon-based-fuels-for-transport/ (Accessed 02 01, 21).

Sabatier, P., and Senderens, J. B. (1902). Nouvelles syntheses du methane. *Comptes Rendus des Séancés de l'Académie des Science*, 514–516.

Saleth, R., and Dinar, A. (2004). in *The Institutional Economics of Water*. Editor E. Elgar (Washington, DC, USA: World Bank and Cheltenham).

Sanna, A. (2013). Advanced Biofuels from Thermochemical Processing of Sustainable Biomass in Europe. *Bioenerg. Res.* 7, 36–47. doi:10.1007/s12155-013-9378-4

Sansaniwal, S. K., Rosen, M. A., and Tyagi, S. K. (2017). Global Challenges in the Sustainable Development of Biomass Gasification: An Overview. *Renew. Sustain. Energ. Rev.* 80, 23–43. doi:10.1016/j.rser.2017.05.215

Semelsberger, T. A., Borup, R. L., and Greene, H. L. (2006). Dimethyl Ether (DME) as an Alternative Fuel. *J. Power Sourc.* 156, 497–511. doi:10.1016/j.jpowsour.2005.05.082

Shah, V., Cheng, Z., Baser, D. S., Fan, J. A., and Fan, L.-S. (2021). Highly Selective Production of Syngas from Chemical Looping Reforming of Methane with CO_2 Utilization on MgO-Supported Calcium Ferrite Redox Materials. *Appl. Energ.* 282, 116111. doi:10.1016/j.apenergy.2020.116111

Shen, W.-J., Jun, K.-W., Choi, H.-S., and Lee, K.-W. (2000). Thermodynamic Investigation of Methanol and Dimethyl Ether Synthesis from CO2 Hydrogenation. *Korean J. Chem. Eng.* 17, 210–216. doi:10.1007/BF02707145

Shi, L., Rossi, R., Son, M., Hall, D. M., Hickner, M. A., Gorski, C. A., et al. (2020). Using Reverse Osmosis Membranes to Control Ion Transport during Water Electrolysis. *Energ. Environ. Sci.* 13 (9), 3138–3148. doi:10.1039/D0EE02173C

Shi, Y., Liu, S., Liu, Y., Huang, W., Guan, G., and Zuo, Z. (2018). Quasicatalytic and Catalytic Selective Oxidation of Methane to Methanol over Solid Materials: a Review on the Roles of Water. *Cataly. Rev.* 62, 313–345. doi:10.1080/01614940.2019.1674475

Shiva Kumar, S., and Himabindu, V. (2019). Hydrogen Production by PEM Water Electrolysis - A Review. *Mater. Sci. Energ. Tech.* 2, 442–454. doi:10.1016/j.mset.2019.03.002

Show, K.-Y., Lee, D.-J., and Chang, J.-S. (2011). Bioreactor and Process Design for Biohydrogen Production. *Bioresour. Technol.* 102 (18), 8524–8533. doi:10.1016/j.biortech.2011.04.055

Sia Partners (2016). Electrified Road Freight Transport Evaluating the Possibilities of External Electric Power Systems for Road Transport. [online] Available at: https://www.sia-partners.com/system/files/document_download/file/2020-06/7._insight_electrified_road_freight_transport.pdf (Accessed January 4, 2021).

Sidhu, S., Graham, J., and Striebich, R. (2001). Semi-volatile and Particulate Emissions from the Combustion of Alternative Diesel Fuels. *Chemosphere* 42 (5-7), 681–690. doi:10.1016/s0045-6535(00)00242-3

Soares, J. F., Confortin, T. C., Todero, I., Mayer, F. D., and Mazutti, M. A. (2020). Dark Fermentative Biohydrogen Production from Lignocellulosic Biomass: Technological Challenges and Future Prospects. *Renew. Sustain. Energ. Rev.* 117, 109484. doi:10.1016/j.rser.2019.109484

Stangeland, K., Li, H., and Yu, Z. (2018). Thermodynamic Analysis of Chemical and Phase Equilibria in CO2 Hydrogenation to Methanol, Dimethyl Ether, and Higher Alcohols. *Ind. Eng. Chem. Res.* 57, 4081–4094. doi:10.1021/acs.iecr.7b04866

Styring, P., and Dowson, G. R. M. (2021). Oxygenated Transport Fuels from Carbon Dioxide : Driving towards Net Zero. *Johnson Matthey Technol. Rev.* 65, 170–179. doi:10.1595/205651321X16063027322661

Styring, P., Jansen, D., De Coninick, H., Reith, H., and Armstrong, K. (2011). Carbon Capture and Utilisation in the green Economy: Using CO2 to Manufacture Fuel, Chemicals and Materials. [online] CO2Chem Media & Publishing Limited, Sheffield, UK. ISBN: 978-0-9572588-1-5. Available at: http://co2chem.co.uk/wp-content/uploads/2012/06/CCU%20in%20the%20green%20economy%20report.pdf (Accessed 04 05, 21).

Styring, P., Quadrelli, E., and Armstrong, K. (2014). *Carbon Dioxide Utilisation*, Elsevier. ISBN: 9780444627469/9780444627483 (eBook).

Sun, W., Wang, G., Li, S., Zhang, R., Yang, B., Yang, J., et al. (2017). Speciation and the Laminar Burning Velocities of Poly(oxymethylene) Dimethyl Ether 3 (POMDME3) Flames: An Experimental and Modeling Study. *Proc. Combustion Inst.* 36, 1269–1278. doi:10.1016/j.proci.2016.05.058

Takeishi, K., and Akaike, Y. (2016). Hydrogen Production by Dimethyl Ether Steam Reforming over Copper Alumina Catalysts Prepared Using the Sol-Gel Method. *Appl. Catal. A: Gen.* 510, 20–26. doi:10.1016/j.apcata.2015.09.027

Teng, H., McCandless, J., and Schneyer, J. (2001). "Thermochemical Characteristics of Dimethyl Ether - an Alternative Fuel for Compression-Ignition Engines,". Technical Paper 2001-01-0154 (SAE International).

Thema, M., Weidlich, T., Hörl, M., Bellack, A., Mörs, F., Hackl, F., et al. (2019). Biological CO2-Methanation: An Approach to Standardization. *Energies* 12 (9), 1670. doi:10.3390/en12091670

Turner, J., Sverdrup, G., Mann, M. K., Maness, P.-C., Kroposki, B., Ghirardi, M., et al. (2008). Renewable Hydrogen Production. *Int. J. Energ. Res.* 32, 379–407. doi:10.1002/er.1372

Uchida, H., and Harada, M. R. (2019). "Application of Hydrogen by Use of Chemical Reactions of Hydrogen and Carbon Dioxide," in *Science and Engineering of Hydrogen-Based Energy Technologies* (London, UK: Elsevier), 279–289.

Ugwu, A., Zaabout, A., Tolchard, J. R., Dahl, P. I., and Amini, S. (2020). Gas Switching Reforming for Syngas Production with Iron-Based Oxygen Carrier-The Performance under Pressurized Conditions. *Int. J. Hydrogen Energ.* 45, 1267–1282. doi:10.1016/j.ijhydene.2019.03.191

UK Department for Business, Energy and Industrial Strategy (2020). *UK Energy Statistics, 2019 & Q4 2019*. London, UK.

Unilever (2020). Carbon Rainbow. Available at: https://www.unilever.com/news/press-releases/2020/unilever-to-invest-1-billion-to-eliminate-fossil-fuels-in-cleaning-products-by-2030.html (Accessed February 01, 2021).

United NationsFramework Convention on Climate Change (2015). "Adoption of the Paris Agreement," in 21st Conference of the Parties (Paris: United Nations).

US deperatment of energy (2021). Fuel Properties Comparison. Alternative Fuels Data Center. [online] Available at: https://afdc.energy.gov/files/u/publication/fuel_comparison_chart.pdf (Accessed March 25, 2021).

Vakili, R., Setoodeh, P., Pourazadi, E., Iranshahi, D., and Rahimpour, M. R. (2011). Utilizing Differential Evolution (DE) Technique to Optimize Operating Conditions of an Integrated Thermally Coupled Direct DME Synthesis Reactor. *Chem. Eng. J.* 168, 321–332. doi:10.1016/j.cej.2011.01.032

Verbeek, R., and Van der Weide, J. (1997). "Global Assessment of Dimethyl-Ether: Comparison with Other Fuels. International Spring Fuels & Lubricants Meeting, Dearborn, Michigan,". Technical Paper 971607 (SAE International).

Vogt, C., Monai, M., Kramer, G. J., and Weckhuysen, B. M. (2019). The Renaissance of the Sabatier Reaction and its Applications on Earth and in Space. *Nat. Catal.* 2, 188–197. doi:10.1038/s41929-019-0244-4 von der Assen, N., and Bardow, A. (2014). Life Cycle Assessment of Polyols for Polyurethane Production Using CO2 as Feedstock: Insights from an Industrial Case Study. *Green. Chem.* 16 (6), 3272–3280. doi:10.1039/C4GC00513A

Wang, S., and Yu, J. (2021). A Comparative Life Cycle Assessment on Lithium-Ion Battery: Case Study on Electric Vehicle Battery in China Considering Battery Evolution. *Waste Manag. Res.* 39 (1), 156–164. doi:10.1177/0734242X20966637

Wang, Z., Paulauskiene, T., Uebe, J., and Bucas, M. (2020). Characterization of Biomethanol-Biodiesel-Diesel Blends as Alternative Fuel for Marine Applications. *J. Mar. Sci. Eng.* 8 (9), 730. doi:10.3390/jmse8090730

Willems, W. (2018). "Sustainable Fuels for Future Mobility: The DME Opportunity for CI-Engines," in 8th International DME Conference, 10th–12th September, 2018 (Sacramento, CA, USA).

Willems, W., Pannwitz, M., Zubel, M., and Weber, J. (2020). Oxygenated Fuels in Compression Ignition Engines. *MTZ Worldw* 81 (3), 26–33. doi:10.1007/s38313-019-0183-0

Williams, C. R., and Bees, M. A. (2013). Mechanistic Modeling of Sulfur-Deprived Photosynthesis and Hydrogen Production in Suspensions ofChlamydomonas Reinhardtii. *Biotechnol. Bioeng.* 111, 320–335. doi:10.1002/bit.25023

World-nuclear.org (2020). Nuclear Power in France | French Nuclear Energy - World Nuclear Association. [online] Available at: https://www.world-nuclear.org/information-library/country-profiles/countries-a-f/france.aspx (Accessed January 5, 2021).

Worldwide Fuel Charter Committee (2019). The Worldwide Fuel Charters. [online] 51–61. Available at: https://www.acea.be/uploads/publications/WWFC_19_gasoline_diesel.pdf (Accessed January 14, 2021).

Xu, H. F., Wang, K. X., Li, W. S., and Zhou, X. P. (2005). Dimethyl Ether Synthesis from Methane by Non Syngas Process. *Catal. Lett.* 100, 53–57. doi:10.1007/s10562-004-3085-x

Yang, Y., Niu, S., Han, D., Liu, T., Wang, G., and Li, Y. (2017). Progress in Developing Metal Oxide Nanomaterials for Photoelectrochemical Water Splitting. *Adv. Energ. Mater.* 7, 1700555.

Zhang, S., Shen, Y., Wang, L., Chen, J., and Lu, Y. (2019). Phase Change Solvents for post-combustion CO2 Capture: Principle, Advances, and Challenges. *Appl. Energ.* 239, 876–897. doi:10.1016/j.apenergy.2019.01.242

Zhang, W. (2010). Automotive Fuels from Biomass via Gasification. *Fuel Process. Technol.* 91, 866–876. doi:10.1016/j.fuproc.2009.07.010

Zimmermann, A. W., Wunderlich, J., Müller, L., Buchner, G. A., Marxen, A., Michailos, S., et al. (2020). Techno-Economic Assessment Guidelines for CO2 Utilization. *Front. Energ. Res.* 8, 5. doi:10.3389/fenrg.2020.00005

Conflict of Interest: The authors declare that the research was conducted in the absence of any commercial or financial relationships that could be construed as a potential conflict of interest.

frontiers
in Energy Research

ORIGINAL RESEARCH
published: 07 June 2021
doi: 10.3389/fenrg.2021.665585

Techno-Economic Optimization of an Integrated Biomass Waste Gasifier–Solid Oxide Fuel Cell Plant

Mar Pérez-Fortes[1]*†, Victoria He[2], Arata Nakajo[1], Jürg Schiffmann[2], François Maréchal[3] and Jan Van herle[1]

[1]Group of Energy Materials (GEM), École Polytechnique Fédérale de Lausanne (EPFL), Sion, Switzerland, [2]Laboratory for Applied Mechanical Design, École Polytechnique Fédérale de Lausanne (EPFL), Neuchâtel, Switzerland, [3]Industrial Process and Energy Systems Engineering (IPESE), École Polytechnique Fédérale de Lausanne (EPFL), Sion, Switzerland

With a growing energy demand in a carbon-constrained society, fuels cells powered by renewable fuels, and specifically solid waste, are seen as interesting contributors to the energy portfolio. The alternative energy industry needs to reduce costs, enhance efficiency, and demonstrate durability and reliability to be economically feasible and attractive. This paper addresses biomass waste gasification in distributed energy systems, using a solid oxide fuel cell (SOFC) to produce electricity and heat. The potential and optimal plant efficiency and layout (i.e., anode off-gas (AOG) recirculation point *via* small-scale turbomachinery and heat exchanger network) are analyzed through a multi-stage approach that includes scenario evaluation and multi-objective optimization *via* a hybrid optimization strategy with heuristics and mathematical programming. The results in this paper summarize the most convenient operating conditions and provide an optimized heat exchanger network (HEN). The AOG recirculation toward the gasifier combustor is the preferred option; the electrical and thermal efficiencies can separately go up to 49 and 47%, respectively. The combined total efficiency ranges between 76 and 82%, and the area of heat exchange, which corresponds to an amount of heat exchanged between 91 and 117 kW, is within 6–14 m^2.

Keywords: bio-waste gasification, solid oxide fuel cell, anode off-gas recirculation, small-scale turbomachinery, process modeling, optimization, mathematical programming, heuristics

Edited by:
Rangan Banerjee,
Indian Institute of Technology Bombay, India

Reviewed by:
Yusuf Bicer,
Hamad Bin Khalifa University, Qatar
Arnaldo Walter,
State University of Campinas, Brazil

***Correspondence:**
Mar Pérez-Fortes
m.d.m.perez-fortes@tudelft.nl

†*Present address: Department of Engineering Systems and Services, Faculty of Technology, Policy and Management, Delft University of Technology (TUDelft), Delft, Netherlands*

Specialty section:
This article was submitted to Process and Energy Systems Engineering, a section of the journal Frontiers in Energy Research

Received: *08 February 2021*
Accepted: *10 May 2021*
Published: *07 June 2021*

Citation:
Pérez-Fortes M, He V, Nakajo A, Schiffmann J, Maréchal F and Van herle J (2021) Techno-Economic Optimization of an Integrated Biomass Waste Gasifier–Solid Oxide Fuel Cell Plant. Front. Energy Res. 9:665585. doi: 10.3389/fenrg.2021.665585

INTRODUCTION

Two important issues that current and future societies must address are energy demand and waste disposal. In this context, the deployment of renewable and waste-derived energy sources could reduce emissions and secure energy access by diversifying supply. Among the waste streams that are available, organic wastes are quite amenable to pre-treatment and further use in biomass-based processes to produce electricity and/or heat. The traditional scheme for electricity production uses large and centralized power plants that inject electricity to the grid. Renewable and locally available sources such as biomass waste are better matched to distributed energy systems, which should be properly designed to cope with population needs and disposable residue resources and their geographical location. The dispersed production and relatively low energy density of waste streams may not allow them to be transported over long distances or aggregated sufficiently for use in central power generation unless co-fired with traditional fuels. In addition, population needs may involve rural development or electricity injection to the grid that is required to alleviate the pressure on large fossil fuel power plants.

In Doty and Turner (2009), the term "distributed generation" (for complete independence from a centralized grid) refers to the generation of combined heat and power (CHP) ranging from several kW's to 25 MW_e. Decentralization of energy production is part of the new energy generation measures, and CHP, for instance, for domestic applications and low dense areas, is an efficient option being explored for at least 20 years (Smith and Few, 2001; Schneider et al., 2021). In particular, Cockroft and Kelly (2006) and Thiers et al. (2010) identified small fuel cell (FC) stationary installations (called "micro-CHP") that can produce power up to 50 kW_e, while large stationary FC systems can be well over 100 kW_e in size. Technologies that compete with FCs at a distributed generation scale of power and/or heat include reciprocating engines, Stirling engines, steam engines, air source heat pumps, photovoltaics, wind turbine systems, and micro-gas turbines. Fuel cell systems comprise the lowest pollutant emissions and highest electrical efficiency options for fueled and dispatchable distributed generation. Stationary FC and biomass gasification systems are seen as more efficient and cleaner options than traditional technologies that can address the combined need to re-use residues while producing electricity and heat (Cottrell et al., 2011).

Biomass as Raw Material

A portfolio of technologies has been advanced to convert biomass into electricity and/or heat. The conversion technology selected depends on the composition and amount of the resource, the desired final product, environmental standards, and economic and project-specific conditions (Faaij, 2006). Mainly, methane- and hydrogen-rich gases can be used most directly in an FC system. The challenging fuels are solid waste and biomass fuels that require additional processes to be used in combination with the FC, such as gasification, pyrolysis, digestion, and fermentation. These processes can produce syngas or producer gas, pyrolysis gas, biogas, and/or ethanol that can each be used in the FC system. Recent research works refer to other bio-hydrogen production concepts that are still in their infancy, such as light-dependent methods of bio-photolysis and photo-fermentation and dark fermentation and water–gas shift (WGS) reaction mediated by photoheterotrophic bacteria. These methods consume CO_2 and mainly use organic waste as the raw material (Kapdan and Kargi, 2006; Kothari et al., 2012). All biomass raw materials need some form of pre-treatment process that depends upon fuel properties to accommodate the inlet material to the processing conditions. The main challenges in the biomass gasification field are tar formation and ash reactivity. A thermochemical treatment option such as gasification followed by FC conversion can both destroy pathogenic bacteria from waste and produce a gas amenable to an electricity generation process.

Fuel Cells for Co-Generation

Current stationary FC systems transform hydrogen-rich gaseous fuels by an electrochemical reaction producing electricity. The hydrogen-rich gaseous fuel can be produced from natural gas, coal, and/or biomass, *via* steam reforming, partial oxidation or gasification, pyrolysis, digestion, fermentation, etc. Fuel cell systems can incorporate internal fuel processing components that provide flexibility to the inlet raw fuel stream. Most current systems are designed to directly operate on natural gas and anaerobic digester gas combined with gas cleanup. Additional hardware is usually required to operate on other fuels such as ethanol, methanol, landfill gas, or other biomass and biogas fuels. Pure hydrogen storage, transportation, and delivery from centralized production is of special concern in terms of 1) the need for a well-established pipeline and/or tractor–trailer networks to secure fuel supply, 2) storage challenges associated with low volumetric energy density, and 3) pumping, transmission, and distribution losses (Dougherty et al., 2009). Onsite hydrogen production and use may overcome these challenges as a short-term solution. Even if an FC can achieve an electrical efficiency greater than 60% (Doherty et al., 2009), if it requires pure hydrogen, then hydrogen production and distribution may negatively influence the whole supply chain and life cycle efficiency depending upon the used feedstock supply, transformation processes, and distribution processes. While integrated high-temperature FC systems can directly operate on natural gas and most biogases, significant challenges in the FC domain include the development of proper materials to bear high temperatures, and integrated operation on biomass-derived fuels in a plant, while increasing cell and stack durability. The selected FC type in this work is a solid oxide fuel cell (SOFC), which, due to its tolerance to CO and CO_2 and high operating temperatures, is well suited for integration with gasification. To date, only a small number of biomass gasification systems in combination with an SOFC have been demonstrated in small scale (Ud Din and Zainal, 2016; Radenahmad et al., 2020).

SOFC Systems and Anode Off-Gas Management

SOFCs are generally implemented in co-generation plants and hybrid (or combined cycle) power plants and for transportation applications. The system efficiency, operating range, and behavior vary depending on the fuel type, energy management, and auxiliary equipment. System studies are therefore of great interest, with investigations using a plurality of approaches such as numerical simulations, experimental analyses, and multi-objective optimizations.

An SOFC is a good candidate to integrate into CHP systems, as the SOFC can provide both electricity and heat, namely, the waste heat from exothermic reactions and from utilization of the high-temperature exhaust gases [anode off-gas (AOG) and cathode off-gas (COG)]. For the latter, the AOG and COG are commonly fed into a burner downstream of the SOFC (AOG containing reactive gases) to generate heat. SOFC-CHP systems are therefore suitable for energy supply at small scale and micro-scale. The overall efficiency (electricity and heat) can reach up to 85–90%. Typical components of SOFC-CHP systems are a gas-cleaning unit, a fuel processor (e.g., steam reformer), an SOFC module, heat exchangers (HEXs), and pressure rise units as well as a DC–AC converter. Heat sinks in SOFC systems are typically fuel and air preheaters, the reformer, and, if existing, also the steam generator and other heat-exchanging units (Choudhury et al., 2013; Buonomano et al., 2015). The selection of an SOFC plant layout therefore depends on different design parameters, such as the operating temperature and pressure of the SOFC stack (pressurized or ambient), the fuel type and necessary fuel-processing units (e.g., internal or external reforming), heat supply for reforming and/or for other heat sinks (e.g., *via* heat recovery or fuel burning), or the steam production method (e.g., through AOG recirculation or external steam generation).

Appropriate off-gas management is of high importance to the overall system efficiency and operation safety and has to be taken into account for the SOFC system design. Generally, the off-gas at the SOFC outlet has high temperatures between 725 and 850°C. The AOG is also high in steam and CO_2 content, as they are the main products of the electrochemical reactions. Other components are H_2, CO, and unreacted educts or fuel gases. Those characteristics make the AOG very suitable for heat recovery, recirculation, or integration into downstream processes. As previously mentioned, the AOG and COG can be burned for heat generation and recovery, or for electricity generation in a downstream micro-gas turbine (Brayton cycle). Another possibility is to recirculate part of the AOG back toward the reformer and stack inlet using turbomachinery or an ejector. AOG recirculation was first implemented by Siemens-Westinghouse in an SOFC-GT system (Hassmann, 2001). The main motivation for AOG recirculation is the coverage of the reformer steam demand by the steam content in the recirculated AOG, omitting the need for external steam supply. This way, the overall system efficiency and simplicity can be improved (Hassmann, 2001; Halinen et al., 2012). In addition, both the recirculated CO_2 and H_2O mitigate the risk for carbon deposition at the SOFC stack inlet (Colpan et al., 2007). Another commonly mentioned reason for AOG recirculation is its potential to increase the electrical output of the stack by recirculating unreacted fuel back to the inlet, hence "increasing the overall fuel utilization" (Dietrich et al., 2011; Peters et al., 2013; Engelbracht et al., 2015; Torii et al., 2016). However, there is a trade-off, as recirculating the AOG can also lead to fuel dilution and thus negatively impact the stack performance, depending on the fuel type, system layout, and operating conditions (Lee et al., 2011; Rokni, 2017).

AOG recirculation and integration is currently not predominantly applied in commercial SOFC-CHP systems, as most of the AOG is thermally converted for heat generation. However, positive effects of AOG recirculation and integration in small-scale SOFC-CHP systems have been determined *via* modeling activities (Zhang et al., 2017; Park et al., 2019), showing the potential and need for further investigations and experimental realizations of AOG integration in SOFC-CHP systems.

In SOFC systems, turbomachinery can be used either as auxiliary systems (e.g., air blower) or to enhance the performance of the system (e.g., AOG recirculator in SOFC-CHP systems and micro-gas turbine for additional power production in SOFC-GT hybrid systems). Here, the focus of turbomachinery lies on the recirculator, as the general goal of the current work is to improve the performance of SOFC systems to make them more attractive and competitive with existing power generation solutions. There are currently only few commercial small-scale gas-bearing–supported turbomachinery systems available, which are suitable for SOFC applications.

The current work focuses on the design of an innovative, highly efficient, and fuel-flexible micro-CHP plant that uses biomass waste as the raw material, and an SOFC to produce electricity and heat, with AOG recirculation. The purpose is to support the design of a pilot plant within the framework of the EU H2020 project BLAZE (Biomass Low cost Advanced Zero Emission small-to-medium scale integrated gasifier-fuel cell combined heat and power plant) *via* process flow modeling and multi-objective (MO) optimization. The results of the current work will be used within the framework of the project to further propose the Bio-SOFC pilot plant process flow diagram (PFD). The results in this paper summarize the most convenient operating conditions and provide an optimized heat exchanger network (HEN). Future research will focus on the role of the recirculator with regard to the SOFC performance and the turbomachinery specificities. Hazelnut shells were preferred in the BLAZE project among different types of residual feedstocks to be used as the raw material. Fifteen types of residual biomass were selected and analyzed based on their availability, physical and chemical properties, and selling and transportation costs. Hazelnut shells were cleaner compared to the other biomass types: lower ash content (1–2%), lower chlorine and sulfur contents, lower moisture content (below 10%), and an adequate shape for gasification (as obtained from the local area where the pilot plant is based in the Abruzzo region at the center of Italy)[1].

Novelty

The current work is a step forward toward the construction of a novel and highly efficient bio-waste-based gasification plant combined with an SOFC, at a pilot scale of 25 kW_e. The boundaries of the study are placed at the pilot plant. The aim is to achieve an overall 90% of plant combined efficiency (50% of electric efficiency, 40% of thermal efficiency). As a reference, small biomass gasification CHP plants using downdraft gasifiers (10–200 kW_e), and small-to-large scale systems using fluidized bed gasifiers (up to 1000 kW_e) coupled with gas engines, have electric efficiencies of up to 25% and combined efficiencies of up to 80% (Bocci et al., 2014). The presented layout counts with a slightly pressurized gasifier, hot syngas–cleaning units, and the AOG recirculated *via* small-scale turbomachinery. This turbomachinery will use steam produced within the plant. The hybrid optimization approach uses a combination of an evolutionary algorithm and mathematical modeling to find the most suitable plant layout and working conditions to reach the target plant efficiency, which can be applied to any other process.

---

[1] BLAZE project public deliverables can be checked at https://www.blazeproject.eu/resources/.

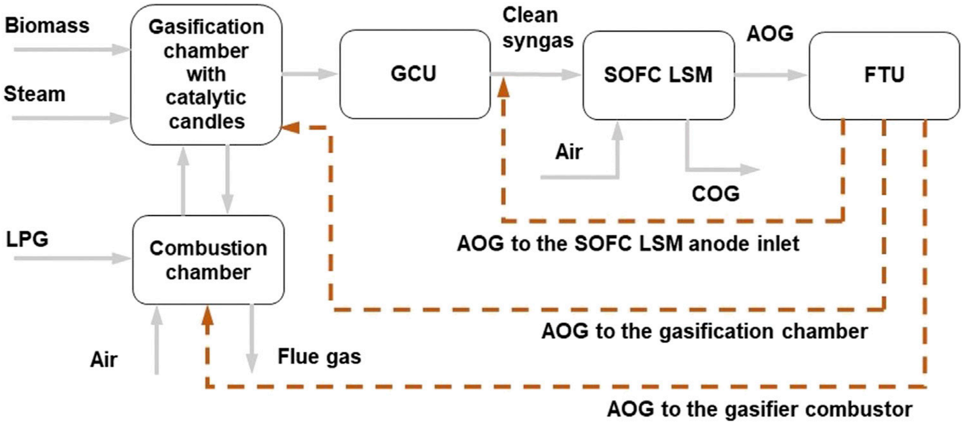

FIGURE 1 | Simplified block flow diagram of the Bio-SOFC plant, pointing out the three recirculation options evaluated. GCU: gas-cleaning units, LSM: large stack module, FTU: fan turbine unit, AOG: anode off-gas, COG: cathode off-gas, and LPG: liquefied petroleum gas.

PROCESS DESCRIPTION

The Bio-SOFC plant uses a dual bubbling fluidized bed gasifier (DBFBG), where steam gasification is separated from combustion, and an SOFC large stack module (LSM) as main technologies. It gasifies biomass waste to produce electricity, at the selected scale of 25 kW_e, and steam. The DBFBG includes ceramic filter candles filled with commercial Ni-catalyst pellets (thus, hot gas cleaning) for particle removal and decomposition of tar and ammonia (Savuto et al., 2019). The heat is transferred from the combustion to the gasification reactor by a sand bed, which acts as a heat carrier (for instance, olivine). Flue gas is produced in the combustor and can act as a heat source in the plant (not only for the gasification process). The hot gas–cleaning units (GCUs), including chloride and sulfur compound separators and tar reformer, together with the previously mentioned catalytic filter candles at the outlet of the gasification chamber, are crucial. They keep the levels of slow tars, fast tars, and sulfur, halogen, and alkali compounds low, to avoid carbon deposition, fouling, and corrosion, specifically as needed by the SOFC LSM. The heat of the gasification process, in the current pilot gasifier, is provided by burning LPG and residual char from gasification in the gasification–combustion reactor. One of the purposes of the current design work is to elucidate the conditions under which the amount of LPG can be minimized, so as to produce electricity completely free (or with minimal use) of fossil fuels.

The syngas stream moves toward the GCU, after some cooling. The clean syngas is then preheated to the required SOFC LSM inlet temperature. The air supply to the gasifier and the fuel cell is controlled by two blowers; both streams are preheated to the desired gasification and fuel cell temperatures. The temperature gradient across the SOFC module is a critical design parameter that is tightly controlled. This determines the mass flowrate of the cathodic air. The COG, before being released, is used to produce hot water. See a simplified block flow diagram (BFD) of the Bio-SOFC plant in **Figure 1**, pointing out the three AOG recirculation options specified hereafter. The turbomachinery, a fan turbine unit (FTU), aims to use the AOG in the Bio-SOFC plant through the best layout configuration, by consuming steam produced in the system. The three main locations where the AOG can be recirculated are 1) the SOFC LSM anode inlet, 2) the gasifier combustor, and 3) the biomass gasification chamber. The main inlet streams are biomass, water, and air; the main outlet streams are flue gas, COG, AOG, hot water, and steam (when produced by heat integration).

The gasifier and the SOFC LSM have to meet specific pressure conditions. In order to use a pressurized gasifier in the Bio-SOFC plant, an ad hoc screw feeder is needed, which has to be appropriately designed to avoid inner hot gas to flow back in the feeder, pyrolyzing inlet biomass. In the SOFC LSM, the anode pressure should always be above the cathode pressure, in a range of 5–30 mbar; it should ideally operate above atmospheric

TABLE 1 | Pressure losses per unit in the Bio-SOFC plant (consortium data). VL: vapor–liquid.

Unit	ΔP (mbar)
Gasifier + filter candles	100
Gasifier combustor	100
GCU	120
SOFC LSM anode	30
SOFC LSM cathode	45
VL separator	20
AOG HEX	10
Burner (GT case)	100

TABLE 2 | Constraints, i.e., range of Bio-SOFC plant modeling values that have to be met (consortium data).

Dependent variable	Condition
Air to the 25 kW_e SOFC	<5600 Nl/min
Cell voltage	>0.7 V
Heat balance gasifier	Heat combustor = heat overall gasification process

pressure. The maximum absolute pressure that the cathode can tolerate is 1.09 bar. Pressure management in the overall plant affects the design of the FTU, as the recirculation pressure can change and depends on the recirculation point. **Table 1** summarizes the pressure losses per unit in the Bio-SOFC plant. **Table 2** summarizes the conditions or constraints that the Bio-SOFC plant should meet. These conditions, as explained in *Methodology*, are checked *via* filtering in the MO optimization approach.

METHODOLOGY

A systematic approach is used to evaluate several candidate design options of the Bio-SOFC plant (named here "scenarios") and to identify the optimal system configurations. System modeling, optimization, and sensitivity analysis are used as evaluation tools. The methodology can be divided into two steps:

1. **Scenario evaluation.** The six scenarios defined take into account the three possible recirculation points, i.e., 1) AOG to the SOFC LSM anode inlet, 2) AOG to the gasifier combustor, and 3) AOG to the gasification chamber (see **Figure 1**), the use of an AOG gas turbine (GT), the possibility of not taking advantage of the AOG calorific value, and the option of not using the FTU for recirculation, but a conventional blower.
2. **MO optimization.** In the scenario evaluation step, one plant layout is selected for optimization. The results of the current step indicate the advised operating conditions from a list of decision variables, and the HEN of the Bio-SOFC plant, according to selected conflictive objectives: electrical and thermal efficiencies ($\mathrm{Eff_{el}}$ and $\mathrm{Eff_{th}}$) and area of heat exchange. Theoretically, the electrical and thermal efficiencies will increase, if the area of heat exchange (cost) increases. The thermal efficiency will decrease, if the available heat is used to generate electricity instead of producing steam.

Process simulation is used to solve the plant mass and energy balances of the Bio-SOFC plant, and it is the starting point of the scenario evaluation and of the process optimization. The selected performance indicators describe not only the objective functions but also all the different metrics considered in the scenario evaluation. Process optimization includes process simulation and process heat management, to elucidate the most suitable operating conditions and HEN for the Bio-SOFC plant, as these are highly influencing aspects of the process performance. See more details in the following paragraphs.

Process Simulation

The mass and energy balance calculations are performed in Aspen Plus V10 software. The Bio-SOFC plant model is zero-dimensional and at the steady state and uses the software in-built library models combined with ad hoc models coded in Fortran. In order to confirm the validity of the Bio-SOFC plant model along its operating conditions, specific technology experts were consulted within the project consortium to provide advice on model parameters, such as efficiencies. Otherwise, literature modeling data were used, as in the case of the gas turbine. The two most important units, the fluidized bed gasifier and the SOFC, were validated by comparison over a range of data that were contrasted with (gasifier model) and derived from (SOFC operation maps) experimental measurements.

In the scenario evaluation, heat integration is assessed by the calculation of the problem table (the feasible heat cascade) and its graphical representation, the grand composite curve (GCC), of the Bio-SOFC plant, at fixed inlet conditions. The problem table is solved in Excel (Kemp, 2007; Towler and Sinnott, 2013). It gives as a result the maximum energy recovery (MER), which is the minimum value of utilities needed.

In the optimization, heat integration is assessed by mixed integer linear programming (MILP) in AMPL (A Mathematical Programming Language, a specific modeling environment for the formulation and solution of mathematical programming models), where variable temperature levels and cooling/heating needs of the Bio-SOFC plant (calculated in the Aspen Plus model) are used as input data. The adapted "SYNHEAT temperature-stage" HEN superstructure of Yee and Grossmann (1990) in Martelli and co-workers (2017) is used in the optimization. The results pinpoint the most efficient combination of cold and hot streams by minimizing the number of connections.

The results of the scenario evaluation, i.e., a preferred layout and the essential trade-offs among the selected performance indicators, are the starting point of the optimization. As overall contextual conditions, it is assumed that inlet streams (air, water, biomass, LPG) are available at 25°C and 1.01325 bar.

Performance Indicators

The list of performance indicators below is used to evaluate the six selected scenarios.

The cold gas efficiency (CGE) calculates the performance of the gasifier by considering the lower heating value (LHV) of the involved streams—the syngas after the filter candles, in the numerator, and the inlet biomass, LPG, and AOG (when available, depending on the scenario) to the gasifier combustor, in the denominator:

$$\boldsymbol{CGE = \frac{\dot{m}_{syngas,ar} \cdot LHV_{syngas,ar}}{\dot{m}_{biomass,ar} LHV_{biomass,ar} + \dot{m}_{LPGs,ar} LHV_{LPG,ar} + \dot{m}_{AOG,ar} LHV_{AOG,ar}}}, \tag{1}$$

where $\dot{m}$ are the mass flowrates in kg/s, the LHV is expressed in kJ/kg, and *ar* refers to "as received" (including moisture content and ashes, when present).

The SOFC efficiency ($\mathrm{Eff_{SOFC}}$) takes into account the gross SOFC LSM power produced ($\mathrm{P_{prod}}$ in kW), divided by the inlet fuel, which is the syngas after the GCU (when available, after AOG mixing):

$$\boldsymbol{Eff_{SOFC} = \frac{P_{prod}}{\dot{m}_{syngas,ar} LHV_{syngas,ar}}}. \tag{2}$$

The electrical efficiency ($\mathrm{Eff_{el}}$) considers the net power produced in the system (that is, the gross power from the SOFC LSM $\mathrm{P_{prod}}$

minus the power consumed by the system's compressors and pumps, in kW) divided by the total inlet calorific value into the system, provided by the biomass and LPG streams:

$$\boldsymbol{Eff}_{el} = \frac{\boldsymbol{P}_{prod} - \left(\sum \boldsymbol{P}_{comp} + \sum \boldsymbol{P}_{pump}\right)}{\dot{\boldsymbol{m}}_{biomass,ar}\boldsymbol{LHV}_{biomass,ar} + \dot{\boldsymbol{m}}_{LPGs,ar}\boldsymbol{LHV}_{LPG,ar}}. \quad (3)$$

The thermal efficiency (Eff_{th}) considers the total amount of heat used to produce hot water at 1.01325 bar and 65°C (Q_{hw} in kW) using the COG stream (from 140 to 50°C), the total amount of heat that is absorbed by the cold utility (Q_{cu} in kW), which in this case is steam produced at 5 bar and 220°C (i.e., the steam conditions needed at the turbine of the FTU), and the thermal power consumed by the turbine of the FTU (Q_{turb} in kW). It is therefore assumed that all the heat absorbed by the cold utility is used to generate steam with a commercial value (at 5 bar and 220°C), even after powering the turbine (at 2.5 bar and around 180°C):

$$\boldsymbol{Eff}_{th} = \frac{\boldsymbol{Q}_{hw} + \boldsymbol{Q}_{cu} - \boldsymbol{Q}_{turb}}{\dot{\boldsymbol{m}}_{biomass,ar}\boldsymbol{LHV}_{biomass,ar} + \dot{\boldsymbol{m}}_{LPGs,ar}\boldsymbol{LHV}_{LPG,ar}}. \quad (4)$$

The CHP performance, or total efficiency (Eff_{tot}), is the sum of Eff_{el} and Eff_{th}. Note that, in the Bio-SOFC plant, not only biomass (in the gasification reactor of the gasifier) but also LPG (in the combustion reactor of the gasifier) is used as a fuel. As mentioned before, one of the main purposes of the plant design is to decrease as much as possible the consumption of the LPG fossil fuel, so as to prioritize the production of renewable electricity.

The selected objective functions used in the optimization are as follows:

1. Eff_{el}
2. Eff_{th}
3. HEN area

The first two objectives are maximized; the last one is minimized. The HEN area is selected as a direct potential variable metric that influences the capital cost of the plant (as the main capital intensive units, sizes and characteristics of the SOFC LSM and gasifier are already fixed and are input conditions in the BLAZE project).

The heat integration problem determines the structure and design variables. The AMPL model solution specifies which cold and hot streams are connected with each other, specifically: 1) at which stage (as defined in the SYNHEAT superstructure), 2) the need for cold and/or hot utilities, 3) the inlet and outlet temperatures of each stream at every stage, and 4) the value of the exchanged heat (Q_{total} in W). From this information, the HEN area is calculated as the sum of all the individual HEXs' areas (A_{ex}, in m^2), as follows:

$$\boldsymbol{A}_{ex} = \frac{\boldsymbol{Q}_{total}}{\boldsymbol{U}_{overall\_cor} \cdot \boldsymbol{LMTD}}. \quad (5)$$

The calculation of the logarithmic mean temperature difference (LMTD) takes into account the inlet and outlet HEX temperatures of the hot (T) and cold (t) streams (Towler and Sinnott, 2013):

$$\boldsymbol{LMTD} = \frac{(\boldsymbol{T}_{in} - \boldsymbol{t}_{out}) - (\boldsymbol{T}_{out} - \boldsymbol{t}_{in})}{\boldsymbol{ln}\,\frac{(\boldsymbol{T}_{in} - \boldsymbol{t}_{out})}{(\boldsymbol{T}_{out} - \boldsymbol{t}_{in})}}. \quad (6)$$

The calculation of the corrected overall heat transfer coefficient ($U_{overall\_cor}$, in $W/m^{2\circ}C$) takes into account the film transfer coefficient of each pair of hot and cold streams (h, $W/m^{2\circ}C$), as a simplification. The heat transfer coefficient is corrected by two factors: a factor of 0.95 that corresponds to a temperature adjustment (Towler and Sinnott, 2013) and a factor of 1.1 that accounts for 10% of area increase due to fouling (Green and Perry, 1999). The film transfer coefficients for each cold and hot stream of the process are estimated based on bibliographic data (non-exhaustive estimation):

$$\boldsymbol{U}_{overall\_cor} = \boldsymbol{U}_{overall} \cdot \frac{0.95}{1.1}, \quad (7)$$

$$\boldsymbol{U}_{overall} = \frac{1}{\frac{1}{\boldsymbol{h}_{hot}} + \frac{1}{\boldsymbol{h}_{cold}}}. \quad (8)$$

Process Optimization

A sequential and systematic approach is used to design and optimize the Bio-SOFC plant. The present work adapts the multi-period approach described by Pérez-Fortes et al. (2019) to consider one unique period, and the queuing MO optimization (QMOO) algorithm is replaced by ev-MOGA, an elitist MO evolutionary algorithm developed by the Predictive Control and Heuristic Optimization Group (CPOH) at Universitat Politècnica de València (Spain), which is available *via* the MATLAB central file exchange (Herrero, 2020). Evolutionary algorithms are heuristic methods that base the optimization strategy on the exploration of the search space (defined by the decision variables and their range of variation); thus, they allow for the optimization of a non-linear and non-continuous system of equations. The sequential steps of the MO optimization methodology consist of 1) the calculation of the mass and energy balances, 2) the system energy integration, and 3) the evaluation of the performance indicators. The ev-MOGA constitutes the master or upper optimization level of the iterative solution process, with the subsequent steps 1), 2), and 3) acting as the slaves or within the lower optimization level. The algorithm is used to identify the most appropriate input values of the defined decision variables, which are varied according to the resulting values of the objective functions. **Figure 2** outlines the main steps of the MO optimization methodology used in the current project. Ten relevant plant variables (see *Input Data*) are selected, and the three objective functions mentioned above (electrical and thermal efficiencies and the total HEX area) are considered. In an evolutionary algorithm, the constraints (or conditions that must be fulfilled) are not enforced but verified by filtering (last step before the loop). In the current project, four constraints are considered, according to SOFC requirements and the heat balance of the allothermal gasifier (see *Input Data*).

In order to keep the mathematical problem (heat management) linear (MILP), the approach considers the

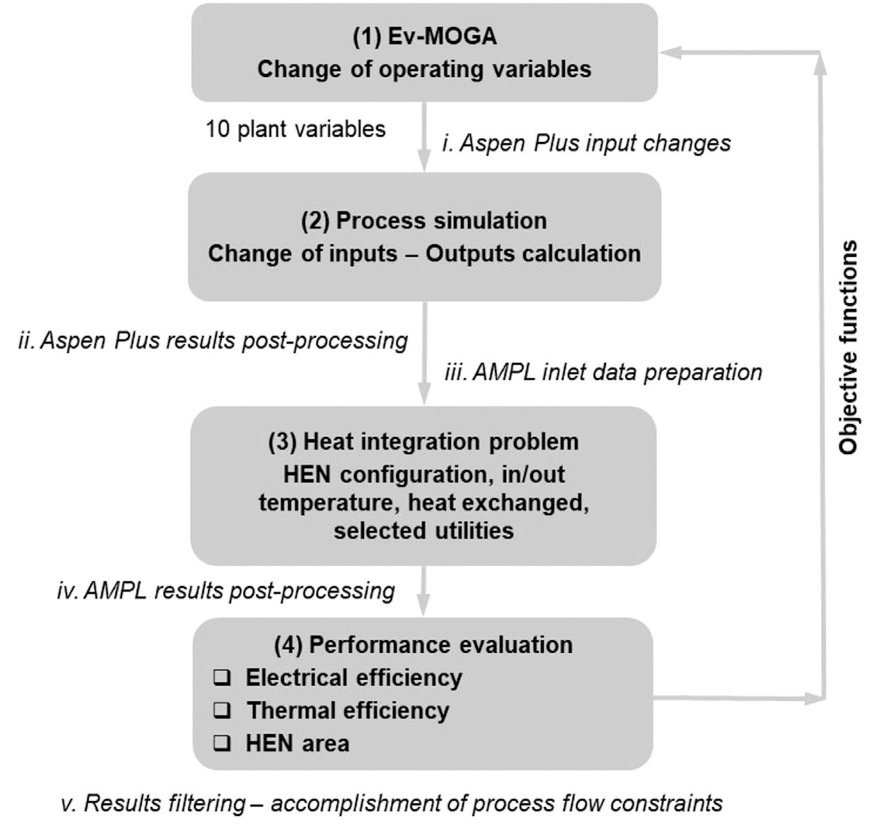

FIGURE 2 | Sequential multi-objective optimization approach for the Bio-SOFC process and HEN design.

optimization of the design specifications (decision variables; among them, temperatures) at the ev-MOGA upper level and the calculation of the HEX areas at a lower level, after solving the optimal matching of streams using the AMPL simultaneous approach. The structure of the HEN is proposed *via* integer variables (binary), considering all the possible matches of hot and cold streams of a stage. The problem is linear by solving the superstructure arrangements: heat transfer flow and energy balances. MATLAB software is used to develop the needed routines for data pre- and post-processing (calculation of the objective functions, filtering, and communication between the software programs Aspen Plus and AMPL). The followed procedure complies with the OSMOSE structure (Industrial Process and Energy Systems Engineering Group, 2020), which is the optimization platform developed by the Industrial Process and Energy Systems Engineering (IPESE) group from EPFL.

As a result of the optimization, the Pareto fronts will allow the decision-maker to visualize the consequences of the selected choice, in terms of performance of one criterion at the expense of the others. Among the selected objectives, maximization of Eff_{el} and maximization of Eff_{th} are conflictive between them, as, in general, one increases if the other decreases (i.e., ideally, $\mathrm{Eff}_{th} = 1 - \mathrm{Eff}_{el}$). The third objective, the HEN area, acts as an economic criterion (capital cost), as the size of the pilot plant is fixed. In this specific case, the operating costs allocated to the utilities are not relevant to optimization, as a unique utility has been selected, the steam that can be used in the process or be sold into the market. In *Selection of Optimum Designs*, the selected non-dominated solutions reported correspond to the extremes of the Pareto frontier and to a weighted distance solution (Euclidean distance to the utopian point—0.4 of Eff_{th} and 0.5 of Eff_{el}, and the minimum HEN area found during the optimization).

Summarizing, the aim of the optimization is twofold: 1) to optimize the process design specifications and 2) to propose an HEN structure. This second point is further described in the next section.

Heat Management

The heat integration problem determines the structure and design variables (inlet and outlet temperatures and HEX areas) of the HEN. The procedure applied here uses as a starting point the work by Pérez-Fortes et al. (2019), which based its approach on the original works by Mian and co-workers (Mian et al., 2016; Martelli et al., 2017). The SYNHEAT algorithm from Martelli et al. (2017) was modified to take into account the multi-period optimization strategy from Mian et al. (2016) in Pérez-Fortes et al. (2019). The same sequential framework idea (upper/lower optimization levels) from Mian et al. (2016) is further adapted here, with different intermediate steps and different upper level algorithms and objective functions, and for a unique period. Another difference as well is that the minimum temperature difference between a hot and a cold stream ($\Delta T_{\min}$) is not considered for optimization but is given as input (30°C).

It was mentioned in *Process Simulation* that two different heat management approaches are used for the scenario evaluation and for the process optimization: pinch analysis and SYNHEAT superstructure, respectively. Pinch analysis using the problem table method was already proposed by Linnhoff and Hindmarsh (1983), where all the streams are combined within temperature intervals to provide a perfect process integration and the minimum external energy requirements. The graphical representation of the problem table is the GCC, and it is used here in *Scenario Evaluation* to analyze the heat management of the Bio-SOFC plant in general and to compare scenarios in particular (i.e., to estimate the cold utility needs).

The SYNHEAT superstructure is used to determine the HEN layout. It stands for the type of stream connection and overall outline, originally proposed by Yee et al. (1990). Parallel and series HEXs can be considered. It assumes constant heat capacities, constant heat transfer coefficients, counter-current HEXs, and isothermal mixers. The proposed representation stands for a "stage-wise" superstructure that allows for matching of different streams; within each stage, potential exchanges between hot and cold streams can happen. In the problem table based on the heat cascade, the number of stages is equal to the number of energy intervals (requiring a large number of exchangers) (Yee et al., 1990). In general, the number of stages will be lower than the maximum number of hot and cold streams, owing that an optimal and practical HEN design should not require a large number of HEXs (i.e., a particular stream should not exchange heat with many streams) (Yee et al., 1990). Overall, the minimum number of HEXs to install is usually the number of process streams and utilities, minus one (Linnhoff and Hindmarsh, 1983). Accordingly, in the current work, three stages have been selected. The total number of cold streams in our process is 4, the total number of hot streams is 8 (without considering the overall evaporation process of the steam needed for the FTU, as is included in the utility), and one utility is considered; the minimum number of HEXs to install is 12. Note that the evaporation process of the utility/steam generation may comprise three bodies—economizer, evaporator, and superheater (thus, for practical purposes, 14 HEXs is the minimum number). Moreover, not all the hot and cold streams can be combined among them; we take into account the forbidden match between air- and fuel-rich streams. As part of the algorithm developed by Martelli et al. (2017), also restricted matches and no-splitting streams are possible.

The Bio-SOFC plant results in a threshold problem, i.e., only requiring a cold utility (the plant produces enough heat for its own process consumption and still has excess of it). In the calculation of $\mathrm{Eff_{th}}$, it is considered that all the system's heat that needs to be released *via* the cold utility is used to produce steam at 5 bar and 220°C (i.e., the steam conditions needed at the turbine of the FTU). The scenario evaluation and the optimization differ in the following:

- In the scenario evaluation, the FTU is modeled, and its ad hoc steam needs and generation are taken into account for every considered layout.
- In the optimization, with the aim of being as flexible as possible with the Bio-SOFC plant possibilities, the FTU is not modeled, but the overall amount of steam produced (and which is available for the turbomachinery) is considered, *via* the SYNHEAT algorithm. Methodologically, inside step (3) in **Figure 2**, there is one more iteration, where the results of the AMPL model are read, and specifically, the cold utility needs are taken into account to calculate the specific amount of steam produced *via* an Aspen Plus model of an evaporator (therefore, there is a flow of information between AMPL and Aspen Plus). As a shortcut in the SYNHEAT algorithm (i.e., to calculate the area of heat exchange), the h value of the cold utility is the one of an evaporator (not distinguishing between the economizer, the evaporator, and the superheater). The specific turbine steam needs have been determined for only the selected Pareto cases. The use of a commercial blower to recirculate the AOG toward the combustor was modeled and evaluated. This device was included in the model used for optimization; with its power consumption, the impact of the flow and temperature of the AOG recirculation toward the combustor in the $\mathrm{Eff_{el}}$ is considered.

TABLE 3 | Cases analyzed in *Scenario Evaluation*. Pressurized gasifier, not fixed HEN, global FU = 0.75, and, when present, VL separation at 20°C (see the corresponding **Supplementary Figures S1–S6**).

Name	Description
Case 1	Base case; Bio-SOFC plant without AOG use
Case 2	AOG recirculation to the gasification chamber
Case 3	AOG recirculation to the SOFC LSM anode inlet
Case 4	AOG recirculation to the gasifier combustor without FTU
Case 5	AOG recirculation to the gasifier combustor with FTU
Case 6	AOG used in a GT

The AMPL MILP problem solves the minimum number of connections among streams using CPLEX, which is the MILP solver by IBM.

PROCESS MODELING

The mass and energy balances are performed in Aspen Plus V10 software. The model uses the Peng–Robinson–Boston–Mathias property method, which applies the Peng–Robinson cubic equation of state with the Boston–Mathias alpha function for the calculation of the thermodynamic properties and steam tables. The model is zero-dimensional, and reactors and HEXs' heat losses are neglected (except in the SOFC LSM). International system units are used.

Table 3 summarizes the selected cases for simulation and comparison, so as to conclude the final layout to be optimized. In these cases, biomass feedstock flow was adapted to produce, in each particular case, 25 $\mathrm{kW_e}$ nominal in the SOFC LSM. **Supplementary Table S1** summarizes the default operating conditions and modeling assumptions of the Bio-SOFC plant model. These correspond specifically to the modeling input in Cases 1 to 6. The details of each unit model are described in the following paragraphs.

Fluidized Bed Gasifier

In the indirectly heated gasifier, the gasification chamber was modeled separated from the combustion chamber to take into account the heating needs (i.e., fuel needed) to have a balanced gasifier. The bibliographic sources used as a reference are Doherty et al. (2013) and Marcantonio et al. (2019). It is assumed that the gasifier works at 1.29325 bar, that it is isothermal (per separate gasifier chamber and combustion chamber), that char is 100% carbon, and that the overall heat needed in the gasification process (the steps that take place in the initial decomposition block, together with RStoic—N, S, and Cl compound formation, RYield—tar production, RGibbs—gasification, and RStoic that simulates the reactions in the filter candles) is provided by the gasifier combustor. The feeding system is not modeled.

The inlet streams to the gasifier are biomass waste, steam (to the gasification chamber), air, LPG (modeled as propane), and AOG in Cases 2–5 (to the combustion chamber). Internally, also a fraction of char, from the gasification process, is burnt into the combustor. The amount of biomass is controlled by a design specification block that varies the amount of inlet waste to reach a gross power output in the SOFC LSM of 25 kW_e. Once the amount of biomass is calculated, the amount of inlet water (which is circulated *via* a pump and converted into steam in an evaporator—sum of the economizer, evaporator, and superheater) is calculated by a calculator block, reaching the specified steam-to-biomass ratio (STB) of 0.5. The amount of LPG is calculated by a design specification block, based on the balance of heat mentioned in the previous paragraph. The amount of inlet air to burn all the fuels in the combustor is calculated in a calculator block that considers a 1.12% excess of air.

The biomass stream, hazelnut shell, is modeled as an unconventional stream (non-conventional solid) that is converted into its elements (conventional components: carbon graphite, H_2, N_2, O_2, S, Cl_2, ash) *via* an RYield reactor (definition of component yields), which uses the ultimate analysis of the considered biomass type. A calculator block is defined for this purpose. Ash is also defined as a non-conventional solid. The decomposed stream goes to an RStoic reactor that simulates the production of H_2S, HCl, and NH_3 from the conversion of the overall amounts of N_2, S, and Cl_2:

$$\frac{1}{2}\boldsymbol{N}_2 + \frac{3}{2}\boldsymbol{H}_2 \rightarrow \boldsymbol{NH}_3 \tag{9}$$

$$\boldsymbol{H}_2 + \boldsymbol{S} \rightarrow \boldsymbol{H}_2\boldsymbol{S} \tag{10}$$

$$\boldsymbol{Cl}_2 + \boldsymbol{H}_2 \rightarrow 2\boldsymbol{HCl} \tag{11}$$

Afterward, the char, inorganics, and volatiles are separated.

- 11% of char is separated and sent toward the gasifier combustor (consortium discussion), together with the ashes (Akhlas et al., 2015). The rest is divided into two streams: 92% going to the gasifier and 8% going to the tar production reactor (Marcantonio et al., 2019).
- The inorganics directly go to the mixing step, before the filter candles.
- The volatile stream, in turn, is also divided into two streams: the main one goes to the gasification block and a fraction of H_2 that is used to produce tar to the tar production reactor.

Tar production, in an RGibbs reactor, considers the synthesis of toluene (C_7H_8), benzene (C_6H_6), and naphthalene ($C_{10}H_8$), as tar representatives, from H_2 and C. The needed stoichiometric amount of H_2 is calculated based on the following tar synthesis reactions and the aim of obtaining a molar proportion of 60% of benzene, 20% of naphthalene, and 20% of toluene:

$$3\boldsymbol{H}_2 + 6\boldsymbol{C} \rightarrow \boldsymbol{C}_6\boldsymbol{H}_6 \tag{12}$$

$$4\boldsymbol{H}_2 + 10\boldsymbol{C} \rightarrow \boldsymbol{C}_{10}\boldsymbol{H}_8 \tag{13}$$

$$4\boldsymbol{H}_2 + 7\boldsymbol{C} \rightarrow \boldsymbol{C}_7\boldsymbol{H}_8 \tag{14}$$

The gasifier, whose inlet streams are steam, volatiles, and a little fraction of char, is modeled with RGibbs, a Gibbs free energy minimization reactor applying the restricted quasi-equilibrium approach *via* Data-Fit from experimental data, from Marcantonio et al. (2019). The gasification reactions are

$$\boldsymbol{C} + \boldsymbol{H}_2\boldsymbol{O} \rightarrow \boldsymbol{H}_2 + \boldsymbol{CO} \tag{15}$$

$$\boldsymbol{C} + \frac{1}{2}\boldsymbol{O}_2 \rightarrow \boldsymbol{CO} \tag{16}$$

$$\boldsymbol{CO} + \boldsymbol{H}_2\boldsymbol{O} \rightarrow \boldsymbol{H}_2 + \boldsymbol{CO}_2 \tag{17}$$

$$\boldsymbol{H}_2 + \frac{1}{2}\boldsymbol{O}_2 \rightarrow \boldsymbol{H}_2\boldsymbol{O} \tag{18}$$

$$\boldsymbol{CH}_4 + \boldsymbol{H}_2\boldsymbol{O} \rightarrow \boldsymbol{CO} + 3\boldsymbol{H}_2 \tag{19}$$

The temperature approach for each reaction is −0.81°C, 1.09°C, −5.27°C, 1.12°C, and −233.4°C, respectively (Marcantonio et al., 2019). The last value has been adapted in the current model to adjust better to the results obtained from the gasifier model in MATLAB (first principle model developed for the existing gasifier). After the gasifier and the tar production, all separated streams are mixed (Marcantonio et al., 2019).

The gasifier combustor is modeled as an isothermal reactor with complete combustion. The inlet air is compressed and heated up to 400°C (600°C in Case 5) before entering the unit. The filter candles (described in the next section) are placed inside the gasifier. The temperature of the syngas going out of the gasifier takes into account this step; it is considered that the filter candles decrease the gasification temperature by 70°C. Before the filter candles, in the pilot plant reactor, there is an in-bed gas-cleaning step that uses calcined dolomite to adsorb tars, NH_3, H_2S, and HCl (Marcantonio et al., 2020). This reactor is not modeled in the current approach (taking into account that this unit does not have a significant contribution to the overall gasifier balance, i.e., mass—syngas composition—and energy balances, except for the contaminant separation), and as an alternative, the contaminants are assumed to be appropriately separated from the main syngas in the downstream GCU. The results of the model (before the filter candles) have been contrasted with the results of the MATLAB model (see **Supplementary**

Table S2), with an acceptable agreement (with the larger discrepancy in CH_4 composition estimation).

Gas-Cleaning Units

The gas-cleaning units in the Bio-SOFC plant include (Marcantonio et al., 2020) the in-bed gas cleaning by a calcined dolomite bed, the catalytic filter candles, the sorbent reactor that separates S compounds, the alkali-based sorbent reactor that separates Cl compounds, and the tar reformer.

As a simplification in the Bio-SOFC plant model, the syngas-cleaning units are the following:

- An RStoic reactor simulating the catalytic filter candles, where methane, toluene, benzene, and naphthalene react with water to produce CO and H_2. These reactions are considered to take place at a temperature that is 70°C lower than the gasification temperature.
- Two heat exchangers that adapt the temperature to 400°C and 550°C, the two selected operating temperatures for S and Cl separation and for tar reforming, respectively.
- The HCl adsorber, H_2S adsorber, and tar reformer that are simply modeled as a component separator that splits all the contaminants from the syngas before the SOFC LSM.

The following reactions take place in the catalytic filter candles, with the specified fractional conversions of methane (0.9), toluene (0.95), benzene (0.92), and naphthalene (0.9) (Marcantonio et al., 2020). These conversion factors belong to an STB of 0.5:

$$\boldsymbol{CH_4} + \boldsymbol{H_2O} \rightarrow 3\boldsymbol{H_2} + \boldsymbol{CO} \tag{20}$$

$$\boldsymbol{C_7H_8} + 7\boldsymbol{H_2O} \rightarrow 11\boldsymbol{H_2} + 7\boldsymbol{CO} \tag{21}$$

$$\boldsymbol{C_6H_6} + 6\boldsymbol{H_2O} \rightarrow 9\boldsymbol{H_2} + 6\boldsymbol{CO} \tag{22}$$

$$\boldsymbol{C_{10}H_8} + 10\boldsymbol{H_2O} \rightarrow 14\boldsymbol{H_2} + 10\boldsymbol{CO} \tag{23}$$

Solid Oxide Fuel Cell Large Stack Module

The SOFC LSM model compiles the modeling approaches in Van herle et al. (2003); EG and G Technical Services, I (2004); Doherty et al. (2009); Pérez-Fortes et al. (2019). In the selected pressurized gasifier configuration, and taking into account the pressure losses in **Table 1**, the anode inlet pressure is 1.07325 bar and cathode inlet pressure is 1.05825 bar. The model is 0D and considers that the inlet gases are heated to a temperature of 700°C, that the outlet temperature (AOG and COG) is 790°C, and that the electrochemical and chemical reactions occur at an average reactor temperature (calculated as an average of the inlet and outlet temperatures—i.e., 745°C with base conditions). The SOFC module is balanced: the outlet power is calculated (see below) and the heat that needs to be evacuated is the result of a heat balance. The model consists of an anode block that is modeled by two RGibbs reactors, one that simulates an internal reformer and another one, downstream the first one, which simulates the combustion step. Both of them, based on inlet species, calculate the phase and chemical equilibriums. Thus, the outlet gas composition is at equilibrium. The second RGibbs receives O_2 from the cathode block, simulated as a component separator that splits O_2 required for the electrochemical reaction. The streams that go out from the anode and cathode are mixed for the heat balance step. The AOG and COG are separated (knowing that all remaining O_2 and N_2 belong to the COG) after the heat balance step (downstream the second RGibbs). The heat loss for the LSM is 2.5 kW (Pérez-Fortes et al., 2019). The inlet amount of air is controlled *via* a design specification block to obtain the desired outlet temperature.

Given the local fuel utilization (FU), the model calculates the needed amount of O_2 in the anode to perform the electrochemical reaction. Note that the local FU is 0.75 when no recirculation affecting the LSM is taking place. As a matter of comparison among the scenarios, a global FU of 0.75 has been fixed. The equivalent amount of H_2 is calculated as in the equations below, considering the overall hydrogen reaction. $H_2(eq)$ comprises the inlet syngas H_2 amount and the H_2 quantity that could be produced from the syngas fractions of CO and CH_4 by the water–gas shift and methane-reforming reactions. It is common to assume that CH_4 is reformed and that CO is shifted to H_2 and, therefore, that only H_2 participates in the electrochemical reaction. To calculate O_2 (needed) and the current density (J), the inlet syngas composition is taken into account:

$$\boldsymbol{H_2} + \frac{1}{2}\boldsymbol{O_2} \rightarrow \boldsymbol{H_2O} \tag{24}$$

$$\boldsymbol{H_2}(\boldsymbol{eq}) = \boldsymbol{H_2}(\boldsymbol{in}) + \boldsymbol{CO}(\boldsymbol{in}) + 4\boldsymbol{CH_4}(\boldsymbol{in}), \tag{25}$$

$$\boldsymbol{H_2}(\boldsymbol{consumed}) = \boldsymbol{FU} \cdot \boldsymbol{H_2}(\boldsymbol{eq}), \tag{26}$$

$$\boldsymbol{O_2}(\boldsymbol{needed}) = \frac{1}{2} \cdot \boldsymbol{H_2}(\boldsymbol{consumed}). \tag{27}$$

The current (I) ("shortcut value" and not representative, as the current depends on the cell connection), current density, and voltage (V_{max} or ideal) are calculated as follows (Van herle et al., 2003; EG and G Technical Services, 2004):

$$\boldsymbol{I_{max}} = \boldsymbol{H_2}(\boldsymbol{eq}) \cdot \boldsymbol{z} \cdot \boldsymbol{F}, \tag{28}$$

$$\boldsymbol{I} = \boldsymbol{FU} \cdot \boldsymbol{I_{max}}, \tag{29}$$

$$\boldsymbol{J} = \frac{\boldsymbol{I}}{\boldsymbol{Area}}. \tag{30}$$

Here, z = 2 (number of electrons transferred) and F = Faraday's constant = 96,485 C/mol.

The calculation of the ΔH and TΔS of the hydrogen oxidation reaction (W) accounts for the difference between the outlet and the inlet steam's enthalpy and entropy values, to estimate the Gibbs free energy (ΔG):

$$\boldsymbol{W_{max}} = -\Delta\boldsymbol{G}, \tag{31}$$

$$\boldsymbol{V_{max}} = -\Delta\boldsymbol{G}/\boldsymbol{I}. \tag{32}$$

The calculation of the ASR (Ω/cm^2) considers the overall governing equations from Nakajo et al. (2011), simplified to be included in the current 0D model. It is composed by its activation, ohmic, and concentration loss terms. Therefore, the final power produced in the SOFC LSM takes into account the V_{cell}, which includes the potential losses. The calculated power is an input variable to the SOFC heat balance, as mentioned at the

TABLE 4 | List of the heating and cooling needs of the Bio-SOFC plant (H: heater, C: cooler), their fixed temperature, type of stream, and estimated film transfer coefficient (h, in W/m^{2}°C) (Smith, 2005; Towler and Sinnott, 2013). In order to calculate the exchange area linked to the cold utility, h = 6000 W/m^{2}°C was assumed.

C or H	Temperature range (°C)	Type of stream	h (W/m^{2}°C)
C1	780–400	Syngas	200
C2	Case dependent	AOG	200
C3	960–120	Flue gas	150
C4	790–140	Air	160
C6[a]	140–50	Air	160
H1	61–400	Air	160
H2	400–550	Syngas	200
H3	Case dependent	AOG	200
H4	550–700	Syngas	200
H5	31–700	Air	160
H6EC	25–108	Water	4000
H6EV	108–108	Water–steam	6000
H6S	108–400	Steam	180
H7EC[a]	25–152	Water	4000
H7EV[a]	152–152	Water–steam	6000
H7S[a]	152–220	Steam	180
H8[a]	140–50	Water	4000

[a] *Not present in the optimization.*

beginning of the section. The results of the SOFC LSM model have been contrasted with the values of an operation map provided by the company SOLIDpower (SP), as summarized in **Supplementary Table S3**.

Fan Turbine Unit

This unit is modeled using the compressor and turbine units from Aspen Plus. The (micro)steam turbine of the FTU has to provide all the power needed by the AOG fan, which indeed depends on the flowrate and the composition of the recirculated stream. Depending on the density of the recirculated stream, the needs of the recirculator vary, and thus, the steam expanded in the turbine varies accordingly.

It is assumed that the turbine has an isentropic efficiency of 0.4 and the inlet steam is at 5 bar and 220°C. The discharge pressure is 2.5 bar. The turbofan is assumed to work with an isentropic efficiency of 0.6. The power transfer among devices, emulating the mechanical efficiency, has a factor of 0.8. The used efficiencies are based on the performance of a thermally driven high-speed gas-bearing–supported turbofan first demonstrated by Wagner et al. (2020).

Pressure Changers, Heaters, and Coolers

The balance of plant (BoP) components such as pumps for water supply, blowers for air supply and gas circulation, and heaters and coolers are modeled using standard Aspen Plus library components. The performance of the blowers is determined based on the isentropic efficiencies of 0.6 and mechanical efficiencies of 1. The pumps' efficiencies are 0.8. Coolers and heaters are usually modeled without pressure loss (except otherwise indicated in **Table 1**). For the design of the HEN, a ΔT_{min} of 30°C is assumed. See **Table 4** for a summary of all the HEXs considered, characterized by their temperature range and film transfer coefficients; these data are introduced in the SYNHEAT algorithm.

Gas Turbine

As an AOG alternative, its burning and use in a GT are also considered based on the promising results reported by Facchinetti et al. (2012); Caliandro et al. (2014); Facchinetti et al. (2014), even if the authors already pointed out in Facchinetti et al. (2012) (evaluation of hydrothermal gasification–SOFC) that there is a trade-off between increased system performance and increased system complexity. In that work, the electrical efficiency can go up to 63% by considering a sub-atmospheric inverted Brayton cycle with oxy-combustion, two GTs (one at the anode side and another one at the cathode side), and CO_2 separation *via* steam condensation and one steam production—one utilization level in a steam turbine. In Caliandro et al. (2014), the electrical efficiency of a non-pressurized small-scale gasifier–SOFC system, using an indirect circulating fluidized bed gasifier, goes up to 64.5%, when using a GT and a steam turbine.

All the AOG is therefore sent to a downstream combustor in Case 6. The burner has a stoichiometric (and complete) combustion. The burner has three inlet streams: AOG, air, and steam (in order to increase the expanding mass flow and control the combustion chamber temperature). The AOG enters the unit at 790°C and 1.04325 bar. Air enters at the same pressure and temperature, while steam enters at atmospheric pressure. The inlet amount of steam corresponds to an steam excess ratio of 3 (toward the inlet mass flow of fuel) (Facchinetti et al., 2014). The burner is adiabatic, and the outlet temperature results in 1176°C. This is the turbine inlet temperature. The pressure at the turbine outlet is 0.2029 bar. Between the GT and the downstream compressor, water is condensed so as to decrease compression power: in that way, water is pumped separately. Flue gas and water are compressed up to atmospheric pressure. The flue gas is vented at 140°C.

RESULTS

Scenario Evaluation

The resulting GCCs for the different cases are presented in **Figure 3** (see the detailed hot and cold streams' temperatures and loads in **Supplementary Table S4**). It is clearly seen that the Bio-SOFC plant has a threshold problem, i.e., only cold utility is needed. The regions where the GCC bends back on itself represent regions where net heat can be exchanged between the different temperature intervals (process heat exchange). The different GCCs of the different cases differ in the amount of heat that can be exchanged within the process, the amount of required cold utility (as explained in *Methodology*, in our case, steam at 5 bar, to power the turbine of the FTU unit, which can be produced), and its temperature. See that Case 2 needs notably more heat to produce steam to power the FTU. The main gas responsible for the different "widths" of the GCC is the flue gas from the gasifier combustor, with more or less heat available (different streams' mass flowrate and difference of temperatures). As a consequence, when the flue gas has a higher heat load, the

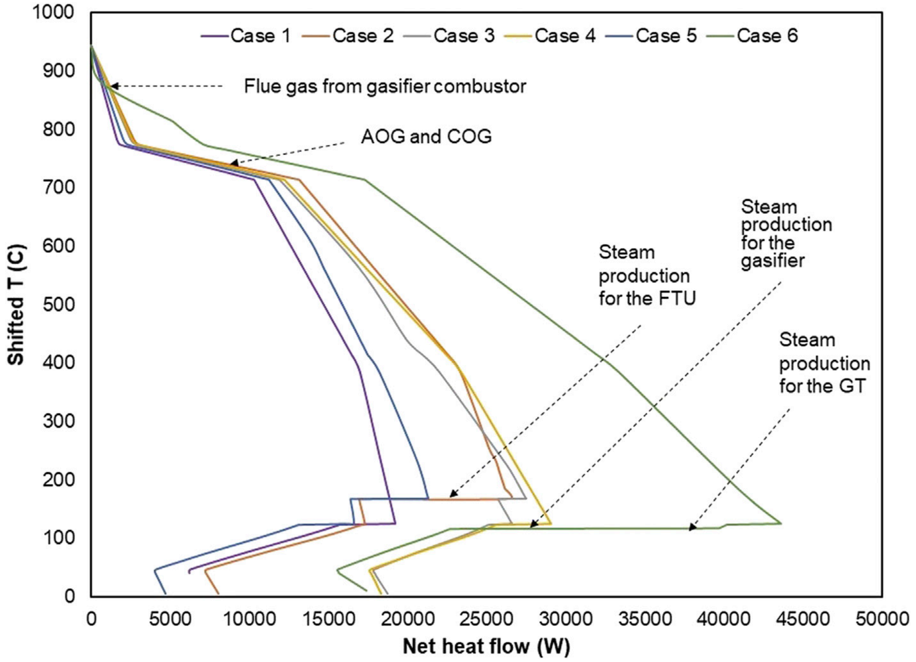

FIGURE 3 | GCCs of Cases 1 to 6.

value of the cold utility is higher. Note the difference between Case 1 and Cases 2, 3, and 4. Case 5 needs less cold utility because the AOG and air streams to the combustor are heated up (thus, the available heat is already used within the process). Case 6 has the largest GCC length, as heat is not only produced in the gasifier combustor *via* LPG but also produced in the GT combustor *via* AOG combustion (with its own streams of inlet air and steam). The less integrated scenarios may have a higher thermal efficiency, as they need more cold utility. However, this is not a situation to be favored, as, in general, higher cold utility needs imply higher LPG demand. Thus, the heat integration results of Case 5 pinpoint the positive effect of decreasing LPG consumption at the expense of higher AOG combustion inlet temperature and steam condensation.

The results of the evaluation of the six cases are summarized in **Supplementary Table S5**. The amount of biomass is controlled to produce 25 kW_e of gross electricity. The net electricity produced is around 24 kW_e in all cases, except when using the GT, the electricity produced goes up to 31.7 kW_e. Case 2 counts with the lowest inlet biomass stream; this is a positive effect of recirculating the AOG toward the gasifier. Lower biomass is needed as, together with the required steam (the AOG in Case 2 has 40% of H_2O in mole basis), the AOG also has carbonaceous species. When the AOG is not used in the gasifier combustor, the inlet amount of LPG is 16.22 kW_{th} (Cases 1 and 6). Case 2, however, needs a higher amount of LPG to close the heat balance in the gasifier. The reason is the higher amount of gas that has to be heated up. The amount of LPG considerably decreases in Cases 3, 4, and particularly 5; when the recirculation ratio toward the inlet stream of the SOFC (RR) is 0.5 (Case 3); and in the last case when the temperature of the AOG and air to the gasifier combustor is increased. In order to calculate the Eff_{el} value, it is seen from the discussed numbers that the larger difference is marked by the remarkable decrease in LPG needs in Case 5 (compared to the biomass inlet decrease in Case 2 and the inlet LPG amounts in Cases 3 and 4).

The syngas produced in the fluidized bed gasifier has the same quality in all the cases (the same inlet biomass and STB), except in Case 2, where the use of AOG instead of steam contributes to produce a larger mass flowrate of syngas, but with a LHV due to dilution (larger CO_2 and H_2O fractions). However, the calorific power of the syngas in Case 2 is overall higher than that for the other cases.

The AOG composition changes in Case 2, when it is recirculated back to the gasifier (higher fractions of CO_2 and H_2O), and changes in Case 3, when it is recirculated back to the SOFC LSM anode inlet (higher fractions of H_2, CO, and CO_2 and lower portion of H_2O). With the Aspen Plus model, voltage is quite similar in all cases, whereas in Case 2, voltage is lower (worst SOFC performance). The amount of air needed is similar as well, except in Cases 2 and 3, where, indeed, AOG composition also changes. However, in order to know more accurate SOFC LSM operating values, it is advised to execute a more exhaustive SOFC stack model.

Note that the largest power consumer in the plant is the air compressor for the SOFC LSM, followed by the air compressor for the gasifier needs. The AOG compressor is used in Cases 2, 3, and 4, whereas in Case 5, only the FTU is considered to completely recirculate the AOG to the gasifier combustor.

The CGE is higher in Case 2 (due to a large calorific power of the overall syngas produced) and in Case 5 (because of the lower amount of LPG needed). The SOFC efficiency is similar in all cases, except in Case 2 (in agreement with its lower operating voltage). The electrical efficiency is 10% larger in Case 5 than in Case 1, revealing the clear benefit of using the AOG within the plant. The electrical efficiency is 45% in Case 6, compared to 44% in Case 5, when the GT is used. The cooling water that can be generated *via* COG cooling is also evaluated. The value of cold utility reported, as explained in *Methodology*, assumes that all the heat that needs to be evacuated from the system is useful heat to produce marketable steam. From the results obtained, $\mathrm{Eff_{th}}$'s are higher in Cases 3, 4, and 6. The total efficiency is higher in Case 6, followed by Cases 3 and 4, Case 5, and Cases 2 and 1. However, as mentioned before, thermal efficiency will always be higher when more LPG is consumed. Therefore, as a criterion for scenario selection for optimization, the $\mathrm{Eff_{el}}$ is considered overall; the AOG use in the gasifier combustor decreases the use of LPG, and more if inlet temperatures are increased. The recirculation of the AOG to the gasifier and to the SOFC results in more diluted syngas entering the SOFC LSM (thus, in a worse overall system performance). The results of $\mathrm{Eff_{el}}$ of Cases 5 and 6 are very similar. However, Case 6 has a more complex layout and consumes more LPG than Case 5.

The larger compression pressure requirement in the FTU happens in Case 5. However, the steam needs are lower than those in Case 2 as, hypothetically, it is assumed that the AOG can be compressed at 20°C (vs. 200°C that so far has been demonstrated in the technology, since the steam in the turbine is at 220°C, to avoid large temperature gradients and steam condensation in the gas bearings). If compression is at 200°C, the total power needed from the turbine is 209 W instead of 162 W, 16.5 kg/h instead of 10.16 kg/h of steam consumed. Note that it is still less than that in Case 2 (even though all the AOG stream is of concern), as steam has been separated from the AOG (thus resulting in less flowrate to compress).

As a conclusion of this evaluation, Case 5 is the selected layout for optimization. The internal use of AOG in the Bio-SOFC plant proves to be positive to increase the $\mathrm{Eff_{el}}$ while decreasing the amount of LPG, pursuing the green production of electricity. The use of the FTU is also strategically selected for optimization, as it can use steam generated within the plant to compress the AOG, thus not decreasing the amount of net electricity produced (Case 4 AOG fan consumption—0.129 W vs. 10.19 kg/h of steam needed). The steam released after the turbine expansion is still marketable steam.

Within the BLAZE project context, the net present value of the base Case 5 was studied, considering pilot plant values. Among the overall investment, the SOFC LSM contributes the most, followed by the gasifier and feeding system, HEN, reactors, and vessels. Operating costs overcome revenues. The most influencing variable in the net present value is the inside battery limits investment. Further R&D is needed to decrease it[2].

Optimization

Supplementary Figure S7 presents the Bio-SOFC plant layout to be optimized, including the variables considered for optimization, in red. The optimization variables are summarized in the next section, whereas the process constraints are listed in **Table 2**. The forbidden matches correspond to prohibited hot–cold stream connections in the HEN design due to possible flammability issues.

Input Data

The generation of green electricity is a design priority. Thus, the AOG recirculation toward the gasifier combustor was the preferred recirculation option. The temperatures of inlet air (TH1) and AOG to the combustor (TH3) were identified as key to achieve zero LPG. Moreover, the lower the amount of steam in the AOG (which depends on TC2), the better towards zero LPG consumption, to consume less compression power and to require less combustion heat in the gasifier combustor. The main operating variables of the gasifier, i.e., the STB, the temperature of the inlet steam (TH6S), and the gasification temperature (TGasif), as well as the main operating variables of the SOFC LSM, i.e., fuel cell inlet temperature ($\mathrm{T_{in}}$ SOFC, the same for the anode and cathode) and FU, are considered decision variables. The hot GCU works at a range of temperatures, with a fixed and complete contaminants' separation fraction, which is assumed not to vary. The chloride and sulfur compounds' abatement units and the tar reformer operating temperatures are therefore optimized. **Table 5** summarizes the decision variables and their possible range of variation.

The forbidden matches are heat exchange connections to avoid, in the Bio-SOFC plant, between fuel-rich and oxygen-rich streams to prevent explosion. In the Bio-SOFC plant, these streams correspond to the following heaters (H) and coolers (C):

- C1: Syngas cooling down after the gasifier
- C2: AOG cooling down for steam separation
- C4: COG cooling down
- H1: Air inlet to the burner
- H2: Syngas between cleaning units
- H3: AOG going to the gasifier combustor
- H4: Syngas going to the SOFC
- H5: Air inlet to the SOFC

The flammability limits are defined as the lowest and highest concentrations of combustibles in air at normal conditions of pressure and temperature (at 1 bar and 20°C); within these limits, the mixture will be burnt if ignited (Towler and Sinnott, 2013). Selecting as a reference the values from Case 5, the compositions of the fuel gases and oxygen-rich gases of the Bio-SOFC system affected by H's and C's mentioned above are summarized in **Table 6** and **Table 7**. The possible mixtures of combustible and oxygen-rich streams are calculated in **Table 8**. The possible flammable mixtures are marked in bold and underlined in the table. The forbidden matches are therefore (C4,H4), (C4,H2), (C1,H5), (C1,H1), and (C2,H1).

Influence of Variables

The output data generated while performing the optimization (independent and control variable values) provide an amount

---

[2] BLAZE project public deliverables can be checked at https://www.blazeproject.eu/resources/.

TABLE 5 | Decision variables for optimization (between brackets, reference in **Supplementary Figure S7**).

Decision variable	Range	Starting value
1. FU on the SOFC LSM (FU)	0.6–0.8	0.75
2. STB in the gasifier (STB)	0.33–0.98	0.5
3. Temperature of gasification (TGasif)	750–850°C	850°C
4. Fuel cell inlet temperature (T_{in} SOFC)	690–750°C	700°C
5. AOG cooling temperature (TC2)	20–300°C	20°C
6. Temperature of inlet air to the gasifier combustor (TH1)	100–760°C	700°C
7. Temperature of inlet steam to the gasifier (TH6S)	200–400°C	200°C
8. Operating temperature of chloride and sulfur compounds' abatement units (TC1)	200–450°C	400°C
9. Operating temperature of the tar reformer (TH2)	550–700°C	550°C
10. AOG inlet temperature to the gasifier combustor (TH3)	20–760°C	400°C

TABLE 6 | Composition of fuel gases in the Bio-SOFC plant.

Component/mole fraction	Syngas	AOG_{ar}	AOG_{dry}
H_2	0.49	0.13	0.26
CO	0.24	0.057	0.11
CH_4	0.005	0	0
CO_2	0.11	0.30	0.61
H_2O	0.14	0.51	0.02

TABLE 7 | Air and COG compositions in the Bio-SOFC plant.

Component/mole fraction	Air	COG
O_2	0.21	0.19
N_2	0.79	0.81

of information that can be used to analyze the variable's impact on the selected optimization objectives. The electrical efficiency is higher when FU, inlet AOG temperature, and air temperature (TH3 and TH1) to the gasifier combustor increase. On the contrary, Eff_{el} increases when the STB and the gasification temperature decrease. Regarding FU, electricity production is certainly improved as a larger fuel conversion is considered. As widely analyzed in the scenario evaluation, the temperature of the inlet gasifier combustor stream tends to be higher to decrease LPG consumption. In relation to the gasifier operation, see **Supplementary Tables S6, S7** for the effects of the STB and TGasif on relevant gasifier output values. The gasification reactions where steam is involved are endothermic, so the heat of combustion increases as the STB raises. The consumptions of LPG and biomass raise with the STB. The higher the STB, the higher the steam fraction in the syngas. The steam content affects the performance of the SOFC LSM. The more the steam in the SOFC, the more the biomass is needed to produce the same amount of power. Therefore, lower STBs are favored in the optimization.

Analogously, a higher steam fraction in the SOFC LSM is avoided when selecting lower gasification temperatures (moreover, in dry composition, H_2 and CO fractions are higher at lower temperatures). Furthermore, LPG and biomass consumptions increase when the gasification temperature raises. In the variables analysis, it is seen that the higher the CGE, the better the Eff_{el}. The lower the inlet LPG and amount of air to the combustor, the better the Eff_{el}. These last three are dependent variables that are linked to the aimed LPG consumption reduction.

The thermal efficiency is "biased" by a worse system integration, as all the cold utility heat can be used to produce marketable steam, thus increasing the Eff_{th}. Influencing and conflicting variables compared to Eff_{el} are TGasif, TH1 and TH3, and gasifier combustor inlet LPG and air (thus, an increased consumption of LPG would need more steam as the cold utility). Lower T_{in} SOFC and TC2 improve Eff_{th}, as less heat is integrated (needed) within the process.

The HEN area is fairly independent of the influence of the selected decision and control variables (see also the Pareto shape in the next section). Nevertheless, it slightly depends on the T_{in} SOFC; the largest HEX in the Bio-SOFC plant corresponds to H5 (inlet SOFC warming up).

Selection of Optimum Designs

Figure 4 shows the Pareto front and its projection on different planes. The optimization process was executed several times, obtaining a total of 38,028 points. This total number of executed scenarios was filtered, first to only keep the cases that converged in Aspen Plus and AMPL and second to only consider the cases that respect the constraints listed in **Table 2**. The Pareto front and its projections reveal that there exists a trade-off between Eff_{th} and Eff_{el} and between Eff_{el} and HEN area. On the contrary, a higher Eff_{th} requires less HEN area.

From these results, the extremes of the Pareto front are selected (see the columns Eff_{el}, Eff_{th}, and HEN area in **Table 9**). Moreover, the utopian point is used as an ideal of the criteria values to find the closer solutions from the Pareto front. The utopian coordinates are $Eff_{el} = 0.5$, $Eff_{th} = 0.4$, and for the HEN area, the minimum area found in the whole range of executed scenarios was selected. The weighted distance to the utopian point is considered in the colored scale of **Figure 5**. Marked by yellow squares are the 20 closer points to the utopian point. The weight given to the Eff_{el} and Eff_{th} is the same (i.e., 1), while the weight given to the HEN area is 1/100 (considered a less critical objective in the BLAZE project, so as to favor the other two criteria). See the first

TABLE 8 | Combustible and oxygen-rich stream mixtures, compared to the upper and lower flammability limits in air (Towler and Sinnott, 2013).

Component/mole fraction	Syngas (C1) + air SOFC (H5)	Syngas (C1) + air COMB (H1)	Syngas (H2,H4) + COG (C4)	AOG$_{dry}$ (H3) + COG (C4)^a	AOG$_{ar}$ (C2) + air COMB (H1)^b	Lower limit	Upper limit
H_2	**0.0327**^{c}	**0.27**	**0.0333**^{c}	0.0093	**0.072**	0.041	0.742
CO	0.016	**0.13**	0.0166	0.004	0.031	0.125	0.742
CH_4	0.00035	0.003	0.00036	0	0	0.053	0.14

^{a}*Even after checking with FU = 0.6, STB = 0.33, TGasif = 760, H_2 fraction reaches 2 %, still well below the 4% limit.*

^{b}*When checked for the air SOFC flow (which is about 16 times higher than the mass flow of the air COMB), H_2 fraction hardly reaches 2%. Thus, we consider that this match does not need to be forbidden.*

^{c}*Not exactly inside the limits, but selected due to their proximity.*

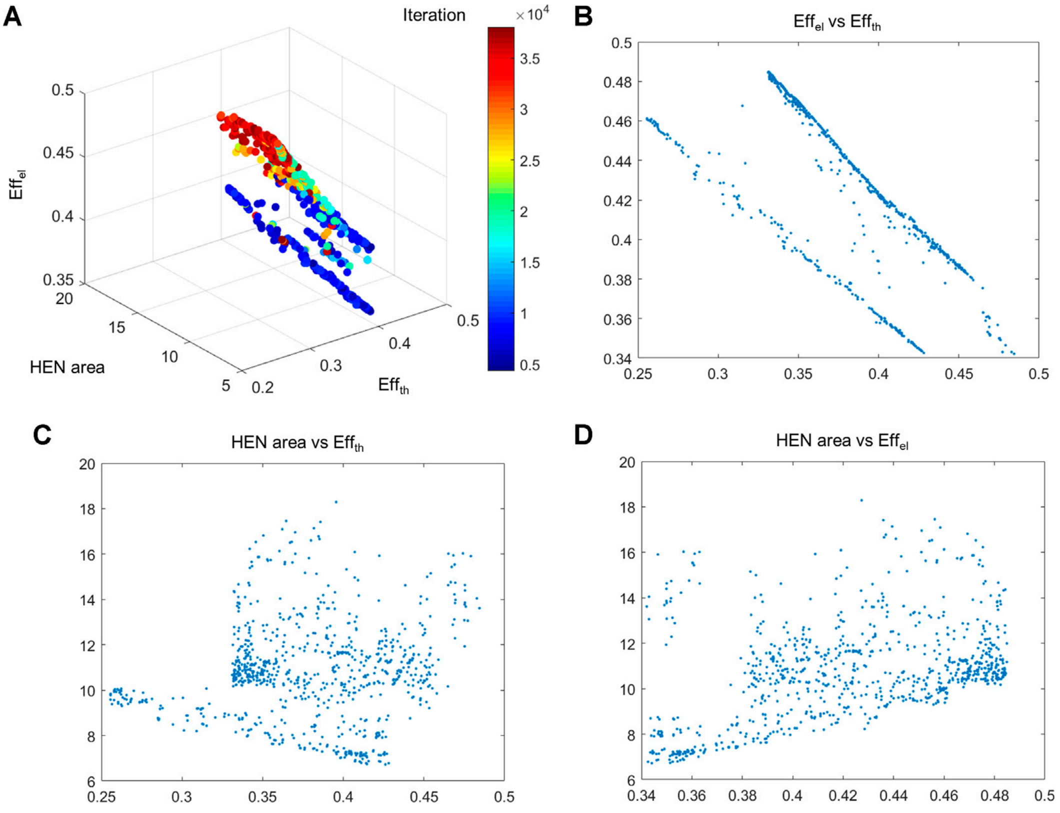

FIGURE 4 | Pareto front of the Bio-SOFC plant (Case 5) optimization. Trade-off among Effel, Effth, and HEX area.

column of **Table 9** for the data corresponding to the closest point to the utopian point.

In **Supplementary Figure S8**, the values of the optimization variables (**Table 5**) of the Pareto points are plotted, sorted by distance (from closer to further) from the utopian point. The most important variables in the Bio-SOFC plant are (in order) as follows:

- FU (var1), which tends to be on the upper limit (above 0.75).
- The AOG cooling temperature (var5), which is low enough to separate steam (below 40°C).
- The SOFC inlet temperature (var4), which tends to be on the lower limit (690–700°C).
- The STB (var2), which tends to be on the lower limit (below 0.4).
- The gasification inlet temperature (var3), which tends to be on the lower limit (around 750–780°C).
- The inlet air temperature to the combustor (var6), usually closer to the upper limit (above 500°C).
- The inlet AOG temperature to the combustor (var10), which tends to be above 100°C.

The selected ranges of temperature for the gasification steam (var7) and the chloride and sulfur compounds' abatement units (var8) and tar reformer (var9) have no impact on the results. The latter is particularly interesting, as it reveals that, for the

TABLE 9 | Selected optimal process designs (extremes of the Pareto front and closest point to the utopian point) and performance.

Variable/performance criteria	Distance utopian	Eff_{el}	Eff_{th}	HEN area
FU	0.780	0.800	0.715	0.746
STB	0.333	0.330	0.967	0.330
TGasif (°C)	782.5	751.2	837.5	839.5
T_{in} SOFC (°C)	690.0	690.4	697.5	690.0
TC2 (°C)	28.7	25.9	26.2	186.9
TH1 (°C)	550.1	745.8	132.4	101.5
TH6S (°C)	321.3	398.6	356.9	221.8
TC1 (°C)	279.4	200.0	236.1	428.6
TH2 (°C)	643.0	551.0	634.3	626.7
TH3 (°C)	508.7	756.6	245.3	263.2
Eff_{el}	0.4547	0.4873	0.3443	0.3493
Eff_{th}[a]	0.3558	0.3052	0.4736	0.4093
Eff_{tot}	0.8105	0.7925	0.8179	0.7587
Area (m^2)	9.980	11.543	13.614	6.727
Steam generated (kg/h)	14.606	10.027	29.977	26.360
Cooling water produced (kg/h)	155.826	153.954	190.537	161.233
Steam to the gasifier (kg/h)	3.261	3.158	10.696	3.371
LPG (kg/h)	0.173	0.000	0.902	1.196
Recirculation compressor (kW) @ TC2	0.122	0.115	0.153	0.360
Steam needed in the FTU (kg/h) @ TC2	9.63	9.13	12.10	28.05
Steam needed in the FTU (kg/h) @ 200°C	15.11	14.35	19.05	[b]

[a] *Considering gas in the FTU fan @ 200°C.*

[b] *TC2 is already close to 200°C; AOG is recirculated with steam.*

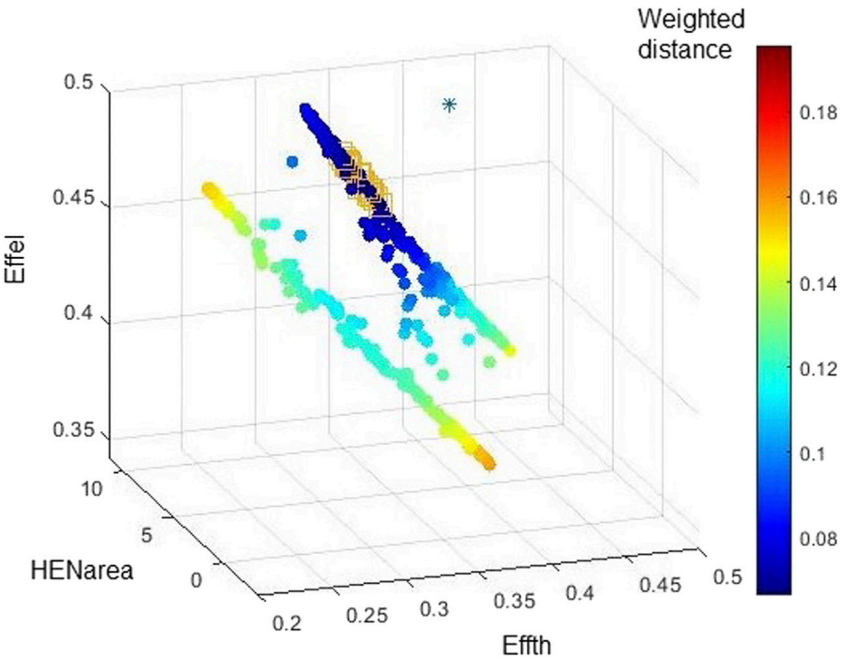

FIGURE 5 | Pareto front and sorting of solutions based upon the utopian point (star point).

specific case of the Bio-SOFC plant, the temperature of the GCU is not crucial for the final efficiency of the plant. However, it was assumed that the efficiency of the GCU units was independent of temperature, and moreover, in the Bio-SOFC plant, production of waste heat is not an issue, as the high-temperature heat is a valuable stream that generates profitable steam. At equality of performance, and in exergy terms, it is not advised to go further down in temperature for the GCU, when the needed temperature downstream is around 700°C.

The results in **Table 9** reveal a total efficiency around 80%. For the solution that is closer to the utopian point, the electrical efficiency is 45%, the thermal efficiency is 36%, and the HEN area is 10 m^2. LPG consumption is zero in the case where Eff_{el} is maximized. In the case where the HEN area is minimized, the LPG consumption is not a crucial variable. Note that the steam consumption of the FTU turbine is below the steam generated in the plant when the AOG is at TC2. However, as explained before, the AOG cannot have such a low temperature. At 200°C, the steam needs could be only covered by the optimum configuration with the largest Eff_{th}. As an alternative, if the FTU is not used, the power consumed by a commercial fan used to provide the ΔP required by the AOG is in the row "Recirculation compressor (kW) @ TC2" in **Table 9**.

The results presented are the extremes of the Pareto front and the utopian point, based on the reported weights above. However, other Pareto solutions from the Pareto front can be selected depending on the decision criteria of the decision-maker, for instance, zero LPG consumption or the calculated exergy efficiency, if priority is given to energy degradation. For instance, for the selected Pareto solutions, the exergy efficiency varies between 34 and 52%, being higher when the electrical efficiency is higher (note that, in the Bio-SOFC plant, the temperatures of the hot and cold utilities were fixed).

Heat Exchanger Network Design

The HEN structures for each of the reported optimum points are summarized in **Supplementary Tables S8–S11**. The reported variables in the tables follow the nomenclature described in the methodology, with capital T corresponding to the hot source (and 1 referring to the inlet, 2 to the outlet). The fourth and fifth columns refer to the stage where heat exchange takes place (as defined in the SYNHEAT algorithm). Therefore, a stream with different stages (which is the case for several hot streams in the current results, not for the cold ones) means that this stream counts with series (up to 3) HEXs. A stream with the same stage several times means that parallel HEXs are considered. End-CU refers to a connection with the cold utility (in this case, generating steam at the conditions required by the FTU).

As general characteristics, the Bio-SOFC plant may count with 12 HEXs with C4–H5 being the most important HEXs (exchange between inlet and outlet air streams of the SOFC LSM). C3 (flue gas) can be combined in many ways, as it is the largest hot source of the Bio-SOFC plant. When combined with H5 (T_{in} SOFC), the HEN area decreases considerably (see **Supplementary Table S11**). C4 (COG) and C3 (flue gas) are indeed the main hot sources.

CONCLUSION

This paper summarizes the different scenario evaluations and the optimization performed to propose a micro-CHP bio-waste gasification–SOFC plant layout and working conditions within the framework of the EU H2020 project BLAZE. Two particularities of this plant are 1) the AOG recirculation and 2) the use of small-scale turbomachinery to make it possible. The main locations where the AOG could be recirculated were 1) the SOFC LSM anode inlet, 2) the gasifier combustor, and 3) the gasification chamber. The AOG recirculation toward the gasifier combustor was selected as the preferred layout for implementation. The optimization of this layout pinpointed the most important plant variables for plant operation: FU (above 0.75), AOG cooling temperature (which has to be low enough to allow steam condensation), SOFC inlet temperature (between 690 and 700°C), STB (below 0.4), gasification inlet temperature (which tends to be on the lower limit), and inlet air temperature to the combustor and inlet AOG temperature to the combustor (which tend to the upper limits). Four optimum designs were selected, i.e., the extremes of the Pareto front (maximum Eff_{el}, maximum Eff_{th}, and minimum HEN area) and the nearest design to the utopian point. The HEN of selected optimal solutions was described (in total, 15 HEXs are foreseen), with a total area of heat exchange between 6 and 14 m^2, which corresponds to an amount of heat exchanged between 91 and 117 kW. The COG and flue gas are the main hot sources, and the consumption of LPG can be avoided, or at least minimized. The most important HEX is the one that exchanges heat between the inlet and outlet air streams of the SOFC LSM. The electrical and thermal efficiencies went up to 49 and 47%, respectively. The combined total efficiency ranges between 76 and 82%. For comparison, current small biomass gasification CHP plants coupled with gas engines have electric efficiencies of up to 25%, and combined efficiencies of up to 80%. The final pilot plant implementation decision will come from the adjustment and consideration as baseline of the optimization results to the strategic decision of the project consortium in terms of steam and LPG consumptions, and, of course, of practical implementation considerations.

DATA AVAILABILITY STATEMENT

The original contributions presented in the study are included in the article/**Supplementary Material**, and further inquiries can be directed to the corresponding author.

AUTHOR CONTRIBUTIONS

MP-F conceptualized the idea. MP-F and AN performed the methodology. MP-F, VH, and AN were involved in modeling and result analysis. MP-F and VH wrote the paper. MP-F edited the paper. MP-F, VH, AN, JS, FM, and JV discussed about the results and reviewed the paper. FM and JV obtained the resources, and JS and JV acquired the funding.

FUNDING

The BLAZE project has received funding from the European Union's Horizon 2020 Research and Innovation Programme under Grant Agreement No. 815284.

ACKNOWLEDGMENTS

Thanks are due to Andrea Di Carlo for gasifier modeling sharing and the biomass- and gasification-related discussions, to Ligang Wang, Jan Pieter Ouweltjes, and Gabriele Prosperi for the provision of data for SOFC validation, to Ilaria Mirabelli and Robert Makkus for the GCU provision of data, to Prof. Enrico Bocci and Prof. Jack Brouwer for the fruitful discussions, and to Alberto Mian for his support during the development of the modeling approach.

SUPPLEMENTARY MATERIAL

The Supplementary Material for this article can be found online at: https://www.frontiersin.org/articles/10.3389/fenrg.2021.665585/full#supplementary-material

REFERENCES

Akhlas, J., Baesso, S., Bertucco, A., and Ruggeri, F. (2015). Coal Gasification by Indirect Heating in a Single Moving Bed Reactor: Process Development & Simulation. *AIMS Energy 3*, 635–665. doi:10.3934/energy.2015.4.635

Bocci, E., Sisinni, M., Moneti, M., Vecchione, L., Di Carlo, A., and Villarini, M. (2014). State of Art of Small Scale Biomass Gasification Power Systems: A Review of the Different Typologies. *Energ. Proced.* 45, 247–256. doi:10.1016/j.egypro.2014.01.027

Buonomano, A., Calise, F., d'Accadia, M. D., Palombo, A., and Vicidomini, M. (2015). Hybrid Solid Oxide Fuel Cells-Gas Turbine Systems for Combined Heat and Power: A Review. *Appl. Energ.* 156, 32–85. doi:10.1016/j.apenergy.2015.06.027

Caliandro, P., Tock, L., Ensinas, A. V., and Maréchal, F. (2014). Thermo-economic Optimization of a Solid Oxide Fuel Cell - Gas Turbine System Fuelled with Gasified Lignocellulosic Biomass. *Energ. Convers. Manage.* 85, 764–773. doi:10.1016/j.enconman.2014.02.009

Choudhury, A., Chandra, H., and Arora, A. (2013). Application of Solid Oxide Fuel Cell Technology for Power Generation-A Review. *Renew. Sustainable Energ. Rev.* 20, 430–442. doi:10.1016/j.rser.2012.11.031

Cockroft, J., and Kelly, N. (2006). A Comparative Assessment of Future Heat and Power Sources for the UK Domestic Sector. *Energ. Convers. Manage.* 47, 2349–2360. doi:10.1016/j.enconman.2005.11.021

Colpan, C. O., Dincer, I., and Hamdullahpur, F. (2007). "Effect of Recirculation on Carbon Deposition for Direct Internal Reforming Solid Oxide Fuel Cells," In Proc. 3rd Internat. Energy, Exergy, and Environ. Symposium. Editor A. F. Miguel, A. H. Reis, and R. N Rosa 1–5 July 2007, Évora, Portugal

Cottrell, C. A., Grasman, S. E., Thomas, M., Martin, K. B., and Sheffield, J. W. (2011). Strategies for Stationary and Portable Fuel Cell Markets. *Int. J. Hydrogen Energ.* 36, 7969–7975. doi:10.1016/j.ijhydene.2011.01.056

Dietrich, R.-U., Oelze, J., Lindermeir, A., Spitta, C., Steffen, M., Küster, T., et al. (2011). Efficiency Gain of Solid Oxide Fuel Cell Systems by Using Anode Offgas Recycle - Results for a Small Scale Propane Driven Unit. *J. Power Sourc.* 196, 7152–7160. doi:10.1016/j.jpowsour.2010.09.016

Doherty, W., Reynolds, A., and Kennedy, D. (2009). Modelling and Simulation of a Biomass Gasification-Solid Oxide Fuel Cell Combined Heat and Power Plant Using aspen Plus. Proc. 22nd Internat. Conf. Eff., Cost, Optim., Simul. Environ. Impact Energ. Syst. Foz Do IguaÇu, Brazil, 1711–1720.

Doherty, W., Reynolds, A., and Kennedy, D. (2013). ASPEN PLUS Simulation of Biomass Gasification in a Steam Blown Dual Fluidised Bed. *Mat. Proc. Energy: Commun. Curr. Res. Technol. Develop.* Editor A. F. Méndez-Vilas (Formatex Research Centre), 212–220.

Doty, S., and Turner, W. C. (2009). *Energy Management Handbook*. 7th ed. The Fairmont Press, Inc. and CRC Press (Taylor & Francis Group)

Dougherty, W., Kartha, S., Rajan, C., Lazarus, M., Bailie, A., Runkle, B., et al. (2009). Greenhouse Gas Reduction Benefits and Costs of a Large-Scale Transition to Hydrogen in the USA. *Energy Policy* 37, 56–67. doi:10.1016/j.enpol.2008.06.039

EG and G Technical Services, I (2004). *Fuel Cell Handbook*. 7 Edition. West Virginia: Fuel Cell, 1–352. doi:10.1002/zaac.200300050

Engelbracht, M., Peters, R., Blum, L., and Stolten, D. (2015). Analysis of a Solid Oxide Fuel Cell System with Low Temperature Anode Off-Gas Recirculation. *ECS Trans.* 68, 283–292. doi:10.1149/06801.0283ecst

Faaij, A. P. C. (2006). Bio-energy in Europe: Changing Technology Choices. *Energy Policy* 34, 322–342. doi:10.1016/j.enpol.2004.03.026

Facchinetti, E., Gassner, M., D'Amelio, M., Maréchal, F., and Favrat, D. (2012). Process Integration and Optimization of a Solid Oxide Fuel Cell - Gas Turbine Hybrid Cycle Fueled with Hydrothermally Gasified Waste Biomass. *Energy* 41, 408–419. doi:10.1016/j.energy.2012.02.059

Facchinetti, E., Favrat, D., and Marechal, F. (2014). Design and Optimization of an Innovative Solid Oxide Fuel Cell-Gas Turbine Hybrid Cycle for Small Scale Distributed Generation. *Fuel Cells* 14, 595–606. doi:10.1002/fuce.201300196

Green, D. W., and Perry, R. H. (1999). *Perry's Chemical Engineers' Handbook - Heat Transfer Equipment Section*. New York, USA: McGraw-Hill Education

Halinen, M., Thomann, O., and Kiviaho, J. (2012). Effect of Anode Off-Gas Recycling on Reforming of Natural Gas for Solid Oxide Fuel Cell Systems. *Fuel Cells* 12, 754–760. doi:10.1002/fuce.201200047

Hassmann, K. (2001). SOFC Power Plants, the Siemens-Westinghouse Approach. *Fuel Cells* 1 (1), 78–84. doi:10.1002/1615-6854(200105)1:1<78::aid-fuce78>3.0.co;2-q

Herrero, J. M. (2020). *Ev-MOGA Multiobjective Evolutionary Algorithm*.

Industrial Process and Energy Systems Engineering Group (2020). *Resources from IPESE Group*. Lausanne, Switzerland: EPFL website.

Kapdan, I. K., and Kargi, F. (2006). Bio-hydrogen Production from Waste Materials. *Enzyme Microb. Technology* 38, 569–582. doi:10.1016/j.enzmictec.2005.09.015

Kemp, I. C. (2007). *Pinch Analysis and Process Integration. A User Guide on Process Integration for the Efficient Use of Energy*. 2nd ed. Burlington, MA, USA: Butterworth-Heinemann, Elsevier

Kothari, R., Singh, D. P., Tyagi, V. V., and Tyagi, S. K. (2012). Fermentative Hydrogen Production - an Alternative Clean Energy Source. *Renew. Sustainable Energ. Rev.* 16, 2337–2346. doi:10.1016/j.rser.2012.01.002

Lee, T. S., Chung, J. N., and Chen, Y.-C. (2011). Design and Optimization of a Combined Fuel Reforming and Solid Oxide Fuel Cell System with Anode Off-Gas Recycling. *Energ. Convers. Manage.* 52, 3214–3226. doi:10.1016/j.enconman.2011.05.009

Linnhoff, B., and Hindmarsh, E. (1983). The Pinch Design Method for Heat Exchanger Networks. *Chem. Eng. Sci.* 38, 745–763. doi:10.1016/0009-2509(83)80185-7

Marcantonio, V., Bocci, E., and Monarca, D. (2019). Development of a Chemical Quasi-Equilibrium Model of Biomass Waste Gasification in a Fluidized-Bed Reactor by Using Aspen Plus. *Energies* 13, 53. doi:10.3390/en13010053

Marcantonio, V., Bocci, E., Ouweltjes, J. P., Del Zotto, L., and Monarca, D. (2020). Evaluation of Sorbents for High Temperature Removal of Tars, Hydrogen Sulphide, Hydrogen Chloride and Ammonia from Biomass-Derived Syngas by Using Aspen Plus. *Int. J. Hydrogen Energ.* 45, 6651–6662. doi:10.1016/j.ijhydene.2019.12.142

Martelli, E., Elsido, C., Mian, A., and Marechal, F. (2017). MINLP Model and Two-Stage Algorithm for the Simultaneous Synthesis of Heat Exchanger Networks, Utility Systems and Heat Recovery Cycles. *Comput. Chem. Eng.* 106, 663–689. doi:10.1016/j.compchemeng.2017.01.043

Mian, A., Martelli, E., and Maréchal, F. (2016). Framework for the Multiperiod Sequential Synthesis of Heat Exchanger Networks with Selection, Design, and Scheduling of Multiple Utilities. *Ind. Eng. Chem. Res.* 55, 168–186. doi:10.1021/acs.iecr.5b02104

Nakajo, A., Wuillemin, Z., Metzger, P., Diethelm, S., Schiller, G., Van herle, J., et al. (2011). Electrochemical Model of Solid Oxide Fuel Cell for Simulation at the Stack Scale I. Calibration Procedure on Experimental Data. *J. Electrochem. Soc.* 158, B1083–B1101. doi:10.1149/1.3596433

Park, Y. J., Min, G., and Hong, J. (2019). Thermodynamic Optimization of a SOFC-CHP System with Exhaust Gas Recirculation Employing an In-House Numerical Simulator. *ECS Trans.* 91, 2097–2104. doi:10.1149/09101.2097ecst

Pérez-Fortes, M., Mian, A., Srikanth, S., Wang, L., Diethelm, S., Varkaraki, E., et al. (2019). Design of a Pilot SOFC System for the Combined Production of Hydrogen and Electricity under Refueling Station Requirements. *Fuel Cells (Weinh)* 19, 389–407. doi:10.1002/fuce.201800200

Peters, R., Deja, R., Blum, L., Pennanen, J., Kiviaho, J., and Hakala, T. (2013). Analysis of Solid Oxide Fuel Cell System Concepts with Anode Recycling. *Int. J. Hydrogen Energ.* 38, 6809–6820. doi:10.1016/j.ijhydene.2013.03.110

Radenahmad, N., Azad, A. T., Saghir, M., Taweekun, J., Bakar, M. S. A., Reza, M. S., et al. (2020). A Review on Biomass Derived Syngas for SOFC Based Combined Heat and Power Application. *Renew. Sustainable Energ. Rev.* 119, 109560. doi:10.1016/j.rser.2019.109560

Rokni, M. (2017). Addressing Fuel Recycling in Solid Oxide Fuel Cell Systems Fed by Alternative Fuels. *Energy* 137, 1013–1025. doi:10.1016/j.energy.2017.03.082

Savuto, E., Di Carlo, A., Steele, A., Heidenreich, S., Gallucci, K., and Rapagnà, S. (2019). Syngas Conditioning by Ceramic Filter Candles Filled with Catalyst Pellets and Placed inside the Freeboard of a Fluidized Bed Steam Gasifier. *Fuel Process. Technol.* 191, 44–53. doi:10.1016/j.fuproc.2019.03.018

Schneider, T., Ruf, F., Müller, D., and Karl, J. (2021). Performance of a Fluidized Bed-Fired Stirling Engine as Micro-scale Combined Heat and Power System on wood Pellets. *Appl. Therm. Eng.* 189, 116712. doi:10.1016/j.applthermaleng.2021.116712

Smith, M. A., and Few, P. C. (2001). Domestic-scale Combined Heat-And-Power System Incorporating a Heat Pump: Analysis of a Prototype Plant. *Appl. Energ.* 70, 215–232. doi:10.1016/s0306-2619(01)00033-2

Smith, R. (2005). *Chemical Process Design and Integration*. West Sussex, United Kingdom: John Wiley & Sons.

Thiers, S., Aoun, B., and Peuportier, B. (2010). Experimental Characterization, Modeling and Simulation of a wood Pellet Micro-combined Heat and Power Unit Used as a Heat Source for a Residential Building. *Energy and Buildings* 42, 896–903. doi:10.1016/j.enbuild.2009.12.011

Torii, R., Tachikawa, Y., Sasaki, K., and Ito, K. (2016). Anode Gas Recirculation for Improving the Performance and Cost of a 5-kW Solid Oxide Fuel Cell System. *J. Power Sourc.* 325, 229–237. doi:10.1016/j.jpowsour.2016.06.045

Towler, G., and Sinnott, R. (2013). *Chemical Engineering Design: Principles, Practice and Economics of Plant and Process Design*. 2nd ed. Waltham, MA, USA: Butterworth-Heinemann, Elsevier

Ud Din, Z., and Zainal, Z. A. (2016). Biomass Integrated Gasification-SOFC Systems: Technology Overview. *Renew. Sustainable Energ. Rev.* 53, 1356–1376. doi:10.1016/j.rser.2015.09.013

Van herle, J., Maréchal, F., Leuenberger, S., and Favrat, D. (2003). Energy Balance Model of a SOFC Cogenerator Operated with Biogas. *J. Power Sourc.* 118, 375–383. doi:10.1016/s0378-7753(03)00103-4

Wagner, P., Wuillemin, Z., Constantin, D., Diethelm, S., Van herle, J., and Schiffmann, J. (2020). Experimental Characterization of a Solid Oxide Fuel Cell Coupled to a Steam-Driven Micro Anode Off-Gas Recirculation Fan. *Appl. Energ.* 262, 114219. doi:10.1016/j.apenergy.2019.114219

Yee, T. F., and Grossmann, I. E. (1990). Simultaneous Optimization Models for Heat Integration-II. Heat Exchanger Network Synthesis. *Comput. Chem. Eng.* 14, 1165–1184. doi:10.1016/0098-1354(90)85010-8

Yee, T. F., Grossmann, I. E., and Kravanja, Z. (1990). Simultaneous Optimization Models for Heat Integration-I. Area and Energy Targeting and Modeling of Multi-Stream Exchangers. *Comput. Chem. Eng.* 14, 1151–1164. doi:10.1016/0098-1354(90)85009-Y

Zhang, L., Xing, Y., Xu, H., Wang, H., Zhong, J., and Xuan, J. (2017). Comparative Study of Solid Oxide Fuel Cell Combined Heat and Power System with Multi-Stage Exhaust Chemical Energy Recycling: Modeling, experiment and Optimization. *Energ. Convers. Manage.* 139, 79–88. doi:10.1016/j.enconman.2017.02.045

Conflict of Interest: The authors declare that the research was conducted in the absence of any commercial or financial relationships that could be construed as a potential conflict of interest.

GLOSSARY

$\mathbf{A_{ex}}$ Heat exchanger area (m^2)

AMPL A Mathematical Programming Language

AOG Anode off-gas

ar as-received basis

BLAZE Biomass Low cost Advanced Zero Emission small-to-medium scale integrated gasifier-fuel cell combined heat and power plant

BoP Balance of plant

C*X* Cooler (X corresponds to a number; nomenclature in the PFD)

CGE Cold gas efficiency

CHP Combined heat and power

COG Cathode off-gas

DBFBG Dual bubbling fluidized bed gasifier

$\mathbf{Eff_{el}}$ Electrical efficiency

$\mathbf{Eff_{th}}$ Thermal efficiency

$\mathbf{Eff_{SOFC}}$ SOFC efficiency

$\mathbf{Eff_{tot}}$ Total (CHP) efficiency

ev-MOGA Multi-objective evolutionary algorithm developed by the Predictive Control and Heuristic Optimization Group (CPOH) at Universitat Politècnica de València (Spain)

FC Fuel cell

FTU Turbine-driven fan unit or fan turbine unit

FU Fuel utilization

GCC Grand composite curve

GCU Gas-cleaning unit

GT Gas turbine

h Film transfer coefficient (W/m$^{2\circ}$C)

HEN Heat exchanger network

HEX Heat exchanger

H*X* Heater (X corresponds to a number; nomenclature in the PFD)

LHV Lower heating value (kJ/kg)

LMTD Logarithmic mean temperature difference (°C)

LPG Liquefied petroleum gas

m mass flowrate (kg/s)

MER Maximum energy recovery

MILP Mixed integer linear programming

MO Multi-objective

PFD Process flow diagram

$\mathbf{P_{comp}}$ Power consumed by the compressors/fans of the system (kW)

$\mathbf{P_{prod}}$ Gross power produced by the SOFC LSM (kW)

$\mathbf{P_{pump}}$ Power consumed by the pumps of the system (kW)

$\mathbf{Q_{cu}}$ Heat that is absorbed by the cold utility (kW)

$\mathbf{Q_{hw}}$ Heat used to produce hot water at 1.01325 bar and 65°C (kW)

$\mathbf{Q_{turb}}$ Thermal power consumed by the turbine of the FTU (kW)

RR Recirculation ratio

SOFC LSM Solid oxide fuel cell large stack module

STCR Steam-to-carbon ratio

STB Steam-to-biomass ratio

T Temperature (°C)

$\mathbf{T_{in}}$ Stream inlet temperature before a heat exchange (°C)

$\mathbf{T_{out}}$ Stream outlet temperature after a heat exchange (°C)

$\mathbf{\Delta T_{min}}$ Minimum temperature difference between a hot and a cold stream (°C)

U Heat transfer coefficient (W/m$^{2\circ}$C)

VL Vapor–liquid

frontiers
in Energy Research

ORIGINAL RESEARCH
published: 11 June 2021
doi: 10.3389/fenrg.2021.682522

Low Moisture Anhydrous Ammonia Pretreatment of Four Lignocellulosic Materials—Distillers Dried Grains With Solubles, Corn Gluten Feed, Corn Fiber, and Oil Palm Frond

Nazira Mahmud[1,2] ***and Kurt A. Rosentrater***[1]*

[1]Department of Agricultural and Biosystems Engineering, Iowa State University, Ames, IA, United States, [2]Faculty of Industrial Sciences and Technology, Universiti Malaysia Pahang, Kuantan, Malaysia

Lignin and hemicellulose structures in cellulosic materials serve as a barrier for enzyme reactions. A pretreatment step is often needed to break these components to allow the biomass to be utilized as a source of value-added products. Various available pretreatment methods possess common drawbacks of the high amount of liquid and chemical requirements, harsh process conditions, and the high amount of waste produced, which driving up the production costs of bioproducts. Low moisture anhydrous ammonia (LMAA) pretreatment capable of eliminating those drawbacks. In this study, Distillers Dried Grains with Solubles (DDGS), corn gluten feed (CGF), corn fiber (CF), and oil palm frond (OPF) with different moisture contents were subjected to LMAA pretreatment at the specific ammonia loading rate, 1 h ammoniation, and 75°C incubation temperature. This pretreatment successfully decreased the lignin content of the materials, increased their percentage of α-cellulose, and improved enzymatic digestibility for most of the materials tested. The effect of moisture content (30 and 50% db) was found to be more significant than that of incubation time (24 and 72 h).

Keywords: lignocellulose, biomas, LMAA pretreatment, ammonia, biorefinery and biofuel, bioproducts, pretreatment, lignin removal

Edited by:
Ana Somoza-Tornos,
University of Colorado Boulder,
United States

Reviewed by:
Ernesto Mura,
Indipendent Researcher, Germany
Mohamad Nasir Mohamad Ibrahim,
Universiti Sains Malaysia, Malaysia

****Correspondence:***
Kurt A. Rosentrater
karosent@iastate.edu

Specialty section:
This article was submitted to
Process and Energy Systems
Engineering,
a section of the journal
Frontiers in Energy Research

Received: *18 March 2021*
Accepted: *01 June 2021*
Published: *11 June 2021*

Citation:
Mahmud N and Rosentrater KA (2021)
Low Moisture Anhydrous Ammonia
Pretreatment of Four Lignocellulosic
Materials—Distillers Dried Grains With
Solubles, Corn Gluten Feed, Corn
Fiber, and Oil Palm Frond.
Front. Energy Res. 9:682522.
doi: 10.3389/fenrg.2021.682522

INTRODUCTION

Pretreatment is a crucial step in any type of lignocellulosic-based bioproduct production. Through pretreatment, the recalcitrant structure of lignocellulosic materials is loosened and disrupted, thus enhancing enzyme penetration and hydrolysis of the biomass crystalline backbone structure. However, pretreatment has also been found to potentially increase the production cost of the lignocellulosic-based bioproducts, either because of the cost of intensive processing or the amount of chemicals required. Conventional pretreatment methods such as chemical and mechanical pretreatment essentially require high chemical loading, high energy consumption, a large amount of water, and a need for waste treatment. Other pretreatment approaches have been developed to eliminate these drawbacks; one of them, physicochemical pretreatment, combines the advantages of chemical pretreatment and physical pretreatment. Typical physical pretreatment would require an energy cost of approximately >20% of operating cost (Baruah et al., 2018). Nuruddin et al. (2016) highlighted that the tandem operation of physical and chemical pretreatment could significantly reduce the energy cost from the reduction of intensity of each single pretreatment (Nuruddin et al., 2016). Chemical pretreatment incurs not only high operating cost from the large volume of chemical used and waste produced, formation of undesired inhibitor compounds and severe cellulose degradation but also from high capital cost due to high corrosion level of equipment as in acid pretreatment (Taylor et al., 2019; Stoklosa et al., 2021). Therefore, physicochemical pretreatment is seen as a viable way to increase the value of some underutilized materials.

Ammonia-based physicochemical pretreatments have been among those most explored by researchers because of the attractive properties of ammonia (NH_3) as a pretreatment agent, including the effects of swelling, delignification, and preservation (Li and Kim, 2011; Yoo et al., 2011). Among these pretreatment methods include ammonia fiber explosion (AFEX), ammonia recycle percolation (ARP), and low liquid ammonia (LLA) pretreatment. These pretreatments still require either high consumption of energy or liquids, thus are not considered feasible for commercial application. AFEX, ARP and LLA run at approximately 60–120, 150–210, and 30°C, respectively. While the high amount of water washing requirement is essential to reduce the alkalinity of the materials, which will then generate a large sum of wastewater in addition to the use of aqueous pretreatment chemical itself (Kim et al., 2016). Not long ago, low moisture anhydrous ammonia (LMAA) pretreatment was introduced, which employs gaseous ammonia (NH_3) as the pretreatment agent at nearly ambient operating conditions (Yoo et al., 2011). The use of gaseous NH_3 results in a substantial reduction of liquid requirements and also since it is gas, it could easily be removed from the materials with the aid of vacuum or slight increase in temperature, eliminating the need for additional water washing step to remove the residual NH_3. The study on LMAA pretreatment is still limited with most works focused on specific biomass such as corn stover (Yoo et al., 2011; Cheng and Rosentrater, 2016; Guo et al., 2017; Yang and Rosentrater, 2017), sweet sorghum bagasse (Stoklosa et al., 2021), ryegrass (Yasuda et al., 2015) and napiergrass (Yasuda et al., 2013), limiting the feasibility evaluation for its wider application. Regardless, LMAA pretreatment of corn stover has yielded promising results in a large scale reactor, suggesting the possibility of effectively using LMAA pretreatment for larger-scale application (Cheng and Rosentrater, 2016; Yang and Rosentrater, 2017).

This study subjected distillers dried grains with solubles (DDGS), corn gluten feed (CGF), corn fiber (CF), and oil palm fronds (OPF), which are undervalued and underutilized materials, to the LMAA pretreatment process. DDGS, CGF, and CF are generated in abundance from corn processing plants as co-products and currently have relatively low economic value. The current market for these materials is primarily in animal feed manufacturing and only a small proportion as low-cost food additives. In 2019–2020, U.S. DDGS and CGF exports were down by 7 and 26% respectively compared to the previous year (Richman, 2021). CF is often mixed with corn gluten feed therefore rarely been exported. Similarly, oil palm fronds (OPF) are abundantly generated throughout the year in palm oil plantation areas. In Malaysia, between 44 and 51 × 10^6 t of OPF is annually produced (Goh et al., 2010; Awalludin et al., 2015), with the amount higher during replanting periods. There is no current commercial application of OPF. Attempts to utilize it in ruminants feed production and wood manufacturing did not yield promising results (Bals et al., 2006).

Revenues from these materials are not comparable to those of the primary manufacturing products, i.e., ethanol from corn wet and dry milling, and oil from palm oil mills. The growth of the palm oil industry has resulted in continuous generation of OPF (Ooi et al., 2017; Rizal et al., 2018), and the relatively slow current ethanol market (2020) has resulted in a greater desire of corn processing industries to increase their co-products value and market (Cooper et al., 2021).

The similarity of these materials is the high content of non-fermentable polysaccharides (cellulose, and hemicellulose), which is of important polymer feedstock for biorefinery and other bio-based structural product. The LMAA pretreatment has the potential to make these polysaccharides more available by removal or disruption of the recalcitrant lignin. It is important to ensure that the utilization of these waste materials to be at the lowest economic effect possible to increase the whole life-cycle value of the primary product. Hence, this study proposed a way to utilize such co-products and other waste materials in a possibly lower-cost approach using LMAA pretreatment (Mahmud and Rosentrater, 2020). The study focused on investigating the effects of LMAA pretreatment on DDGS, CGF, CF, and OPF. The efficiencies of LMAA pretreatment were evaluated in terms of the reduction in lignin content, increase in available cellulose, and also improvement in the percentage of enzymatic digestibility, which could indicate its suitability especially for a biochemical process for generation of higher value compounds.

MATERIALS AND METHODS

Materials

DDGS was obtained from Absolute Energy, L.L.C. (St. Ansgar, IA, United States), CGF was obtained from Grain Processing Corporation (Muscatine, IA, United States), and CF was obtained from Honeyville, Inc. (North Ogden, UT, United States). OPF was obtained from an oil palm plantation site in Malaysia. OPF was cleaned, dried, and chopped into 1 cm pieces. The compositions of each of the raw materials are summarized in **Table 1**. The moisture content of all raw materials was determined according to the NREL LAP standard method (Sluiter et al., 2008). The moisture content of the raw materials was adjusted to 30% dry basis (db) and 50% dry basis (db) by addition of water and steeped for 24 h.

Enzyme

Cellulase enzyme (Celluclast® 1.5 L) used was purchased from Sigma Aldrich Corp. (St. Louis, MO, United States) with a determined activity of 65 FPU/ml.

Low Moisture Anhydrous Ammonia Pretreatment

LMAA pretreatment was conducted in a 0.9 L reactor (Parr Instrument Co., Moline, IL, United States). Anhydrous

TABLE 1 | Composition of untreated lignocellulosic biomass used in the study.

Biomass	Compositions (%)				
	α-cellulose	Hemicellulose	AIL	ASL	Ash
DDGS	15.33 ± 1.03	39.33 ± 3.14	9.91 ± 2.36	1.19 ± 0.05	8.00 ± 0.00
CGF	26.67 ± 1.03	22.00 ± 0.89	15.56 ± 1.72	2.36 ± 0.19	8.27 ± 0.00
CF	22.67 ± 4.13	41.00 ± 4.98	7.78 ± 0.86	3.17 ± 0.26	2.33 ± 0.00
OPF	49.33 ± 6.77	17.67 ± 4.41	25.60 ± 0.54	0.33 ± 0.01	5.50 ± 0.00

Values are mean of triplicate analysis with ± standard deviation. AIL, acid insoluble lignin; ASL, acid soluble lignin. DDGS, distillers dried grains with solubles; CGF, corn gluten feed; CF, corn fiber; OPF, oil palm frond; DDGS, distillers dried grains with solubles; CGF, corn gluten feed; CF, corn fiber; OPF, oil palm frond.

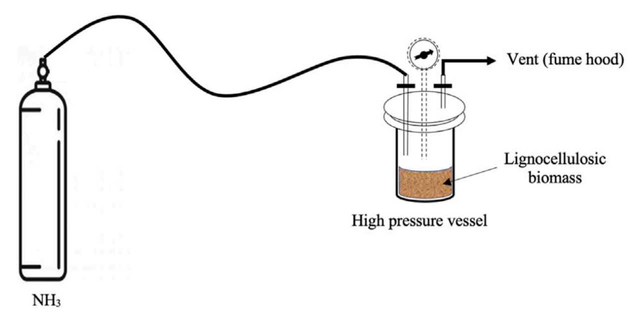

FIGURE 1 | Experimental set-up of the LMAA pretreatment.

ammonia (NH_3) loading was 0.09 g/g biomass for DDGS, CGF, and CF, and 0.18 g/g biomass for OPF. This was based on a previous study, which highlighted that materials with higher lignin content should be treated with a higher dosage of ammonia loading (Cheng and Rosentrater, 2016). In this regard, OPF used in this work contains similar lignin content compared to corn stover used in their work. NH_3 was introduced into the reactor filled with raw materials while monitoring the pressure (**Figure 1**). The reactor was held for 1 h after which the lid was removed in the fume hood for 15 min to enable evaporation of the NH_3. The ammoniated raw materials were transferred into glass bottle with screw cap and subjected to incubation at 75°C for 24 and 72 h in a convection oven. When the incubation process had been completed, the glass bottle caps were removed for 1 h to allow surplus NH_3 to evaporate. The whole pretreatment procedure was according to (Cheng and Rosentrater, 2016; Yang and Rosentrater, 2017).

Compositional Analyses

Holo-, Alpha-, and Hemicellulose Determination

Holocellulose and α-cellulose content of the pretreated samples were determined using the Wise method (Wise et al., 1946). Hemicellulose content obtained by subtracting the holocellulose content with the α-cellulose content.

Lignin and Carbohydrate Determination

Lignin content determination was according to the NREL LAP standard method (Sluiter et al., 2012). The acid-insoluble lignin (AIL) content was determined based on a gravimetric method while the acid-soluble lignin (ASL) content was determined at 320 nm using Cary 8454 UV/Vis Diode Array Spectrophotometer (Agilent Technologies, Santa Clara, CA, United States). Absorptivity at lambda max value (ε) of 30 L/g cm was used to calculate the percentage of soluble lignin for all types of raw materials (Noureddini and Byun, 2010; Nomanbhay et al., 2013). The glucose content was determined using HPLC equipped with Bio-Rad Aminex HPX-87H column (Bio-Rad Laboratories, Hercules, CA, United States), Varian 356-LC refractive index detector (Varian, Inc., CA, United States), guard column and autosampler based on the following conditions: injection volume—10 μl; mobile phase—0.01 N HPLC grade sulfuric acid; flow rate—0.6 ml/min; column temperature—65°C; detector temperature—as close as possible the column temperature; detector—refractive index; run time—20 min. A set of sugar recovery standards (SRS) was prepared to determine degradation losses, which is used to compensate for degradation losses of the samples.

Equations 1–4 were used to calculate the percentage of lignin and glucose in the sample after hydrolysis, where AIR, acid-insoluble residue; ODW, oven dry weight; $Wt._C$, weight of crucible; $Wt._P$, weight of protein; V, volume; correction factor = 0.9. The protein content of each raw materials was assumed at 31.4% (Pedersen et al., 2014), 25.1% (Miron et al., 2001), 9.9% (Noureddini and Byun, 2010), and 5.3% (Khalil et al., 2012) for DDGS, CGF, CF, and OPF, respectively.

$$\% AIL = \frac{(Wt._{C+AIR}(g) - Wt._{C}(g)) - (Wt._{C+ash}(g) - Wt._{C}(g)) - Wt._{P}(g)}{ODW_{sample}(g)} \times 100 \tag{1}$$

$$\% ASL = \frac{UV_{abs} \times V_{filtrate}(mL) \times Dilution}{\varepsilon\,(L/g.cm) \times ODW_{sample}\,(g) \times Pathlength\,(cm)} \times 100 \tag{2}$$

$$\% Recovery\ sugar = \frac{Sugar\ conc._{(after\ hydrolysis)}\,(mg/mL)}{Sugar\ conc._{(before\ hydrolysis)}\,(mg/mL)} \times 100 \tag{3}$$

$$\% Glucose = \frac{Sugar\ conc.(mg/mL) \times Correction\ factor \times V_{filtrate}\,(mL)}{\%\ recovery\ sugar \times ODW_{sample}(g)} \times 100 \tag{4}$$

Enzymatic Digestibility Test

Enzymatic digestibility test was conducted according to the NREL LAP standard method (Selig et al., 2008). The cellulase enzyme loading was 60 FPU/g cellulose. The mixture was incubated at

50°C and 150 rpm in an incubator shaker (Excella E24 Incubator Shaker Series, New Brunswick Scientific, Edison, NJ, United States). Samples were taken at 24 h intervals for up to 120 h. Percentage of digestions were calculated in term of glucan digestibility based on **Eq. 5**, where 0.9 is a correction factor for calculating 6-cabon polymeric sugars from corresponding monomeric sugars.

$$\%\ Digestion = \frac{Cellulose\ digested\ (g)}{Cellulose\ added\ (g)} \times 100 \times 0.9 \quad (5)$$

Non-linear changes in percentage digestibility over time were modeled by developing a regression trendline using the Hanes-Woolf approach, where the kinetic rate constants were determined by linear regression on a time over digestibility versus time plot.

Experimental Design and Data Analysis

The independent variables tested for each feedstock were moisture content (30% db and 50% db) and LMAA incubation time (untreated (UT), 24, and 72 h). Untreated samples of each feedstock were subjected to the same analyses and served as a control. The measured dependent variables were α-cellulose (wt. %), hemicellulose (wt. %), AIL (wt. %), ASL (wt. %), and glucan contents (wt. %), along with enzymatic digestibilities percentages. All experimental procedures were run in triplicate and average data with standard deviation were presented.

Statistical analyses were conducted using JMP Pro 13.1.0 (SAS Institute, Cary, NC, United States) statistical software. Comparisons amongst mean values of results from the moisture content factor were conducted using paired Student's t-test. Tukey's Honestly Significant Difference (HSD) test was used for multiple pairwise comparisons amongst mean values of results from the incubation time factor, as well as the interaction between factors. The analyses were conducted at α = 0.05.

TABLE 2 | *p*-values of individual and interaction effects after LMAA pretreatment[a].

		DDGS		
Factor	**α-cellulose**	**Hemicellulose**	**AIL**	**ASL**
MC	0.1116	0.2780	0.9599	0.7453
Time	0.0086	<0.0001	0.0264	<0.0001
MC[a]Time	0.4217	0.7255	0.8573	0.2644
		CGF		
Factor	**α-cellulose**	**Hemicellulose**	**AIL**	**ASL**
MC	0.0191	0.1408	0.3538	0.2313
Time	0.0024	<0.0001	0.0001	<0.0001
MC[a]Time	0.2027	0.4915	0.7657	0.6271
		CF		
Factor	**α-cellulose**	**Hemicellulose**	**AIL**	**ASL**
MC	0.0482	0.0005	0.5725	0.0013
Time	<0.0001	<0.0001	0.0537	0.0570
MC[a]Time	0.3324	0.0158	0.7202	0.0358
		OPF		
Factor	**α-cellulose**	**Hemicellulose**	**AIL**	**ASL**
MC	0.2244	0.6510	0.0864	0.0001
Time	0.0338	0.0300	<0.0001	<0.0001
MC[a]Time	0.6679	0.8740	0.4162	<0.0001

[a]Ho = the mean values of compositions from all factors are not significantly different at α = 0.05. MC, moisture content; Time, incubation time; AIL, acid insoluble lignin; ASL, acid soluble lignin; DDGS, distillers dried grains with solubles; CGF, corn gluten feed; CF, corn fiber; OPF, oil palm frond.

RESULTS AND DISCUSSIONS

Effect of Moisture Content and Incubation Time on Biomass Compositions

Variations in incubation time and moisture content have resulted in different amounts of α-cellulose, hemicellulose, AIL, and ASL for all types of materials tested. **Table 2** summarizes the *p*-values of each factor at α = 0.05. Results for main and interaction effects of factors on materials compositions after LMAA pretreatment are shown in **Tables 3**, **4**, respectively.

Distillers Dried Grains With Solubles

Incubation time had a significant effect on DDGS compositions (**Table 2**). There was no significant difference in the compositions at the moisture contents tested, suggesting that working at lower MC will insignificantly affect sample compositions. The results (mean values) for the main effect (**Table 3**) and the interaction effect (**Table 4**) show that different incubation times resulted in significant differences in mean values of compositions between level UT and the others but not always significantly different between levels 24 and 72, suggesting that 24 h is a sufficient incubation time for DDGS.

The highest cellulose content recorded was 27.33 wt. % from 30% MC DDGS treated for 24 h (**Table 4**). Similarly, the same parameters resulted in no significant differences in the mean of hemicellulose and AIL, but not for ASL. It could be observed that cellulose in DDGS was slightly decreased as incubation time increased to 72 h, suggesting that a longer incubation period might enhance cellulose degradation, either partially into glucose or fully into the carbon unit. The latter is undesirable in the biochemical process because it would decrease the substrate available for the fermentation process. Results of glucan content (**Figure 2**) show that total glucan in the sample was not decreased, perhaps eliminating the possibility of occurrence for the latter scenario mentioned above.

Corn Gluten Feed

In CGF, *p*-values of <0.05 were recorded with respect to a time factor, indicating that different times resulted in significantly different compositions. In spite of this, based on the results in **Tables 3**, **4**, significant differences in compositions were recorded only between levels UT and 24, and levels UT and 72 but not always between levels 24 and 72. Varying the MC resulted in no significant difference in mean values of compositions (except for α-cellulose content). α-cellulose content in CGF was decreased after the pretreatment compared to that of untreated samples,

TABLE 3 | Main effects of factors on biomass compositions after LMAA pretreatment. a, b, c these signify significant differences.

DDGS

Factor	Levels	α-cellulose (wt. %)	Hemicellulose (wt. %)	AIL (wt. %)	ASL (wt. %)
Time (h)	UT	15.33 ± 1.03^{b}	39.33 ± 3.14^{a}	9.91 ± 2.36^{a}	1.19 ± 0.05^{c}
	24	25.33 ± 4.13^{a}	5.67 ± 4.14^{b}	5.79 ± 3.44^{ab}	1.91 ± 0.08^{b}
	72	22.33 ± 7.42^{ab}	9.00 ± 6.49^{b}	4.34 ± 2.69^{b}	2.09 ± 0.08^{a}
MC (% db)	30	22.89 ± 6.48^{a}	16.67 ± 17.36^{a}	6.72 ± 3.66^{a}	1.72 ± 0.42^{a}
	50	19.11 ± 5.93^{a}	19.33 ± 15.94^{a}	6.64 ± 3.81^{a}	1.73 ± 0.41^{a}

CGF

Factor	Levels	α-cellulose (wt. %)	Hemicellulose (wt. %)	AIL (wt. %)	ASL (wt. %)
Time (h)	UT	26.67 ± 1.03^{a}	22.00 ± 0.89^{a}	15.56 ± 1.72^{a}	2.36 ± 0.19^{c}
	24	20.00 ± 3.79^{b}	4.42 ± 2.89^{b}	6.91 ± 1.88^{b}	3.06 ± 0.14^{b}
	72	20.67 ± 4.50^{b}	3.42 ± 2.63^{b}	7.32 ± 3.34^{b}	3.55 ± 0.34^{a}
MC (% db)	30	20.67 ± 4.80^{b}	10.78 ± 8.55^{a}	10.51 ± 4.54^{a}	3.06 ± 0.60^{a}
	50	24.22 ± 3.53^{a}	9.11 ± 9.96^{a}	9.35 ± 5.03^{a}	2.92 ± 0.52^{a}

CF

Factor	Levels	α-cellulose (wt. %)	Hemicellulose (wt. %)	AIL (wt. %)	ASL (wt. %)
Time (h)	UT	22.67 ± 4.13^{b}	41.00 ± 4.98^{a}	7.78 ± 0.86^{a}	3.17 ± 0.26^{a}
	24	35.00 ± 3.74^{a}	24.33 ± 7.78^{b}	4.99 ± 2.23^{a}	3.41 ± 0.36^{a}
	72	36.33 ± 5.13^{a}	17.25 ± 11.68^{b}	4.99 ± 2.23^{a}	3.44 ± 0.29^{a}
MC (% db)	30	29.33 ± 6.40^{b}	32.94 ± 7.84^{a}	5.64 ± 2.23^{a}	3.53 ± 0.31^{a}
	50	33.33 ± 8.43^{a}	22.11 ± 15.30^{b}	6.20 ± 2.32^{a}	3.15 ± 0.18^{b}

OPF

Factor	Levels	α-cellulose (wt. %)	Hemicellulose (wt. %)	AIL (wt. %)	ASL (wt. %)
Time (h)	UT	49.33 ± 6.77^{b}	17.67 ± 4.41^{a}	25.60 ± 0.54^{a}	0.33 ± 0.01^{c}
	24	$56.00 \pm 2.83^{a,b}$	$12.58 \pm 4.59^{a,b}$	12.10 ± 3.69^{b}	0.55 ± 0.03^{b}
	72	57.00 ± 3.52^{a}	8.17 ± 5.53^{b}	11.48 ± 3.82^{b}	0.62 ± 0.13^{a}
MC (% db)	30	52.67 ± 4.90^{a}	12.22 ± 6.80^{a}	17.65 ± 6.31^{a}	0.54 ± 0.18^{a}
	50	55.56 ± 6.23^{a}	13.39 ± 5.60^{a}	15.13 ± 8.37^{a}	0.46 ± 0.11^{b}

Values are mean of triplicate analysis with ± standard deviation, and levels not connected by the same letter are significantly different at α = 0.05. MC, moisture content; Time, incubation time; UT, untreated; AIL, acid insoluble lignin; ASL, acid soluble lignin; DDGS, distillers dried grains with solubles; CGF, corn gluten feed; CF, corn fiber; OPF, oil palm frond. a, b, c these signify significant differences.

possibly indicating that the pretreatment conditions applied were too much for CGF, causing degradation of α-cellulose.

Analysis of glucan content (**Figure 2**) shows a slight reduction of total glucan in 30% MC CGF, possibly indicating sugar degradation. This effect was not observed in 50% MC CGF. Pretreatment conducted on 50% MC CGF recorded a significantly less α-cellulose degradation than that of 30% MC CGF. However, the results between 24 and 72 h incubation times were not significantly different.

Corn Fiber

The effect of MC on CF compositions was more apparent than those of DDGS and CGF, with a significant difference in the results except for AIL content. Sample with 50% MC recorded significantly higher α-cellulose, lower hemicellulose, and lower ASL. Conversely, there was no statistically significant difference in mean values of compositions between levels 24 and 72 of the incubation time, suggesting that 24 h LMAA incubation time might be sufficient for CF. The α-cellulose content recorded for 50% MC CF treated for 24 h (38 wt. %) were not significantly different from those of 72 h (39.33 wt. %) (**Table 4**). Other compositions exhibited similar trends. There was a statistically significant interaction between all factors for hemicellulose and ASL content (**Table 2**).

Oil Palm Frond

For OPF, there was no significant difference of α-cellulose recorded for the different MC tested. This was also true for hemicellulose and AIL content, but not for ASL content. Different incubation time was mostly giving a significant difference of results at levels 0 and 24, and between levels 0 and 72, but not always between levels 24 and 72. Only the mean of ASL content has recorded a statistically significant interaction between all factors (**Table 2**). The cellulose content recorded for 50% MC OPF treated for 24 h (58 wt. %) was insignificantly different from those of 72 h (59.33 wt. %), possibly indicating that these parameters (50% MC and 24 h) are sufficient for LMAA pretreatment of OPF.

From the results, lower MC (30%) in the DDGS and OPF was observed to not giving a statistically significant difference in α-cellulose content after LMAA pretreatment from those for 50% MC biomass, suggesting its suitability for future use. For CGF and CF, significantly higher α-cellulose content was recorded at higher MC (50%). According to Yang and

TABLE 4 | Interaction effects of factors on biomass compositions after LMAA pretreatment.

DDGS

Time (h) MC (% db)	α-cellulose (wt. %)		Hemicellulose (wt. %)		AIL (wt. %)		ASL (wt. %)	
	30	50	30	50	30	50	30	50
UT	15.33 ± 1.03^{a}		39.33 ± 3.14^{a}		9.91 ± 2.36^{a}		1.19 ± 0.05^{c}	
24	27.33 ± 0.02^{a}	23.33 ± 0.02^{a}	3.83 ± 0.02^{b}	7.50 ± 0.02^{b}	5.34 ± 3.23^{a}	6.24 ± 6.47^{a}	1.86 ± 0.08^{b}	1.95 ± 0.07^{a,b}
72	26.00 ± 0.02^{a}	18.67 ± 0.03^{a}	6.83 ± 0.02^{b}	11.17 ± 0.03^{b}	4.91 ± 3.23^{a}	3.78 ± 0.81^{a}	2.11 ± 0.10^{a}	2.06 ± 0.05^{a}

CGF

Time (h) MC (% db)	α-cellulose (wt. %)		Hemicellulose (wt. %)		AIL (wt. %)		ASL (wt. %)	
	30	50	30	50	30	50	30	50
UT	26.67 ± 1.03^{a}		22.00 ± 0.89^{a}		15.56 ± 1.72^{a}		2.36 ± 0.19^{c}	
24	17.33 ± 0.01^{b}	22.67 ± 0.01^{a,b}	6.00 ± 0.01^{b}	2.83 ± 0.01^{b}	7.99 ± 0.71^{b}	5.82 ± 1.77^{b}	3.14 ± 0.17^{a,b}	2.98 ± 0.03^{b,c}
72	18.00 ± 0.01^{b}	23.33 ± 0.01^{a,b}	4.33 ± 0.04^{b}	2.50 ± 0.02^{b}	7.98 ± 3.53^{b}	6.66 ± 3.53^{b}	3.69 ± 0.20^{a}	3.41 ± 0.43^{a,b}

CF

Time (h) MC (% db)	α-cellulose (wt. %)		Hemicellulose (wt. %)		AIL (wt. %)		ASL (wt. %)	
	30	50	30	50	30	50	30	50
UT	22.67 ± 4.13^{b}		41.00 ± 4.98^{a}		7.78 ± 0.86^{a}		3.17 ± 0.26^{c}	
24	32.00 ± 0.01^{a,b}	38.00 ± 0.01^{a}	31.00 ± 0.01^{a,b}	17.67 ± 0.02^{b,c}	4.16 ± 1.77^{a}	5.83 ± 3.53^{a}	3.72 ± 0.02^{a}	3.10 ± 0.19^{c}
72	33.33 ± 0.03^{a}	39.33 ± 0.01^{a}	26.83 ± 0.04^{b}	7.67 ± 0.02^{c}	4.99 ± 3.53^{a}	4.99 ± 1.77^{a}	3.69 ± 0.06^{a,b}	3.19 ± 0.10^{b,c}

OPF

Time (h) MC (% db)	α-cellulose (wt. %)		Hemicellulose (wt. %)		AIL (wt. %)		ASL (wt. %)	
	30	50	30	50	30	50	30	50
UT	49.33 ± 6.77^{a}		17.67 ± 4.41^{a}		25.60 ± 0.54^{a}		0.33 ± 0.01^{c}	
24	54.00 ± 0.01^{a}	58.00 ± 0.01^{a}	12.33 ± 0.03^{a}	12.83 ± 0.05^{a}	13.68 ± 4.46^{b}	10.52 ± 4.46^{b}	0.55 ± 0.03^{b}	0.56 ± 0.02^{b}
72	54.67 ± 0.02^{a}	59.33 ± 0.01^{a}	6.67 ± 0.04^{a}	9.67 ± 0.07^{a}	13.68 ± 2.23^{b}	9.27 ± 5.58^{b}	0.73 ± 0.04^{a}	0.50 ± 0.03^{b}

Values are means of triplicate analysis with ± standard deviation, and levels not connected by the same letter are significantly different at α = 0.05. MC, moisture content; Time, incubation time; UT, untreated; AIL, acid insoluble lignin; ASL, acid soluble lignin; DDGS, distillers dried grains with solubles; CGF, corn gluten feed; CF, corn fiber; OPF, oil palm frond. a, b, c these signify significant differences.

Rosentrater (2017), LMAA pretreatment performance was optimum at 50% MC for corn stover, in comparison to the same materials at 20 and 80% MC. In this regard, looking more detail into the structure and compositions of each material used in this work, OPF is more closely resembles that of corn stover, however, corn stover required a higher MC requirement might be due to slightly higher cellulose content in it (Mensah et al., 2021). In other aspect, this also proves the requirement of moisture in LMAA pretreatment, although it varies with the cellulose content of materials (Kim et al., 2016; Yang and Rosentrater, 2017; Stoklosa et al., 2021). The difference in MC requirement could also be attributed to the difference in water absorption behavior that somehow related to the compositional difference in materials, which will be described in the following paragraph. α-cellulose content was assumed to be the most critical component because it gives the most sugar (glucose) for the fermentation process and is a high purity material for bio-based structural as such nanocellulose development (Phanthong et al., 2018), this was used to decide the most effective parameters for the LMAA pretreatment process. Following α-cellulose, hemicellulose also potentially can supply sugar (xylose) to the system (Mahmud and Rosentrater, 2020). It was observed that hemicellulose contents at the selected MC (30% for DDGS and OPF, and 50% for CGF and CF) were slightly less than those of the other MC, although the reason for the trend is unclear.

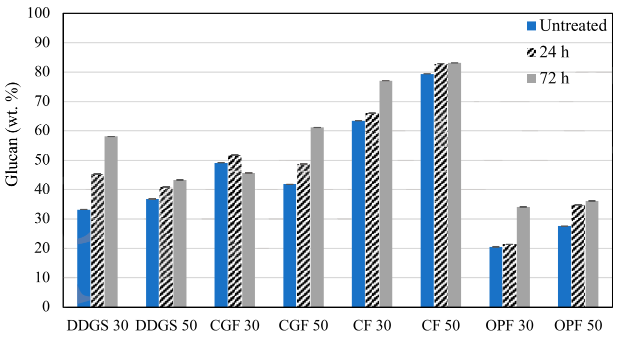

FIGURE 2 | Glucan content in the biomass after LMAA pretreatment. Error bars represent ± standard deviations. DDGS, distillers dried grains with solubles; CGF, corn gluten feed; CF, corn fiber; OPF, oil palm frond. Numbers in the x-axis indicate moisture content designation.

In the LMAA pretreatment process, it was hypothesized that water molecules present in the biomass bind with NH_3 molecules during ammoniation and form ammonium ions (NH^{4+}) and

TABLE 5 | Biomass compositions after LMAA pretreatment and comparison with other published pretreatment processes.

DDGS

Components (wt. %)	**LMAA**[a]	**LMAA** Zhang (2013)	**AFEX** Bals et al. (2006)
Cellulose	27.33	25.40[b]	Nd
Hemicellulose	3.83	8.76[c]	66.19[d]
AIL	5.34	13.34	nm
Ash	9.33	3.97	7.06
Other	57.73	48.53	26.75

CF

Components (wt. %)	**LMAA**[e]	**NaOH** Gáspár et al. (2005)	**$NaOH + H_2O_2$** Gáspár et al. (2005)	**Extrusion** Myat and Ryu (2014)
Cellulose	38.00	46.07	59.89	25.13
Hemicellulose	17.67	31.00	19.71	31.84
AIL	5.83	3.53	3.11	7.40
Ash	3.33	3.60	2.51	2.30
Other	35.17	15.80	14.78	33.33

OPF

Components (wt. %)	**LMAA**[e]	**SAA** Jung et al. (2012)	**DA** Siti Sabrina et al. (2013)	**Autohydrolysis** Sabiha-Hanim et al. (2011)
Cellulose	58.00	44.69[f]	46.5	48.69
Hemicellulose	12.83	12.12[g]	20.28	6.73
AIL	10.52	19.30	11.41	22.45
Ash	5.80	nm	9.28	nm
Other	12.85	23.89	12.53	22.13

DDGS, distillers dried grains with solubles; CF, corn fiber; OPF, oil palm frond. Values from published works were adjusted according to the initial compositions of materials used in this study except for Noureddini and Byun (2010). AIL, acid insoluble lignin.

[a] *LMAA, low moisture anhydrous ammonia (30% MC, 24 h incubation); AFEX, ammonia fiber expansion;*

[b] *Assumed equivalent to glucan.*

[c] *Assumed equivalent to xylan.*

[d] *Calculated according to xylan.*

[e] *LMAA, low moisture anhydrous ammonia (50% MC, 24 h incubation); NaOH, soaking in sodium hydroxide; NaOH+ H_2O_2, soaking in sodium hydroxide and hydrogen peroxide; SAA, soaking in aqueous ammonia; DA, dilute acid pretreatment; Autohydrolysis, heated in autoclave. Noureddini and Byun (2010) LMAA (60% MC, 80°C, 0.1 g NH_3/g biomass, 168 h pretreatment), (Guo et al., 2017) AFEX (60% MC, 80°C, 0.6 g NH3/g biomass), nd, not detected; nm, not measured. Pedersen et al. (2014) NaOH/NaOH + H_2O_2 (25% NaOH, 0.6% H_2O_2, 120°C, 120 min). Miron et al. (2001) Extrusion (300 rpm screw speed, 30% MC, 140°C, 3 mm die diameter, 100 g/min feed rate). Khalil et al. (2012) SAA (7% NH_3, 80°C, 20 h).*

[f] *Calculated according to glucan.*

[g] *Calculated according to xylan, nm, not measured. Selig et al. (2008) DA (0.01 M H2SO4, 60°C, 12 h). Mensah et al. (2021) Autohydrolysis (121°C, 15 psi, 60 min).*

hydroxyl ions (OH^-) that react with lignin (Yoo et al., 2011). Water molecules can also form hydrogen bonds with cellulose, which causes swelling of the cellulose crystalline structure, resulting in micro-cracks and later increasing accessibility of enzymes (Yoo et al., 2011; Célino et al., 2014). For CGF and CF, for which a significant amount of starch is part of their compositions, water might be absorbed into the starch in addition to that absorbed into the other cellulosic structure. Therefore, in total, more amount of water was absorbed as bound water, providing more sites for NH_3-H_2O reactions, justifying the requirement of higher MC by these materials. For OPF, although the presence of high cellulose might enhance water absorption and therefore potentially produce a higher α-cellulose content after the pretreatment, no significant differences were found between 50 and 30% MC samples. For DDGS, which consists of a low amount of starch and cellulose, only a small amount of water was retained in its structure to provide the pretreatment effect. The addition of more water to DDGS might result in its only being kept in the structure as free water and thus not contribute to any reaction with NH_3 (Yoo et al., 2011).

Several previous studies have reported that water absorption capacity was less in protein than in starch and cellulose, explaining the results of this study (Greer and Stewart, 1959; Wang et al., 2007). The approximate starch content in DDGS, CGF, and CF, are 6% (Pedersen et al., 2014), 20% (Schroeder, 2012), and 17.77% (Noureddini and Byun, 2010), respectively. For the incubation time factor, longer time (72 h) resulted in no significant overall effect on the materials, especially in terms of α-cellulose content, which was in contrast to the previous study (Yang and Rosentrater, 2017). This might be attributed to the higher NH_3 loading applied during ammoniation, which might be suitable for materials used in this work, speeding up the digestion reaction within the structural materials.

Other than increasing the α-cellulose available in the materials compared to that in untreated materials (except for CGF), the LMAA pretreatment decreased the hemicellulose and AIL content for all materials. While the ASL content for all materials after pretreatment was increased, this was not particularly valuable information in biochemical processing,

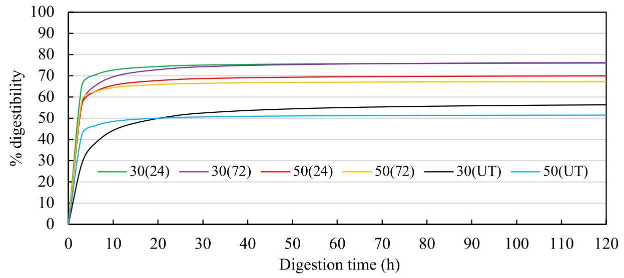

FIGURE 3 | Enzymatic digestibility curves for treated DDGS. In the legend, the first numbers indicate the MC (%db), the numbers in the parentheses indicate the incubation time (h). Hanes-Woolf linear regressions used to estimate the digestibilites over time were 30 (24): Y = 0.0131x + 0.0065; 30 (72): Y = 0.013x + 0.0138; 50 (24): Y = 0.0142x + 0.0106; 50 (72): Y = 0.0148x + 0.0071; 30(UT): Y = 0.0173x + 0.0529; 50(UT): Y = 0.0193x + 0.0131. UT indicates untreated DDGS.

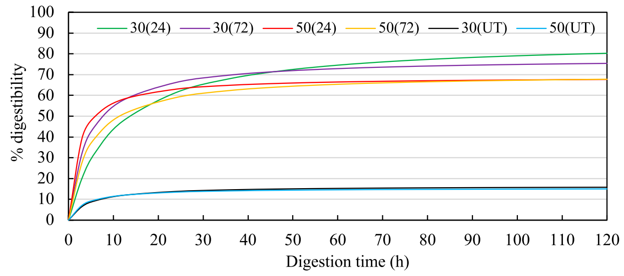

FIGURE 5 | Enzymatic digestibility curves for treated CF. In the legend, the first numbers indicate the MC (%db), the numbers in the parentheses indicate the incubation time (h). Hanes-Woolf linear regressions used to estimate the digestibilites over time were 30 (24): Y = 0.0115x + 0.1147; 30 (72): Y = 0.0128x + 0.055; 50 (24): Y = 0.0145x + 0.0328; 50 (72): Y = 0.0142x + 0.0659; 30(UT): Y = 0.0609x + 0.2771; 50(UT): Y = 0.0647x + 0.2278. UT indicates untreated CF.

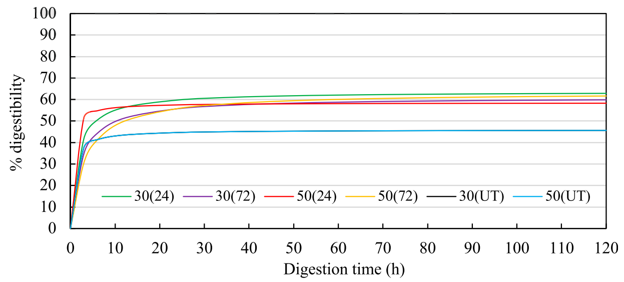

FIGURE 4 | Enzymatic digestibility curves for treated CGF. In the legend, the first numbers indicate the MC (%db), the numbers in the parentheses indicate the incubation time (h). Hanes-Woolf linear regressions used to estimate the digestibilites over time were 30 (24): Y = 0.0157x + 0.0248; 30 (72): Y = 0.0164x + 0.0372; 50 (24): Y = 0.0171x + 0.007; 50 (72): Y = 0.0158x + 0.051; 30(UT): Y = 0.0218x + 0.0144; 50(UT): Y = 0.0218x + 0.0144. UT indicates untreated CGF.

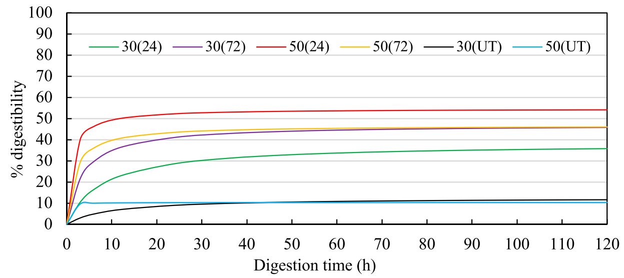

FIGURE 6 | Enzymatic digestibility curves for treated OPF. In the legend, the first numbers indicate the MC (%db), the numbers in the parentheses indicate the incubation time (h). Hanes-Woolf linear regressions used to estimate the digestibilites over time were 30 (24): Y = 0.0262x + 0.2085; 30 (72): Y = 0.0212x + 0.0752; 50 (24): Y = 0.0183x + 0.0199; 50 (72): Y = 0.0214x + 0.038; 30(UT): Y = 0.0798x + 0.7621; 50(UT): Y = 0.0964x + 0.0235. UT indicates untreated OPF.

because this fraction would be removed from the system either during filtration or evaporated by the drying process (a moisture reduction process that is required before the waste can be fed into the boiler).

The *p*-values from statistical analysis (**Table 2**) support the results described. *p*-values lower than 0.05 indicated no evidence that varying the associated factors would lead to a different mean value. Most interaction effects of the factors in all type of materials tested reflected insignificant results at α = 0.05, showing no evidence that effects of time differed with different materials MC, as reported by Cheng and Rosentrater (2016), Yang and Rosentrater (2017). Only several compositions for several types of materials, the mean of ASL content for CF and OPF, and the mean of hemicellulose content for CF, exhibited a significant interaction effect. It was rather weak supporting data for the selection of the best working conditions. **Table 5** summarizes the comparison of materials compositions after the pretreatment process recorded in this study with the available results from others for DDGS, CF, and OPF. No previous research on CGF pretreatment was available for comparison. It has been proven that LMAA provides a competitive way of biomass pretreatment at a potentially lower cost than other pretreatment approaches (Yoo et al., 2011; Mahmud and Rosentrater, 2019).

TABLE 6 | *p*-values of main and interaction effects on enzymatic digestibilities of the LMAA-treated biomass.

Factor	DDGS	CGF	CF	OPF
Incubation time	0.6008	0.4266	0.8222	0.6706
MC	0.0531	0.7653	0.4389	0.0146
Digestion time	0.2434	0.4511	0.0035	0.2341
MC × Incubation time	0.9443	0.9092	0.4937	0.0376
MC × Digestion time	0.9265	0.8310	0.0665	0.7046
Incubation time × Digestion time	0.8517	0.8503	0.2875	0.9937
MC × Incubation time × Digestion time	0.7378	0.4745	0.2547	0.8889

Factors: MC – 30 and 50% db; Incubation time – 24 and 72 h; Digestion time – 24 and 72 h. DDGS, distillers dried grains with solubles; CGF, corn gluten feed; CF, corn fiber; OPF, oil palm frond.

Effect of Moisture Content and Pretreatment Time on Enzymatic Digestibility

Figures 3–6 show the results for enzymatic digestibility tests. The percentage digestibility of all LMAA pretreated materials was higher than that of untreated materials (UT), indicating that LMAA pretreatment was successful in allowing more penetration of hydrolysis enzyme to the cellulose. The highest digestibility values recorded at the end of hydrolysis for DDGS, CGF, and CB were from those with 30% MC and treated for 24 h, with 76.02%, 62.87%, and 80.28% digestibility, respectively. The highest digestibility percentage recorded for OPF was 54.15%, from those with 50% MC and treated for 24 h. These equivalents to about 32%, 28%, 82% and 81% increase in digestibility compared to those of UT samples for DDGS, CGF, CF and OPF, respectively. As a comparison (Yang and Rosentrater, 2017), recorded a 64% increase in digestibility of LMAA pretreated corn stover, whereas 80%, 6.4% increase in digestibility were recorded for corn stover pretreated with other ammonia pretreatments, which were aqueous ammonia and AFEX pretreatment, respectively (Kim and Lee, 2007; Baruah et al., 2018). While (Jung et al., 2012) recorded ~64% digestibility of aqueous pretreated OPF. The percentages of digestibilities generally increased as digestion time increased. For the commercial application of the process, from an economic standpoint, 24 h of reaction would be considered sufficient for all type of biomass tested, since there was no significant difference between the percentage digestibility values at 24 and 72 h (**Table 6**). However, this is dependent on the concentration of enzyme used, with comparison (Yang and Rosentrater, 2017) required longer digestibility time due to low concentration of cellulase (45 FPU/ml).

p-values of the main effects revealed no significant difference in digestibility resulting from most of the factors tested. The exception was observed in the main effect of MC for OPF and the main effect of digestion time for CF, in which the digestion of 50% MC OPF was significantly higher than that of 30% MC, and the digestion of CF at 72 h was significantly higher than that at 24 h. With respect to the most significant parameters giving the best yield of α-cellulose, the highest percentage digestibility recorded for DDGS was 73.66% (30% MC and 24 h incubation), for CGF was 57.50% (50% MC and 24 h incubation), for CF was 66.26% (50% MC and 24 h incubation), and for OPF was 52.28% (50% MC and 24 h incubation).

CONCLUSION

In this study, DDGS, CGF, CF, and OPF were treated using LMAA pretreatment. DDGS required lesser MC (30%) for the process, while the other biomass candidates exhibited better results (increase in α-cellulose and enzymatic digestibilities) from pretreatment at 50% MC. The two LMAA incubation times tested produced statistically insignificant differences in results for all materials tested, leading to a conclusion of 24 h pretreatment is the best. Enzymatic hydrolysis conducted after the LMAA pretreatment process increased the digestibility of the biomass compared to those not treated; DDGS - 76.02%, CGF - 62.87%, CF - 80.28%, and OPF - 54.15%. These results have proven the potential of LMAA-treated materials for value-added product production especially in the production of higher value compounds through biochemical conversion. OPF is a major agricultural waste in oil palm plantation shown a promising future in increasing profits of the plantation owner. This study also highlights the potential of corn milling co-products to be used in a variety of applications other than in the feed manufacturing market. Additionally, some published techno-economic analyses have concluded significantly lower operating cost for biorefineries that adopt LMAA treatment. This justifies continued work in this area to ensure more concrete findings. Future studies should include more variety in ammonia loadings to determine the effect of higher concentrations on digestion, of which the analysis could be conducted in more detail through chromatography analysis. Moreover, this study concluded that 24 h digestion time was sufficient for enzyme digestion, potentially giving more yield to the biorefinery. It is worth investigations the correlation of enzyme concentration and ammonia loading with enzyme digestibility performance.

DATA AVAILABILITY STATEMENT

The raw data supporting the conclusions of this article will be made available by the authors, without undue reservation.

AUTHOR CONTRIBUTIONS

KR conceived and supervised the research, and revised and edited the manuscript. NM conducted the research, conducted the analysis, and drafted the manuscript.

REFERENCES

Awalludin, M. F., Sulaiman, O., Hashim, R., and Nadhari, W. N. A. W. (2015). An Overview of the Oil Palm Industry in Malaysia and its Waste Utilization Through Thermochemical Conversion, Specifically via Liquefaction. *Renew. Sust. Energ. Rev.* 50, 1469–1484. doi:10.1016/j.rser.2015.05.085

Bals, B., Dale, B., and Balan, V. (2006). Enzymatic Hydrolysis of Distiller's Dry Grain and Solubles (DDGS) Using Ammonia Fiber Expansion Pretreatment. *Energy Fuels* 20, 2732–2736. doi:10.1021/ef060299s

Baruah, J., Nath, B. K., Sharma, R., Kumar, S., Deka, R. C., Baruah, D. C., et al. (2018). Recent Trends in the Pretreatment of Lignocellulosic Biomass for Value-Added Products. *Front. Energ. Res.* 6, 1–19. doi:10.3389/fenrg.2018.00141

Célino, A., Fréour, S., Jacquemin, F., and Casari, P. (2014). The Hygroscopic Behavior of Plant Fibers: A Review. *Front. Chem.* 1, 43. doi:10.3389/fchem.2013.00043

Cheng, M., and Rosentrater, K. A. (2016). "Optimization of Low Moisture Anhydrous Ammonia (LMAA) Pretreatment for Corn Stover Enzymatic Digestibility during Hydrolysis Process", in 2016 ASABE Annual International Meeting, Orlando, FL, July 17-20, 2016.

Cooper, G., McCaherty, J., Huschitt, E., Schwarck, R., and Wilson, C. (2021). *2021 Ethanol Industry Outlook*. Washington, DC. Available at: www.ethanolrfa.org.

Gáspár, M., Juhász, T., Szengyel, Z., and Réczey, K. (2005). Fractionation and Utilisation of Corn Fibre Carbohydrates. *Process Biochem.* 40, 1183–1188. doi:10.1016/j.procbio.2004.04.004

Goh, C. S., Tan, K. T., Lee, K. T., and Bhatia, S. (2010). Bio-Ethanol From Lignocellulose: Status, Perspectives and Challenges in Malaysia. *Bioresour. Technol.* 101, 4834–4841. doi:10.1016/j.biortech.2009.08.080

Greer, E. N., and Stewart, B. A. (1959). The Water Absorption of Wheat Flour: Relative Effects of Protein and Starch. *J. Sci. Food Agric.* 10, 248–252. doi:10.1002/jsfa.2740100409

Guo, M., Jin, T., Nghiem, N. P., Fan, X., Qi, P. X., Jang, C. H., et al. (2017). Assessment of Antioxidant and Antimicrobial Properties of Lignin From Corn Stover Residue Pretreated with Low-Moisture Anhydrous Ammonia and Enzymatic Hydrolysis Process. *Appl. Biochem. Biotechnol.* 184, 350–365. doi:10.1007/s12010-017-2550-0

Jung, Y. H., Kim, S., Yang, T. H., Lee, H. J., Seung, D., Park, Y.-C., et al. (2012). Aqueous Ammonia Pretreatment, Saccharification, and Fermentation Evaluation of Oil Palm Fronds for Ethanol Production. *Bioproc. Biosyst. Eng.* 35, 1497–1503. doi:10.1007/s00449-012-0739-8

Khalil, H. P. S. A., Jawaid, M., Hassan, A., Paridah, M. T., and Zaidon, A. (2012). "Oil Palm Biomass Fibres and Recent Advancement in Oil Palm Biomass Fibres Based Hybrid Biocomposites," in *Composites and Their Applications*. 1st Edn, Editor Hu, N. (London, United Kingdom: Intech Publication), 187–220.

Kim, J. S., Lee, Y. Y., and Kim, T. H. (2016). A Review on Alkaline Pretreatment Technology for Bioconversion of Lignocellulosic Biomass. *Bioresour. Technol.* 199, 42–48. doi:10.1016/j.biortech.2015.08.085

Kim, T. H., and Lee, Y. Y. (2007). Pretreatment of Corn Stover by Soaking in Aqueous Ammonia at Moderate Temperatures. *Appl. Biochem. Biotechnol.* 137–140, 81–92. doi:10.1007/s12010-007-9041-7

Li, X., and Kim, T. H. (2011). Low-Liquid Pretreatment of Corn Stover With Aqueous Ammonia. *Bioresour. Technol.* 102, 4779–4786. doi:10.1016/j.biortech.2011.01.008

Mahmud, N., and Rosentrater, K. A. (2019). Techno-Economic Analysis of Low Moisture Anhydrous Ammonia (LMAA) Pretreatment for Butanol Production From Oil Palm Frond. *Biomass. Convers. Biorefin.* Available at 14 December 2019. doi:10.1007/s13399-019-00564-5

Mahmud, N., and Rosentrater, K. A. (2020). Techno-Economic Analysis (TEA) of Different Pretreatment and Product Separation Technologies for Cellulosic Butanol Production From Oil Palm Frond. *Energies* 13, 181. doi:10.3390/en13010181

Mensah, M. B., Jumpah, H., Boadi, N. O., and Awudza, J. A. M. (2021). Assessment of Quantities and Composition of Corn stover in Ghana and Their Conversion into Bioethanol. *Scientific Afr.* 12, e00731. doi:10.1016/j.sciaf.2021.e00731

Miron, J., Yosef, E., and Ben-Ghedalia, D. (2001). Composition and *In Vitro* Digestibility of Monosaccharide Constituents of Selected Byproduct Feeds. *J. Agric. Food Chem.* 49, 2322–2326. doi:10.1021/jf0008700

Myat, L., and Ryu, G.-H. (2014). Characteristics of Destarched Corn Fiber Extrudates for Ethanol Production. *J. Cereal Sci.* 60, 289–296. doi:10.1016/j.jcs.2014.06.006

Nomanbhay, S. M., Hussain, R., and Palanisamy, K. (2013). Microwave-Assisted Alkaline Pretreatment and Microwave Assisted Enzymatic Saccharification of Oil Palm Empty Fruit Bunch Fiber for Enhanced Fermentable Sugar Yield. *J. Sustain. Bioenergy Syst.* 3, 7–17. doi:10.4236/jsbs.2013.31002

Noureddini, H., and Byun, J. (2010). Dilute-Acid Pretreatment of Distillers' Grains and Corn Fiber. *Bioresour. Technol.* 101, 1060–1067. doi:10.1016/j.biortech.2009.08.094

Nuruddin, M., Hosur, M., Uddin, M. J., Baah, D., and Jeelani, S. (2016). A Novel Approach for Extracting Cellulose Nanofibers From Lignocellulosic Biomass by Ball Milling Combined With Chemical Treatment. *J. Appl. Polym. Sci.* 133, 42990. doi:10.1002/app.42990

Ooi, Z. X., Teoh, Y. P., Kunasundari, B., and Shuit, S. H. (2017). Oil Palm Frond as a Sustainable and Promising Biomass Source in Malaysia: A Review. *Environ. Prog. Sustain. Energy* 36, 1864–1874. doi:10.1002/ep.12642

Pedersen, M. B., Dalsgaard, S., Knudsen, K. E. B., Yu, S., and Lærke, H. N. (2014). Compositional Profile and Variation of Distillers Dried Grains With Solubles From Various Origins With Focus on Non-starch Polysaccharides. *Anim. Feed Sci. Technol.* 197, 130–141. doi:10.1016/j.anifeedsci.2014.07.011

Phanthong, P., Reubroycharoen, P., Hao, X., Xu, G., Abudula, A., and Guan, G. (2018). Nanocellulose: Extraction and Application. *Carbon Resour. Convers.* 1, 32–43. doi:10.1016/j.crcon.2018.05.004

Rizal, N., Ibrahim, M., Zakaria, M., Abd-aziz, S., Yee, P., and Hassan, M. (2018). Pre-Treatment of Oil palm Biomass for Fermentable Sugars Production. *Molecules* 23, 1381. doi:10.3390/molecules23061381

Sabiha-Hanim, S., Noor, M. A. M., and Rosma, A. (2011). Effect of Autohydrolysis and Enzymatic Treatment on Oil Palm (Elaeis Guineensis Jacq.) Frond Fibres for Xylose and Xylooligosaccharides Production. *Bioresour. Technol.* 102, 1234–1239. doi:10.1016/j.biortech.2010.08.017

Schroeder, J. W. (2012). *Corn Gluten Feed: Composition, Storage, Handling, Feeding, and Value*. North Dakota State University. Available at: https://library.ndsu.edu/ir/bitstream/handle/10365/4796/as1127.pdf?sequence=1.

Richman, S. (2021). *2020 U.S. Distillers Grains Exports & Imports Statistical Summary*. Ellisville, MO. Available at: www.ethanolrfa.org.

Selig, M., Weiss, N., and Ji, Y. (2008). *Enzymatic Saccharification of Lignocellulosic Biomass*. Available at: www.doe.gov.

Siti Sabrina, M. S., Roshanida, A. R., and Norzita, N. (2013). Pretreatment of Oil Palm Fronds for Improving Hemicelluloses Content for Higher Recovery of Xylose. *J. Teknol.* 62, 39–42. doi:10.11113/jt.v62.1877

Sluiter, A., Hames, B., Hyman, D., Payne, C., Ruiz, R., Scarlata, C., et al. (2008). Determination of Total Solids in Biomass and Total Dissolved Solids in Liquid Process Samples. Technical Report: NREL/TP-510-42621. Available at: www.doe.gov.

Sluiter, A., Hames, B., Ruiz, R., Scarlata, C., Sluiter, J., Templeton, D., et al. (2012). *Determination of Structural Carbohydrates and Lignin in Biomass*. Available at: www.doe.gov.

Stoklosa, R. J., Moore, C., Latona, R. J., and Nghiem, N. P. (2021). Butyric Acid Generation by *Clostridium tyrobutyricum* From Low-Moisture Anhydrous Ammonia (LMAA) Pretreated Sweet Sorghum Bagasse. *Appl. Biochem. Biotechnol.* 193, 761–776. doi:10.1007/s12010-020-03449-w

Taylor, M., Alabdrabalameer, H., and Skoulou, V. (2019). Choosing Physical, Physicochemical and Chemical Methods of Pre-treating Lignocellulosic Wastes to Repurpose into Solid Fuels. *Sustainability* 11, 3604. doi:10.3390/su11133604

Wang, L. Z., Liu, L., Holmes, J., Kerry, J. F., and Kerry, J. P. (2007). Assessment of Film-Forming Potential and Properties of Protein and Polysaccharide-Based Biopolymer Films. *Int. J. Food Sci. Tech.* 42, 1128–1138. doi:10.1111/j.1365-2621.2006.01440.x

Wise, L. E., Murphy, M., and Adieco, A. A. D. (1946). A Chlorite Holocellulose, its Fractionation and Bearing on Summative Wood Analysis and Studies on the Hemicelluloses. *Pap. Trade J.* 122, 35–43.

Yang, M., and Rosentrater, K. A. (2017). Small-Scale Low-Moisture Anhydrous Ammonia (LMAA) Pretreatment of Corn stover. *Biomass Bioenergy* 97, 38–42. doi:10.1016/j.biombioe.2016.12.013

Yasuda, M., Takenouchi, Y., Nitta, Y., Ishii, Y., and Ohta, K. (2015). Italian Ryegrass (*Lolium multiflorum* Lam) as a High-Potential Bio-Ethanol Resource. *Bioenerg. Res.* 8, 1303–1309. doi:10.1007/s12155-015-9582-5

Yasuda, M., Takeo, K., Nagai, H., Uto, T., Yui, T., Matsumoto, T., Ishii, Y., and Ohta, K. (2013). Enhancement of Ethanol Production From Napiergrass (*Pennisetum purpureum Schumach*) by a Low-Moisture Anhydrous Ammonia Pretreatment. *J. Sustain. Bioenergy Syst.* 3, 179–185. doi:10.4236/jsbs.2013.33025

Yoo, C. G., Nghiem, N. P., Hicks, K. B., and Kim, T. H. (2011). Pretreatment of Corn stover Using Low-Moisture Anhydrous Ammonia (LMAA) Process. *Bioresour. Technol.* 102, 10028–10034. doi:10.1016/j.biortech.2011.08.057

Zhang, W. (2013). *Analysis of Properties to Distillers Dried Grains with Solubles (DDGS) and Using Destoner and Low Moisture Anhydrous Ammonia (LMAA) to Utilize DDGS*. Ames, IA: Iowa State University.

Conflict of Interest: The authors declare that the research was conducted in the absence of any commercial or financial relationships that could be construed as a potential conflict of interest.

frontiers in Energy Research

ORIGINAL RESEARCH
published: 24 June 2021
doi: 10.3389/fenrg.2021.676233

Economic and Environmental Assessment of Plastic Waste Pyrolysis Products and Biofuels as Substitutes for Fossil-Based Fuels

*Adrián Pacheco-López[1†], Fabian Lechtenberg[1†], Ana Somoza-Tornos[1,2], Moisès Graells[1] and Antonio Espuña[1]**

[1]*Department of Chemical Engineering, Universitat Politècnica de Catalunya, Campus Diagonal-Besòs, Barcelona, Spain,* [2]*Renewable and Sustainable Energy Institute (RASEI), University of Colorado Boulder, Boulder, CO, United States*

Edited by:
Valerie Eveloy,
Khalifa University, United Arab Emirates

Reviewed by:
Tuan Amran Tuan Abdullah,
University of Technology Malaysia, Malaysia
Thokchom Subhaschandra Singh,
National Institute of Technology, Manipur, India

****Correspondence:***
Antonio Espuña
antonio.espuna@upc.edu

[†]These authors have contributed equally to this work and share first authorship

Specialty section:
This article was submitted to Process and Energy Systems Engineering, a section of the journal Frontiers in Energy Research

Received: *04 March 2021*
Accepted: *06 May 2021*
Published: *24 June 2021*

Citation:
Pacheco-López A, Lechtenberg F, Somoza-Tornos A, Graells M and Espuña A (2021) Economic and Environmental Assessment of Plastic Waste Pyrolysis Products and Biofuels as Substitutes for Fossil-Based Fuels. Front. Energy Res. 9:676233. doi: 10.3389/fenrg.2021.676233

The global economy is shifting toward more sustainable sources of energy. The transportation sector is a remarkable example of this fact, where biofuels have emerged as promising alternatives to traditional fossil fuels. This work presents a techno-economic and environmental assessment of existing liquid fuels in hard-to-decarbonize sectors and their emerging renewable substitutes. The comparison focuses on fossil-based, biomass-derived, and plastic waste-sourced fuel alternatives that can be used in spark-ignition (gasoline) and compression-ignition (diesel) engines. Results for diesel substitutes prove the superior performance of plastic waste pyrolysis oil in terms of production cost reduction (–25% compared to diesel) and “well-to-tank” life cycle impact reduction (−54% human health, −40% ecosystems, −98% resources). Consequently, research and development toward the conversion of plastic waste into fuels should be extended to make the technology more accessible and robust in terms of fuel quality. On the contrary, the results for gasoline alternatives are not as conclusive: bioethanol and ethanol from plastic pyrolysis have a considerably lower impact on resource scarcity than gasoline (–80% and –35% respectively) and higher on the other two life cycle endpoint categories, but they have higher production costs compared to gasoline (+57% and +130% respectively). While blends of gasoline with pyrolysis-sourced ethanol can reduce the impact on human health and ecosystems, blends with bioethanol have a lower impact on resource scarcity and increase economic profitability. This allows fuel providers to offer tradeoff solutions in the form of blends based on their priorities.

Keywords: techno-economic assessment, life cycle assessement, plastic waste management, biofuels, energy sustainability, pyrolysis oil, transport decarbonization

---

Abbreviations: B0-B100, Blends of biodiesel with fossil diesel. The number indicates the volumetric percentage of biodiesel; CEPCI, Chemical Engineering Plant Cost Index; E0-E100, Blends of bioethanol with fossil gasoline. The number indicates the volumetric percentage of bioethanol; LCA, Life Cycle Assessment; PE, Polyethylene; PP, Polypropylene; TTW, Tank-to-Wheels; WPE, Plastic Waste Pyrolysis Ethanol; WPE0-WPE100, Blends of WPE with fossil gasoline. The number indicates the volumetric percentage of WPE; WPO, Plastic Waste Pyrolysis Oil; WPO0-WPO100, Blends of WPO with fossil diesel. The number indicates the volumetric percentage of WPO; WTT, Well-to-Tank; WTW, Well-to-Wheels.

INTRODUCTION

Current economies are transitioning to carbon-free energy sources, but there is still a need for liquid fuels for "hard-to-decarbonize" sectors (mainly aviation, shipping, and road transportation). The demand for diesel and gasoline for road transportation increased between 2000 and 2017 by 11.4%, with a diesel to gasoline usage ratio of 2.5 (Fuels Europe, 2018). Aviation and marine shipping are even harder to decarbonize, for instance through electrification, due to the higher involved mass and range, thus they will continue to rely on the use of liquid fuels (Gray et al., 2021). Cleaner fuels will be key to the transition to a more sustainable future. Biofuels have been widely studied but pose some challenges, mainly on land use, as they compete with the food supply chain.

The upcycling of plastic waste to produce chemicals and fuels with identical properties to those obtained from fossil sources has gained public interest because it slows down resource depletion and diverts waste that would traditionally end up in landfills (Lopez et al., 2017; Miandad et al., 2016). The chemical recycling of plastic waste will play a vital role in closing material loops and shifting toward a circular economy paradigm. Among the different alternatives for the material recovery of plastics (e.g., pyrolysis, gasification, and cracking), pyrolysis stands out for offering the possibility of recovering valuable chemicals (Dahlbo et al., 2018). It even allows the recovery of the plastic monomer, thereby offering the possibility to close the concerning carbon loops in the plastic supply chain. However, these technologies have been mostly developed and tested at the lab and pilot scale and there are several barriers to their industrial implementation such as technological, financial, managerial, performance limitations, and social barriers, among others (Araujo Galvão et al., 2018). For instance, PLASTIC ENERGY^{TM} operates a 5,000 t/year mixed plastic waste pyrolysis pilot plant in Seville, Spain. This pilot project has led to collaborations with big companies in the oil and plastics market. An example is the construction of a semi-commercial plastic waste recycling, and a pyrolysis oil refinery project is due to be constructed in 2021 in Gleen in the Netherlands (SABIC, 2019).

While fuel products ultimately end up as carbon dioxide (CO_2) in the environment, other chemical products, such as plastics, have a variety of end-of-life alternatives, including incineration, landfill, and mechanical or chemical recycling. Recently, Somoza-Tornos et al. (2020) compared alternatives using techno-economic and Life Cycle Assessment (LCA). The authors concluded that recovering chemicals (specifically ethylene from polyethylene) from plastic waste offers an economic incentive and a positive environmental impact by avoiding the burden of direct incineration and especially dealing with landfill, which stands as the least preferable option where all the plastic value is lost in a non-degradable graveyard. Additionally, they applied similar methods to select the best alternatives from plastic waste upcycling into chemicals in recent contributions (Pacheco-López et al., 2020; Somoza-Tornos et al., 2021).

This study provides a techno-economic and environmental assessment of diesel and gasoline substitutes, namely biodiesel, bioethanol, plastic waste pyrolysis oil, and plastic waste pyrolysis ethanol. Through this assessment, the advantages and disadvantages of each pathway are revealed. The first part of this study assesses alternative feedstock and pathways to obtain a fuel that can be used as a diesel substitute. The second part deals with ways to produce ethanol as a gasoline substitute. To that end, literature data has been compiled to track the cost of already mature pathways while estimations of the cost of pyrolysis products are based on a techno-economic assessment. The environmental impact is compared through an LCA approach.

MATERIALS AND METHODS

This section introduces the scope of the current work and presents the chosen functional unit used in the study. The proposed polypropylene (PP) pyrolysis process is explained along with the followed techno-economic and environmental assessment procedures.

Scope

The scope of this contribution lies in the production of fuels for the direct replacement of fossil fuels in non-modified engines. **Figure 1** compares alternatives: fossil-based diesel and gasoline are compared against biodiesel and bioethanol as well as plastic waste pyrolysis oil and plastic waste pyrolysis ethanol, respectively.

Biomass has emerged as a promising alternative feedstock to produce fuels of similar quality as fossil-based products while creating a closed carbon cycle. However, adverse effects such as competition with the food and water sector as well as intense land usage and other kinds of environmental impact must be analyzed on a case-by-case basis to choose the most suitable feedstock (Herrmann et al., 2018).

Pyrolysis products from plastic waste can have a wide range of compositions and properties depending mainly on the following conditions: type of plastic, catalyst, and most importantly temperature (Lopez et al., 2017). High temperature pyrolysis breaks the polyolefin into smaller compounds, leading to higher gas yields. Low temperature pyrolysis on the other hand leads to higher oil yields with increasingly heavier compounds as the temperature is reduced.

It must be acknowledged that alternative fuels and engines for transportation purposes such as electricity (Glitman et al., 2019) or hydrogen (Sharma and Krishna Ghoshal, 2015) will play an important role in the transition to a more sustainable transportation sector. However, during this transition period, it will be a natural step to utilize the machines that are already available and predominantly produced nowadays, that is 52.3% gasoline and 29.9% diesel engines (ACEA, 2020). Therefore, the approach proposed will focus on targeting fuels suitable for traditional engine vehicles, complying with their technical requirements and exhaust emissions standards.

The full life cycle assessment of fuel is often referred to as "Well-to-Wheel" analysis and it comprises two phases: 1) the "Well-to-Tank" phase, which consist of all the steps from raw material procurement over processing until obtaining the final fuel, and 2) the "Tank-to-Wheel" phase, which describes the combustion of a fuel in an engine (Edwards et al., 2014; Brinkman et al., 2005). This work assesses the Well-to-Tank phase. This

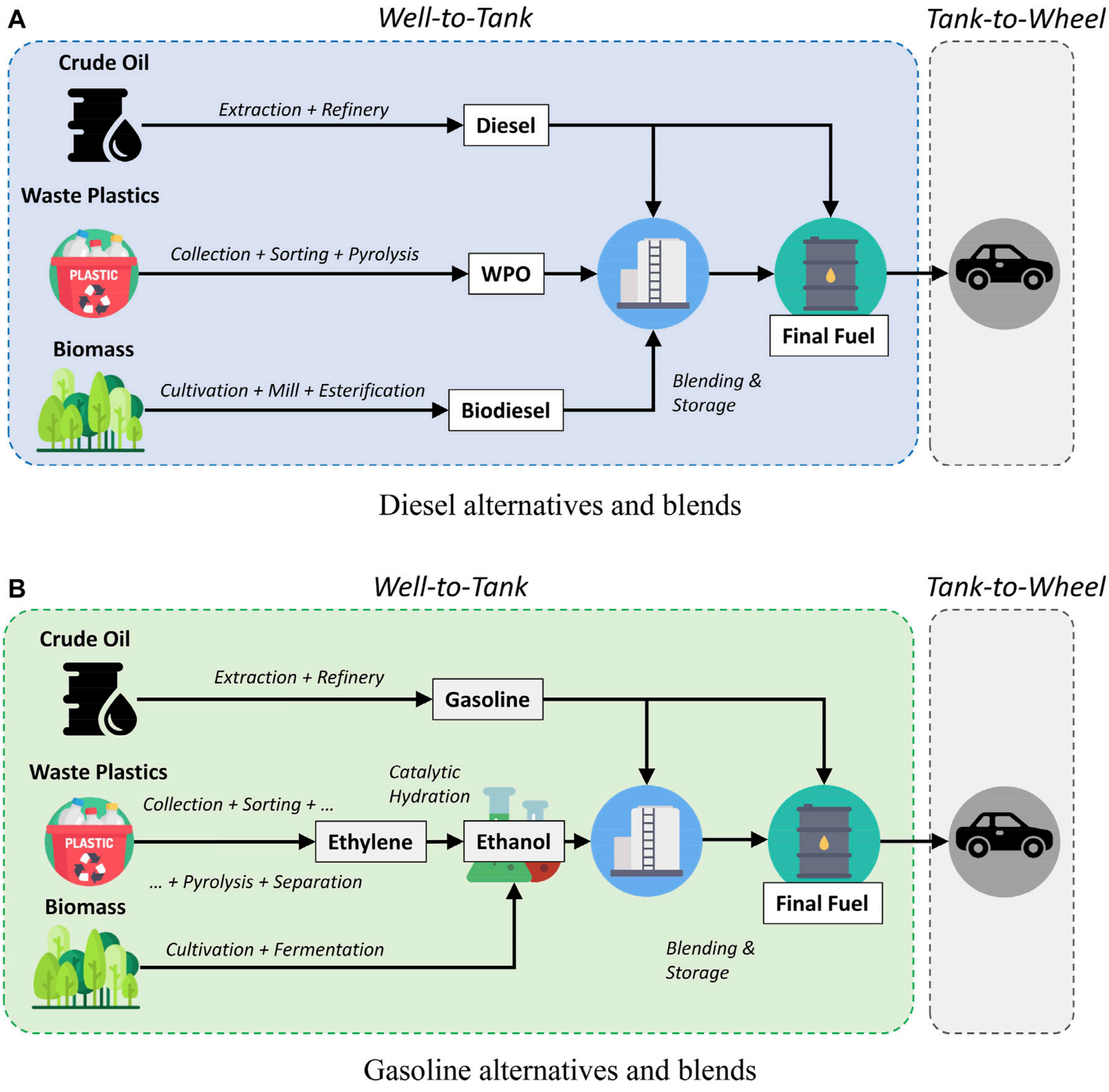

FIGURE 1 | Scope of investigation for the production pathways to **(A)** diesel and **(B)** gasoline.

approach was chosen due to the variation of the emission values reported in the literature for different raw materials and conversion procedures in the pyrolysis path (Damodharan et al., 2019). Energy demand and emissions in the Well-to-Tank phase can be estimated more reliably due to the steadiness of the process, while the Tank-to-Wheels phase is more variable and the results depend on a big set of variables and conditions. It is important to remark that all data was collected or extrapolated to refer to the year 2019.

Diesel Substitutes

Diesel is a mixture of hydrocarbons in the boiling point range from 150 to 380°C, traditionally obtained from fractioning crude oil in refineries. Its use in car engines has been commercialized for over 100 years. The considered pathways and alternatives for diesel engines are represented in **Figure 1A**.

Oils obtained from the catalytic low temperature pyrolysis of plastic waste have proven usable in conventional diesel engines (Wong et al., 2015). Damodharan et al. (2019) present an exhaustive overview of the research that has been carried out in the field during the last 20 years. From their review, it is evident that detailed performance criteria (e.g., heat release, nitrogen oxides, smoke emissions, etc.) in engine tests vary significantly from study to study. However, a clear consensus is that the oils can be used without complications and engine modifications in low blending ratios with conventional low sulfur diesel. Chandran et al. (2020) concluded that a content of 30% volume (v/v) of Plastic Waste Pyrolysis Oil (WPO) in diesel allows for long-term operation without engine modifications while Singh et al. (2020) reported that ratios of up to 50% are feasible under a slight increase in carbon monoxide (CO) emissions at high loads.

Biodiesel obtained from vegetable oils, animal fats or waste cooking oil appears as another sustainable alternative to fossil-based diesel. The basic principle of producing biodiesel is the transesterification of oils and fats to obtain smaller esters and glycerin, a mixture that has been used commercially in diesel engines since the early 1990s (Pahl, 2009). Similar to WPO, pure biodiesel can be used as-is in modified diesel engines and usually in blends up to 20% v/v with fossil-based diesel without any modifications to the engine (Alleman et al., 2016).

Gasoline Substitutes

A widely employed gasoline substitute is ethanol. It is the second aliphatic alcohol (C_2H_5OH) and has a wide range of applications: it can act as a solvent, conservative, disinfectant, and precursor to various other chemical products (e.g., acetic acid, ethyl esters, etc.). This study focuses on its application as a fuel substitute in internal combustion engines (Ilves et al., 2018). It can be blended with diesel at low ratios but its most common use is blended with gasoline in spark ignition engines.

The path to obtaining ethanol from plastic waste is depicted in **Figure 1B**. Somoza-Tornos et al. (2020) presented a detailed techno-economic and life cycle assessment of an 18.9 t/h polyethylene (PE) waste pyrolysis plant with high purity (99.5%) and ethylene yield of 46%. The gas mixture leaving the furnace is subsequently separated into its compounds through heat integrated cryogenic distillation. Ethanol can then be obtained from ethylene through hydration. Ethanol obtained from this route is referred to from here on as Plastic Waste Pyrolysis Ethanol (WPE).

Traditionally, ethanol is obtained from biomass (i.e., bioethanol). A variety of feedstock can be used for that purpose: for instance, while sugarcane is widely employed in Brazil, the main feedstock for bioethanol in the United States is corn. Obtaining ethanol from these feedstock follows in principle the same steps: pretreatment (milling), fermentation, and distillation (Canilha et al., 2012). As a renewable resource, bioethanol contributes to sustainability in the transportation sector. However, the main controversies surrounding bioethanol are associated with its land usage and competition with the food sector. Additionally, in many cases, its cost exceeds those of fossil-based fuel.

Pathway Selection

The business as usual pathways considered in this study are fossil-based fuels sourced from crude oil. The assessed costs and impacts cover the extraction and refining processes based in Europe.

Biofuels can be obtained from a variety of raw materials that are grouped as first-, second-, and third-generation. The pathways selected in this study are the first-generation fuels that are obtained from generally edible biomass. They were chosen because of their high maturity and easy to gather, reliable data for comparison. The biodiesel pathway studied herein covers acquisition and processing based on the mixture of raw materials employed in Europe, that is dominated by rapeseed (European Commission, 2020). For bioethanol also, the European mixture is studied, which mostly consists of maize, wheat, and sugar beet (European Commission, 2020).

TABLE 1 | Fuel properties for unit conversion.

Fuel	Density (kg/L) (Edwards et al., 2007)	Lower heating values (GJ/kg) (Kavalov, 2004)
Gasoline	0.7550	2.685×10^{-2}
Ethanol	0.7895	4.133×10^{-2}
Diesel	0.8450	3.727×10^{-2}
Biodiesel	0.8800	4.225×10^{-2}
WPO	0.7714	4.187×10^{-2}

Plastic waste pyrolysis oil to substitute diesel can be obtained from different types of plastic. Here, PP is chosen as raw material because its derived oils were shown to perform better in engines than those obtained from other plastics (Mangesh et al., 2020). The pyrolysis process is simulated in this study to obtain equipment dimensions for the techno-economic assessment and energy and emission values for the life cycle assessment. As a substitute of a gasoline additive, the pathway to produce ethanol from the pyrolysis of polyethylene (PE) is chosen due to its favorable ethylene yield, as reported by Kannan et al. (2014). The costs and impacts of the complete pathway are estimated using references for the pyrolysis process and the subsequent hydration steps. All calculations assume the costs and impacts in Europe.

Functional Unit

Among all data found in the literature and the results obtained from commercial simulators and LCA tools for techno-economic and environmental assessment, there are properties defined through different functional units. Some properties refer to the amount of fuel such as liters or kilograms, however, not all fuels store the same amount of energy and therefore different fuels can deliver different amounts of energy. For that reason, an energy dimension is chosen as a functional unit, in particular Gigajoules (GJ). In order to adapt fuel properties to this functional unit, fuel density is used to convert liters to kilograms when necessary, and Lower Heating Values to convert kilograms to GJ. The conversion factors considered are shown in **Table 1**.

Process Simulation: Polypropylene Pyrolysis

This work presents a process simulation of low temperature polypropylene pyrolysis. **Figure 2** depicts the flowsheet of the process including material and energy balances. The polymer pyrolysis heat demand is determined using Aspen Plus V11 with the POLYNRTL package. The group contribution-based property model allows an estimation of the polymer properties and thus the necessary heat for running the reaction. The condensation of the pyrolysis products is simulated in Aspen Hysys V11 using the Peng-Robinson equation of state to obtain accurate values of the hydrocarbon equilibrium and cooling demand.

Polypropylene is modeled as a 20-segment isotactic oligomer of propylene ($C_{63}H_{128}$, Molar mass 885.7 g/mol). A pseudo-stoichiometry has been obtained from the pyrolysis product

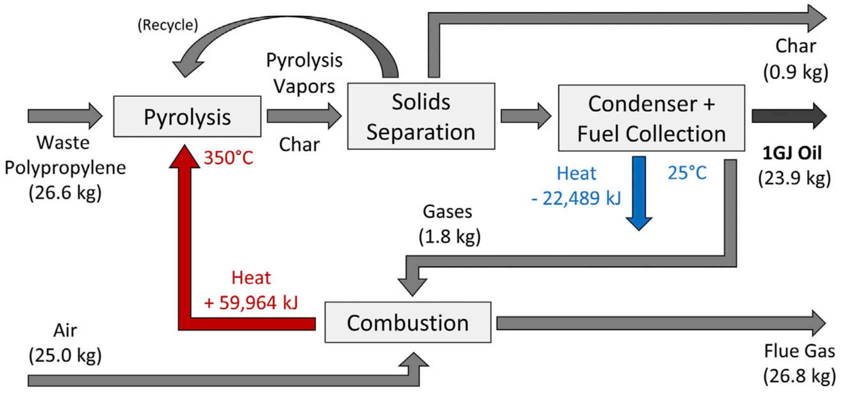

FIGURE 2 | Schematic representation of material and energy balances of the PP pyrolysis process. A possible recycling structure is indicated but not utilized in this work.

TABLE 2 | Polypropylene pyrolysis products adapted from Mangesh et al. (2020).

Type	C-range	Compound	Formula	Composition (% wt)
Alkane	C_{11}–C_{20}	Pentadecane	$C_{15}H_{32}$	2.9
	C_{21}–C_{30}	Pentacosane	$C_{25}H_{52}$	74.9
Alkene	C_1–C_{10}	Pentene	C_5H_{10}	7.1
	C_{11}–C_{20}	Pentadecene	$C_{15}H_{30}$	7.4
Aromatic	–	Benzene	C_6H_6	0.8
Gas	C_1–C_4	Methane	CH_4	3.4
Char	C	Carbon	C	3.6

composition and oil yields reported by Mangesh et al. (2020). The cited study uses colorless 2 mm sized shreds of polypropylene obtained from bottles, cans, and containers. Conversion of 100 g samples took place in the presence of 25 g of micro-mesoporous zeolite ZSM-5 catalyst in a 250 mm stainless-steel reactor under vacuum. Reaction time is 30 min at 350°C. Further details on catalyst preparation and product characterization can be found in Mangesh et al. (2020). The pyrolysis product is a complex mixture of hydrocarbons. These products have been grouped into classes according to their characteristics and each class has been represented by a single component (**Table 2**). Further details on the estimation of pyrolysis oil properties and simulation in Aspen software can be found in the **Supplementary Material**.

A 710 GJ/h production plant capacity was chosen, which corresponds to the plastic waste output (450 t/day) of a city with around 8 million people such as London. The process is simulated in steady-state mode. The plastic feed enters the pyrolysis reactor at 25°C and 1 bar. A heat of 14.7 MW is required to drive the decomposition reaction at 350°C and 1 bar. To that end, the 1.3 t/h product gas stream is burned in a furnace with an 80% efficiency and 20% air excess. After leaving the reactor, the solid char phase is separated from the liquid and gas phase through mechanical separation (e.g., filtering). The fluid products are cooled down to 25°C in an adiabatic condenser with a 5.6 MW cooling demand that is supplied by a cooling water utility. Heat and material losses in piping and the solid separation are neglected. For further details about this process, refer to the **Supplementary Material**.

Techno-Economic Assessment

The techno-economic assessment performed herein compares the production costs of the different pathways. Breakdowns of these costs into capital expenses (CapEx), operational expenses (OpEx), and raw material costs are obtained to determine major cost drivers in each pathway. Market prices are collected to show the possible profit margin of each pathway and blends of fuels. **Tables 3**, **4** detail the gathered data and its sources along with the results of the techno-economic assessment for each alternative. When available, price averages were taken over the period ranging from 2016 to 2020. All economic data for fossil fuels and biofuels were collected from literature sources.

WPO production cost is estimated following the method used in Gonzalez-Garay et al. (2017) and developed in chapter 6.2 from Sinnott and Towler (2020). The annual capital and operating costs are estimated. They are divided by the annual production to obtain unitary production costs. A detailed explanation of this cost estimation procedure is further developed in **Section 1.3 of the Supplementary Material**. Since currently WPO is not a traded product, its price has been estimated as equal to that of fossil diesel. The production costs of WPE are calculated using references for pyrolysis, separation (Somoza-Tornos et al., 2020), and catalytic hydration (Ayaou et al., 2020). In other words, the production cost of WPE is estimated as the sum of costs for the PE pyrolysis, the separation of the gas products, and the conversion of ethylene to ethanol processes.

When necessary, costs are extrapolated to 2019 using the Chemical Engineering Plant Cost Index (CEPCI) (Jenkins 2020) and converted from dollars into euros with the average exchange rate for 2019 (1€ = 1.1225$). Additionally, all prices and costs are adapted to refer to the chosen functional unit (i.e., €/GJ) using **Table 1**.

TABLE 3 | Production cost breakdown of diesel and alternatives. Densities and Lower Heating Values used are shown in **Table 1**.

	Fossil diesel	Biodiesel	WPO[g]
CAPEX (€/GJ)	1.71[a]	1.32[c]	0.19
OPEX (€/GJ)	1.14[a]	2.11[c]	0.31
Feedstock (€/GJ)	10.20[a]	19.48[c]	9.30
Total cost[f] (€/GJ)	13.06[a]	22.90[d]	9.80
Market price (€/GJ)	16.94[b]	18.94[e]	18.72

[a] *Estimated using data from* U.S. Energy Information Administration (2019a).

[b] *Prices from* European Commission (2021).

[c] *Breakdown from* International Renewable Energy Agency (2013).

[d] *From* Organisation for Economic Co-operation and Development (2020).

[e] *Prices from* Eurostat - European Commission (2020).

[f] *Costs updated to 2019 with CEPCI (*Jenkins, 2020*); converted to euros with an average 2019 exchange rate of 1.1225 €/$.*

[g] *This work, section* "Techno-Economic Assessment"*, market price considered equal to fossil diesel.*

TABLE 4 | Production cost breakdown of gasoline and alternatives. Densities and Lower Heating Values used are shown in **Table 1**.

	Fossil gasoline	Bioethanol	WPE[g]
CAPEX (€/GJ)	1.77[a]	1.39[c]	6.42
OPEX (€/GJ)	1.18[a]	10.65[c]	12.42
Feedstock (€/GJ)	11.78[a]	11.12[c]	15.03
Total cost[f] (€/GJ)	14.73[a]	23.16[d]	33.87
Market price (€/GJ)	17.67[b]	27.62[e]	27.62

[a] *Estimated using data from* U.S. Energy Information Administration (2019b).

[b] *Prices from* European Commission (2021).

[c] *Breakdown from* International Renewable Energy Agency (2013).

[d] *From* Organisation for Economic Co-operation and Development (2020).

[e] *Prices from* Eurostat - European Commission (2020).

[f] *Costs updated to 2019 with CEPCI (*Jenkins, 2020*); converted to euros with average 2019 exchange rate of 1.1225 €/$.*

[g] *This work, section* "Techno-Economic Assessment"*, market price considered equal to bioethanol.*

For the proposed blends between traditional fuels and their substitutes, the prices are estimated using **Eq. 1**, where v^{alt} is the volumetric fraction of alternative in fossil fuel blend, $LHV^{alt/fos}$ the lower heating value and $Cost^{alt/fos}$ the cost of the pure alternative or fossil fuels.

$$Cost^{Blend}\left(v^{alt}\right) = \frac{\left(1 - v^{alt}\right) \cdot \left(LHV^{fos} \cdot Cost^{fos} - LHV^{alt} \cdot Cost^{alt}\right) + LHV^{alt} \cdot Cost^{alt}}{\left(1 - v^{alt}\right) \cdot \left(LHV^{fos} - LHV^{alt}\right) + LHV^{alt}} \quad (1)$$

Environmental Assessment

The environmental assessment performed in this study is a cradle-to-gate, or as previously introduced, Well-to-Tank, LCA following the ISO 14040:2006 standards (ISO, 2016). To compare values between different fuels, the functional unit is set to the amount of fuel equivalent to 1 GJ of Lower Heating Values. For the fossil-based fuels and biofuels, the life cycle inventories from the EcoInvent database v3.4 (Wernet et al., 2016) were retrieved and the results of the final impact are analyzed through ReCiPe2016 methodology (Huijbregts et al., 2017) with the SimaPro software (Goedkoop et al., 2014) using the hierarchical approach.

TABLE 5 | Net flows of the PP pyrolysis process and EcoInvent entries used for modeling and LCA.

Concept	Amount per GJ of fuel	EcoInvent v3.4 entry
By-products		
Char (kg)	0.939	—
Raw materials		
Polypropylene (kg)	26.605	Waste polyethylene, for recycling, sorted (Europe without Switzerland) | market for waste polyethylene, for recycling, sorted
Utilities		
Net electricity consumption (kWh)	7.368×10^{-2}	Electricity, high voltage (Europe without Switzerland) | market group for
Cooling water (kWh)	7.881	Electricity, high voltage (Europe without Switzerland) | market group for
Water (kg)	1×10^{-4}	Water, deionized, from tap water, at user (Europe without Switzerland) | market for water, deionized, from tap water, at user
Equipment		
Steel (kg)	1.075×10^{-4}	Steel, chromium steel 18/8 (RER)| steel production, converter, chromium steel 18/8
Direct emissions (fuel combustion)		
CO_2 (kg)	5.278	—
H_2O (kg)	3.129	—
N_2 (kg)	17.03	—
O_2 (kg)	1.314	—

For the plastic waste pyrolysis pathways, no pre-defined inventories are available in EcoInvent. The WPO inventory was obtained through the mass and energy balances from the process simulation. The complete inventory is shown in **Table 5**. A cut-off approach for the PP waste inlet is assumed (i.e., waste is free from primary material burden) (Gentil et al., 2010). Thus, the environmental impacts of PP waste are assumed to be only associated to the sorting process. The impacts of PP sorting are approximated to those of polyethylene sorting due to data availability and the similar properties of both polymers in terms of chemistry and application. The impact of cooling water is calculated as the electricity required for pumping assuming a conversion factor of 9.5 kWh/MWh of cooling energy and considering 10% extra water to compensate for evaporation and other losses. The environmental impact associated with the furnace and side equipment units is estimated using the corresponding steel requirements, considering a lifetime of 25 years. The environmental impact of WPO is compared to the impact obtained from:

- Diesel ["*Diesel (Europe without Switzerland) | petroleum refinery operation*"] and,
- Biodiesel ["*Vegetable oil methyl ester (Europe without Switzerland) | esterification of rape oil*"]

The entry for biodiesel production in Europe without Switzerland from only rape oil is selected because it is the dominating feedstock for biodiesel production in Europe and EcoInvent database offers no inventory for mixed production of the other raw materials.

Similar to the approach used in techno-economic assessment, the environmental impact from the pyrolysis of PE waste into ethylene were retrieved from Somoza-Tornos et al. (2020) and allocated according to the economic weight of each product. Then, the subsequent impact associated with the hydration of ethylene into ethanol is assumed to be equivalent to the same operation in the case of fossil-based ethanol. Considering the stoichiometric relation (0.61 kg ethylene/kg ethanol):

$$Impact^{WPE} = Impact^{Fossil-Ethanol} - 0.61 \cdot \left(Impact^{Fossil-Ethylene} - Impact^{Pyrolysis-Ethylene}\right) \tag{2}$$

with:

- Fossil Ethanol ["*Ethanol, without water, in 99.7% solution state, from ethylene (RER)| ethylene hydration*"];
- Fossil Ethylene ["*Ethylene, average (RER)| production*"];
- Pyrolysis Ethylene (Somoza-Tornos et al. (2020)).

Once the impact of ethanol from plastic waste pyrolysis is calculated, it is compared to the impact of:

- Gasoline ["*Petrol, unleaded (Europe without Switzerland) | petroleum refinery operation*"].
- Bioethanol ["*Ethanol, without water, in 99.7% solution state, from fermentation (Europe without Switzerland) | dewatering of ethanol from biomass, from 95 to 99.7% solution state*"].

RESULTS AND DISCUSSION

This section presents the results from the techno-economic and environmental assessment performed on diesel and gasoline alternatives, as well as a discussion on tradeoffs between all alternatives.

Techno-Economic Assessment

As described above, the study comprises two lines. First, the assessment of alternatives for diesel-based engines. Second, the comparison of gasoline alternatives, and then the assessment of possible blends.

Diesel Alternatives

Table 3 shows the cost breakdown and market prices for WPO, biodiesel, and diesel. It can be seen that the production of pure fossil-diesel and WPO are economically profitable (i.e., their production costs are below their market prices), while biodiesel production is not. This is due to the cost considered for biodiesel raw materials (mainly rapeseed oil, methanol/ethanol, and sodium hydroxide), which represents approximately 85% of production costs (22.90 €/GJ). This value is considerably higher than in the other two alternatives (9.81 €/GJ for PP waste and 13.06 €/GJ for crude oil). However, it is possible to obtain biodiesel using biomass waste or other non-edible biomass sources as feedstock, such as used cooking oil, waste animal fats, or other kinds of waste biomass, which are not assessed in this study.

It is worth noting that the calculated WPO total cost of 9.80 €/GJ (0.410 €/kg) is much larger than the cost of 1.07 €/GJ (0.045 €/kg) at the same plant scale (710 GJ/h), using household plastic waste estimated by Fivga and Dimitriou (2018). A conversion rate of 1.15 €/£ and the lower heating value of WPO of 0.04187 GJ/kg were used for this conversion. The difference stems from the assumed plastic waste feedstock cost (0.39 €/kg vs. 0 €/kg). This shows that the feedstock cost for plastic waste is a parameter that greatly influences the production cost and consequently the economic feasibility of the derived fuels. However, despite the conservative assumption taken in this work, WPO still stands as the most economically competitive alternative. Note that the price of plastic waste has been assumed to be equal to the cost of mixed plastic waste sorting and collection.

Figure 3A shows the range of blends between fossil diesel and biodiesel, and how blending affects the production costs and average market prices. According to these results, blends up to 50% v/v biodiesel are economically acceptable. This confirms that one of the most used biodiesel blends, B20 (total cost: 14.84 €/GJ vs. market price: 17.30 €/GJ), is still economically competitive overall, although the profit margin is significantly reduced compared to fossil diesel. Following the same procedure, production costs and market prices for blends of fossil diesel with WPO are estimated, leading to the results shown in **Figure 3B**. In this case, any blend would be economically profitable and the profit margin increases with the proportion of WPO used in the blend. A typical blend that could be used in current diesel vehicles is WPO30, which can be considered profitable from an economic standpoint.

Figure 4 depicts the cost and market price comparison for traditional fossil diesel and two proposed blends with biodiesel and WPO. The blend with the best economic performance is WPO30 (total cost: 12.09 €/GJ vs. market price: 17.47 €/GJ) against fossil diesel (total cost: 13.06 €/GJ vs. market price: 16.94 €/GJ) and commercial blend with biodiesel (total cost: 14.84 €/GJ vs. market price: 17.30 €/GJ). The cost driver in these three cases is the feedstock cost.

From an economic point of view, the diesel and WPO standalone alternatives are profitable. Between these two alternatives, WPO is cheaper to produce. WPO is not a product available in the market; therefore, its price is estimated as equivalent to that for fossil diesel, which may add an important source of uncertainty to the study. However, its energy content is similar to fossil diesel, thus the price estimation is acceptable. Therefore, any blend between diesel and WPO would be economically profitable, with very similar results, and theoretically, a WPO100 would be the most profitable option.

Gasoline Alternatives

To assess the different fuel alternatives for gasoline engines, the production costs of gasoline are compared to European sourced bioethanol and plastic waste based ethanol. Cost

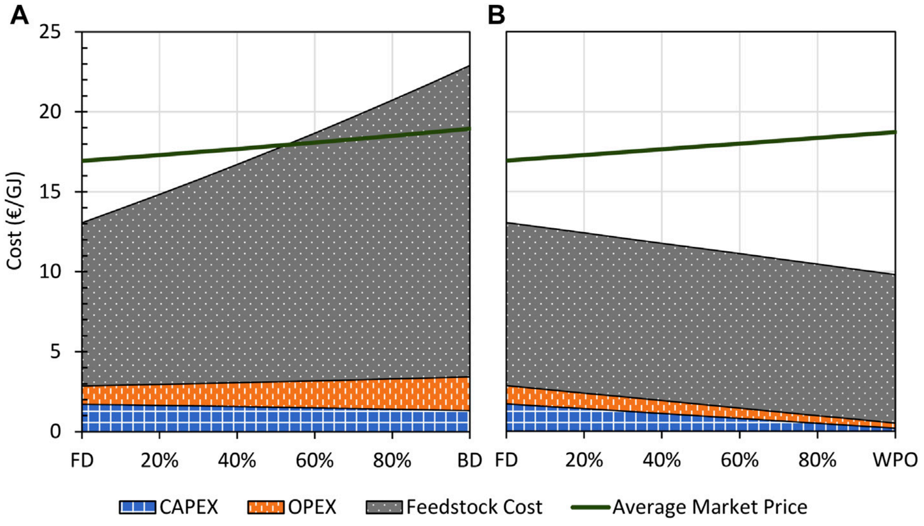

FIGURE 3 | (A) Production cost breakdown for different blends of diesel and biodiesel and theoretical blend market price. Horizontal axis labels represent biodiesel weight percentage in the final blend. **(B)** Production cost breakdown for different blends of diesel and WPO and theoretical blend market price. Horizontal axis labels represent the WPO weight percentage in the final blend. FD: fossil diesel. BD: biodiesel. WPO: plastic waste pyrolysis oil (for references, see **Table 3**).

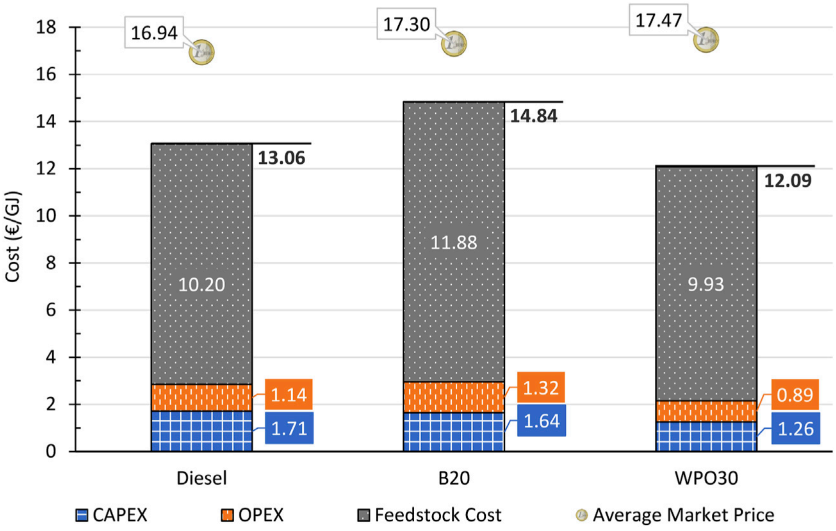

FIGURE 4 | Economic comparison of traditional diesel against proposed blends with biodiesel (B20) and WPO (WPO30). B20: Diesel/Biodiesel blend 80/20% v/v. WPO30: Diesel/Plastic waste pyrolysis oils 70/30% v/v (for references, see **Table 3**).

breakdowns for these three routes are shown in **Table 4**, along with the reference market price for ethanol. Results show that the traditional way of obtaining bioethanol is economically competitive (total cost: 23.16 €/GJ vs. market price: 27.62 €/GJ). In contrast, the pyrolysis route is not competitive (total cost: 33.87 €/GJ). Capital and operational expenses are high due to complex and energy intensive gas separation and subsequent hydration steps.

Figure 5A shows the production cost breakdown and price for all tentative blends of gasoline and bioethanol. The results show that any blend would be economically competitive and feasible to use according to current market prices (17.67 €/GJ for gasoline and 27.62 €/GJ for ethanol), but the profit margin would grow slightly when the percentage of bioethanol is increased. **Figure 5B** depicts the production cost of blends of gasoline and WPE. In this case, WPE/gasoline blends are competitive up to approximately 40% v/v with a total cost equal to its market price of 20.60 €/GJ, showing that they would be feasible to implement for the unmodified engines at the

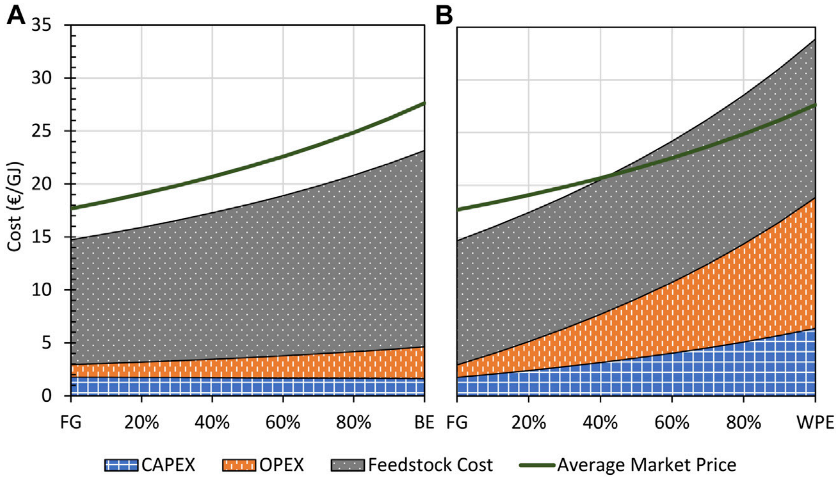

FIGURE 5 | (A) Production cost breakdown for different blends of gasoline and bioethanol and theoretical blend market price. Horizontal axis labels represent bioethanol weight percentage in the final blend. **(B)** Production cost breakdown for different blends of gasoline and WPE and theoretical blend market price. Horizontal axis labels represent the WPE weight percentage in the final blend. FG: fossil gasoline. BE: bioethanol. WPE: plastic waste pyrolysis-sourced ethanol (for references, see **Table 4**).

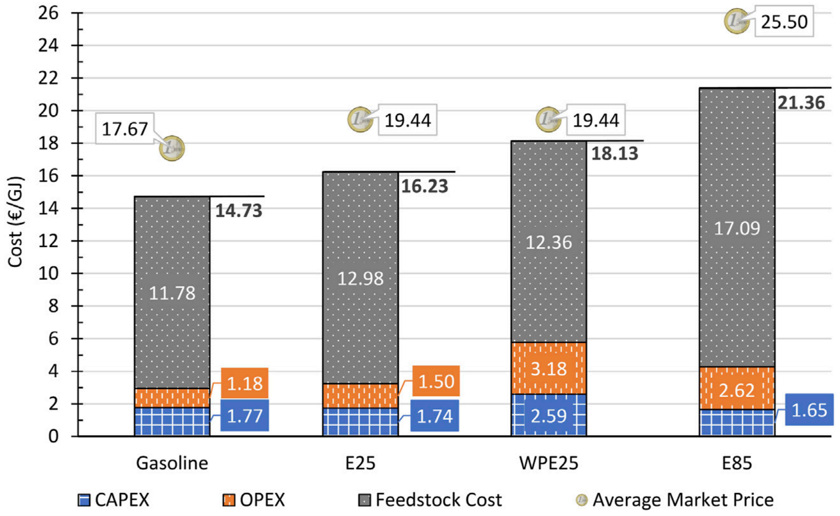

FIGURE 6 | Economic comparison of traditional gasoline against commercial bioethanol blends and proposed WPE blend. E25: gasoline/bioethanol blend 75/25% v/v. WPE25: gasoline/plastic waste pyrolysis-sourced ethanol blend 75/25% v/v. E85: gasoline/bioethanol blend 15/85% v/v (for references, see **Table 4**).

recommended blending ratios (usually 25% v/v). Similar to the diesel case, in **Figure 6**, traditional gasoline is compared against two typically commercially available gasoline-bioethanol blends (E25 and E85), and an equivalent case is proposed using WPE instead (WPE25). Any of these alternatives would be economically feasible, but provided that pure bioethanol is the most profitable alternative, E85 is the most profitable bioethanol/gasoline blend (total costs: 23.16 and 21.36 €/GJ vs. market prices: 27.62 and 25.50 €/GJ respectively). To sum up, the larger the amount of bioethanol added to gasoline, the more economically profitable the blend would be, assuming the market price behaves as modeled herein.

Environmental Assessment

The environmental assessment is performed similarly to the economic assessment presented in the previous section. First, diesel alternatives are compared, and then the possible blends are evaluated. Subsequently, the ethanol obtained from two different routes are compared, and their blends with gasoline evaluated. They are assessed in terms of harmonized impact scores at midpoint and endpoint levels, which focus mainly on three areas: human health, ecosystem quality, and resource scarcity,

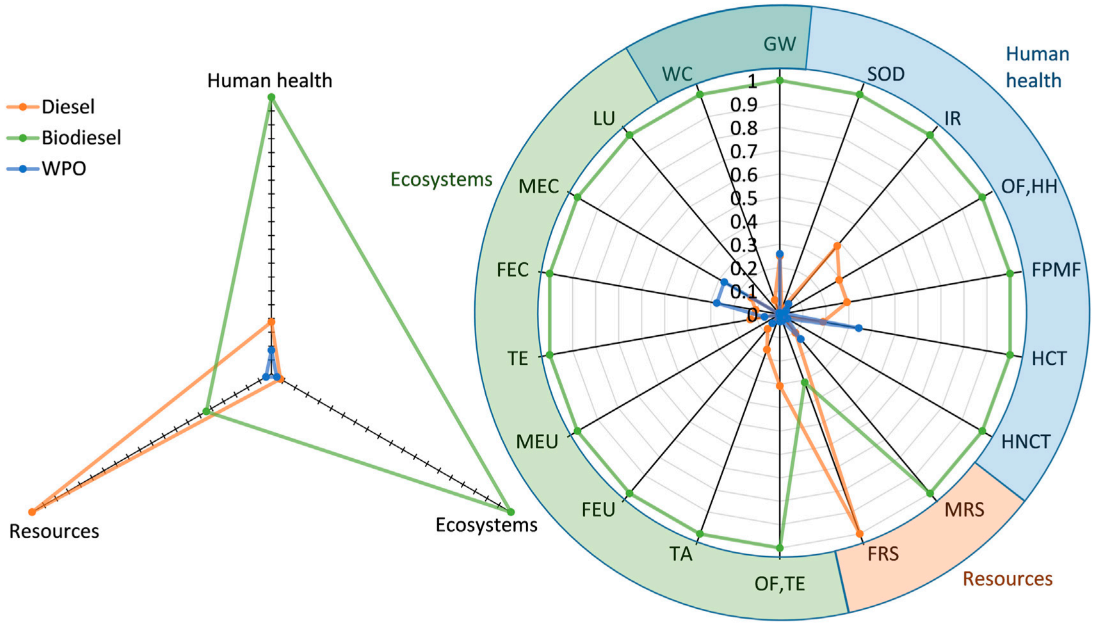

FIGURE 7 | Normalized LCA endpoint and midpoint indicators comparison for diesel, biodiesel, and WPO production pathways. GW: global warming; SOD: stratospheric ozone depletion; IR: ionizing radiation; OF, HH: ozone formation, human health; FPMF: fine particulate matter formation; OF, TE: ozone formation, terrestrial ecosystems; TA: terrestrial acidification; FEU: freshwater eutrophication; MEU: marine eutrophication; TE: terrestrial ecotoxicity; FEC: freshwater ecotoxicity; MEC: marine ecotoxicity; HCT: human carcinogenic toxicity; HNCT: human non-carcinogenic toxicity; LU: land use; MRS: mineral resource scarcity; FRS: fossil resource scarcity; WC: water consumption. WPO: plastic waste pyrolysis oil. Endpoint and midpoint values are available in **Supplementary Table S2**.

as proposed in ReCiPe2016 methodology (Huijbregts et al., 2017). To facilitate the comparison and representation of the different impact scores, the endpoints and midpoints values are normalized with respect to the highest value among the alternatives.

To assess midpoint impacts, the focus is set on the ones driving the endpoints impacts results:

- The human health endpoint is mainly driven by global warming and fine particulate matter formation impacts.
- Ecosystems quality is driven by global warming, land use, and terrestrial acidification.
- Resource scarcity is led by fossil resource scarcity.

Diesel Alternatives

For the three analyzed diesel alternatives, **Figure 7** depicts the LCA results on radar plots with normalized impact at midpoint and endpoint levels. As expected, the use of fossil diesel involves a higher impact on resource scarcity than any other alternative (13.04 vs. 3.54 and 0.31 USD2013/GJ for biodiesel and WPO respectively). Biodiesel, on the other hand, has a higher impact on human health and ecosystems (18.67×10^{-5} DALY/GJ and 17.58×10^{-7} species·yr vs. 3.50×10^{-5} DALY/GJ and 0.66×10^{-7} species·yr for diesel). By contrast, the production of WPO from polypropylene *via* the proposed process has a lower impact in all categories compared to the other two alternatives (0.31 USD2013/GJ, 1.6×10^{-5} DALY/GJ and 0.39×10^{-7} species yr). This is because waste is valorized, producing a valuable fuel and the process is comparatively simpler and environmentally friendlier.

The impact of biodiesel is significantly higher than for fossil-based diesel and WPO on human health and ecosystems, which are driven by global warming (55.34 vs. 12.15 and 12.70 kg equivalent carbon dioxide (CO_2eq)/GJ respectively), fine particulate matter formation (136×10^{-3} vs. 35×10^{-3} and 2.4×10^{-3} kg $PM_{2.5}$eq/GJ respectively), and land use (155.2 vs. 0.111 and 0.106 m^2 crop eq/GJ respectively). On the other hand, fossil resource scarcity is considerably higher for fossil diesel (29.0 kg oil eq/GJ) than the other alternatives (10.21 kg oil eq/GJ for biodiesel and 0.90 kg oil eq/GJ for WPO).

It is important to highlight that, even though the biofuel alternative in principle closes the carbon cycle by depleting the CO_2 from the atmosphere (1.98 kg CO_2/kg rape seed) that is emitted during fuel combustion, its whole production phase entails considerable global warming impact and impact on ecosystems in general. These stem from intense land usage, water consumption and the use of fertilizers for harvesting energy crops. A significant amount of global warming impact comes from dinitrogen monoxide (N_2O) emissions that have a 298 times higher greenhouse gas effect than CO_2 (Solomon et al., 2007). First-generation fuel feedstock in principle entails an additional carbon debt from cutting down forests and grasslands that act as carbon storage, which will eventually be released over a period of time. This kind of carbon debt is referred to as land use change and is considered a major source of emission

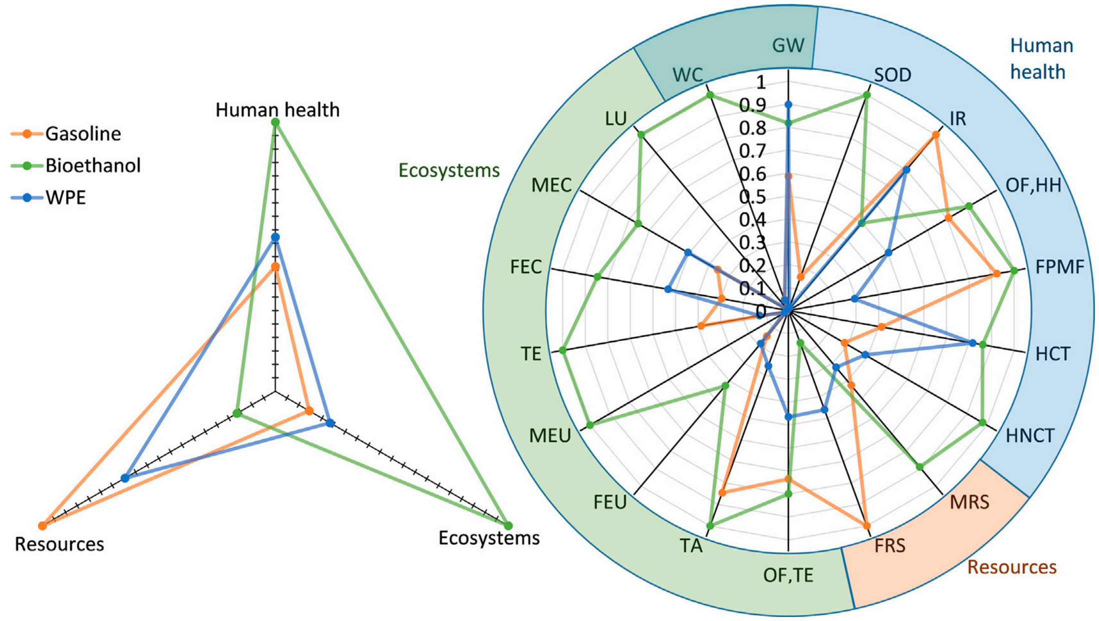

FIGURE 8 | Normalized LCA endpoint and midpoint indicators comparison for gasoline, bioethanol and WPE production pathways. GW: global warming; SOD: stratospheric ozone depletion; IR: ionizing radiation; OF,HH: ozone formation, human health; FPMF: fine particulate matter formation; OF,TE: ozone formation, terrestrial ecosystems; TA: terrestrial acidification; FEU: freshwater eutrophication; MEU: marine eutrophication; TE: terrestrial ecotoxicity; FEC: freshwater ecotoxicity; MEC: marine ecotoxicity; HCT: human carcinogenic toxicity; HNCT: human non-carcinogenic toxicity; LU: land use; MRS: mineral resource scarcity; FRS: fossil resource scarcity; WC: water consumption. WPE: plastic waste pyrolysis-sourced ethanol. Endpoint and midpoint values are available in **Supplementary Table S3**.

in the life cycle of first-generation fuels. Adding this impact to the assessment leads to most first-generation fuels having higher global warming potential than fossil fuels (Jeswani et al., 2020).

Gasoline Alternatives

Figure 8 shows the endpoint and midpoint indicators for the three proposed ways of obtaining ethanol and gasoline. In the same line to the findings for diesel alternatives, the biomass-sourced ethanol has a higher impact on human health and ecosystems than the other alternatives and the lowest on resources (10.14×10^{-5} DALY/GJ, 6.19×10^{-7} species·yr and 2.31 USD2013/GJ). Gasoline has the highest impact on resources but lowest on the other two endpoints (4.70×10^{-5} DALY/GJ, 0.90×10^{-7} species·yr and 13.93 USD2013/GJ) and pyrolysis-sourced ethanol have intermediate impact values on human health, ecosystems, and resources (5.81×10^{-5} DALY/GJ, 1.45×10^{-7} species·yr and 9.00 USD2013/GJ).

When compared to gasoline, bioethanol has a considerably higher impact on human health and ecosystems and a lower impact on resources. WPE shows a similar tendency but smaller difference with gasoline, that is, slightly higher impact on human health and ecosystems and slightly lower on resources.

The highest impact on global warming corresponds to WPE and bioethanol (41.95 and 38.14 vs. 17.78 kg CO_2eq/GJ respectively for WPE, bioethanol, and gasoline), additionally, the highest impact on fine particulate matter formation corresponds to bioethanol (75×10^{-3} vs. 45×10^{-3} and 22×10^{-3} kg $PM_{2.5}$eq/GJ respectively for bioethanol, gasoline, and WPE), which drives it to the highest human health endpoint impact among the other alternatives. The highest impact on ecosystems corresponds to bioethanol, driven mostly by its high impact on land use (42.6 vs. 0.23 and 0.14 m^2 crop eq/GJ respectively for WPE and gasoline). On the other hand, fossil resource scarcity is higher on gasoline (31.1 vs. 22.1 and 7.2 kg oil eq/GJ respectively for WPE and bioethanol).

Remarks on Engine Performance

After the production phase, the fuels enter the use phase where they generate an additional impact on the environment. Engine tests for different blends at varying operating conditions are commonly used to identify the performance and emission values of fuel in a test engine.

In the case of diesel, biodiesel, and WPO the literature findings vary vastly from study to study. Adaileh and Alqdah (2012) report that biodiesel obtained from waste cooking oil provided a significant reduction in carbon monoxide and unburned hydrocarbons, but increases in nitrogen oxide emissions and brake-specific fuel consumption. Similar differences can be observed in the case of WPO, as described in the review by Damodharan et al. (2019) and more recent studies by Singh et al. (2020) and Singh et al. (2021).

The differences observed between biodiesel and WPO engine performance can be explained by the different composition and properties of the fuels under study, stemming from different feedstock types and quality, the catalyst used during conversion, experimental procedure, etc. As previously mentioned, more in-depth studies are required to assess the final environmental impact for each case individually.

Bioethanol is commonly found to enhance engine performance while also reducing emission values (Thangavelu, 2016). This implies that the inclusion of the use phase would favor ethanol over gasoline in terms of environmental impact. There is a consensus that ethanol fuel has no considerable variations in composition from study to study.

Economic and Environmental Tradeoffs

In order to devise the potential of each of the alternatives and their potential blends, a tradeoff evaluation has been performed attending to economic and environmental results. First, diesel alternatives and second, gasoline alternatives were studied, and the resulting proposals are discussed from a global point of view.

Diesel Alternatives

Considering global economic and environmental performance, any blending of diesel and WPO would be more profitable than fossil diesel alone, and any biodiesel/diesel blend. Indeed, WPO appears to be a very promising alternative, with outstanding performance in comparison to biodiesel as a diesel alternative, and it is recommended that the highest blending ratio that internal combustion engines can admit are used (without compromising performance or stability).

Gasoline Alternatives

Bioethanol has better economic performance than any other alternative considered in this study. Regarding gasoline/ethanol blends, bioethanol is economically competitive at any ratio because of the specific market prices of these blends, while WPE should not exceed 40% v/v to ensure economic feasibility. From the environmental point of view, WPE shows better overall results than other choices and blends with gasoline would entail a lower impact on human health and ecosystems than gasoline-bioethanol blends.

To find a tradeoff between economic and environmental performance, and considering typical blending ratios (25% v/v), WPE seems to be a good choice. When compared individually to gasoline, its environmental impact on human health is 20% lower, while for bioethanol it is 40% higher; on ecosystems, its impact is 5% higher while for bioethanol it is 350% higher; and on resources, both WPE and bioethanol have a lower impact than gasoline (58 and 89% lower respectively). In reverse, the profit margin of WPE25 vs. E25 would be around 59% lower.

Global Analysis of Alternatives

From a global perspective and bearing in mind the kinds of fuel considered in this work, one alternative could potentially be devised as better than the rest. The results show that the use of WPO as a fuel is a very promising option to replace fossil fuels and biofuels, since it has shown the best economic and environmental results among the considered options. Although it is important to underline that this technology is not yet as developed as the rest and it needs to be scaled up.

CONCLUSION

This work presents an overview and assessment of the most widely used fuel sources for "hard-to-decarbonize" sectors and compares them with emerging solutions. On one hand, biofuels have gained wide attention due to their potential to close the carbon cycle and preserve fossil resources. However, first-generation biofuels can have a considerable impact on ecosystems and human health, as has been confirmed in this study for the case of biodiesel and bioethanol in Europe. On the other hand, fuels derived from plastic waste sources are gaining increasing interest due to their capability to displace the problem of waste management. The comparative techno-economic and life cycle assessment between fossil-, bio- and plastic waste pathways in this study yield the following insights:

- A contribution is made to waste-to-resource modeling through the simulation of a low temperature waste pyrolysis process of polypropylene.
- Techno-economic assessment reveals that the production (Well-to-Tank) of oils derived from waste polypropylene (namely WPO) are more economically competitive (9.80 vs 13.06 €/GJ for diesel and 22.90 €/GJ for biodiesel).
- Life cycle assessment shows that WPO performs better in all three ReCiPe2016 impact categories (ecosystems, human health, and resources) than the fossil and biodiesel alternatives due to its low emissions stemming from procedural simplicity and low energy demand.
- Converting the pyrolysis products of polyethylene into high purity ethanol (WPE) to be used in gasoline engines is economically non-competitive (33.8 €/GJ) compared to bioethanol (23.2 €/GJ) and fossil gasoline itself (14.7 €/GJ). This comes from the more complex processing including the separation of gaseous pyrolysis products and subsequent catalytic hydration.
- Similar to biodiesel, bioethanol performs worse in ecosystems and human health but better in resources than fossil gasoline for the aforementioned reasons. As opposed to WPO, WPE production is more complex and energy intensive, thus, it is placed in between gasoline and bioethanol in all categories.

Based on these findings, the products from plastic waste pyrolysis appear as a very promising alternative and, more specifically, the use of PP waste pyrolysis oil (WPO) as a diesel substitute shows great potential to partially replace fossil fuels. Additionally, it would help to deal with the growing problem of waste disposal. WPE, on the other hand, is more costly to produce and less environmentally friendly due to the additional separation and hydration steps. Although it offers a certain profit margin and tradeoff solutions in the impact categories between gasoline and bioethanol, it should be considered only if the conversion from a valuable chemical product (ethylene) to ethanol for the sake of fuel production is reasonable. Thus, research efforts should focus on the direct utilization of plastic waste oils in engines due to the aforementioned reasons. Real data from emerging commercial projects should be collected and assessed to further validate the findings of this study.

Future work must consider the extension of the system boundaries to the use phase of the alternative fuels since fuel quality can vary heavily depending on the used feedstock. Moreover, material and energy balances, thus costs and impacts will change depending on the type and quality of plastic waste. Accordingly, not only alternative feedstock for plastics, but also biomass based pathways might be included in the assessment, with a special focus on identifying weak spots to increasing economic competitiveness and the environmental friendliness of each alternative.

DATA AVAILABILITY STATEMENT

The original contributions presented in the study are included in the article/**Supplementary Material**, further inquiries can be directed to the corresponding author.

AUTHOR CONTRIBUTIONS

Conceptualization: AS-T, AP-L, FL; Methodology: AS-T, AP-L, FL; Software: AS-T, FL; Validation: MG, AE; Formal Analysis: AS-T, AP-L, FL; Investigation: AS-T, AP-L, FL; Resources: AS-T, AP-L, FL; Data Curation: AS-T, AP-L, FL; Writing—Original Draft: AS-T, AP-L, FL; Writing—Review and Editing: AP-L, FL; Visualization: AP-L, FL; Supervision: MG, AE; Project Administration: MG, AE; Funding Acquisition: MG, AE.

FUNDING

This study received financial support from the Spanish Competitiveness, Industry, and Economy Ministry and the European Regional Development Fund, both funding the research Project AIMS (DPI 2017-87435-R).

ACKNOWLEDGMENTS

AP-L thankfully acknowledges the financial support of the Spanish Ministry of Science, Innovation, and Universities (grant ref. PRE 2018-087135). FL gratefully acknowledges the Universitat Politècnica de Catalunya and Banco Santander for the financial support of his predoctoral grant FPI-UPC. **Figure 1** was made with icons designed by Freepik, Smashicons and DinosoftLabs from www.flaticon.com.

SUPPLEMENTARY MATERIAL

The Supplementary Material for this article can be found online at: https://www.frontiersin.org/articles/10.3389/fenrg.2021.676233/full#supplementary-material

REFERENCES

ACEA (2020). Fuel Types of New Cars. European Automobile Manufacturers' Association. Available at: https://www.acea.be/press-releases/article/fuel-types-of-new-cars-petrol-52.3-diesel-29.9-electric-6.8-market-share-fi (Accessed March 1, 2021)

Adaileh, W. M., and Alqdah, K. S. (2012). Performance of Diesel Engine Fuelled by a Biodiesel Extracted from a Waste Cocking Oil. *Energ. Proced.* 18, 1317–1334. doi:10.1016/j.egypro.2012.05.149

Alleman, T. L., McCormick, R. L., Christensen, E. D., Fioroni, G., Moriarty, K., and Yanowitz, J. (2016). *Biodiesel Handling and Use Guide*. 5th Edn, Golden, Colorado; Cincinnati, OH, United States: National Renewable Energy Laboratory; Eco Engineering. doi:10.2172/1332064

Araujo Galvão, G. D., De Nadae, J., Honorato Clemente, D., Chinen, G., and de Carvalho, M. M. (2018). Circular Economy: Overview of Barriers. *Proced. CIRP* 73, 79–85. doi:10.1016/j.procir.2018.04.011

Ayaou, B., Bodson, A., Dehottay, L., Farai, R., Farcy, A., Hendrickx, D., et al. (2020). *Ethanol Production by Catalytic Hydration of Ethylene*, Liege, Belgium: Liège Université Library Press, 1–21.

Brinkman, N., Wang, M., Weber, T., and Arlington, T. (2005). Well-to-Wheels Analysis of Advanced Fuel/Vehicle Systems - A North American Study of Energy Use, Greenhouse Gas Emissions, and Criteria Pollutant Emissions. Energy, no. May. Available at: http://www.transportation.anl.gov/pdfs/TA/339.pdf (Accessed April 18, 2021). doi:10.2172/1218344

Canilha, L., Chandel, A. K., Dos Santos. Milessi, T. S., Fernandes Antunes, F. A., Antunes, F. A. F., da Costa Freitas, W. L., et al. (2012). Bioconversion of Sugarcane Biomass into Ethanol: An Overview about Composition, Pretreatment Methods, Detoxification of Hydrolysates, Enzymatic Saccharification, and Ethanol Fermentation. *J. Biomed. Biotechnol.* 2012, 1–15. doi:10.1155/2012/989572

Chandran, M., Tamilkolundu, S., and Murugesan, C. (2020). Characterization Studies: Waste Plastic Oil and its Blends. *Energy Sourc. A: Recovery, Utilization, Environ. Effects* 42 (3), 281–291. doi:10.1080/15567036.2019.1587074

Dahlbo, H., Poliakova, V., Mylläri, V., Sahimaa, O., and Anderson, R. (2018). Recycling Potential of Post-Consumer Plastic Packaging Waste in Finland. *Waste Manage.* 71, 52–61. doi:10.1016/j.wasman.2017.10.033

Damodharan, D., Rajesh Kumar, B., Gopal, K., De PouresDe Poures, M. V., and Sethuramasamyraja, B. (2019). Utilization of Waste Plastic Oil in Diesel Engines: A Review. *Rev. Environ. Sci. Bio/Technol.* 18, 681–697. doi:10.1007/s11157-019-09516-x

Edwards, R., Larivé, J. F., Rickeard, D., and Werner, W. (2014). *WELL-TO-TANK (WTT) Report*. Version 4a. Ispra, Italy: Joint Research Center of the EU (JRC). doi:10.2790/95629

Edwards, R., Larive, J. F., Vincent, M., and Rounveirolles, P. (2007). WELL-TO-WHEELS ANALYSIS of FUTURE AUTOMOTIVE FUELS and WELL-To-WHEELS Report. Europe Version 2c (March): 88. Available at: www.co2star.eu/publications/Well_to_Tank_Report_EU.pdf (Accessed February 22, 2021).

European Commission (2020). *EU Agricultural Outlook for Markets, Income and Environment 2020 - 2030*, Brussels: European Commission, DG Agriculture and Rural Development. Available at: https://ec.europa.eu/info/sites/default/files/food-farming-fisheries/farming/documents/agricultural-outlook-2020-report_en.pdf (Accessed April 22, 2020). doi:10.2762/252413

European Commission (2021). Weekly Oil Bulletin | Energy. Available at: https://ec.europa.eu/energy/data-analysis/weekly-oil-bulletin_en (Accessed February 22, 2021).

Eurostat - European Commission (2020). Statistical Classification of Economy Activity in the European Union (NACE 2). 2019 Annual Detailed Data by PRODCOM List. Available at: http://ec.europa.eu/eurostat/web/prodcom/data/excel-files-nace-rev.2 (Accessed November 26, 2020).

Fivga, A., and Dimitriou, I. (2018). Pyrolysis of Plastic Waste for Production of Heavy Fuel Substitute: A Techno-Economic Assessment. *Energy* 149 (April), 865–874. doi:10.1016/j.energy.2018.02.094

Fuels Europe (2018). Statistical Report. Available at: https://www.fuelseurope.eu/wp-content/uploads/FuelsEurope-Statistical-Report-2018.pdf (Accessed February 28, 2021).

Gentil, E. C., Damgaard, A., Hauschild, M., Finnveden, G., Eriksson, O., Thorneloe, S., et al. (2010). Models for Waste Life Cycle Assessment: Review of Technical Assumptions. *Waste Manage.* 30 (12), 2636–2648. doi:10.1016/j.wasman.2010.06.004

Glitman, K., Farnsworth, D., and Hildermeier, J. (2019). The Role of Electric Vehicles in a Decarbonized Economy: Supporting a Reliable, Affordable and Efficient Electric System. *Electricity J.* 32 (7), 106623. doi:10.1016/j.tej.2019.106623

Goedkoop, M., Ponsioen, T., and Meijer, E. (2014). Introduction to LCA with SimaPro. Available at: https://www.pre-sustainability.com/introduction-to-lca (Accessed December 16, 2020).

Gonzalez-Garay, A., Gonzalez-Miquel, M., and Guillen-Gosalbez, G. (2017). High-Value Propylene Glycol from Low-Value Biodiesel Glycerol: A Techno-Economic and Environmental Assessment under Uncertainty. *ACS Sustain. Chem. Eng.* 5 (7), 5723–5732. doi:10.1021/acssuschemeng.7b00286

Gray, N., McDonagh, S., O'Shea, R., Smyth, B., and Murphy, J. D. (2021). Decarbonising Ships, Planes and Trucks: An Analysis of Suitable Low-Carbon Fuels for the Maritime, Aviation and Haulage Sectors. *Adv. Appl. Energ.* 1 (February), 100008. doi:10.1016/j.adapen.2021.100008

Herrmann, R., Jumbe, C., Bruentrup, M., and Osabuohien, E. (2018). Competition between Biofuel Feedstock and Food Production: Empirical Evidence from Sugarcane Outgrower Settings in Malawi. *Biomass Bioenergy* 114 (July), 100–111. doi:10.1016/j.biombioe.2017.09.002

Huijbregts, M. A. J., Steinmann, Z. J. N., Elshout, P. M. F., Stam, G., Verones, F., Vieira, M., et al. (2017). ReCiPe2016: A Harmonised Life Cycle Impact Assessment Method at Midpoint and Endpoint Level. *Int. J. Life Cycle Assess.* 22 (2), 138–147. doi:10.1007/s11367-016-1246-y

Ilves, R., Küüt, A., and Olt, J. (2019). Ethanol as Internal Combustion Engine Fuel. *Ethanol: Sci. Eng.*, 215–229. doi:10.1016/B978-0-12-811458-2.00008-0

International Renewable Energy Agency (2013). Road Transport: The Cost of Renewable Solutions. IRENA Report, Preliminary Findings. Available at: https://irena.org/-/media/Files/IRENA/Agency/Publication/2013/Road_Transport.pdf. (Accessed February 25, 2020).

ISO (2016). ISO 14040:2006 - Environmental Management — Life Cycle Assessment — Principles and Framework. Available at: https://www.iso.org/standard/37456.html (Accessed March 1, 2021).

Jenkins, S. (2020). Chemical Engineering Plant Cost Index. Chemical Engineering. Available at: https://www.chemengonline.com/pci-home (Accessed April 18, 2021).

Jeswani, H. K., Chilvers, A., and Azapagic, A. (2020). Environmental Sustainability of Biofuels: A Review. *Proc. R. Soc. A* 476, 20200351. doi:10.1098/rspa.2020.0351.

Kannan, P., Al Shoaibi, A., and Srinivasakannan, C. (2014). Temperature Effects on the Yield of Gaseous Olefins from Waste Polyethylene via Flash Pyrolysis. *Energy Fuels* 28 (5), 3363–3366. doi:10.1021/ef500516n

Kavalov, B. (2005). Biofuel potentials in the EU. European Commission, Directorate-General Joint Research Centre, Institute for Prospective Technological Studies (IPTS), EUR 21012 EN. Available at: http://ftp.jrc.es/EURdoc/eur21012en.pdf (Accessed April 18, 2021).

Lopez, G., Artetxe, M., Amutio, M., Bilbao, J., and Olazar, M. (2017). Thermochemical Routes for the Valorization of Waste Polyolefinic Plastics to Produce Fuels and Chemicals. A Review. *Renew. Sustain. Energ. Rev.* 73 (November 2016), 346–368. doi:10.1016/j.rser.2017.01.142

Mangesh, V. L., Padmanabhan, S., Tamizhdurai, P., and Ramesh, A. (2020). Experimental Investigation to Identify the Type of Waste Plastic Pyrolysis Oil Suitable for Conversion to Diesel Engine Fuel. *J. Clean. Prod.* 246, 119066. doi:10.1016/j.jclepro.2019.119066

Miandad, R., Barakat, M. A., Aburiazaiza, A. S., Rehan, M., and Nizami, A. S. (2016). Catalytic Pyrolysis of Plastic Waste: A Review. *Process Saf. Environ. Prot.* 102, 822–838. doi:10.1016/j.psep.2016.06.022

Organisation for Economic Co-operation and Development (2020). OECD Statistics (OECD-FAO Agricultural Outlook 2020-2029 - EU - Biofuels Available at: https://stats.oecd.org/. (Accessed April 22, 2021).

Pacheco-López, A., Somoza-Tornos, A., Muñoz, E., Capón-García, E., Graells, M., and Espuña, A. (2020). Synthesis and Assessment of Waste-To-Resource Routes for Circular Economy. *Computer Aided Chem. Eng.* 48, 1933–1938. doi:10.1016/B978-0-12-823377-1.50323-2

Pahl, G. (2009). Biodiesel: Growing a New Energy Economy. *Choice Reviews Online* Vol. 46, 46-3271. doi:10.5860/choice.46-3271

SABIC (2019). Sustainable Developent Goals Roadmap. Available at: https://www.sabic.com/assets/en/Images/Sustainable-Development-Goals-2019-Roadmap_tcm1010-21094.pdf (Accessed March 1, 2021).

Sharma, S., and Ghoshal, S. K. (2015). Hydrogen the Future Transportation Fuel: From Production to Applications *Renew. Sustain. Energ. Rev.* 43, 1151–1158. doi:10.1016/j.rser.2014.11.093

Singh, R. K., Ruj, B., Sadhukhan, A. K. P., Gupta, P., and Tigga, V. P. (2020). Waste Plastic to Pyrolytic Oil and its Utilization in CI Engine: Performance Analysis and Combustion Characteristics. *Fuel* 262 (November 2019), 116539. doi:10.1016/j.fuel.2019.116539

Singh, T. S., Rajak, U., Dasore, A., Muthukumar, M., and Verma, T. N. (2021). Performance and Ecological Parameters of a Diesel Engine Fueled with Diesel and Plastic Pyrolyzed Oil (PPO) at Variable Working Parameters. *Environ. Tech. Innovation* 22, 101491. doi:10.1016/j.eti.2021.101491

Sinnott, R., and Towler, G. (2020). Costing and Project Evaluation. *Chem. Eng. Des.*, 275–369. doi:10.1016/b978-0-08-102599-4.00006-0

Solomon, S. D., Qin, M., Manning, R. B., Alley, T., Berntsen, N. L., and Bindoff, N. L. (2007). Technical Summary. in *Climate Change 2007: The Physical Science Basis. Contribution of Working Group I to the Fourth Assessment Report of the Intergovernmental Panel on Climate Change*, Cambridge, United Kingdom; New York, NY, USA: Cambridge University Press. Available at: https://www.ipcc.ch/site/assets/uploads/2018/05/ar4_wg1_full_report-1.pdf. (Accessed April 1, 2021)

Somoza-Tornos, A., Gonzalez-Garay, A., Pozo, C., Graells, M., Espuña, A., and Guillén-Gosálbez, G. (2020). Realizing the Potential High Benefits of Circular Economy in the Chemical Industry: Ethylene Monomer Recovery via Polyethylene Pyrolysis. *ACS Sustain. Chem. Eng.* 8 (9), 3561–3572. doi:10.1021/acssuschemeng.9b04835

Somoza-Tornos, A., Pozo, C., Graells, M., Espuña, A., and Puigjaner, L. (2021). Process Screening Framework for the Synthesis of Process Networks from a Circular Economy Perspective. *Resour. Conservation Recycling* 164 (August 2020), 105147. doi:10.1016/j.resconrec.2020.105147

Thangavelu, S. K., Ahmed, A. S., and Ani, F. N. (2016). Review on Bioethanol as Alternative Fuel for Spark Ignition Engines. *Renew. Sustain. Energ. Rev.* 56, 820–835. doi:10.1016/j.rser.2015.11.089

U.S. Energy Information Administration (2019a). Diesel Prices and Outlook. Available at: https://www.eia.gov/energyexplained/diesel-fuel/prices-and-outlook.php (Accessed February 23, 2021).

U.S. Energy Information Administration (2019b). Factors Affecting Gasoline Prices. Available at: https://www.eia.gov/energyexplained/gasoline/factors-affecting-gasoline-prices.php (Accessed February 23, 2021).

Wernet, G., Bauer, C., Steubing, B., Reinhard, J., Moreno-Ruiz, E., and Weidema, B. (2016). The Ecoinvent Database Version 3 (Part I): Overview and Methodology. *Int. J. Life Cycle Assess.* 21 (9), 1218–1230. doi:10.1007/s11367-016-1087-8

Wong, S. L., Ngadi, N., Abdullah, T. A. T., and Inuwa, I. M. (2015). Current State and Future Prospects of Plastic Waste as Source of Fuel: A Review. *Renew. Sustain. Energ. Rev.* 50, 1167–1180. doi:10.1016/j.rser.2015.04.063

Conflict of Interest: The authors declare that the research was conducted in the absence of any commercial or financial relationships that could be construed as a potential conflict of interest.

frontiers
in Energy Research

ORIGINAL RESEARCH
published: 23 July 2021
doi: 10.3389/fenrg.2021.690725

Life Cycle Assessment of Green Diesel Production by Hydrodeoxygenation of Palm Oil

Antonio Arguelles-Arguelles[1], *Myriam Adela Amezcua-Allieri*[2]* and
Luis Felipe Ramírez-Verduzco[2]*

[1]Posgraduate Department, Mexican Institute of Petroleum, Mexico City, Mexico, [2]Biomass Conversion Divison, Research Direction of Hydrocarbon Conversion, Mexican Institute of Petroleum, Mexico City, Mexico

Transition to a new energy low carbon pool requires the gradual replacing of fossil fuels with other cleaner energies and biofuels. In this work, the environmental impact of renewable diesel production using an attributional life cycle assessment was evaluated by considering five stages: palm plantation-culture-harvest, palm oil extraction, palm oil refining, green (renewable) diesel production, and biofuel use. The functional unit was established as 1.6×10^{-2} m^3 (13.13 kg) of renewable diesel. The results show that the production of renewable diesel by Hydro-processed Esters and Fatty Acids is more environmentally friendly than fossil diesel production. In particular, the analysis showed that the CO_2 emission decreases around 110% (i.e. mitigation occurred) compared with conventional diesel production. However, renewable diesel production has a relevant environmental impact in the human toxicity category due to the high consumption of agrochemicals during palm culture.

Keywords: environmental impact, green diesel, palm oil, life cycle (impact) assessment, biofuel

OPEN ACCESS

Edited by:
Luis Puigjaner,
Universitat Politecnica de Catalunya,
Spain

Reviewed by:
Murugesan Arthanarisamy,
KSR college of Technology, India
Mariano Martín,
University of Salamanca, Spain

Correspondence:
Luis Felipe Ramírez-Verduzco
lframir@imp.mx
Myriam Adela Amezcua-Allieri
mamezcua@imp.mx

Specialty section:
This article was submitted to
Process and Energy Systems
Engineering,
a section of the journal
Frontiers in Energy Research

Received: *04 April 2021*
Accepted: *28 May 2021*
Published: *23 July 2021*

Citation:
Arguelles-Arguelles A,
Amezcua-Allieri MA and
Ramírez-Verduzco LF (2021) Life Cycle
Assessment of Green Diesel
Production by Hydrodeoxygenation of
Palm Oil.
Front. Energy Res. 9:690725.
doi: 10.3389/fenrg.2021.690725

INTRODUCTION

The severe environmental problems related to the greenhouse effect and global warming have instigated a search for new and alternative energy sources to reduce the use of fuels derived from petroleum. One alternative is the use of biofuels, which are environmentally friendly (Guo et al., 2015). However, reliable tools are required to determine how friendly biofuels are for the environment. Life Cycle Assessment (LCA) is a methodology commonly used to evaluate the effect on the environment caused by industrial processes and services, from acquisition, manufacture, use, and maintenance of the raw material, until the final disposal of the product or service. Thus, LCA is one suitable tool for environmental decision-making (Curran, 2006).

Researchers have reported several LCA studies for biofuels in the last decades (Sampattagul et al., 2009; Ashnani et al., 2014; Piemonte et al., 2014; Uctug et al., 2017; Fortes et al., 2018; Parajuli et al., 2018; Tabatabaei et al., 2019; Chiriboga et al., 2020; Fridrihsone et al., 2020), showing environmental benefits because it can help moderate the impact of global warming and reduce dependence on fossil fuels. Parajuli et al. (Parajuli et al., 2018) described LCA within a biorefinery context, identifying that

---

Abbreviations: DCB, Dichlorobenzene; FFB, Fresh Fruit Bunches; FU, Functional Unit; GHG, Greenhouse Gas; ha, Hectare; HEFA, Hydro-processed Esters and Fatty Acids; LCA, Life Cycle Assessment; R11, Trichloromethane; RD, Renewable Diesel; T, Ton; ULSD, Ultra-Low Sulfur Diesel.

the main effects of the system integration were in the reduction of Greenhouse Gas (GHG) emissions, fossil fuel consumption, eutrophication potential, and freshwater ecotoxicity, compared to a conventional mixed crop-livestock system, without the biogas conversion facility and the green biorefinery. However, it is necessary to move towards the large-scale replacement of conventional energy resources with renewable ones to turn to the circular economy model. Although some studies have claimed carbon neutrality, further studies assessing the environmental impact from cradle-to-grave are required to precisely determine the potential of any renewable fuel to absorb CO_2.

The increase in "clean fuel" production focuses on mitigating pollutants from vehicle exhaust in response to the problems of petroleum-derived fuels. Biodiesel and renewable diesel (RD) are two biofuels that have been the subject of interest in recent years as potential substitutes for diesel fuel. Both biofuels use the same raw material (vegetable oils or animal fats). However, they have different chemical properties because their production occurs in different ways.

Biodiesel is a mixture of Fatty Acid Alkyl Esters (FAAEs). Biodiesel can be produced through the transesterification reaction between triacylglycerides and some alcohol (Peiró et al., 2010; Nanaki and Koroneos, 2012; Escobar et al., 2014; Carneiro et al., 2017; Fernandez et al., 2017; Alagumalai et al., 2020; Chamkalani et al., 2020; Seela et al., 2020; Jacob et al., 2021; Mukhopadhyay and Chakraborty, 2021). On the other hand, RD is a mixture of oxygen-free hydrocarbons, mainly alkanes, commonly being obtained by hydrotreating (Kalnes et al., 2007; Sotelo-Boyas et al., 2011; Ramírez-Verduzco and Hernández-Sánchez, 2020).

RD offers advantages over biodiesel. RD has a higher energy density and heating value than biodiesel because of the lack of oxygen atoms. RD also has a higher cetane number (~70) than biodiesel (~50). RD has storage stability and is compatible with petroleum diesel at any concentration (Kalnes et al., 2007; Sotelo-Boyas et al., 2011; Ramírez-Verduzco and Hernández-Sánchez, 2020). In addition, GHG emissions from RD are more than 80% lower than petroleum diesel and about 40% less than biodiesel (Kalnes et al., 2007). However, RD has two main disadvantages. First, the RD has poor cold flow properties [*v.g.* cloud point of 291.15 K (Ramírez-Verduzco and Hernández-Sánchez, 2020)], causing the formation of solids and deposits into the engines, especially in cold weather or winter seasons (Soo-Young, 2014; Kumar et al., 2018; Douvartzides et al., 2019). Secondly, RD reactions consume a significant amount of hydrogen (Sotelo-Boyas et al., 2011; Ramírez-Verduzco and Hernández-Sánchez, 2020).

Biofuels have to meet the regulatory requirements that guarantee quality and performance according to standards. Currently, the RD is still under research and development. RD has the inconvenience of flow cold properties, an aspect that needs to be improved. The best way to use this biofuel is by mixing it with ultra-low sulfur diesel (ULSD), which has a fossil origin.

In recent years hydrotreating has become a more common way to produce RD, known as Hydro-processed Esters and Fatty Acids (HEFA). This process involves decarboxylation, decarbonylation, and deoxygenation reactions (Kalnes et al., 2007; Sotelo-Boyas et al., 2011; Ramírez-Verduzco and Hernández-Sánchez, 2020). Some companies have been producing and commercializing RD. Such as Neste Oil, Petrobras, SK-Innovation, and UOP/Eni, through catalytic processes to carry out the hydrodeoxygenation of triacylglycerides.

Although efforts have been made to study the LCA of biodiesel (Peiró et al., 2010; Nanaki and Koroneos, 2012; Sandoval et al., 2014; Carneiro et al., 2017; Fernandez et al., 2017; Chamkalani et al., 2020; Mukhopadhyay and Chakraborty, 2021), according to the best of our knowledge, there are no LCA studies for RD production through palm oil hydrotreating. Considering that the production of biofuels is accompanied by their LCA is of vital importance to estimate emissions, this research postulates that it is possible to mitigate GHG emissions during the production and use of RD.

This study examines the environmental impact associated with the production and use of RD through LCA, a subject that is of interest to stakeholders from the petroleum industry, and other companies and researchers looking for green alternatives.

MATERIALS AND METHODS

An attributional LCA from cradle-to-grave of RD production and use in Mexico was performed according to ISO 14040 (ISO 14040, 2006) and ISO 14044 (ISO 14044, 2006), collecting the necessary input information from various sources such as companies, the administration of the Mexican government, and research centers (Kalnes et al., 2007; Mendez, 2010; Sandoval, 2011; Sandoval-Esquivez, 2011; Neste Oil Company, 2013; Nucci et al., 2014; Mesa and Piñeros, 2018; Sun et al., 2018). This information was requested and collected for all stages involved during the life cycle of RD (**Figure 1**).

Functional Unit

A functional unit (FU) of $1.6 \times 10^{-2}\,m^3$ (13.13 kg) of RD was established based on the average production of African palm per hectare in Mexico (13.39 T/ha) (Ornelas-Ruiz-, 2021), considering that in each hectare planted, there is an average of 143 palm plants. Therefore, FU derives from the production of one of the 143 plants/ha.

System Boundaries

LCA boundaries were established from cradle-to-grave. The five stages selected were palm plantation-culture-harvest, palm oil extraction, palm oil refining, hydrodeoxygenation of refined palm oil, and RD production and use (**Figure 1**). The geographical area for the RD life cycle process was located at Veracruz state (for palm plantation-culture-harvest to palm oil extraction) and Mexico City (for palm refining and RD production). The environmental impact of infrastructure for every production stage was excluded in this work (Hernández, 2010).

FIGURE 1 | Stages included in LCA of RD obtained by HEFA process.

TABLE 1 | Life cycle inventory.

Stage	Inputs	Input value (g)	Outputs	Output value (g)	Energy (KW)	Water use (m^3)
Culture	Fertilizers	9,018.9	FFB	93,630	2.8	378.108
	Pesticides	345	—	—	—	—
Palm oil extraction	FFB	93,630	Palm oil	18,726	Vapor	0.0936
			Sludge	56,178	39.9	
			Empty clusters and husk	27,152	—	
			Palmist oil	1778	Electricity	
			Palm fiber	12,171	2.3	
Palm oil refining	Palm oil	18,726	Refined palm oil	15,916	—	0.0041
			Free fatty acid	620	Vapor	
	Phosphoric acid	17.9			0.16	
			Clay	1740	—	
			Shell trace	291	Electricity	
	Bentonite	883			1.4	
			Gums	589	—	
HEFA	Refined palm oil	15,916	RD	13,130	Vapor	0.0068
			Water	1,133	0.2	
			Propane	818	—	
	Hydrogen	337	CO_2	849	Electricity	
			CO	276	1.4	

Assumptions

In this work, various assumptions have been established to simplify the LCA. Due to a lack of information, the energy required to distribute water on the culture stage was not considered. For fresh fruit bunches (FFB), we based calculations on the supposition that they were transported by tractors (with up to 8T of capacity) from plantations to the extraction plant. This would involve articulated truck (Euro 0–4 type) transport of crude palm oil with 27 T of capacity. The land-use change for palm plantations was not considered. A complete conversion of the biofuel hydrocarbon content into CO2 during combustion was assumed. Mass allocation methods for the assignment of co-product impacts were used. A scenario with data obtained from companies, Mexican government administration, or research centers was assumed. The location of the palm culture was presumed in Texistepec, Veracruz State. The origin of the palm oil was presumed to come from FFB, performing its extraction in the plant known as Aceites de Palma SA de CV, which has industrial facilities and high capacity in Mexico, located at Acayucan (Veracruz State), 13.3 km away from the Texistepec. The palm refining and RD production was considered to occur in Mexico City. Pollutants from vehicle exhaust were assumed to be equal for RD and ULSD. The H_2 was presumed to come from the catalytic reforming process of a Mexican refinery, considering those with excess H_2 capacity.

Life Cycle Inventory

Inputs (resources necessary for production) and outputs (products, co-products, emissions, and waste) were identified and quantified (**Table 1**) (Kalnes et al., 2007; Sandoval, 2011; Mendez, 2019; Sandoval-Esquivez, 2011; Neste Oil Company, 2013; Nucci et al., 2014; Mesa and Piñeros, 2018; Sun et al., 2018).

Impact Categories

The impact categories selected for the LCA that were simulated in this work are: global warming, acidification, eutrophication, ozone layer depletion, photochemical smog, and human toxicity. Those categories were selected based on their importance in terms of C fingerprint and GHG and previous reports of biofuels, and comparing them with fossil diesel and other biofuels.

Software

The LCA of RD was simulated in the CCalC2 software (V1.1) developed by the University of Manchester, which was selected due to its vast database and its user-friendly accessibility. Two

TABLE 2 | Blue and green water use.

Water use	Stage	Blue water (m^3/FU)	Green water (m^3/FU)
Agricultural	Planting and harvesting	108.57	269.43
Agricultural	Nursery	0.102	0
Agricultural	Pre-nursery	0.006	0
Process	Palm oil refining	0.0041	0
Process	Green diesel production	0.0068	0
Process	Palm oil extraction	0.0936	0
Total	LCA for RD	108.78 m^3	269.43 m^3

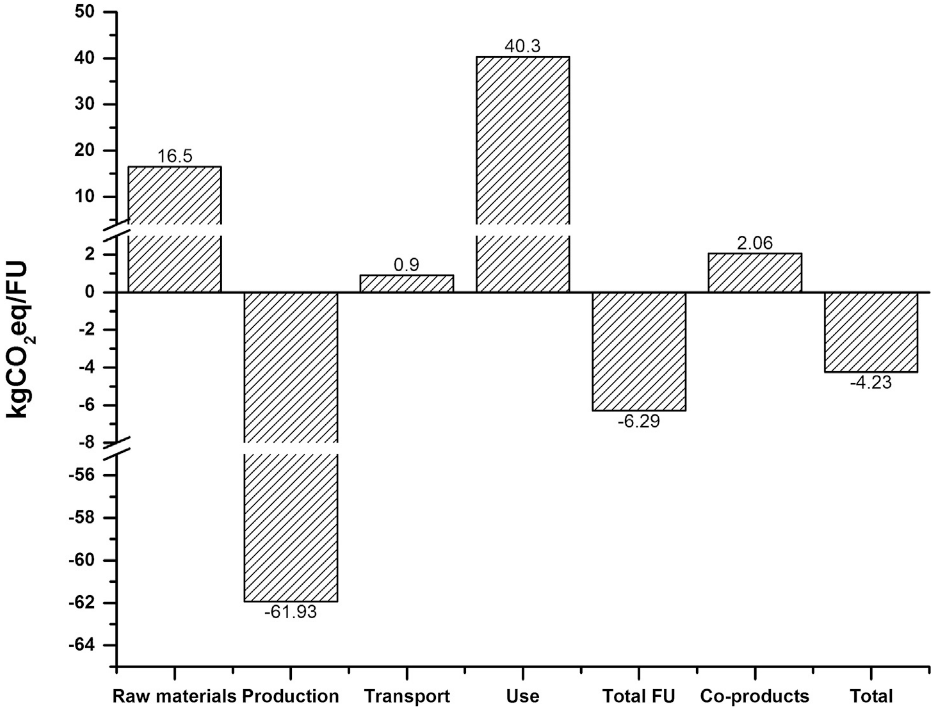

FIGURE 2 | Carbon footprint.

simulation runs of the LCA with bioethanol as a standard before addressing the RD were used to ensure the consistency and coherence of results with data reported in the literature (Mortimer et al., 2004).

RESULTS AND DISCUSSION

This section contains the main results found in this work for the environmental impact categories, comparing RD and RD-ULSD blend respect fossil diesel and other biofuels. It also describes the sensitivity analysis and alternative scenario proposals to improve the base case.

Before addressing the RD, the LCA of bioethanol was simulated from two different sources, sugar beet and wheat. GHG emissions of 43.9 and 49.1 gCO_2 eq./MJ were obtained with the CCaLC2 software, respectively. Those values were close to the 39± 3 and 44± 3 gCO_2 eq./MJ reported by Mortimer et al. (2004).

In terms of RD, our simulation shows that the water needed to produce 1.6×10^{-2} m^3 of RD in Mexico was 378.2 m^3 (**Table 2**), using more than 99% of this water for agriculture in the palm plantation and 0.1045 m^3 during the processing of the palm fruit until obtaining the RD.

Palm culture has high water requirements for good development, more than 150 mm per month. The water footprint measured with the Pfister method (40) is 82.2 m^3, derived from the multiplication of the total blue water used in the life cycle by the corresponding water stress index for each country. Palm culture has high water requirements for good development, more than 150 mm per month.

The water footprint for RD production is equivalent to 0.142 m^3/MJ, a relevant impact compared with other biofuels. For example, some studies performed in the United States have shown that the water footprint of rapeseed biodiesel and beet bioethanol is 6×10^{-2} and 2×10^{-2} m^3/MJ, respectively (Gerbens-Leenes and Hoekstra, 2010).

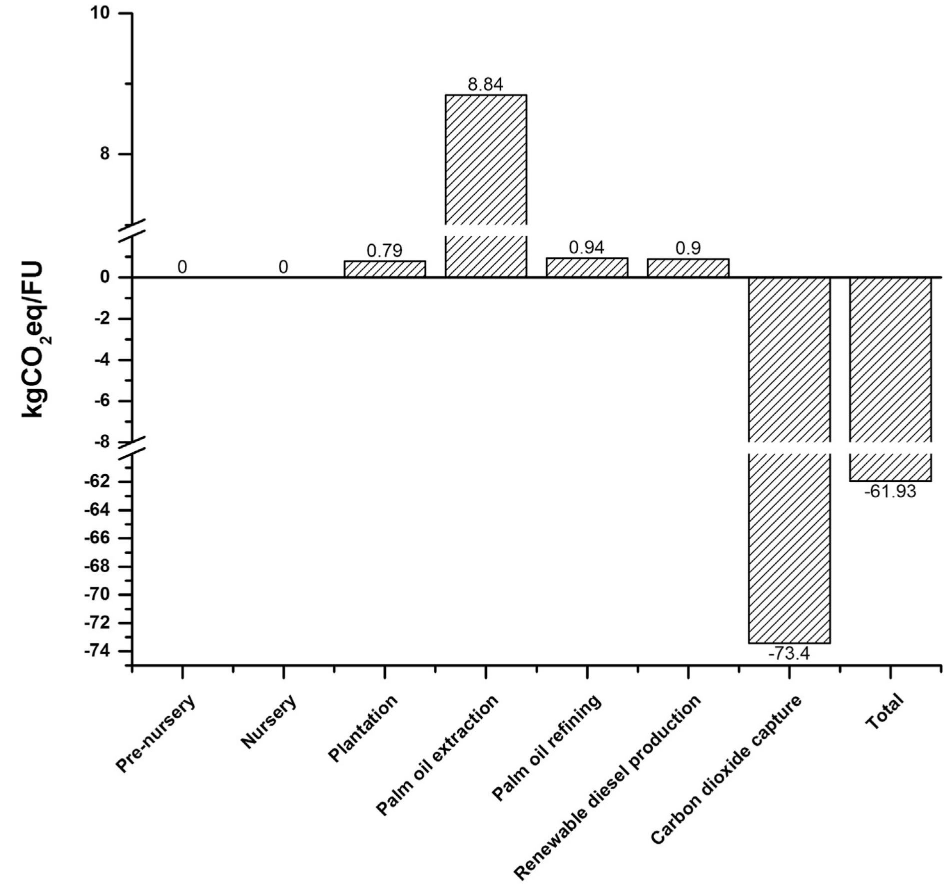

FIGURE 3 | Carbon footprint for the production stages.

Environmental Impacts of RD Production

Regarding global warming, **Figure 2** shows the carbon footprint. The highest emissions are mainly due to fuel combustion and palm oil processing. The last category includes everything necessary to obtain each material in the system, such as extraction/production, energy, and emissions, among others.

Within the production process shown in **Figure 3**, the stage with the highest generation of emissions is palm oil extraction, caused by the large amount of energy used in the production of steam required for the palm fruit treatment.

There is a total emission of −4.23 kg of CO_2, which corresponds to −7.32 gCO_2eq/MJ for RD production. 108.3% of reduction in CO_2/FU was obtained when our results are compared with the average emissions from extraction and use of fossil diesel (87.54 gCO_2eq/MJ) (Eriksson and Ahlgren, 2013).

The acidification potential for RD production is 229 gSO_2eq/FU (**Figure 4**). Considering that biofuel has zero sulfur content, it does not generate SO_2 emissions during its use. The emissions of this impact (17.4%) occur during the production of the required energy for oil extraction, refining, and RD production. The rest of the emissions are mainly related to palm culture supplies, like the triple superphosphate, which contributes to 128 gSO_2eq/FU).

Regarding eutrophication, Palm culture requires large amounts of fertilizers, mainly phosphorus-, and nitrogen-based, which are used at least twice a year during plantation, increasing the amounts of fertilizer in the last years of palm life when the production curve decreases. The phosphate equivalent emissions generated in the RD production are mostly (>95%) derived from the use of fertilizers during the culture stage within the production chain (**Figure 4**).

Concerning ozone layer depletion, the amount of trichlorofluoromethane (R11) emitted is 1.75 mg in the production of 1.6×10^{-2} m^3 of RD (**Figure 4**). At least 95% of the ozone layer depletion potential is related to the procurement/production of raw materials, while the remainder is related to energy production and transportation.

Regarding photochemical smog, the RD production causes 12.1 g of ethene eq (**Figure 4**). 27.5% of the emissions come from the generation of energy (electricity and steam) used in the production stages (oil extraction, oil refining, and oil conversion by the HEFA process). 69.4% of emissions occur during raw material production. Triple superphosphate is the principal cause for 42.3% of the emissions in the photochemical smog category.

Human toxicity is the most significant impact evaluated in RD production, reaching 36.8 kg of Dichlorobenzene (DCB) eq (**Figure 4**). Palm production (pre-nursery, nursery, and culture) generates around 54.5% emissions of the total due to

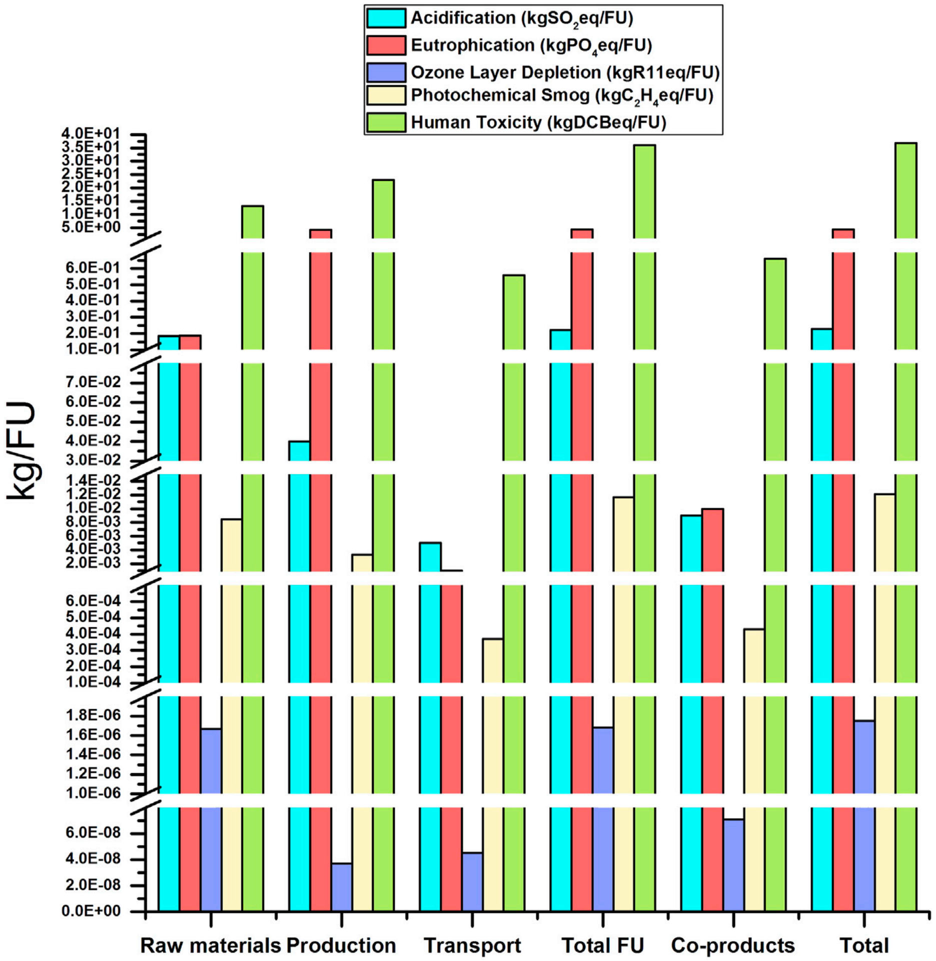

FIGURE 4 | Emissions on each impact category.

TABLE 3 | Emissions in the impact categories.

Impact category	Units	Diesel[a]	B100	ME50	RD
Global warming	gCO$_2$eq/MJ	79.93	61.35	68.56	−7.32
Acidification	gSO$_2$eq/MJ	0.547	0.7	0.476	0.396
Eutrophication	gPO$_4$eq/MJ	0.127	1.78	0.331	7.67
Ozone layer depletion	mgCFC-11eq/MJ	0.012	0.006	0.007	0.003
Photochemical smog	gC$_2$H$_4$eq/MJ	0.033	—	—	0.021
Human toxicity	g1,4-DCBeq/MJ	7.37	64.11	9.63	63.67

[a] *Data from Ecoinvent 2.1.*

the use of pesticides, insecticides, and herbicides during the culture stage, such as carbofuran, glyphosate, benomyl, and mainly methyl bromide.

The oil extraction, oil refining, and RD production process contribute 8% of the total emissions. This impact mainly comes from the generation of energy necessary in the above three stages.

Obtaining raw materials is of particular note, accounting for 35.9% of total emissions. The fertilizers generate a relevant environmental impact in which triple superphosphate is again the pollutant source that contributes the most to human toxicity potential.

Comparison of the Environmental Impact of RD Production and Use With Biodiesel and Fossil Diesel

RD presents a notable decrease to conventional diesel in global warming, ozone layer depletion, photochemical smog, 109.1, 75, and 36.4% (**Table 3**). It also exhibits a competitive environmental advantage regarding the other two biofuels, biodiesel at 100% (B100), and RD by microemulsion at 50% of mixture in volume (ME50) (Arpornpong et al., 2015).

Regarding acidification potential, RD has about a 27.6% reduction in emissions than conventional diesel. RD has a minor impact compared to ME50 (a second-generation biofuel) and B100 in this category.

For the eutrophication and human toxicity potential categories, RD has a significant environmental impact, about 60 and 8.6 times more than conventional diesel, respectively.

TABLE 4 | Effect of use of RD-ULSD blend on emissions.

Impact category	Units	Blend at 25% of RD and 75% of ULSD in volume
Global warming	gCO_2eq/MJ	63.83
Acidification	gSO_2eq/MJ	0.51
Eutrophication	gPO_4eq/MJ	2.01
Ozone layer depletion	mgR11eq/MJ	0.01
Photochemical smog	gC_2H_4/MJ	0.03
Human toxicity	g1,4-DCBeq/MJ	21.44

Environmental impact in eutrophication principally occurs in the plantation-culture-harvest stage.

The use of inorganic fertilizers, such as triple superphosphate during palm culture, represents a common practice in Mexico. This practice significantly increases eutrophication. Additionally, the use of herbicides and pesticides in Mexico has generated toxicity problems, such as respiratory diseases in people and contamination of aquifers and soil.

Other substances that are also harmful to health and are highly toxic include methyl bromide and carbofuran, which are commonly used as agrochemicals during palm culture by farmers in Mexico.

Emissions Derived From the RD-ULSD Blend

For this study, the chemical and yield characteristics of an RD synthesized by HEFA were considered, the details of this process are reported in previous work (Ramírez-Verduzco and Hernández-Sánchez, 2020) and described briefly below.

RD was produced in a reactor using a NiMo/γ-Al_2O_3 catalyst at the following operating conditions, such as temperature, pressure, liquid hourly space velocity (LHSV), and H_2/oil ratio equal to 613 K, 4,903 kPa, 1.0 h^{-1}, and 935 std. m^3/m^3 respectively. For the LCA, the use of H_2 was assumed to come from the catalytic reforming process of a Mexican refinery, considering those with excess H_2 capacity.

The HEFA process consists of two reaction steps. First, the obtention of diglycerides occurs, including monoglycerides, carboxylic acids, and propane. This happens through the hydrogenation of double bonds and C-O bond cleavage. Second, carboxylic acids convert into final products through three parallel reactions (deoxygenation, decarboxylation, and decarbonylation). The products are alkanes water, CO_2, and CO.

Although RD obtained by HEFA met most of the chemical and physical characteristics required by the Mexican standard for diesel (Official Mexican Standard NOM-016-CRE-2016), the RD did not meet the regulatory requirement for low-temperature flow properties (pour and cloud points). The Mexican standard for the pour point from March to October requires a maximum of 273 K, while from November to February, a maximum of 268 K. The cloud point depends on the temperature conditions for proper diesel distribution. However, Mexico's average lowest temperature is around 272.4 K. Our experimental measurements for the pour and cloud points were 288 and 291 K, respectively. Therefore, we do not recommend the direct use of RD in engines for cold regions. Instead, we propose mixing RD with ULSD (<10 ppm S). We performed a study on the establishment of the adequate mixing percentage and use this mixture to complement our LCA and ensure proper engine operation. We obtained a mixture that ensures regulatory compliance for the flow properties at low temperature is 25 and 75% by volume of RD and ULSD, respectively. Because this mixture had a pour point of 267.4 K and a cloud point of 269.3 K, those values comply satisfactorily with the Mexican standard. Then we estimated the environmental impact for the blend by simulating the LCA (**Table 4**). According to our study, a mixture of RD with Mexican ULSD would reduce GHG emissions by 27% over single fossil diesel. However, the blend increases the impact in eutrophication (~16 times) and human toxicity (~3 times) more than single fossil diesel.

Sensitivity Analysis

Through sensitivity analysis, we used inputs with uncertainty to verify the variability of the results in stages or specific data and detect ranges for which the simulated information is or not the desired outcome (Curran, 2015).

We performed the sensitivity analysis by considering four parameters, energy use, palm harvest efficiency, oil refining yield, and HEFA yield. **Table 5** shows the results of this analysis. The simulations carried out with a 20% variation in energy use show that, except for the eutrophication potential (which remains constant), all categories are affected to a greater or lesser extent as the amount of energy used decreases, the different impacts also decrease. The simulations carried out with a 20% variation in the oil palm harvest efficiency reveal that as efficiency increases, emissions also increase in the global warming category and emissions decrease for the other categories of environmental impact. The simulations carried out with a 10% variation in the oil refining yield reveal that as it increases, the environmental impact on the global warming category also increases, while the rest decrease. The simulations carried out with a 10% variation in the HEFA yield reveal that as it is higher, the environmental impact on the global warming category also increases, while the rest decrease.

From the above, we notice an advantage of renewable energy use in the life cycle through sensitivity analysis. In contrast, generating power by burning fossil fuels is not a recommended option since it increases emissions in five impact categories. Only emissions in the eutrophication category remain constant.

The sensitivity analysis also indicates that the plantation efficiency and production yields (mainly in palm oil refining and the HEFA process) could modify the impact depending on

TABLE 5 | Effect of production parameters on emissions.

Impact category	Energy use (–/+ 20%)	Palm efficiency (–/+ 20%)	Oil refining yield (–/+ 10%)	HEFA yield (–/+ 10%)
Global warming (gCO_2eq/MJ)	−12.1–−1.8	−1.3–9.8	−16.8–0.1	−16–-0.37
Acidification (gSO_2eq/MJ)	0.38–0.42	0.35–0.47	0.36–0.44	0.36–0.44
Eutrophication (gPO_4eq/MJ)	7.7	6.4–9.6	6.9–8.5	6.9–8.5
Ozone layer depletion (mgR11eq/MJ)	2.9×10^{-3}—3.2×10^{-3}	2.6×10^{-3} –3.6×10^{-3}	2.7×10^{-3}—3.3×10^{-3}	2.7×10^{-3}—3.3×10^{-3}
Photochemical smog (gC_2H_4eq/MJ)	1.9×10^{-2}–2.2×10^{-2}	1.9×10^{-2}–2.4×10^{-2}	1.9×10^{-2}—2.3×10^{-2}	1.9×10^{-2}—2.3×10^{-2}
Human toxicity (g1,4-DCBeq/MJ)	62.7–65.5	54.3–77.9	58.1–70.6	57.9–70.8

the situation. As an illustration, if we could get better efficiency and production yields, the environmental impact will decrease in five out of the six categories (excluding global warming having an inverse behavior). Taking this into account, changes in cultivation practices are relevant, to achieve more palm fruit per hectare and improve the refining palm oil and HEFA process, enabling a higher yield during both stages.

Alternative Scenarios as Better Practices

The goal for the alternative scenarios is to identify opportunity areas in the value chain of RD production. This indicates how to achieve a reduction in environmental impact in the life cycle by modifying the base scenario and the results of the improvement proposals are described here.

The substitution of conventional pesticides by biopesticides contributes to having a notorious reduction of the emissions concerning the baseline scenario. The emissions decreased 60 and 10% in the categories of human toxicity and ozone layer depletion. While for global warming, photochemical smog and acidification decreased 5%. In terms of the change of location, we propose an alternate scenario where the palm plantation and oil extraction were in Acapetahua, Chiapas. This location has ideal weather for palm production. It also has an oil extraction plant of the company OLEO SUR located in the state of Chiapas as the principal palm producer in Mexico. Oil refining occurs in the same company as the extraction in Coatzacoalcos-Veracruz. The RD production is now in Minatitlán, Veracruz. The results show that the change of location between the stages of the process generates a slight increase in global warming, acidification, human toxicity, and the rest of the categories remain constant. This is because the transport of inputs and by-products is higher. For the mature plantation, the LCA of RD has an environmental impact generated from palm culture until RD production.

The palm begins to produce fruit about two years after sowing. This simulation represents the emissions generated for a mature plantation, not considering the environmental impact of pre-nursery and nursery. It is worth mentioning that the plantation palm is mature about six years after transplanting palm. Mature crops reduce the potential for emissions in all the categories evaluated, highlighting 66.6% in water footprint and 21.5% in human toxicity. In the case of the CO_2 capture, we assume that the carbon emitted by RD combustion comes from biomass, which captures CO_2 for the biomass itself, therefore, global warming is the only modified category. Although it increases considerably in the baseline scenario, it presents a reduction of 42.7% compared to fossil diesel.

CONCLUSION

Considering that the production of biofuels accompanied by their LCA is of vital importance to reduce emissions, this research demonstrated that it is possible to mitigate the amount of GHG emissions during the production and use of RD.

The LCA of RD demonstrated that biofuel significantly reduces GHG emissions than its fossil counterpart by about 110%.

RD production has lower emissions than conventional diesel. There is a low environmental impact in terms of acidification, ozone layer depletion, and photochemical smog. In both cases, there was a high impact on human toxicity and eutrophication.

Palm culture has high water requirements for good development, more than 150 mm per month, causing a higher water footprint than other biofuels.

RD has poor cold flow properties (pour and cloud point), making it difficult to use in cold regions. It is, therefore, necessary to mix it with ULSD to comply with fuel quality regulations. An adequate mixing percentage may vary depending on the average ambient temperature conditions and standards.

Raw material obtention has a higher environmental impact, mainly due to fertilizers and hydrogen. Selecting adequate supplies is relevant to reduce environmental impact.

Fossil fuels account for 80% of energy use, which affects every category evaluated. We recommend the use of renewable energy to reduce impact during RD production.

The efficiency of palm plantations is a factor that considerably affects the impact potentials. Soil studies, modification of fertilization techniques, and replacement of agrochemicals with bioproducts are some methods of improving plantation performance and significantly reducing environmental impact.

The environmental impact caused by RD production is higher in the first years of palm culture, decreasing at the mature culture stage.

RD could be a sustainable option to reduce the use of conventional fossil diesel. However, our study has limitations imposed by the technology used in Mexico for the plantation-culture-harvest of palm and the maturity level of the RD production technology.

RD production technologies are still in development, being less mature than diesel hydrodesulfurization processes in terms of producing fossil diesel. Therefore, future work should focus on monitoring the evolution of RD production technology through LCA studies. Some examples of technological challenges are the following: Research for ecological agriculture, biopesticides, and bio-stimulants. The development of new active catalysts will allow for the use of less severe operating conditions for the RD production process. Use renewable sources for the energy production and H_2 required in the RD production process, and it is necessary to ensure optimal use of by-products and waste such as light gases, CO_2, and CO.

DATA AVAILABILITY STATEMENT

The original contributions presented in the study are included in the article/Supplementary Material, further inquiries can be directed to the corresponding authors.

AUTHOR CONTRIBUTIONS

AA-A collected the inventory data and performed the LCA simulation. LR-V translated and edited the document and made graphics of figures 2–4 with the Origin software, reviewed results of HEFA process. MA-A conceptualized and supervised the work, reviewed the results of LCA and reviewed and edited the document.

FUNDING

CONACyT and Energy Secretary financed the research through CEMIE-Bio. AA-A received a scholarship from CONACyT for post-graduate studies.

ACKNOWLEDGMENTS

We carried out this work as part of the Y.61023 project Clúster CEMIE-Bio Bioturbosina. The authors thank the Instituto Mexicano del Petróleo for making the conclusion of this work possible. AA-A acknowledges an M. Sc. Scholarship from CONACyT.

REFERENCES

Alagumalai, A., Mathimani, T., Pugazhendhi, A., Atabani, A. E., Brindhadevi, K., and Duc Canh, N. (2020). Experimental Insight into Co-combustion Characteristics of Oxygenated Biofuels in Modified DICI Engine. *Fuel* 278, 118303. doi:10.1016/j.fuel.2020.118303

Arpornpong, N., Sabatini, D. A., Khaodhiar, S., and Charoensaeng, A. (2015). Life Cycle Assessment of palm Oil Microemulsion-Based Biofuel. *Int. J. Life Cycle Assess.* 20, 913–926. doi:10.1007/s11367-015-0888-5

Ashnani, M. H. M., Johari, A., Hashim, H., and has ani, E. (2014). Life Cycle Assessment of palm Oil Biodiesel Production in Malaysia. *Appl. Mechanic. Mater.* 465-466, 1080–1108. doi:10.4028/www.scientific.net/AMM.465-466.1080

Carneiro, M. L. N. M., Pradelle, F., Braga, S. L., Gomes, M. S. P., Martins, A. R. F. A., Turkovics, F., et al. (2017). Potential of Biofuels from Algae: Comparison with Fossil Fuels, Ethanol and Biodiesel in Europe and Brazil through Life Cycle Assessment (LCA). *Renew. Sustain. Energ. Rev.* 73, 632–653. doi:10.1016/j.rser.2017.01.152

Chamkalani, A., Zendehboudi, S., Rezaei, N., and Hawboldt, K. (2020). A Critical Review on Life Cycle Analysis of Algae Biodiesel: Current Challenges and Future Prospects. *Renew. Sustain. Energ. Rev.* 134, 110143. doi:10.1016/j.rser.2020.110143

Chiriboga, G., De La Rosa, A., Molina, C., Velarde, S., and Carvajal, G. (2020). Energy Return on Investment (EROI) and Life Cycle Analysis (LCA) of Biofuels in Ecuador. *Heliyon* 6, 1–11. doi:10.1016/j.heliyon.2020.e04213

Curran, M. A. (2006). *Data from: Scientific Applications International Corporation. Life Cycle Assessment: Principles and Practice.* Cincinnati, OH: U.S. Environmental Protection Agency. (EPA), EPA/600/R-06/060. Available at: https://cfpub.epa.gov/si/si_public_record_report.cfm?Lab=NRMRL&dirEntryId=155087

Curran, M. A. (2015). *Life Cycle Assessment Student Handbook. A Guide for Environmentally Sustainable Products*. USA: HardcoverScrivener Publishing LLC. John Wiley & Sons.

Neste Oil Company (2013). Data from: NExBTL Renewable Diesel Singapore Plant, Technical Report. Singapore: Neste Proprietary Publication. Available at: https://www.neste.com/about-neste (Accessed December 12, 2020).

Douvartzides, S. L., Charisiou, N. D., Papageridis, K. N., and Goula, M. A. (2019). Green Diesel: Biomass Feedstocks, Production Technologies, Catalytic Research, Fuel Properties and Performance in Compression Ignition Internal Combustion Engines. *Energies* 809, 1–42. doi:10.3390/en12050809

Eriksson, M., and Ahlgren, S. (2013). Data from: LCAs of Petrol and Diesel, Institutionen for Energi Och Teknik. Southampton: Swedish University of Agricultural Sciences. Available at: https://pub.epsilon.slu.se/10424/17/ahlgren_s_and_eriksson_m_130529.pdf (Accessed December 12, 2020).

Escobar, N., Ribal, J., Clemente, G., and Sanjuán, N. (2014). Consequential LCA of Two Alternative Systems for Biodiesel Consumption in Spain, Considering Uncertainty. *J. Clean. Prod.* 79, 61–73. doi:10.1016/j.jclepro.2014.05.065

Fernandez, I. A. P., Liu, D. H., and Zhao, J. (2017). LCA Studies Comparing Alkaline and Immobilized Enzyme Catalyst Processes for Biodiesel Production under Brazilian Conditions. *Resour. Conserv. Recy.* 119, 117–127. doi:10.1016/j.resconrec.2016.05.009

Fortes, S., Costa, M., Queiroz, L., and Jacob-Lopes, E. (2018). Life Cycle Assessment (LCA) of Third-Generation Biodiesel Produced Heterotrophically by *Phormidium Autumnale*. *Open Biotech. J.* 12, 270–281. doi:10.2174/1874070701812010270

Fridrihsone, A., Romagnoli, F., and Cabulis, U. (2020). Environmental Life Cycle Assessment of Rapeseed and Rapeseed Oil Produced in Northern Europe: A Latvian Case Study. *Sustain* 12, 1–21. doi:10.3390/su12145699

Gerbens-Leenes, W., and Hoekstra, A. Y. (2010). Data from: Burning Water: the Water Footprint of Biofuel-Based Transport. Available at: https://research.utwente.nl/en/publications/burning-water-the-water-footprint-of-biofuel-based-transport. Groningen: UNESCO-IHE. Research Report Series No. 44.

Guo, M., Song, W., and Buhain, J. (2015). Bioenergy and Biofuels: History, Status, and Perspective. *Renew. Sustain. Energ. Rev.* 42, 712–725. doi:10.1016/j.rser.2014.10.013

Hernández, F. (2010). *Análisis técnico, económico y medioambiental de los potenciales sustitutos de los hidrocarburos en el mercado español de los combustibles para automoción*. Madrid, Spain: Universidad Politécnica de Madrid. [dissertation/Ph.D.'s thesis]. [España].

ISO 14040 (2006). Environmental Management - Life Cycle Assessment-Principles and Framework. Available at: https://www.iso.org/standard/37456.html (Accessed December 12, 2020).

ISO 14044 (2006). Environmental Management - Life Cycle Assessment - Requirements and Guidelines. Available at: https://www.iso.org/standard/38498.html (Accessed December 12, 2020).

Jacob, A., Ashok, B., Alagumalai, A., Chyuan, O. H., and Le, P. T. K. (2021). Critical Review on Third Generation Micro Algae Biodiesel Production and its Feasibility as Future Bioenergy for IC Engine Applications. *Energ. Convers. Manage.* 228 (2), 113655. doi:10.1016/j.enconman.2020.113655

Kalnes, T., Marker, T., and Shonnard, D. R. (2007). Green Diesel: a Second Generation Biofuel. *Int. J. Chem. React. Eng.* 5 (1). doi:10.2202/1542-6580.1554

Kumar, V., Sindhu, R. K., and Kumar, S. (2018). Comparative Analysis of green Diesel versus Petro-Diesel in Compression Ignition Engine. *Biosci. Biotech. Res. Comm.* 11, 128–135. doi:10.21786/bbrc/11.1/18

Méndez, C. (2019). *Refinación de aceite crudo de palma acondicionado como carga a un proceso de hidrodesoxigenación (HDO)*. Mexico City: Instituto Mexicano del Petróleo. [dissertation/master's thesis]. [México].

Mesa, H., and Piñeros, L. (2018). *Fabricación y montaje de los equipos para una planta extractora de aceite de palma*. Colombia: Universidad Piloto de Colombia. [dissertation/master's thesis]. [Colombia].

Mortimer, N. D., Elsayed, M. A., and Horne, R. E. (2004). *Energy and Greenhouse Gas Emissions for Bioethanol Production from Wheat Grain and Sugar Beet*. January: Final Report for British Sugar plc. Report No. 23/1.

Mukhopadhyay, P., and Chakraborty, R. (2021). LCA of Sustainable Biodiesel Production from Fried *Borassus Flabellifer* Oil in Energy-Proficient Reactors: Impact Assessment of Multi Fuel-Additives on Pour point, NOx and Engine Performance. *Sustainable Energ. Tech. Assessments* 44, 100994. doi:10.1016/j.seta.2021.100994

Nanaki, E. A., and Koroneos, C. J. (2012). Comparative LCA of the Use of Biodiesel, Diesel and Gasoline for Transportation. *J. Clean. Prod.* 20 (1), 14–19. doi:10.1016/j.jclepro.2011.07.026

Nucci, B., Puccini, M., Pelagagge, L., Vitolo, S., and Nicolella, C. (2014). Improving the Environmental Performance of Vegetable Oil Processing through LCA. *J. Clean. Prod.* 64, 310–322. doi:10.1016/j.jclepro.2013.07.049

Ornelas-Ruiz-, P. (2021). Data from: Servicio de Información Agroalimentaria y Pesquera, Gobierno de México. Available at: https://www.gob.mx/siap (Accessed December 12, 2020).

Parajuli, R., Dalgaard, T., and Birkved, M. (2018). Can Farmers Mitigate Environmental Impacts through Combined Production of Food, Fuel and Feed? A Consequential Life Cycle Assessment of Integrated Mixed Crop-Livestock System with a green Biorefinery. *Sci. Total Environ.* 619-620, 127–143. doi:10.1016/j.scitotenv.2017.11.082

Peiró, L. T., Lombardi, L., Méndez, G. V., and Durany, X. G. (2010). Life Cycle Assessment (LCA) and Exergetic Life Cycle Assessment (ELCA) of the Production of Biodiesel from Used Cooking Oil (UCO). *Energy* 35 (2), 889–893. doi:10.1016/j.energy.2009.07.013

Pfister, S., Koehler, A., and Hellweg, S. (2009). Assessing the Environmental Impacts of Freshwater Consumption in LCA. *Environ. Sci. Technol.* 43, 4098–4104. doi:10.1021/es802423e

Piemonte, V., Di Paola, L., and Russo, V. (2014). An LCA Study on Feedstocks and Processes for Biofuels Production. *Chem. Eng. Trans.* 37, 517–522.

Ramírez-Verduzco, L. F., and Hernández-Sánchez, M. J. (2020). Blends of Green Diesel (Synthetized from Palm Oil) and Petroleum Diesel: A Study on the Density and Viscosity. *Bioenerg. Res. In press*. doi:10.1007/s12155-020-10183-y

Sampattagul, S., Suttibut, C., and Kiatsiriroat, T. (2009). LCA/LCC of Jatropha Biodiesel Production in Thailand. *Int. J. Renew. Energ.* 4, 33–42. doi:10.14456/iire.2009.1

Sandoval, A. (2011). Data from: Paquete tecnológico palma de aceite: Establecimiento y Mantenimiento. Available at: https://franciscodelgado.tripod.com/palmamexico.pdfSAGARPA. Centro de Investigación Regional Pacífico Sur

Sandoval-Esquivez, A. (2011). Data from: Paquete tecnológico palma de aceite (*Elaeis guinnensis jacq.*) Producción. SAGARPA. Centro de Investigación Regional Pacífico Sur https://docplayer.es/10763640-Produccion-de-planta-paquete-tecnologico-palma-de-aceite-elaeis-guinnensis-jacq-paquete-tecnologico-palma-de-aceite.html.

Seela, C. R., AlagumalaiPugazhendhi, A. A., and Pugazhendhi, A. (2020). Evaluating the Feasibility of Diethyl Ether and Isobutanol Added Jatropha Curcas Biodiesel as Environmentally Friendly Fuel Blends. *Sustain. Chem. Pharm.* 18 (7), 100340. doi:10.1016/j.scp.2020.100340

Soo-Young, N. (2014). Application of Hydrotreated Vegetable Oil from Triglyceride Based Biomass to CI Engines - A Review. *Fuel* 115, 88–96. doi:10.1016/j.fuel.2013.07.001

Sotelo-Boyas, R., Liu, Y., and Minowa, T. (2011). Renewable Diesel Production from the Hydrotreating of Rapeseed Oil with Pt/Zeolite and NiMo/Al2O3 Catalyst. *Eng. Chem. Res.* 50, 2791–2799. doi:10.1021/ie100824d

Sun, P., Elgowainy, A., Wang, M., Han, J., and Henderson, R. J. (2018). Estimation of U.S. Refinery Water Consumption and Allocation to Refinery Products. *Fuel* 221, 542–557. doi:10.1016/j.fuel.2017.07.089

Tabatabaei, M., Aghbashlo, M., Najafi, B., Hosseinzadeh-Bandbafha, H., Faizollahzadeh Ardabili, S., Akbarian, E., et al. (2019). Environmental Impact Assessment of the Mechanical Shaft Work Produced in a Diesel Engine Running on Diesel/biodiesel Blends Containing Glycerol-Derived Triacetin. *J. Clean. Prod.* 223, 466–486. doi:10.1016/j.jclepro.2019.03.106

Uctug, G., Modi, D. N., Modi, D. N., and Mavituna, F. (2017). Life Cycle Assessment of Biodiesel Production from Microalgae: A Mass and Energy Balance Approach in Order to Compare Conventional with *In Situ* Transesterification. *Ijcea* 8, 355–356. doi:10.18178/ijcea.2017.8.6.683

Conflict of Interest: The authors declare that the research was conducted in the absence of any commercial or financial relationships that could be construed as a potential conflict of interest.

frontiers
in Energy Research

PERSPECTIVE
published: 05 August 2021
doi: 10.3389/fenrg.2021.707867

Synthetic Fuels in a Transport Transition: Fuels to Prevent a Transport Underclass

Peter Styring*, **Emily L. Duckworth** and **Edward G. Platt**

UK Centre for Carbon Dioxide Utilisation, Chemical & Biological Engineering, Sir Robert Hadfield Building, The University of Sheffield, Sheffield, United Kingdom

The Paris Agreement set policy scenarios to address mitigating against the climate emergency, by reducing greenhouse gas emissions to limit the temperature increase to 1.5°C. There has been a drive toward electrifying transport, with battery electric vehicles (BEVs) at the forefront. Reliance on single-technology policy development can lead to consequential impacts, often not considered, or dismissed. Energy cannot be created or destroyed but can be transformed. While BEVs may represent zero tailpipe emissions, the battery energy must be sourced elsewhere. An ideal policy scenario will come from "renewable" sources; however, current global energy mixes require the electricity to come from carbon-burning point source emitters. Therefore, the emissions are deferred to low socioeconomic regions. The move to ban new internal combustion engine (ICE) vehicle sales has been accelerated. High BEV costs will preclude low-income groups from making purchases. Such groups typically rely on used cars for mobility. Without considered consequential policy analysis, transport underclasses may result, where private transport is only accessible by the wealthy. Synthetic fuels derived from CO_2 represent a social bridge in the energy transition, also helping to accelerate toward net zero. The Covid-19 lockdown provided a unique opportunity to experience an environment with reduced transport-related emissions. Global studies allowed the consequential effects of pollution reduction to be studied. These are surprising and offer the opportunity for policies, driven by science, to be developed. Here, we consider the consequential effects of clean air policies, and how these can be used to propose dynamic responses to policy recommendations.

Keywords: synthetic fuel, policy development, electric vehicle, ICE, net zero carbon, social impact

Edited by:
Luis Puigjaner,
Universitat Politecnica de Catalunya,
Spain

Reviewed by:
Veera Gnaneswar Gude,
Mississippi State University,
United States
Felix Charles Penrice Leach,
University of Oxford, United Kingdom

***Correspondence:**
Peter Styring
p.styring@sheffield.ac.uk

Specialty section:
This article was submitted to Sustainable Energy Systems and Policies,
a section of the journal
Frontiers in Energy Research

Received: *11 May 2021*
Accepted: *09 July 2021*
Published: *05 August 2021*

Citation:
Styring P, Duckworth EL and Platt EG (2021) Synthetic Fuels in a Transport Transition: Fuels to Prevent a Transport Underclass.
Front. Energy Res. 9:707867.
doi: 10.3389/fenrg.2021.707867

INTRODUCTION

The drive toward "net zero" required to meet the necessary challenges of the Paris Climate Accord (UNFCCC, 2015), proposed at the 21st United Nations Conference of Parties (COP21) and ratified at COP22, together with subsequent amendments (IPCC et al., 2018), requires significant technological and behavioral changes if the global temperature rise is to be limited to 1.5°C or lower. The accord requires significant reduction in anthropogenic greenhouse gas (GHG) emissions. Most efforts have been and are being concentrated on the energy sector; however, action is needed in the transport sector (CCC, 2019). Urban and national transport has been considered as the easiest to de-fossilize through a drive toward battery electric vehicles (BEVs). This is true for the reduction of tailpipe emissions (tank or socket to wheel) but becomes less so when emissions are considered over the complete life cycle of the vehicle emissions (well, or more accurately renewable energy source, to wheel) (Moro and Lonza, 2018; Brand et al., 2020; Carbon Brief, 2020; Dixon et al., 2020). Furthermore, we need to consider the consequential effects of focusing on a single aspect of the transport transition. Net zero technologies will only be successful if they are accompanied by net zero behaviors. What remains clear is the commitment to achieving net zero by 2050. Synthetic transport fuels may aid its acceleration until an EV transition is accomplished and legacy liquid fuel vehicles phased out. There have been a number of studies that consider different approaches to the decarbonization of future transport systems (Royal Society, 2019; Senecal and Leach, 2019; Senecal and Leach, 2021), but the Covid lockdown of 2020 has given a unique insight into what may happen if road transport emissions are significantly reduced.

Net zero is defined as the removal of unavoidable emissions from the atmosphere using technological or natural interventions (sequestration or offsetting). Also key to this is the need to avoid emissions or at least reduce them. A full understanding of the impact of fossil fuel replacement on emissions and the effect of conventional fuel prohibition on social justice is required. During the COVID-19 pandemic, an unintended consequence of lockdowns, and so reductions in road traffic, has been an insight into what a low-emission future may look like (Brimblecombe and Lai 2020; Wang et al., 2020). In this study, we consider what efforts can be made to accelerate the transition to net zero by using synthetic chemical fuels to power legacy internal combustion engines (ICEs) while BEVs become fully established.

It is clear that we must take a systemic approach rather than considering isolated policies, as unintended negative consequences must be avoided. In this respect, we consider the negative potential for increasing social injustice and the creation of a transport underclass if we do not consider the long-term consequences of ill-thought-out policy actions. By applying a theory of change approach, we propose a possible solution to a multifaceted approach to accelerate toward net zero.

THE REALITY OF MOBILITY

Mobility is at the center of international economies. To ensure stable and prosperous futures, we need to have the capability to move people, food, and commodity goods locally, nationally, and internationally. The first law of thermodynamics states that in a closed system, energy cannot be created or destroyed and that it can only be converted from one form to another. We have used Earth's fossil resources to create the energy we need, including power generation and mobility. The reason we used these sources is that they are dense in energy and are easily converted through combustion. However, this produces unwanted side products such as carbon dioxide (CO_2), nitrogen and sulfur oxide gases (NO_x and SO_x), and particulate matter (PM), such as soot and nanoparticles. These side products are unfortunately harmful to the environment and health. Despite the development of cleaner combustion engines, emissions persist. Policy has driven technology development, including legislation to replace lead in petrol during the 1980s, to the United Kingdom policy incentives for diesel vehicles in 2001. While diesel fuel produces less of the greenhouse gas (GHG) carbon dioxide than petrol, there are increased NO_x and PM emissions which can contribute to respiratory illnesses. The panacea of transport is the so-called zero-emission vehicle that is technically impossible to produce because of the first law of thermodynamics and the subject of many misconceptions.

Achieving a net zero emissions policy by 2050 currently seems ambitious (EU, 2019). However, predictions thirty years into the future are difficult, and while the Committee on Climate Change (CCC, 2019) set legally binding five-year carbon budgets, they concede that these contain inherent uncertainties. It is reasonable to suggest that battery technology and energy harvesting from solar and wind sources will undergo significant improvements (IEA, 2020a) and that car design and manufacture will result in lighter, more efficient performance and energy conversion. However, we will still be using legacy ICEs for the foreseeable future.

The fear is that a radical move toward abolishing ICEs will result in a transport social underclass where lower socioeconomic groups become transport impoverished. Taking the United Kingdom as an example, we may be able to find some solace in the rationale behind a transition. The United Kingdom government has said it will ban the sale of new petrol (gasoline) and diesel vehicles by 2030, bringing forward its initial ambition by ten years. It will also ban the sale of new hybrid vehicles by 2035. Many from low-income communities rely on cheap, used vehicles to reach their place of employment. The new legislation will prohibit new ICE vehicle sales, not used vehicles. Petrol vehicles typically have a life of 10 years or 100,000 miles and diesels 20 years or 200,000 miles, with an average vehicle life of 13.9 years (SMMT, 2020). This would give an upper limit of twenty years to the vehicle lifetime. By 2050 all ICE vehicles will have naturally reached the end of their life, and only BEVs will exist on the used car market, which looks like a reasonable transition strategy. However, it relies on rapid improvement in battery technologies and social interventions, as the current battery lifetime will limit their long-term viability in a low-cost used BEV market. Interventions will need to address the reconditioning of batteries for resale. Robust policies need to be in place at the local and national levels to develop mass transit systems that allow convenient, clean, and cheap travel with efficient interconnectivity. Logan et al. (2020) have carried out a recent analysis of such a transition in the United Kingdom that points the way to possible solutions.

Synthetic fuels have a role to play in accelerating defossilization of transport in the period between 2030 and 2050. Furthermore, the current policy does not cover commercial heavy goods vehicles, so synthetic liquid fuels to replace diesel will play an increasingly important role (Styring et al., 2021). We have used a theory of change approach (**Figure 1**) to evaluate the transition to fully electric mobility, identifying gaps and hot spots in the process and policy development. Direct air capture (DAC) of CO_2 emissions from

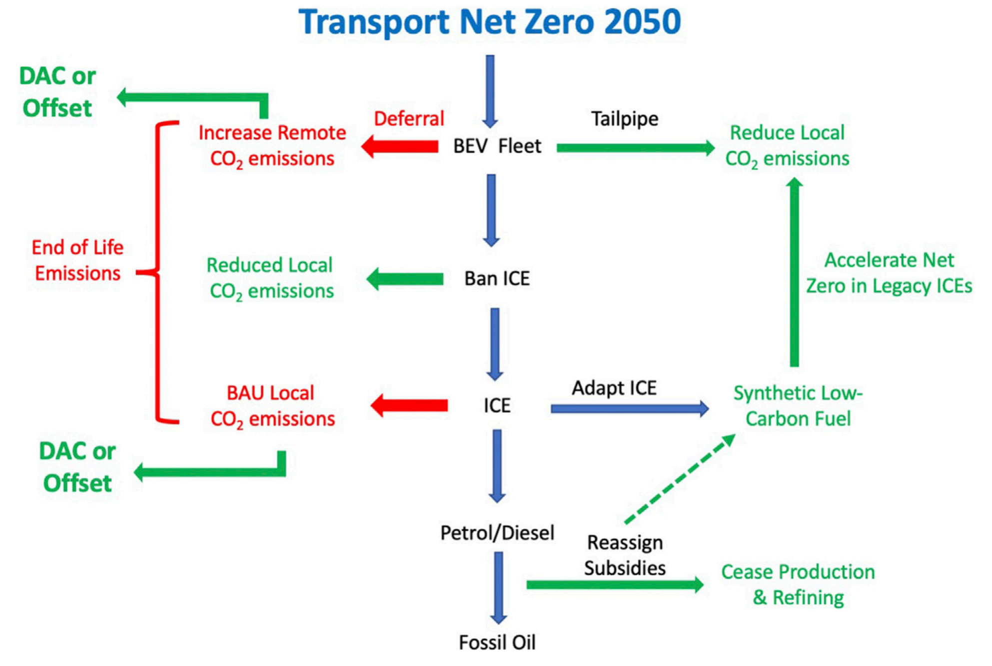

FIGURE 1 | Theory-of-change approach to accelerated transport defossilization.

the atmosphere is one method to achieve net zero; however, it is currently expensive and not available at scale (McQueen et al., 2021).

We see that in focusing on transport as a pathway to net zero, BEVs fuelled by 100% renewable energy sources are seen as the solution. While the tailpipe CO_2 emissions will be zero in this scenario, there will still be production and end-of-life decommissioning emission embodied in the system.

SYNTHETIC FUELS

The internal combustion engine is not the problem; the fuel is. The human body requires fuel to survive. If we use the wrong fuel, the body responds accordingly, a feature that is clearly shown in the link between junk food and obesity. If the ICE has been developed over decades to become more and more efficient, then maybe the engine is not the problem but the fuels we use are. The Royal Society (2019) published a policy briefing that considered alternative fuels for transport. Hydrocarbons such as petrol, diesel, and kerosene can be made synthetically using waste carbon–containing feedstock, which reduces fossil-carbon consumption. CO_2 is still produced, but this is now second-life carbon (Styring et al. 2021). However, synthetic hydrocarbons still produce particulate emissions and NO_x due to their combustion chemistry. Dimethyl ether (DME) is a direct replacement or drop-in fuel for diesel engines, needing a small modification to the fuel delivery system and the injection timing (Styring and Dowson, 2021). A typical diesel engine such as that found in a Ford Mondeo will emit around 250 g CO_2 per km traveled, while Ford has reported that if DME is used instead, the emissions drop to 3 g per km (Lee et al., 2016; Willems, 2018). As the emissions associated with the manufacture and decommissioning of the vehicle are essentially the same as those of the conventional diesel vehicle, the life-cycle emission profile is considerably better than even a BEV's. Ellingsen et al. (2016) stated the true emissions of a BEV over the cradle-to-grave analysis, which means that to meet net zero criteria, a medium-size car needs to drive 70,000 km before tailpipe emission reduction is met. This is the crossover point or breakthrough, where the embedded and use emissions from a BEV first equal and then fall below the emissions for a conventional and equivalent ICE vehicle. The study demonstrates that only mini (Class A) cars show favorable life-cycle emission reduction relative to fossil-fueled cars and that a small diesel car shows better full-life emission characteristics than larger BEVs. If we relate DME emissions to the Ellingsen life cycle evaluation, then the crossover point is significantly reduced, so less mileage is required before the DME vehicle shows improvement over the BEV equivalent.

UNINTENDED CONSEQUENCES IN THE SYSTEM

The 2020 Covid-19 lockdown and consequential reduction in traffic emissions provided an insight into future transport scenarios. While expected reductions in atmospheric CO_2 and NO_2 levels were observed, there were unexpected increases in PM levels. This was observed by groups in China (Brimblecombe and Lai 2020;Wang et al., 2020), where the lockdown was particularly strict, and by us in Sheffield, United Kingdom (Alam et al., 2021),

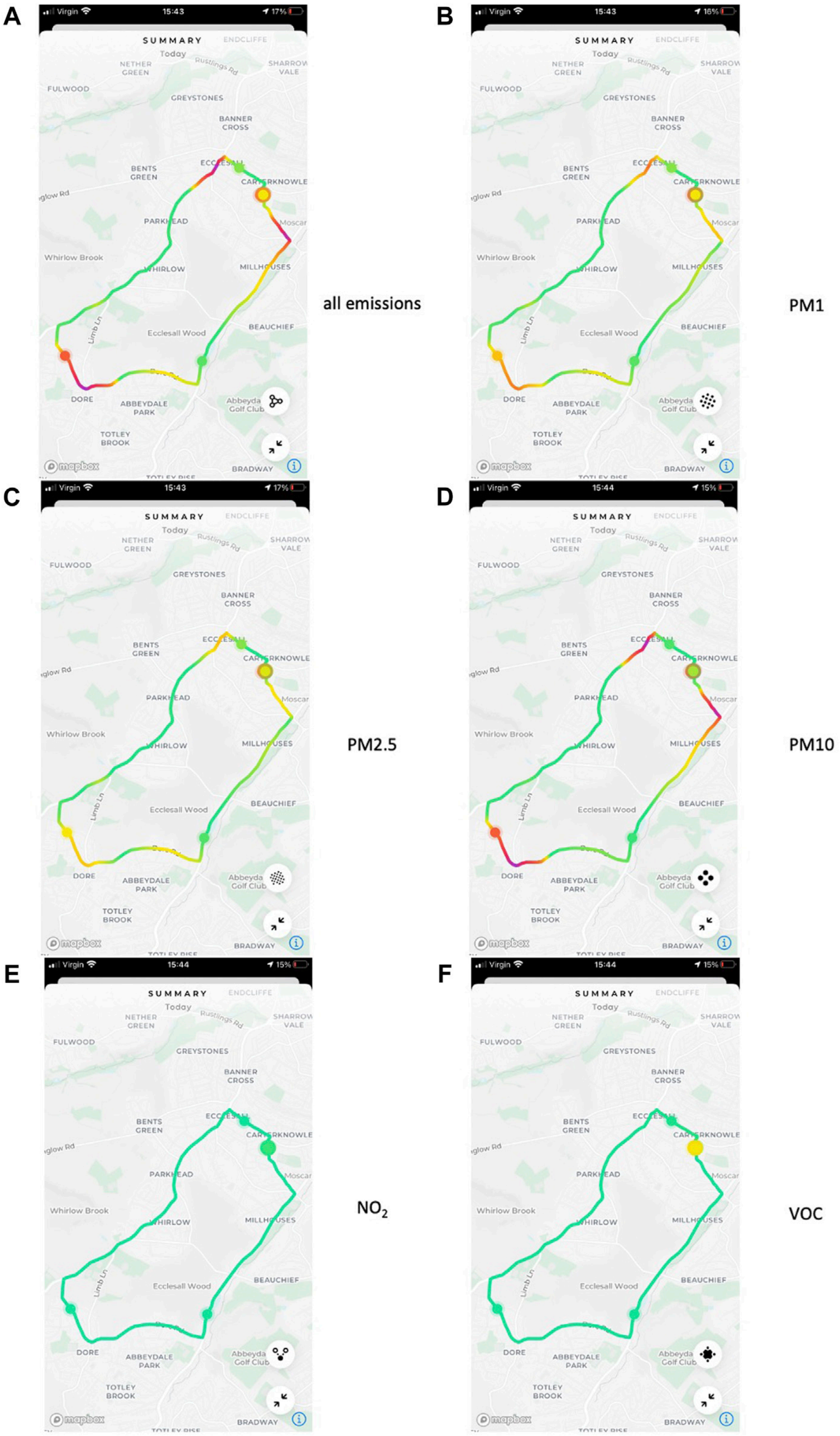

FIGURE 2 | Emission data during United Kingdom Lockdown 3. Wind was blowing at 9 mph from the southwest. Light traffic and no obvious wood fires, except wood-burning stoves in Dore (Flow 2 data). The circular pictograms refer to the species analysis as given in the chemical labels at the side of each figure.

using a Flow 2 sensor (PlumeLabs 2021) mounted on a bicycle, as shown in **Figure 2**.

PM2.5s are particles with diameters less than 2.5 μm and are not only breathed in by humans but respired; taken into the lung capillaries and distributed around the body. While such particles are themselves hazardous to health, they are also able to carry nanoparticles (PM0.1 and below), which include viruses, into the body, thereby increasing their risk to health. The GPS-emission plots shown in **Figure 2** were recorded during the first United Kingdom lockdown. Further details are reported in the **Supplementary Material**. The combined emission data (**A**) show three hot spots for hazardous emissions, as depicted by the color of the data. Green is safe, while purple is hazardous to health, with intermediate shades depicting a range of hazards (see the **Supplementary Material** for color coding). The nitrogen oxide data (**E**) and volatile organic compound (VOC) data (**F**) show very low levels of emissions, which correlates well with there being very little road traffic. Three hot spots relate to PM emissions, particularly PM10 and PM1. As the NO_2 levels are low, these cannot be associated with road traffic, and two of the sites (Ecclesall and Millhouses) are suburban, while the third (Dore) is semirural, suggesting that the emission is not agricultural. Some of the emissions in Dore are due to wood-burning stoves, but the link between each of the sites was the presence of local bakeries which were allowed to remain open during the lockdown. So, in this period, the emissions were linked to cooking and heating activities rather than transport-related emissions. An explanation for similar observations of high PM levels at low NO_2 emission levels was also being developed in China, where lockdown restrictions were even more severe (Brimblecombe and Lai, 2020; Wang et al., 2020). Under normal conditions, solar radiation reacts with oxygen to produce ozone, which in turn reacts with NO_x to yield other products. In the absence of any significant amounts of NO_x from vehicle exhausts, the ozone reacts with volatile organic compounds such as methane and cooking emissions in the atmosphere to produce particulate matter (PM) which increases the atmospheric concentration. These studies are continuing to aid an understanding of the atmospheric chemistry, which changes as the emission portfolio is altered through interventions. Particulate emissions are also associated with non-combustion vehicle emissions such as brake and tire abrasion in BEVs; however, there were no significant correlations between the observed PM emissions and vehicular activity during the lockdown.

POLICY INTERVENTIONS

Many political manifestos aspire to achieve net zero using a suite of technological and policy interventions. However, these generally make assumptions that technologies already exist or are close to commercialization, while the maturity of these may be overestimated. A common proposal is that CCS technologies will be available at scale by 2050. While such facilities have been operating in Norway for over fifty years, the global capacity, the majority of which is enhanced fossil oil recovery, is currently around 40 million tonnes per annum. By contrast, total global emissions are around 1,000 times higher (Global CCS Institute, 2021). The European Union policy document "A Cleaner Planet for All" shows that widespread CCS will not be available until around 2050 and still not at a scale to make a significant impact on global emissions (EU, 2019). A second assumption is that EVs will decarbonize the transport sector. There will always be embedded emissions from vehicle production and disposal at the end of life and electricity generation from fossil resources until a 100% renewable electricity grid is achieved, and so CCS will be necessary to remove these emissions. A third policy involves carbon offsetting through the planting of trees and indeed forests, which is the so-called afforestation. We have already considered the first two assumptions, but what about the third?

Policy makers often propose planting trees as a solution to offset CO_2 emissions. Whilst trees can mitigate some CO_2 emissions, there is a lack of discussion on the extent of this capability. Various factors affect a tree's ability to absorb CO_2, such as tree species, age, and climate. To estimate the amount of CO_2 sequestrated per year per tree, numeric tables which give values based on the tree's age and species (US Department of Energy, 1988) can be used. A single tree can sequestrate 1.66 kg CO_2/year in its first year of growth. Whilst the sequestration rate does increase past the first year, so does tree mortality. This decreases the net CO_2 stored in two ways; when a tree is dead, it can no longer absorb CO_2, and second, on decomposition, it emits CO_2 and, more problematically, methane, which has 24 times the GHG potential of CO_2.

To explain the scale on which trees would need to be planted to offset emissions, a scenario is proposed where an average diesel car with a CO_2 emission of 122.1 gCO2/km (DFT, 2015, DVLA) travels 10,000 miles annually, emitting approximately 1,965 kg CO_2. It would take 1,180 trees to offset these emissions each year. Currently, there are over 38 million United Kingdom registered cars, so over 45 billion trees would need to be planted annually to offset United Kingdom private car emissions alone. Furthermore, with growing vehicle ownership, this number could rise even further (DFT, 2020). To plant that many trees, a land area of 22.5 million Ha would be needed; the United Kingdom land area is approximately 24.3 million Ha (Office for National Statistics, 2021).

There also need to be policy interventions that incentivize behavioral change. Technology alone cannot solve the problem without public acceptance. If a social underclass is to be avoided, there needs to be a balance between mandatory legislation and responsible fuel use. The electrification policy needs to include provisions for the transition of legacy vehicles including low carbon fuel subsidies. Together with policy interventions and financial easing of the transition, there also need to be fiscal measures in place to incentivize defossilization while at the same time disincentivizing fossil carbon use.

FISCAL MEASURES

Many technologies in their early development cycles require significant investment above that of the counterfactual to encourage technological, consumer, and behavioral change. This is certainly the case in the transport sector, where fossil fuels are relatively inexpensive but also attract state subsidies to maintain a security of supply. It is reasonable to propose that as the transition away from fossil-based resources takes effect, there should also be a transition away from conventional supply chains to the new, greener technologies. Furthermore, the VAT on synthetic, low-carbon fuels could be subject to zero sales tax, at least in the early years of transition, while at the same time applying VAT at the upper rate to fossil carbon fuels (PGES, 2021). There is also a strong need for a robust and realistic carbon tax or emission tax to be applied to the full range of emitters, from point source energy and industrial sources to transport and domestic emissions. The current carbon price does not deter emitters, and the International Energy Agency (IEA) have suggested that a higher value is needed (IEA, 2020b).

DISCUSSION AND RECOMMENDATIONS

We need to reduce emissions if we are to avoid irreversible climate change. This can only be achieved by using a multifaceted approach where policy, technology development, financial incentives, and behavioral change work together. It is reasonable to conclude that the 2050 net zero policy is achievable in principle, but we should be aware that paradigm technology shifts are required.

- Net zero as an aspiration can only be achieved by radical change in attitudes, behaviors, and technologies. This includes taking a more active approach to transport such as walking and cycling and the introduction of more interconnected mass transit systems.
- BEVs are not zero-emission vehicles over the complete life cycle. They can produce zero tailpipe emissions, but the other emissions are transferred to other locations, often in low socioeconomic areas of states. While not covered in detail, we should also be aware of embodied emission, including increased production and decommissioning costs, and increased brake and tire wear.
- BEVs will not provide the answer to road transport emissions if they are treated as an isolated technology. Full systemic life cycle assessment is needed from the cradle to the grave, not just the mobility emissions.
- When considering a whole system, the interdependency of different policy interventions should be considered. Unintended consequences should be included in a risk analysis of mitigation strategies, including changes in atmospheric chemistry that are promoted.
- It is unlikely that afforestation as a carbon offsetting policy will be effective given the area of land required and the timescales involved. A transition of subsidies, away from fossil fuels and toward low-carbon technologies, is required, and this needs to be accompanied by a transition in the skill sets of workforces to ensure a stable economy. Synthetic fuels provide a route to accelerate a transition.
- Fiscal interventions will be essential (reduction in the VAT for low-carbon fuels and a sensible carbon tax), coupled with financial support, if a socially just low-carbon transport revolution is to be realized.
- Care must be taken so that a transport underclass is not created. Small vehicle defossilization will most likely be achieved using BEVs, but synthetic low-emission fuels can help bridge the gap between ICEs and new electrified mobility in the transition period between 2030 and 2050.
- While it is acknowledged that BEVs will provide the long-term solution for private ground transportation, long-haul road transport, aviation, and maritime vessels will prove more difficult to defossilize, and so alternative ICE fuels based on recycled waste carbon feedstock may prove to be lower carbon options to accelerate the transition to net zero.

DATA AVAILABILITY STATEMENT

The data analyzed in this study is subject to the following licenses/restrictions: emissions data used in some of the article are available in a Faraday Discussion. Details will be made available on request. Requests to access these datasets should be directed to p.styring@sheffield.ac.uk.

AUTHOR CONTRIBUTIONS

PS led the analysis of the policy and the theory of change. ED conducted the offsetting analysis, and EP assisted in the air quality analysis.

ACKNOWLEDGMENTS

We thank the Engineering and Physical Sciences Research Council for funding the research under the UKRI Interdisciplinary Centre for Circular Chemical Economy programme (EP/V011863/1).

SUPPLEMENTARY MATERIAL

The Supplementary Material for this article can be found online at: https://www.frontiersin.org/articles/10.3389/fenrg.2021.707867/full#supplementary-material

REFERENCES

Alam, M. S., Bloss, W., Brean, J., Brimblecombe, P., Chan, C., Chen, Y., et al. (2021). General Discussion: Aerosol Formation and Growth; VOC Sources and Secondary Organic Aerosols. *Faraday Discuss.* 226, 479–501. doi:10.1039/D1FD90011K

Brand, C., Anable, J., Ketsopoulou, I., and Watson, J. (2020). Road to Zero or Road to Nowhere? Disrupting Transport and Energy in a Zero Carbon World. *Energy Policy* 139, 111334. doi:10.1016/j.enpol.2020.111334

Brimblecombe, P., and Lai, Y. (2020). Diurnal and Weekly Patterns of Primary Pollutants in Beijing under COVID-19 Restrictions. *Faraday Discuss.* 226, 138–148. Advanced article. doi:10.1039/d0fd00082e

Carbon Brief (2020). *Factcheck: How Electric Vehicles Help to Tackle Climate Change*. London: Carbon Brief. Available at: www.carbonbrief.org/factcheck-how-electric-vehicles-help-to-tackle-climate-change (Accessed May 8, 2021).

CCC (2019). *Climate Change Committee*. London: Committee on Climate Change Available at: www.theccc.org.uk/wp-content/uploads/2019/05/Net-Zero-The-UKs- contribution-to-stopping-global-warming.pdf (Accessed March 8, 2021).

DFT (2020). *Department for Transport. (2020). Vehicle Licensing Statistics: July to September 2020 Data Tables* London: Department for Transport. [Data set]. Available from: www.gov.uk/government/statistics/vehicle- licensing-statistics-july-to-september-2020 (Accessed February 17, 2021).

DFT (2015). *Department for Transport. DVLA (2015). Average CO_2 Emissions of Newly Registered Cars* . [Data set] London: Department for Transport. Available from: https://www.gov.uk/government/publications/new-car-carbon-dioxide-emissions#history (Accessed February 17, 2021).

Dixon, J., Bukhsh, W., Edmunds, C., and Bell, K. (2020). Scheduling Electric Vehicle Charging to Minimise Carbon Emissions and Wind Curtailment. *Renew. Energ.* 161, 1072e1091. doi:10.1016/j.renene.2020.07.017

Ellingsen, L. A. W., Singh, B., and Strømman, A. H. (2016). “The Size and Range Effect: Lifecycle Greenhouse Gas Emissions of Electric Vehicles,” *Environ. Res. Lett.* 11, 054010. doi.org/doi:10.1088/1748-9326/11/5/054010

EU (2019). *Communication from the Commission to the European Parliament, the European Council, the Council, the European Economic and Social Committee* Belgium: European Union, Brussels. Available from: https://eur-lex.europa.eu/legal- content/EN/TXT/?uri=CELEX:52018DC0773 (Accessed March 8, 2021).

Global CCS Institute (2021). *Global Carbon Capture and Storage Institute* Australia: Global CCS Institute, Melbourne. Available from: https://www.globalccsinstitute.com/resources/global-status-report/ (Accessed March 8, 2021).

IEA (2020a). *International Energy Agency* Paris: IEA. Available at: www.iea.org/reports/world-energy-outlook-2020/achieving-net-zero-emissions-by-2050 (Accessed March 8, 2021).

IEA (2020b). *Price Level of Selected Carbon Pricing Instruments Covering the Power Sector*. as of April 2020. Paris: IEA. Available from: www.iea.org/data-and-statistics/charts/price-level-of-selected-carbon-pricing-instruments-covering-the-power-sector-as-of-april-2020 (Accessed March 8, 2021).

Lee, U., Han, J., Wang, M., Ward, J., Hicks, E., Goodwin, D., et al. (2016). Well-to-Wheels Emissions of Greenhouse Gases and Air Pollutants of Dimethyl Ether from Natural Gas and Renewable Feedstocks in Comparison with Petroleum Gasoline and Diesel in the United States and Europe. *SAE Int. J. Fuels Lubr.* 9 (3), 546–557. doi:10.4271/2016-01-2209

Logan, K. G., Nelson, J. D., and Hastings, A. (2020). Electric and Hydrogen Buses: Shifting from Conventionally Fuelled Cars in the UK. *Transportation Res. D: Transport Environ.* 85, 102350. doi:10.1016/j.trd.2020.102350

McQueen, N., Gomes, K. V., McCormick, C., Blumanthal, K., Pisciotta, M., and Wilcox, J. (2021). A Review of Direct Air Capture (DAC): Scaling up Commercial Technologies and Innovating for the Future. *Prog. Energ.* 3, 032001. doi:10.1088/2516-1083/abf1ce

Moro, A., and Lonza, L. (2018). Electricity Carbon Intensity in European Member States: Impacts on GHG Emissions of Electric Vehicles. *Transportation Res. Part D: Transport Environ.* 64, 5–14. doi:10.1016/j.trd.2017.07.012

Office for National Statistics (2021). *Standard Area Measurements (2020) for Administrative Areas in the United Kingdom. [Data Set] Office for National Statistics* London: Office for National Statistics. Available at: https://geoportal.statistics.gov.uk/datasets/e919e5a1647f426595650429937b7ad5 Available from: geoportal.statistics.gov.uk/datasets/standard-area-measurements-2019-for-administrative-areas-in-the-united-kingdom (Accessed February 15, 2021).

PGES (2021). *All Party Parliamentary Group for Energy Studies, “What Are the Energy Policies that Will Drive an Independent UK to Net Zero while Fuelling the Economy?”. Energy Policy Document* London: The All-Party Parliamentary Group for Energy Studies (PGES). Available from: https://pges.org.uk/wp-content/uploads/2021/03/PGES-Inquiry-Report-FINAL.pdf (Accessed March 9, 2021).

PlumeLabs (2021). *PlumeLabs* Paris: Plume Labs. https://plumelabs.com/en/ (Accessed March 8, 2021).

Royal Society (2019). *Synthetic Transport Fuels, Policy Briefing*. London, England: The Royal Society.

Senecal, K., and Leach, F. (2021). *Racing toward Zero: The Untold Story of Driving Green*. USA: SAE International. ISBN 978-1-4686-0146-6.

Senecal, P. K., and Leach, F. (2019). Diversity in Transportation: Why a Mix of Propulsion Technologies Is the Way Forward for the Future Fleet. *Results Eng.* 4, 100060. doi:10.1016/j.rineng.2019.100060

SMMT (2020). *Average Vehicle Age* London: The Society of Motor Manufacturers and Traders. Avaialable at: www.smmt.co.uk/industry-topics/sustainability/average-vehicle-age/ (Accessed May 8, 2021).

Styring, P., and Dowson, G. R. M. (2021). Oxygenated Transport Fuels from Carbon Dioxide : Driving towards Net Zero. *Johnson Matthey Technology Rev.* 65, 170–179. doi:10.1595/205651321x16063027322661

Styring, P., Dowson, G. R. M., and Tozer, I. O. (2021). Synthetic Fuels Based on Dimethyl Ether as a Future Non-fossil Fuel for Road Transport from Sustainable Feedstocks. *Front. Energ. Res.* 9, 663331. doi:10.3389/fenrg.2021.663331

UNFCCC (2015). *United Nations Framework Convention on Climate Change* Bonn: United Nations Framework Convention on Climate Change. Available at: unfccc.int/sites/default/files/english_paris_agreement.pdf. (Accessed 8, March2021).

US Department of Energy (1988). *Method for Calculating Sequestration by Trees in Urban and Suburban Settings*. Washington, DC: United States Department of Energy, Energy Information Administration. Available from: www3.epa.gov/climatechange/Downloads/method-calculating-carbon-sequestration-trees-urban-and-suburban-settings.pdf (Accessed March 8, 2021).

IPCC (2018). “Summary for Policymakers,” in *Global Warming of 1.5°C. An IPCC Special Report on the Impacts of Global Warming of 1.5°C above Pre-industrial Levels and Related Global Greenhouse Gas Emission Pathways, in the Context of Strengthening the Global Response to the Threat of Climate Change, Sustainable Development, and Efforts to Eradicate Poverty*. Editors V. Masson-Delmotte, P. Zhai, H. O. Pörtner, D. Roberts, J. Skea, P. R. Shukla, et al. (Geneva, Switzerland: World Meteorological Organization), 32. Available at: www.ipcc.ch/sr15/faq/faq-chapter-1/ (Accessed March 8, 2021).(eds.)].

Wang, Y., Wen, Y., Wang, Y., Zhang, S., Zhang, K. M., Zheng, H., et al. (2020). Four-Month Changes in Air Quality during and after the COVID-19 Lockdown in Six Megacities in China. *Environ. Sci. Technol. Lett.* 7, 802–808. doi:10.1021/acs.estlett.0c00605

Willems, W. (2018). “Sustainable Fuels for Future Mobility: The DME Opportunity for CI- Engines,” in (paper presented at the 8th International Conference on DME, Sacramento, CA, USA, 2018.

Conflict of Interest: The authors declare that the research was conducted in the absence of any commercial or financial relationships that could be construed as a potential conflict of interest.

frontiers
in Energy Research

ORIGINAL RESEARCH
published: 10 August 2021
doi: 10.3389/fenrg.2021.682609

Economic Evaluation of Combined Heat and Power Integrated With Food Waste-Based Ethanol Production

Noor Intan Shafinas Muhammad[1,2] *and Kurt A. Rosentrater*[1]*

[1]*Agricultural and Biosystems Engineering Department, Iowa State University, Ames, IA, United States,* [2]*Faculty of Civil Engineering Technology, Universiti Malaysia Pahang, Kuantan, Malaysia*

The concern of food waste (FW) impact on the environment, societies, and economies, has triggered many researchers to find alternative ways to utilize these materials. FW can be high in glucose and other sugars (depending upon the food used) and has the potential to be converted into value-added products such as ethanol. Ethanol is an organic material that has a high demand from different industries for products such as fuel, beverages, pharmaceuticals, and other industrial applications. FW fermentation to produce ethanol may be a promising method, and might results in positive impacts on economies. However, it is a challenge for the product price to compete with that of corn ethanol due to low yield and the inconsistency of FW composition. Thus, to increase the profitability, a conventional fermentation plant integrated with a combined heat and power (CHP) system might be a great combination, and was analyzed in this study. Solid waste stream from the process can be converted into energy and could reduce the utility cost. Therefore, the main focus of this study is to evaluate the economic impact of this integrated system by estimating the minimum selling price (MSP) using techno-economic analysis (TEA) and compare to conventional plants without CHP. Results from this analysis showed that the MSE value for this integrated system was $1.88 per gallon ($0.50 per liter). This study suggests that an integrated system with CHP was found to be more economical and attractive to be implemented on a commercial scale.

Keywords: food waste, ethanol, CHP (combined heat and power), techno-economic analysis, biofuel, industrial fermentation

OPEN ACCESS

Edited by:
Luis Puigjaner,
Universitat Politecnica de Catalunya,
Spain

Reviewed by:
Ahmed Rezk,
Aston University, United Kingdom
Rajesh S. Kempegowda,
Inrigo As, Norway

****Correspondence:***
Kurt A. Rosentrater
Karosent@iastate.edu

Specialty section:
This article was submitted to
Process and Energy Systems
Engineering,
a section of the journal
Frontiers in Energy Research

Received: *18 March 2021*
Accepted: *17 June 2021*
Published: *10 August 2021*

Citation:
Shafinas Muhammad NI and
Rosentrater KA (2021) Economic
Evaluation of Combined Heat and
Power Integrated With Food Waste-
Based Ethanol Production.
Front. Energy Res. 9:682609.
doi: 10.3389/fenrg.2021.682609

INTRODUCTION

Every year, the world generates about 1.3 billion tons of food waste (FW) through supply food chain stages including at the consumer level. In addition to that, this waste is expected to increase due to several factors such as managerial and technical limitation, global population, modernization, and living style (Gustavsson et al., 2011; Aschemann-Witzel et al., 2015). In the United States, 76.1% of the FW will be sent to the landfills as a final destination (EPA 2018). Furthermore, FW could lead to various problems such as to the environment, society, the ecosystem, and the economy (Papargyropoulou et al., 2014).

Prevention is the best option in the FW management hierarchy, followed by recycling, energy recovery, and disposal. Thus, by considering the amount of valuable nutrients in the FW, recycling using the biological platform in producing other value-added products would be a great approach. This method is expected to have a good impact on the economy and the environment compared to the thermochemical technology.

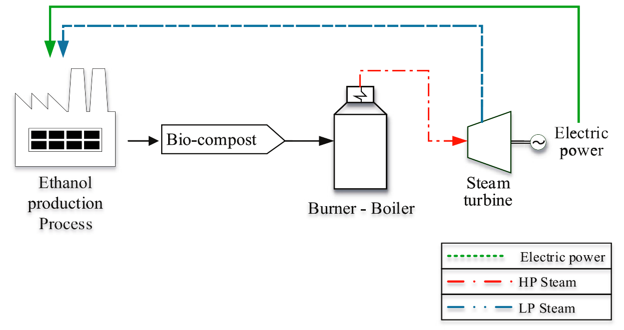

FIGURE 1 | Combined heat and power (CHP) schematic diagram.

Anaerobic digestion (AD) and fermentation are relatively a matured technology that could produce energy such as biogas and ethanol respectively. However, according to Pham et al., 2015, an AD method will add a negative impact on the environment and be more costly.

In a study performed by Shafinas and Rosentrater, ethanol conversion from FW fermentation without enzymes was shown to have good potential from an economic perspective. Even though the distillation column was identified as an energy-intensive process, the minimum selling price (MSP) value was the lowest compared to the membrane separation process. From the economic analysis, the MSE for FW fermentation without enzymes and 2-step distillation system was found to be $2.41/gal (Muhammad and Rosentrater 2020a). This value is in between corn ethanol price and cellulosic ethanol. However, the ethanol price from FW fermentation is expected to be more economical if the production process could integrate with the combined heat process (CHP) by producing in-site energy to minimizing the utility cost.

CHP is an integrated system that could produce electric power and steam on site. The advantages of embedded on site the plant are to avoid losses in distribution and transportation from the electrical power grid. The CHP is not considered as technology, but a method in applying technologies. Therefore, the implementation of this system could increase energy efficiency, minimize the emission, reduce utility cost, and promote sustainable development. Various studies have been suggested to use the integrated system in the ethanol fermentation plant due to advantages as mentioned above (Daianova et al., 2012; Raj, Iniyan, and Goic 2011; Eriksson and Kjellström 2010; Dias, Lima, and Mariano 2018).

The concept of CHP is direct combustion of the solid waste stream that will convert chemical energy into heat energy. The consistent of the heat source from the boiler will turn water into high-pressure steam. By using the Rankine cycle principle, the steam turbine can produce electricity. The backpressure steam turbine is commonly used in the industrial plant because of the low capital cost, simple configuration, and high efficiency (DOE 2016). The steam exhausts from the system will be recovered and used directly to a process and steam distribution. The biomass moisture content of biomass should be in the range of 15–55% before it can be directly burnt in the combustion system (Pirouti et al., 2010). Details of the overall process are shown in the schematic diagram in **Figure 1**.

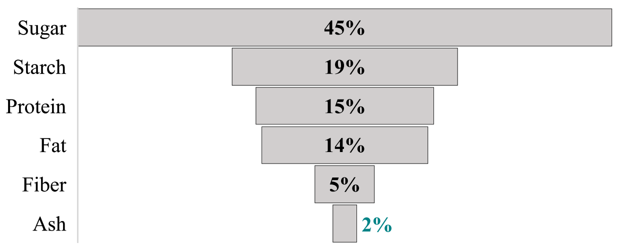

FIGURE 2 | FW composition.

In this study, FW fermentation without enzymes integrated with the CHP process is modeled. The process model and conditions are similar to a study done by Muhammad and Rosentrater but with an additional energy cogeneration model (Muhammad and Rosentrater 2020b). The primary target of this study is to evaluate and compare the economic performance between with and without the integrated system. The techno-economic analysis will be performed to estimate the minimum selling price ($/gal) and compared with previous studies. The sensitivity analysis will be performed to identify the impact of the processing parameter on economic feasibility.

METHODOLOGY

Process Modeling

Figure 2 shows the FW composition used in this study. This information was based upon data collected in our laboratory. The fermentation process was modeled using anaerobic conditions without any hydrolysis enzymes added, and ethanol yield was set to 2.2% (w/w) (based on laboratory results). The yield is considered higher compared to the previous study (Suwannarat and Ritchie 2015).

SuperPro Designer V9.0 software was used to simulate the integrated conceptual fermentation plant and evaluate the performance on a commercial scale. The daily plant feedstock is supposed to be 2000 Mg, and assuming no cost.

A 2-step distillation process was used to separate the ethanol from the fermentation broth followed by a purification process through a molecular sieve. The waste stream from this process was considered as a co-product that can be utilized as liquid fertilizer and bio-compost. Previous study found that by selling these co-products to other industries it could maximize the profit. (Muhammad and Rosentrater 2020a). However, in this study, bio compost was being utilized to generate heat and power by using the CHP system. The moisture content of bio compost was maintained at 40% by weight before being combusted in the burner. The chemical energy will be converted into heat energy to generate steam in the boiler. High-pressure steam turns the steam turbine which satisfies the thermodynamic cycle that changes heat to mechanical works. The turbine drives the generator and finally generates electric power and then will be used back in the facilities. In this study, assume that no surplus electricity can be sold to the grid.

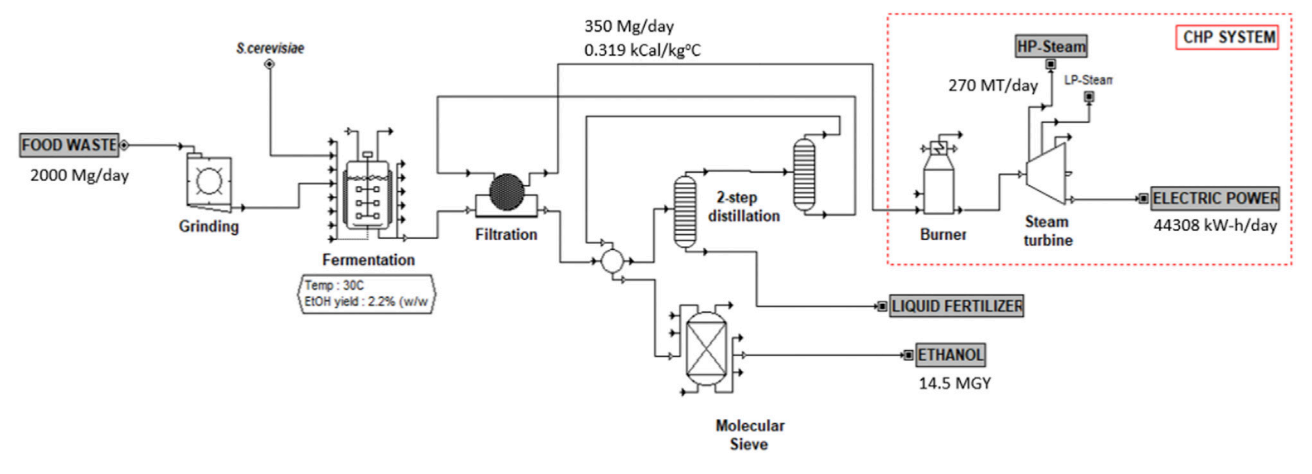

FIGURE 3 | Process flow diagram of FW fermentation with integrated CHP.

TABLE 1 | Detailed investment of CHP integrated with FW fermentation plant.

Assumption of investment Peters et al. (2003); Brown and Brown (2014)

TPEC (Total Purchased Equipment)	Value estimate by SuperPro Simulation (2018 dollars)
Purchased equipment installation	39% of TPEC
Instrument and control	26% of TPEC
Piping	31% of TPEC
Electrical system	10% of TPEC
Building (including services)	29% of TPEC
Yard improvements	12% of TPEC
Services facilities	55% of TPEC
TIEC (Total Installed Equipment Cost)	202%
Indirect cost	
Engineering	32% of TPEC
Construction	24% of TPEC
Legal and contractors' fees	23% of TPEC
TIC (Total Indirect Cost)	
Project Contingency	20% of TIC + TIEC
FCI (Fixed Capital Investment)	TIC + TIEC + Contingency
Non-depreciated Direct Cost	
Working Capital	15% of FCI
Land	6% of TPEC
TPI (Total Project Investment)	FCI + WC + Land
Lang Factor	5.46

TABLE 2 | Utility prices (EIA 2017).

Utility component	Prices
Electricity (¢/kW-h)	5.5
Water (¢/gal) (¢/L)	0.350 (0.09)
Steam ($/Mg)	12.00
Cooling water ($/Mg)	0.05
Chilled water ($/Mg)	0.40

Furthermore, the exhaust steam from the steam turbine will be captured and used for the heating system. The process diagram flow is illustrated in **Figure 3**.

The size and quantity of equipment, utilities and energy consumptions, transportation cost, labor, and raw material needed were determined by mass and energy balance from the simulation. The plant had 7,900 operating hours per year.

Techno-Economic Assumptions

Techno-economic analysis (TEA) is used to evaluate the economic viability of the CHP plant integrated with the FW based ethanol production plant. Equipment purchased cost was taken from the SuperPro Designer V9.0 software and indexed to 2018 dollars. The methodology to calculate the project investment expenditure was adopted from Peters et al., 2003. In addition to that, 3.02 installation factor was used as it is a common assumption factor for a biorenewable facilities plant. Discounted cash flow analysis spreadsheet was performed to estimate the MSE price ($/gal) with predetermined internal rate of return to generate a net present value (NPV) of zero (Brown and Brown 2014). The IRR value was set to 10% to allow the ethanol product cost to have a competitive price in the market Most of the financial assumptions have been adapted from National Renewable Energy Laboratory Reports (NREL) (Wright et al., 2010; Tao et al., 2014). The main assumptions made in this study are listed below.

- Plant capacity: 2000 Mg/day (t/day)
- Plant feedstock: FW with 78% moisture content
- Plant distance: 12 mi (19.3 km) radius (Poliafico and Murphy 2007)
- Plant life: 20 y
- Equity financed: 100%
- The internal rate of return (IRR): 10% (Short, Packey, and Holt 1995)
- General plant depreciation: 7 y with 200% double declining balance (DDB)
- CHP plant depreciation: 20 y with 150% double declining balance (DDB)

TABLE 3 | Assumptions for operator requirements for various types of process equipment (Brown and Brown 2014).

Equipment type	Operators per unit per shift
Boilers	1.0
Electric generating plants	3.0
Crushers, mills, grinders	1.0
Evaporators	0.2
Furnace	0.5
Heat exchangers	0.1
Reactors/bioreactors	0.5
Clarifiers and thickeners	0.2
Mixers	0.3
Rotary and belt filters	0.2
Screens	0.05

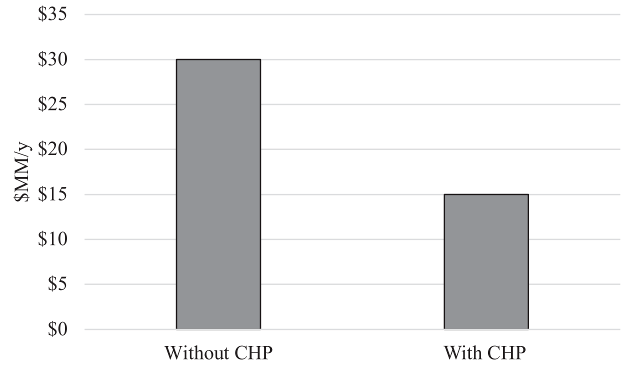

FIGURE 4 | Annual utility cost (million USD/year).

TABLE 4 | Sensitivity analysis parameters for FW fermentation process integrated with CHP.

Parameters	Optimistic	Base case	Pessimistic
Plant distance-miles radius (km radius)	8 (12.9)	12 (19.3)	24 (38.6)
Plant Capacity- Mg/day	1,000	2000	3,000
Liq. fertilizer resale value-¢/gal (¢/L)	40 (10.6)	30 (7.9)	20 (5.3)
Ethanol yield (% w/w) wet basis	2.9	2.2	1.5
Fix capital cost ($MM)	407	585	757

- CHP feedstock: bio compost with 40% moisture content
- Contingency factor: 20% from total installed equipment and indirect cost
- Construction period: 2.5 years with total capital investment spent with 8, 60 and 32% for first, second and third year respectively.
- Startup period: 6 months with considering 50% of revenues, 75% variable cost and 100% fixed expenses will be achieved.

There were three major cost areas used in the discounted cash flow analysis to estimate MSE ($/gal): Total projet investment (TPI), variabel cost ($/y) and the fixed operating cost ($/y). The detailed investment costs are shown in **Table 1** upon assumption.

Variable cost consists of the raw material cost, transportation cost, and utility cost. The utility cost depends on the energy balance of the whole process and the prices for each utulity component as shown in **Table 2**. The fixed cost consists of operating labor cost, laboratory cost, overhead, maintenance, local taxes, and insurances. The labor costs depend on the number of operators required per equipment, as listed in **Table 3**.

Economies of scale will be performed to evaluate the reduction of the product value while increasing daily feedstock volume from 10 to 5,000 Mg. From this analysis, the range of optimum feedstock value with the lower MSE value will be estimated for the future study.

Sensitivity Analysis

Further analysis is required to identify which parameter has the most significant impact on MSE value. A sensitivity analysis is a method used by modifying one parameter value while maintaining others. **Table 4** shows the sensitivity analysis parameters selected for this analysis. These parameters are identified as a powerful impact on plant economic performance.

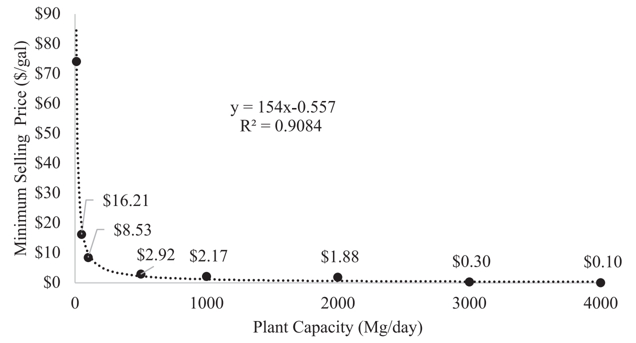

FIGURE 5 | Economies of scale for FW fermentation process integrated with CHP.

RESULTS AND DISCUSSION

Economic Analysis

This plant is designed with 2000 Mg/day of FW as a feedstock. The mass and energy balance was obtained from the simulation result. From the discounted cash flow analysis, the MSE price was estimated to $1.88 per gallon ($0.50 per liter) with yielding an NPV of zero and 10% IRR. Results from this analysis reveals that the integrated process is found to be the most economical process

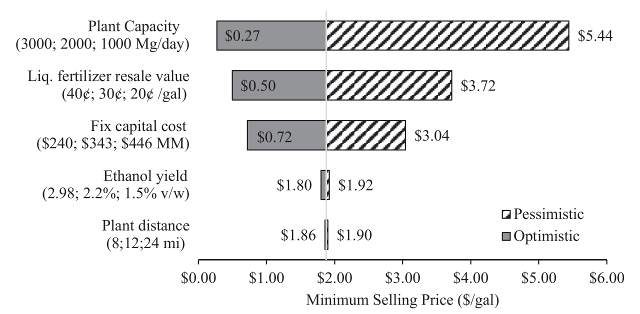

FIGURE 6 | Sensitivity analysis of FW fermentation process integrated with CHP (Optimistic is the best case scenario simulation, pessimistic is the worst case scenario simulation).

compared to the other studies from Muhammad (Muhammad 2019).

The CHP integrated plant has a value for total installed equipment cost (TIEC) and total project investment (TPI) of $221 MM and $400 MM respectively. In addition to that, the annual utility cost ($/y) without credit power and heat from CHP was $30 MM annually as detailed in **Figure 4**. However, this value reduces more than 50% by using energy generated from CHP. This finding shows that the fermentation process integrated with CHP has a significant impact on reducing the product cost.

Economies of scale for this study are represented in **Figure 5**. From the graph, there is a power relationship of –0.557 between MSE and feedstock size. It also shows that with the feedstock rate varying between 10 and 4,000 Mg per day, the MSE of ethanol ranges from $74.16 to $0.10 per gallon of ethanol. The MSE keep decreasing because there is surplus of electricity that exceeds demand. Thus, it will be sold to the grid. However, higher feedstock capacity is impossible due to the logistic problem. FW is made up of organic materials that are easily contaminated by other organisms. Therefore, proper storage is required in a loading area. Therefore it will incur the cost of operation and is not economically viable.

Sensitivity Analysis

Figure 6 shows the sensitivity analysis for this study. From the tornado chart, it indicates that feedstock plant capacity is the most influential parameter in estimating the MSE value. Increasing the amount of FW feedstock to the plant from 1,000 Mg/day to 3,000 Mg/day will decrease the value of MSE from $5.44 to $0.27 per gallon.

CONCLUSIONS

This techno-economic analysis evaluates the cost of integrated CHP with FW fermentation process in producing ethanol as the primary product. From the discussions above, waste stream can be converted into heat and power energy and utilized back to the process. This process could reduce the annual utilities cost by up to 50%. The results from discounted cash flow analysis showed that the MSE value for an integrated system is lower compared to previous study as discussed above given by $1.88 per gallon ($0.50 per liter) and $2.41 per gallon ($0.64 per liter) respectively. This finding would justify that integrated CHP with ethanol production plant is more economically attractive and more energy efficient.

Additionally, from the sensitivity analysis, results showed that the variability of feedstock plant capacity at ±100% would give an MSE value in the range of $0.27 to $5.44 per gallon. Based on the economics of scale, the graph shows that the MSE value is decreasing when the feedstock plant capacity increases. As expected, it occurs because of surplus electricity which will be sold to the grid to improve profitability. However, a higher amount of feedstock will require an extensive storage facility which is not modeled in this study. Therefore, further optimization study is recommended to be done to find the optimal feedstock plant including the storage facilities. This information is one of the essential aspects for the investors and shareholders for future consideration.

DATA AVAILABILITY STATEMENT

The raw data supporting the conclusions of this article will be made available by the authors, without undue reservation.

AUTHOR CONTRIBUTIONS

NS conducted the research, conducted the analysis, and drafted the manuscript. KR conceived the project, provided supervision, and edited the manuscript.

REFERENCES

Aschemann-Witzel, J., de Hooge, I., Amani, P., Bech-Larsen, T., and Oostindjer, M. (2015). Consumer-Related Food Waste: Causes and Potential for Action. *Sustainability* 7 (6), 6457–6477. doi:10.3390/su7066457

Brown, R. C., and Brown, T. R. (2014). "Economics of Biorenewable Resources," in *Biorenewable Resources Engineering New Products From Agriculture*. 2nd ed. (Ames, Iowa: Wiley Blackwell), 307.

Daianova, L., Dotzauer, E., Thorin, E., and Yan, J. (2012). Evaluation of a Regional Bioenergy System with Local Production of Biofuel for Transportation, Integrated with a CHP Plant. *Appl. Energ.* 92, 739–749. doi:10.1016/J.APENERGY.2011.08.016

Dias, M. O. S., Lima, D. R., and Mariano, A. P. (2018). "Techno-Economic Analysis of Cogeneration of Heat and Electricity and Second-Generation Ethanol Production from Sugarcane," in *Advances In Sugarcane Biorefinery* (London, UK: Elsevier), 197–212. doi:10.1016/B978-0-12-804534-3.00010-0

DOE (2016). *Combined Heat and Power Technology Fact Sheet Series*. U.S. Department of Energy. Available at: https://www.energy.gov/sites/prod/files/2016/09/f33/CHP-SteamTurbine.pdf (Accessed July 01, 2020).

EIA (2017). *Iowa State Energy Profile*. U.S. Energy Information Administration. Available at: https://www.eia.gov/state/print.php?sid=IA (Accessed July 01, 2020).

EPA (2018). *Advancing Sustainable Materials Management: 2015 Fact Sheet Assessing Trends in Material Generation, Recycling, Composting, Combustion* *with Energy Recovery and Landfilling in the United States*. Available at: https://www.epa.gov/sites/production/files/2018-07/documents/2015_smm_msw_factsheet_07242018_fnl_508_002.pdf (Accessed July 01, 2020).

Eriksson, G., and Kjellström, B. (2010). Assessment of Combined Heat and Power (CHP) Integrated with Wood-Based Ethanol Production. *Appl. Energ.* 87 (12), 3632–3641. doi:10.1016/J.APENERGY.2010.06.012

Gustavsson, J., Cederberg, C., Sonesson, U., van Otterdijk, R., and Meybeck, A. (2011). *Global Food Losses and Food Waste: Extent, Causes and Prevention.* Rome, Italy. doi:10.1098/rstb.2010.0126

Muhammad, N. I. S. (2019). *Comparative Assessment of the Economic and Environmental Impacts of Food Waste Fermentation on Value-Added Products*. Graduate Theses and Dissertations Iowa State University. Available at: https://lib.dr.iastate.edu/etd/17063.

Muhammad, N. I. S., and Rosentrater, K. A. (2020a). Economic Assessment of Bioethanol Recovery Using Membrane Distillation for Food Waste Fermentation. *Bioengineering* 7 (1), 15. doi:10.3390/bioengineering7010015

Muhammad, N. I. S., and Rosentrater, K. A. (2020b). Techno-Economic Evaluation of Food Waste Fermentation for Value-Added Products. *Energies* 13 (2), 436. doi:10.3390/en13020436

Papargyropoulou, E., Lozano, R., K. Steinberger, J., Wright, N., and Ujang, Z. b. (2014). The Food Waste Hierarchy as a Framework for the Management of Food Surplus and Food Waste. *J. Clean. Prod.* 76, 106–115. doi:10.1016/J.JCLEPRO.2014.04.020

Peters, M. S., Timmerhaus, K. D., and West, R. E. (2003). *Plant Design and Economics for Chemical Engineers*. 5th ed. Boston: McGraw-Hill.

Pham, T. P. T., Kaushik, R., Parshetti, G. K., Mahmood, R., and Balasubramanian, R. (2015). Food Waste-To-Energy Conversion Technologies: Current Status and Future Directions. *Waste Manage.* 38, 399–408. doi:10.1016/J.WASMAN.2014.12.004

Pirouti, M., Wu, J., Ekanayake, J., and Jenkins, N. (2010). “Dynamic Modelling and Control of a Direct-Combustion Biomass CHP Unit,” In 45th International Universities Power Engineering Conference UPEC2010, Cardiff, UK, 1–6.

Poliafico, M., and Murphy, J. D. (2007). *Anaerobic Digestion in Ireland : Decision Support System*. Ireland: Department of Civil, Structural and Environmental EngineeringCork Institute of Technology.

Raj, N. T., Iniyan, S., and Goic, R. (2011). A Review of Renewable Energy Based Cogeneration Technologies. *Renew. Sustainable Energ. Rev.* 15 (8), 3640–3648. doi:10.1016/J.RSER.2011.06.003

Short, W., Packey, D. J., and Holt, T. (1995). “A Manual for the Economic Evaluation of Energy Efficiency and Renewable Energy Technologies,” in *A Manual for the Economic Evaluation of Energy Efficiency and Renewable Energy Technologies* (Golden, CO). doi:10.2172/35391

Suwannarat, J., and Ritchie, R. J. (2015). Anaerobic Digestion of Food Waste Using Yeast. *Waste Manage.* 42, 61–66. doi:10.1016/j.wasman.2015.04.028

Tao, L., Schell, D., Davis, R., Tan, E., Elander, R., and Bratis, A. (2014). “NREL 2012 Achievement of Ethanol Cost Targets: Biochemical Ethanol Fermentation via Dilute-Acid Pretreatment and Enzymatic Hydrolysis of Corn Stover,” in *NREL 2012 Achievement of Ethanol Cost Targets: Biochemical Ethanol Fermentation via Dilute-Acid Pretreatment and Enzymatic Hydrolysis of Corn Stover* (United States: Golden, CO). doi:10.2172/1129271

Wright, M. M., Daugaard, D. E., Satrio, J. A., and Brown, R. C. (2010). Techno-Economic Analysis of Biomass Fast Pyrolysis to Transportation Fuels. *Fuel* 89, S2–S10. doi:10.1016/J.FUEL.2010.07.029

Conflict of Interest: The authors declare that the research was conducted in the absence of any commercial or financial relationships that could be construed as a potential conflict of interest.

frontiers in Energy Research

ORIGINAL RESEARCH
published: 01 September 2021
doi: 10.3389/fenrg.2021.718310

The Role of Biowaste: A Multi-Objective Optimization Platform for Combined Heat, Power and Fuel

Rafael Castro-Amoedo[1]*, **Nicolas Morisod**[2], **Julia Granacher**[1] **and François Maréchal**[1]

[1]Industrial Process and Energy Systems Engineering (IPESE), École Polytechnique Fédérale de Lausanne, Lausanne, Switzerland, [2]Satom SA, Monthey, Switzerland

Biomass, bioenergy and negative emission technologies are inherent to the future design of energy systems. Urban clusters have a growing demand for fuel, heat and electricity, which is both a challenge and an opportunity for biomass-based technologies. Their deployment should meet demand, while minimizing environmental impact and staying cost-competitive. We develop a systematic approach for the design, evaluation and ranking of biomass-to-X production strategies under uncertain market conditions. We assemble state-of-the-art and innovative conversion technologies, based on feedstock, by-products and waste characteristics. Technical specifications, as well as economic and environmental aspects are estimated based on literature values and industry experts input. Embedded into a bi-level mixed-integer linear programming formulation, the framework identifies and assesses current and promising strategies, while establishing the most robust and resilient designs. The added value of this approach is the inclusion of sub-optimal routes which might outperform competing strategies under different market assumptions. The methodology is illustrated in the anaerobic digestion of food and green waste biomass used as a case study in the current Swiss market. By promoting a fair comparison between alternatives it highlights the benefits of energy integration and poly-generation in the energy transition, showing how biomass-based technologies can be deployed to achieve a more sustainable future.

Keywords: multi criteria decision analysis, energy system design, biomass, decision-making, uncertainty analysis, robust design, decision support, environmental policy

Edited by:
Ana Somoza-Tornos,
University of Colorado Boulder,
United States

Reviewed by:
Emmanuel Ogbe,
ExxonMobil, United States
Mariano Martín,
University of Salamanca, Spain

***Correspondence:**
Rafael Castro-Amoedo
rafael.amoedo@epfl.ch

Specialty section:
This article was submitted to Process and Energy Systems Engineering, a section of the journal Frontiers in Energy Research

Received: *31 May 2021*
Accepted: *20 July 2021*
Published: *01 September 2021*

Citation:
Castro-Amoedo R, Morisod N, Granacher J and Maréchal F (2021) The Role of Biowaste: A Multi-Objective Optimization Platform for Combined Heat, Power and Fuel. Front. Energy Res. 9:718310. doi: 10.3389/fenrg.2021.718310

1 INTRODUCTION

The global energy system is changing due to the need of curbing greenhouse gas emissions. The large majority of European countries have set ambitious goals by defining a carbon-neutral policy by 2050. Achieving a sustainable future relies not only on the introduction of renewable feedstocks and energy sources but also on efficient and integrated systems. Energy from biomass is one of the most widely explored research fields in energy and environmental science. Defined as a carbon-neutral energy source, biomass can be regarded as a promising energy storage option, compensating for the progressive phase-out of fossil fuels. In this context, Sepulveda et al. (Nestor, 2021) have recently highlighted the role of firm low-carbon technologies in balancing future energy systems, decisively contributing for cost-effective zero-emission systems. The policy-enhanced requirement to generate negative CO_2 emissions places biomass in the center of renewable energy use (IRENA, 2016). As of 2018, modern bioenergy [1] roughly represented half of the generated renewable energy while accounting for only 5% of global final energy consumption (REN21, 2020). The potential to achieve a higher share exists: as a versatile feedstock, biomass has a large plethora of downstream processing options, including the production of different fuels, on top of heat and electricity.

Future energy strategies plan a massive deployment of renewable energy, intensifying periods of surplus electricity (summer) with periods of intense demand (winter). As pointed out by Candra, Hartmann, and Nelles (Candra et al., 2018) the greater the share of renewables, the more frequently the price of electricity will approach zero. For debottlenecking the offset of demand and supply and its implication on electricity price, chemical storage can be applied. In periods with surplus electricity, chemical storage - offered by thermochemical biomass conversion - benefits from a cheap (or even free) electricity market, while electricity production is economically unattractive. We should not be surprised then to find a growing need for flexible poly-generation systems that can easily accommodate seasonal fluctuations.

As a broad category, biomass is a limited resource disputed for food, feed and fuel as recently reviewed by Muscat et al. (2020). The ongoing debate pertains to the competition for land, water, labor and capital. Biowaste, however, does not suffer from such competition. A growing concern with sustainability metrics and circular economy regards it as a resource, questing for attractive economic and environmental conversion routes, beyond the prime safe disposal concern. Urban biowaste, in particular, represents the organic residue issuing from households, municipalities, and industries that is separately collected from other municipal solid waste fractions (Steubing et al., 2010). It accounts for food waste (FW) residues from either households or professionals and municipal residues such as garden leftovers and sweepings, commonly labeled as green waste (GW). In Switzerland, as pointed out by Burg et al. (2019), urban biowaste generation has been steadily increasing for the past 20 years. Steubing et al. (2010) noted that from a current sustainable energy potential of 8.2 PJ, only 5.5 PJ (67%) is presently used. The study does not mention, however, the efficiency of the conversion processes. The unused biowaste potential triggers, besides a clear energy loss, an additional problem from an environmental perspective due to the natural partial decomposition of organic fractions into nitrous oxide (N_2O) and methane (CH_4).

Burg et al. (2019) went further and estimated the long-term (up to 2050) potential of wet bioenergy resources in Switzerland by means of a Monte Carlo simulation. Based on an increasing trend in consumer patterns and waste generation, side by side with better management policies and consumer engagement, the study calls for and validates long-term investment in biomass-to-energy infrastructure. In particular, anaerobic digestion and biogas generation are expected to dominate biowaste management policy by 2050. However, the study does not explore different digestate (the remainder of anaerobic digestion) disposal alternatives or biogas downstream processing but rather assumes their use as a fertilizer and an energy source, respectively. Moreover, the approach foregoes the potential risk of soil contamination as highlighted in Nkoa (2014), and misses the important energy system perspective of employing biogas as a chemical building block.

Collection and transport of biomass to conversion facilities are non-negligible factors. Schnorf et al. (2021) studied key biomass transport chains in Switzerland and identified the cost as the main barrier to biomass transport, whereas energetic and environmental benefits largely justify the involved logistics. On economic grounds, break-even distances range from 36 to 477 km, depending on the feedstock, and requiring between 0.4 and 5% of its embodied energy. The decentralized fashion of urban biowaste collection, spatially distributed according to population demographics, sets an average distance between source nodes and treatment facilities below 30 km - thereby not jeopardizing the transportation of biomass from an economic point of view.

Current state-of-the-art technologies for energy production, such as combined heat and power (CHP), rely heavily on fossil fuels. The defossilization of the energy sector opens the door to new technologies, such as heat pumps or geothermal wells, along with more versatile feedstocks. Urban biowaste, in particular, can be converted to store energy products by a variety of means, such as digestion, gasification or liquefaction. As borne out by Celebi et al. (2019), a combination of technologies is particularly suitable not only to address high-temperature heat needs but also to boost system and conversion efficiency. While digestion produces biogas, the co-generation of digestate can be thermally valued in either gasification or liquefaction units, producing excess heat in the medium-to high-temperature range by cooling down producer gas and liquid products, respectively. Enhanced heat integration allows further recovery which can be used for electricity production (via expansion/steam turbine), process integration with different energy-intensive stages such as drying or even the integration with other industrial clusters.

Biomass gasification is a thermochemical process designed to obtain value-added products (CH_4, H_2, CO, CO_2), from potentially low-cost feedstocks, combining high efficiency (Gassner and Maréchal, 2012) and desirably low investment and operating costs. Urban biowaste and digestate, oftentimes readily available, constitute a potentially free feedstock, making them a viable and promising energy source. Moreover, gasification is able to handle lignocellulosic rich streams which anaerobic digestion - the state-of-the art technology for biowaste - cannot. According to Sikarwar et al. (2016) the three most common gasifiers - the fixed bed, the fluidized bed and the entrained flow - contribute to the gasification capacity of handling a wide range of biomass compositions, making it a suitable technology to value seasonal-dependent waste fractions. Gasification comprises several steps prior to the gasifier such as feedstock drying, pyrolysis and partial combustion. Air is the most common gasifying media, but oxygen, steam of carbon monoxide are also used. However, investment costs can be as

---

[1] excludes biomass used for cooking and heating in inefficient stoves.

much as three times the one of incineration (Sikarwar et al., 2016).

Watery feedstocks, among which food waste or digestate, are better handled by catalytic hydrothermal gasification (CHTG), in which water is kept at supercritical conditions, prompting inorganic salts precipitation. It overcomes the need for the pre-drying step associated with conventional gasification, since it requires a pumpable (below 20 wt% solids) input material. CHTG, when compared to conventional gasification, shows higher overall conversion efficiency and reduced tar formation (Mian et al., 2015). However, it requires both high-pressure (above 220 bar) and high-temperature (above 400°c) conditions which impact the investment cost. Nevertheless, as pointed out by Sikarwar et al. (2016) the poly-generation concept of biomass gasification brings flexibility and increased efficiency due to potential mass and heat integration synergies.

Several authors, among which Granacher (2019), have addressed gasification and liquefaction technologies for biomass. Damartzis and Zabaniotou (2011) reviewed and ranked different biomass-to-biofuels gasification designs based on economic and environmental performance metrics. Korberg et al. (2021) highlighted the use of gasification to valorize different biomass types in a low-carbon future scenario, while Magagula et al. (2021) simulated and investigated ways to promote energy-neutral gasification processes. Segurado et al. (2019) reviewed polygeneration systems coupled with biomass gasification; although hindered from the economic perspective, biomass gasification requires more study and would profit from optimization frameworks that are able to capture different market realities. Mian et al. (2015) studied hydrothermal gasification of microalgae in a multi-objective optimization framework; Gassner and Maréchal developed a thermo-economic optimization decision-support methodology for lignocellulosic biomass, whereas Celebi et al. (2019) developed a similar concept for woody biomass. Castro-Amoedo et al. (2020) considered both gasification and liquefaction for sewage sludge. Together these studies provide important insights into the thermochemical pathways to convert different types of feedstock. Cheng et al. (2020) reviewed a large number of studies on urban biowaste and emphasized the need to develop a wide range of value-added products, promoting a bio-based circular economy, rather than focusing on the peculiar aspects of anaerobic digestion and composting.

Research Gaps and Objectives

Biomass treatment technologies are manifold and hold promising potential. Their combination and potential synergies are of uttermost importance in a fast and evolving energy system. The literature is abundant with examples of single conversion technologies, but rather neglects holistic and integrated approaches, especially when embedding uncertainty features.

In this work we provide a strategic perspective on how to move toward economically and environmentally sound biowaste conversion systems, by considering a systematic approach. Developing a methodology to simultaneously assess, compare and rank system designs, contributes to close the gap in the future bio-based economy. Indeed, the discussion is of particular relevance in the context of rapid urbanization, increasing environmental awareness and regulations, and the interaction between environment and energy systems. We critically assess, in an operational context, the economic, environmental and thermodynamic aspects of solutions. A two-level optimization framework, using a mixed-integer linear programming (MILP) model is built to study system designs under different pricing and market conditions - showing how they can provide benefits to the local energy ecosystem.

By applying our modeling framework to a cluster of 400,000 people equivalent, this work provides a prime example on the opportunities arising from the poly-generation of heat, electricity and fuels in urban biowaste treatment. We expand on the benefits of anaerobic digestion by showing that, when coupled with biogas upgrade and digestate treatment units, it opens the door to inexpensive fuel production, whether in the form of synthetic natural gas, formic acid or both. Constant biowaste generation and a non-limiting demand for each final product are assumed. Different economic assumptions introduce flexibility to handle volatile resource prices while profiting from changes across the year, such as carbon-free or zero-marginal cost renewable electricity production. The insights we derive are applicable to other biomass-based systems and should contribute to broadening the discussion on the best strategy for handling biomass feedstocks and meeting the current and future energy demand.

The paper is outlined as follows: in **Section 2** the methodology is outlined, starting with the conversion modeling strategy, followed by the energy integration model and mathematical formulation, and leading to the evaluation and ranking system. The specifications of the case study are discussed alongside modeling options. In **Section 3**, we apply the methodology to the case study; system designs are clustered, analyzed, evaluated and ranked, highlighting the robustness of the procedure, but also bottlenecks and limitations. **Section 4** concludes the work, arguing on the suitability of the methodology to handle biomass-based challenges and contribute to the future energy system.

2 METHODS AND APPLICATION

The optimization of complex integrated energy systems, as mentioned in Maronese et al. (2015) and Tock and Maréchal (2015), is very time consuming, underscoring the need to develop and use a methodology that sets-up simple parameterized models. Thermodynamic, economic and environmental aspects need to be considered simultaneously for identifying promising designs inside an intricate structure without requiring complex solving strategies. A master-slave partition on a bi-level optimization methodology (**Figure 1**) is developed for this purpose. The master level controls multi-objective framework by sending optimization inputs to the MILP - which works at the slave level - further retrieving design variables and performance indicators. It is a variation of the comprehensive **A**nalyse **G**enerate **I**nterpret **R**eport and React (AGIR) approach, first proposed by Maréchal and Kalitventzeff (1997). Therein, the **A**nalyse step

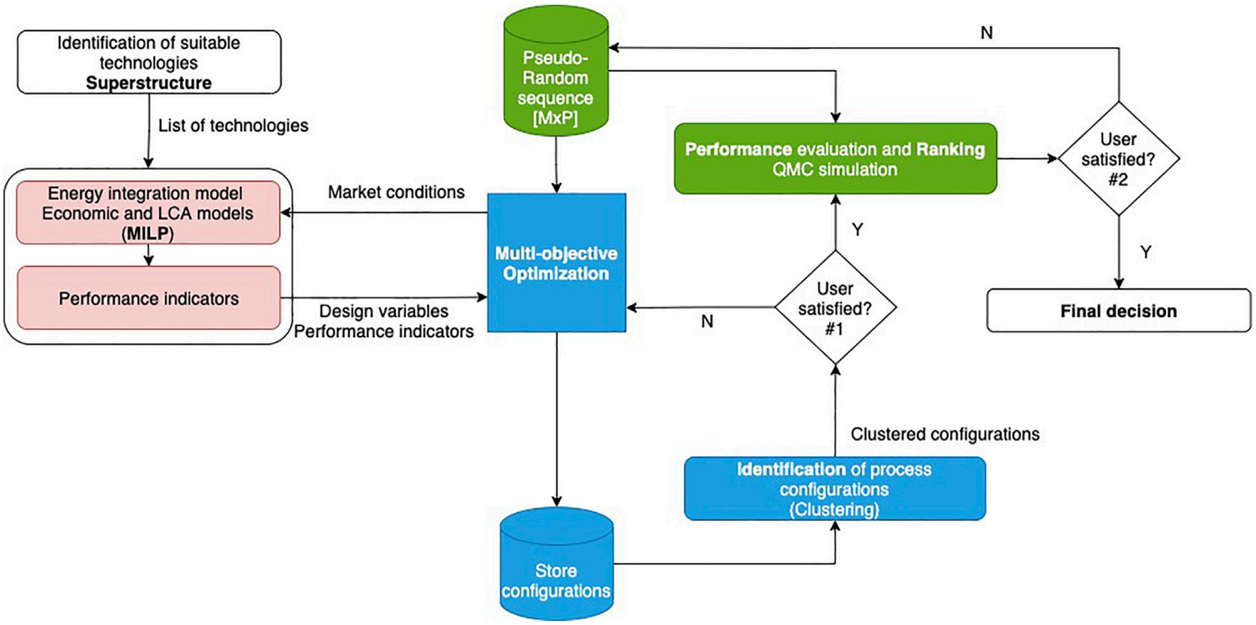

FIGURE 1 | Solution generation procedure; blue and red shapes refer to the master and slave level, respectively. Green shapes are user controlled.

consists in the definition of system boundaries and identification of possible system units with their corresponding economic and environmental models. In the **G**enerate step, optimization tools are used to create a list of system configurations by activating and sizing units while defining appropriate operating conditions. **I**nterpret creates meaningful indicators for the associated values of decision values, whereas **R**eport and React is responsible for the user interaction part, ultimate responsible to define, upon proper interpretation, a new AGIR procedure.

2.1 Superstructure

A superstructure is built by aggregating into a single entity all process models related to the conversion of the feedstock to different products and by-products. There is no practical limit to the number of process models to be added, provided they are suitable to handle the feedstocks and intermediate products.

A superstructure defines the main process steps - setting up thermodynamic and technically feasible operating conditions - while accounting for physical and chemical transformations, in addition to resource needs and heat requirements. Options for heat recovery and the energy conversion system (utility systems) are added, such as heat pumps, Rankine cycles and gas boilers. A similar superstructure concept was developed by Santibañez-Aguilar et al. (2013), Maronese et al. (2015) and Castro-Amoedo et al. (2020).

The quantity and quality of available data shapes the accuracy of the overall model. Flowsheeting software (e.g., Aspen) can be used for a conversion technology or a utility system, while models not involving thermodynamic considerations are based on literature values. Each model defines an interface with the rest of the process, with the internal mathematical formulation used to describe input/output relations appearing as a blackbox for the energy integration and process synthesis model. This feature allows combining models from different software and literature sources. The major challenge is the accurate representation of operating conditions on mass and energy balances; these balances define material conversion but also heat (with corresponding temperature levels θ_k, if applicable) and power requirements, further used for energy integration. To build a thermo-environomic representation for the energy integration optimization problem, an economic model is used to estimate operating and investment costs, whereas a life cycle assessment one links material and energy flows with the corresponding life cycle inventory process. A key attribute of this approach is the embedded linearity of all features with respect to a reference size - therefore assuming constant efficiency.

2.2 Energy Integration Model

The total cost of the process is minimized by computing thermodynamically feasible energy targets. These targets are achieved by optimizing heat recovery and combining heat, power and fuel generation while activating different conversion units - hence defining the least expensive energy conversion system. The problem is solved using a MILP (described in **Section 2.3**).

The energy integration model relies on the definition and identification of hot and cold stream profiles and respective minimum approach temperature, which allows to define hot and cold composite curves. Pinch identification (Linnhoff and Hindmarsh, 1983; Maréchal and Kalitventzeff, 1998a) and graphical analysis enable further process suggestions and improvements regarding conversion technologies and heat integration. The quality of process integration has a direct impact on the process performance, and should be tackled by key performance indicators.

2.3 Mathematical Formulation

The overall problem follows a MILP formulation, allowing for the inclusion of the discrete (binary) and continuous behavior of the system, while ensuring the required robustness. Discrete time intervals $t \in \mathbf{T} = \{1, 2, \ldots, t_t\}$, with duration t^t_{op}, are employed to account for time-dependent variables and parameters, capturing the dynamic nature of the problem. The system is represented through units belonging to the set **U**, grouped in 2 subsets: process units (**PU**) and utility units (**UU**). The former represent units added with a fixed size (**Eq. 8**), associated with either a demand and/or a system imperative (e.g., waste collection), while the latter represent energy technologies and markets used to satisfy process units - sized between a minimum ($f^{\min}_u$) and maximum ($f^{\max}_u$) values (**Eq. 6**). Each unit can supply, demand or convert resources ($r \in \mathbf{R}$) and heat, within temperature intervals $k \in \mathbf{K} = \{1, 2, \ldots, n_k\}$.

The MILP objective is the minimization of total cost - Tc (**Eq. 1**). Operating expenditures - Opex (**Eq. 2**) account for fixed ($c^{\mathrm{op},1}_u$) and variable ($c^{\mathrm{op},2}_u$) units operating cost, as well as resources import ($\tilde{c}^-_{r,t}$) and export ($\tilde{c}^+_{r,t}$) costs, associated with the amount imported ($\dot{M}^-_{r,t}$) and exported ($\dot{M}^+_{r,t}$), respectively. Annualized capital expenditures - Capex (**Eq. 3**) - consider fixed ($\tilde{c}^{\mathrm{inv},1}_u$) and variable ($\tilde{c}^{\mathrm{inv},2}_u$) fractions, annualized with a project lifetime ($\tilde{n}$) and an interest rate ($\tilde{i}$). Binary variables ($y_{u,t}$, y_u) are used for utility selection and continuous variables ($f_{u,t}$, f_u) for unit sizing (**Eq. 7**)

The ϵ constraint method is used for multi-objective optimization, by constraining the environmental impact (**Eq. 5**). Sobol sampling is used to generate different values of ϵ_m; $s_{m,\epsilon}$ refers to the entrances on the sampling matrix $S_{M,P}$; ϵ^{max} and ϵ^{min}, to upper and lower boundaries coming from single optimization of the environmental impact, respectively. The approach works as a grid in the objective domain, with M market scenarios generation and P uncertain parameters, the latter identified by a ($\tilde{}$) on the respective definition.

$$\min_{f_u,\, y_u,\, f_{u,t},\, y_{u,t}} \quad \mathrm{Tc} = \mathrm{Opex} + \mathrm{Capex} \tag{1}$$

with:

$$\mathrm{Opex} = \sum_{t=1}^{t_t} \left(\sum_{u=1}^{n_u} \left(c^{\mathrm{op},1}_u y_{u,t} + c^{\mathrm{op},2}_u \cdot f_{u,t} \right) + \sum_{r=1}^{n_r} \left(\tilde{c}^-_{r,t} \cdot \dot{M}^-_{r,t} - \tilde{c}^+_{r,t} \cdot \dot{M}^+_{r,t} \right) \right) \cdot \frac{1}{\dot{M}^-_{biowaste,t}} \cdot t^t_{op} \qquad [\$/\mathrm{t_{biowaste}}] \tag{2}$$

$$\mathrm{Capex} = \sum_{u=1}^{n_u} \frac{\tilde{i}\,(1+\tilde{i}\,)^{\tilde{n}}}{(1+\tilde{i}\,)^{\tilde{n}} - 1} \left(c^{\mathrm{inv},1}_u y_u + c^{\mathrm{inv},2}_u f_u \right) / \sum_{t=1}^{t_t} \dot{M}^-_{biowaste,t} \cdot t^t_{op} \qquad [\$/\mathrm{t_{biowaste}}] \tag{3}$$

$$\mathrm{Impact} = \sum_{t=1}^{t_t} \left(\sum_{u=1}^{n_u} \left(c^{\mathrm{imp}}_u f_{u,t} \right) + \sum_{r=1}^{n_r} \left(k^-_{r,t} \cdot \dot{M}^-_{r,t} - k^+_{r,t} \cdot \dot{M}^+_{r,t} \right) \right) \cdot \frac{1}{\dot{M}^-_{biowaste,t}} \cdot t^t_{op} \leq \epsilon_m \qquad [\mathrm{Env.Impact/t_{biowaste}}] \tag{4}$$

$$\epsilon_m = \epsilon^{min} + s_{m,\epsilon} \cdot (\epsilon^{max} - \epsilon^{min}), \quad m = 1, \ldots, M \tag{5}$$

$$f^{\min}_u y_{u,t} \leq f_{u,t} \leq f^{\max}_u y_{u,t}, \quad \forall u \in \mathbf{U},\ \forall t \in \mathbf{T} \tag{6}$$

$$y_{u,t} \leq y_u, \qquad f_{u,t} \leq f_u \quad \forall u \in \mathbf{U},\ \forall t \in \mathbf{T} \tag{7}$$

$$f^{\max}_u = f^{\min}_u = 1, \quad \forall u \in \mathbf{PU} \tag{8}$$

Material and energy flow models contain physical properties used to define both mass and energy requirements. $\dot{m}^+_{r,u,t}$ and $\dot{m}^-_{r,u,t}$ define the reference mass flowrate of resource r produced and consumed, respectively, in unit u at time step t. **Equation 9** establishes that requirements for each resource are satisfied by inside production and imports. The resource consumption interacts with the overall resource balance and ensures that import, export and production are balanced, as formulated in **Eq. 10**. The mass balance is closed for each resource layer (**Eq. 11**), with the amount of resource r per consuming/supplying unit j/i in time step t ($\dot{M}^-_{r,j,t}/\dot{M}^+_{r,j,t}$) balanced by internal needs and connection flowrates of resource r between supplying unit i (**SU**) and consuming unit j (**CU**) given by $\dot{m}_{r,i,j,t}$ - (**Eqs. 12**, **13**).

$$\sum_{u=1}^{n_u} f_{u,t} \cdot \dot{m}^+_{r,u,t} + \dot{M}^-_{r,t} - \sum_{u=1}^{n_u} f_{u,t} \cdot \dot{m}^-_{r,u,t} \geq 0, \quad \forall r \in \mathbf{R}, \forall t \in \mathbf{T} \tag{9}$$

$$\sum_{u=1}^{n_u} f_{u,t} \cdot \dot{m}^+_{r,u,t} + \dot{M}^-_{r,t} - \dot{M}^+_{r,t} - \sum_{u=1}^{n_u} f_{u,t} \cdot \dot{m}^-_{r,u,t} = 0, \quad \forall r \in \mathbf{R}, \forall t \in \mathbf{T} \tag{10}$$

$$0 = \sum_r f_{u,t} \cdot (\dot{m}^+_{r,u,t} - \cdot \dot{m}^-_{r,u,t}), \quad \forall u \in \mathbf{U}, \forall t \in \mathbf{T} \tag{11}$$

$$\dot{M}^-_{r,j,t} + \sum_{i=1}^{n_i} \dot{m}_{r,i,j,t} = f_{j,t} \cdot \dot{m}^-_{r,j,t} \quad \forall r \in \mathbf{R}, \forall j \in \mathbf{CU}, \forall t \in \mathbf{T} \tag{12}$$

$$\dot{M}^+_{r,i,t} = f_{i,t} \cdot \dot{m}^+_{r,i,t} - \sum_{j=1}^{n_j} \dot{m}_{r,i,j,t} \quad \forall r \in \mathbf{R}, \forall i \in \mathbf{SU}, \forall t \in \mathbf{T} \tag{13}$$

The approach developed in Maréchal and Kalitventzeff (1998b), based on the work of Linnhoff and Hindmarsh (1983) is used to satisfy the minimum energy requirements. The energy balance is closed in each temperature interval k (**Eq. 14**) and residual heat ($R_{t,k}$) flows from higher (k) to lower ($k-1$) temperature (θ) levels. Following thermodynamic feasibility, cascaded heat flows are positive, and values in both the first and the last interval k are zero (**Eq. 15**). $q_{u,t,k}$ is the reference heat load for unit u in time step t and temperature interval k.

$\forall k \in \mathbf{K}$ with $\theta_{k+1} \geq \theta_k$

$$\sum_{u=1}^{n_u} \dot{q}_{u,t,k} \cdot f_{u,t} + \dot{R}_{t,k+1} - \dot{R}_{t,k} = 0 \quad \forall t \in \mathbf{T} \tag{14}$$

$$\dot{R}_{t,k} \geq 0, \quad \dot{R}_{t,1} = \dot{R}_{t,nk+1} = 0 \quad \forall t \in \mathbf{T} \tag{15}$$

The MILP problem is written in AMPL (AMPL et al., 2013) and solved by IBM ILOG CPLEX Optimization Studio (IBM ILOG Cplex, 2009). Indices, sets, variables and parameters used in the formulation are resumed in the Nomenclature section.

TABLE 1 | Key performance indicators.

KPI	Description	
Opex	Operating expenditure	[\$/$t_{biowaste}$]
Capex	Investment expenditure	[\$/$t_{biowaste}$]
Tc	Total cost	[\$/$t_{biowaste}$]
Impact	Environmental impact	[$kgCO_2/t_{biowaste}$]
ϵ	Global efficiency	[–]
ϵ_{el}	Electrical efficiency	[–]
ϵ_{th}	Thermal efficiency	[–]
ϵ_{ch}	Chemical efficiency	[–]
Pbt	Pay-back time	[y]
Cf	Complexity factor	[-]

2.4 Performance Indicators

Distinct process options are evaluated on thermodynamic, economic and environmental aspects (**Table 1**). They are suitable to compare and rank solutions, allowing for simultaneous bench-marking with similar studies and publications. Thermodynamic indicators such as efficiencies are able to capture the quality and extent of process integration and heat recovery, but also the efficiency of a chemical conversion. Electrical (**Eq. 16**), thermal (**Eq. 17**), chemical (**Eq. 18**) and global (**Eq. 19**) efficiencies are thus considered. Δh^0 reports to the lower heating value on a dry basis of the respective products. Economic metrics comprise financial indicators (Capex, Opex and Tc) but also the pay-back time (**Eq. 20**), which evaluates the time needed for investment recovery. A complexity factor (**Eq. 21**) accounts for the number of activated technologies, with lower values representing simpler systems.

$$\epsilon_{el} = \frac{M^{+}_{elec}}{\Delta h^{0}_{bw}\dot{m}^{-}_{bw} + M^{-}_{elec}} \tag{16}$$

$$\epsilon_{th} = \frac{M^{+}_{heat}}{\Delta h^{0}_{bw}\dot{m}^{-}_{bw} + M^{-}_{elec}} \tag{17}$$

$$\epsilon_{ch} = \frac{\Delta h^{0}_{Biocrude}\dot{m}^{+}_{Biocrude} + \Delta h^{0}_{SNG}\dot{m}^{+}_{SNG} + \Delta h^{0}_{FA}\dot{m}^{+}_{FA}}{\Delta h^{0}_{bw}\dot{m}^{-}_{bw} + M^{-}_{elec}} \tag{18}$$

$$\epsilon = \frac{\Delta h^{0}_{Biocrude}\dot{m}^{+}_{Biocrude} + \Delta h^{0}_{SNG}\dot{m}^{+}_{SNG} + \Delta h^{0}_{FA}\dot{m}^{+}_{FA} + M^{+}_{elec} + M^{+}_{heat}}{\Delta h^{0}_{bw}\dot{m}^{-}_{bw} + M^{-}_{elec}} \tag{19}$$

$$\text{Pbt} = \frac{\sum_{u=1}^{n_u} c_u^{\text{inv1}} y_u + c_u^{\text{inv2}} f_u}{\Delta\text{Opex}} \tag{20}$$

$$\text{Cf} = \frac{\sum_{u=1}^{n_u} y_u,\ \forall u\colon y_u = 1}{\sum_{u=1}^{n_u} y_u} \tag{21}$$

2.5 Solution Generation and Clustering

Varying market settings - at the random sequence generator level - ensures the generation of configurations which, under constant/nominal market conditions, would not emerge. The procedure is controlled by the master (multi-objective optimization) level and executed by the slave MILP model. The former is responsible for receiving random Sobol parameters and forward them to the latter that minimizes total cost, while deciding on the existence and size of each superstructure unit. The master level stores configurations and repeats the procedure for the M market scenarios generated.

The generation procedure is neither sensitive to repeated solutions nor to numerically-close ones. Indeed, solutions exist with designs close enough to be considered identical in practical applications. By applying clustering, the number of relevant solutions is reduced according to a similarity measure. The number of clusters is decided based upon state-of-the-art Silhouette (Rousseeuw, 1987) and Elbow (Davies and Bouldin, 1979) methods, following data normalization, which removes the mean and scales data to unit variance. The K-medoids algorithm is used for clustering, relying upon the set of existing solutions for centroid representation, avoiding therefore non-realistic centroids as provided by the k-means algorithm. As clustering is not based on KPIs but rather on configurations, sub-optimal solutions under current market conditions are selected, which might then become optimal on a different set of market values.

2.6 Ranking and Performance Evaluation

The use of a quasi Monte-Carlo (QMC) simulation, making use of a low-discrepancy Sobol sequence, recomputes performance indicators for each cluster centroid and for each set of market conditions. The use of a quasi-random sequence is associated with higher sampling efficiency, compared to classic pseudo-random methods (Hou et al., 2019), which justifies its increasing use in sensitivity and uncertainty analysis. This procedure allows to bound and rank solutions, but also to produce statistical insights. For each set of market conditions and for each KPI, a solution is rewarded with 1 point if it is among the top-three performances. Scores are then normalized, outlining the design with the best probabilistic performance globally (defining a total score) and per KPI - thus promoting a robust, informed and reliable decision-making procedure. As design problems involve decisions on a long time-horizon (normally 10–20 years), the need to account for market variability and unpredictability is paramount. In that regard, et al. (Moret et al., 2017) highlighted the relevance of economic scenarios on energy planning systems and signaled the risk of using *a priori* selection of uncertain parameters.

2.7 Main Highlights of the Methodology

Although our method can run with no user intervention, it would benefit from an interactive user - focusing on providing thoughtful and subjective insight. Based upon the solutions ranking, the user evaluates the suitability of each configuration while taking into account the objective criteria provided by optimization (user satisfied #2, **Figure 1**). If satisfied, the process ends and proceeds for decision. If not, provided the designs are judged adequate, the user can control and change the parameters at the QMC simulation step, recomputing performance indicators and retrieving new results until an acceptable outcome is reached. On the other hand, if a reasonable design is not reached (user satisfied #1, **Figure 1**), steering market conditions at the master level

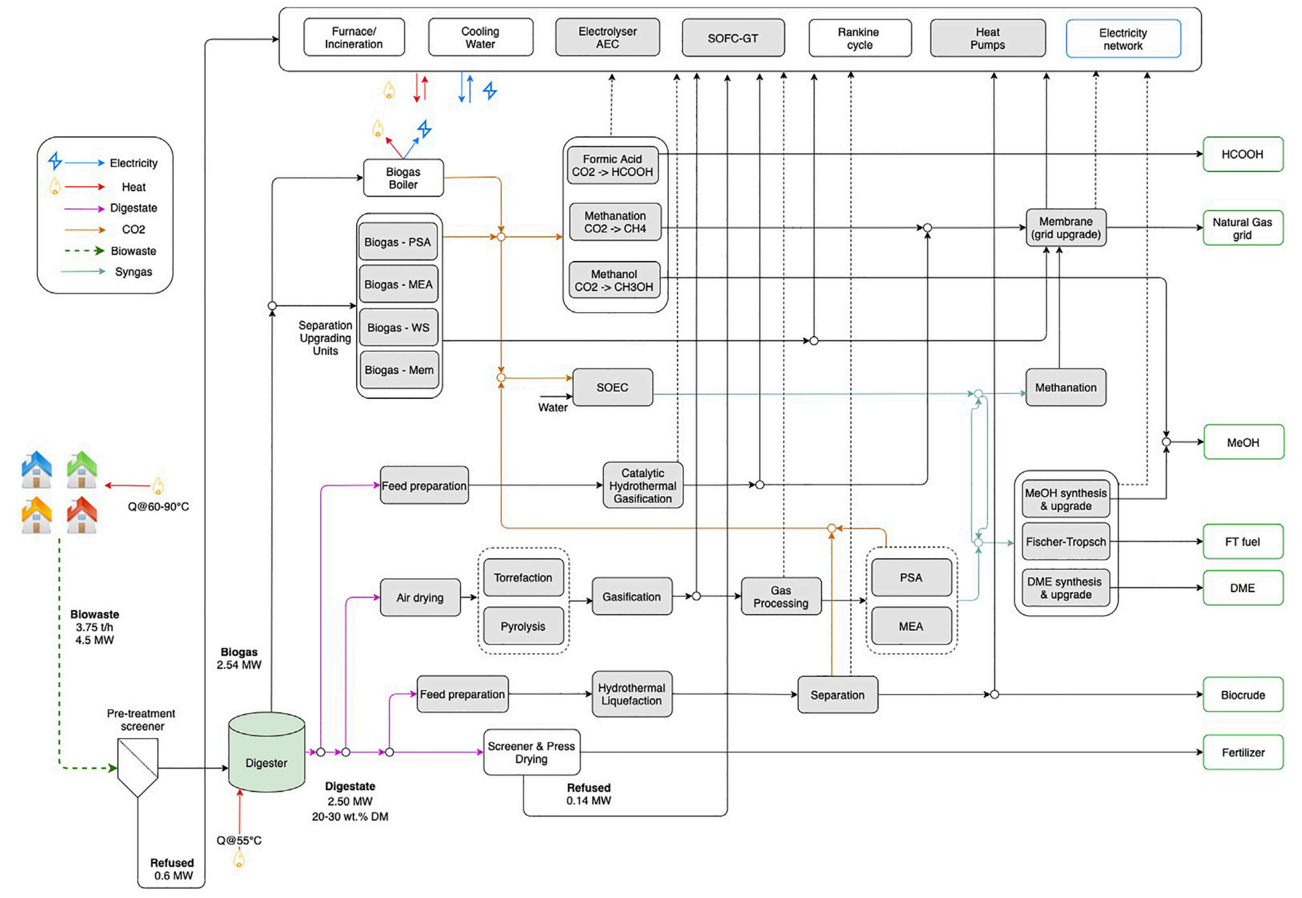

FIGURE 2 | Urban biowaste superstructure with average yearly values. Gray fill units are proposed investments. WS - water scrubbing; Mem - polymeric dry membranes.

will generate a new set of configurations. The robustness of the model allows for minimal involvement, mainly circumscribed to a phase when a large set of solutions is available. This reinforces the confidence of non-specialists in optimization tools and promotes engagement, reducing the likelihood of missing good solutions.

2.8 Case-Study Application

A biowaste superstructure is depicted in **Figure 2**, with connections for different combined heat, power and fuel strategies. The units in gray require investment, updated to 2019 values using the chemical engineering plant cost index (CEPCI). Biowaste generation of 3.75 t/h and 4.5 MW corresponds to 400,000-person equivalent, which is used as the reference population. The network diagram (**Supplementary Appendix Figure A9**) shows both the source nodes and the biowaste treatment facility. A monthly resolution (twelve time steps) covering a full year of operation is used to capture the variation of seasonal parameters and make use of data provided by the industrial partner.

Superstructure Modeling

Models are the core of the conversion process description, allowing to formulate the transformation from feedstock to final value-added products. Surrogate and blackbox models, which are simplified representations of complex systems, originate from literature values, experts input or detailed simulation models in flowsheet software. Belsim (2018) and Al-Malah (2016), both simulation software, use compositions and characteristics of digestate to generate simplified models. Each model has a reference flow or size (e.g., reference input digestate) that is linearly scaled considering input/output of mass and energy flows. Regardless of the size, constant efficiency is assumed; costs have a linear dependency with unit's size. **Supplementary Appendix Tables A7** and **A8** summarize key assumptions and input/output values. In particular, temperature-enthalpy profiles are defined and fixed for each conversion unit, therefore not subjected to optimization. **Supplementary Appendix Tables A5** and **A6** describe environmental and economic assumptions, respectively. In this section only the most relevant modeling strategies are presented.

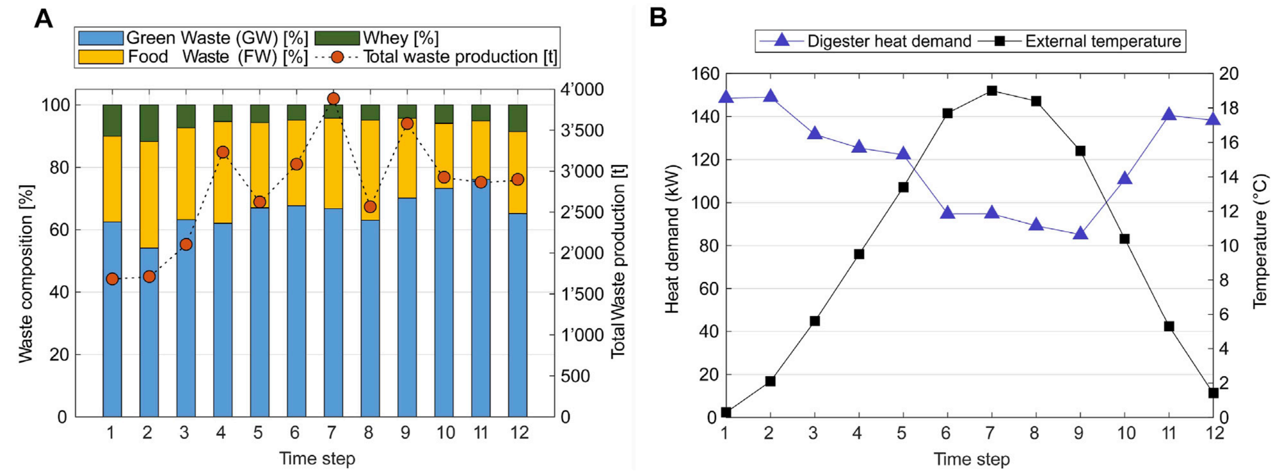

FIGURE 3 | Seasonal effect on: **(A)** biowaste quantities and composition identified by total production and sub-biowaste type; **(B)** external temperature and digester heat demand.

Our case study limits impact categories to global warming potential (GWP) using the IPCC 2013 GWP100a impact method. Its widespread use and bench-marking potential motivated the choice. However, it might not be the most adequate indicator to tackle digestate use as a fertilizer or even future concerns with the use and production of some conversion technologies; impact categories relative to land, waste or other biological levels could be considered. Subsidies and gate-fees, which are difficult to estimate, were also excluded.

Feedstock and Pre-treatment

Anaerobic digesters are able to handle different organic waste fractions, provided contamination is kept to a minimum. Three biowaste fractions ($s \in \mathbf{S}$) are considered: green waste (GW), food waste (FW) and whey. GW is ground and sieved to guarantee a maximum particle size of 10 cm, and FW is ground and mixed with water - ensuring a pumpable sludge prior to digester inlet. Whey does not undergo any pre-treatment prior to its use.

Digester

The digester is modeled as a semi-continuous reactor, working on the thermophilic range (55°c), with a variable residence time. Biowaste quantities and composition (**Figure 3A**) reflect seasonality, which impacts the digester residence time, while external temperature influences digester heat demand (**Figure 3B**). Following the approach of Wellinger, Murphy et al. (2013) and Castro-Amoedo (2019), biogas generation is modeled as a first-order kinetic reaction (**Eq. 22**).

$$Biogas_{s,t} = \frac{M_{s,t} \cdot TS_{s,t} \cdot VS_{s,t} \cdot BMP_{s,t} \cdot \left(1 - e^{-k_{s,t} \cdot tr_t}\right)}{CH_4 \text{ fraction}} \tag{22}$$

$M_{s,t}$, $TS_{s,t}$, $VS_{s,t}$, $BMP_{s,t}$ and $k_{s,t}$ represent respectively the mass, total solids, volatile solids, bio-methane potential and the kinetic parameter of feedstock s in time-step t. tr_t represents the residence time per time-step t and CH_4 fraction corresponds on average to 0.5344. All parameters have been reconciled by mean square error minimization using real data from 2019 (**Supplementary Appendix Figure A10**). The values are in line with those reported by Holliger et al. (2017) for the same treatment facility.

Biogas and CO_2 Upgrade

Biogas can be used on a conventional boiler to co-generate heat and electricity or in separation units which are able to split its main components - CH_4 and CO_2 - for additional upgrading. Pressure Swing adsorption (PSA), monoethanolamine (MEA), Water scrubbing and polymeric dry membranes were considered according to their suitability for biogas upgrading, as discussed by Allegue and Hinge (2012) and Wien Institute of Chem (2012). These technologies were not the object of detailed flowsheet simulation, but properties described by Murphy et al. (2013), Kohl and Nielsen (1997), Huertas et al. (2011) and Urban (2009) were used and summarized accordingly. Production of SNG requires at least 96% CH_4 fraction (Celebi et al., 2019), with the level of H_2S below 5 ppm, to avoid corrosion and potential oxidation to sulfur dioxide, a highly environmentally impactful gas (Allegue and Hinge, 2012).

Different C1-chemicals can be obtained by promoting CO_2-based upgrading routes:

- Formic acid: produced according to the process described in Jens et al. (2019) comprising the reaction of CO_2 and H_2 at 50°c and 94 bar, with subsequent by-products removed by distillation. A reactive distillation column at 200 mbar and 180°c produces formic acid with adequate market purity.
- Methane: The Sabatier reaction which combines CO_2 and H_2 as described in Suciu et al. (2019).
- Methanol: Adiabatic reactor as described in Rihko-Struckmann et al. (2010) working at 220°c and 50 bar, followed by a flash unit and a distillation column for methanol purification.

Digestate

The digestate, a carbon- and oxygen-rich sludge, is mainly composed of undigested volatile fractions and lignocellulosic components, and contains approximately 50% of the biowaste inlet energy. Four different conversion pathways are considered:

- Catalytic hydrothermal gasification (CHTG): the main steps involved are feedstock preparation (hydrolysis), salt separation, fixed bed catalytic reaction, water absorption tower and membrane upgrade. The modeling follows the description of Mian et al. (2015) and is adapted to digestate characteristics.
- Gasification: comprises air drying and optional torrefaction and pyrolysis which reduces the amount of heat needed for gasification. Circulated fluidized bed and entrained flow reactors with both indirect- and direct-heat were considered for the intermediate syngas production. The modeling approach described in Gassner and Maréchal (2012) and Celebi et al. (2019) was used. Depending on the gasifier technology, different compositions of syngas are to be expected; a gas processing step, comprising a water-gas shift reactor finely tunes the composition for downstream fuel generation coupled with CO_2 separation units. Final specification is fuel dependent. Di-methyl ether (DME) should be produced with 99.88 vol%, at 25°c and 1 bar; Fischer-Tropsch (FT) fuel at 25°c and 1 bar; Methanol (MeOH) with 99.4 vol%, at 25°c and 1 bar, and substitute natural gas (SNG) at 96%, 25°c and 50 bar. Thermal profiles are described in **Supplementary Appendix Table A8.**
- Hydrothermal liquefaction (HTL): Liquefaction has a filtration preparation step to ensure a cake with 20 wt% solids followed by a reactor, which operates at 340°c and 220 bar. A three-phase separation stage originates biocrude, a CO_2-rich gaseous stream and a solid residue (biochar) routed to thermal valorisation. The values and structure used are adapted from Castro-Amoedo et al. (2020) and Biller et al. (2018) to the digestate characteristics.
- Discard/Fertilizer: State-of-the-art digestate disposal comprising screening, mechanical water removal step and air drying, with a fraction thermo-valorized and the remaining disposed as fertilizer.

Utilities

The utilities section consists of additional technologies that allow closing the energy balance. The co-generation solid oxide fuel cell-gas turbine (SOFC-GT) is modeled according to Facchinetti et al. (2011) and Suciu et al. (2019) whereas the co-generation solid oxide electrolysis cell (SOEC) and the alkaline electrolyser (AEC) are adapted from Wang et al. (2018) and Suciu et al. (2019). Celebi et al. (2019) used a steam boiler fired by natural gas as a representative proxy of the European boiler family. The same consideration and modeling approach is taken in this work. Steam, produced in a Rankine cycle, is the industrial heat carrier per excellence due to good heat transfer properties, as well as preferable prices and high safety. The generation level is set at high pressure (50 bar) and distributed according to different pressure levels, chosen according to the temperature-enthalpy profiles. A superstructure approach as described in Wallerand et al. (2018), is used for heat pumps with pressure levels chosen to fit the temperature requirements of digester and district heating network. Neither the refrigeration fluid (ammonia) nor the pressure levels are subject to optimization.

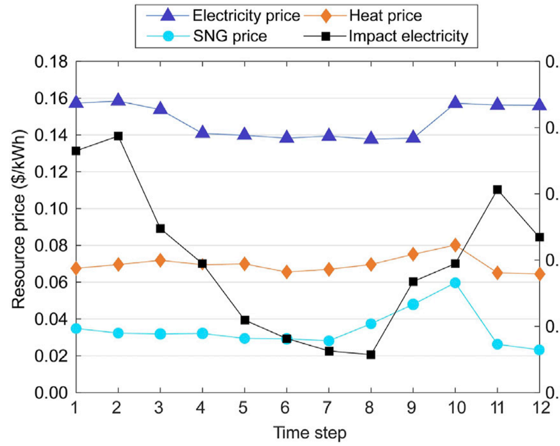

FIGURE 4 | Seasonal effect on electricity, heat and SNG price and electricity environmental impact for the reference year 2019.

2.9 Market Conditions

Distinct configurations are expected under different market conditions and economic assumptions. Resource prices, such as electricity, SNG and heat, have a seasonality trend which is particularly relevant for energy systems design. **Figure 4** shows the monthly average resource prices obtained from industry and local providers for 2019 - used as the representative year - alongside the electricity grid carbon intensity for Switzerland, obtained using the tool described in Kantor and Santecchia (2019). The use of heating oil, heat pumps, electricity and natural gas contribute to the price of heat according to their share, retrieved from the Ecoinvent database (Wernet et al., 2016).

Motivated by growing electricity demand and renewable energy penetration, uncertainty associated with energy systems is considered to be on the high-level. Therefore a 50% variation on the seasonal trend is considered (**Table 2**). Prices for different fuels are the average between 2016 and 2019 (Comtrade Comtrade, 2021), and a medium-level uncertainty (30%) is considered. We further assume that Fischer-Tropsch fuels can replace diesel and therefore show a similar market cost, while biocrude, due to the need of a pre-processing step, replaces crude oil on a 50% basis. Kim et al. (2013) considered three levels of investment cost uncertainty linked with biomass-to-fuels technology maturity and complexity; the medium range value of 30% is here taken. The interest rate is employed to discount investment and assess project profitability, taking an average value of 0.08, which should reflect the risk and premium associated with investment. Due to a low level of maturity associated with some technologies, 50% variation is used.

TABLE 2 | Market considerations and parameter uncertainty range; * diesel price; ** half of crude oil price. Uniform distribution are assumed for all parameters.

Generation-parameter	Unit	Nominal value	Variation (%)
Price electricity	[$/kWh]	Seasonal	50
Price SNG	[$/kWh]	Seasonal	50
Price heat	[$/kWh]	Seasonal	50
Price DME	[$/t]	830	30
Price FA	[$/t]	650	30
Price MeOH	[$/t]	400	30
Price FT-fuel	[$/t]	1,060(*)	30
Price biocrude	[$/t]	400(**)	30
Carbon electric grid	[kgCO_2 −eq/kWh]	Seasonal	50
Investment cost	[$]	Technology dependent	30
Interest rate	[-]	0.08	50

Ranking-parameter	Unit	Range
CO_2 tax	[$/t_{CO_2}$	[0–1,000]
SNG premium	[$/MWh_{SNG}$]	[0–340]
Waste tax	[$/cap.year]	[0–24]

The ranking and evaluation phase (**Section 2.6**) counts, in addition to all the parameters from the generation phase, with three additional taxation-based parameters: 1) a CO_2 tax which allows to translate into monetary units a solution's environmental impact; 2) a premium on SNG that is common practice in Europe to promote the upgrade of biogas to grid-level quality and 3) an additional waste tax, that could be used to help financing greener solutions. The values were chosen based upon the generation phase: for each solution and market condition the value of the three taxes were computed to break-even with the solution with the lowest total cost. The values are within acceptable market ranges and prospect policies.

3 RESULTS AND DISCUSSION

The continuous generation of biowaste and the ongoing pressure on natural resources urges for flexible energy systems, whereas increasing complexity claims for comprehensive approaches. Our two-stage approach embraces the challenge and attempts to provide useful insight and quantitative decision support, leaving subjective duties to the user. An urban biowaste case-study validates the pertinence of the methodology. The MILP formulation comprises 74,650 variables (3,978 binary) and 47,873 constraints. The mipgap was set to 0.01% and the solving time is 23 min on a 8-Core Xeon 2.4 GHz processor with 16.0 Gb of RAM. The MILP is solved 1,000 (M = 1,000) times for different generation parameters (p = 11) combination.

3.1 Solutions Clustering and Solution Identification

The original solutions were sorted based on thirty-seven dimensions in the feature space, which correspond to the used MILP decision variables. Based upon the Silhouette and Elbow methods - **Supplementary Appendix Figure A11** - 10 clusters are chosen to conveniently represent the set of 197 unique solutions. The optimization procedure, as described in our methodology, is used to generate a database of solutions built on different market assumptions, instead of relying on a fixed (and highly uncertain) set of market values. Solutions are characterized by their intrinsic aspects: energy flows (**Figure 5A**), technology activation (**Figure 5B**) and efficiencies (**Figure 5C**), rather than by performance indicators.

Investment foreshadows a shift from biogas as a fuel to its use as a chemical building block. Indeed, configurations with moderate investments rely on importing electricity - profiting from periods with low costs and excess supply - to maximize the production of formic acid. Higher investments also entail the co-production of SNG. This trend is further supported by an increasingly complex technology mix (b): formic acid production and electrolysis are the first investments, whereas for higher values, gasification technologies and biogas purification units are activated; the use of heat pumps is activated for the highest values of investment, which are simultaneously associated with the highest global efficiency. The shift toward fuel production is notorious for a wide range of investment, corroborated by a large chemical contribution to the global efficiency (c).

Figure 6 depicts the grand composite curve of two configurations: without investment (corresponding to the current scenario) and with the largest average one (141 $\$/t_{bw}$). In the former, biogas is used as a fuel to drive a Rankine cycle which supplies both the internal digester needs and a district heating system, whereas the use of gasification units coupled with heat pumps on the latter changes the heat integration configuration. The system is better integrated with low temperature heat supplied by heat pumps, biogas upgrade, and digestate headed toward gasification units, further enhancing heat recovery and integration, while simultaneously producing SNG.

Solutions are further evaluated by economic criteria which use the same parameters distribution (although not mandatory) of the generation stage, accrued by a tax on CO_2 emissions, a premium on SNG, and a waste tax.

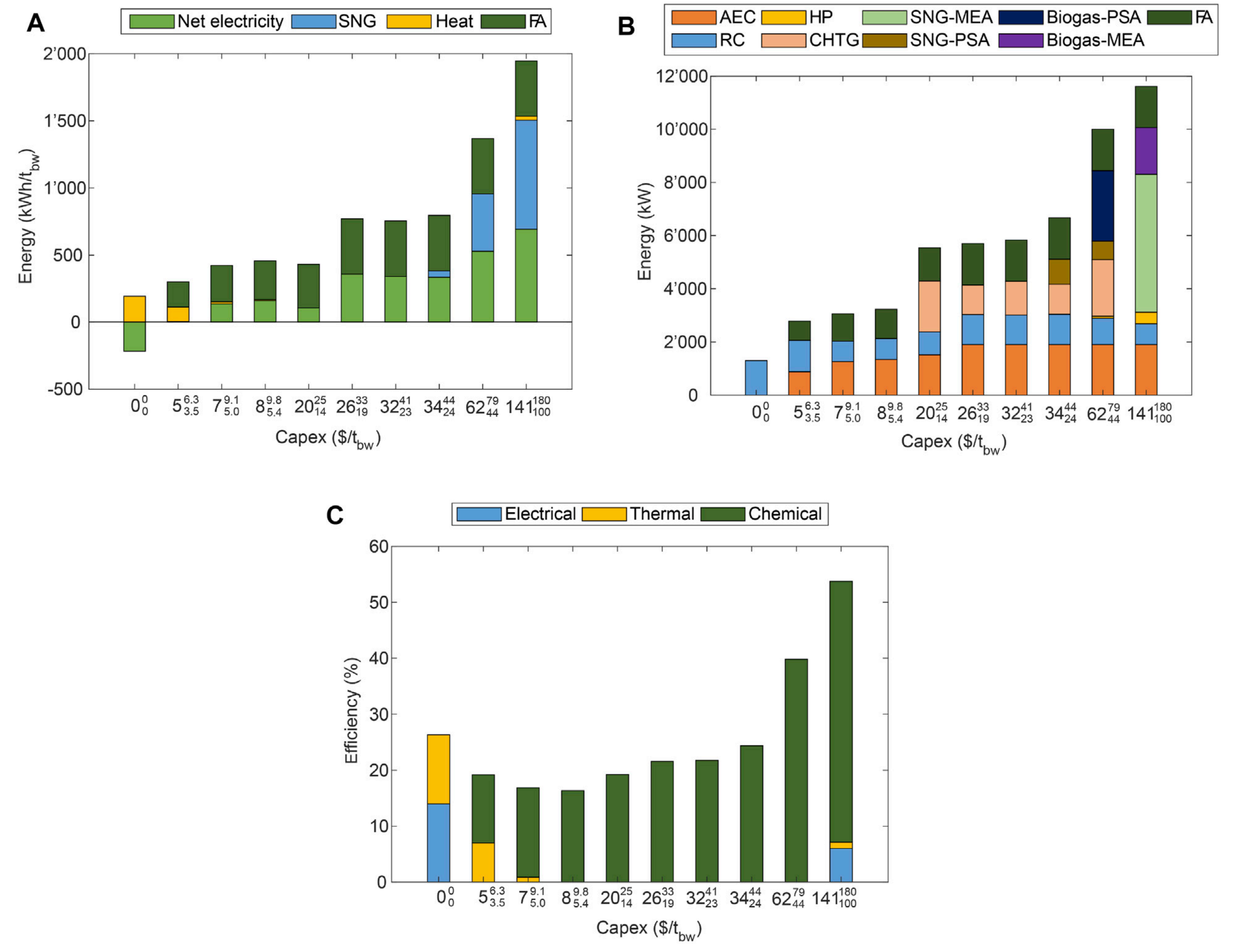

FIGURE 5 | System configurations, highlighting **(A)** energy flows, **(B)** technology activation and **(C)** efficiencies as a function of Capex: central value represents the average, whereas sub- and superscript represent the 95% CI.

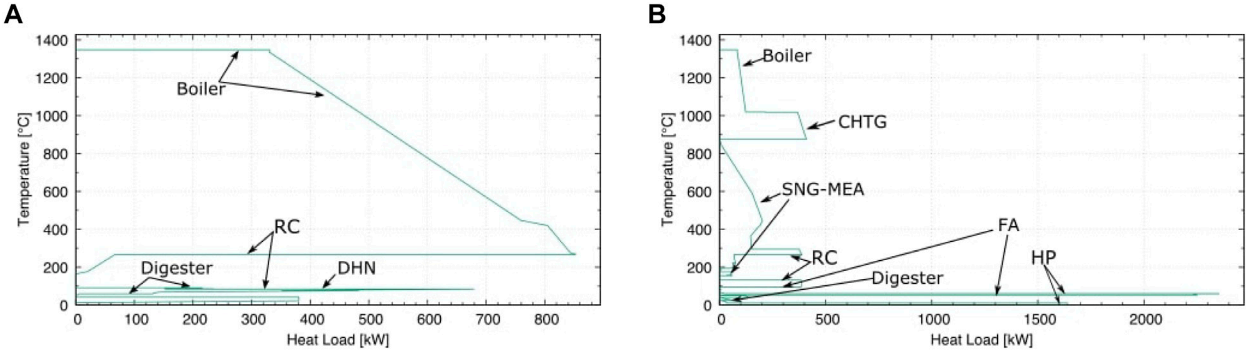

FIGURE 6 | Grand composite curves (GCC) of **(A)** reference case (no investment) and **(B)** maximum average investment. GCC are a graphical representation of the heat cascade, showing the excess heat availability at each temperature interval. RC - Rankine cycle, HP - heat pumps, DHN - district heating network, FA - formic acid production.

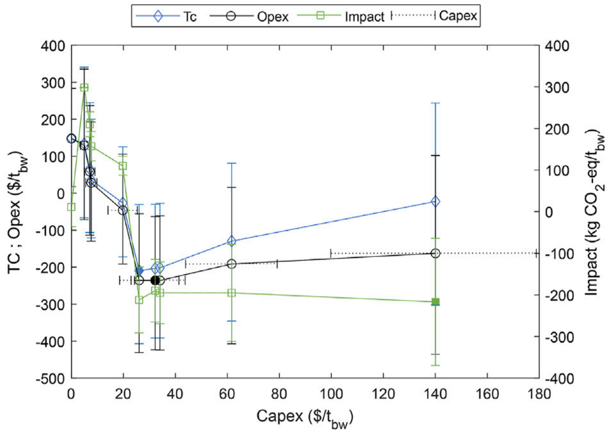

FIGURE 7 | Pareto trade-off. Vertical lines represent the 95% confidence interval (CI) in total cost (Tc), operating cost (Opex) and environmental impact (impact). Horizontal dashed lines represent the 95% CI on capital expenditures (Capex). Filled markers portray solutions with the average lowest values. Trend lines are for visual support only.

TABLE 3 | Quasi Monte-Carlo simulation results (10,000) per solution and per KPI. The central value represents the mean; sub- and superscript account for the upper and lower range of the 95% CI.

Capex	Tc	Opex	Impact	Pbt	Global eff	Cf
[$/t_{bw}$]	[$/t_{bw}$]	[$/t_{bw}$]	[kgCO_2eq/t_{bw}]	[y]	[-]	[-]
0_{0}^{0}	148_{17}^{283}	148_{17}^{283}	12_{-36}^{59}	0_{0}^{0}	26.3	0.05
$5_{3.5}^{6.3}$	134_{-67}^{341}	129_{-71}^{335}	298_{298}^{299}	$1.0_{0}^{2.7}$	19.2	0.23
$7_{5.0}^{9.1}$	65_{-107}^{245}	58_{-114}^{237}	210_{180}^{240}	$1.8_{0}^{3.2}$	16.8	0.23
$8_{5.4}^{9.8}$	35_{-121}^{200}	28_{-130}^{192}	158_{122}^{193}	$1.26_{0.2}^{2.0}$	16.8	0.32
20_{14}^{25}	-26_{-172}^{126}	-46_{-192}^{106}	110_{87}^{133}	$0.9_{0.5}^{1.5}$	19.3	0.32
26_{19}^{33}	-209_{-407}^{-31}	-235_{-431}^{-56}	-212_{-291}^{-133}	$0.6_{0.3}^{0.9}$	21.6	0.27
32_{23}^{41}	-203_{-391}^{-30}	-236_{-423}^{-63}	-190_{-265}^{-115}	$0.7_{0.4}^{1.1}$	21.8	0.36
34_{24}^{44}	-202_{-391}^{-27}	-236_{-424}^{-61}	-195_{-269}^{-121}	$0.7_{0.4}^{1.1}$	24.4	0.41
62_{44}^{79}	-130_{-346}^{81}	-191_{-407}^{15}	-195_{-312}^{-78}	$1.6_{0.9}^{2.8}$	39.8	0.41
141_{100}^{180}	-23_{-302}^{244}	-163_{-435}^{102}	-217_{-369}^{-64}	$13.8_{1.9}^{14}$	53.8	0.36

3.2 Market Conditions and Ranking

Market conditions are used for solution generation but are also part of performance indicator calculation. The use of different market conditions renders solutions more or less attractive, depending on the list of performance indicators and priorities. **Figure 7** shows Opex, Tc and Impact as a function of Capex, resulting from a QMC simulation. Increasing investment entails on average, as expected, a reduction in operating cost; however, for the low range of investments (below 26 $\$/t_{bw}$), the environmental impact follows an increasing trend. This can be explained by a shift toward electricity import and a low quantity of added-value chemical production, which is nevertheless enough to justify a significant average decrease in total cost performance. Filled markers identify two relevant solutions for decision-makers and practitioners: the solution with average minimum total cost (blue, diamond) and the solution with average minimum environmental impact (green, square). The wide confidence interval range depicts overlapping situations in which other solutions might have lower total cost and environmental impact. A robust approach is thus warranted to rank and choose among solutions.

The use of traditional Pareto trade-off analysis hinders the comparison between more than three KPIs, constraining the amount of information that can be obtained. **Table 3** expands on the graphical information by including all the considered KPIs: the central position corresponds to the average value and the 95% confidence interval is represented by the sub- and superscript values; values are sorted by increasing Capex and negative values correspond to profit (or negative emissions) situations.

The reference configuration, entailing zero investment, is the most penalizing design in average economic terms. Increasing investment, even as little as 5 $\$/t_{bw}$, promotes a 10% average reduction reduction in total cost, associated with the added-value of formic acid production. However, the impact substitution credit is not enough to either cover the burden associated with production or the electricity imports. Only for higher investments (greater than 26 $\$/t_{bw}$), and thus increased formic acid production, does the system convert itself into a net negative emission system; for these set of solutions not only environmental impact but also costs reach their average minimum. If we take a closer look, environmental impact is consistently negative above 26 $\$/t_{bw}$, which is a remarkable result: properly managed, urban biowaste constitutes a net CO_2 sink, asserting its relevance in the prospective environmental policies. Solutions' pay-back time (except the largest investment) does not surpass 3 years, which stands low compared with typical lifetime of engineering projects.

As a thermodynamic KPI, global efficiency only reaches higher than the reference value for the highest investments which are associated with SNG co-production and also with a greater number of units, which can be understood as a need for more process equipment, workers and safety measures. In all the intermediate investments, despite a more complex system, the shift toward value-added chemicals does not encompass a more efficient system.

Decision-making based on averages is commonplace in engineering applications. However, using averages forestalls deeper analyses and relations. The use of confidence intervals instead, protects against uncertainty to a much higher degree, which is paramount in energy systems. For example, depending on market conditions the reference solution can be either an environmental burden or a net emissions sink. Other solutions and KPIs show a similar dichotomy.

The use of a ranking system allows arguing then on a probabilistic base, conditioned to the set of market parameters (**Table 4**). Based upon the parameters distribution, each configuration is ranked according to the probability of belonging to the three best alternatives for the set of KPIs - which are ultimately a user-defined choice. Due to the absence of investment, the reference solution outperforms all the others in Capex, pay-back time and complexity factor, although statistically underperforming in other economic and environmental impact categories. On the other end of the spectrum, solutions with the highest investment perform statistically better on Impact, Opex, total cost, and global efficiency, albeit with an increased complexity degree.

Some caveats on the interpretation are warranted: the number and type of KPIs, their weighting on the total score and the assumed parameters distribution, all of which play a significant role in ranking and evaluation. For instance, a different set of priorities is likely to radically change the decision: based only on mathematical objectives (ranking P1, blue), the solution with the average investment of

TABLE 4 | Solutions probabilistic ranking (normalized) ranged by increasing capex and pertaining to two ranking systems: P1, containing only MILP objectives; P2 adding thermodynamic and configuration indicators. Highlighted scores achieve the highest global performance assuming uniform weights.

Solutions (average capex)	0	5	7	8	20	26	32	34	62	141
Capex	33.3%	33.0%	33.3%	–	–	–	–	–	–	–
Tc	–	–	–	–	–	33.0%	31.6%	32.7%	1.8%	0.7%
Opex	–	–	–	–	–	27.7%	25.9%	31.4%	6.7%	8.3%
Impact	–	–	–	–	–	33.3%	11.4%	16.7%	16.6%	21.9%
Pay-back time	33.3%	21.0%	17.7%	13.3%	–	14.5%	–	–	–	0.1%
Global eff	33.0%	–	–	–	–	–	–	–	33.0%	33.0%
Complexity factor	33.0%	33.0%	33.0%	–	–	–	–	–	–	–
Total score (P1)	8.3%	8.3%	8.3%	0.0%	0.0%	23.5%	17.2%	20.2%	6.3%	7.7%
Total score (P2)	18.9%	12.4%	12.0%	1.9%	0.0%	15.5%	9.8%	11.5%	8.3%	9.1%

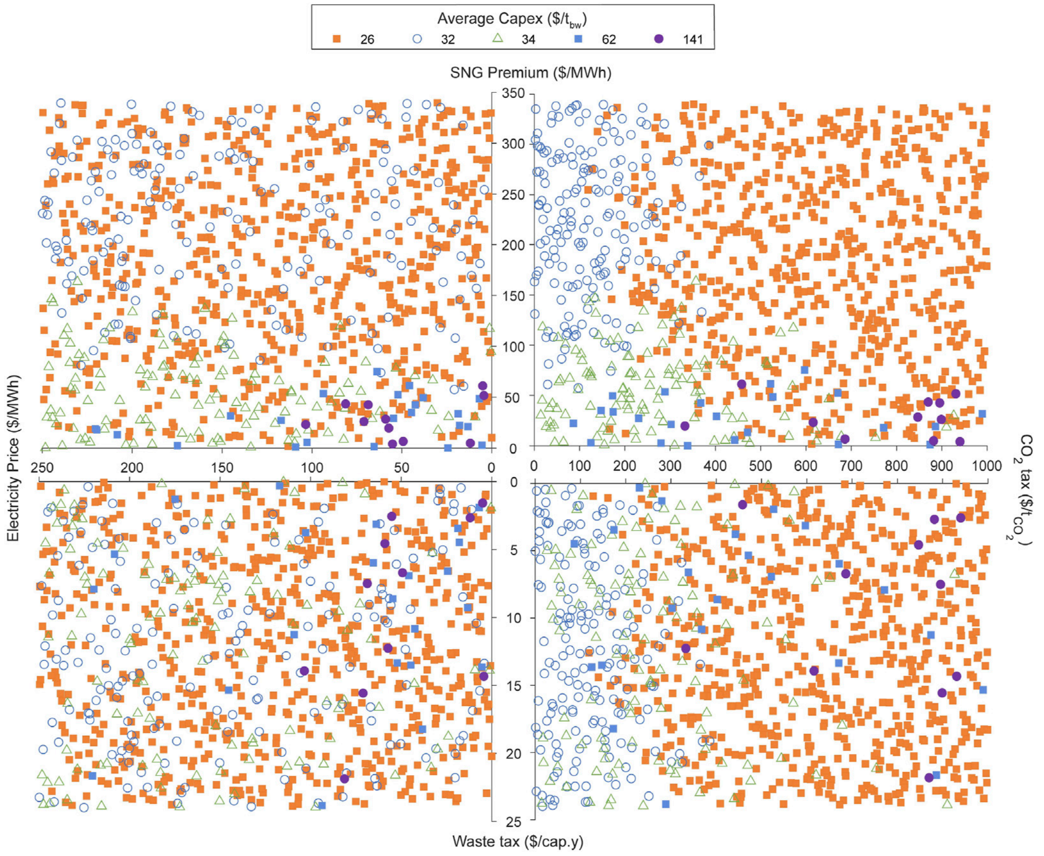

FIGURE 8 | Solutions achieving the lowest total cost for different parameters combination. Symbols represent design configurations labeled according to their average capex ($/t^{bw}).

26 $/t$_{bw}$ outperforms in approximately one quarter of all market scenarios. The inclusion of other user indicators (P2), under the assumption of uniform weights, sharply decreases the interest of that design while promoting the reference one, which performs statistically better in 19% of the cases. The solution with an average investment of 20 $/t$_{bw}$ is never amid the top-three configurations in any KPI, which perfectly showcases the decouple of solution generation and ranking. Decision-maker intervention and subjective analysis is crucial for fine tuning and analysis.

The user has available a large set of parameters that are ultimately responsible for solution ranking and might serve as guidelines in policy-making. **Figure 8** shows solutions (identified by their average investment) that achieve the lowest total cost for each market configuration. Only 1,000 points and four parameters are shown for the sake of clarity and simplicity. The right side underlines the role of the CO_2 tax as the main driver in total cost. For values above 300 $/t_{CO_2}$ and regardless of other parameters, the solution with an average investment of 26 $\$/t_{bw}$ is systematically preferred (but for lower values of SNG premium and waste tax, whereupon it competes with high investment designs), translated by an investment in catalytic hydrothermal gasification for digestate upgrade, and the production of formic acid after biogas upgrade. For more modest carbon tax values the solution of 32 $\$/t_{bw}$ is preferred for high SNG incentives and waste taxes, whereas the solution with 34 $\$/t_{bw}$ dominates in the lower range. Both solutions promote gasification, with the latter combining both dry and hydrothermal options. The left side of the figure, despite less trend informative, reinforces the predominant role of carbon taxation. Nonetheless, solutions with low average investment are associated with higher electricity price, waste tax and SNG premium, while high investment options dominate markets with low costs of electricity and waste tax.

4 CONCLUSION

Sustainable development goals comprise the gradual replacement of fossil fuels, progressive deployment of renewable energy and negative CO_2 emissions. Biomass is able to address all of these dimensions, thus its critical role in the energy transition. In this work we propose a two-stage optimization approach for the design of robust energy systems, applied to an anaerobic digestion plant which is, according to Burg et al. (2019), the present and future dominant conversion technology for urban biowaste treatment in Switzerland.

The applied methodology addresses the challenge of biogas separation and upgrading, while dealing with complex and difficult to digest lignocellulosic fractions. Biogenic CO_2 and surplus electricity periods promote fuel synthesis, contributing to close the gap between electricity supply and demand, and therefore improving the system resilience. We show that greater diversity, which is represented by activating different technologies, reduces costs, emissions and promotes efficiency. The use of heat pumps - activated on the high-range of investment - associated with heat integration strategies, greatly contributes for a far superior system with increased efficiency. Synergies are explored and translated into user-defined metrics, showcasing the added-benefit to the local energy ecosystem.

The main advantage of our approach lies in the use of different market conditions for solution generation and clustering, avoiding the bias toward configurations that marginally outperform under prevailing market conditions. Indeed, the uncertainty associated with existing energy systems asks for frameworks that allow a systematic analysis of market settings - enabling the emergence of sub-optimal designs. As performance indicators are not the driver for solution generation, but are rather used for ranking and evaluation, their number can be easily adapted to account for user preferences or multi-stakeholders positions. The robustness of the approach is highlighted in the use of an approach for design ranking and evaluation. Moderate investment solutions (between 26 and 34 $\$/t_{bw}$) are more robust, as they statistically achieve lower values of total cost and lower environmental impacts, by combining gasification units (dry and hydrothermal options) with biogas separation and CO_2 upgrade to formic acid.

Policy-makers could also benefit from our approach. Feed-in tariffs, institutional incentives for substitute natural gas production, a CO_2 tax or a consumer waste tax can be calculated from this work. The developed methodology is thus appropriate to handle exogenous uncertainty embedded in a multi-period framework, with systematic generation, evaluation and ranking of system configurations. With our approach, we believe and hope to contribute for an interdisciplinary effort to address the clean energy transition in which cutting-edge biomass-based models are paramount.

DATA AVAILABILITY STATEMENT

The raw data supporting the conclusions of this article will be made available by the authors, without undue reservation.

AUTHOR CONTRIBUTIONS

RC-A: conceptualization, methodology, modeling, results generation and analysis; data validation and visualisation; writing - original draft preparation and corrections. NM: modeling and data visualisation. JG: conceptualization, validation, writing-reviewing and editing. FM: supervision and conceptualization; writing-reviewing and editing.

ACKNOWLEDGMENTS

The authors would like to acknowledge SATOM SA, especially Mr. Daniel Baillifard and Mr. Julian Dovat for the precious discussions on organic waste valorization and detailed technical information which contributed to the accuracy of this study. The authors financially acknowledge the European Union's Horizon 2020 research and innovation programme under the Marie Sklodowska-Curie grant agreement No 754354 and No SEP-210500079, and the Swiss Competence Center for Energy Research SCCER-EIP.

SUPPLEMENTARY MATERIAL

The Supplementary Material for this article can be found online at: https://www.frontiersin.org/articles/10.3389/fenrg.2021.718310/full#supplementary-material

REFERENCES

Allegue, L. B., and Hinge, J. (2012). Biogas and Bio-Syngas Upgrading. Danish Technological Institute. Tech. Rep. Dec.

"AMPL" (2013). *Encyclopedia of Operations Research and Management Science*. Editor I. Saul and C. F. Gass and Michael Boston, MA: Springer US, 52. doi:10.1007/978-1-4419-1153-7283

Al-Malah, K. I. (2016). Introducing aspen plus in Aspen Plus® (Hoboken, NJ: John Wiley & Sons, Inc), 1–47.

Belsim (2018). Software – Belsim Vali v4. Available at: https://belsim.com/2021.

Biller, P., Johannsen, I., dos Passos, J. S., and Ottosen, L. D. M. (2018). Primary Sewage Sludge Filtration Using Biomass Filter Aids and Subsequent Hydrothermal Co-liquefaction. *Water Res.* 130, 58–68. doi:10.1016/j.watres.2017.11.048

Burg, V., Bowman, G., Hellweg, S., and Thees, O. (2019). Long-Term Wet Bioenergy Resources in Switzerland: Drivers and Projections until 2050. *Energies.* 12, 3585. doi:10.3390/en12183585

Candra, D., Hartmann, K., and Nelles, M. (2018). Economic Optimal Implementation of Virtual Power Plants in the German Power Market. *Energies.* 11, 2365. doi:10.3390/en11092365

Castro-Amoedo, R. (2019). "Wastewater Management towards a Sustainable futureDairy Production: A Study Case". en. In Proceedings of the 32nd International Conference on Efficiency, Cost, Optimization, Simulation and Environmental Impact of Energy Systems - ECOS 2019. CONF. Wroclaw, PolandInstitute of Thermal Technology, Silesian University of Technology, 565.

Castro-Amoedo, R., Damartzis, T., Granacher, J., and Maréchal, F. (2020). System Design and Performance Evaluation of Wastewater Treatment Plants Coupled with Hydrothermal Liquefaction and Gasification. *Front. Energ. Res.* 8, 2296–598X. doi:10.3389/fenrg.2020.568465

Celebi, A. D., Sharma, S., Ensinas, A. V., and Maréchal, F. (2019). Next Generation Cogeneration System for Industry - Combined Heat and Fuel Plant Using Biomass Resources. *Chem. Eng. Sci.* 204, 59–75. doi:10.1016/j.ces.2019.04.018

Cheng, S. Y., Tan, X., Show, P. L., Rambabu, K., Banat, F., Veeramuthu, A., et al. Incorporating Biowaste into Circular Bioeconomy: A Critical Review of Current Trend and Scaling up Feasibility. In: *Environ. Technology Innovation* 19 (2020), p. 101034. doi:10.1016/j.eti.2020.101034

Comtrade Comtrade (2021). UN Comtrade: International Trade Statistics. Available at: https://comtrade.un.org/data/. 2021.

Damartzis, T., and Zabaniotou, A. (2011). Thermochemical Conversion of Biomass to Second Generation Biofuels through Integrated Process Design-A Review. *Renew. Sustainable Energ. Rev.* 15 (1), 366–378. doi:10.1016/j.rser.2010.08.003

Davies, D. L., and Bouldin, D. W. (1979). A Cluster Separation Measure. *IEEE Trans. Pattern Anal. Mach. Intell.* PAMI-1, 224–227. doi:10.1109/TPAMI.1979.4766909

Facchinetti, E., Favrat, D., and Marechal, F. (2011). Innovative Hybrid Cycle Solid Oxide Fuel Cell-Inverted Gas Turbine With CO2 Separation. *Fuel Cells.* 11 (4), 565–572. doi:10.1002/fuce.201000130

Gassner, M., and Maréchal, F. (2012). Thermo-Economic Optimisation of the Polygeneration of Synthetic Natural Gas (SNG), Power and Heat from Lignocellulosic Biomass by Gasification and Methanation. *Energy Environ. Sci.* 5 (2), 5768–5789. doi:10.1039/C1EE02867G

Gassner, M., Vogel, F., Heyen, G., and Maréchal, F. (2011). Optimal Process Design for the Polygeneration of SNG, Power and Heat by Hydrothermal Gasification of Waste Biomass: Process Optimisation for Selected Substrates. *Energ. Environ. Sci.* 4 (5), 1742–1758. doi:10.1039/C0EE00634C

Granacher, J. (2019). "Potential of Hydrothermal Black Liquor Gasification Integrated in Pulp Production Plant". en. In Proceedings of ECOS 2019. CONF. Wroc0142aw, PolandSilesian University of Technology, 2299.

Henchoz, S., Weber, C., Maréchal, F., and Favrat, D. (2015). Performance and Profitability Perspectives of a CO2 Based District Energy Network in Geneva's City Centre. *Energy.* 85, 221–235. doi:10.1016/j.energy.2015.03.079

Holliger, C., Fruteau de Laclos, H., and Hack, G. (2017). "Methane Production of Full-Scale Anaerobic Digestion Plants Calculated From Substrate's Biomethane Potentials Compares Well with the One Measured On-Site". English. *Front. Energ. Res.* 5, 2296–598X. doi:10.3389/fenrg.2017.00012

Hou, T., Nuyens, D., Roels, S., and Janssen, H. (2019). Quasi-Monte Carlo Based Uncertainty Analysis: Sampling Efficiency and Error Estimation in Engineering Applications. *Reliability Eng. Syst. Saf.* 191, 106549. doi:10.1016/j.ress.2019.106549

Huertas, J. I., Giraldo, N., and Izquierdo, S. (2011). ""Removal of H2S and CO2 from Biogas by Amine Absorption". en," in *Mass Transfer in Chemical Engineering Processes* (Rijeka, Croatia: InTech).

IBM ILOG Cplex (2009). "V12. 1: User's Manual for CPLEX". *Int. Business Machines Corporation.* 46 (53), 157.

IRENA (2016). Global Renewables Outlook: Energy Transformation 2050. Available at: www.irena.org/publications/2020/Apr/Global-Renewables-Outlook-2020.

Jens, C. M., Scott, M., Liebergesell, B., Westhues, C. G., Schäfer, P., Franciò, G., et al. (2019). Rh-Catalyzed Hydrogenation of CO2 to Formic Acid in DMSO-Based Reaction Media: Solved and Unsolved Challenges for Process Development. *Adv. Synth. Catal.* 361 (2), 307–316. doi:10.1002/adsc.201801098

Jørgen, H., and Laura Bailon, Al. (2014). Biogas Upgrading Evaluation of Methods for H2S Removal. Danish Technological Institute. en. Tech. Rep. Danish Technol. Inst. , 31.

Kantor, I., and Santecchia, A. (2019). Ecological Risk Assessment. en. Tech. Rep. 1669, 27–51. doi:10.1002/9781119483342.ch4

Kim, J., Sen, S. M., and Maravelias, C. T. (2013). An Optimization-Based Assessment Framework for Biomass-To-Fuel Conversion Strategies. *Energ. Environ. Sci.* 6 (4), 1093–1104. doi:10.1039/C3EE24243A

Kohl, A. L., and Nielsen, R. (1997). *Gas Purification. Eng.* 5th ed. Houston, Tex: Gulf Pub.

Korberg, A. D., Mathiesen, B. V., Clausen, L. R., and Skov, I. R. (2021). The Role of Biomass Gasification in Low-Carbon Energy and Transport Systems. *Smart Energy.* 1, 1000062666–1000069552. doi:10.1016/j.segy.2021.100006

Linnhoff, B., and Hindmarsh, E. (1983). The Pinch Design Method for Heat Exchanger Networks. *Chem. Eng. Sci.* 38 (5), 745–763. doi:10.1016/0009-2509(83)80185-7

Magagula, S., Han, J., Liu, X., and Sempuga, B. C. (2021). Targeting Efficient Biomass Gasification. *Chin. J. Chem. Eng.* 33, 268–278. doi:10.1016/j.cjche.2020.11.027

Maréchal, F., and Kalitventzeff, B. (1997). Identification of the Optimal Pressure Levels in Steam Networks Using Integrated Combined Heat and Power Method. *Chem. Eng. Sci.* 52 (17), 2977–2989. doi:10.1016/S0009-2509(97)00102-4

Maréchal, F., and Kalitventzeff, B. (1998a). Process Integration: Selection of the Optimal Utility System. *Comput. Chem. Eng.* 22, S149–S156. doi:10.1016/s0098-1354(98)00049-0

Maréchal, F., and Kalitventzeff, B. (1998b). Energy Integration of Industrial Sites: Tools, Methodology and Application. *Appl. Therm. Eng.* 18 (Nov), 921–933. doi:10.1016/S1359-4311(98)00018-0

Maronese, S., Ensinas, A. V., Mian, A., Lazzaretto, A., and Maréchal, F. (2015). Optimum Biorefinery Pathways Selection Using the Integer-Cuts Constraint Method Applied to a MILP Problem. *Ind. Eng. Chem. Res.* 54 (28), 7038–7046. doi:10.1021/acs.iecr.5b01439

Mian, A., Ensinas, A. V., and Marechal, F. (2015). Multi-objective Optimization of SNG Production from Microalgae Through Hydrothermal Gasification. *Comput. Chem. Eng.* 76, 170–183. doi:10.1016/j.compchemeng.2015.01.013

Moret, S., Codina Gironès, V., Bierlaire, M., and Maréchal, F. (2017). Characterization of Input Uncertainties in Strategic Energy Planning Models. *Appl. Energ.* 202, 597–617. doi:10.1016/j.apenergy.2017.05.106

Murphy, J., and Baxter, D. (2013). *The Biogas Handbook: Science, Production and Applications. Woodhead Publishing Series in Energy Number 52.* Editor A. Wellinger (Oxford: Woodhead Publishing).

Muscat, A., de Olde, E. M., de Boer, I. J. M., and Ripoll-Bosch, R. (2020). The Battle for Biomass: A Systematic Review of Food-Feed-Fuel Competition. *Glob. Food Security.* 25, 100330. doi:10.1016/j.gfs.2019.100330

Nestor, A. (2021). Sepulveda et al. "The Design Space for Long-Duration Energy Storage in Decarbonized Power Systems". *Nat. Energ.* 6, 506–516. doi:10.1038/s41560-021-00796-8

Nkoa, R. (2014). Agricultural Benefits and Environmental Risks of Soil Fertilization with Anaerobic Digestates: a Review. *Agron. Sustain. Dev.* 34, 473–492. doi:10.1007/s13593-013-0196-z

REN21 (2020). *Renewables Global Status Report*. Paris: REN21 Secretariat

Rihko-Struckmann, L. K., Peschel, A., Hanke-Rauschenbach, R., and Sundmacher, K. (2010). Assessment of Methanol Synthesis Utilizing Exhaust CO2for Chemical Storage of Electrical Energy. *Ind. Eng. Chem. Res.* 49 (21), 11073–11078. doi:10.1021/ie100508w

Rousseeuw, P. J. (1987). Silhouettes: A Graphical Aid to the Interpretation and Validation of Cluster Analysis. *J. Comput. Appl. Mathematics.* 20, 53–65. doi:10.1016/0377-0427(87)90125-7

Rubio-Maya, C., Uche-Marcuello, J., Martínez-Gracia, A., and Bayod-Rújula, A. A. (2011). Design Optimization of a Polygeneration Plant Fuelled by Natural Gas and Renewable Energy Sources. *Appl. Energ.* 88, 449–457. doi:10.1016/j.apenergy.2010.07.009

Santibañez-Aguilar, J. E., Ponce-Ortega, J. M., Betzabe González-Campos, J., Serna-González, M., and El-Halwagi, M. M. (2013). Optimal Planning for the Sustainable Utilization of Municipal Solid Waste. *Waste Management* 33, 2607–2622. doi:10.1016/j.wasman.2013.08.010

Schmidt, O., Gambhir, A., Staffell, I., Hawkes, A., Nelson, J., and Few, S. (2017). Future Cost and Performance of Water Electrolysis: An Expert Elicitation Study. *Int. J. Hydrogen Energ.* 42 (52), 30470–30492. doi:10.1016/j.ijhydene.2017.10.045

Schnorf, V., Trutnevyte, E., Bowman, G., and Burg, V. (2021). Biomass Transport for Energy: Cost, Energy and CO2 Performance of forest wood and Manure Transport Chains in Switzerland. *J. Clean. Prod.* 293, 125971. doi:10.1016/j.jclepro.2021.125971

Segurado, R., Pereira, S., Correia, D., and Costa, M. (2019). Techno-economic Analysis of a Trigeneration System Based on Biomass Gasification. *Renew. Sustainable Energ. Rev.* 103, 501–514. doi:10.1016/j.rser.2019.01.008

Sikarwar, V. S., Zhao, M., Clough, P., Yao, J., Zhong, X., Memon, M. Z., et al. (2016). An Overview of Advances in Biomass Gasification. *Energ. Environ. Sci.* 9, 2939–2977. doi:10.1039/C6EE00935B

Snowden-Swan, L. J., Zhu, Y., Jones, S. B., Elliott, D. C., Schmidt, A. J., Hallen, R. T., et al. (2016). Hydrothermal Liquefaction and Upgrading of Municipal Wastewater Treatment Plant Sludge: A Preliminary Techno-Economic Analysis. *en. Tech. Rep.* Pnnl-25464, 1258731. doi:10.2172/1258731

Steubing, B., Zah, R., Waeger, P., and Ludwig, C. (2010). Bioenergy in Switzerland: Assessing the Domestic Sustainable Biomass Potential. *Renew. Sustainable Energ. Rev.* 14, 2256–2265. doi:10.1016/j.rser.2010.03.036

Suciu, R., Stadler, P., Kantor, I., Girardin, L., and Maréchal, F. (2019). Systematic Integration of Energy-Optimal Buildings With District Networks. *Energies.* 12, 2945. doi:10.3390/en12152945

Tock, L., Gassner, M., and Maréchal, F. (2010). Thermochemical Production of Liquid Fuels from Biomass: Thermo-Economic Modeling, Process Design and Process Integration Analysis. *Biomass and Bioenergy* 34 (12), 1838–1854. doi:10.1016/j.biombioe.2010.07.018

Tock, L., and Maréchal, F. (2015). Decision Support for Ranking Pareto Optimal Process Designs under Uncertain Market Conditions. *Comput. Chem. Eng.* 83, 165–175. doi:10.1016/j.compchemeng.2015.06.009

TU Wien Institute of Chemical engineering (2012). Biogas to Biomethane: Technology Review. *Eng. Tech. Rep.*

Turton, R. (2018). *Analysis, Synthesis and Design of Chemical Processes. en.* 5th edition. Boston, MA: Prentice-Hall.

Urban, W. (2009). *Technologien und Kosten der Biogasaufbereitung und Einspeisung in das Erdgasnetz : Ergebnisse der Markterhebung 2007-2008*. German: Results of Market Survey 2007-2008. Fraunhofer UMSICHT, 123.

Wallerand, A. S., Kermani, M., Kantor, I., and Maréchal, F. (2018). Optimal Heat Pump Integration in Industrial Processes. *Appl. Energ.* 219, 68–92. doi:10.1016/j.apenergy.2018.02.114

Wang, L., Pérez-Fortes, M., Madi, H., Diethelm, S., herle, J. V., and Maréchal, F. (2018). Optimal Design of Solid-Oxide Electrolyzer Based Power-To-Methane Systems: A Comprehensive Comparison between Steam Electrolysis and Co-electrolysis. *Appl. Energ.* 211, 1060–1079. doi:10.1016/j.apenergy.2017.11.050

Wernet, G., Bauer, C., Steubing, B., Reinhard, J., Moreno-Ruiz, E., and Weidema, B. (2016). The Ecoinvent Database Version 3 (Part I): Overview and Methodology. *Int. J. Life Cycle Assess.* 21 (9), 1218–1230. doi:10.1007/s11367-016-1087-8

Zhu, Y., Biddy, M. J., Jones, S. B., Elliott, D. C., and Schmidt, A. J. (2014). Techno-Economic Analysis of Liquid Fuel Production From Woody Biomass via Hydrothermal Liquefaction (HTL) and Upgrading. *Appl. Energ.* 129, 384–394. doi:10.1016/j.apenergy.2014.03.053

Conflict of Interest: Author NM was employed by company Satom SA.

The remaining authors declare that the research was conducted in the absence of any commercial or financial relationships that could be construed as a potential conflict of interest.

NOMENCLATURE

$\boldsymbol{u} \in \mathbf{U}$ Units $\mathbf{U}$ = {Gasification, CHTG,HTL,PSA, MEA, … }**Utility Units** $\mathbf{UU} = \mathbf{U} \setminus \mathbf{PU}$

$\boldsymbol{u} \in \mathbf{PU}$ Process Units $\mathbf{PU}$ = {urbanbiowaste generation}

$\boldsymbol{u} \in \mathbf{U}$ Units $\mathbf{U}$ = {Gasification, CHTG,HTL,PSA, MEA, … }**Utility Units** $\mathbf{UU} = \mathbf{U} \setminus \mathbf{PU}$

$\boldsymbol{i} \in \mathbf{SU}$ Supply Units $\mathbf{SU}$ = {Gasification, CHTG,HTL,PSA, MEA, … }

$\boldsymbol{j} \in \mathbf{CU}$ Consuming Units $\mathbf{CU}$ = {Gasification, CHTG,HTL,PSA, MEA, … }

$\boldsymbol{r} \in \mathbf{R}$ Resources $\mathbf{R}$ = {electricity, cooling water,SNG,biocrude,FA, … }

$\boldsymbol{k} \in \mathbf{K}$ Temperature intervals $\mathbf{K} = \{1 \ldots n_k\}$

$\boldsymbol{t} \in \mathbf{T}$ Time steps $\mathbf{T} = \{1 \ldots t_t\}$

$\boldsymbol{f_u}/\boldsymbol{f_{u,t}}$ Sizing factor of unit u/in time step t [-]

$\boldsymbol{y_u}/\boldsymbol{y_{u,t}}$ Binary variable to use or not unit u/in time step t [-]

$\boldsymbol{g_{i,j}}$ Binary variable connecting producing unit i to consuming unit j [-]

$\dot{m}_{r,i,j,t}$ Flowrates of resource r between supplying unit i and consumer unit j in time step t [kg/h] or [m^3/h] or [kW]

$\dot{M}^{+}_{r,t}$ Exported quantity of resource r in time step t [kg/h] or [m^3/h] or [kW]

$\dot{M}^{-}_{r,t}$ Imported quantity of resource r in time step t [kg/h] or [m^3/h] or [kW]

$\dot{R}_{t,k}$ Residual heat in the temperature interval k in time step t [kW]

$t^{\mathbf{op}}_{t}$ Operating time per time step t [h/time step]

f^{min}_{u}/f^{max}_{u} Minimum/Maximum size of unit u [−]

$c^{-}_{r,t}/c^{+}_{r,t}$ Reference cost of importing/exporting resource r at time step t [\$/Ref. flow]

$c^{\mathbf{op}}_{u}$ Specific operating cost of unit u [\$/Ref. flow]

$c^{\mathbf{inv},1}_{u}/c^{\mathrm{inv},2}_{u}$ Specific fixed/variable investment cost of unit u [\$]/[\$/Ref. flow]

$c^{\mathbf{imp},1}_{u}/c^{\mathrm{imp},2}_{u}$ Specific fixed/variable environmental impact of unit u [Impact]/[Impact/Ref. flow]

$k^{-}_{r,t}/k^{+}_{r,t}$ Reference environmental impact of importing/exporting resource r at time step t [Env. Impact/Ref. flow]

$\dot{m}^{+}_{r,u,t}/\dot{m}^{-}_{r,u,t}$ Reference mass flowrate of produced/consumed resource r in unit u at time step t [kg/h] or [m^3/h] or [kW]

$\dot{q}_{u,t,k}$ Reference heat load of unit u in time step t and temperature interval k [kW]

$\dot{m}^{L}_{r,i,j,t}/\dot{m}^{U}_{r,i,j,t}$ Minimum and maximum transport limits of resource r between origin i and destination j at time step t [Flow]

$\boldsymbol{n}/\boldsymbol{i}$ Investment lifetime/Investment interest rate [years]/[-]

bw biowaste

SNG substitute Natural gas

FA formic acid

DME di-methyl ether

MeOH methanol

FT fischer-Tropsch fuel

WW wastewater

AEC alkaline Electrolysis cell

FW food waste

GW green waste

Opex operational expenditures

Capex capital expenditures

Tc total cost

Cf complexity factor

Pbt pay-back time

KPI key performance indicator

QMC quasi Monte-Carlo

MEA monoethanolamine

PSA pressure swing adsorption

HTL hydrothermal liquefaction

CHTG catalytic hydrothermal gasification

DHN district heating network

RC rankine cycle

HP heat pump(s)

frontiers
in Energy Research

ORIGINAL RESEARCH
published: 17 September 2021
doi: 10.3389/fenrg.2021.742109

Two Sides of the Same Coin—Explaining the Acceptance of CO_2-Based Fuels for Aviation Using PLS-SEM by Considering the Production and Product Evaluation

Lisanne Simons, Linda Engelmann, Katrin Arning*†*and Martina Ziefle*

Chair of Communication Science and Human-Computer Interaction Center, RWTH Aachen University, Aachen, Germany

Edited by:
Luis Puigjaner,
Universitat Politecnica de Catalunya,
Spain

Reviewed by:
Carlos Pozo,
Universitat Politecnica de Catalunya,
Spain
Anna-Gesina Hülemeier,
University of Münster, Germany

***Correspondence:**
Linda Engelmann
engelmann@comm.rwth-aachen.de

†Present Address:
Katrin Arning,
Hochschule Ansbach, Ansbach,
Germany

Specialty section:
This article was submitted to
Process and Energy Systems
Engineering,
a section of the journal
Frontiers in Energy Research

Received: *15 July 2021*
Accepted: *12 August 2021*
Published: *17 September 2021*

Citation:
Simons L, Engelmann L, Arning K and Ziefle M (2021) Two Sides of the Same Coin—Explaining the Acceptance of CO_2-Based Fuels for Aviation Using PLS-SEM by Considering the Production and Product Evaluation. Front. Energy Res. 9:742109. doi: 10.3389/fenrg.2021.742109

In the present study, we studied the acceptance of CO_2-based fuels for aviation as a product manufactured using Carbon Capture and Utilization (CCU). CCU can be regarded as the cornerstone for a circular approach. We focused on understanding whether the evaluation of CCU as a production method is related to the social acceptance of the resulting product. We applied an empirical quantitative approach using an online questionnaire targeted at German, Spanish, Dutch, and Norwegian respondents (N = 2,187). For both CCU and the fuel, lay perceptions in terms of perceived benefits and barriers were assessed, as well as their affective evaluation. Additionally, the acceptance of the end-product was surveyed. Using partial least squares structural equation modeling (PLS-SEM), we gained a better understanding of how the acceptance of CO_2-based fuels for aviation is formed. We found that the evaluation of CCU was mainly indirectly related to the acceptance of the product through relationships with the evaluation of the fuels. The perception of the benefits of CCU did affect the benefit perception of CO_2-based fuels the most, followed closely by the affective evaluation of the fuels. For the perception of the barriers of CO_2-based fuels, the perceived barriers of CCU were again the strongest predictor, followed by the affective evaluation of the fuels. We identified a moderate predictive power for the acceptance of CO_2-based fuels. The relationship with the perceived benefits of the fuels was the most relevant, followed by barrier perceptions, the affective evaluation of the fuels, and finally the benefit perception of CCU. Overall, the findings yield first insights into the role of the evaluation of CCU and CO_2-based fuels for aviation for the formation of the product's acceptance. The outcomes are useful for informing the product's and CCU's technical development and policy making. Additionally, they aid in the design of public information about CCU and support the development of sensible communication strategies for the successful market roll-out of CCU and CO_2-based fuels.

Keywords: CO2-based fuels for aviation, carbon capture and utilization, social acceptance, perception, affective evaluation, PLS-SEM

1 INTRODUCTION

In parallel with the growing public awareness of climate change and its potential consequences for future life on Earth, the number of (international) research efforts aiming to mitigate climate change has significantly increased in recent years (Foley et al., 2017). When supported by technical, economic, and political systems, such efforts might help to reduce the use of fossil resources by increasing the roll-out of renewable energy sources. Additionally, they could help to integrate more efficient processes and production lines that will reduce energy consumption altogether. In this regard, another aim is to develop green products, such as low-carbon chemicals and materials, that are produced with a circular economy in mind (Tenhunen and Pöhler, 2020). A circular economy refers to the use of multiple methods from different fields—e.g., science, process engineering, economics, ecology, and policy—to target closed material cycles, develop or rearrange production chains, and reframe consumption behaviors (Moreau et al., 2017; Morseletto, 2020). Alongside standardized approaches such as techno-economic and life cycle analyses, within a frame of reference, material and energy flows are analyzed and compared. In this way, ecological and environmental effects, resource depletion, and potential human-health consequences can holistically be assessed (Klöpffer, 2014; von der Assen and Bardow, 2014; Finkbeiner, 2014; International Standard Organization, 1997).

It is increasingly understood that circular economy efforts have strong social, policy, and governance components (Sovacool et al., 2015; Moreau et al., 2017; Boudet, 2019; Kirchherr and Piscicelli, 2019; Hartley et al., 2020), even though the majority of research activities still focus on technical and economic factors. Sovacool and colleagues (Sovacool et al., 2015; Sovacool et al., 2018) called for the systematic and consequent integration of social science knowledge and methods in the development and deployment of energy systems. In this way we can learn about the perception of potential barriers and risks of novel energy technologies (Slovic and Peters, 2006; Huijts et al., 2012; Emmerich et al., 2020), and use the social acceptance of these innovations for a successful energy transition (Moreau et al., 2017; Boudet, 2019). This is possible because studies on public perception and social acceptance can inform technical research and industry efforts about potential acceptance pitfalls quite early on in the development process (Arning et al., 2020). Additionally, such studies can help to launch public information strategies (Offermann-van Heek et al., 2020; Kluge et al., 2021), as well as tailor public education (Liebe and Dobers, 2019; Hartley et al., 2020) to the needs of consumers. Last, but not the least, acceptance research helps to foster a transparent communication between all involved stakeholders (Zaunbrecher and Ziefle, 2016; Boudet, 2019; Kluge et al., 2021) and might help to integrate and educate the public about the economic and ecological necessity to systematically rethink technology development in line with sustainability.

In the last couple of years, a general increase in studies dealing with social acceptance in renewable energy technologies can be observed. Such studies both deal with the acceptance of different energy technologies—e.g., wind (e.g., Devine-Wright et al., 2017; Fischhendler et al., 2021), biomass (e.g., Mather-Gratton et al., 2021), solar (e.g., Kratschmann and Dütschke, 2021), and hydrogen (e.g., Ricci et al., 2008)—and different CO_2-based end products—like fuels (Linzenich et al., 2019b; Engelmann et al., 2020) and insulation boards (Arning et al., 2021; Simons et al., 2021). Nevertheless, few studies combine public perception and acceptance while investigating more than one aspect or production step relevant from a circular economy perspective (Arning et al., 2018b; Offermann-van Heek et al., 2020).

In line with this research gap, this work studied the acceptance of one example of a product produced using the circular economy technology Carbon Capture and Utilization (CCU): CO_2-based fuels for aviation[1]. CO_2-based fuels are not an entirely circular product yet. However, it can be integrated within a circular economy approach in the sense that—in contrast to the rather linear production and consumption of traditional jet fuel from fossil resources—the CO_2-based fuel production pathway "bends" the line (to become a curve) and CO_2 use from direct air capture would then be the final step to complete circularity (to make the curve become a circle). This change would be different to the traditional production and consumption of jet fuel from fossil resources in the sense that the traditional process chain is linear in the prevailing linear economic model. We focused on understanding whether the social acceptance of the product is related to the public perception of CCU as the technology used to produce it. More specifically, we aimed to get a better understanding of whether, and if so to what extent, end users include their perception of CCU in their acceptance judgment of the product, rather than merely considering their evaluation of the product itself. To our knowledge, no previous study considered this aspect for any CO_2-based product.

The present article first establishes a theoretical basis for the study's aim. We then outline the logic of the empirical procedure alongside the research question and hypotheses. Next, we describe the measurement instrument and method, including a description of the sample and an explanation of the applied partial least squares structural equation modeling approach. Subsequently, the results section provides insights into the evaluation of CCU and CO_2-based fuels and presents the identified structural model and its quality evaluation. Finally, the findings are discussed and the limitations and prospects for future research are outlined.

2 PRODUCTION OF CO_2-BASED FUELS AS A LOW-CARBON AND SUSTAINABLE ALTERNATIVE

CCU is a circular economy approach that is currently being developed and employed. The main idea behind CCU is to reuse captured CO_2 as feedstock for the production of carbon-based materials and products (von der Assen and Bardow, 2014). In this way, CCU not only is valuable because of its potential

---

[1] In the remainder of this work (CO_2-based) fuels always refer to CO_2-based fuels for aviation.

contribution to mitigating climate change (Kätelhön et al., 2019), but also enables the more sustainable production of a variety of products: chemicals such as ethylene, methanol, and olefines (Kätelhön et al., 2019; Mustafa et al., 2020); also products such as construction materials, polymers, and fuels can be produced by using the CO_2 for mineral carbonation (Zimmermann et al., 2020b; Chauvy and De Weireld, 2020). Through the production of CO_2-based fuels, CCU can help to supply energy sources to nonelectrifiable mobility sectors that experience difficulties in switching to carbon-free fuel alternatives such as hydrogen. An example of such a mobility sector is the aviation sector (International Energy Agency, 2019).

Nevertheless, there are still some hurdles to overcome before the implementation of CCU reaches its full potential. First, the conversion of CO_2, as well as several other production steps, can be energy-intensive (Zimmermann et al., 2020a). To ensure an overall carbon-neutral CO_2 reuse, enough low-carbon energy sources must thus be available (Wich et al., 2020). Moreover, the widespread industrial implementation of CCU requires the construction of new plants, or adaptation of existing ones. This can include high-pressure processes and involves high investment costs. Additionally, all of this will happen in a sector that knows a slow market adoption (Zimmermann et al., 2020a). However, when these conditions for CCU are met, estimations predict that the greenhouse gases (GHG) emitted during the production of one ton of CO_2-based fuel—measured in CO_2 equivalents (CO_2e)—could be 34% less than the GHGs emitted during the production of one ton of a reference conventional fuel (Zakkour et al., 2018).

There are multiple ways to produce CO_2-based fuels: e.g., Fischer-Tropsch-synthesis that converts syngas into liquid hydrocarbons, or the production of methanol, dimethyl ether, or oxymethylene ether (e.g., Matzen and Demirel, 2016; Bongartz et al., 2018; Deutz et al., 2018; Dieterich et al., 2020). In the present study we considered a CCU process based on the separation of CO_2 from the flue gas streams of the exhaust of industrial plants, before the CO_2 is emitted. There are also several possible processes to separate the CO_2 from the flue gas, i.e., membrane adsorption, cryogenic separation, or the use of a physical solvent (Mustafa et al., 2020). Depending on the source of the flue gas, it can be necessary to purify the captured CO_2 before reusing it. If this is the case, the applied purification procedure depends on circumstances such as the CO_2 output flow rates and the type of impurities in the stream (Pieri et al., 2018; Pires da Mata Costa et al., 2021). After purification, the previously compressed CO_2 in some cases requires (if it is not converted in the existing plant) transport through pipelines, or using trucks or trains, depending on the properties of the gas stream and other external factors, such as transport distance (Pieri et al., 2018). Finally, the CO_2 is converted into CO_2-based fuels. The present study assumed a direct electrocatalytic conversion in a co-ionic membrane reactor. During the conversion, CO_2 is converted into chemical energy carriers in the form of hydrocarbons. The eCOCO$_2$ project and its interdisciplinary consortium[2] is studying this approach (eCCO$_2$, 2016).

3 SOCIAL ACCEPTANCE OF SUSTAINABLE TECHNOLOGIES

For CCU, as for all other sustainable innovations and related products and technologies, its social acceptance is a prerequisite for its successful market adoption. In the past, it has become apparent that in the case of renewable energy sources such as wind turbines a lack of local acceptance can manifest itself in the form of active protest (Ellis and Ferraro, 2016; Scherhaufer et al., 2017; Azarova et al., 2019). For these reasons, knowledge on the acceptance, and drivers of the acceptance, must be integrated in the development and deployment of innovations. To gather this knowledge, communication and social science methodologies should be incorporated in research efforts. Misperceptions about public attitudes, which could lead to erroneous decisions and miscommunication, can then be prevented by means of a thorough investigation of factors influencing acceptance, thereby also decreasing the chance of protests or opposition (Devine-Wright et al., 2017). Furthermore, the social insights can be used to regard the public's information needs when formulating targeted communication strategies. This allows the public to make decisions based on objectively oriented information (Offermann-van Heek et al., 2020). Altogether, the importance of the integration of social technology acceptance has increased in recent years, as can be derived from its inclusion in studies in fields like policy making and analysis (Akerboom et al., 2020; Bjø nå vold et al., 2020), and supply chain design (d'Amore et al., 2020).

According to the classification of Wüstenhagen et al. (2007), the social acceptance of sustainable, or renewable, technological innovations consists of three dimensions. First, the socio-political acceptance refers to the general acceptance or public support of a technology. For CCU, this refers to both the general technological approach of recycling CO_2 by converting it into other products, as well as the usage of these end products. Second, community acceptance describes the local acceptance of those who personally experience proximity to a CCU plant, e.g., because of the location of their home or their role as local decision makers. These stakeholders can show a positive attitude through acceptance, or a negative one through a rejection of the technology which possibly results in protests. Finally, the third dimension regards the market acceptance, which specifically refers to the acceptance and adoption by the consumers and investors. To understand the social acceptance of a sustainable technology, these three dimensions need to be studied separately, in combination with each other, and over longer periods of time.

We defined *acceptance* as the active adoption of a sustainable technology or product, to be distinguished from a merely reactive acceptance of the technology or product (Dethloff, 2004). In its most basic form, acceptance can thus be seen as a general willingness to use the innovation. In a broader perspective, acceptance also covers the underlying cognitive perceptions of a technology (e.g., assumptions and mental models about a technology, (perceived) knowledge as well as factual domain knowledge) and its affective evaluation (feelings, risk affects, and concerns about the innovation and the technology) (Huijts et al., 2012; Arning et al., 2019; Huijts et al., 2019;

---

[2] https://ecocoo.eu/.

Linzenich et al., 2019b). There is empirical evidence that acceptance can be regarded as adoption decision of persons to (not) use a technical product and this decision is influenced by cognitive and affective (risk) evaluations (Joffe, 2003; Linzenich et al., 2019b; Huijts et al., 2019; Engelmann et al., 2020). Going a step further, it also includes actions and attitudes that manifest itself in the active support of the innovation, for example by speaking out and promoting it (Huijts et al., 2012). Finally, the acceptance of a sustainable innovation could be manifested in a preference for the technology or product compared to comparable conventional alternatives. For that reason, previous research has often weighed the preference of individual product or production attributes, such as fuels, against one another to determine which technology and technological circumstances are most preferable (e.g., Hackbarth and Madlener, 2013; Hackbarth and Madlener, 2016; Linzenich et al., 2019a). We therefore also included the preference for a sustainable technology or product, compared to previously used conventional approaches, in our interpretation of acceptance. Altogether, acceptance is a complex construct which is challenging to accurately capture directly, especially if it regards generally unknown innovations (Fine, 1986; Sinkovics et al., 2002). It is assessed by measuring a behavioral intention, since the intent of a planned future action has a direct influence on acceptance, as has been noted in previous models that studied social acceptance in the context of sustainable energy technologies (e.g., Huijts et al., 2012; Broman Toft et al., 2014; Arning et al., 2021).

4 SOCIAL ACCEPTANCE OF CARBON CAPTURE AND UTILIZATION (PRODUCTS) AND CO_2-DERIVED FUELS

One part of the social science studies on CCU-related topics is dedicated to examining the *CCU technology* in general and the underlying infrastructure and process steps. Besides the practical challenges associated with CCU that must be tackled to implement the technology on a widespread basis—i.e., technical issues, high costs, and legal barriers (Scheelhaase et al., 2019), these studies helped to identify the barriers laypeople perceive as part of the public perception of CCU. Although laypeople's perceptions are not necessarily factual risks, gaining an understanding of these perceived risks and (usage) barriers is necessary to be able to design communication strategies and clarify misconceptions that could lead to a rejection of the technology and its products (Engelmann et al., 2020). One such often identified barrier regards CCU's questionable sustainability. Laypeople, e.g., think that CCU is an excuse to continue emitting CO_2 or that increased CO_2 emissions are merely delayed (Jones et al., 2014; Arning et al., 2017). Interestingly, whereas laypeople were ambivalent about the existence of unidentified risks of CCU as a technology, potential health risks resulting from the technology's deployment were rather dismissed (Offermann-van Heek et al., 2018).

Besides the barriers, studies also identified the perceived benefits of the CCU approach. Generally speaking, the public perceives CCU as beneficial and useful (Arning et al., 2018a). The best evaluated benefits are environmental, e.g., it buys more time in the mitigation of climate change, reduces the use of fossil resources, and reduces CO_2-emissions (Jones et al., 2014; Jones et al., 2017). Another example of a perceived advantage was the possible economic benefit of CCU, e.g., because of job generation (Offermann-van Heek et al., 2018).

Regarding the general acceptance of CCU, it was found to be positive, but tentative with scores not much higher than the midpoint of the scale, whereas local acceptance of CCU installations was still moderate but somewhat lower (Arning et al., 2020). In another study, CCU was found to be more positively accepted than Carbon Capture and Storage (CCS), in which the captured CO_2 is merely stored instead of reused (Arning et al., 2019). Moreover, some previous studies focused on understanding the drivers behind the acceptance of CCU. Arning et al. (2018b) found that as a CO_2 source, a steel plant was preferred over a chemical or coal-fired plant. The study also found that for the acceptance of CCU, profitability is the most decisive factor, thereby being more important than the obtained end product and the source of the CO_2. Nonpublic financing was the preferred way to make CCU profitable, indicating that there is little willingness to pay for the implementation of CCU installations among laypeople. In line with the theories described in **Section 3**, other studies found that the acceptance of CCU primarily increases as the benefits for the technology are increasingly perceived. An increase in acceptance was also seen when the technology was increasingly perceived to be mature and innovative. Contrarily, perceived barriers—e.g., risks connected to the use and disposal of CCU products—have been found to reduce the acceptance (Linzenich et al., 2019b; Offermann-van Heek et al., 2020).

As aforementioned, the specific acceptance of CCU products should be included in acceptance studies as well. Even though laypeople perceived relatively few barriers for such products, sustainability doubts, increased (energy) costs, and a possibly reduced product quality were still identified as possible acceptance hurdles (Jones et al., 2014, 2015; Arning et al., 2017; Arning et al., 2018a). Regarding the benefits of CCU consumer products—e.g., mattresses—laypeople again perceived environmental and economic benefits, e.g., the contribution to climate change mitigation and job opportunities, respectively (Jones et al., 2015; Arning et al., 2018a).

CCU products are generally positively accepted. The products studied so far include CO_2-based mattresses and beverages infused with recycled CO_2 (Offermann-van Heek et al., 2018). Their acceptance is usually reflected in laypeople's expressed willingness to use and buy CCU products (Arning et al., 2018a). Moreover, van Heek et al. (2017b) identified acceptance-relevant factors for CCU products. These included the disposal conditions and the saved fossil resources resulting from their replacement by CO_2. Contrarily, the amount of CO_2 that can be stored in a product was less relevant for its acceptance. Additionally, the benefit and barrier perceptions of the CCU products had a direct positive and negative effect, respectively, on the acceptance of the products (Offermann-van Heek et al., 2018).

Regarding specific CCU products, some studies found CO_2-based fuels to be the preferred CCU product compared to other possible manufactured goods, such as e.g., fertilizer or mattresses (Arning et al., 2018b; Offermann-van Heek et al., 2018). In general, laypeople assessed CO_2-based fuels to be safer, more eco-friendly, less toxic, cleaner, and less harmful than their conventional counterparts (Engelmann et al., 2020). The product was also better accepted than the individual CCU production steps—the capture, transport, and conversion of CO_2—required to make the product (Offermann-van Heek et al., 2020).

Finally, a few studies have started to build a bridge between the evaluation of CCU as a technology and the resulting products. Lutzke and Árvai (2021) found that for carbonized beverages, the source from which the CO_2 is captured can influence the willingness to use a resulting CO_2-based product. In this case, an increased negative evaluation of CCU also decreased the product's acceptance. Arning et al. (2018a) did study laypeople's perceptions of CCU and mattresses as a CCU product in a single study, but did not examine possible relationships between the two evaluations. Additionally, Offermann-van Heek et al., 2020 identified a rather small fuel production site in the form of a biogas plant, which does not require the transport of CO_2, as the best case scenario for the production of CO_2-based fuels. However, their methodology does not allow the derivation of conclusions about the role of the perception of the infrastructure on the perception of the product. The first approaches to dovetailing CCU as a technological process with the resulting products have thus been established, but both aspects still need to be combined in a detailed and systematic way.

5 DERIVATION AND JUSTIFICATION OF EMPIRICAL PROCEDURE

Since the acceptance of CCU is a complex phenomenon for which multiple dimensions and stakeholders should be considered (Wüstenhagen et al., 2007), acceptance studies should focus not only on understanding the acceptance of CCU as a technology, but also on the acceptance of the resulting CCU products. We believe that the latter is thereby of especially great importance because without the public's adoption of the products—through the subtle act of choosing, or at least tolerating, them—the CCU technology will not be able to thrive. Additionally, a rejection of the produced CCU products will lead to a loss of resources such as time and investments used to employ the CCU technology. For these reasons, this study focused on obtaining a better understanding of the public acceptance of CO_2-based fuels for aviation as an example of a CCU product. As such, it considered aspects of the socio-political and market acceptance proposed by Wüstenhagen et al. (2007) (**Section 3**).

However, we recognize that the acceptance and perception of CCU as a production method is important as well. A strong rejection of the technology could hinder its successful roll-out if it leads to active opposition and protests or lack of funding. Additionally, one could assume that the consumers use their evaluation of the technology when evaluating the resulting product, since CCU products cannot exist without the CCU production technology. Even though the findings discussed in **Section 4** show that studies have gathered diverse insights on several aspects of both CCU as a technology and the resulting products, to our knowledge, the relationship between the evaluation of CCU and the acceptance and evaluation of CCU products has not been covered in previous studies. Based on this research gap, we formulated the following research question to guide the study described in the present article:

What role, if any, does the evaluation of CCU as a production method play in the formation of the acceptance of CO_2-based fuels for aviation as an example of a CCU product?

Answering this research question could be very valuable for the design of communication strategies for the product's and technology's market roll-out, since it helps to pinpoint what the communication should focus on.

5.1 Hypotheses

Because of the explorative approach of the study, we defined a broad range of hypotheses to aid in answering the research question. We thereby focused on the cognitive and affective evaluation of the technology and product as possible drivers behind acceptance (Huijts, 2018). These evaluations are assumed to have a greater influence on the formation of acceptance than, e.g., the demographic characteristics of the respondents (Liu et al., 2019).

First, the cognitive determinants include the perceived benefits and barriers (Liu et al., 2019). As aforementioned, the role of such perceptions of a product or technology on the acceptance of that product or technology has been well established by previous theories and findings (e.g., Huijts et al., 2012; Arning et al., 2020; Engelmann et al., 2020). In line with these previous findings, as well as our goal of exploring the possible relationships between CCU and the acceptance of CO_2-based fuels for aviation, we propose the following hypotheses:

H1$_a$: The benefit perception of CO_2-based fuels is positively related to the acceptance of CO_2-based fuels.
H1$_b$: The barrier perception of CO_2-based fuels is negatively related to the acceptance of CO_2-based fuels.
H1$_c$: The benefit perception of CCU is positively related to the acceptance of CO_2-based fuels.
H1$_d$: The barrier perception of CCU is negatively related to the acceptance of CO_2-based fuels.

In this regard we also explored the possibility of indirect relationships through relationships between the perception of CCU and the perception of CO_2-based fuels using the following hypotheses:

H2$_a$: The benefit perception of CCU is positively related to the benefit perception of CO_2-based fuels.

H2$_b$: The benefit perception of CCU is negatively related to the barrier perception of CO_2-based fuels.
H2$_c$: The barrier perception of CCU is positively related to the barrier perception of CO_2-based fuels.
H2$_d$: The barrier perception of CCU is negatively related to the benefit perception of CO_2-based fuels.

Second, the cognitive determinants are distinguished from the affective attitude toward a technology or product. Affect can be regarded as an emotional evaluation that is made rather intuitively (Slovic and Peters, 2006; Cousse et al., 2020). This has been found to affect judgments directly, as well as through its relationship with perceived risks—in our case barriers—and benefits (Finucane et al., 2000; Linzenich et al., 2019b). For this we proposed the following hypotheses:

H3$_a$: The affective evaluation of CO_2-based fuels is positively related to the acceptance of CO_2-based fuels.
H3$_b$: The affective evaluation of CO_2-based fuels is positively related to the benefit perception of CO_2-based fuels.
H3$_c$: The affective evaluation of CO_2-based fuels is negatively related to the barrier perception of CO_2-based fuels.
H3$_d$: The affective evaluation of CCU is positively related to the acceptance of CO_2-based fuels.
H3$_e$: The affective evaluation of CCU is positively related to the benefit perception of CCU.
H3$_f$: The affective evaluation of CCU is negatively related to the barrier perception of CCU.

Finally, the possible relationship between the affective evaluation of the technology and the evaluation of the product was explored as well:

H4$_a$: The affective evaluation of CCU is positively related to the affective evaluation of CO_2-based fuels.
H4$_b$: The affective evaluation of CCU is positively related to the benefit perception of CO_2-based fuels.
H4$_c$: The affective evaluation of CCU is negatively related to the barrier perception of CO_2-based fuels.

6 METHODS

In this section, we will cover the used measurement instrument, data collection and preparation approach, final sample, the applied PLS-SEM procedure, and the additional statistical tests.

6.1 The Measurement Instrument

As a measurement instrument, we used a quantitative online questionnaire generated using the survey software by *Qualtrics*[3]. Porteron et al. (2019) and Lotz (2020) For the development and selection of items for the questionnaire different sources were consulted: 1) input from previous (CCU) acceptance studies (**Section 4**); 2) discussions and exchange with project partners of the *Horizon2020 eCOCO$_2$* consortium[2] (supported by literature review (e.g., Porteron et al., 2019 and Lotz, 2020)), in combination with; 3) validated items scales if available. All items included in the analysis can be found in the supplementary materials (**Supplementary Table S1**). The original German questionnaire was translated for its use in Spain, Norway, and Netherlands. Whereas the German and the Dutch versions were prepared within the authors' group, a translation agency was consulted for the Norwegian and Spanish translations. All translated surveys were subsequently pretested and cross-checked by native speakers of the respective languages. Moreover, the ethical board of the Faculty of Humanities at RWTH Aachen University checked and approved the survey's ethical acceptability.

Before starting, the respondents completed a few screening questions to control for a representative sample—regarding nationality, age, gender, education, and home region—of respondents between 18 and 70 years of age. Subsequently, the respondents received a brief introduction on the survey's topic, were reminded of their rights, and informed on how the data would be handled [with regard to the data privacy standards of the DSGVO (Schwartz, 2019)].

In the main part of the questionnaire, question blocks were alternated with increasingly detailed explanations of the production process. The provided explanations were easily and objectively formulated, and checked for technical correctness by experts in the field of CCU[4]. The first explanation briefly covered the overall production process of CO_2-based fuels using CCU. This allowed the respondents to indicate their affective evaluation, benefit perception, and barrier perception of CCU as a production process for the fuels. In the subsequent parts of the questionnaire, the respondents received five further, more detailed, explanations covering: the separation, purification, transport, and conversion conversion of CO_2, as well as CO_2-based fuels for aviation as an end product. This enabled the respondents to then indicate their affective evaluation, benefit perception, barrier perception, and acceptance of CO_2-based fuels for aviation.

In **Section 6.4.2** the used questions are considered in more detail. All multiple-item measurements used six-point scales—ranging from *0 = most negative answer* to *5 = most positive answer*. Within the questionnaire blocks queried with Likert scales, the statements to be evaluated were presented in a randomized order.

6.2 Data Collection and Preparation

Data were collected in the fall of 2020 using the paid services of a market research company. Data collection targeted German, Dutch, Spanish, and Norwegian respondents. To ensure a good quality dataset the survey included two quality checks, during which the respondents were asked to select a specific response and were marked as *failed quality check* if they failed to do so. After this quality check and further cleaning[5] we ended up with a final dataset

---

[3]https://www.qualtrics.com.

[4]An English translation of these explanations can be found in the supplementary material.

[5]From the sample of 9,738 participants who at least started the survey, respondents were removed because of: full quotas; incomplete data sets; speeding, i.e., all participants whose response time was below 35 percent of the median duration, and; internally inconsistent answering patterns, i.e., cases that indicated (dis) agreement for two items phrasing the same statement oppositely.

of N = 2,187 respondents. On average, participants took 23.2 min (SD = 9.6 min) to fully complete the survey.

If necessary, we recoded the data so that 0 always referred to the most negative answer from the question's point of view, and 5 to the most positive. We also computed a grouping variable for the respondents' education. The different nationalities received a different question on their highest achieved level of education in line with the used system in the respective countries. We grouped the answers to these questions into a single variable using a low, medium, and high level of education based on the International Standard Classification of Education (ISCED)[6] (Eurostat Statistics Explained, 2011). An overview of the grouping can be found in the supplementary material (**Supplementary Tables S2–S5**).

6.3 Sample

Of the N = 2,187 respondents in the sample after cleaning, 48% were male (n = 1,052) and 52% were female (n = 1,135). By design, the ages ranged between 18 and 70 years (fixed quotas set for each country). The average age was M = 45.0 (SD = 14.5). Most of the respondents completed a medium (n = 1,005, 46%) or high (n = 820, 37%) level of education. A relatively small share of the respondents completed a low level of education (n = 362, 17%). Finally, of the respondents, 25% were German (n = 543), 25% were Spanish (n = 545), 25% were Dutch (n = 549), and 25% were Norwegian (n = 550). In the supplementary material, **Supplementary Table S6** depicts how well the collected sample represents the aimed sample, which was based on the representative distributions in the included countries. Regarding age and gender, our sample represented the respective populations fairly well. However, for the respondents' education and region there were more discrepancies. Additionally, **Supplementary Table S7** in the supplementary material summarizes the descriptive data for the constructs in the final model (**Section 7.2**) for each country. Even though occasional differences between the included countries occurred, the present study aimed to take a cross-national, pan-European view. We therefore only use and interpret the overall sample in the remainder of the present article.

Finally, we also assessed the participants' previous experience with CO_2-based fuel production using three items[7]. Overall, we found that the previous experience with CO_2-based fuel production was rather low (M = 1.6, SD = 0.3) for all countries (Norway: M = 1.2, SD = 0.9; Germany: M = 1.5, SD = 0.8); the Netherlands: M = 1.6, SD = 0.9; Spain: M = 2.0, SD = 0.9).

6.4 Partial Least Squares Structural Equation Modeling (PLS-SEM)—Procedure

In this subsection, we report on the PLS-SEM procedure starting with the theoretical background of the methodological approach, followed by the description of how the model selection was accomplished. We also outline the procedures of model specification and evaluation. The latter includes the reflective and formative measurement evaluation, as well as the structural model evaluation.

6.4.1 Partial Least Squares Structural Equation Modeling

To test the hypotheses introduced in **Section 5**, we applied partial least squares structural equation modeling (PLS-SEM). As extensively described by Hair et al. (2017), SEM is a multivariate analysis technique. It thus allows the simultaneous exploration of multiple variables. Although other kinds of SEM exist as well, the PLS approach is especially well equipped for exploratory research. A model designed using PLS-SEM consists of two model layers that are analyzed simultaneously. The first is the *measurement model* (*outer model*). In social science research, the concepts included in a study are often abstract and cannot be measured directly. Instead, they are measured using several items (manifest variables, indicators) which are then combined to form a construct (latent variable) (Sarstedt et al., 2016). The relationships between the included constructs and their indicators are referred to as the *measurement model*. The second is the *structural model* (*inner model*), which consists of the relationships between the different constructs. In the present study, the *structural model* will be used to evaluate the hypotheses.

There are two ways to measure latent variables which are represented differently in the *measurement model*. For *reflective measurements*, the indicators "are considered to be error-prone manifestations of an underlying construct with relationships going from the construct to its indicators" (Bollen, 1989; as cited in Sarstedt et al., 2016, p. 4000). Such indicators can thus be seen as "a representative sample of all the possible items available within the conceptual domain of the construct" (Nunnally and Bernstein, n.d., as cited in Sarstedt et al., 2016, p. 4000). To give an example, in our study, the construct of *support* (**Section 6.4.2**) can be considered as an example for reflective measurement, as statements about one's support of an object are interchangeable and omitting a supporting statement does not change the content of the construct. For *formative measurements* "the indicators form the construct by means of linear combinations" (Diamantopoulos, 2006, as cited in Sarstedt et al., 2016, p. 4000). Contrary to reflective measurements, the values of the indicators of formative measurements are not assumed to have the construct as a common cause. Instead, the indicators are aspects of the construct and the relationships run from the indicators to the construct (Hair et al., 2017, p. 73). Formative constructs are present, for example, in the case of *barriers* and *benefits* of a technology, since omitting a beneficial or detrimental facet can change the content of the construct.

Additionally, our *measurement model* included single-indicator constructs—which are reflective by nature—as well as higher-order constructs (HOCs). In a HOC, several lower-order constructs (LOCs) act as the indicators of the construct.

---

[6] https://ec.europa.eu/eurostat/statistics-explained/index.php/International_Standard_Classification_of_Education_(ISCED)#Implementation_of_ISCED_2011_.28levels_of_education.29.

[7] 1:"I have a great interest in the production of CO_2-based fuels."; 2: "I know a lot about the production of CO_2-based fuels." and 3: "I have never thought about the issue of the production of CO_2-based fuels."

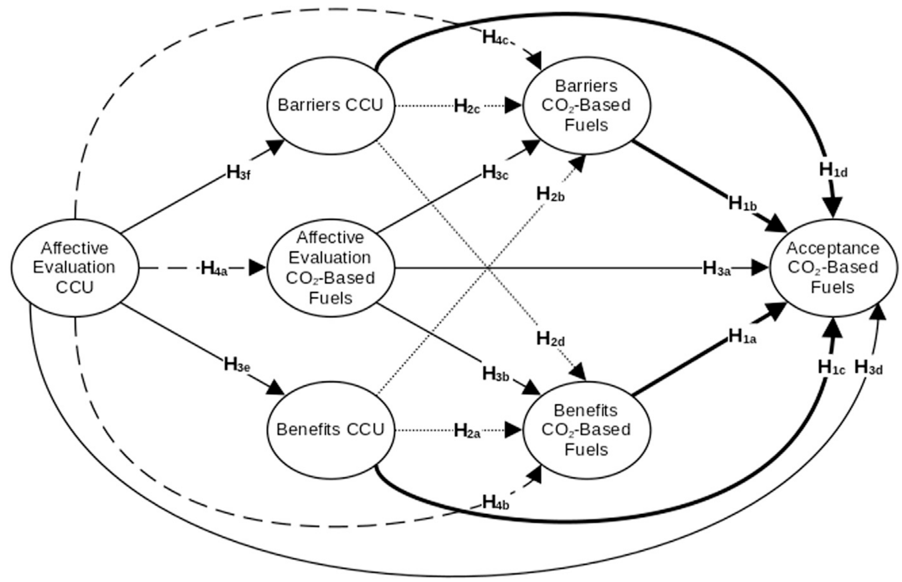

FIGURE 1 | Overview of hypotheses. The thick solid lines indicate the hypothesized direct relationships between perception and acceptance (H_1); the dotted lines indicate the hypothesized relationships between the perception of CCU and the perception of CO_2-based fuels (H_2); the thin solid lines indicate the hypothesized relationships between the affective evaluations and perception and acceptance (H_3); and the long-dashed lines indicate the hypothesized relationships between the affective evaluation of CCU and the evaluation and perception of CO_2-based fuels (H_4).

These LOCs are constructs with their own indicators and measurement type (Sarstedt et al., 2019). In the present study, the use of HOCs allows the easier interpretation of the subcomponents (LOC) that are considered as part of the model's abstract concepts (HOC).

Finally, in the *structural model*, constructs can be exogenous, endogenous, or both. Exogenous constructs explain (an)other construct(s) in the model, whereas endogenous constructs are being explained by (an)other construct(s) (Hair et al., 2017, p. 46). Since *Affective Evaluation CCU* explains others included in the model, it represents an exogenous construct, whereas *Affective Evaluation* CO_2*-Based Fuels*—while explaining other constructs itself—is being explained by the former, therefore functioning as an endogenous construct.

6.4.2 Model Specification

We defined our original structural model based on the hypotheses described in **Section 5.1**. The structural model is depicted in **Figure 1**. In the graphic, the ovals refer to the structural model's constructs and the paths run from the exogenous to the endogenous constructs. A complete overview of the constructs, indicators (abbreviations), and items they refer to is provided in **Supplementary Table S1** in the supplementary material.

The *Affective Evaluation CCU* (*CUAE1—CUAE6*) and *Affective Evaluation* CO_2*-Based Fuels* (*FAE1—FAE6*) were the only two non-HOC constructs in the model. These constructs referred to the feelings the respondents had about CCU as a production method, and CO_2-based fuels as an end product, respectively. This was measured using two semantic differentials that consisted of the same six opposing adjective pairs. The adjective pairs were inspired by Engelmann et al. (2020). The affective evaluation is likely to be different if different adjective pairs are used. The constructs thus resemble formative, measurements.

The constructs for the benefits and barriers of CCU, and the benefits and barriers of CO_2-based fuels, were HOCs. They were based on benefit and barrier perceptions used in previous studies on CCU (e.g., Arning et al., 2019) and CCU products (e.g., Offermann-van Heek et al., 2018; Engelmann et al., 2020; Simons et al., 2021), as well as extensive discussions with the project partners of the *Horizon2020 eCOCO*$_2$ consortium^2. These HOCs for the perception also resembled formative measurements because the inclusion of other benefit and barrier aspects likely changes the construct. The multiple-item LOCs for these perception HOCs resembled formative measurements as well, since different items highlighting different aspects of the LOCs likely exist.

The HOC *Benefits CCU* had two multiple-indicator LOCs. The *Environmental Benefits CCU* referred to CCU's benefits for the environment and consisted of five indicators (*CUBEN1—CUBEN5*). The *Policy Benefits* referred to policy-related benefits of CCU and consisted of four indicators (*CUBEN6—CUBEN9*). Additionally, the HOC included two single-indicator constructs that highlighted a specific benefit for which the given name is self-explanatory: *Employment Opportunities* (*CUBEN10*) and *Raise Awareness* CO_2 *Reuse* (*CUBEN11*).

The HOC *Barriers CCU* also had two multiple-indicator LOCs. The *Policy Barriers* referred to policy-related barriers of CCU and consisted of four indicators (*CUBAR1—CUBAR4*). The *Sustainability Barriers* referred to barriers related to the environmental sustainability of the production method and consisted of four indicators (*CUBAR5—CUBAR8*). The HOC also included one single-indicator construct that highlighted a specific barrier: *Scale Barrier* (*CUBAR9*), which referred to the observation that CCU will not contribute to the reduction of CO_2 emissions if it is only applied in Europe. The HOC *Benefits* CO_2-*Based Fuels* only had *Environmental Benefits Fuels* as a multiple-indicator LOC. It consisted of three indicators (*FBEN1—FBEN3*) and referred to environmental benefits of using CO_2-based fuels for aviation. Additionally, the HOC had three single-indicator LOCs: *Future of Flying* (*FBEN4*) referred to the possibility of continuing flying after fossil resources have been exhausted; *Sustainability Aviation* (*FBEN5*) referred to the product's potential to do something to increase the sustainability of air travel; and *Increased Quality* (*FBEN6*) referred to the increased quality of the product because of the use of CO_2.

Finally, the HOC *Barriers* CO_2-*Based Fuels* consisted of five single-indicator LOCs. Three of these are self-explanatory: *Increased Prices Air Tickets* (*FBAR1*), *Insufficient Research* (*FBAR3*), and *Decreased Quality* (*FBAR5*). Moreover, *Safety Risk* (*FBAR2*) referred to the fear that the fuels pose a safety risk because existing motors were not built for them, and *Less Motivation to Fly Less* (*FBAR4*) referred to the fear that people will be less motivated to change their flying behavior for environmental reasons when the CO_2-based fuels are used.

The final construct, which was a HOC as well, regarded the acceptance of CO_2-based fuels for aviation. In line with the used definition of acceptance (**Section 3**), it referred to people's willingness to use, support, and prefer the product. *Acceptance* CO_2-*Based Fuels* consisted of three LOCs and resembled a formative measurement, since including other acceptance aspects likely changes the construct. The items for the indicators of the LOCs were presented as a Likert scale question. The first was a single-indicator LOC *Willingness to Use* (*FCA1*), more specifically this referred to the respondents' willingness to fly in an airplane driven by CO_2-based fuels. Moreover, the LOC *Support* consisted of two indicators (*FCA2*, *FCA3*) and referred to the respondents' support of CO_2-based fuels for air travel. *Support* resembled a reflective measurement, since one either supports the product or not, and it is thus an overlying construct for its indicators. For the same reason, the final LOC, *Preference*, also resembled a reflective measurement. It consisted of three indicators (*FCA4—FCA6*) and referred to the respondents' preference of CO_2-based fuels compared to conventional options.

6.4.3 Model Evaluation

The model was implemented and evaluated using the programming language *R* and the *SEMinR* package[8] (Ray et al., 2021). With N = 2,187 respondents, the sample was large enough to be used for our hypothesized model (**Section 6.4.2**) (Hair et al., 2017, p. 47). During the analysis, we refined the hypothesized model through several iterations to find a final model with a good quality. To do so, we first refined the measurement model through the step-wise removal of indicators that did not adhere to the quality criteria, removing the worst one in each iteration. When the measurement model sufficed, the structural model was evaluated and refined by removing the worst relationship that did not meet the quality criteria in each iteration, until the structural model sufficed as well. In **Section 7**, we only outlined the results for the final model. To evaluate the measurement model, different quality criteria were used for formative and reflective measurements. Since all HOCs were formative, their quality was evaluated using the criteria for formative measurements. The quality of the HOCs' LOCs was evaluated separately based on their measurement type (Sarstedt et al., 2019). Moreover, there are no quality criteria for single-indicator constructs. Finally, we applied bootstrapping with 5,000 repetitions to the model. This was done to be able to assess several quality criteria that use the bootstrapped confidence interval (*CI*).

Reflective measurement evaluation. We reported the loadings (λ) and assessed the internal consistency reliability, convergent reliability, and discriminant validity according to the guidelines by (Hair et al., 2017, p. 136–143). The *internal consistency reliability* refers to how well the different indicators fit together. To assess this we reported Cronbach's alpha (α) as the lower bound of the true reliability and the composite reliability (ρ_C) as the upper bound. To meet the criterion, both the values had to be ≥ 0.60 and ≤ 0.90. The *convergent reliability* considers "the extent to which a measure correlates positively with alternative measures of the same construct" (Hair et al., 2017, p. 137). To measure this, we considered the average variance extracted (AVE) and the outer indicator loadings. When AVE $\geq$ 0.50 and $\lambda \geq 0.70$ there was convergent reliability. The *discriminant validity* is "the extent to which a construct is truly distinct from other constructs by empirical standards" (Hair et al., 2017, p. 138). This was measured using the heterotrait-monotrait ratio (HTMT) by assessing the bootstrapped *CI*s. If the *CI*s did *not* contain the value 1, there was sufficient discriminant validity.

Formative measurement evaluation. We reported the original estimate weight (w) and the mean weight of the bootstrapping (M). As quality measures, we assessed the collinearity, as well as the significance and relevance of the indicators according to the guidelines by Hair et al. (2017, p. 163–175). We could not assess the convergent validity—"the extent to which a measure correlates positively with other (e.g., reflective) measures of the same construct using different indicators"—since we did not measure the same constructs in multiple ways. *Collinearity* refers to whether indicators of the same construct highly correlate. For formative measurements, indicators are expected not to show collinearity. This was assessed using the variance inflation factor (VIF), which showed that there was no collinearity if VIF ≤ 5. For the *significance and relevance* of the indicators, the outer weight (w) was evaluated. A positive w signifies relevance. The significance of the weight was assessed using the t-statistic of the two-tailed t-test, which had to be $t >$ 1.65. Additionally, significance was implied if the bootstrapping *CI* did not contain 0.

Structural model evaluation. The evaluation of the structural model was also conducted based on the guidelines by Hair et al. (2017, p. 205–215). For each relationship, we reported the

---

[8] https://CRAN.R-project.org/package=seminr.

original estimate β and the bootstrapped mean estimate M. The β value refers to the strength of the relationship: if the exogenous construct changes by x, the endogenous construct changes by $x \times beta$. We first assessed the *collinearity* of each endogenous construct with multiple exogenous constructs pointing toward it using the VIF. There was no collinearity if VIF ≤5. Then, we evaluated the *significance* of the relationships using the t-statistic of the two-tailed t-test and the bootstrapped *CI*. A relationship was significant if $t > 1.65$—p was reported as well—and *CI* did not contain 0. To see whether the impact of an exogenous construct on an endogenous construct was substantial, the *effect size* f^2 was calculated and interpreted as follows: $f^2 = 0.02$ (small effect), $f^2 = 0.15$ (medium effect), $f^2 = 0.35$ (large effect). Finally, we looked at the *in-sample predictive power* of the constructs using R^2 and R^2_{adj} which were interpreted as follows: $R^2 \leq 0.10$ (lack of predictive power), $R^2 = 0.25$ (weak power), $R^2 = 0.50$ (moderate power), $R^2 = 0.75$ (substantial power).

6.5 Additional Statistical Analyses

To get an idea of how the constructs used in the PLS-SEM model were evaluated, we additionally analyzed them separately. To do so, we computed a value for the constructs by taking the mean of its indicators in the final model. For the HOCs, we used the LOC's single indicators and did not separately consider the LOCs. For all of these constructs, Cronbach's was $\alpha \geq 0.70$ (**Supplementary Table S1** in the supplementary material). As descriptive statistics, we reported the sample's mean evaluation (*M*) and standard deviation (*SD*). To test whether the mean evaluation was significantly different from the midpoint of the scale—which lay at 2.5—we used one sample t-tests. An evaluation significantly higher than the midpoint of the scale indicated a significant tendency toward the positive. There were no evaluations lower than the midpoint of the scale. We also used paired samples t-tests to test whether the single adjective pairs of the affective evaluation of CCU and CO_2-based fuels were evaluated significantly different[9]. For both of these tests, the level of significance was set at $\alpha = 0.05$ and Cohen's d was calculated as the effect size. The latter was interpreted as follows: $d = 0.20$ (small effect), $d = 0.50$ (medium effect), and $d = 0.80$ (large effect) (Cohen 1988, 1992, as cited in Field, 2018, p. 176).

7 RESULTS

In this section we will describe the respondents' evaluation of CCU and CO_2-based fuels for aviation, the results of the final model based on PLS-SEM, and the final model compared to the hypothesized model. Additionally, we will take a look at the strength of the predictions and predictors.

TABLE 1 | Descriptive statistics and results of one sample t-test with 2.5 for the evaluation of the constructs for CCU and CO_2-based fuels.

	M	*SD*	*t* (2,186)	*p*	*d*
Acceptance CO_2-based fuels	3.22	0.89	37.6	<0.001	0.80
Benefits CO_2-based fuels	3.30	0.84	44.6	<0.001	0.95
Barriers CO_2-based fuels	2.63	0.90	6.88	<0.001	0.15
Affective evaluation CO_2-based fuels	3.18	1.08	29.2	<0.001	0.62
Benefits CCU	3.10	0.83	33.9	<0.001	0.72
Barriers CCU	2.70	0.78	9.28	<0.001	0.20
Affective evaluation CCU	2.96	1.05	20.4	<0.001	0.44

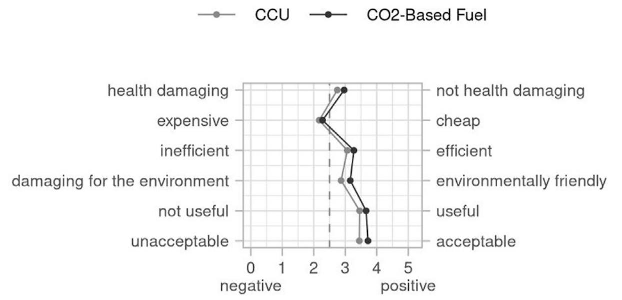

FIGURE 2 | Results of the affective evaluation of CCU and CO_2-based fuels ($N = 2,187$).

7.1 Evaluation of Carbon Capture and Utilization and CO_2-Based Fuels

Table 1 depicts the results of the paired-samples t-tests with the midpoint of the scale for the constructs. It shows that the respondents accepted the use of CO_2-based fuels rather than rejecting it, agreed to the perception of the fuels' benefits, as well as the perception of its barriers. For the perception of CCU as a production method, both the benefits and the barriers were also perceived rather than not. Regarding the perception of both CCU and the fuel, the effect size for the difference between the evaluation and the midpoint of the scale was negligible and small, respectively, for the barrier perception, but large and medium, respectively, for the benefit perception.

The table also includes the affective evaluation of CCU and the fuels. These evaluations can directly be compared since the same adjective pairs were used in both semantic differentials. On average, the affective evaluation tended toward the positive for both CCU and the fuels. In **Figure 2**, the evaluations of the single adjective pairs for CCU and the fuels are depicted. For all adjective pairs, CO_2-based fuels were evaluated a bit more positively than CCU, and all of these differences were significant (**Table 2**).

7.2 Partial Least Squares Structural Equation Modeling—Model Evaluation

7.2.1 Measurement Model Evaluation

The results for the reflective LOCs are depicted in **Table 3**. They show that the convergent validity and internal consistency

---

[9] Before conducting paired t-tests it was checked if assumptions are met and normal distribution was present. In case of sporadic outliers we additionally checked whether nonparametric testing yielded same significance and since this was the case we stayed with the interpretation of these results.

TABLE 2 | Results of paired samples t-test for differences in the affective evaluation of CCU and CO_2-based fuels.

	CCU		**CO_2-based fuels**		***t* (2,186)**	***p***	***d***
	M	***SD***	***M***	***SD***			
Unacceptable–acceptable	3.45	1.34	3.72	1.28	–10.9	<0.001	–0.21
Not useful–useful	3.46	1.38	3.66	1.32	–7.83	<0.001	–0.15
Damaging for the environment–environmentally friendly	2.87	1.53	3.16	1.38	–9.45	<0.001	–0.20
Inefficient–efficient	3.07	1.30	3.27	1.32	–7.59	<0.001	–0.16
Expensive–cheap	2.17	1.28	2.28	1.36	–3.72	<0.001	–0.079
Health damaging–not health damaging	2.75	1.38	3.00	1.30	–7.93	<0.001	–0.16

TABLE 3 | Evaluation of the reflective lower-order constructs (LOC): original estimate loading (λ), internal consistency reliability (α, ρ_C), and convergent validity (AVE).

Construct	**Indicator**	**λ**	**α**	**ρ_C**	**AVE**
Acceptance of CO_2-based fuels: support	FCA2	0.89	0.67	0.86	0.75
	FCA3	0.84			
Acceptance of CO_2-based fuels: preference	FCA4	0.87	0.79	0.88	0.70
	FCA5	0.85			
	FCA6	0.79			

TABLE 4 | Evaluation of the formative constructs and lower-order constructs (LOC): collinearity (VIF) and indicator weight (original estimate *w*, bootstrap mean *M*, t-statistic t (2,187), *p*-value).

Construct	**Indicator**	**VIF**	**Weights**			
			w	***M***	***t* (2,187)**	***p***
Benefits CCU: environmental benefits CCU	CUBEN1	2.28	0.22	0.22	5.74	<0.001
	CUBEN2	2.09	0.29	0.29	7.70	<0.001
	CUBEN3	1.81	0.16	0.16	4.15	<0.001
	CUBEN4	2.44	0.26	0.26	6.38	<0.001
	CUBEN5	2.17	0.27	0.27	6.90	<0.001
Benefits CCU: policy benefits	CUBEN6	1.78	0.20	0.20	5.03	<0.001
	CUBEN7	1.67	0.51	0.51	14.6	<0.001
	CUBEN8	1.88	0.31	0.31	8.24	<0.001
	CUBEN9	1.55	0.21	0.21	6.25	<0.001
Barriers CCU: policy barriers	CUBAR1	1.31	0.20	0.20	3.63	<0.001
	CUBAR2	1.44	0.36	0.36	6.37	<0.001
	CUBAR3	1.32	0.45	0.45	8.56	<0.001
	CUBAR4	1.22	0.35	0.35	6.49	<0.001
Barriers CCU: sustainability barriers	CUBAR5	1.38	0.36	0.36	5.30	<0.001
	CUBAR6	1.46	0.39	0.39	6.30	<0.001
	CUBAR7	1.37	0.32	0.32	5.08	<0.001
	CUBAR8	1.29	0.27	0.27	4.46	<0.001
Affective evaluation CCU	CUAE1	3.62	0.23	0.23	4.92	<0.001
	CUAE2	3.53	0.28	0.28	6.42	<0.001
	CUAE3	2.97	0.15	0.15	3.46	<0.001
	CUAE4	1.82	0.25	0.25	7.27	<0.001
	CUAE5	1.19	0.16	0.16	5.34	<0.001
	CUAE6	2.40	0.22	0.21	5.75	<0.001
Benefits CO_2-based fuels: environmental benefits fuels	FBEN1	2.11	0.51	0.51	15.6	<0.001
	FBEN2	1.92	0.29	0.29	8.66	<0.001
	FBEN3	1.88	0.34	0.34	10.5	<0.001
Affective evaluation CO_2-based fuels	FAE1	4.97	0.26	0.26	5.75	<0.001
	FAE2	5.32	0.34	0.34	7.34	<0.001
	FAE3	3.36	0.11	0.11	3.05	= 0.001
	FAE4	2.67	0.16	0.16	4.37	<0.001
	FAE5	1.40	0.13	0.13	4.74	<0.001
	FAE6	2.76	0.19	0.19	5.61	<0.001

TABLE 5 | Evaluation of the formative higher-order constructs (HOC) based on its lower-order constructs (LOC): collinearity (VIF) and indicator weight (original estimate *w*, bootstrap mean *M*, t-statistic t (2,187), *p*-value).

HOC	LOC	VIF	Weights			
			w	*M*	*t* (2,187)	*p*
Benefits CCU	Environmental benefits CCU	3.80	0.64	0.64	14.1	<0.001
	Policy benefits	3.49	0.22	0.22	4.77	<0.001
	Employment opportunities	1.56	0.097	0.097	3.26	= 0.001
	Raise awareness use of CO_2	2.23	0.14	0.14	3.80	<0.001
Barriers CCU	Policy barriers	2.18	0.75	0.75	12.6	<0.001
	Sustainability barriers	2.18	0.31	0.32	4.61	<0.001
Benefits CO_2-based fuels	Environmental benefits fuels	2.43	0.64	0.64	21.0	<0.001
	Future of flying	1.62	0.12	0.12	4.30	<0.001
	Sustainability aviation	2.06	0.28	0.28	9.95	<0.001
	Increased quality	1.15	0.15	0.14	6.13	<0.001
Barriers CO_2-based fuels	Safety risk	1.49	0.53	0.52	8.82	<0.001
	Insufficient research	1.28	0.20	0.20	3.11	= 0.001
	Decreased quality	1.37	0.50	0.50	8.96	<0.001
Acceptance CO_2-based fuels	Willingness to use	1.95	0.12	0.12	4.22	<0.001
	Support	1.79	0.58	0.58	19.9	<0.001
	Preference	1.79	0.45	0.45	14.3	<0.001

reliability were granted. The discriminant validity of these measurements was also established, since none of the *CI*'s for the indicators contained 1. The results for the formative constructs and LOCs are depicted in **Table 4** and show that for most constructs the indicators did not show collinearity. Only for the *FAE2* of *Affective Evaluation* CO_2*-Based Fuels* the VIF >5. This indicator was nevertheless included in the final model to keep the indicators of this construct similar to the ones for *Affective Evaluation CCU*. To control for the effect of this procedure, and checking if the less restrictive handling of the VIF in this item is decisive for the overall model, an alternative analysis was run in which this indicator was discarded. Owing to the fact that the differences in rounding to the second decimal place produced little to no differences for the interpretation of relevant values in the model evaluation, *FAE2* was retained for modeling in favor of a basis of comparison in the measurement of the affective component of the model. Moreover, the results in the table reveal that all indicators were significant and relevant for their constructs based on their positive and significant weights. Additionally, the *CI*'s for all indicators did not contain 0, which also indicated their significance.

Finally, the results of the formative HOCs are depicted in **Table 5**. None of the LOCs showed collinearity. They were also all significant and relevant for the HOCs based on their positive and significant weights, as well as the *CI*'s that did not contain 0.

Overall, the measurement model thus sufficiently met the quality criteria. In the next step, the structural model was evaluated.

7.2.2 Structural Model Evaluation

The results of the structural model evaluation can be found in **Table 6**. The table shows that there was no collinearity in the model. All path coefficients were significant based on the t-statistic and the *CI*s not containing 0. The effect of five relationships was small, of four medium, and of the final two large.

The in-sample predictive power was very weak for *Barriers CCU* (R^2 = 0.13) and *Barriers* CO_2*-Based Fuels* (R^2 = 0.17). For *Benefits CCU* (R^2 = 0.30) and *Affective Evaluation* CO_2*-Based Fuels* (R^2 = 0.45) it was weak. And finally, for *Benefits* CO_2*-Based Fuels* (R^2 = 0.56) and *Acceptance* CO_2*-Based Fuels* (R^2 = 0.57) the in-sample predictive power was moderate (Hair et al., 2018).

7.3 Complete Model: Hypotheses Validation

Through nine iterations we converted our hypothesized model (**Section 6.4.2**) into a model that sufficiently fulfilled the quality criteria (**Section 7.2**). The final model is depicted in **Figure 3**. In this graphic, the LOCs that serve as indicators for the HOCs are included (gray rectangles) besides the HOCs in the structural model (black ovals). The single indicators for the non-HOCs and LOCs are not represented in the graphic, but can be found in the supplementary material. Compared to the hypothesized model, several single-indicator LOCs were removed from the final model because they were not significant for the respective HOC: *Scale Barrier* of the HOC *Barriers CCU*, as well as *Increased Prices Air Tickets* and *Less Motivation to Fly Less* of the HOC *Barriers* CO_2*-Based Benefits*.

The hypotheses were evaluated by comparing the hypothesized structural model (**Figure 1**) to the structural model of the final model (**Figure 3**). In these graphics, relationships are represented by a path from the exogenous to the endogenous construct.

First, we looked at the direct relationships from the perception to the acceptance of CO_2-based fuels for aviation (H_1). Only for the barriers of CCU (H_{1d}) we found no significant relationship. The benefits of CO_2-based fuels (H_{1a}) and the benefits of CCU

TABLE 6 | Evaluation of the structural model: path coefficient evaluation [original estimate *β*, bootstrapped mean *M*, confidence interval (*CI*), t-test statistic *t* (2,187), and significance (*p*)], effect size (f^2), and collinearity (VIF).

Exogeneous construct	Endogeneous construct	Path coefficient						f^2	VIF
		β	*M*	*CI*		*t* (2,187)	*p*		
				2.5%	97.5%				
Barriers CO_2-based fuels	Acceptance CO_2-based fuels	–0.21	–0.21	–0.24	–0.17	11.6	<0.001	0.091	1.10
Benefits CO_2-based fuels	Acceptance CO_2-based fuels	0.45	0.45	0.40	0.50	18.6	<0.001	0.20	2.27
Affective evaluation CCU	Affective evaluation CO_2-based fuels	0.67	0.67	0.64	0.70	41.0	<0.001	0.81	—
Affective evaluation CCU	Barriers CCU	–0.36	–0.37	–0.41	–0.32	15.8	<0.001	0.15	—
Affective evaluation CCU	Benefits CCU	0.55	0.55	0.51	0.59	27.6	<0.001	0.43	—
Affective evaluation CO_2-based fuels	Barriers CO_2-based fuels	–0.19	–0.19	–0.24	–0.14	7.64	<0.001	0.038	1.14
Affective evaluation CO_2-based fuels	Benefits CO_2-based fuels	0.42	0.42	0.37	0.46	17.6	<0.001	0.24	1.42
Affective evaluation CO_2-based fuels	Acceptance CO_2-based fuels	0.17	0.17	0.12	0.22	7.01	<0.001	0.035	1.90
Barriers CCU	Barriers CO_2-based fuels	0.30	0.31	0.26	0.36	12.1	<0.001	0.099	1.14
Benefits CCU	Benefits CO_2-based fuels	0.44	0.44	0.39	0.48	18.8	<0.001	0.30	1.42
Benefits CCU	Acceptance CO_2-based fuels	0.14	0.14	0.090	0.18	5.69	<0.001	0.023	1.86

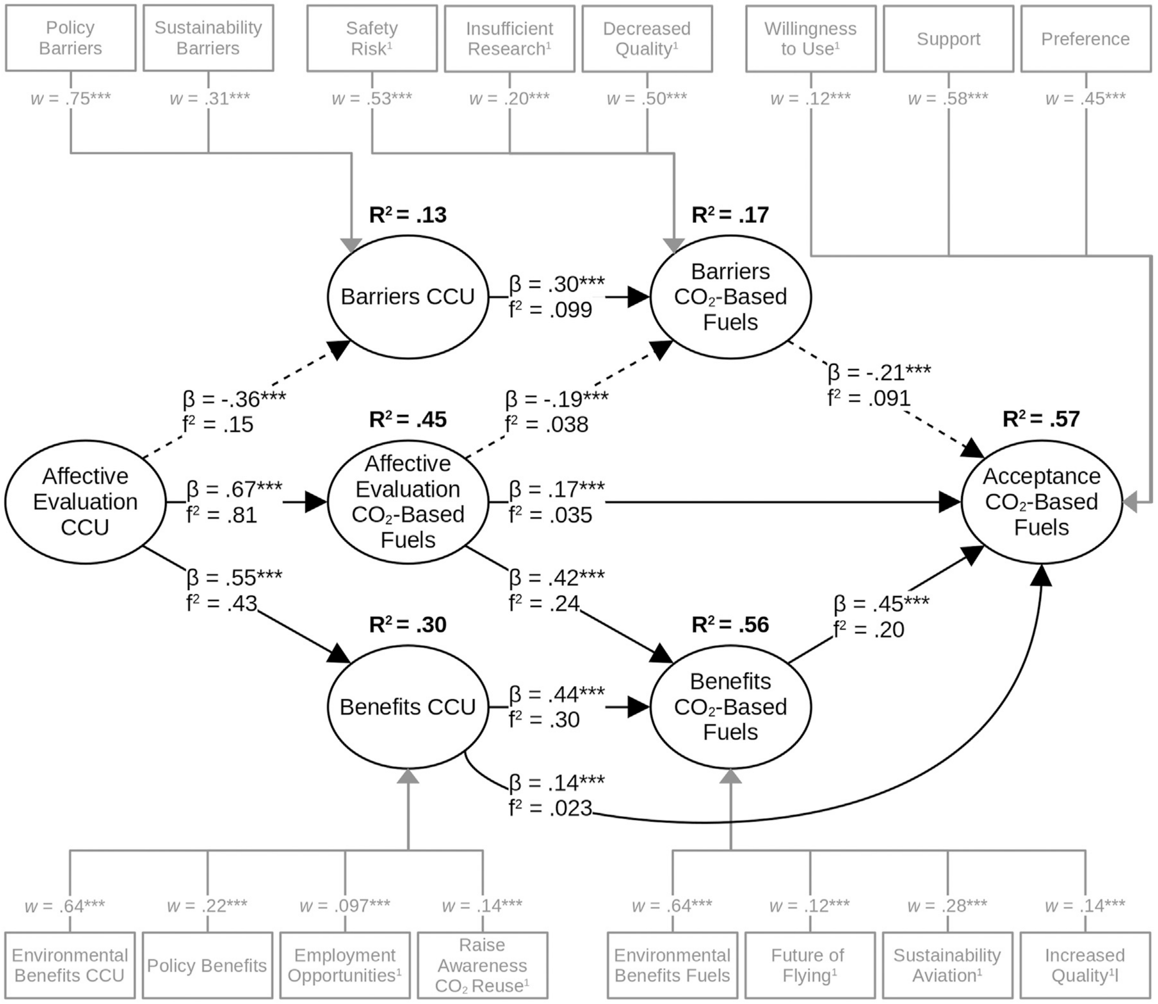

FIGURE 3 | Final structural equation model with subcomponents of higher-order components. The graphic includes original estimate weights *w*, path coefficients *β* (all $***p < 0.001$), effect sizes f^2, and explained variances R^2. Dashed paths indicate a negative path coefficient. ¹ signifies a single-indicator composite.

(H_{1c}) were positively related to the acceptance, and the barriers of CO_2-based fuels (H_{1b}) were negatively related to the acceptance.

Second, we considered the relationships from the perception of CCU to the perception of CO_2-based fuels (H_2). We found significant positive relationship between the perceptions of benefits of CCU and CO_2-based fuels (H_{2a}) and between the perceptions of barriers of CCU and CO_2-based fuels (H_{2c}). Between the benefits of CCU and the barriers of CO_2-based fuels (H_{2b}) and vice versa (H_{2d}) we found no significant relationships.

Subsequently, the relationships from the affective evaluations to the perception and acceptance were evaluated (H_3). The affective evaluation of CO_2-based fuels was positively related to the acceptance of the fuels (H_{3a}), but the affective evaluation of CCU was not significantly directly related to the acceptance (H_{3d}). Moreover, the affective evaluation of CO_2-based fuels was positively related to the benefits of the fuels (H_{3b}) and negatively related to its barriers (H_{3c}). Similarly, positive and negative relationships were found between the affective evaluation of CCU and the benefits (H_{3e}) and barriers (H_{3f}) of CCU, respectively.

The last hypotheses to consider were the relationships from the affective evaluation of CCU to the affective evaluation and perception of CO_2-based fuels (H_4). We found no direct significant relationship between the affective evaluation of CCU and the benefits (H_{4b}) and barriers (H_{4c}) of CO_2-based fuels. However, there was a significant positive relationship between the affective evaluation of CCU and the affective evaluation of CO_2-based fuels (H_{4a}).

Finally we looked at the strength of the predictions and predictors. As aforementioned, we found a moderate in-sample predictive power for the acceptance of CO_2-based fuels. The relationship with the benefits of CO_2-based fuels was thereby most relevant. This was followed by the barrier perception and affective evaluation of the fuels, and finally the benefit perception of CCU. For predicting the benefits of CO_2-based fuels—with a moderate in-sample predictive power—the benefits of CCU were most relevant, closely followed by the affective evaluation of the fuels. For the barriers of CO_2-based fuels—with a weak in-sample predictive power—the barriers of CCU were also most relevant followed by the affective evaluation of the fuels, but the gap between the strength of both predictors was larger. The affective evaluation of CCU was the only predictor for the barriers of CCU, the benefits of CCU, and the affective evaluation of CO_2-based fuels in the model. It is thereby noteworthy that this single predictor resulted in a moderate in-sample predictive power for the affective evaluation of the fuels.

8 DISCUSSION

In the short term, merely trying to limit CO_2-emissions will likely not suffice to mitigate climate change (Peters and Geden, 2017). It is therefore important that circular economy approaches—for which Carbon Capture and Utilization (CCU) is a cornerstone, which reuse (otherwise) emitted CO_2, are developed and adopted as well. A prerequisite for the successful roll-out of CCU is its social acceptance, which includes the public's acceptance of CCU products.

In this study, we focused on the acceptance of one such product: CO_2-based fuels for aviation. To our knowledge, the study was the first to aim at gaining a better understanding of the role the evaluation of CCU as a production method plays on the acceptance of a CCU product. We applied a quantitative approach integrating a large European sample. We used partial least squares structural equation modeling for our exploratory research aim because it allowed us to evaluate a large number of variables simultaneously, thereby considering the relationships between these latent variables and also the quality of the latent variables themselves.

The present study yielded a better understanding of how the acceptance of CO_2-based fuels is formed. Based on this knowledge, this final section answers the study's research question: **What role, if any, does the evaluation of CCU as a production method play in the formation of the acceptance of CO_2-based fuels for aviation as an example of a CCU product?** Additionally, the knowledge is used to formulate guidelines for the development of communication and information strategies. Finally, we reflect on the study's limitations and resulting future research prospects.

8.1 The Role of the Cognitive Evaluation of Barrier and Benefit Perceptions on Acceptance Evaluations

First, we considered the role of the cognitive evaluation, in the form of the perceived benefits and barriers of CCU and CO_2-based fuels, for the acceptance of the product. Generally, the fuels were accepted, but not strongly yet. This is in line with previous findings on the acceptance of this (Engelmann et al., 2020), and other CCU product(s) (Offermann-van Heek et al., 2018). For both the fuels and CCU, the benefits were perceived, and a higher benefit perception was related to a higher acceptance of CO_2-based fuels. The relationship between the benefits of a CCU product and the acceptance of this product is in line with previous research (e.g., Huijts et al., 2012; Offermann-van Heek et al., 2018). However, the role of the benefits of CCU for the acceptance evaluation of the CCU product is a new insight. The benefits of CCU only have a weak direct affect on the acceptance compared with the other acceptance predictors. However, they are also indirectly related to the acceptance of the fuels through their direct relationship with the benefits of the fuels. For both benefit perceptions, the environment-related benefits played a substantial role, confirming previous findings (Offermann-van Heek et al., 2018; Arning et al., 2021).

The barriers of CCU and CO_2-based fuels were perceived as well. However, the barrier perceptions were less pronounced in comparison with the perceived benefits (as taken from the descriptive statistics and the lower effect sizes of perceived barriers of both product and technology). Perceived barriers had a moderating effect on acceptance through the direct positive relationship with the barriers of the product. The stronger the barriers for CO_2-based fuels are perceived, the lower the acceptance of the product. Moreover, it is noteworthy that compared to the previously identified lack of sustainability of CCU as a relevant barrier (Jones et al., 2014; Arning et al., 2017), barriers related to lacking policy seemed to be more important for the model. This reflects laypeople's policy expectations and addresses the need for the informed formation of policies for CCU (Moreau et al., 2017; Hartley et al., 2020). The barriers for the fuels highlighted safety concerns as well as doubts concerning reductions in product quality. This allows us to speculate about the relationship between the barriers of CCU and the product. An increased questioning of appropriate policy strategies may be accompanied by doubts about the characteristics of the end product.

Moreover, the benefits of CCU do not seem to influence the barriers of CO_2-based fuels and vice versa. This can be seen as empirical evidence that benefit perception and barrier perception are not inversely related and do not exclude each other. Instead, consumers see both positive and negative aspects of CO_2-based fuels for aviation simultaneously. This phenomenon of perceiving both sides (in varying weights) to some extent is quite typical for the evaluation of technical innovations and acceptance (e.g., Huijts et al., 2019; Offermann-van Heek et al., 2018). In the adoption process, consumers see the benefits and the barriers on different levels—in terms of personal and societal consequences—and weigh both. This results in the acceptance decision.

8.2 The Role of the Affective Evaluation on Acceptance Evaluations

Besides the cognitive evaluation of a product or technology, to be able to explain the acceptance, it is important to also consider the public's affective evaluation of the product or technology (Finucane et al., 2000). The affective evaluations of CCU and CO_2-based fuels were both positive on average. However, for all included adjective pairs, the fuels were evaluated more positively than CCU although small effect sizes have to be taken into account. This confirms previous findings that found the end product to be viewed more positively than the necessary production steps (Offermann-van Heek et al., 2020). For the present study this means that the fuel is perceived to be less health-damaging and more cheap, efficient, environmentally friendly, useful, and acceptable than CCU as the technology used to make the fuel. One possible explanation is a lack of understanding of the technology as opposed to a perceived understanding of the fuel as a product. Even though climate change is increasingly recognized as an (environmental) threat, it can still be difficult to understand complex technological approaches aimed at mitigating climate change, such as CCU. This, in turn, can create uncertainty when assessing the benefits or risks of the technology. In contrast, CO_2-based fuels—which laypeople have also not been able to experience yet—replace known, conventionally used, and well-established products such as kerosene. Fuels in general are thus more tangible and laypeople might have been able to more easily assess and evaluate their use.

The affective evaluation of CO_2-based fuels was directly related to the acceptance of the product, and also acted as a mediator through relationships with its benefit and barrier perception. The higher the affective evaluation, the higher the acceptance. The affective evaluation of CCU was not directly related to the acceptance, nor to the benefit and barrier perception of the product. However, it was related to the benefit and barrier perception of CCU, as well as the affective evaluation of the fuels. Indirectly, an increased positive affective evaluation of CCU is thus still related to an increased acceptance.

Despite the new perspective provided by the integration of both technology and product, the results of the model partially confirm previous research findings. The direct effect of the affective evaluation of the product on its acceptance is in line with previous findings for CCU as a technological approach, for which Linzenich et al. (2019b) found that affect in the form of risk perceptions directly influenced its acceptance. Interestingly, Liu et al. (2019) differentiated between positive and negative affects—which our measurement instrument did not due to the opposite polarity of the semantic differentials—when investigating their impact on the acceptance of self-driving vehicles: People's behavioral intention was only influenced by positive affect, whereas negative affect did not have a direct impact. Also a study by Arning et al. (2020) identified an effect of the positive affective evaluation on the acceptance of the CCU technology, but did not for the negative affect in terms of perceived threats.

Our model shows that besides the cognitive evaluation—which involves a rational weighing of advantages and disadvantages—affect is a central component in shaping the acceptance of CO_2-based fuels for aviation. As a new insight, we extended this knowledge by having identified the indirect effect of the affective technology evaluation on the product's acceptance.

8.3 Evaluation of Carbon Capture and Utilization and the Acceptance of CO_2-Based Fuels

To answer the research question: Overall we found that the evaluation of CCU as a production method was mostly indirectly related to the acceptance of the CO_2-based fuels through moderating effects through relationships with the evaluation of the fuels. The only exception was the benefit perception of CCU, which was directly related to the acceptance. However, relative to acceptance's relationship with the benefit and barrier perception and affective evaluation of the fuel, the direct relationship with acceptance was weak both in terms of β and effect size. We believe there are two possible explanations for the lack of a direct relationship between the evaluation of CCU and acceptance. First, respondents might have a harder time evaluating a complex unknown technology like CCU based on basic information alone and might therefore be more careful in their evaluation (Zaunbrecher and Ziefle, 2016). It might be easier for them to evaluate a product that is said to be similar to products they are more familiar with. Therefore, the technology might be rather neglected when evaluating the product. This argument is stressed by the more positive affective evaluation of the fuel compared to CCU—which is in line with previous findings on perceptions of CCU and CO_2-

based fuels (Arning et al., 2021)—even though the fuel would not exist without the technology. Alternatively, consumers might generally care less about the production method of products, as long as the product itself has a good quality and is safe. Although a direct comparison between the relevance of production type and a resulting product from a lay perspective has not been drawn so far to our knowledge, assumptions can nevertheless be made from previous research. For the roll-out of a CCU plant, the perceived importance of technology attributes showed that, apart from the fact that CO_2 can be stored and thus fossil resources saved, aspects relating to the involvement of the public in planning or the type of plant operator had comparatively little to very little relevance (Arning et al., 2021). This indicates that laypeople focus on potential benefits of the production rather than on roll-out conditions that could directly affect them, e.g., in the form of citizen participation.

Even though the evaluation of the product was thus more important for the acceptance of CO_2-based fuels, the evaluation of CCU still played an indirect role as it had moderating effects through benefit and barrier perceptions as well as its affective component. The affective evaluation of CCU even seems to play a substantial role in predicting the affective evaluation of the fuels, since as its only predictor in the model it managed to explain 45% of the variance for this construct. Affective evaluations in energy technology acceptance are known to considerably impact social acceptance (Slovic et al., 1982; Huijts et al., 2012; Huijts, 2018), especially in the beginning of the innovation management process when people do not have much familiarity with the technology and cannot yet assess the adverse and long-term consequences of development on them (Midden and Huijts, 2009; Bögel et al., 2018). Thus, affective responses give valuable insights into “archaic” reactions to uncertainty and unknown consequences connected to technical innovations and related transformation processes (Renn et al., 2011), especially in the early phase of the production process.

8.4 Insights for Communication and Information Strategies and Managerial Recommendations

The strategy for the public communication resulting from the insights of the study can be divided into a general and specific level.

At a *general* level, the successful implementation of changes in the energy transition will deeply affect social processes and needs societal support. Therefore, the transition and roll-out of energy technology innovations requires a carefully planned and systematically implemented communication. This allows the early identification of acceptance conflicts and controversial perspectives of the involved parties and enables their resolution through discourse (Drews and Van den Bergh, 2016). Communication strategies should closely reflect the perceptions and acceptance of the public (Offermann-van Heek et al., 2018; Kluge et al., 2021). Since acceptance decisions for technical innovations typically simultaneously consider the perceived benefits and barriers, both the advantages and potential drawbacks should be communicated transparently (Offermann-van Heek et al., 2018; Linzenich et al., 2019b). Not doing so, and instead predominately reporting the obvious advantages—as might be recommended by marketing approaches—can lead to public distrust in authorities as well as distrust in the technology, product, and perceived honesty of information providers. This happens whenever the public feels that information is being concealed. Especially industry and politics for which the public tends to assume other predominant motives for innovation—e.g., market claims, economic benefits, or election-related motives—instead of truly supporting a sustainable energy supply, are viable for such mistrust (Offermann-van Heek et al., 2018; Linzenich et al., 2019b).

On a more *specific* level, relating to the outcomes of the present study, not only the product features of CO_2-based fuels need to be addressed in public communication strategies, but also the production process. Even though the direct relationship between process-related components and product acceptance was not very strong, it still played a substantial indirect role. It could thus be shown that focusing exclusively on end-consumption in the form of the fuel as a product would disregard elementary aspects—in this case the technological production approach—when informing the public. Without including the production approach, one would miss out on empowering the public with appropriate information (about advantages and disadvantages) for informed participation (e.g., in the form of adapted consumption and travel behavior), which is becoming increasingly important in times of the ever more urgent pursuit of reaching the 1.5°C target. Also with regard to the acceptance of other goods that could be produced in a circular economy fashion, communication about the technical possibilities and pathways is of significant importance. Laypeople, of course, do not have the same competence as technical experts, which allows them to understand all the technical details. The communication therefore has to follow a clear strategy aimed at generating tailored understandable information for differing individual information needs for both, aspects of product and production as well as the impact and importance of circular economy approaches. This could be especially important for the perception of potential barriers. Compared to the perceived benefits of CCU and CO_2-based fuels, the barriers were perceived less strongly, which indicates that general acceptance is unlikely to be hindered by major adoption obstacles. However, we have to acknowledge that the barriers were still somewhat perceived—$M = 2.70$ for CCU and $M = 2.63$ for CO_2-based fuels, out of the maximum of second 5.00 second, and that their influence was strong enough to be included in the model. If specific groups of consumers perceive the barriers more strongly, this could increase their effect on acceptance for these consumers. In general, but especially for these groups, the barriers should thus be included in communication strategies. In the model, policy and sustainability barriers were included for CCU, i.e., doubts about the policies for CCU and environmental sustainability of the technology. For the CO_2-based fuels for aviation as a CCU product, safety risks and the possibly decreased quality of the novel fuel seemed to be important barriers. Stressing the whole picture of the technical approach and the innovation would thus help not only to deliver the impact of each step in the technology process and their relation to the overall goal to reduce climate-related goals, but also to provide transparency with respect to the technology innovation that is needed by the public to support climate-related measures. Last but not the least an open communication policy is essential for the public that they are taken seriously and involved.

At this moment, informing the public and communicating a technological innovation usually follows a top-down approach. The solution to preventing the anticipated or feared resistance toward, and boycott of, the product seems to be to quite superficially and nontransparently inform the public at the end of the development process. This approach possibly seems to be the simplest and most effective, especially since the lay public, naturally, does not have the expertise to adequately evaluate the technical processes. From a technical expert point of view, it might probably be the most obvious and convenient to assume that if the public is not confronted with the possible disadvantages, they will not even think of rejecting the product or technology. However, in the long term, such "hiding" communication strategies will not be successful and fall short. This is not only explained by lacking honesty toward, and consideration of the information needs of, the public and the resulting uninformedness perceived by the public, as well as their feeling of being kept out of the loop. More so, it neglects that (non-)acceptance reactions in the population often reflect decision conflicts between societal goals, local impacts, and individual motives (Evans et al., 2013; Feinberg and Willer, 2013). Those decision conflicts reach deep into a person's identity and touch their daily living circumstances. For that reason, it must be assumed that they do not simply disappear over time.

Laypeople—this group does include not only the broader public, but also policy and decision makers on different levels and in different organizations—are unlikely to engage with the product if they do not have the opportunity to familiarize themselves with the product, the technology, and its societal benefits, or if they feel like they are not being adequately considered and assume that there is not enough transparency to allow them to get familiar with the idea, and the consequences of the innovation. Therefore, open information is an inevitable precondition of a successful roll-out (Brunsting et al., 2013; Gölz and Wedderhoff, 2018; Arning et al., 2020) A balanced, honest, and trustful communication strategy is advisable. This should confirm the already positively experienced aspects—e.g., environmental benefits and employment opportunities, but also discuss, recognize, or in the case of misconceptions, invalidate, the perceived barriers. From a managerial perspective, it seems to be a timely issue of outstanding importance to systematically inform research, applications, governance, and policy to support the circular economy approach and to claim the area-wide economic and ecological necessity to rethink technology processes and products in line with circular economy activities and sustainable innovations.

8.5 Limitations and Future Research

Finally, we considered which further potential limitations of the study should be picked up in further research. Several key-points that related to different theoretical, empirical, and methodological issues were identified.

Considering construct ambiguity. First, we were not able to validate the convergent validity of the formative constructs. Future studies should aim to validate these quality criteria by implementing reflective measures measuring the same construct in the measurement instrument (Hair et al., 2017). However, more importantly, constructs are never a perfect representation of the latent variables they aim to represent. Instead, they should be seen as an approximation of these latent variables (Sarstedt et al., 2016). In addition, by definition, formative constructs do not necessarily cover the entire latent variable but rather aspects of the variable. The use of other benefits, barriers, and adjective pairs thus likely changes the constructs. Since the items used were based on extensive literature study and discussions with experts, we do believe in their validity for CCU and CO_2-based fuels. A crucial issue in such explorative studies is the development and selection of appropriate items with a good item quality. However, especially in such novel fields, there are not always already validated items that can be used for the acceptance evaluation and the PLS-SEM modeling. In the present study, we therefore pursued a mixture out of an exploratory and validated approach. On the one hand, we developed items that reflected content coming from the exchange with technical experts; on the other hand, we reused items that have been extracted from previous (CCU) acceptance studies (**Section 4**) and validated scales that were available. Future studies should replicate the suitability and item quality of these items and should check if further items can be identified from qualitative research, which then should be included in the model to see whether it changes the relationships between the constructs. Additionally, social science studies on CCU (products) have consistently reported that the general public's awareness of the technology is regrettably low (Offermann-van Heek et al., 2018; Linzenich et al., 2021). This can be attributed to the fact that, so far, no CCU product is available on the market and the population has thus not gotten the chance to gain hands-on experience. Future studies should track whether and how acceptance and perception outcomes change when this is possible, and more information becomes available.

Considering out-of-sample predictive power and causality. The identified model is only valid to explain the hypothesized relationships within our sample. Based on the used approach and analysis, the model's out-of-sample predictive power cannot be granted. Moreover, because of the correlational nature of structural equation modeling, causal conclusions cannot be drawn based on this approach (Bullock et al., 1994). Although our model was valid to assess the hypotheses in the present study, future (experimental) studies should aim to validate the assumed predictiveness and causality the model conveys.

Considering single production steps. So far, we did not include the acceptance evaluations of the single production steps—i.e., separation, purification, transport, and conversion of CO_2—and compare them with, and relate them to, the acceptance evaluations for the product, CO_2-based fuels for aviation. Even though the SEM procedure yielded a first understanding of the role of the evaluation of the production process in the formation of acceptance for the product, it remains important to analyze the single steps separately. This will provide insights into whether all the single steps of the circular economy approach are perceived, understood, and evaluated equally. Additionally, it could identify whether there are specific hurdles in the perception of the production steps that require additional communication efforts.

Considering local acceptance. In the present study, we addressed the public acceptance of CO_2-based fuels for aviation as an example of a CCU product, thereby touching aspects of the socio-political and market acceptance proposed by Wüstenhagen et al. (2007). However, any infrastructure for CCU plants is embedded in various land-use scenarios—i.e., the properties of the plant, its location, and its infrastructural needs—which need to be explored from a local perspective. Compared to the general public, the acceptance evaluations of those who personally experience proximity to the CCU plant could differ. The fears of people living in close proximity to the plant, as well as the perceptions of communal (local) decision makers who have to take into account inhabitants' voices, have to be considered. Future studies should aim to include local acceptance aspects in the model to be able to consider all dimensions simultaneously and gain a more complete view on the acceptance.

Considering user diversity and further acceptance drivers. The constructs in the model described in the present study had a low or moderate in-sample predictive power. This is likely the result of our focus on the role of the evaluation of CCU and CO_2-based fuels for explaining the acceptance of the product. We did not analyze demographic factors on acceptance yet and did also not include further (psychological) factors in our model (this would have exceeded the scope of the paper and also space restrictions). However, based on other acceptance models (Huijts et al., 2012) and the results of previous CCU acceptance studies (van Heek et al., 2017b; Offermann-van Heek et al., 2018; Arning et al., 2019) we know that these play an important role in explaining acceptance as well. Including user diversity factors—like *trust*, *innovativeness*, and *self-efficacy*—in future studies will increase the understanding of the acceptance of CO_2-based fuels. Additionally, it will help to explain what drives the perception and affective evaluation of CCU and the product, which our model showed play a substantial role in explaining acceptance (R^2 = 0.57). This knowledge helps to formulate targeted communication strategies for different consumer groups, and increase the likelihood of a successful market roll-out of the technology and product (Sovacool et al., 2018; Linzenich et al., 2019b; Liebe and Dobers, 2019). As part of this, we should also look into national differences. In our sample we included participants from four European countries—Spain, Norway, Germany, and Netherlands—but did so far not consider differences between these countries[10]. However, if research focuses on national acceptance differences, social and cultural norms and other diversity factors should be considered to explain the potential differences (Tellis et al., 2003; Zheng et al., 2021), since nationalities differ for myriad factors, e.g., socioeconomic situation and familiarity with green energies. This will help to understand and address differences in culturally defined openness to innovation within, and across, European markets regarding CO_2-based fuels.

Considering further aspects of public communication. Even though the present study provided first insights into the aspects important for the communication of CO_2-based fuels for aviation, there may still be other important aspects for the successful communication of circular economy products and procedures. This should be explored empirically. As such, it needs to be studied which information—including type and depth of detail—on CO_2-based fuels is required. Additionally, it should be considered which information channels and media are preferred, and, more so, which media is trusted by the public in terms of reliability, actuality, and objectivity of the information. Altogether we should question which information instances are credible in the eyes of the public and which degree of complexity is tolerated by both the information providers and receivers (e.g., Offermann-van Heek et al., 2018; Kluge et al., 2021).

Considering further circular economy products and application fields. Finally, the findings at hand are only valid for the acceptance of CO_2-based fuels for aviation. The extent of the general validity of the results for other CO_2-based products, or circular economy approaches, remains unclear. It would be interesting for future studies to identify which acceptance factors are product specific, and which apply across different circular economy products. Whereas there might be universal acceptance principles—e.g., the fear of harm, economic burden, nature protection, personal comfort, and living standard, there might also be quite product-specific factors—e.g., proximity to the body of CCU products (van Heek et al., 2017a; Arning et al., 2018a) like CCU-based clothing, food packaging, or cosmetics. The consideration of different product categories as well as different technology routes in the production of CO_2-based goods in future studies would furthermore provide the opportunity to study tradeoffs between aspects such as production route and product.

DATA AVAILABILITY STATEMENT

The raw data supporting the conclusion of this article will be made available by the authors, without undue reservation.

ETHICS STATEMENT

The studies involving human participants were reviewed and approved by the Ethikkommission der Fachgruppe 7.3 "Empirische Humanwissenschaften" an der Philosophischen Fakultät der RWTH Aachen (Ethics Committee of the Division 7.3 "Empirical Human Sciences" at the Faculty of Arts and Humanities at RWTH Aachen). The participants provided their written informed consent to participate in this study.

---

[10] For a first glance into descriptive findings and differences across countries, a table can be found in the supplementary materials.

AUTHOR CONTRIBUTIONS

All authors listed have made a substantial, direct and intellectual contribution to the work, and approved it for publication. LS and LE were responsible for the methodology, conduction of the described study, data curation, validation of the data. KA conceptualized the empirical questionnaire study on which the SEM model was based. LS did the formal analysis and visualization. MZ was responsible for the funding acquisition and LE for the project management. LE, MZ, and LS did the final editing of the paper.

FUNDING

This project has received funding from the European Union's Horizon 2020 research and innovation programme under grant agreement No 838077. The funding source was further not involved in conducting the study.

ACKNOWLEDGMENTS

We thank the eCOCO$_2$ colleagues for their openness and willingness to sharing their experience and technical knowledge, which helped us to create reliable explanations on the CCU technology and CO$_2$-based fuels. Thanks also to Miriam Lorenzo and Lilian Kojan for their research support. Special thanks go to two reviewers for their thoughtful comments and discussions on an earlier version of the manuscript. Last but not least we would like to thank the guest editor of this special issue, Luis Puigjaner for his general support in motivating and editing the paper.

SUPPLEMENTARY MATERIAL

The Supplementary Material for this article can be found online at: https://www.frontiersin.org/articles/10.3389/fenrg.2021.742109/full#supplementary-material

REFERENCES

Akerboom, S., Botzen, W., Buijze, A., Michels, A., and van Rijswick, M. (2020). Meeting Goals of Sustainability Policy: Co2 Emission Reduction, Cost-Effectiveness and Societal Acceptance. An Analysis of the Proposal to Phase-Out Coal in the netherlands. *Energy Policy* 138, 111210. doi:10.1016/j.enpol.2019.111210

Arning, K., Linzenich, A., Engelmann, L., and Ziefle, M. (2021). More green or Less Black ? How Benefit Perceptions of CO2 Reductions vs. Fossil Resource Savings Shape the Acceptance of CO2-based Fuels and Their Conversion Technology. *Energ. Clim. Change* 2, 100025. doi:10.1016/j.egycc.2021.100025

Arning, K., Offermann-van Heek, J., Linzenich, A., Kaetelhoen, A., Sternberg, A., Bardow, A., et al. (2019). Same or Different? Insights on Public Perception and Acceptance of Carbon Capture and Storage or Utilization in Germany. *Energy policy* 125, 235–249. doi:10.1016/j.enpol.2018.10.039

Arning, K., Offermann-van Heek, J., Sternberg, A., Bardow, A., and Ziefle, M. (2020). Risk-benefit Perceptions and Public Acceptance of Carbon Capture and Utilization. *Environ. Innovation Societal Transitions* 35, 292–308. doi:10.1016/j.eist.2019.05.003

Arning, K., van Heek, J., and Ziefle, M. (2018a). Acceptance Profiles for a Carbon-Derived Foam Mattress. Exploring and Segmenting Consumer Perceptions of a Carbon Capture and Utilization Product. *J. Clean. Prod.* 188, 171–184. doi:10.1016/j.jclepro.2018.03.256

Arning, K., van Heek, J., and Ziefle, M. (2017). Risk Perception and Acceptance of CDU Consumer Products in Germany. *Energ. Proced.* 114, 7186–7196. doi:10.1016/j.egypro.2017.03.1823

Arning, K., Zaunbrecher, B. S., Sternberg, A., Bardow, A., and Ziefle, M. (2018b). Blending Acceptance as Additional Evaluation Parameter into Carbon Capture and Utilization Life-Cycle Analyses. In Proceedings of the 7th International Conference on Smart Cities and Green ICT Systems (SMARTGREENS 2018). 34–43. doi:10.5220/0006683000340043

Azarova, V., Cohen, J., Friedl, C., and Reichl, J. (2019). Designing Local Renewable Energy Communities to Increase Social Acceptance: Evidence from a Choice experiment in Austria, Germany, Italy, and Switzerland. *Energy Policy* 132, 1176–1183. doi:10.1016/j.enpol.2019.06.067

Bjørnåvold, A., Lizin, S., Van Dael, M., Arnold, F., and Van Passel, S. (2020). Eliciting Policymakers' Preferences for Technologies to Decarbonise Transport: A Discrete Choice experiment. *Environ. Innovation Societal Transitions* 35, 21–34. doi:10.1016/j.eist.2019.12.002

Bögel, P., Oltra, C., Sala, R., Lores, M., Upham, P., Dütschke, E., et al. (2018). The Role of Attitudes in Technology Acceptance Management: Reflections on the Case of Hydrogen Fuel Cells in Europe. *J. Clean. Prod.* 188, 125–135. doi:10.1016/j.jclepro.2018.03.266

Bongartz, D., Doré, L., Eichler, K., Grube, T., Heuser, B., Hombach, L. E., et al. (2018). Comparison of Light-Duty Transportation Fuels Produced from Renewable Hydrogen and green Carbon Dioxide. *Appl. Energ.* 231, 757–767. doi:10.1016/j.apenergy.2018.09.106

Boudet, H. S. (2019). Public Perceptions of and Responses to New Energy Technologies. *Nat. Energ.* 4, 446–455. doi:10.1038/s41560-019-0399-x

Broman Toft, M., Schuitema, G., and Thøgersen, J. (2014). Responsible Technology Acceptance: Model Development and Application to Consumer Acceptance of Smart Grid Technology. *Appl. Energ.* 134, 392–400. doi:10.1016/j.apenergy.2014.08.048

Brunsting, S., de Best-Waldhober, M., and Terwel, B. W. (2013). 'I Reject Your Reality and Substitute My Own!' Why More Knowledge about CO2 Storage Hardly Improves Public Attitudes. *Energ. Proced.* 37, 7419–7427. doi:10.1016/j.egypro.2013.06.684

Bullock, H. E., Harlow, L. L., and Mulaik, S. A. (1994). Causation Issues in Structural Equation Modeling Research. *Struct. Equation Model. A Multidisciplinary J.* 1, 253–267. doi:10.1080/10705519409539977

Chauvy, R., and De Weireld, G. (2020). CO 2 Utilization Technologies in Europe: A Short Review. *Energy Technol.* 8, 2000627. doi:10.1002/ente.202000627

Cousse, J., Wüstenhagen, R., and Schneider, N. (2020). Mixed Feelings on Wind Energy: Affective Imagery and Local Concern Driving Social Acceptance in switzerland. *Energ. Res. Soc. Sci.* 70, 101676. doi:10.1016/j.erss.2020.101676

Dethloff, C. (2004). *Akzeptanz und Nicht-Akzeptanz von technischen Produktinnovationen*. Lengerich, Germany: Pabst Science Publ.

Deutz, S., Bongartz, D., Heuser, B., Kätelhön, A., Schulze Langenhorst, L., Omari, A., et al. (2018). Cleaner Production of Cleaner Fuels: Wind-To-Wheel - Environmental Assessment of CO2-based Oxymethylene Ether as a Drop-In Fuel. *Energy Environ. Sci.* 11, 331–343. doi:10.1039/C7EE01657C

Devine-Wright, P., Batel, S., Aas, O., Sovacool, B., Labelle, M. C., and Ruud, A. (2017). A Conceptual Framework for Understanding the Social Acceptance of Energy Infrastructure: Insights from Energy Storage. *Energy Policy* 107, 27–31. doi:10.1016/j.enpol.2017.04.020

Dieterich, V., Buttler, A., Hanel, A., Spliethoff, H., and Fendt, S. (2020). Power-to-liquid via Synthesis of Methanol, DME or Fischer-Tropsch-Fuels: a Review. *Energ. Environ. Sci.* 13, 3207–3252. doi:10.1039/D0EE01187H

Drews, S., and Van den Bergh, J. C. J. M. (2016). What Explains Public Support for Climate Policies? a Review of Empirical and Experimental Studies. *Clim. Pol.* 16, 855–876. doi:10.1080/14693062.2015.1058240

eCOCO2 (2019). *Closing the Loop: From Co2 to fuel.Direct Electrocatalytic Conversion of Co2 into Chemical Energy Carriers in a Co-ionic Membrane Reactor*

Ellis, G., and Ferraro, G. (2016). "The Social Acceptance of Wind Energy. *Where We Stand and the Path Ahead*," in *JRC Science for Policy Report* (Brussels: European Commission).

Emmerich, P., Hülemeier, A.-G., Jendryczko, D., Baumann, M. J., Weil, M., and Baur, D. (2020). Public Acceptance of Emerging Energy Technologies in Context of the German Energy Transition. *Energy Policy* 142, 111516. doi:10.1016/j.enpol.2020.111516

Engelmann, L., Arning, K., Linzenich, A., and Ziefle, M. (2020). Risk Assessment Regarding Perceived Toxicity and Acceptance of Carbon Dioxide-Based Fuel by Laypeople for its Use in Road Traffic and Aviation. *Front. Energ. Res.* 8, 291. doi:10.3389/fenrg.2020.579814

Eurostat Statistics Explained (2011). *International Standard Classification of Education (ISCED).*

Evans, L., Maio, G. R., Corner, A., Hodgetts, C. J., Ahmed, S., and Hahn, U. (2013). Self-interest and Pro-environmental Behaviour. *Nat. Clim Change* 3, 122–125. doi:10.1038/nclimate1662

Federico d'Amore, F., Lovisotto, L., and Bezzo, F. (2020). Introducing Social Acceptance into the Design of Ccs Supply Chains: A Case Study at a European Level. *J. Clean. Prod.* 249, 119337. doi:10.1016/j.jclepro.2019.119337

Feinberg, M., and Willer, R. (2013). The Moral Roots of Environmental Attitudes. *Psychol. Sci.* 24, 56–62. doi:10.1177/0956797612449177

Field, A. (2018). *Discovering Statistics Using IBM SPSS Statistics*. 5 edn.. London: SAGE publications Ltd).

Fine, S. F. (1986). Technological Innovation, Diffusion and Resistance. *J. Libr. Adm.* 7, 83–108. doi:10.1300/J111V07N01_g0910.1300/j111v07n01_09

Finkbeiner, M. (2014). "The International Standards as the Constitution of Life Cycle Assessment: the Iso 14040 Series and its Offspring," in *Background and Future Prospects in Life Cycle Assessment* (Springer), 85–106. doi:10.1007/978-94-017-8697-3_3

Finucane, M. L., Alhakami, A., Slovic, P., and Johnson, S. M. (2000). The Affect Heuristic in Judgments of Risks and Benefits. *J. Behav. Decis. Making* 13, 1–17. doi:10.1002/(SICI)1099-0771(200001/03)13:13.0.CO;2-S10.1002/(sici)1099-0771(200001/03)13:1<1::aid-bdm333>3.0.co;2-s

Fischhendler, I., Herman, L., Barr, A., and Rosen, G. (2021). The Impact of Community Split on the Acceptance of Wind Turbines. *Solar Energy* 220, 51–62. doi:10.1016/j.solener.2021.01.055

Foley, A., Smyth, B. M., Pukšec, T., Markovska, N., and Duić, N. (2017). A Review of Developments in Technologies and Research that Have Had a Direct Measurable Impact on Sustainability Considering the paris Agreement on Climate Change. *Renew. Sustainable Energ. Rev.* 68, 835–839. doi:10.1016/j.rser.2016.11.215

Gölz, S., and Wedderhoff, O. (2018). Explaining Regional Acceptance of the German Energy Transition by Including Trust in Stakeholders and Perception of Fairness as Socio-Institutional Factors. *Energ. Res. Soc. Sci.* 43, 96–108. doi:10.1016/j.erss.2018.05.026

Hackbarth, A., and Madlener, R. (2013). Consumer Preferences for Alternative Fuel Vehicles: A Discrete Choice Analysis. *Transportation Res. D: Transport Environ.* 25, 5–17. doi:10.1016/j.trd.2013.07.002

Hackbarth, A., and Madlener, R. (2016). Willingness-to-pay for Alternative Fuel Vehicle Characteristics: A Stated Choice Study for germany. *Transportation Res. A: Pol. Pract.* 85, 89–111. doi:10.1016/j.tra.2015.12.005

Hair, J. F., Hult, G. T. M., Ringle, C., and Sarstedt, M. (2017). *A Primer on Partial Least Squares Structural Equation Modeling (PLS-SEM)*. 2 edn. Los Angeles: Sage publications, Inc).

Hair, J., Risher, J., Sarstedt, M., and Ringle, C. (2018). When to Use and How to Report the Results of Pls-Sem. *Eur. Business Rev.* 31. doi:10.1108/EBR-11-2018-0203

Hartley, K., van Santen, R., and Kirchherr, J. (2020). Policies for Transitioning towards a Circular Economy: Expectations from the european union (Eu). *Resour. Conservation Recycling* 155, 104634. doi:10.1016/j.resconrec.2019.104634

Huijts, N. M. A., de Vries, G., and Molin, E. J. E. (2019). A Positive Shift in the Public Acceptability of a Low-Carbon Energy Project after Implementation: The Case of a Hydrogen Fuel Station. *Sustainability* 11. doi:10.3390/su11082220

Huijts, N. M. A., Molin, E. J. E., and Steg, L. (2012). Psychological Factors Influencing Sustainable Energy Technology Acceptance: A Review-Based Comprehensive Framework. *Renew. Sustainable Energ. Rev.* 16, 525–531. doi:10.1016/j.rser.2011.08.018

Huijts, N. M. A. (2018). The Emotional Dimensions of Energy Projects: Anger, Fear, joy and Pride about the First Hydrogen Fuel Station in the netherlands. *Energ. Res. Soc. Sci.* 44, 138–145. doi:10.1016/j.erss.2018.04.042

International Energy Agency (2019). *Putting CO2 to Use*. (IEA)

International Standard Organization (1997). *ISO 14040: Environmental Management-Life Cycle Assessment-Principles And Framework*.

Joffe, H. (2003). Risk: From Perception to Social Representation. *Br. J. Soc. Psychol.* 42, 55–73. doi:10.1348/014466603763276126

Jones, C. R., Kaklamanou, D., Stuttard, W. M., Radford, R. L., and Burley, J. (2015). Investigating Public Perceptions of Carbon Dioxide Utilisation (Cdu) Technology: a Mixed Methods Study. *Faraday Discuss.* 183, 327–347. doi:10.1039/c5fd00063g

Jones, C. R., Olfe-Kräutlein, B., Naims, H., and Armstrong, K. (2017). The Social Acceptance of Carbon Dioxide Utilisation: A Review and Research Agenda. *Front. Energ. Res.* 5. doi:10.3389/fenrg.2017.00011

Jones, C. R., Radford, R. L., Armstrong, K., and Styring, P. (2014). What a Waste! Assessing Public Perceptions of Carbon Dioxide Utilisation Technology. *J. CO2 Utilization* 7, 51–54. doi:10.1016/j.jcou.2014.05.001

Kätelhön, A., Meys, R., Deutz, S., Suh, S., and Bardow, A. (2019). Climate Change Mitigation Potential of Carbon Capture and Utilization in the Chemical Industry. *Proc. Natl. Acad. Sci. U S A.* 116, 11187–11194. doi:10.1073/pnas.1821029116

Kirchherr, J., and Piscicelli, L. (2019). Towards an Education for the Circular Economy (Ece): Five Teaching Principles and a Case Study. *Resour. Conservation Recycling* 150, 104406. doi:10.1016/j.resconrec.2019.104406

Klöpffer, W. (2014). "Introducing Life Cycle Assessment and its Presentation in 'LCA Compendium'," in *Background and Future Prospects in Life Cycle Assessment* (Springer), 1–37. doi:10.1007/978-94-017-8697-3_1

Kluge, J., Offermann-van Heek, J., and Ziefle, M. (2021). How Will I Know about Local Energy Projects? A Conjoint-Analysis of Communication Preferences in Germany. *Energ. Res. Soc. Sci.* 75, 102016. doi:10.1016/j.erss.2021.102016

Kratschmann, M., and Dütschke, E. (2021). Selling the Sun: A Critical Review of the Sustainability of Solar Energy Marketing and Advertising in germany. *Energ. Res. Soc. Sci.* 73, 101919. doi:10.1016/j.erss.2021.101919

Liebe, U., and Dobers, G. M. (2019). Decomposing Public Support for Energy Policy: what Drives Acceptance of and Intentions to Protest against Renewable Energy Expansion in germany? *Energ. Res. Soc. Sci.* 47, 247–260. doi:10.1016/j.erss.2018.09.004

Linzenich, A., Arning, K., Bongartz, D., Mitsos, A., and Ziefle, M. (2019a). What Fuels the Adoption of Alternative Fuels? Examining Preferences of German Car Drivers for Fuel Innovations. *Appl. Energ.* 249, 222–236. doi:10.1016/j.apenergy.2019.04.041

Linzenich, A., Arning, K., Offermann-van Heek, J., and Ziefle, M. (2019b). Uncovering Attitudes towards Carbon Capture Storage and Utilization Technologies in Germany: Insights into Affective-Cognitive Evaluations of Benefits and Risks. *Energ. Res. Soc. Sci.* 48, 205–218. doi:10.1016/j.erss.2018.09.017

Linzenich, A., Arning, K., and Ziefle, M. (2021). Acceptance of Energy Technologies in Context: Comparing Laypeople's Risk Perceptions across Eight Infrastructure Technologies in Germany. *Energy Policy* 152, 112071. doi:10.1016/j.enpol.2020.112071

Liu, P., Xu, Z., and Zhao, X. (2019). Road Tests of Self-Driving Vehicles: Affective and Cognitive Pathways in Acceptance Formation. *Transportation Res. Part A: Pol. Pract.* 124, 354–369. doi:10.1016/j.tra.2019.04.004

Lotz, V. (2020). *Public Perception of Alternative Fuels in Aviation – an Empirical Study on the Influence of National Culture on Technology Acceptance*. Unpublished master's thesis. Aachen, Germany: RWTH Aachen University.

Lutzke, L., and Árvai, J. (2021). Consumer Acceptance of Products from Carbon Capture and Utilization. *Climatic Change* 166, 1–20. doi:10.1007/s10584-021-03110-3

Mather-Gratton, Z. J., Larsen, S., and Bentsen, N. S. (2021). Understanding the Sustainability Debate on forest Biomass for Energy in Europe: A Discourse Analysis. *Plos one* 16, e0246873. doi:10.1371/journal.pone.0246873

Matzen, M., and Demirel, Y. (2016). Methanol and Dimethyl Ether from Renewable Hydrogen and Carbon Dioxide: Alternative Fuels Production and Life-Cycle Assessment. *J. Clean. Prod.* 139, 1068–1077. doi:10.1016/j.jclepro.2016.08.163

Midden, C. J. H., and Huijts, N. M. A. (2009). The Role of Trust in the Affective Evaluation of Novel Risks: The Case of CO2Storage. *Risk Anal. Int. J.* 29, 743–751. doi:10.1111/j.1539-6924.2009.01201.x

Moreau, V., Sahakian, M., Van Griethuysen, P., and Vuille, F. (2017). Coming Full circle: Why Social and Institutional Dimensions Matter for the Circular Economy. *J. Ind. Ecol.* 21, 497–506. doi:10.1111/jiec.12598

Morseletto, P. (2020). Targets for a Circular Economy. *Resour. Conservation Recycling* 153, 104553. doi:10.1016/j.resconrec.2019.104553

Mustafa, A., Lougou, B. G., Shuai, Y., Wang, Z., and Tan, H. (2020). Current Technology Development for Co2 Utilization into Solar Fuels and Chemicals: A Review. *J. Energ. Chem.* 49, 96–123. doi:10.1016/j.jechem.2020.01.023

Offermann-van Heek, J., Arning, K., Linzenich, A., and Ziefle, M. (2018). Trust and Distrust in Carbon Capture and Utilization Industry as Relevant Factors for the Acceptance of Carbon-Based Products. *Front. Energ. Res.* 6. doi:10.3389/fenrg.2018.00073

Offermann-van Heek, J., Arning, K., Sternberg, A., Bardow, A., and Ziefle, M. (2020). Assessing Public Acceptance of the Life Cycle of CO2-based Fuels: Does Information Make the Difference?. *Energy Policy* 143, 111586. doi:10.1016/j.enpol.2020.111586

Peters, G. P., and Geden, O. (2017). Catalysing a Political Shift from Low to Negative Carbon. *Nat. Clim Change* 7, 619–621. doi:10.1038/nclimate3369

Pieri, T., Nikitas, A., Castillo-Castillo, A., and Angelis-Dimakis, A. (2018). Holistic Assessment of Carbon Capture and Utilization Value Chains. *Environments* 5, 108. doi:10.3390/environments5100108

Pires da Mata Costa, L., Micheline Vaz de Miranda, D., Couto de Oliveira, A. C., Falcon, L., Stella Silva Pimenta, M., Guilherme Bessa, I., et al. (2021). Capture and Reuse of Carbon Dioxide (Co2) for a Plastics Circular Economy: A Review. *Processes* 9. doi:10.3390/pr9050759

Porteron, S., de Bruijne, E., Den, X. L., Zotz, F., Olfe-Kräutlein, B., Marxen, A., et al. (2019). *Identification and Analysis of Promising Carbon Capture and Utilisation Technologies, Including Their Regulatory Aspects*. Potsdam, Germany: European Commission, Directorate-General for Climate Action.

Ray, S., Danks, N., and Calero Valdez, A. (2021). *Seminr: Domain-specific Language for Building and Estimating Structural Equation Models*.

Renn, O., Klinke, A., and Van Asselt, M. (2011). Coping with Complexity, Uncertainty and Ambiguity in Risk Governance: a Synthesis. *Ambio* 40, 231–246. doi:10.1007/s13280-010-0134-0

Ricci, M., Bellaby, P., and Flynn, R. (2008). What Do We Know about Public Perceptions and Acceptance of Hydrogen? a Critical Review and New Case Study Evidence. *Int. J. Hydrogen Energ.* 33, 5868–5880. doi:10.1016/j.ijhydene.2008.07.106

Sarstedt, M., Hair, J. F., Jr, Cheah, J.-H., Becker, J.-M., and Ringle, C. M. (2019). How to Specify, Estimate, and Validate Higher-Order Constructs in Pls-Sem. *Australas. Marketing J.* 27, 197–211. doi:10.1016/j.ausmj.2019.05.003

Sarstedt, M., Hair, J. F., Ringle, C. M., Thiele, K. O., and Gudergan, S. P. (2016). Estimation Issues with Pls and Cbsem: Where the Bias Lies!. *J. Business Res.* 69, 3998–4010. doi:10.1016/j.jbusres.2016.06.007

Scheelhaase, J., Maertens, S., and Grimme, W. (2019). Synthetic Fuels in Aviation - Current Barriers and Potential Political Measures. *Transportation Res. Proced.* 43, 21–30. doi:10.1016/j.trpro.2019.12.015

Scherhaufer, P., Höltinger, S., Salak, B., Schauppenlehner, T., and Schmidt, J. (2017). Patterns of Acceptance and Non-acceptance within Energy Landscapes: A Case Study on Wind Energy Expansion in Austria. *Energy Policy* 109, 863–870. doi:10.1016/j.enpol.2017.05.057

Schwartz, P. M. (2019). Global Data Privacy: The EU Way. *NYUL Rev.* 94, 771.

Simons, L., Ziefle, M., and Arning, K. (2021). The Social Acceptance Factors for Insulation Boards Produced with Co2-Derived Foam. *Front. Energ. Res.* 9, 422. doi:10.3389/fenrg.2021.717975

Sinkovics, R. R., Stöttinger, B., Schlegelmilch, B. B., and Ram, S. (2002). Reluctance to Use Technology-Related Products: Development of a Technophobia Scale. *Thunderbird Int'l Bus Rev.* 44, 477–494. doi:10.1002/tie.10033

Slovic, P., Fischhoff, B., and Lichtenstein, S. (1982). Why Study Risk Perception? *Risk Anal.* 2, 83–93. doi:10.1111/j.1539-6924.1982.tb01369.x

Slovic, P., and Peters, E. (2006). Risk Perception and Affect. *Curr. Dir. Psychol. Sci.* 15, 322–325. doi:10.1111/j.1467-8721.2006.00461.x

Sovacool, B. K., Axsen, J., and Sorrell, S. (2018). Promoting novelty, Rigor, and Style in Energy Social Science: towards Codes of Practice for Appropriate Methods and Research Design. *Energ. Res. Soc. Sci.* 45, 12–42. doi:10.1016/j.erss.2018.07.007

Sovacool, B. K., Ryan, S. E., Stern, P. C., Janda, K., Rochlin, G., Spreng, D., et al. (2015). Integrating Social Science in Energy Research. *Energ. Res. Soc. Sci.* 6, 95–99. doi:10.1016/j.erss.2014.12.005

Tellis, G. J., Stremersch, S., and Yin, E. (2003). The International Takeoff of New Products: The Role of Economics, Culture, and Country Innovativeness. *Marketing Sci.* 22, 188–208. doi:10.1287/mksc.22.2.188.16041

Tenhunen, A., and Pöhler, H. (2020). *A Circular Economy of Plastics: A Vision of Redesigning Plastics Value Chains*. doi:10.32040/2020.978-951-38-8824-4

van Heek, J., Arning, K., and Ziefle, M. (2017a). Differences between Laypersons and Experts in Perceptions and Acceptance of CO2-utilization for Plastics Production. *Energ. Proced.* 114, 7212–7223. doi:10.1016/j.egypro.2017.03.1829

van Heek, J., Arning, K., and Ziefle, M. (2017b). Reduce, Reuse, Recycle: Acceptance of CO 2 -utilization for Plastic Products. *Energy Policy* 105, 53–66. doi:10.1016/j.enpol.2017.02.016

von der Assen, N., and Bardow, A. (2014). Life Cycle Assessment of Polyols for Polyurethane Production Using CO2 as Feedstock: Insights from an Industrial Case Study. *Green. Chem.* 16, 3272–3280. doi:10.1039/C4GC00513A

Wich, T., Lueke, W., Deerberg, G., and Oles, M. (2020). Carbon2Chem-CCU as a Step toward a Circular Economy. *Front. Energ. Res.* 7, 162. doi:10.3389/fenrg.2019.00162

Wüstenhagen, R., Wolsink, M., and Bürer, M. J. (2007). Social Acceptance of Renewable Energy Innovation: An Introduction to the Concept. *Energy Policy* 35, 2683–2691. doi:10.1016/j.enpol.2006.12.001

Zakkour, P., Cook, G., Akai, M., Itaoka, K., Chae, S., and Kemper, J. (2018). *Towards Greenhouse Gas Accounting Guidelines for Carbon Dioxide Capture and Utilisation Technologies*.

Zaunbrecher, B. S., and Ziefle, M. (2016). Integrating Acceptance-Relevant Factors into Wind Power Planning: A Discussion. *Sustainable Cities Soc.* 27, 307–314. doi:10.1016/j.scs.2016.08.018

Zheng, X., Wang, R., Hoekstra, A. Y., Krol, M. S., Zhang, Y., Guo, K., et al. (2021). Consideration of Culture Is Vital if We Are to Achieve the Sustainable Development Goals. *One Earth* 4, 307–319. doi:10.1016/j.oneear.2021.01.012

Zimmerman, A., Müller, L., Wang, Y., Langhorst, T., Wunderlich, J., Marxen, A., et al. (2020a). *Techno-economic Assessment Life Cycle Assessment Guidelines for Co2 Utilization*, version 1.1. doi:10.3998/2027.42/162573

Zimmermann, A. W., Wunderlich, J., Müller, L., Buchner, G. A., Marxen, A., Michailos, S., et al. (2020b). Techno-economic Assessment Guidelines for Co2 Utilization. *Front. Energ. Res.* 8, 5. doi:10.3389/fenrg.2020.00005

Conflict of Interest: The authors declare that the research was conducted in the absence of any commercial or financial relationships that could be construed as a potential conflict of interest.

Advantages of publishing in Frontiers

OPEN ACCESS
Articles are free to read
for greatest visibility
and readership

FAST PUBLICATION
Around 90 days
from submission
to decision

HIGH QUALITY PEER-REVIEW
Rigorous, collaborative,
and constructive
peer-review

TRANSPARENT PEER-REVIEW
Editors and reviewers
acknowledged by name
on published articles

Frontiers
Avenue du Tribunal-Fédéral 34
1005 Lausanne | Switzerland

Visit us: www.frontiersin.org
Contact us: frontiersin.org/about/contact

REPRODUCIBILITY OF RESEARCH
Support open data
and methods to enhance
research reproducibility

DIGITAL PUBLISHING
Articles designed
for optimal readership
across devices

FOLLOW US
@frontiersin

IMPACT METRICS
Advanced article metrics
track visibility across
digital media

EXTENSIVE PROMOTION
Marketing
and promotion
of impactful research

LOOP RESEARCH NETWORK
Our network
increases your
article's readership